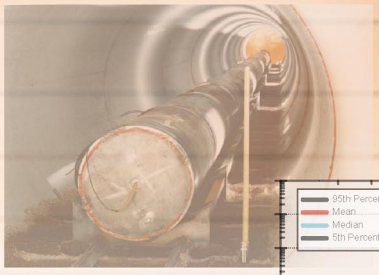

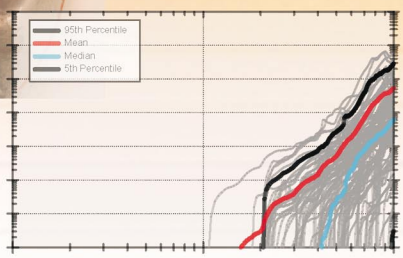

FY01 Supplemental Science and Performance Analyses,

Volume 2: Performance Analyses

U.S. Department of Energy
Office of Civilian Radioactive Waste Management

July 2001

QA: QA

TDR-MGR-PA-000001 REV 00

July 2001

FY01 Supplemental Science and Performance Analyses, Volume 2: Performance Analyses

By
BSC

Prepared for:
U.S. Department of Energy
Yucca Mountain Site Characterization Office
P.O. Box 30307
North Las Vegas, Nevada 89036-0307

Prepared by:
Bechtel SAIC Company, LLC
1180 Town Center Drive
Las Vegas, Nevada 89144

Under Contract Number
DE-AC08-01RW12101

QA: QA

TDR-MGR-PA-000001 REV 00

July 2001

FY 01 Supplemental Science and Performance Analyses

Volume 2:
Performance Analyses

By
BSC

Prepared for:
U.S. Department of Energy
Yucca Mountain Site Characterization Office
P.O. Box 30307
North Las Vegas, Nevada 89036-0307

Prepared by:
Bechtel SAIC Company, LLC
1180 Town Center Drive
Las Vegas, Nevada 89144

Under Contract Number
DE-AC08-01RW12101

DISCLAIMER

This report was prepared as an account of work sponsored by an agency of the United States Government. Neither the United States Government nor any agency thereof, nor any of their employees, nor any of their contractors, subcontractors or their employees, makes any warranty, express or implied, or assumes any legal liability or responsibility for the accuracy, completeness, or any third party's use or the results of such use of any information, apparatus, product, or process disclosed, or represents that its use would not infringe privately owned rights. Reference herein to any specific commercial product, process, or service by trade name, trademark, manufacturer, or otherwise, does not necessarily constitute or imply its endorsement, recommendation, or favoring by the United States Government or any agency thereof or its contractors or subcontractors. The views and opinions of authors expressed herein do not necessarily state or reflect those of the United States Government or any agency thereof.

Prepared by:

Jerry A McNeish for P. Swift — 7.17.01

P.N. Swift et al.
Lead Author

Date

Checked by:

David E. Mohn FOR L.C. Powell — 7/17/01

L.C. Powell et al.
Discipline Primary Checker

Date

Approved by:

Jerry A McNeish — 7.17.01

J.A. McNeish
Responsible Manager
Total System Performance Assessment

Date

ACKNOWLEDGMENTS

The following individuals have contributed to the technical content and preparation of this document:

Authors/Analysts

B.W. Arnold
K. Coppersmith
E. Devonec
B. Dunlap
N. Graves
K.E. Jenni
D.A. Kalinich
K.P. Lee
J.D. Matties
J.A. McNeish
S.P. Miller
L.D. Rickertsen
D. Sevougian
P.N. Swift
M.L. Wilson

Checkers

N. E. Biggar
G. Freeze
D. Hoxie
W. Hunt
D.E. Mohr
J. McCord
A.S. Mobasheran
L.C. Powell (Discipline Primary Checker)
J.L. Ramsey
G.J. Saulnier
L. Rottinghaus
R.D. Zimmerman

Reviewers

D. Beckman
G.S. Bodvarsson
S.J. Cereghino
D. Dobson
A.A. Eddebbarh
G.E. Gdowski
J.F. Gibbons
J.L. King
C.L. Lugo
M.A. Lugo
R. MacKinnon
E. Miller
G.H. Nieder-Westermann
J. Nowak
B.A. Robinson
A. Simmons
A.J. Smith
C. Stockman
T. Summers
S.H. Swenning
Y. Tsang
G. Valentine
M. Zhu
P. Mast
R. Quittmeyer

Technical Editors

J.L. Boone
C.K. Dodson
M.C. Therien

Technical Support

J. Avvakoumides
C.E. Cisneros
N. Connerley
S.D. Crawford
K.K. Fong
L.C. Grisham
A.M. Hunter
R. Hyman
V.Y. Kelly
L. Lechel
M.W. Lee
S.L. Martin
S. Royall
C.M. Sales
C.A. Stewart

Graphics

R.K. Chandler
R.J. Danat
L.G. Feedar
J.A. Gibes
J.E. Lloyd
L.R. McKinley
R.C. Sandgren
W.D. Young

This work was supported by the Yucca Mountain Site Characterization Office as part of the Civilian Radioactive Waste Management Program, which is managed by the U.S. Department of Energy, Yucca Mountain Site Characterization Project.

INTENTIONALLY LEFT BLANK

CONTENTS

Page

CONTENTS (Continued)

Page

FIGURES

Page

FIGURES (Continued)

Page

FIGURES (Continued)

Page

FIGURES (Continued)

Page

FIGURES (Continued)

Page

FIGURES (Continued)

Page

FIGURES (Continued)

Page

INTENTIONALLY LEFT BLANK

TABLES

Page

INTENTIONALLY LEFT BLANK

ACRONYMS

AMR	analysis model report
BDCF	biosphere dose-conversion factor
CDF	cumulative distribution function
CSNF	commercial spent nuclear fuel
DLL	dynamic link library
DOE	U.S. Department of Energy
DTN	Data Tracking Number
EBS	engineered barrier system
EPA	U.S. Environmental Protection Agency
HLW	high-level waste
HTOM	higher-temperature operating mode
LTOM	lower-temperature operating mode
NRC	U.S. Nuclear Regulatory Commission
PA	performance assessment
RH	relative humidity
S&ER	Yucca Mountain Science and Engineering Report
SCC	stress corrosion cracking
SCCD	Stress Corrosion Cracking Dissolution
SCM	Software Configuration Management
SSPA	Supplemental Science and Performance Analysis Report
SZ	saturated zone
TH	thermal-hydrologic
THC	thermal-hydrologic-chemical
THM	thermal-hydrologic-mechanical
TSPA	total system performance assessment
TSPA-SR	Total System Performance Assessment for the Site Recommendation
UZ	unsaturated zone

INTENTIONALLY LEFT BLANK

1. INTRODUCTION

The U.S. Department of Energy (DOE) is considering the possible recommendation of a site at Yucca Mountain, Nevada, for the potential development of a geologic repository for the disposal of high-level radioactive waste and spent nuclear fuel. To facilitate public review and comment, in May 2001 the DOE released the *Yucca Mountain Science and Engineering Report* (S&ER) (DOE 2001 [DIRS 153849]), which presents technical information supporting the consideration of the possible site recommendation. The report summarizes the results of more than 20 years of scientific and engineering studies. A decision to recommend the site has not been made: the DOE has provided the S&ER and its supporting documents as an aid to the public in formulating comments on the possible recommendation.

This *FY01 Supplemental Science and Performance Analyses* report (SSPA) has been prepared to describe the results of additional technical studies related to the performance of a potential Yucca Mountain repository. The S&ER and its supporting documents describe the extensive scientific studies that have been conducted; however, important uncertainties will always remain in any assessment of the performance of a potential repository over thousands of years (DOE 2001 [DIRS 153849], Sections 1.5, 4.1, and 4.4). One part of the DOE approach to recognizing and managing these uncertainties is a commitment to continued testing and analysis and to the continued evaluation of the technical basis supporting the possible recommendation of the site.

This report, the SSPA, has been prepared to address several specific aspects of the existing uncertainties related to the performance of a potential Yucca Mountain repository. The SSPA describes new information developed since the completion of the models supporting the S&ER, including its key supporting references, the *Total System Performance Assessment for the Site Recommendation* (TSPA-SR) (CRWMS M&O 2000 [DIRS 153246]) and the analysis model reports (AMRs) and process model reports cited therein.

This SSPA consists of two volumes. The first volume, *FY01 Supplemental Science and Performance Analyses, Volume 1 – Scientific Bases and Analyses* (BSC 2001 [DIRS 154657]), focuses on the technical work conducted in each process model area, encompassing uncertainty quantification, updated science and models, and lower-temperature operating mode (LTOM) analyses. This volume, *FY01 Supplemental Science and Performance Analyses, Volume 2 - Performance Analyses*, describes the total system performance assessment (TSPA) analyses conducted using the updated information documented in Volume 1. The SSPA has been prepared in accordance with the *Technical Work Plan for FY01 Supplemental Science and Performance Analyses: Volume 1 – Scientific Bases and Analyses, Volume 2 – Performance Analyses* (BSC 2001 [DIRS 155055]). For an expanded discussion of the background for these reports, see SSPA Volume 1 (BSC 2001 [DIRS 154657], Section 1.1).

1.1 GOALS AND SCOPE

Based on internal reviews of the S&ER (DOE 2001 [DIRS 153849]) and other documents, the DOE identified and performed several types of analyses to supplement the treatment of uncertainty in support of the consideration of a possible site recommendation. The information in this report is intended to supplement, not supplant, the information contained in the AMRs

supporting the S&ER. In general, the studies and analyses described in this document provide additional information of three types:

- **Unquantified Uncertainties Analysis**–Specific uncertainties that were not treated explicitly in the S&ER and the TSPA-SR are quantified. Unquantified uncertainties include parameter bounds, conceptual models, assumptions, and in some cases, input parameters consisting of statistically biased or skewed distributions. The primary goals of this effort were to provide insights into the importance of the unquantified uncertainties and the degree of conservatism in the overall assessment of the performance of a potential repository described in the TSPA-SR.

- **Updates in Scientific Information**–New information has been developed for some of the process models that are important to performance. This work includes new experimental results, new conceptual models, and new analytical approaches, as well as results of continued research. It also identifies and discusses multiple lines of evidence that have been used directly, to support modeling, or indirectly, to develop confidence in modeling results. The primary goals of this effort were to provide insights into the impact of the new scientific results and improved models (i.e., those updated since completion of the models supporting the S&ER), and to develop additional confidence in the models and parameters used for total system performance assessment (TSPA).

- **Lower-Temperature Operating Mode Analysis**–Because some of the processes that can affect performance are a function of the environment in the potential repository (e.g., temperature and humidity), the uncertainties associated with models of these processes also depend on the environmental variables. In particular, operating the potential repository at temperatures above 96°C would result in water boiling and condensing, which requires models of flow and transport that are more complex-and possibly more uncertain-than models at lower temperatures. Therefore, the effects of a range of thermal operating modes on projected system performance, including lower operating temperatures in the potential repository (e.g., below 96°C at the drift wall or below 85°C at the waste package surface), have been evaluated. The uncertainties associated with various process models have been analyzed over a range of temperatures. The primary goals of evaluating a range of thermal operating modes were to provide insights into the effect of thermal parameters on predicted performance of a potential repository, including uncertainty of those predictions, and to increase confidence in the predicted performance of a potential repository over a range of thermal conditions.

The three types of supplemental information have been evaluated in terms of the impact on process model results, as described in SSPA Volume 1, and in terms of the impacts on TSPA results, which are described in this volume.

1.2 OVERVIEW OF ANALYSIS PROCESS

Performance assessment is a method of forecasting how a potential repository system, or parts of this system, designed to contain radioactive waste is expected to behave over time. One goal of performance assessment (PA) is to aid in determining whether the potential repository system

can meet established performance requirements. Other applications include identifying which barriers and processes significantly affect performance, explicitly presenting uncertainty in projections, and providing information to guide future design and testing activities. The TSPA is a comprehensive quantitative analysis where the results of detailed conceptual and numerical models of each of the individual and coupled processes are combined into a single probabilistic model that can be used to project how a potential repository will perform over time. Detailed background on the definition, philosophy, regulatory requirements for, and the development and use of a TSPA is described in the TSPA-SR (CRWMS M&O 2000 [DIRS 153246], Section 1.1.1).

Based on the results of the three types of supplemental information, described above and documented in SSPA Volume 1, two types of analyses of the performance of the potential repository were conducted using TSPA and are documented in this volume. First, a set of sensitivity analyses was conducted to evaluate the effects of incorporating the updated models and representations (based on the unquantified uncertainties, new scientific information, and updates necessary to evaluate a LTOM) one at a time. Then, the updated models and representations were abstracted and aggregated to produce a modified TSPA model, referred to as the supplemental TSPA model, that captures the combined effects of those alternative representations. This supplemental TSPA model was used to evaluate system performance over a range of thermal operating modes. The supplemental TSPA model results were compared with results of the TSPA-SR to provide insights into the cumulative effects of all model changes on the system results.

Section 2 of this volume describes the method and approach used to conduct the TSPA sensitivity analyses and the uses of the supplemental TSPA model. The following sections briefly describe the types of insights that can be drawn from those analyses.

1.2.1 Potential Insights from Sensitivity Analyses

TSPA results can be reviewed at the system level and at the subsystem level. System-level results refer to one of the key outputs of the TSPA model: estimated annual dose from radiological exposure to materials released from the potential repository and received by a critical group of individuals that reside on a transport pathway from the potential repository to the biosphere. TSPA analyses produce estimates of the annual dose over the time of the analyses. Subsystem-level results refer to intermediate results of the TSPA model. Intermediate results include, for example, seepage flow rate at the drift wall and the transport time of specific radionuclides in the saturated zone (SZ). Subsystem- and system-level results can provide insight into the effect of newly quantified uncertainties, newly updated technical and scientific information, and potential impacts of changes in thermal operating mode.

Sensitivity analyses make it possible to trace a specific model update to a specific change in system-level results: that is, to a change in estimated expected annual dose. Because the results produced at the system level are dose estimates, these system-level sensitivity analyses can result in insights about the overall degree of conservatism or non-conservatism in the results of other analyses using TSPA models.

In cases where sensitivity analyses do not show impacts on the system-level results, analyses that are focused on subsystem-level results help to isolate and show the immediate implications of model updates. The subsystem-level analyses emphasize the impact on intermediate results where changes can be tied most directly to the specific process model updates being evaluated. Subsystem-level results can provide insights into the importance of the specific input to system-level performance, and into the degree of conservatism or non-conservatism in previous model assumptions. For example, if an updated representation involves making a large change to an input parameter to a process model, and the results of that process model or the abstracted model change little or not at all, then system performance is not sensitive to that particular input. Thus subsystem results can be used to provide insights into whether the updated representations have the potential to impact the overall total system performance. These conclusions need to be made cautiously. Many of these sensitivity analyses were run individually, and individually many showed little effect, but it is possible that combinations of parameters might have a large effect.

In addition, if the new representation is believed to provide a better or more realistic representation of uncertainty, or incorporates new technical information, subsystem results can be compared with subsystem results from the TSPA-SR models and representations. For example, if a model has been updated based on new experimental results, and the subsystem results show much better performance (i.e., greater ability to limit radionuclide release and transport) at the subsystem level, it can be concluded that the previous representation was conservative; that is, it under-estimated the performance of that subsystem. Similarly, if a new representation results in much poorer performance at the subsystem level, it might be concluded that the previous representation was non-conservative; that is, it over-estimated performance of that subsystem. Again, caution is needed in drawing conclusions since "local" conservatism relative to subsystem behavior does not necessarily mean conservatism at the total system level.

1.2.2 Potential Insights from the Supplemental TSPA Model

The supplemental TSPA model combines a large number of the individual process-level updates from the three types of information produced and described in Volume 1 into a single TSPA model. Analyses with the supplemental TSPA model have also been conducted at the system level and the subsystem level. At the system level, results from different implementations of the TSPA can be compared to produce a range of insights into overall performance. Results from the supplemental TSPA model are compared with results from the TSPA-SR model (see Section 4) to help understand the aggregated implications of all updated models and representations. This comparison may also have implications for understanding the overall degree of conservatism or non-conservatism that may be associated with the TSPA results presented in the TSPA-SR. The results of the supplemental TSPA model under the assumptions associated with different thermal operating conditions can be compared to develop insights into thermal effects. Of particular interest is whether there are differences in the expected annual dose and the uncertainty in that estimated dose over time under different thermal conditions.

Finally, the subsystem-level analyses conducted with the supplemental TSPA model include examinations of the subsystem performance to changes due to thermal operating modes. These show which components of the total system are sensitive to temperatures in the potential repository, and show the implications of different thermal modes for performance at the subsystem level. This can be important in that some processes may be thermally affected, but

that effect will only be discernable at the subsystem level and not at the system level. Again, conclusions about the system-level implications of different thermal operating modes based on subsystem-level results must be made cautiously. Since many of these sensitivity analyses are being run individually, there is a possibility that coupled processes will not be captured in these subsystem-level analyses.

1.3 OUTLINE OF REPORT

This report, consisting of two volumes, describes supplemental information and analyses that have been performed, the results of which have been incorporated into a TSPA. SSPA Volume 1 (BSC 2001 [DIRS 154657]) focuses on the technical work conducted in each process model area, encompassing uncertainty quantification, updated science and models, and lower-temperature operating mode analyses. Volume 2 describes the supplemental TSPA analyses conducted using the SSPA Volume 1 updated information.

Table 1.3-1 shows the supplemental analyses that have been produced, the rationale for obtaining that supplemental information (i.e., unquantified uncertainties, updated scientific information, or lower-temperature operating mode analyses), and the section in Volume 1 of this report where the work is documented.

The last two columns of the table identify whether and how the supplemental information was evaluated in a TSPA analysis. Most of the specific items shown in the table were analyzed through a TSPA sensitivity analysis, and many were included in the supplemental TSPA model. The methods and approaches used to conduct the sensitivity analyses and development of the supplemental TSPA model are discussed in Section 2 of this volume. As can be seen in the table, some topics were evaluated only through the process-level analyses described in Volume 1. Some topics were evaluated through TSPA sensitivity analyses only, and were not included in the supplemental TSPA model. This is usually because the sensitivity analyses show a minor effect on system performance. As discussed in Section 2 and subsequent sections of this volume, the performance analyses provide a more quantitative means of evaluating the significance of the supplemental information. These analyses support the evaluations of the subsystem significance discussed for each process model in Volume 1. The performance analyses indicated in the last two columns of Table 1.3-1 are discussed in Sections 3 and 4 of this volume.

The contents of each of the sections of this volume are as follows:

- Section 1 provides the goals and scope of the volume, including a description of the types of TSPA analyses that have been conducted.

- Section 2 describes the method and approach used to evaluate the implications of the updated technical information for TSPA results. It describes the method and approach used to evaluate the performance implications of newly quantified uncertainties and updated models and representations, as well as the method and approach used for thermal sensitivity analyses.

- Section 3 summarizes subsystem-level results and describes the results of TSPA sensitivity analyses for each of the updated representations described in Volume 1.

- Section 4 describes the TSPA results incorporating the updated models and representations into a supplemental TSPA model, and describes analyses conducted with that supplemental TSPA model to evaluate the sensitivity of performance to alternative thermal operating modes. This section also compares the results of the supplemental TSPA model (see Section 1.2.2) to the results from TSPA-SR. The comparisons provide insight into the overall changes in expected annual doses that result from the aggregated model updates.

- Section 5 summarizes the results of these evaluations.

Appendix A, *Data Tracking Information for Supplemental Science and Performance Analyses*, provides the information necessary to identify and compare results from the TSPA-SR with results from the supplemental TSPA model. The Appendix also identifies the tracking information relating to the Records Information System and Technical Data Management System through which the simulation model runs can be retrieved.

1.4 QUALITY ASSURANCE

An activity evaluation was performed for this work activity in accordance with AP-2.21Q, *Quality Determinations and Planning for Scientific, Engineering, and Regulatory Compliance Activities* [DIRS 154534], and it was determined that activities supporting the development of this work and activities documented in this technical product are quality-affecting activities. This technical product and associated activities have been prepared subject to the requirements of the *Quality Assurance Requirements and Description* (DOE 2000 [DIRS 149540]) and implementing procedures. This document was prepared in accordance with the *Technical Work Plan for FY01 Supplemental Science and Performance Analyses: Volume 1 - Scientific Bases and Analyses, Volume 2 - Performance Analyses* (BSC 2001 [DIRS 155055]). There are no deviations from the technical work plan in this technical product.

The activity evaluation and a Process Control Evaluation for Supplement V, prepared in accordance with AP-SV.1Q, *Control of the Electronic Management of Information* [DIRS 153202], are attached to the technical work plan. Section 10 of the technical work plan describes the controls that will be used in the electronic management of information for this work activity. The technical work plan provides important planning details and should be consulted if questions or issues arise related to this document and the work activities it describes.

As described in Section 1.1, the goal of the additional analyses presented in this technical report is to provide insights into the effects of uncertainty and conservatisms and optimisms that were not evaluated in the family of analysis model reports that supported the S&ER (DOE 2001 [DIRS 153849]) and the TSPA-SR (CRWMS M&O 2000 [DIRS 153246]). Additional analyses are presented to examine the potential performance-related effects associated with operating the potential repository over a range of thermal operating modes. To provide these insights, the baselined models and analyses used as the technical basis for the TSPA-SR and the S&ER have been modified or extended beyond the bounds utilized in the TSPA-SR. These alternative

representations are provided to evaluate the sensitivity of model performance to these unquantified uncertainties and to incorporate thermal dependencies into the conceptual representations used in the PA. These alternative representations supplement those documented in the supporting references to the TSPA-SR or the S&ER. While it may be necessary to modify a parameter distribution or model to examine the effects of these alternative representations, the models used as a basis for the TSPA-SR are not changed; these examinations are exploratory sensitivity analyses that provide insights into system behavior. In many respects, these analyses are no different than the types of sensitivity analyses, barrier importance analyses, and neutralization analyses that were presented in the TSPA-SR and the *Repository Safety Strategy: Plan to Prepare the Safety Case to Support Yucca Mountain Site Recommendation and Licensing Considerations* (CRWMS M&O 2000 [DIRS 153225]). If any of the revised models or analyses documented in this technical report are deemed to be more appropriate for the intended use of evaluating performance of a potential repository, they will be validated and documented in accordance with the quality assurance requirements for models and analyses in AP-3.10Q, *Analyses and Models* [DIRS 154517]. Until such time, they are considered scoping in nature to provide insights into the importance of uncertainty that was not explicitly evaluated in the TSPA-SR. Additional discussions regarding the applicability of quality assurance requirements to the SSPA is presented in SSPA Volume 1 (BSC 2001 [DIRS 154657], Section 1.5).

Software codes used in this study (see Section 2.3) were obtained from Software Configuration Management (SCM) in accordance with AP-SI.1Q, *Software Management* [DIRS 154886]. All qualified codes were appropriate for the intended use and were used only within the range of validation.

INTENTIONALLY LEFT BLANK

Table 1.3-1. Summary of Supplemental Models and Analyses

Key Attributes of System	Process Model (Section of S&ER)	Topic of Supplemental Scientific Model or Analysis	Reason for Supplemental Scientific Model or Analysis			Section of Volume 1	Performance Assessment Treatment of Supplemental Scientific Model or Analysis (Discussed in Volume 2)	
			Unquantified Uncertainty Analysis	Update in Scientific Information	Lower-Temperature Operating Mode Analysis		TSPA Sensitivity Analysis[a]	Included in Supplemental TSPA Model[b]
Limited Water Entering Emplacement Drifts	Climate (4.2.1)	Post-10,000-year climate model		X		3.3.1	X	X
	Net Infiltration (4.2.1)	Infiltration for post-10,000-year climate model		X		3.3.2	X	X
	Unsaturated Zone (UZ) Flow (4.2.1)	Flow in PTn		X		3.3.3		
		Three-dimensional flow fields for lower-temperature design; flow fields for post-10,000 yr climate, lateral flow; variable thickness of PTn; fault property uncertainty		X	X	3.3.4		
		Effects of lithophysal properties on thermal properties		X		3.3.5		
	Coupled Effects on UZ Flow (4.2.2)	Mountain-scale thermal-hydrologic (TH) effects		X	X	3.3.5		
		Mountain-scale thermal-hydrologic-chemical (THC) effects		X	X	3.3.6		
		Mountain-scale thermal-hydrologic-mechanical (THM) effects		X	X	3.3.7		
	Seepage into Emplacement Drifts (4.2.1)	Flow-focussing within heterogeneous permeability field; episodic seepage	X		X	4.3.1, 4.3.2, 4.3.5	X	X
		Effects of rock bolts and drift degradation on seepage	X			4.3.3, 4.3.4		
	Coupled Effects on Seepage (4.2.2)	Thermal effects on seepage	X		X	4.3.5	X	X
		THC effects on seepage	X		X	4.3.6		
		THM effects on seepage		X	X	4.3.7		

Table 1.3-1. Summary of Supplemental Models and Analyses (Continued)

Key Attributes of System	Process Model (Section of S&ER)	Topic of Supplemental Scientific Model or Analysis	Reason for Supplemental Scientific Model or Analysis			Section of Volume 1	Performance Assessment Treatment of Supplemental Scientific Model or Analysis (Discussed in Volume 2)	
			Unquantified Uncertainty Analysis	Update in Scientific Information	Lower-Temperature Operating Mode Analysis		TSPA Sensitivity Analysis[a]	Included in Supplemental TSPA Model[b]
Long-Lived Waste Package and Drip Shield	Water Diversion Performance of engineered barrier system (EBS) (4.2.3)	Multiscale TH model, including effects of rock dryout	X		X	5.3.1		X
		Thermal property sets	X	X		5.3.1		X
		Effect of in-drift convection on temperatures, humidities, invert saturations, and evaporation rates	X		X	5.3.2		
		Composition of liquid and gas entering drift	X		X	6.3.1	X	X
		Evolution of in-drift chemical environment	X		X	6.3.3	X	X
		Thermo-Hydro-Chemical model comparison to plug-flow reactor and fracture plugging experiment		X		6.3.1		
		Rockfall		X		6.3.4		
	In-Drift Moisture Distribution (4.2.5)	Environment on surface of drip shields and waste packages	X			5.3.2 7.3.1		
		Condensation under drip shields	X			8.3.2	X	
		Evaporation of seepage	X		X	8.3.1 5.3.2	X	X
		Effect of breached drip shields or waste package on seepage	X		X	8.3.3	X	X
		Waste package release flow geometry (flow-through, bathtub)	X			8.3.4	X	
	Drip Shield Degradation and Performance (4.2.4)	Local chemical environment on surface of drip shields (including magnesium and lead) and potential for initiating localized corrosion	X			7.3.1		

Table 1.3-1. Summary of Supplemental Models and Analyses (Continued)

Key Attributes of System	Process Model (Section of S&ER)	Topic of Supplemental Scientific Model or Analysis	Reason for Supplemental Scientific Model or Analysis			Section of Volume 1	Performance Assessment Treatment of Supplemental Scientific Model or Analysis (Discussed in Volume 2)	
			Unquantified Uncertainty Analysis	Update in Scientific Information	Lower-Temperature Operating Mode Analysis		TSPA Sensitivity Analysis[a]	Included in Supplemental TSPA Model[b]
Long-Lived Waste Package and Drip Shield	Waste Package Degradation and Performance (4.2.4)	Local chemical environment on surface of waste packages (including magnesium and lead) and potential for initiating localized corrosion	X			7.3.1		
		Aging and phase stability effects on Alloy 22	X	X		7.3.2	X	
		Uncertainty in weld stress state following mitigation	X			7.3.3	X	X
		Weld defects	X			7.3.3	X	X
		Early failure due to improper heat treatment	X		X	7.3.6	X	X
		General corrosion rate of Alloy 22: temperature dependency	X		X	7.3.5	X	X
		General corrosion rate of Alloy 22: uncertainty/variability partition	X			7.3.5	X	X
		Long-term stability of passive films on Alloy 22	X			7.3.4		
		Stress threshold for initiation of stress corrosion cracking (SCC)	X	X		7.3.3	X	X
		Probability of non-detection of manufacturing defects		X		7.4.3	X	X
		Number of defects		X		7.3.5	X	X
		Distribution of crack growth exponent (repassivation slope)	X	X		7.3.7	X	X
Limited Release of Radionuclides from the Engineered Barriers	In-Package Environments (4.2.6)	Effect of high-level waste (HLW) glass degradation rate and steel degradation rate on in-package chemistry	X		X	9.3.1	X	X
	Cladding Degradation and Performance (4.2.6)	Effect of initial perforations, creep rupture, SCC, localized corrosion, seismic failure, rock overburden failure, and unzipping velocity on cladding degradation	X		X	9.3.3	X	X

Table 1.3-1. Summary of Supplemental Models and Analyses (Continued)

Key Attributes of System	Process Model (Section of S&ER)	Topic of Supplemental Scientific Model or Analysis	Reason for Supplemental Scientific Model or Analysis			Section of Volume 1	Performance Assessment Treatment of Supplemental Scientific Model or Analysis (Discussed in Volume 2)	
			Unquantified Uncertainty Analysis	Update in Scientific Information	Lower-Temperature Operating Mode Analysis		TSPA Sensitivity Analysis[a]	Included in Supplemental TSPA Model[b]
Limited Release of Radionuclides from the Engineered Barriers	DOE high-level radioactive waste Degradation and Performance (4.2.6)	HLW glass degradation rates	X	X	X	9.3.1		
	Dissolved Radionuclide Concentrations (4.2.6)	Solubility of neptunium, thorium, plutonium, and technetium	X	X	X	9.3.2	X	X
	Colloid-Associated Radionuclide Concentrations (4.2.6)	Colloid mass concentrations	X			9.3.4	X	
	EBS (Invert) Degradation and Transport (4.2.6, 4.2.7)	Diffusion inside waste package	X	X		10.3.1	X	X
		Transport pathway from inside waste package to invert	X	X		10.3.2		
		Sorption inside waste package	X	X		10.3.4	X	X
		Sorption in invert	X	X		10.3.4	X	X
		Diffusion through invert	X			10.3.3	X	X
		Colloid stability in the invert	X			10.3.5		
		Microbial transport of colloids	X	X		10.3.6		

Table 1.3-1. Summary of Supplemental Models and Analyses (Continued)

Key Attributes of System	Process Model (Section of S&ER)	Topic of Supplemental Scientific Model or Analysis	Reason for Supplemental Scientific Model or Analysis			Section of Volume 1	Performance Assessment Treatment of Supplemental Scientific Model or Analysis (Discussed in Volume 2)	
			Unquantified Uncertainty Analysis	Update in Scientific Information	Lower-Temperature Operating Mode Analysis		TSPA Sensitivity Analysis[a]	Included in Supplemental TSPA Model[b]
Delay and Dilution of Radionuclide Concentrations by the Natural Barriers	UZ Radionuclide Transport (Advective Pathways; Retardation; Dispersion; Dilution) (4.2.8)	Effect of drift shadow zone - advection/diffusion splitting	X		X	11.3.1	X	X
		Effect of drift shadow zone – concentration boundary condition on EBS release rates	X			11.3.1		
		Effect of matrix diffusion	X			11.3.2, 11.3.3		
		Three-dimensional transport			X	11.3.2		
		Effect of coupled thermo-hydrologic, thermo-hydro-chemical, and thermo-hydro-mechanical processes on transport		X	X	11.3.5		
	SZ Radionuclide Flow and Transport (4.2.9)	Groundwater specific discharge	X	X		12.3.1	X	
		Effective diffusion coefficient in volcanic tuffs	X			12.3.2	X	
		Flowing interval spacing				12.3.2	X	
		Flowing interval (fracture) porosity	X			12.3.2	X	
		Effective porosity in the alluvium	X			12.3.2	X	
		Correlation of the effective diffusion coefficient with matrix porosity	X			12.3.2	X	
		Bulk density of the alluvium	X	X		12.3.2	X	X

Table 1.3-1. Summary of Supplemental Models and Analyses (Continued)

Key Attributes of System	Process Model (Section of S&ER)	Topic of Supplemental Scientific Model or Analysis	Reason for Supplemental Scientific Model or Analysis			Section of Volume 1	Performance Assessment Treatment of Supplemental Scientific Model or Analysis (Discussed in Volume 2)	
			Unquantified Uncertainty Analysis	Update in Scientific Information	Lower-Temperature Operating Mode Analysis		TSPA Sensitivity Analysis[a]	Included in Supplemental TSPA Model[b]
Delay and Dilution of Radionuclide Concentrations by the Natural Barriers	SZ Radionuclide Transport (4.2.9)	Retardation for radionuclides irreversibly sorbed on colloids in the alluvium	X	X		12.3.2	X	
		No matrix diffusion in volcanic tuffs case				12.5.2	X	
		Presence or absence of alluvium				12.5.2	X	
		Sorption coefficient in alluvium for iodine and technetium	X	X		12.3.2	X	X
		Sorption coefficient in alluvium for neptunium and uranium	X	X		12.3.2	X	
		Sorption coefficient for neptunium in volcanic tuffs	X			12.3.2	X	
		K_c model for groundwater colloid concentrations plutonium and americium		X		12.5.2	X	
		Enhanced matrix diffusion in volcanic tuffs				12.5.2	X	
		Effective longitudinal dispersivity	X	X		12.3.2	X	
		New dispersion tensor		X		12.3.2		
		Flexible design			X	12.3.2		
		Different conceptual models of the large hydraulic gradient and their effects on the flow path and specific discharge		X		12.3.1		
		Hydraulic head and map of potentiometric surface		X		12.3.1		

Table 1.3-1. Summary of Supplemental Models and Analyses (Continued)

Key Attributes of System	Process Model (Section of S&ER)	Topic of Supplemental Scientific Model or Analysis	Reason for Supplemental Scientific Model or Analysis			Section of Volume 1	Performance Assessment Treatment of Supplemental Scientific Model or Analysis (Discussed in Volume 2)	
			Unquantified Uncertainty Analysis	Update in Scientific Information	Lower-Temperature Operating Mode Analysis		TSPA Sensitivity Analysis[a]	Included in Supplemental TSPA Model[b]
Delay and Dilution of Radionuclide Concentrations by the Natural Barriers	Biosphere (4.2.10)	Receptor of interest	X			13.3.1		
		Comparison of dose assessment methods	X			13.3.2		
		Radionuclide removal from soil by leaching	X			13.3.3		
		Uncertainties not captured by the GENII-S computer code	X			13.3.4		
		Influence of climate change on groundwater usage and biosphere dose conversion factors (BDCF)	X			13.3.5, 13.3.7		
		BDCF for groundwater and igneous releases		X		13.3.6, 13.3.8 13.4	X	X
Low Mean Annual Dose Considering Potentially Disruptive Events	Volcanism/Igneous Activity (4.3.2)	Probability of dike intersection of repository for the operating mode described in S&ER		X		14.3.3.1		X
		Scaling factors to evaluate impacts of repository design changes			X	14.3.3.2		
		Contribution to release of Zone 1 and Zone 2		X		14.3.3.3	X	
		Sensitivity to waste particle size distribution		X		14.3.3.4	X	
		New wind speed data		X		14.3.3.5	X	X
		Explanation of method for handling ash/waste particle size and density		X		14.3.3.6		
		Volcanism inputs for supplemental TSPA model		X		14.3.3.7		X
		New aeromagnetic data		X		14.3.3.8		

NOTE: [a] Discussed in Section 3.
[b] Discussed in Section 4.

INTENTIONALLY LEFT BLANK

2. METHODS AND APPROACH

The goals of the work described here are to provide insights into the implications of newly quantified uncertainties, updated science, and evaluations of lower operating temperatures on the performance of a potential Yucca Mountain repository and to increase confidence in the results of the TSPA described in the S&ER (DOE 2001 [DIRS 153849]). The primary tool used to evaluate the implications of the three types of supplemental information (see Section 1.1 of this volume) described in SSPA Volume 1 (BSC 2001 [DIRS 154657]) is the use of performance assessment (PA) and a TSPA model. The sections below describe the various TSPA analyses conducted and how they support the goals of developing insights and confidence.

2.1 TSPA AND THE PERFORMANCE ASSESSMENT PYRAMID

An overview of the definition and uses of PA and TSPA is provided in Section 1.2 of this volume, and the regulatory, technical, and philosophical bases for the use of PA and TSPA are described in detail in the TSPA-SR (CRWMS M&O 2000 [DIRS 153246]). The TSPA-SR document also describes the details of the TSPA-SR model, which is used as the basis for the analyses conducted for this report. A summary of the general approach used to conduct a PA is provided below.

The Performance Assessment Pyramid (Figure 2-1) illustrates how the detailed processes and components that comprise the technical bases for the total system model are distilled into progressively more abstracted models, culminating in an analysis of total system performance. The breadth of the lowest level of the pyramid represents the complete suite of technical information available, including site characterization and design data and information (i.e., the field and laboratory studies that are the first step in understanding the system). The next higher level indicates how these data are used to develop conceptual models and numerical process models of how the individual system components are expected to perform under the anticipated repository-relevant conditions.

The next level represents the synthesis of information from the lower levels of the pyramid into computer models. At this point, the subsystem behavior may be described by linking process models together into abstractions or abstracted models, and at this point PA modeling usually begins. The term abstraction is used to indicate the extraction of essential information from the detailed process models. Essential information is that required to determine the effect of a particular process on the overall system performance, including the uncertainties. The abstraction must represent the characteristics of the component model, and the uncertainties associated with the model, well enough for the TSPA to be a useful representation of the system.

The top level shows the final distillation of information into the most critical aspects necessary to represent the total system. At this level, all of the models are linked together in the TSPA model. The TSPA model is used to forecast total system behavior over future time periods ranging up to 1,000,000 years. These performance estimates, and their associated uncertainties, provide a basis for comparison with regulatory standards for specified time periods (e.g., 10,000 years) that are intended to ensure long-term public health and safety.

The evaluations documented in SSPA Volume 1 focused on the lower levels of the pyramid: on updated evaluations of uncertainty, new scientific information, LTOM analyses, their incorporation into the conceptual and numerical process models, and the abstraction of this information for use in performance assessment. The evaluations documented here focus on the higher levels of the pyramid (i.e., on the results of the TSPA model) using newly abstracted models based on updated conceptual and numerical process models. Many of the uncertainties in the process models have been quantified and propagated through the abstraction process, and the TSPA results reflect those uncertainties.

2.2 SUPPLEMENTAL PERFORMANCE EVALUATIONS

Supplemental performance evaluations were conducted to examine what implications the supplemental scientific models and analyses developed since completion of the models that support the S&ER (DOE 2001 [DIRS 153849]). As described in SSPA Volume 1 (BSC 2001 [DIRS 154657]), process models were updated based on available supplemental information. The rationale for collecting and evaluating the supplemental information (quantification of uncertainties, updated scientific information, and LTOM analyses) has no impact on the type of TSPA analyses conducted. In the supplemental performance evaluations, the updated conceptual and process models described in SSPA Volume 1 were abstracted and incorporated into a TSPA model using a process identical to the abstraction process described in detail in the TSPA-SR (CRWMS M&O 2000 [DIRS 153246], Section 3). Two types of analyses were conducted. *TSPA sensitivity analyses* refer to TSPA analyses in which only one or a few components of the TSPA-SR model are updated with the newly abstracted models, and the results are compared with the TSPA-SR results. The supplemental TSPA model was developed by simultaneously incorporating a number of the updated components into the TSPA-SR model. A number of topics from SSPA Volume 1 were evaluated through TSPA sensitivity analyses and included in the supplemental TSPA model (Table 1.3-1). The methods and approach for both types of analyses are described below.

2.2.1 TSPA Sensitivity Analyses

TSPA sensitivity analyses were conducted for some of the updated models or representations described in SSPA Volume 1 and summarized in Table 1.3-1. TSPA sensitivity analyses were conducted for those updated models or representations judged by the Yucca Mountain Site Characterization Project to have the potential to influence TSPA results based on analyses described in SSPA Volume 1. For each of the topics indicated for TSPA sensitivity analysis, the updated representations were abstracted and incorporated into the TSPA-SR model one at a time. One-off sensitivity analyses were conducted to evaluate the implications of each of the model changes on the estimated performance of the potential repository. One-off sensitivity analysis are evaluations where one (or a few) parameters, or a single component model, are changed at a time to evaluate and demonstrate the effect of those specific assumptions and changes on model results. All of the one-off sensitivity analyses used the TSPA-SR nominal case (the base case) as the basis for comparison. Comparisons of the TSPA results from a one-off sensitivity analysis with the results of the TSPA-SR model provide insights into the implications of the updated model, and thus into the implications and importance of the supplemental information that provided the basis for the updated model.

Comparisons of results from the TSPA sensitivity analyses and the TSPA-SR results are done on two levels: the system level and the subsystem level. System-level evaluations and comparisons focus on the highest-level TSPA model result: the estimated annual dose. Subsystem-level evaluations and comparisons focus on the implications of the updated representations on intermediate model results, at a level below that of dose estimates.

As discussed previously (see Section 1.2 of this volume), sensitivity analyses make it possible to trace a specific model update to a specific change in system-level results: that is, to a change in estimated expected annual dose. Because the results produced at the system level are dose estimates, these system-level sensitivity analyses can result in insights about the overall degree of conservatism or non-conservatism in other TSPA model results. Sensitivity analyses focused on subsystem-level results help to isolate and show the implications of model updates. They emphasize the impact on intermediate results where changes can be tied most directly to the specific process model updates being evaluated.

The types of insights that can be produced from the TSPA sensitivity analyses are discussed in more detail in Section 1.2 of this volume. The TSPA sensitivity analyses and their results are described in Section 3 of this volume.

2.2.2 Supplemental TSPA Model

Comparing the results of the TSPA sensitivity analyses with the results of the TSPA-SR model illustrates the impact of the supplemental information for individual topics in isolation. To gain insights into cumulative and coupled effects when several of the model components are updated, the supplemental TSPA model was developed. The supplemental TSPA model includes updated abstractions for the topics indicated in Table 1.3-1, but only some of the supplemental information was carried all the way through the TSPA pyramid to the highest level of abstraction and incorporated into the supplemental TSPA model. In deciding which topics to include in this supplemental TSPA model, the Yucca Mountain Site Characterization Project used the results of TSPA sensitivity analyses and professional judgement and experience with TSPA models to select topics related to the waste package judged to be most sensitive to thermal effects. The environments affecting the long-lived waste package have an important influence on expected annual dose histories (as shown in the sensitivity analyses described in Section 3 of this volume); examining the LTOM was an important objective of the studies conducted for this report.

Results of the supplemental TSPA model are compared with results of the TSPA-SR (see Section 4). These comparisons provide insights into the cumulative effects of multiple model changes on system results and add to the insights on the implications of the supplemental information that result from the TSPA sensitivity analyses. The types of insights that can be produced by the supplemental TSPA model, and comparisons with the TSPA-SR model results, are discussed in more detail in Section 1.2 of this volume.

The supplemental TSPA model also provides the platform for a set of thermal sensitivity analyses. The goals for developing and evaluating the supplemental information on the LTOM were to provide insights into the effect of thermal parameters on predicted performance of the potential repository, including uncertainty in those predictions, and to increase confidence in the predicted performance of the potential repository over a range of thermal conditions

(see Section 1 of this volume). The design and mode of operations for the potential repository described in the S&ER (DOE 2001 [DIRS 153849], Section 2.1.4) are expected to be flexible enough to meet a range of potential thermal conditions or goals. For process models where thermal load potentially has an impact on the modeling and model results, analyses were conducted to evaluate the manner in which the process models, parameters, and results would vary under different thermal loading, focusing particularly on a LTOM.

The supplemental TSPA model was used to evaluate the system-level performance of the potential repository under different thermal operating modes. Specifically, two thermal operating modes were evaluated with the supplemental TSPA model: the thermal operating mode described in the S&ER (the higher-temperature operating mode, HTOM), and an alternative LTOM wherein average maximum temperatures on the waste package do not exceed 85ºC following closure of the potential repository. The development of the LTOM is described in SSPA Volume 1 (BSC 2001 [DIRS 154657], Section 2.3). The expected annual dose estimates from these two supplemental TSPA model implementation are compared directly to gain insight into differences in performance that may result from different thermal operating conditions (see Section 4.2 of this volume).

2.3 COMPUTER SOFTWARE USE

The software used for the SSPA, the version number, qualification status, and operating system are listed in Table 2.3-1. The computer type on which software is run is indicated by the operating system listed in the table. The Windows NT 4.0 operating system is run on a personal computer (PC), and the SUN operating systems are run on SUN computers. Codes listed as Qualified were obtained from Software Configuration Management in accordance with AP-SI.1Q, *Software Management* [DIRS 154886]. Codes for which qualification status is listed as "5.10" have been submitted to Software Configuration Management and are used in the SSPA in accordance with AP-SI.1Q [DIRS 154886], Section 5.10, which allows these codes to be used as they undergo qualification. These codes are documented in Deficiency Report BSC-01-D-088 or Corrective Action Report BSD-01-C-002. Codes with 5.10-status have been developed by the TSPA modelers and are considered appropriate for use in the TSPA model.

2.3.1 Data Retrieval

The supplemental TSPA model files and associated external files necessary to reproduce the results are documented in Appendix A. For each case, the "*.gsm" file is the GoldSim file that contains the SSPA model and the results of the simulation. As described in Appendix A, this file (along with the GoldSim code) is all that is needed to view the model and the results presented in Sections 3 and 4.

2.3.2 Software

ASHPLUME–ASHPLUME V1.4LV-dll is a volcanic ash dispersion and deposition code used to evaluate the consequences of extrusive volcanic events through the potential repository. The software estimates the distribution of ash and radioactive waste released into the biosphere during volcanic events that intercept the potential repository. ASHPLUME uses a variety of eruption and environmental parameters as input, and it outputs ash and radioactive waste

concentrations at selected locations on the ground surface. ASHPLUME V1.4LV-dll is a modified version of ASHPLUME V1.0 (Jarzemba et al. 1997 [DIRS 100987]). ASHPLUME V1.4LV-dll is qualified, appropriate for this application, and is used only within the range of validation in accordance with its qualification under AP-SI.1Q [DIRS 146376].

Bath_10–Bath_10 is a dynamic link library (DLL) that uses input from GoldSim to randomly select a column from a text file (BathCDFs.txt). Each column in this file represents a different cumulative distribution function (CDF). This CDF then is used to determine when groundwater flow will enter and leave the emplacement drift.

CWD–CWD is a software routine that calculates the cumulative probability distribution for the occurrence and size of closure weld defects in the waste packages given the non-detection probability and the fraction for defects to be considered.

FEHM–FEHM performs UZ particle transport simulations. Two versions of FEHM (V2.10 and V2.12) were used for the SSPA. At each time step, FEHM reads a set of pre-generated flow fields and performs UZ particle transport simulation, the results of which are used as input by GoldSim for the SZ model. FEHM V2.10 currently is undergoing qualification under AP-SI.1Q [DIRS 154886] for Windows NT. FEHM V2.12 is a modification to FEHM V2.10 and is in the process of being qualified under AP-SI.1Q [DIRS 154886].

GoldSim–Three versions of GoldSim (V6.04.000, V6.04.007, and V7.17.200) were used for the SSPA. GoldSim V6.04.000 and V6.04.007 were used to maintain consistency with the TSPA-SR runs in the comparisons. These versions of GoldSim were baselined under AP-SI.1Q [DIRS 146376]. Version 6.04.000 qualification was initiated prior to the effective date of AP-SI.1Q [DIRS 154886]. Therefore, qualification of Version 6.04.000 was completed under AP-SI.1Q [DIRS 146376]. GoldSim V7.17.200, currently undergoing qualification, was used to incorporate updates to the software necessary to support evolution of the TSPA model for the supplemental TSPA analysis runs. GoldSim was developed by Golder Associates as an update to the baseline software, RIP V5.19.01 (Golder Associates 1999 [DIRS 151395]). In addition to the capabilities of RIP, new TSPA calculation software is required for downloading parameter values from a database. GoldSim is a Windows-based program that is computationally similar to RIP, which was used for TSPA calculations for the Viability Assessment (DOE 1998 [DIRS 100550]). GoldSim is designed so that probabilistic simulations can be represented graphically. GoldSim fulfills the specific functional requirements for the SSPA. GoldSimV6.04.000 and V6.04.007 are appropriate for this application and are used only within the range of validation in accordance with AP-SI.1Q [DIRS 146376].

GVP (Gaussian Variance Partitioning)–GVP V1.02 was developed to incorporate measurement uncertainty and corrosion rate variability into the calculations of waste package degradation. To assess waste package failure distribution over time in the potential repository, only the fraction of the total variance is needed because of variability in the waste package degradation simulations. Gaussian variance partitioning is applied to separate the contributions of uncertainty from their elicited distributions. The routine accesses corrosion rates located in an external file and GoldSim stochastic variables. The output of GVP is a distribution table of variability in uncertainty. GVP provides a clearer demonstration of the sensitivity of the TSPA-SR models to uncertainty and variability. GVP is qualified as a multiple-use software

routine in accordance with AP-SI.1Q [DIRS 146376], Section 5.1.2. It is appropriate for this application and is used only within the range of validation in accordance with its qualification under AP-SI.1Q [DIRS 146376].

MAKEPTRK–MAKEPTRK V2.0 provides input information required by the code FEHM to define transport models and nodal assignments. For TSPA, only the nodal assignments were used. MAKEPTRK is qualified as a single-use software routine in accordance with AP-SI.1Q [DIRS 146376], Section 5.1.1. It is appropriate for this application and is used only within the range of validation in accordance with AP-SI.1Q [DIRS 146376].

MFD (Manufacturing Defects Calculation)–MFD V1.01 was developed to calculate the frequency of occurrence and size of flaws potentially found in the waste package closure welds based on uncertainties within the potential repository. Flaw density and size distributions are used as the parameter for a Poisson distribution used to represent the frequency of occurrence of flaws in a given length of closure weld. Its output, flaw sizes as a probability density function on each closure weld, is used to support WAPDEG analysis and is linked to GoldSim. MFD V1.01 is qualified as a multiple-use software routine in accordance with AP-SI.1Q [DIRS 146376], Section 5.1.2. It is appropriate for this application and is used only within the range of validation in accordance with its qualification under AP-SI.1Q [DIRS 146376].

MkTable–MkTable was developed for preprocessing data used in simulating long-term degradation of the waste packages. It is appropriate for this application and is used only within the range of validation in accordance with its qualification under AP-SI.1Q [DIRS 154886].

Patch_Fail_Lag–Patch_Fail_Lag is a DLL that runs in real time with the TSPA model. It lags the patch failure curves for the drip shield and the waste package by the waste package failure time. The lagged curves are used in cladding degradation calculations. This is done because in the GoldSim program, the source element will start looking at these curves only after the waste package fails.

PDFCDF–PDFCDF extracts data from the GoldSim output files (the dose rate statistic file and the dose rate history file). It then calculates a probability density function and CDF data of the dose rates at a given time, or it calculates the probability density function and CDF for the time when the dose rate reaches a specific value.

POST10K_BINS–POST10K_BINS is a routine that extracts infiltration rates corresponding to nodes in the potential repository identified in a user-prescribed file. The nodes are assumed to be categorized in bins, and the format of the file follows that of the "zone" file used in FEHM.

PREWAP–PREWAP V1.0 is an executable file developed for constructing the WAPDEG input file by using pH, Chloride, and thermohydrology data extracted from various tables to generate reformatted output tables of in-drift (drip shield and waste package) and in-package chemistry parameters that are used as input to the WAPDEG routine. The PREWAP file is executed to generate the WAPDEG data file before invoking the TSPA-SR model. PREWAP is qualified as a single-use software routine in accordance with AP-SI.1Q [DIRS 146376], Section 5.1.1. It has been reused for Volume 2 of the SSPA and is being qualified per AP-SI.1Q [DIRS 154886].

PROCESSBTC–PROCESSBTC is a code used to post process the response curves generated from one-dimensional SZ radionuclide transport simulations. It takes a response curve generated by one-dimensional SZ simulation as input and filters out points having the same value within a continuous time period. The code then carries out interpolation to smooth the curve based on user inputs on total number of points expected for the response curve. The results are used as generic SZ response functions by SZ_CONVOLUTE for calculating SZ response curves based on UZ source terms and expected climate scenarios at Yucca Mountain.

Rewrite_Percolation_Data–Rewrite_Percolation_Data is a routine that regenerates percolation flux time histories for the potential repository. The new data will be based on the new extended climate sequences. Output from Rewrite_Percolation_Data is used as input to other routine(s) supporting the TSPA model.

SCCD (Stress Corrosion Cracking Dissolution)–SCCD V2.0 was developed to predict crack initiation and propagation in closure weld manufacturing defects and incipient weld cracks. A reference table based on stress and strain intensity as a function of crack depth is modified by SCCD and used as input to WAPDEG. The resulting waste package failure histories are then returned to GoldSim. SCCD is qualified as a multiple-use software routine in accordance with AP-SI.1Q [DIRS 146376], Section 5.1.2. It is appropriate for this application and is used only within the range of validation in accordance with its qualification under AP-SI.1Q [DIRS 146376].

SeepagedllMk2_uu–SeepagedllMk2_uu is a variation of Seepagedllv2 that incorporates changes required for the supplemental TSPA model.

Seepagedllv2uu–Seepagedllv2uu is a variation of Seepagedllv2 which incorporates changes required for the one-off analysis supporting the unquantified uncertainty analysis.

Seepagedllv2–Seepagedllv2 V1.0 calculates the seepage fraction and flux of water that will enter the drift and could potentially contribute to the degradation of the engineered systems and release and transport radionuclides within the drifts. The routine was developed using an analysis abstracted from the seepage process modeling that generated probability distributions that represent the uncertainty and spatial variability of seepage. The resulting output is passed to GoldSim. Seepagedllv2 is qualified as a single-use software routine in accordance with AP-SI.1Q [DIRS 146376], Section 5.1.1. It has been reused for Volume 2 of the SSPA and is being qualified per AP-SI.1Q [DIRS 154886].

SOILEXP–SOILEXP calculates the cumulative soil removal factor used to calculate radionuclide concentration at deposition points over the life of the potential repository. The SOILEXP routine receives input from GoldSim, calculates the cumulative soil removal factor for the time interval, and passes the result back to GoldSim. SOILEXP is qualified as a single-use software routine in accordance with AP-SI.1Q [DIRS 146376], Section 5.1.1. It has been reused for Volume 2 of the SSPA and is being qualified per AP-SI.1Q [DIRS 154886].

SZ_CONVOLUTE–SZ_CONVOLUTE is used to compute radionuclide concentration and dose at the accessible environment based on SZ transport calculations. Two versions of SZ_CONVOLUTE (V2.0 and V2.1) were used for the SSPA. SZ_CONVOLUTE V2.0 is

qualified and was obtained from Software Configuration Management. SZ_CONVOLUTE V2.1 is a modification to Version 2.0 (incorporating changes in response to changes in the long-term climate model) that was developed to calculate SZ response curves based on UZ radionuclide source terms, generic SZ responses, and the expected climate scenario. SZ_CONVOLUTE V2.0 is the result of minor modifications made to SZ_CONVOLUTE V1.0 (CRWMS M&O 1998 [DIRS 101112]). The modifications include a change to the format of the breakthrough curve input file. SZ_CONVOLUTE V1.0 reads the breakthrough curve for each of 100 realizations from 100 separate files. SZ_CONVOLUTE V2.0 reads the breakthrough curves for all 100 realizations from a single file and includes a provision to allow the GoldSim model to track a subset of the total radionuclide inventory. SZ_CONVOLUTE V2.0 incorporates an approximate method for computing concentration and dose at the accessible environment that used the generic SZ transport calculation as a basis. It requires input of data files containing generic SZ breakthrough curves that have been calculated for a constant mass flux input. Any number of radionuclides, source regions, and breakthrough monitoring locations may be used. UZ mass flux information is required for each nuclide at each source location. Generic SZ breakthrough curves also are required for each nuclide originating at each source region and reaching each monitoring location. Information concerning the UZ breakthrough concentration, the current simulation time, the current climate state, and the number of radionuclides are supplied through the routine call from GoldSim. The output information returned to GoldSim through the routine call is the breakthrough concentration multiplied by the current time step at each time. Breakthrough information is supplied for each nuclide origination at each source location and reaching each monitoring location. SZ_CONVOLUTE V2.0 is qualified, appropriate for this application and is used only within the range of validation in accordance with its qualification under AP-SI.1Q [DIRS 146376]. SZ_CONVOLUTE V2.1 is being qualified in accordance with AP-SI.1Q [DIRS 154886], Section 5.10.

T2_BINNING–T2_BINNING V1.0 was used to generate repository-release bins based on surface infiltration information. T2_BINNING groups nodes into five bins that correspond to prescribed infiltration ranges. The nodes belong to a pre-defined region in the potential repository from the three-dimensional site-scale UZ model. T2_BINNING is qualified as a single-use software routine in accordance with AP-SI.1Q [DIRS 146376], Section 5.1.1. It has been reused for Volume 2 of the SSPA and has been qualified per AP-SI.1Q [DIRS 154886]. It is appropriate for this application and is used only within the range of validation in accordance with its qualification.

Transform_Perc_files_into_Tables–Transform_Perc_files_into_Tables is a routine to reformat output files produced by Rewrite_Percolation_Data_Files.f90 for plotting. From these files, it reads the percolation time histories for each locations, and writes them to a new file under a table format (rows = time steps, columns = locations). The new files can be opened in Sigma Plot or Excel to produce horsetail plots of percolation time histories.

WAPDEG–WAPDEG V4.0 was developed to simulate waste package degradation using a stochastic approach. Two versions of WAPDEG V4.0 were used in the SSPA (Table 2.3-1). WAPDEG V4.0 (CRWMS M&O 2000 [DIRS155166]) is used in the supplemental TSPA model. WAPDEG V4.0 (BSC 2001 [DIRS 155316]) was used in the unquantified uncertainty runs to maintain consistency for comparison with the TSPA-SR. WAPDEG V4.0 is an improved version of WAPDEG 3.09, which was used for waste package degradation analysis for the

viability assessment of the potential Yucca Mountain repository (DOE 1998 [DIRS 100550]). WAPDEG consists of two parts: the WAPDEG DLL and the WAPDEG executable program. The WAPDEG DLL is designed to be called by the GoldSim program. It evaluates and applies initiation thresholds of various corrosion and other degradation processes as a function of time-dependent exposure conditions. The penetration rate of active degradation processes as a function of exposure conditions is also evaluated. WAPDEG generates output for time-histories of failures and subsequent degradation (i.e., number of penetrations) for each waste package barrier. WAPDEG V4.0 (BSC 2001 [DIRS 155316]) is being qualified in accordance with AP-SI.1Q [DIRS 154886], Section 5.10. WAPDEG V4.0 (CRWMS M&O 2000 [DIRS 155166]) is appropriate for this application and is used only within the range of validation in accordance with AP-SI.1Q [DIRS 146376].

Writefiles–Writefiles is a DLL that runs in real time with the Goldsim program sample_glacial_distributions.gsm. This routine produces output files for each bin, for each glacial flow field, for each infiltration scenario, and for each fuel type. These files contain percolation flux for each location. The output files are used as input to the rewrite_percolation_data.f90 routine that generates percolation flux data for the long term climate model, which is an input to the TSPA model.

Writefiles_new is a variation of Writefiles that is necessary to address changes to the climate model.

WT_BINNING–WT_BINNING V1.0 was used to generate UZ radionuclide collect bins at the UZ-SZ interface. WT_BINNING groups nodes at or below a prescribed water table into one of four quadrants defined for the SZ model. WT_BINNING is qualified as a single-use software routine in accordance with AP-SI.1Q [DIRS 146376], Section 5.1.1. It is appropriate for this application and is used only within the range of validation in accordance with AP-SI.1Q [DIRS 146376].

WTRISE–This software routine post-processes a FEHM ".ini" file to incorporate a water table rise. It modifies the saturation of nodes located beneath the prescribed water table and creates a large sink so that radionuclides are immediately transported out of the UZ domain.

INTENTIONALLY LEFT BLANK

Table 2.3-1. Software and Software Routines

Computer Code	Version	STN/CSCI	Qualification Status	Operating System	Reference
ASHPLUME	1.4LV-dll	10022-1.4LV-dll-00	Qualified	Windows NT 4.0	CRWMS M&O 2000 [DIRS 154748]
Bath_10	1.0	10539-1.0-00	5.10	Windows NT 4.0	BSC 2001 [DIRS 155165]
CWD	1.0	10363-1.0-00	5.10	Windows NT 4.0	CRWMS M&O 2000 [DIRS 152624]
FEHM	2.10	10086-2.10-00	5.10 for Windows NT	Windows NT 4.0	Los Alamos National Laboratory 2000 [DIRS 132447]
FEHM	2.12	10086-2.12-00	5.10	Windows NT 4.0	LANL 2001 [DIRS 155412]
GoldSim	6.04.007	10344-6.04.007-00	Qualified	Windows NT 4.0	Golder Associates 2000 [DIRS 151202]
GoldSim	6.04.000	10310-6.04.000-00	Qualified	Windows NT 4.0	Golder Associates 2001 [DIRS 155089]
GoldSim	7.17.200	10344-7.17.200-00	5.10	Windows NT 4.0	BSC 2001 [DIRS 155182]
GVP	1.02	10341-1.02-00	Qualified	Windows NT 4.0	CRWMS M&O 2000 [DIRS 155433]
MAKEPTRK	2.0	10491-2.0-00	Qualified	Sun OS 5.7	Los Alamos National Laboratory 2001 [DIRS 155175]
MFD	1.01	10342-1.01-00	Qualified	Windows NT 4.0	CRWMS M&O 2000 [DIRS 155434]
MkTable	1.00	10505-1.00-00	Qualified	Windows NT 4.0	BSC 2001 [DIRS 154921]
Patch_Fail_Lag	1.0	10532-1.0-00	5.10	Windows NT 4.0	BSC 2001 [DIRS 155176]
PDFCDF	1	10558-1.0-00	5.10	Windows NT 4.0	BSC 2001 [DIRS 155413]
POST10K_BINS	1.0	10538-1.0-00	5.10	Windows NT 4.0	BSC 2001 [DIRS 155179]
PREWAP	1.0	10533-1.0-00	5.10	Windows NT 4.0	BSC 2001 [DIRS 155181]
PROCESSBTC	1.0	10556-1.0-00	5.10	Windows NT 4.0	BSC 2001 [DIRS 155414]
Rewrite_Percolation_Data	1.0	10501-1.0-00	5.10	Windows NT 4.0	BSC 2001 [DIRS 155180]
SCCD	2.0	10343-2.0-00	Qualified	Windows NT 4.0	CRWMS M&O 2000 [DIRS 155178]
SeepagedllMk2_uu	1.0	10534-1.0-00	5.10	Windows NT 4.0	BSC 2001 [DIRS 155177]
Seepagedllv2uu	1.0	10535-1.0-00	5.10	Windows NT 4.0	BSC 2001 [DIRS 155174]
Seepagedllv2	1.0	10496-1.0-00	5.10	Windows NT 4.0	BSC 2001 [DIRS 155172]

Table 2.3-1. Software and Software Routines (Continued)

Computer Code	Version	STN/CSCI	Qualification Status	Operating System	Reference
SOILEXP	1.0	10492-1.0-00	5.10	Windows NT 4.0	BSC 2001 [DIRS 155171]
SZ_CONVOLUTE	2.0	10207-2.0-00	Qualified	Windows NT 4.0	CRWMS M&O 2000 [DIRS 155423]
SZ_CONVOLUTE	2.1	10207-2.1-00	5.10	Windows NT 4.0	CRWMS M&O 2000 [DIRS 155424]
T2_BINNING	1.0	10490-1.0-00	Qualified	Windows NT 4.0	Los Alamos National Laboratory 2001 [DIRS 155170]
Transform_Perc_files _ into_Tables	1.0	10530-1.0-00	5.10	Windows NT 4.0	BSC 2001 [DIRS 155168]
WAPDEG	4.0	10000-4.0-02	5.10	Windows NT 4.0	BSC 2001 [DIRS 155316]
WAPDEG	4.0	10000-4.0-00	Qualified	Windows NT 4.0	CRWMS M&O 2000 [DIRS 155166]
Writefiles	1.0	10527-1.0-00	5.10	Windows NT 4.0	BSC 2001 [DIRS 155164]
Writefiles_new	1.0	10560-1.0-00	5.10	Windows NT 4.0	BSC 2001 [DIRS 155437]
WT_BINNING	1.0	10489-1.0-00	Qualified	Windows NT 4.0	Los Alamos National Laboratory 2001 [DIRS 155163]
WTRISE	1.0	10537-1.0-00	5.10	Sun OS 5.7	Sandia National Laboratories 2001 [DIRS 117132]

NOTE: STN = software tracking number; CSCI = computer software configuration item.

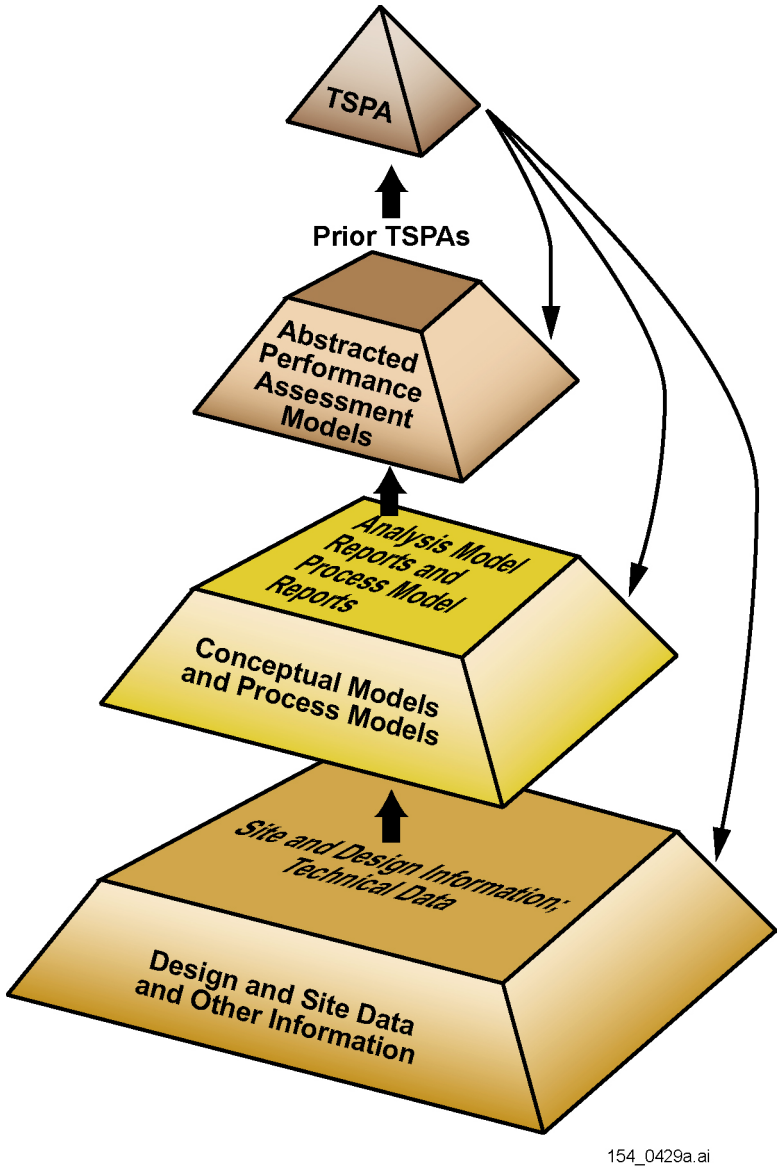

154_0429a.ai

NOTE: TSPA = Total System Performance Assessment.

Figure 2-1. The Performance Assessment Pyramid

INTENTIONALLY LEFT BLANK

3. TSPA SENSITIVITY ANALYSES: EVALUATIONS OF UNCERTAINTY AND NEW INFORMATION

In this section, the results of supplemental analyses conducted using the TSPA-SR (CRWMS M&O 2000 [DIRS 153246]) models and input parameters, modified to provide insights into the potential effects of specific uncertainties that were not fully evaluated in TSPA-SR, are documented. All analyses described in this section were conducted as one-off comparisons in which all models and input parameters are the same as those used in the TSPA-SR, except for the model or parameter being examined. SSPA results documented in this section, therefore, are suitable for direct comparison to results of the TSPA-SR. All differences in performance measures (including total system annual dose rates and intermediate measures where appropriate) between these results and those in TSPA-SR are caused only by the changes in the selected models and inputs.

Comparing results of the one-off analyses to those of the TSPA-SR illustrates the impact of uncertainties in individual components in isolation, but it does not allow full insight into the cumulative and coupled effects when additional uncertainties in all components are considered. In Section 4, results of analyses conducted using an updated supplemental TSPA model are presented. These results include model improvements and better treatments of uncertainties in the major subsystem components.

GoldSim (Versions 6.04.000, 6.04.007, and 7.17.200) calculations conducted for the supplemental TSPA analyses have been archived in the Record Information System and are listed in Appendix A with their respective reference identification for accessibility. Excluding the figures that identify a specific source in another document (e.g., Figures 3.1.1-1 and 3.1.1-2), the simulation runs corresponding to the figures in this section are specified in Appendix A. The electronic media tapes referenced in Appendix A, which can be retrieved using the references documented, identify the source file information used to produce the figures. Appendix A also provides a brief discussion of the process necessary to run the GoldSim simulations. Calculations conducted as part of the TSPA-SR are archived in the Technical Data Management System, listed with their data tracking numbers in Appendix A, and presented in the TSPA-SR (CRWMS M&O 2000 [DIRS 153246], Appendix G).

3.1 TSPA-SR SYSTEM-LEVEL EVALUATION OF NOMINAL PERFORMANCE

Results of the TSPA-SR for nominal performance have been documented in detail (CRWMS M&O 2000 [DIRS 153246], Section 4.1). The nominal performance scenario includes all features, events, and processes that are expected to occur during the first 10,000 years, but it does not include human intrusion or unlikely disruptive events, such as igneous activity (CRWMS M&O 2000 [DIRS 153246], Section 2.1.1). The TSPA-SR nominal performance analyses address two periods: 100,000 years after permanent closure and 1,000,000 years after permanent closure. The first period focuses on performance for 10,000 years, with the analyses extended to 100,000 years to evaluate robustness of the system with respect to 10,000-year performance. The second period is considered to evaluate the peak annual dose, which occurs between 100,000 and 1,000,000 years in most realizations.

System-level results from the TSPA-SR are summarized briefly in this section for convenience when comparing results of one-off sensitivity analyses described later in Section 3. Subsystem-level performance analyses are summarized in later subsections, as appropriate, for comparison to one-off analysis results.

3.1.1 TSPA-SR Nominal Performance Results for One Hundred Thousand Years

TSPA-SR results for 100,000 years of nominal performance are presented in Figure 3.1.1-1. In the upper panel, 300 simulated annual dose histories and some statistical measures of the annual dose distribution are shown to illustrate the temporal evolution of annual dose to the receptor and the uncertainty associated with that annual dose projection. The mean curve is generated by averaging the 300 annual dose values at each time step. The percentile curves are generated by determining the location of the given percentile at each time step (for example, the median curve is generated by determining the annual dose that has half of the calculated annual doses below it at each time step). There is a considerable amount of variability in the projections of annual dose; however, because the models used in TSPA-SR for waste package performance resulted in no package failures until approximately 10,500 years after closure, the calculated annual dose is zero for all of the 300 realizations for the nominal scenario during the first 10,000 years. The differences in results for different realizations at later times are caused by the differences in the input parameters. The spread in annual dose (Figure 3.1.1-1) largely is related to uncertainties in waste package degradation processes (CRWMS M&O 2000 [DIRS 153246], Section 5.1).

The total annual dose (Figure 3.1.1-1, upper panel) is the sum of the annual doses attributed to each radionuclide in the groundwater at the point of use. Figure 3.1.1-1 (lower panel) shows the mean annual dose histories for the most important radionuclides, and Figure 3.1.1-2 shows pie charts for the mean contribution of radionuclides to the total annual dose at four different times. Figure 3.1.1-1 shows that, from the time of closure to approximately 40,000 years, the dominant annual dose contributors are the more mobile radionuclides (i.e., technetium-99 and iodine-129). As time progresses, less mobile radionuclides (which have lower solubility and slower transport through the UZ and SZ) become more important, and by approximately 60,000 years, the annual dose is dominated by neptunium-237 and colloidally-transported plutonium-239. For completeness, Figure 3.1.1-3 shows the mean annual dose histories for the rest of the radionuclides that were tracked in the TSPA simulation. These radionuclides make small contributions to the total annual dose.

3.1.2 TSPA-SR Nominal Performance Results for One Million Years

Although the regulatory period specified by the U.S. Nuclear Regulatory Commission (NRC) proposed rule (10 CFR 63.113(b), 64 FR 8640 [DIRS 101680]) is limited to the first 10,000 years after closure, TSPA analyses have been extended to 100,000 years to assure that no dramatic degradation of performance occurs after the 10,000-year compliance period. Analyses of nominal performance also have been extended to 1,000,000 years to provide estimates of the overall peak dose during the period of geologic stability, as required by the U.S. Environmental Protection Agency (EPA) (40 CFR Part 197.35, 64 FR 46976 [DIRS 105065]).

The TSPA-SR base-case model for nominal performance was used (without modification) to calculate annual doses for 1,000,000 years (Figure 3.1.2-1; CRWMS M&O 2000

[DIRS 153246], Section 4.1.3). Peak mean annual dose is about 490 mrem/yr, occurring at about 270,000 years. The dominant radionuclide contributing to the peak annual dose is neptunium-237, with lesser contributions from thorium, radium, and plutonium (Figure 3.1.2-2). The range of annual doses from the individual realizations is less at later times than that shown before 100,000 years because uncertainty in some key aspects of the engineered and natural barriers decreases with time. In particular, after about 100,000 years waste packages and drip shields have been sufficiently degraded that releases from nearly all packages contribute to total dose.

The TSPA-SR base-case model was developed to provide a defensible basis for evaluating 10,000-year performance, rather than to provide a realistic evaluation of uncertainty in peak dose. The TSPA-SR therefore included sensitivity analyses of 1,000,000-year performance to examine the effects of alternative models for long-term climate change and secondary-phase effects on actinide solubilities (CRWMS M&O 2000 [DIRS 153246], Section 4.1.3). These sensitivity analyses have been superseded by the results of more recent analyses (see Sections 3.2.1.2 and 3.2.7).

3.2 SUBSYSTEM-LEVEL EVALUATIONS: NOMINAL PERFORMANCE

This section describe results of one-off sensitivity analyses conducted by modifying the models and input parameters used in the TSPA-SR base case (CRWMS M&O 2000 [DIRS 153246]). Except for the model or parameter being examined, the one-off sensitivity analyses were conducted using the same models and input parameters as those used in TSPA-SR base case, and therefore differences in performance measures between these results and those of the TSPA-SR provide insights into the importance of uncertainty in individual model components. Analyses are presented for each of the major modeling subsystems, and the results are displayed as system-level annual dose histories for nominal performance and as intermediate performance measures, where appropriate. All analyses described in this section use 100 realizations of the TSPA base-case model (as modified for the one-off sensitivity analyses), and the results are compared to those of the TSPA-SR base case (as described in Section 3.1).

3.2.1 Evaluation of Unsaturated Zone Flow

The UZ-flow component of the TSPA includes climate, infiltration, and mountain-scale flow subcomponents (CRWMS M&O 2000 [DIRS 153246], Sections 3.2.1, 3.2.2, and 3.2.3). Climate refers to the characteristic meteorological conditions, which are required to determine the hydrology within and around Yucca Mountain. In particular, temperature and precipitation are important inputs to the infiltration model. Net infiltration is the penetration of water through the ground surface to a depth where it can no longer be withdrawn by evaporation or transpiration by plants. The net infiltration is the upper boundary condition for groundwater flow in the UZ. Mountain-scale UZ flow refers to the percolation of groundwater through the rock strata above the water table. Upon reaching the drifts containing the waste packages, this water can accelerate radionuclide mobilization and release, and it provides the primary medium for transport of radionuclides away from the potential repository under nominal conditions. Aspects of UZ flow at the drift scale (i.e., more detailed consideration of flow immediately around the drifts) are discussed in Sections 3.2.2 and 3.2.9.

In Section 3.2.1.1, the UZ-flow results for TSPA-SR (CRWMS M&O 2000 [DIRS 153246], Section 3.2) are summarized. In Section 3.2.1.2, an extended climate model is presented. As explained further in Section 3.2.1.2, the base-case climate model was originally developed for the 10,000-year regulatory period and has no climate changes after 2,000 years. The extension of the model to later times is referred to as the extended climate model, and includes additional climate changes out to 1 million years in the future. Information about the extended climate model has already been presented in the TSPA-SR (CRWMS M&O 2000 [DIRS 153246], Section 3.2.5), but it is summarized here because it was not part of the TSPA-SR base case and it is used here for an additional TSPA sensitivity analysis.

As shown in Table 1.3-1, additional analyses related to UZ flow are discussed in SSPA Volume 1 (BSC 2001 [DIRS 154657], Chapter 3), but the extended climate analysis is the only one that was carried through to TSPA simulations. Implementation of the extended climate model involves aspects of climate (BSC 2001 [DIRS 154657], Section 3.3.1), infiltration (BSC 2001 [DIRS 154657], Section 3.3.2), and mountain-scale flow (BSC 2001 [DIRS 154657], Section 3.3.4). The other UZ-flow analyses provide useful information about UZ flow and its uncertainties, but do not present new abstractions for use in TSPA simulations (see BSC 2001 [DIRS 154657], Sections 3.3.3.5, 3.3.5.6, 3.3.6.4, and 3.3.7.5).

3.2.1.1 Review of Previous Results

Future climate changes are included in TSPA simulations by modeling infiltration and flow for a sequence of discrete climate states. The climate in the base-case TSPA-SR model consists of three periods: 600 years with present-day climate, followed by 1,400 years of a monsoon climate, and then a glacial-transition climate for the remainder of the simulation (CRWMS M&O 2000 [DIRS 153246], Figure 3.2-3 and Table 3.2-1). By monsoon is meant a climate with a strong summer rain pattern, as is currently found in parts of the southwestern U.S. The glacial-transition climate is cooler than present-day and possibly significantly wetter, with relatively cool, dry summers and cool, wet winters (CRWMS M&O 2000 [DIRS 151940], Section 3.5.1.4). Each climate state has a range of possible behaviors, represented by bounding analog meteorological sites. However, the upper-bound climate analogs still fall under the definition of semiarid.

In order to represent infiltration uncertainty in TSPA simulations, three infiltration maps were generated for each climate state. They are termed the low-, medium-, and high-infiltration cases. The modeled repository-average net infiltration (i.e., the average net infiltration for the area of the potential repository) ranges from 0.4 mm/yr for present-day climate with low infiltration to 37 mm/yr for glacial-transition climate with high infiltration (CRWMS M&O 2000 [DIRS 153246], Table 3.2-2). According to the infiltration model, the monsoon climate has higher net infiltration than the present-day climate and the glacial-transition climate has higher net infiltration than the monsoon climate, except for the low-infiltration case. The increase in net infiltration for the monsoon climate is a result of greater precipitation. The additional increase in net infiltration for the glacial-transition climate is a result of the colder temperatures, which reduce the amount of evapotranspiration. The glacial-transition low-infiltration case has lower infiltration than the monsoon low-infiltration case because of a more uniform seasonal distribution of precipitation. The average intensity and frequency of precipitation events for the glacial-transition low-infiltration case are not sufficient to overcome evapotranspiration from the

root zone (USGS 2000 [DIRS 123650], Section 6.11.3). The relative probabilities of the three infiltration cases were derived by means of a detailed infiltration uncertainty analysis (CRWMS M&O 2000 [DIRS 143244]). The infiltration probabilities obtained from the analysis are 17 percent for low, 48 percent for medium, and 35 percent for high (CRWMS M&O 2000 [DIRS 153246], Table 3.2-2). These probabilities establish a discrete distribution of infiltration that is used for sampling during TSPA simulations. Thus, 17 percent of the realizations in a TSPA simulation are run with the low-infiltration results, 48 percent of the realizations are run with the medium-infiltration results, and 35 percent of the realizations are run with the high-infiltration results.

The combination of three climate states (present-day, monsoon, and glacial-transition) and three infiltration cases (low, medium, and high) led to nine flow cases that were simulated using the mountain-scale UZ flow model. The average infiltrations (CRWMS M&O 2000 [DIRS 153246], Table 3.2-2) also represent the average flux over the repository at the top boundary of the flow model. The probabilities for the three infiltration cases apply also to the UZ flow fields derived from those infiltration cases. The percolation flux at the potential repository is similar to the infiltration imposed at the surface because there is little lateral flow above the repository, but the percolation flux at the water table is distributed differently because of significant lateral diversion between the level of the potential repository and the water table, especially in the northern portion of the potential repository area (e.g., CRWMS M&O 2000 [DIRS 153246], Figure 3.2-8). The differences in behavior between the northern and southern parts of the model domain occur because the Calico Hills nonwelded tuff is largely zeolitized in the north, resulting in a low-permeability zone and extensive perched water (CRWMS M&O 2000 [DIRS 151940], Figure 3.7-9), which causes lateral diversion (hundreds of meters in some locations) to more permeable fault zones in the simulation. Further discussions of the extent and effects of the perched-water zones, including alternative models that have been considered, are presented elsewhere (CRWMS M&O 2000 [DIRS 151940], Section 3.7.3.3). Recent work has indicated a potential for additional lateral diversion in the nonwelded hydrogeologic units above the potential repository (BSC 2001 [DIRS 154657], Section 3.3.3). These effects have not yet been included in TSPA simulations, but the non-inclusion is expected to be conservative (BSC 2001 [DIRS 154657], Sections 3.3.3.5 and 3.3.3.8).

The computed mean annual dose to receptors is moderately sensitive to infiltration and UZ flow, as has been shown by conducting TSPA simulations with infiltration fixed at the estimated high or low values, rather than sampling values from the distribution established for the TSPA-SR base case (CRWMS M&O 2000 [DIRS 153246], Section 5.2.1.1). The calculated dose to receptors for the high-infiltration case is slightly higher than for the TSPA-SR base case, but the calculated dose to receptors for the low-infiltration case is a factor of 3 to 10 lower than the TSPA-SR base case (CRWMS M&O 2000 [DIRS 153246], Figure 5.2-1).

3.2.1.2 An Extended Climate Model

The TSPA-SR base-case climate model (CRWMS M&O 2000 [DIRS 153246], Section 3.2.1) was developed for the 10,000-year regulatory period, and it has no climate changes after 2,000 years. An extended climate model for the time period from 10,000 years to 1 million years has also been developed (CRWMS M&O 2000 [DIRS 153038]). In this climate model, six climate states were determined for the post-10,000-year climate sequence: interglacial,

monsoon, intermediate, and three different full-glacial climates. The present-day climate is an interglacial climate, and the present-day climate is used as an analog for future interglacial climates. The intermediate climate is the same as the glacial-transition climate used in the TSPA-SR base-case model (CRWMS M&O 2000 [DIRS 153038], Section 6.1). Preceding each glacial state in the climate sequence is a period called intermediate/monsoon when the climate alternates between those two states (CRWMS M&O 2000 [DIRS 153038], Table 6-6). For TSPA simulations, the climate sequence was simplified by combining the alternating intermediate and monsoon climates into a single intermediate climate state. This approximation is acceptable for TSPA because the monsoon climate is estimated to occur for less than 7 percent of the intermediate/monsoon climate (CRWMS M&O 2000 [DIRS 153038], Section 7). Furthermore, the intermediate climate is, on average, wetter than the monsoon climate (e.g., see CRWMS M&O 2000 [DIRS 153246], Table 3.2-2), keeping in mind that intermediate climate is the same as glacial-transition climate. Therefore, combining the alternating intermediate and monsoon climates into the intermediate climate state is conservative. However, the monsoon climate still occurs from 600 years to 2,000 years in the extended climate definition, as in the TSPA-SR base case (CRWMS M&O 2000 [DIRS 153246], Table 3.2-1).

The extended climate model, as it has been abstracted for use in TSPA simulations, is summarized in the TSPA-SR (CRWMS M&O 2000 [DIRS 153246], Section 3.2.5). The extended climate model is the same as the TSPA-SR base-case climate model until 38,000 years, when the first glacial period is estimated to occur. The next glacial periods occur at 106,000 years and 200,000 years in the model. The glacial periods are 8,000 to 40,000 years in duration and recur approximately every 90,000 years on average (CRWMS M&O 2000 [DIRS 153246], Table 3.2-4). The repository-average net infiltration for the glacial states ranges from 17 mm/yr for the lowest low-infiltration case to 110 mm/yr for the highest high-infiltration case (CRWMS M&O 2000 [DIRS 153246], Table 3.2-6). These infiltration values are not the same as those reported in SSPA Volume 1 (BSC 2001 [DIRS 154657], Table 3.3.2-3) because the table in SSPA Volume 1 presents averages over the domain of the UZ model, whereas the TSPA-SR (CRWMS M&O 2000 [DIRS 153246], Table 3.2-6) presents averages over the potential repository area.

A sensitivity analysis was conducted in which the extended climate model (CRWMS M&O 2000 [DIRS 153246], Section 3.2.5) was used, but the rest of the model was the same as the TSPA-SR base case. A comparison of the computed mean annual dose to receptors for this analysis with that for the TSPA-SR base case is shown in Figure 3.2.1-1. Each TSPA simulation is a combination of the low-, medium-, and high-infiltration cases (see Section 3.2.1.1). The probabilities for the infiltration cases are the same for both simulations. The calculated dose to receptors peaks during the glacial climates because of the increased seepage during those periods. There is relatively little change in dose during the first glacial climate (which begins at 38,000 years) because the simulated drip shields and waste packages are still largely intact at that time (CRWMS M&O 2000 [DIRS 153246], Figures 4.1-8 and 4.1-9), and they divert most of the seepage water around the waste packages during that period. The seep flow rate increases during the glacial climates and decreases during the interglacial climates, as compared to the TSPA-SR base case. The interglacial periods occur at 65,000 years, 137,000 years, etc. (CRWMS M&O 2000 [DIRS 153246], Table 3.2-4). Despite the large increase in infiltration during the glacial periods, the number of waste packages that are subjected to seepage increases compared

to the TSPA-SR base case by less than 20 percent (TSPA runs SR00_047nm5 and UU01_020nm6; see Appendix A).

3.2.2 Evaluation of Seepage

Seepage can be described as the movement of liquid water into waste-emplacement drifts. The basic conceptual model for seepage is that openings (such as drifts) in unsaturated media act as capillary barriers and divert water around them (CRWMS M&O 2000 [DIRS 153246], Section 3.2.4). For seepage to occur in the conceptual model, the fractures at the drift wall must be locally saturated. Drift walls can become locally saturated either by disturbance to the flow field caused by the drift opening or by heterogeneity in the permeability field that creates channeled flow and local ponding. Water that seeps into the drifts can accelerate radionuclide mobilization and function as a transport medium within the waste packages and the drifts.

In Section 3.2.2.1, the seepage results for TSPA-SR (CRWMS M&O 2000 [DIRS 153246], Section 3.2.4) are summarized. In Section 3.2.2.2, an updated seepage model is presented, based on new work discussed in SSPA Volume 1 (BSC 2001 [DIRS 154657], Section 4.3.1). In Section 3.2.2.3, effects of flow focusing on seepage are presented (BSC 2001 [DIRS 154657], Section 4.3.2). In Section 3.2.2.4, the effects of episodic flow on seepage are presented (BSC 2001 [DIRS 154657], Section 4.3.5.5.1). In Section 3.2.2.5, effects of rock bolts and drift degradation on seepage are discussed (BSC 2001 [DIRS 154657], Sections 4.3.3 and 4.3.4). In Section 3.2.2.6, thermal effects on seepage are presented (BSC 2001 [DIRS 154657], Section 4.3.5). In Section 3.2.2.7, the results of combining the effects from the previous sections are presented. As shown in Table 1.3-1, SSPA Volume 1 also contains analyses of THC and THM effects on seepage (BSC 2001 [DIRS 154657], Sections 4.3.6 and 4.3.7), but those sections do not present new abstractions for use in TSPA simulations (BSC 2001 [DIRS 154657], Sections 4.3.6.6 and 4.3.7.5).

3.2.2.1 Review of Previous Results

Seepage is variable in space because of variability in percolation flux and heterogeneity in fracture hydrologic properties. In addition, seepage may be affected by changes in drift shape as the drift degrades, the presence of rock bolts used for ground support, emplacement-drift ventilation, and the heat output from the decaying radioactive waste.

During the early heating period, drainage of thermally mobilized water can lead to relatively high water fluxes above the drifts; some of the water may seep into the drifts and lead to a brief period of relatively high seepage. In the TSPA-SR base-case model, which is for a relatively high-temperature operating mode, most locations in the potential repository have temperatures above boiling during the heating period (e.g., Figure 3.2.2-10 in Section 3.2.2.6) and reduced saturation for some distance into the host rock. During this period, seepage may be suppressed; however, the TSPA-SR base-case seepage-abstraction model does not take credit for this effect (CRWMS M&O 2000 [DIRS 153246], Section 3.3.3.2.3). Finally, there is the return to ambient temperature during the cooling period, which may take tens of thousands of years. However, the thermal perturbation to flow above the drift is predicted to be insignificant after a few hundred years (CRWMS M&O 2001 [DIRS 154594], Section 6.3.8). Superimposed on the thermal perturbation is the change in infiltration over time. Flow and seepage will not return to their

present-day conditions, but rather, return to wetter, glacial-transition conditions (see Section 3.2.1). Also, there are potentially changes to hydrologic properties in the surrounding rock caused by coupled processes (THC and THM processes). However, such hydrologic-property changes are neglected in the TSPA-SR base-case model (CRWMS M&O 2000 [DIRS 153246], Section 3.3.3.1.2).

Within the TSPA-SR base-case model, seepage is characterized by four quantities: the seepage fraction (fraction of waste-package locations that have seepage), the mean seep flow rate for locations with seepage, the standard deviation of seep flow rate for locations with seepage, and a flow-focusing factor that represents the effects of flow channeling because only a subset of fractures are actively flowing. Uncertainty distributions were developed for these four quantities, with the first three being functions of the local percolation flux and the fourth being a function of the infiltration case, that is, the distribution of the flow-focusing factor is different for the low-, medium-, and high-infiltration cases. Values for each of these four quantities are sampled from the uncertainty distributions for each model realization (CRWMS M&O 2000 [DIRS 153246], Section 3.2.4.3; CRWMS M&O 2000 [DIRS 148384], Section 6.3.1.2).

Thermal effects on the amount of seepage are taken into account by using the thermally perturbed percolation flux 5 m above the drifts from the multiscale thermal hydrology model as the input to the seepage-abstraction model (CRWMS M&O 2000 [DIRS 153246], Section 3.3.3.2.3). At 5 m from the drifts, flow is not expected to be significantly perturbed by the capillary barrier effect of the drift, and also will not usually be within the boiling dry-out zone. Because the percolation flux is taken from a location that does not dry out, water seeps into the drifts throughout the heating period in the TSPA-SR base-case model (see Section 3.2.2.6).

During TSPA-SR simulations, seepage histories are averaged within environmental groups (CRWMS M&O 2000 [DIRS 153246], Section 3.3.2). An environmental group is a group of waste packages modeled to have the same environmental conditions (seepage, chemistry, temperature, etc.) within the TSPA model. In the TSPA-SR base case, the division into environmental groups is based on infiltration during the glacial-transition climate (0 to 3 mm/yr, 3 to 10 mm/yr, 10 to 20 mm/yr, 20 to 60 mm/yr, and 60+ mm/yr), waste type (commercial spent nuclear fuel [CSNF] and codisposal waste, which refers to waste packages that have both high-level glass waste and DOE-owned spent nuclear fuel), and seepage state (seepage at all times, seepage some of the time, and no seepage).

There are 30 environmental groups, resulting from five infiltration bins, times two waste types, times three seepage states (CRWMS M&O 2000 [DIRS 153246], Section 3.3.2). There is little or no difference between the groups with seepage some of the time and seepage all of the time. The packages with seepage only some of the time typically do not have seepage during the early dry period (i.e., during the present-day climate), but then have seepage all the time during the wetter glacial-transition climate. Thus, during the glacial-transition climate, when waste packages start failing, waste packages with seepage some of the time or seepage all of the time generally all have seepage.

In the TSPA-SR base case, an average of only about 13 percent of the waste packages are subjected to seepage. The average seepage fraction varies from about 8 percent for waste

packages in locations where infiltration is 0 to 3 mm/yr up to about 20 percent for waste packages in locations where infiltration is 60+ mm/yr (CRWMS M&O 2000 [DIRS 153246], Table 4.1-1). This relatively small change in seepage fraction across a relatively large range of infiltrations results from the use of the flow-focusing factor, which has the effect of reducing the seepage fraction (if flow is focused into high-flow pathways, then the packages outside those pathways will not have seepage) and increasing the seep flow rate for those packages that are subject to seepage. Because of the nonlinearity of seepage as a function of percolation flux, the total amount of seepage is higher with flow focusing than it is without focusing, even though fewer waste packages are affected. As a result, the computed annual dose is higher with flow focusing, although the increase is only a factor of three at most (CRWMS M&O 2000 [DIRS 153246], Section 5.2.1.2 and Figure 5.2-2a).

3.2.2.2 Updated Seepage Model and Abstraction

Since the TSPA-SR base case was defined, additional testing and modeling of seepage has been performed and documented in revised AMRs (CRWMS M&O 2001 [DIRS 153045]; CRWMS M&O 2000 [DIRS 153314]; CRWMS M&O 2001 [DIRS 154291]). The most important change from the previous versions of these reports is that the revisions include some seepage data for the Topopah Spring lower lithophysal unit, the unit in which most of the potential repository might be located. Previously, seepage data were only available for the Topopah Spring middle nonlithophysal unit. The data and models indicate that the seepage threshold (the percolation flux above which seepage occurs) is higher in the lower lithophysal unit than in the middle nonlithophysal unit, primarily because of higher fracture permeability. The revised seepage abstraction (CRWMS M&O 2001 [DIRS 154291]) accounts for the differences between these two units by developing distributions of uncertainty and spatial variability separately for the lithophysal and nonlithophysal units. However, the TSPA model does not differentiate between host units, so in the final revised seepage abstraction the two sets of results are combined and weighted by the fraction of the repository in each rock type, which is approximately 80 percent lithophysal and 20 percent nonlithophysal (CRWMS M&O 2001 [DIRS 154291], Table 11). The inclusion of results for the lower lithophysal unit, with a higher seepage threshold, results in lower estimates of the seepage fraction (the fraction of waste-package locations that receive seepage) in the revised seepage abstraction.

A sensitivity analysis was conducted in which the revised seepage abstraction was used, but the rest of the model was the same as the TSPA-SR base case. Figure 3.2.2-1 shows a comparison between the mean annual dose for the case with the revised seepage abstraction and the TSPA-SR base case. The results are essentially the same except near 60,000 years, where the sensitivity case is higher than the TSPA-SR base case. That difference was traced to one realization (number 53) in which the seep flow rate was nearly ten times higher than in the TSPA-SR base case for some environmental groups, causing the pulse of advective releases from the initial cladding failures in the CSNF to occur earlier than in the TSPA-SR base case (Figure 3.2.2-2).

The distributions of seep flow rate are different in the updated seepage abstraction compared to those in the TSPA-SR base case, but not greatly different. For example, Figure 3.2.2-3 presents a comparison of the mean seep flow rate for two of the environmental groups. In this figure and similar figures to come, the increase in seepage after 2,000 years is caused by the change from

monsoon climate to glacial-transition climate. The seepage fractions in the updated seepage abstraction are lower because of the inclusion of the lower-lithophysal seepage data: on average, less than half as many waste packages are exposed to seepage in the updated seepage case (TSPA runs SR00_047nm5 and UU01_032nm5; see Appendix A).

3.2.2.3 Effects of Flow Focusing on Seepage

Variations in flow on large scales (hundreds of meters) are accounted for in the mountain-scale UZ flow model (CRWMS M&O 2000 [DIRS 151940], Section 3.7). Variations in flow on small scales (a few meters) are accounted for in the drift-scale seepage model (CRWMS M&O 2000 [DIRS 151940], Sections 3.9.4 and 3.9.5). A flow-focusing factor was developed to account for the possibility of flow channeling on intermediate scales of tens of meters (CRWMS M&O 2001 [DIRS 154291], Section 6.4.3). Such focusing potentially could concentrate flow from an area of tens of meters square onto a drift segment containing a waste package, thereby increasing the local percolation flux and seepage at that location. However, if flow is concentrated in one location, conservation of water mass requires that flow be reduced in other areas.

The distributions of the flow-focusing factor used in the TSPA-SR base-case model are based on estimates of spacing of actively flowing fractures in the mountain-scale flow model (CRWMS M&O 2000 [DIRS 151940], Section 3.9.6.3). Recent work has addressed the spatial variability of UZ flow on intermediate scales more directly: flow was simulated in two dimensions with heterogeneous fracture permeability and mesh spacing less than 1 m for a number of cases (BSC 2001 [DIRS 154657], Section 4.3.2). The resulting estimated distributions of percolation flux at repository depth all are similar, indicating flow enhancements (i.e., increases in the ratio of simulated flux to the mean infiltration rate) that usually are less than a factor of 3 and always less than a factor of about 6. In contrast, the uncertainty distributions for the flow-focusing factor that were defined for the TSPA-SR base-case seepage abstraction had a much broader range from 1 to 47 (CRWMS M&O 2000 [DIRS 151940], Section 3.9.6.3). As discussed in SSPA Volume 1 (BSC 2001 [DIRS 154657], Section 4.3.2.6), the flow-focusing factor implied by the new modeling can be bounded by a distribution that is exponentially distributed, with a minimum focusing factor of 1 and a mean focusing factor of 2. This distribution was substituted for the TSPA-SR base-case distribution for a TSPA sensitivity analysis. The comparison of the computed mean annual dose for this case with the TSPA-SR base case is shown in Figure 3.2.2-4.

The dose comparison shows little difference between the two TSPA simulations even though there is a significant difference in the amount of seepage. The difference in seepage is illustrated in Figure 3.2.2-5, which shows the mean seep flow rate for one of the environmental groups (CSNF, 20 to 60 mm/yr infiltration, seeping some of the time). Because of the lesser amount of flow focusing in the sensitivity case, the mean seep flow rate is lower in that case by nearly a factor of 10. By definition, the mean seep flow rate is the seep flow rate averaged only over locations that have seepage. With flow focusing, the percolation flux is higher in the locations that have percolation, which then produces higher seep rates in those locations. At the same time, less flow focusing makes the seepage fractions higher in the sensitivity case; approximately 50 percent more waste packages are exposed to seepage in that case than in the TSPA-SR base case (TSPA runs SR00_047nm5 and UU01_019nm5; see Appendix A). The number of waste packages that always receive seepage actually declines, but the number of waste packages that

receive seepage only some of the time increases. A high flow-focusing factor increases the chances of seeping all the time, because the focusing enhancement can increase the local percolation flux above the seepage threshold flux even during the dry, present-day climate.

Comparisons of advective releases from the engineered-barrier system for technetium-99 and neptunium-237 are shown in Figure 3.2.2-6. The advective releases are not as different as would be expected from the difference in seepage between this sensitivity case and the TSPA-SR base case. The simulated releases largely are limited by the rate at which the waste inventory is exposed (e.g., by waste-package and cladding failure) and available for transport. In addition, much of the radionuclide release is diffusive rather than advective, especially for technetium-99 (CRWMS M&O 2000 [DIRS 153246], Section 4.1.2), and diffusive releases are not affected by seepage in the TSPA model. Together, the large amount of diffusive release and the relatively small change in the advective release as the seepage changes lead to the small change in doses shown in Figure 3.2.2-4.

3.2.2.4 Effects of Episodic Flow on Seepage

Episodic flow effects were not included in the TSPA-SR base-case seepage-abstraction model because episodic flow caused by episodic infiltration at the surface was considered to be unlikely at the depth of the potential repository (CRWMS M&O 2001 [DIRS 154291], Section 5). However, another possible mechanism for episodic flow is discussed in SSPA Volume 1 (BSC 2001 [DIRS 154657], Section 4.3.5.5), where a conceptual model is presented for episodic flow caused by accumulation of water at fracture asperities followed by drainage after buildup of sufficient water pressure. An asperity is a place where a fracture narrows and therefore is less permeable to fluid flow. As discussed in SSPA Volume 1 (BSC 2001 [DIRS 154657], Section 4.3.5.6.2), this type of episodic flow has not been observed in Yucca Mountain, and it might not be possible under ambient conditions to trap water for long enough because of possible dissipation by imbibition into the matrix or evaporation. However, because episodic flow pulses could lead to greater seepage into drifts, the possible implications of asperity-induced episodic flow for seepage and potential repository performance are presented in this section.

A method for including episodic flow in the seepage abstraction was presented in *Abstraction of Drift Seepage*, although it was not included in the final abstraction (CRWMS M&O 2001 [DIRS 154291], Section 6.4.4). However, that method can now be used to evaluate the effects of asperity-induced episodic flow on seepage. In the abstraction method, episodic flow is parameterized by an episodicity factor, which is the fraction of time that flow occurs. The distribution of episodicity factors used for this sensitivity analysis is a log-uniform distribution between 10^{-4} and 1 (BSC 2001 [DIRS 154657], Section 4.3.5.6).

The implementation of episodicity in the seepage abstraction is similar to the implementation of flow focusing. Both effects tend to increase the total amount of seepage, but in different ways (CRWMS M&O 2001 [DIRS 154291], Sections 6.4.3.2 and 6.4.4). Flow focusing tends to increase the mean seep flow rate and decrease the seepage fraction. Episodic flow also tends to increase the mean seep flow rate (though not as much as flow focusing does), but it also increases the seepage fraction. The seepage fraction increases because, for a given average percolation flux, if flow occurs only part of the time, the flux is higher during the periods when

flow does occur, and the higher flux gives a higher estimate of seepage fraction because seepage fraction increases with percolation flux.

A sensitivity analysis was conducted in which the episodicity distribution was included in the seepage abstraction, but all other parts of the model were the same as the TSPA-SR base case. A comparison was made between the mean annual dose for that case and the base case (Figure 3.2.2-7), and the mean annual dose for the sensitivity case is higher than the TSPA-SR base case after about 40,000 years. The first general-corrosion penetrations of the waste packages occur at about 40,000 years. Before that, no seepage water enters the waste packages in the TSPA-SR model (CRWMS M&O 2000 [DIRS 153246], Section 4.1.2).

The dose increase is caused by the increase in seep flow rate and seepage fraction described above. The mean seep flow rate is illustrated in Figure 3.2.2-8 for CSNF in the 20 to 60 mm/yr infiltration bin. The figure shows that, compared to the TSPA-SR base case, the average seep flow rate increases for the always-seeping locations and decreases for the sometimes-seeping locations. The number of waste packages that sometimes receive seepage actually declines, but the number of waste packages that always receive seepage increases significantly. A low episodicity factor (i.e., much smaller than 1) increases the chances of seeping all the time because the higher flux during the episodic flow periods can push the local percolation flux above the seepage threshold flux even during the dry, present-day climate. In the TSPA-SR base case, more waste packages receive seepage some of the time than receive seepage all the time; whereas in this sensitivity case with episodic flow, more packages receive seepage all the time than receive seepage some of the time. In both cases, the group with more packages has the higher mean seep flow rate. The number of waste packages exposed to seepage in this sensitivity case increases to more than twice the number exposed in the TSPA-SR base case (TSPA runs SR00_047nm5 and UU01_018nm5; see Appendix A).

3.2.2.5 Effects of Drift Degradation and Rock Bolts on Seepage

The updated seepage abstraction model (see Section 3.2.2.2) includes an enhancement of seep flow rate by 50 percent to account for potential effects of drift degradation and the presence of rock bolts on seepage (CRWMS M&O 2001 [DIRS 154291], Section 6.4.1). The base-case seepage-abstraction model (see Section 3.2.2.1) includes a similar enhancement of 55 percent (CRWMS M&O 2000 [DIRS 151940], Section 3.9.6.3). Recent work addressing these effects in more detail has found less impact on seepage than the earlier work on which the seepage abstraction was based (BSC 2001 [DIRS 154657], Sections 4.3.3 and 4.3.4). These recent results show that there is probably no significant increase of seepage because of drift degradation or the presence of rock bolts, but it was also noted that TSPA results are not expected to be sensitive to a change of only 50 percent in the seep flow rates (BSC 2001 [DIRS 154657], Section 4.3.4.6). Because there is uncertainty about the effects of drift degradation on seepage, with significant increases in seepage possible in some locations, the 50-percent seepage enhancement is retained for the analyses in this report. No further sensitivity analyses are presented in this section.

3.2.2.6 Thermal Effects on Seepage

The TSPA-SR base-case model is conservative in its treatment of thermal effects on seepage. Seepage increases are included when there is drainage of thermally mobilized water above the

drifts, but seepage reductions because of evaporation by heat from the waste are not included. These effects are implemented using the percolation flux from 5 m above the emplacement drifts as input to the seepage-abstraction model (CRWMS M&O 2000 [DIRS 148384], Section 6.3.1.2); 5 m is far enough away from the drifts that it is not usually within the boiling, dry-out zone. Several recent analyses have been conducted to estimate the amount of seepage reduction during the period when there is a vaporization barrier around the drifts (BSC 2001 [DIRS 154657], Section 4.3.5). Those analyses found that little, if any, liquid flow reaches the drifts when there is an above-boiling zone around them.

An alternative model is evaluated in which seepage is reduced to zero when the drift wall is above boiling. This change has no effect on dose in the nominal scenario because all waste packages and drip shields remain intact until well past the boiling period in the TSPA-SR base-case nominal scenario (e.g., CRWMS M&O 2000 [DIRS 153246], Figures 4.1-8 and 4.1-9). Thus, to determine if there is some effect, this sensitivity analysis was performed using a case in which there are no drip shields and there is a patch failure in each waste package at 100 years after closure. This is the same as the case with neutralized waste packages and drip shields, which was previously analyzed for the *Repository Safety Strategy: Plan to Prepare the Safety Case to Support Yucca Mountain Site Recommendation and Licensing Considerations* (CRWMS M&O 2000 [DIRS 153225], Volume II, Section 3.4.2).

Figure 3.2.2-9 shows a comparison of the mean annual dose for this sensitivity case with the case that has neutralized waste packages and drip shields and the TSPA-SR base-case seepage model. The calculated doses are reduced for approximately the first 500 years because of the reduction in advective releases caused by eliminating seepage while the drifts are above boiling. Diffusive releases also are relatively low during this period (in both cases) because heat from the waste packages reduces the moisture content, and thus the diffusion coefficient, in the invert. Figure 3.2.2-10 shows time-histories of drift-wall temperature that were used for the five infiltration bins. Information about the infiltration bins and the thermal hydrologic model can be found in the TSPA-SR (CRWMS M&O 2000 [DIRS 153246], Sections 3.3.2 and 3.3.3.) The figure shows that the drift walls are only above boiling temperature (at the repository elevation, the boiling temperature is approximately 96°C) for about 300 years or less, depending on the infiltration bin; thus the seepage model is only changed from the base-case seepage model for about 300 years. The change in seepage for CSNF with 20 to 60 mm/yr infiltration and seepage some of the time is shown in Figure 3.2.2-11. As expected, the mean seep flow rate is only different from the base case for a little over 300 years.

In SSPA Volume 1 (BSC 2001 [DIRS 154657], Section 4.3.5.6), an alternative model is recommended in which seepage is reduced by a sampled factor between 0 and 0.2 when the drift wall is above boiling rather than being set to 0 during this period. As with the alternative thermal seepage formulation discussed above, this change would only affect seepage during the first few hundred years, and would therefore not affect results of the TSPA-SR base-case nominal scenario. A separate analysis with this small change was not performed, but the results would be expected to be between the two curves on Figure 3.2.2-9 and Figure 3.2.2-11. In addition, the alternative recommended in SSPA Volume 1 (BSC 2001 [DIRS 154657], Section 4.3.5.6) is considered along with other seepage modifications in Section 3.2.2.7.

3.2.2.7 Combined Effects on Seepage

In this section, results are presented for a sensitivity analysis in which the changes of the preceding sections are combined. This alternative seepage model includes:

- The updated seepage abstraction (see Section 3.2.2.2)
- The updated distribution for the flow-focusing factor (see Section 3.2.2.3)
- The distribution of the episodicity factor (see Section 3.2.2.4)
- The reduction in seepage by a sampled factor between 0 and 0.2 when the drift wall is above boiling (see Section 3.2.2.6).

As above (see Section 3.2.2.6), to see the effect of changes in seepage during the boiling period, this sensitivity analysis was performed using the case with neutralized waste packages and drip shields (CRWMS M&O 2000 [DIRS 153225], Volume II, Section 3.4.2). The comparison of mean annual dose for this sensitivity case with the case that has neutralized waste packages and drip shields and the TSPA-SR base-case seepage model is shown in Figure 3.2.2-12. For the modified seepage model, the mean annual dose is about a factor of two higher than the TSPA-SR base case at all times. Because the thermal seepage-reduction factor is sampled between 0 and 0.2, there is only one tenth as much seep flow, on average, as in the TSPA-SR base case when the drift wall is above boiling. However, the seepage reduction apparently causes no reduction in dose during the boiling period similar to the reduction when seepage was eliminated (see Section 3.2.2.6). The results show that even a small amount of seepage is enough to provide for release of the highly soluble species (in particular, technetium-99 and iodine-129). The neutralization of waste packages and drip shields makes this case more advection-dominated than was the TSPA-SR base case, especially at early times (compare Figure 3.2.2-13 with CRWMS M&O 2000 [DIRS 153246], Figure 4.1-13).

The change in seepage for CSNF with 20 to 60 mm/yr infiltration and seepage some of the time is shown in Figure 3.2.2-14. The mean seep flow rate in this environmental group for the combined seepage modifications is lower than in the TSPA-SR base-case seepage model by a factor of a little over two at late times, and by a factor of ten or more during the boiling period. The mean annual dose increases even though the mean seep flow rate decreases because the number of waste packages exposed to seepage triples (TSPA runs SR00_047nm5 and UU01_035nm5; see Appendix A). Over one-third of the waste packages are in locations with seepage in the modified seepage model. The increase in seepage fraction occurs because two changes, lower flow-focusing factors and inclusion of episodicity, tend to increase the seepage fraction (see Sections 3.2.2.3 and 3.2.2.4), while only one change, inclusion of data from the lower-lithophysal unit in the seepage abstraction, tends to reduce the seepage fraction (see Section 3.2.2.2).

3.2.3 Analyses of In-Drift TH Conditions

The TSPA-SR base-case TH analyses (CRWMS M&O 2000 [DIRS 153246], Section 3.3.3) include estimates of temperature and relative humidity (RH) within the emplacement drifts.

Several models are used to determine the scale of effects, the variability of thermal and hydrologic properties across the potential repository, heat transfer, and liquid and gas flow processes that determine the TH conditions. These analyses also include variability in infiltration and percolation flux across the site. In addition, the TH analyses consider the effects of pre-closure ventilation by reducing the heat generated by the emplaced waste by the amount removed by the ventilation air. These analyses do not consider drying of the rock by the ventilation air, or the associated change in thermal and flow properties.

Only limited sensitivity studies of the importance of in-drift TH conditions, with respect to the estimate of annual dose, have been provided (CRWMS M&O 2000 [DIRS 153246]). Sensitivity of calculated performance to in-drift temperatures is shown in the comparison of the results for the designs with and without backfill. The results for these two cases (CRWMS M&O 2000 [DIRS 153246], Section 4.6) suggest that there is little difference between the two estimates of system performance. However, the approach to the assessment of thermal effects in some of the models (e.g., use of bounding approximations) limits their usefulness in sensitivity studies. The sensitivity to in-drift TH conditions can be inferred, to some extent, from studies (CRWMS M&O 2000 [DIRS 153246], Sections 5.2.1 and 5.3.1) that examined the range of flow conditions in the UZ because variations in UZ percolation fluxes result in variations in in-drift moisture fluxes.

3.2.4 Analyses of In-Drift Physical and Chemical Environments

In this section, the supplemental analyses of degradation of and chemistry within the emplacement drifts are discussed. Discussions of emplacement drift degradation focus on analyses of uncertainty in the estimates of rock fall, the attendant effects on near-field flow and seepage into the drift, and damage to EBS components. The discussion of in-drift chemistry focuses on the supplemental work done regarding the chemistry of the incoming seepage and the evolution of the chemistry within the emplacement drift.

3.2.4.1 Drift Degradation

Drift degradation analyses (CRWMS M&O 2000 [DIRS 153246], Section 3.3.1) include predictions of rock fall into the emplacement drift, assessment of damage to EBS components, and changes to near-field flow and seepage due to alteration of the drift profile. Results of the analyses indicate that few drifts would suffer significant degradation and that the effects of degradation would be small deformations of the drifts.

Sensitivity and uncertainty analyses have not been conducted for drift degradation. Uncertainties are considered, however, in the development and application of the rock fall model. In the model, blocks of rock defined by the intersection of fractures near the emplacement drifts are considered (CRWMS M&O 2000 [DIRS 153246], Section 3.3.1.3). Fractures are represented in the model by a multiplier for fracture trace length and a correction for sub-horizontal fractures. The range of variability in fracture data is captured through Monte Carlo simulations of rock mass. To account for uncertainties associated with seismic, thermal, and time-dependent effects on rock fall, the locking effect of lateral confinement by the rock mass is ignored and joint strength is reduced.

Sensitivity studies of drift degradation are reported in SSPA Volume 1 (BSC 2001 [DIRS 154657], Section 6.3.4). These studies examine uncertainties in the rock fall model multiplier and in the correction for sub-horizontal fractures, consider a wide range in the size of the fractures to determine the effects on rock fall, and are conducted using a large number of realizations in the Monte Carlo simulations. The results do not show significant increases in the estimate of the size or density of rock fall over that obtained previously. Consequently, TSPA calculations of their effects on the estimate of annual dose have not been conducted.

3.2.4.2 In-Drift Chemistry

In the TSPA-SR base-case model, estimates of the composition of liquids and gases entering the drifts are made using a THC model (CRWMS M&O 2000 [DIRS 153246], Section 3.3.3). This model is used to predict drift-scale chemical composition of seepage water and associated gas-phase chemistry, including the effects of heating. There are uncertainties in thermodynamic input data, the ambient water composition and partial pressure of carbon dioxide within the surrounding rock and surface soil, and in the phases that are important in the associated geochemical reactions. These uncertainties may be important for estimating the overall dynamics of the system and may, therefore, be important in determining the chemistry of incoming water. The chemical reactions are directly related to the temperature and amount of water, both of which are better constrained than are the rates of reaction, and may define the incoming chemistry even if the other factors are uncertain. Nevertheless, these uncertainties were not quantified, and their importance to performance of the potential repository is not explicitly considered in previous analyses.

The previous analyses also considered evolution of the chemistry within the emplacement drift (CRWMS M&O 2000 [DIRS 153246], Section 3.3.4). In addition to changing temperature and moisture conditions, the modeling considered the precipitation of salts on the surface of the drip shield and other components. This precipitation results from evaporation of the water and subsequent re-dissolution of the salts when water drips or condenses onto the components under cooler conditions at later times. The model used for the analyses is based on literature data that describe the minerals and salts produced by evaporative concentration and the relationship between solution composition and RH. This model is incomplete and there are uncertainties in the estimates it produces. These uncertainties were not assessed in the previous analyses.

Supplemental subsystem analyses to address these uncertainties are reported in SSPA Volume 1 (BSC 2001 [DIRS 154657], Section 6.3). The effects of uncertainties in the incoming water composition and partial pressure of carbon dioxide on the chemistry of the water in the drift invert are reported in SSPA Volume 1 (BSC 2001 [DIRS 154657], Section 6.3.1). The analyses consider the importance of better-constrained thermodynamic and kinetic data and better represent the ambient water chemistry and the temperature dependence of that chemistry. The analyses also consider the effect of a more representative host rock mineralogy and find important contributions from fluorides not considered previously.

Supplemental subsystem analyses were conducted to examine estimates of the evolved chemistry of water in the drift (BSC 2001 [DIRS 154657]). Uncertainties in the thermodynamic database and the model for evolution of solids and water during evaporation over time were evaluated

(BSC 2001 [DIRS 154657], Section 6.3.3). Where data are lacking (e.g., the low humidity range), bounding simplifications are used to overcome limitations in the model.

These developments are used to define a new range for the in-drift (including the invert) chemistry that is used in the estimate of annual dose. The new estimate has been compared with the results using the TSPA-SR base-case model (Figure 3.2.4-1). The conceptual model used for the supplemental estimate of chemistry is summarized in SSPA Volume 1 (BSC 2001 [DIRS 154657], Section 6.4). The results show that there is no significant effect on the estimate of mean annual dose. Although the solubilities of radionuclides are affected by this chemistry, residence time in the invert is a sufficiently small fraction of the transport time that this effect apparently is not significant. This result is consistent with previous sensitivity studies (CRWMS M&O 2000 [DIRS 153246], Section 5.2).

3.2.5 Analyses of Waste Package and Drip Shield Degradation

The model for waste package and drip shield degradation in the TSPA-SR base case (CRWMS M&O 2000 [DIRS 153246], Section 3.4) addresses the environment on the surface of the drip shield and waste package, general corrosion, localized corrosion, SCC in the waste package closure lid, weld regions, the effect of preexisting manufacturing flaws on SCC, microbiologically induced corrosion, and aging and phase stability. The model accounts for temperature and relative humidity at the drip shield and waste package surfaces and in-drift chemical environments.

Several sources of uncertainty are addressed in the TSPA-SR (CRWMS M&O 2000 [DIRS 153246], Section 5.2.3). Additional analyses (BSC 2001 [DIRS 154657], Section 7.3) consider further quantification of the uncertainties in the waste package and drip shield degradation model. The following sections show the effect of these considerations on the estimate of mean annual dose.

The previous waste package degradation model (CRWMS M&O 2000 [DIRS 153246], Section 3.4) has been updated, incorporating the quantified uncertainties in the degradation models (BSC 2001 [DIRS 154657], Section 7.3). Changes to the SCC model (BSC 2001 [DIRS 154657], Section 7.4) include:

- The model for weld flaws in the waste package closure lid weld region has been updated. Changes include refinement of the probability distribution for detection of the flaws and explicit consideration of the fraction of weld flaws that are initially surface-breaking.

- The probability distribution for threshold stress uncertainty has been updated. The range of the probability distribution has been updated to reflect new information about this threshold.

- The probability distribution for the crack growth exponent has been updated. The uncertainty range for the crack growth exponent of the slip dissolution model is updated to reflect new information.

The effect of these changes is indicated in Figure 3.2.5-1. This figure shows the mean annual dose estimate using the TSPA-SR base-case model and that calculated using the same model except that the waste package and drip shield degradation model has been updated as indicated. The differences are not large.

The following sections present analyses of additional uncertainties considered in SSPA Volume 1 (BSC 2001 [DIRS 154657], Section 7.3). These analyses address uncertainties in the models for the aging of Alloy 22, SCC, general corrosion, and early failure of the waste package.

3.2.5.1 Aging of Alloy 22

Recent information regarding aging due to phase instability of Alloy 22 has been considered (BSC 2001 [DIRS 154657], Section 7.3.2). In the TSPA-SR base-case model, aging is addressed by enhancing the corrosion rate by a factor of between 1.0 and 2.5 (CRWMS M&O 2000 [DIRS 153246], Section 3.4.1.6). However, Alloy 22 may be less susceptible to long-range ordering and other phase instability mechanisms than considered in the TSPA-SR base-case corrosion model (BSC 2001 [DIRS 154657], Section 7.3.2). It may also be the case that if phase instability occurs, the effect could be more severe than in that base-case model. To evaluate the potential importance of these considerations, an analysis is conducted using a supplemental model for these effects. In this supplemental model, the probability of aging enhancement to the corrosion rate is chosen to be 0.0001, and the effect of aging is chosen to enhance the general corrosion rate by a factor of 1000.

TSPA results using this model are shown in Figure 3.2.5.1-1. In addition to the change in the representation of the aging enhancement, this supplemental model reflects updates to the TSPA-SR base-case waste package and drip shield model discussed previously (see Section 3.2.5). The specific implementation of the model for this analysis is summarized in Appendix A.

Figure 3.2.5.1-1a compares the calculated mean annual dose using the supplemental model with that using the TSPA-SR base-case model. The supplemental model results in a contribution to the mean annual dose before 10,000 years due to the small fraction of waste packages that fail earlier than in the base-case model due to the enhanced corrosion rate. Although this contribution can be calculated, it is too small to be measured. The remainder of the waste packages do not fail early from an aging enhancement to the corrosion rate and remain intact for much longer than in the base case. The cause is shown in more detail in Figure 3.2.5.1-1b. This figure shows the range of realizations calculated with the supplemental model that result in an annual dose. A small number of these realizations manifests the effect of the enhanced corrosion and results in early failure of the waste package. The majority of the realizations, however, do not show early failure due to the aging enhancement. The average of all of these realizations gives the small contribution to the annual dose in the early period and a delayed mean annual dose from the majority of realizations that have no aging enhancement.

This supplemental analysis shows that the base-case model is conservative after 20,000 years. Before this time, the annual dose in the supplemental model is greater than that in the base-case analysis; however, the estimated mean annual dose is small, even using the extreme parameters of this model. As will be shown in Section 3.2.5.4, the magnitude of this effect is more than a

factor of 10 smaller than that due to other possible effects of early waste package failure. In view of the small effect on mean annual dose before 20,000 years, and in view of the scoping nature of the analysis, it appears reasonable to maintain the general conservative approach to aging enhancement that is used in the TSPA-SR base-case model.

3.2.5.2 Stress Corrosion Cracking

Additional considerations of the sources of uncertainty in the SCC model (BSC 2001 [DIRS 154657], Section 7.3.3) result in supplements to the SCC model (summarized below). The effects of these refinements on the estimate of mean annual dose are evaluated in three calculations that address the expanded range of considerations for the residual stress profile of the closure weld regions (Figure 3.2.5.2-1), the threshold stress for SCC crack initiation (Figure 3.2.5.2-2), and the orientation of the weld flaws (Figure 3.2.5.2-3). The models used for these analyses are discussed in SSPA Volume 1 (BSC 2001 [DIRS 154657], Section 7.3.3), and updates to the base-case degradation model are discussed in Section 3.2.5 of this volume. The effects on waste package degradation of all of these changes are summarized in SSPA Volume 1 (BSC 2001 [DIRS 154657], Section 7.4.2). The implementation of the models for each of these analyses is summarized in Appendix A.

The TSPA-SR base-case SCC model addresses uncertainties in the closure weld residual stress profile by considering a range of values for the upper bound of the uncertainty distribution and by choosing a conservative value from this range for the base-case simulations (BSC 2001 [DIRS 154657], Section 7.3.3.2). The curve for the supplemental analysis (Figure 3.2.5.2-1) is calculated by considering the full range of these values rather than only the single conservative value. Figure 3.2.5.2-1a compares the mean annual dose estimate with this more realistic representation of the uncertainties in the stress profile with the result considering only the single value, and Figure 3.2.5.2-1b shows the full set of realizations for the more realistic representation of the upper bound. The mean annual dose is affected by the delayed initiation of SCC and resulting increased waste package lifetime.

Similarly, the base-case SCC model uses a conservative representation of the threshold stress for crack initiation. In this case, a conservative range represents the uncertainties. Using updated information, the analyses (BSC 2001 [DIRS 154657], Section 7.3.3) consider a more representative range of values, and the results show the effect on the estimate of annual dose (Figure 3.2.5.2-2). As in the case of the analysis of residual stress uncertainty bound, the more realistic model shows a marked decrease in the mean annual dose in the first 50,000 years due to a reduced probability of waste package failure resulting from SCC degradation.

The base-case model also uses a conservative representation for the orientation of weld flaws: the orientation that maximizes crack growth to failure. The supplemental model takes into account new information on the effectiveness of flaw detection techniques and the specifics of weld flaw geometry to provide a more representative fraction of flaws capable of propagating in the radial direction. Figure 3.2.5.2-3 shows the effect of this modification to the model on the estimate of annual dose. As in the other cases, the more realistic representation results in increased waste package resistance to SCC failure of the waste package and delay before release of radionuclides.

3.2.5.3 General Corrosion

The TSPA-SR base-case model addresses uncertainties in the representation of general corrosion in several ways (CRWMS M&O 2000 [DIRS 153246]. Section 3.4.1.2). In particular, the model addresses uncertainty arising from variability in conditions and microstructure in the waste package or drip shield by partitioning the uncertainty between epistemic uncertainty in the general corrosion rate and aleatoric uncertainty due to variability. The sensitivity to this treatment of uncertainty in the general corrosion is examined by comparing the results using a probability distribution for general corrosion that reflects the epistemic uncertainty and the aleatoric uncertainty, with the result using a probability distribution in which only the epistemic uncertainty is taken into account.

The effect neglecting the contribution of variability to the variance in the corrosion probability distribution is shown in Figure 3.2.5.3-1. The implementation of this model is described in the TSPA-SR (CRWMS M&O 2000 [DIRS 153246], Section 3.4.2.2). Figure 3.2.5.3-1a shows the mean annual dose estimated using this base-case model. The probability distribution for general corrosion in this model reflects the epistemic uncertainty in the corrosion rate and the aleatoric uncertainty due to variability. Figure 3.2.5.3-1a also shows the result using the updated model discussed above (see Section 3.2.5). More importantly, the model also includes only the epistemic uncertainty in the general corrosion rate. The implementation of the latter is summarized in Appendix A.

The comparison shows a difference in the estimate of mean annual dose. The neglect of uncertainty due to variability effectively narrows the temporal failure distributions for the drip shield and waste package associated with general corrosion. This narrowing leads to later initial failures of the drip shields and waste packages. In figure 3.2.5.3-1a, the earliest release is delayed in the latter model because of this later initial failure of these components.

A second source of uncertainty in the TSPA-SR base-case model is the temperature dependence of the general corrosion rate. Because the Alloy 22 weight-loss measurement techniques may not be sensitive enough to distinguish such dependence over the range of temperatures covered in those tests, the model does not take into account any temperature dependence of the general corrosion rate of this material. New information, however, is able to indicate this temperature dependence. Supplemental analyses of the temperature dependence of the general corrosion rate for Alloy 22 have been conducted (BSC 2001 [DIRS 154657], Section 7.3.5). Potentiostatic polarization test results provide additional insight into the temperature dependence of general corrosion beyond that provided by the weight-loss measurements. The additional information supports a discernible temperature dependence for general corrosion of Alloy 22. To implement this model, the temperature dependence is calibrated to the base-case model at a temperature of 60ºC (the lower of two temperatures considered in the immersion tests). The net effect of the temperature dependence is that, while waste package temperatures are greater than 60ºC (for approximately the first 10,000 years), Alloy 22 general corrosion rates are higher than in the TSPA-SR base case. After this time, the general corrosion rate is lower and the net effect is that, on average, the rate of waste package failure is much lower in the supplemental model than in the base-case model.

The results of the estimates of annual dose using the updated waste package degradation rate are compared with the results using the base-case (temperature-independent) general-corrosion model in Figure 3.2.5.3-2. The specific implementation of the supplemental model for this analysis is summarized in Appendix A. Figure 3.2.5.3-2a compares the base-case result to the results in which the temperature dependence of the general corrosion rate is developed from the potentiostatic polarization test results. Because the rate of waste package failures is much lower in the first 100,000 years in the supplemental model, the mean annual dose is significantly lower than the base-case result. The variance in the estimate of annual dose using the temperature-dependent model is shown in Figure 3.2.5.3-2b. Because of the larger variance in the degradation rate due to the treatment of uncertainty, variance in the estimate of annual dose using the temperature-dependent model is somewhat larger than that for the base-case general-corrosion model.

3.2.5.4 Early Failure of the Waste Package

Figure 3.2.5.4-1 shows the effect of considering a broader range of early failures than is considered in the TSPA-SR base-case model. That model considers a broad range of possible defects based upon information in the literature regarding component manufacturing processes similar to those that would be employed for the drip shield and waste package (CRWMS M&O 2000 [DIRS 153246], Section 3.4.1.4). However, these considerations did not fully address defects that might occur as a result of improper heat treatment of the waste package closure welds resulting from heat treatment to mitigate potential SCC.

The implications of such improper heat treatment were considered in SSPA Volume 1 (BSC 2001 [DIRS 154657], Section 7.3.6). The analysis resulted in an increased probability for early waste package failure. Figure 3.2.5.4-1 shows the impact of this increased probability on the estimate of mean annual dose. The analysis uses the probability distribution from SSPA Volume 1 (BSC 2001 [DIRS 154657], Section 7.3.6). This probability distribution is applied to waste packages located anywhere in the potential repository. With this probability distribution, most realizations will have no waste packages failing early, some will have a single waste package failing early, and a small fraction will have as many as two failing early. The mean number of waste packages that fail early is on the order of 0.26 (BSC 2001 [DIRS 154657] Section 7.3.6). The analysis makes the conservative assumption that any waste packages identified as being improperly treated suffer substantial breaches of the closure welds soon after beginning to undergo corrosion. In this conservative approach, the entire area of the waste package in the weld region is assumed to be breached. This amounts to 32 patch breaches for the waste packages that fail early. Accordingly, the average number of patches breaches due to early waste package failure is about 8 (0.26×32). The specific implementation of the supplemental model for this analysis is summarized in Appendix A.

In the base case, no release occurs before 10,000 years. In the conservative model, which incorporates failures from improper heat treatment, release before 10,000 years is apparent (Figure 3.2.5.4-1). The mean dose rate resulting from these early failures is low because the number of waste packages calculated to fail early is small. The mean annual dose in this one-off sensitivity study is on the order of 0.01 mrem/year. The only factor permitting the early release of these radionuclides in this calculation is the early failure of the small fraction of waste packages. This analysis is only a sensitivity study and does not necessarily indicate actual

system performance. For example, the role of possible mitigation techniques has not been considered in developing the probability distribution for the supplemental early failure evaluation. Further, the model for early failure, given that it occurs, is non-mechanistic (BSC 2001 [DIRS 154657], Section 7.3.6). This model was developed for estimating order-of-magnitude importance of possible effects. Accordingly, these results should be viewed as merely providing information about potential effects in the event of early waste package failure.

3.2.6 Analyses of Water Diversion Performance of the EBS

The EBS components include the waste package and the drip shield over the waste package. The models for the water diversion performance of these components are discussed in the TSPA-SR (CRWMS M&O 2000 [DIRS 153246], Section 3.6.2.1). In the model for water diversion by the drip shield, all seepage into the drift first falls onto the drip shield. Breaches in the drip shield intercept this flow and permit a fraction of the incoming seepage to flow through the drip shield. The remainder of the water flows directly down to the invert and then drains into the host rock. The fraction of water flowing through the drip shield is the ratio of the summed axial length of the patch breaches in the drip shield to the total length of the drip shield, and all flow intercepted by breaches is assumed to flow through the drip shield. Evaporative reduction of the amount of water contacting the drip shield is ignored in the TSPA-SR base-case model.

The model for water diversion by the waste package in the base-case model specifies that all water transmitted through the drip shield falls onto the waste package. Breaches in the waste package intercept this flow and permit a fraction of the incident water to flow into the waste package. The remainder flows off the waste package, down to the invert, and then into the host rock. The fraction of water flowing into the waste package is the ratio of the summed axial length of the patch breaches in the waste package to the total length of the waste package. As in the case of the drip shield, evaporative reduction of the amount of water contacting the waste package is ignored.

Condensation of water on the underside of the drip shield with subsequent dripping onto the waste package was considered in the *EBS Radionuclide Transport Abstraction* report (CRWMS M&O 2000 [DIRS 153940], Section 6.3.3). However, this process is not included in the base-case model.

Sensitivities to these features of the base-case model are not evaluated in the TSPA-SR (CRWMS M&O, 2000 [DIRS 153246]). However, some of the sensitivities are evaluated in SSPA Volume 1 (BSC 2001 [DIRS 154657], Section 8.3). These aspects are taken into account here to determine their importance in the estimate of annual dose. These aspects include evaporative reduction of seepage, condensation under the drip shield, constraints on advective flux into the waste package due to the geometry of drip shield and waste package breaches, and accumulation of water within the waste package (bathtub effect).

3.2.6.1 Evaporative Reduction of Seepage

The analyses (BSC 2001 [DIRS 154657], Section 8.3.1) indicate that, because waste packages remain intact during the period when evaporative reduction of the flow might be important, little effect on radionuclide release is expected. Comparison of analyses including this effect with the

results using the TSPA-SR base-case model (Figure 3.2.6.1-1) confirm this expectation: there is no discernible difference between the results with or without the evaporative reduction. The conceptual model for this case is summarized in SSPA Volume 1 (BSC 2001 [DIRS 154657], Section 8.4), and the implementation for this analysis is described in Appendix A.

3.2.6.2 Condensation Under the Drip Shield

Condensation of water on the underside of the drip shield with subsequent dripping onto the waste package is considered in SSPA Volume 1 (BSC 2001 [DIRS 154657], Section 8.3). A bounding estimate of the amount of water that might condense under the drip shield is provided in SSPA Volume 1 (BSC 2001 [DIRS 154657], Section 8.3.2). The model assumes that, if the drip shield is cooler than the invert, a fraction of the water evaporated from the drift invert condenses under the drip shield and drips onto the waste package. For the sensitivity analyses, the fraction of water reaching the waste package is sampled from a uniform probability distribution that ranges between zero and one. Analyses using the base-case model for invert and drip shield temperature indicate condensation under the drip shield throughout the potential repository, even in areas in which no seepage occurs. In this event, there would be advective flow throughout the repository during the early thermal period in spite of the drip shield. However, the amount of water condensing under the drip shield is not large after the first few thousand years.

The resulting mean annual dose calculated using this condensation model is compared with TSPA-SR base-case model results without a model for condensation under the drip shield in Figure 3.2.6.2-1. Because the condensation is not significant while the waste packages remain intact, the analysis is conducted for the juvenile failure scenario in which a single CSNF waste package is breached at 100 years. The juvenile failure scenario is defined in the TSPA-SR (CRWMS M&O 2000 [DIRS 153246], Appendix G), and the results are displayed and explained in the *Repository Safety Strategy: Plan to Prepare the Safety Case to Support Yucca Mountain Site Recommendation and Licensing Considerations* report (CRWMS M&O 2000 [DIRS 148713], Section 3.3). The conceptual model for condensation is summarized in SSPA Volume 1 (BSC 2001 [DIRS 154657], Section 8.4), and the implementation for the calculation of juvenile failure scenario annual dose is described in Appendix A.

Condensation flow in this model changes the estimate of mean annual dose, a change that arises from two considerations. First, flow (due to condensation) occurs in this case even in areas that receive no seepage in the base-case model. Consequently, the probability that the single juvenile failure waste package is in a location with advective flow, and hence is contacted by flowing water and experiencing advective release of radionuclides is increased. Second, the flux from the condensation affects the release from individual waste packages. The release of neptunium-237 is increased because more water is available to dissolve this radionuclide. The magnitude of the release of technetium-99 and iodine-129 is not affected because the release of these radionuclides is controlled by the waste form degradation rate rather than radionuclide solubility limit.

The overall effect of the condensation in this simple model is to increase the peak mean annual dose rate in the first 10,000 years by nearly an order of magnitude. The effect would be negligible in the nominal scenario because the waste packages do not fail in the period when

evaporation might be important. Further, this simple model probably overestimates the effects. For example, the model does not consider the fraction of the evaporated water that condenses on locations that are cooler than the emplacement drift (e.g., the drift wall). In addition, the model does not account for the fact that the drip shield temperature is underestimated and the drift invert temperature is overestimated in the base-case model. Finally, even if there is condensation under the drip shield, the condensate will flow down the underside of the drip shield rather than fall onto the waste package because moisture adheres to the oxide film on the titanium metal. Therefore, it is likely that the effect of condensation would be negligible in a more realistic model.

3.2.6.3 Geometrical Constraint on Flow through the Waste Package

The fraction of water flowing through the waste package may be different from the assumption used in TSPA-SR base-case model to define the fraction. In this conservative model, all of the water flowing through the drip shield is assumed to flow through the waste package. However, there are geometrical constraints on this flow if the waste package breaches are not directly under the drip shield breaches. The analyses in SSPA Volume 1 (BSC 2001 [DIRS 154657], Section 8.3.3) develop a more realistic representation for this fraction. The difference in the resulting estimate of annual dose is shown in Figure 3.2.6.3-1. The implementation of the conceptual model for this analysis is described in Appendix A.

Patch breaches do not develop on the drip shield until about 40,000 years. Consequently, the updated model shows no change in the estimate of mean annual dose from that calculated with the base-case model. After this time, the geometrical constraint reduces the flux through the waste package, resulting in a reduction in the release of neptunium-237 and other solubility-limited radionuclides. The effect is a modest change in the mean annual dose due to this change in the source term.

3.2.6.4 Bathtub Effect

Before development of any breach in the bottom of the waste package, water entering a breach in the top of the waste package would accumulate as in a bathtub. After a breach is formed in the bottom, the water could drain. The impact of this accumulation and subsequent drainage is considered in SSPA Volume 1 (BSC 2001 [DIRS 154657], Section 8.3.4). The accumulation could add to the volume of water contacting the waste form and increase the mass flux of radionuclides released from the waste form. The increased mass of released radionuclides could increase the advective flux of radionuclides transported from the waste package after the bottom of the waste package is breached. The effect would be temporary, lasting only until the accumulated water drains from the waste package.

The effects on estimate of mean annual dose rate are shown in Figure 3.2.6.4-1. The bathtub model used for this analysis is summarized in SSPA Volume 1 (BSC 2001 [DIRS 154657], Section 8.4), and implementation of the model for this calculation is described in Appendix A. The effect on the estimate of mean annual dose rate is small. First, only a fraction of the waste packages in the potential repository are contacted by water, and only a fraction of these have a sufficient delay of breaching in the bottom (after breaching in the top) to provide a significant bathtub effect. In addition, although accumulations in this small fraction of waste packages can

be substantial (on the order of 1 m^3 of water for an average waste package in an area with seepage), the accumulated water drains rapidly and has a short-term effect. Diffusive releases from the EBS depend only on the concentration of radionuclides in the water and not the additional mass and, therefore, are not affected. Advective releases from the EBS are affected, but only over a short period, and the net effect averaged over an entire time step of several hundred years is small.

3.2.7 Analyses of Waste Form Degradation and Radionuclide Release

The waste form degradation and radionuclide release model addresses the inventory of radionuclides in the emplaced waste, in-package chemistry, waste form matrix degradation, CSNF cladding, radionuclide solubility limits, and colloid-associated radionuclide concentrations. Several of these topics have been addressed in supplemental analyses. The topics discussed in the following sections include: in-package chemistry, CSNF cladding degradation, radionuclide solubility limits, and colloid-associated radionuclide concentrations.

3.2.7.1 In-Package Chemistry

The TSPA-SR base-case model for the in-package chemistry is a simple mixing cell (CRWMS M&O 2000 [DIRS 153246], Section 3.5.2.1). This model is used to evolve the incoming water chemistry (assumed to be that of Well J-13 water) as a result of reactions of in-package materials, including the oxidation of in-package metals and the degradation of waste forms. In particular, the model is used to approximate the effect of the degradation reactions in the waste form and the waste form and iron corrosion products of these reactions.

Analyses described in SSPA Volume 1 (BSC 2001 [DIRS 154657]) reconsider the range assumed for the dissolution rates of stainless steel, carbon steel, and the glass HLW form in the codisposal waste packages. These rates, in concert with the fuel exposure rate and the flow rate of water through the waste package, determine the time-dependent chemistry (in particular, the pH of the water). As indicated in SSPA Volume 1 (BSC 2001 [DIRS 154657], Section 9.3.1), the TSPA-SR base-case model uses conservatively high dissolution rates.

The supplemental TSPA analyses consider a model in which these dissolution rates are represented more realistically. The main effects in this model are explained in SSPA Volume 1 (BSC 2001 [DIRS 154657], Section 9.3.1.3.3). The calculation for the CSNF in-package pH shows two lows: one in the early time (about 1 to 50 years, after waste package breach), and another in the period between about 10,000 to 200,000 years. These bracket a period of near neutral pH. These pH lows can be attributed to dissolution of carbon steel in the early time and stainless steels in the latter. The period of neutral pH is facilitated primarily by the buffering by $Fe(OH)_3(s)$, which precipitated during dissolution of the carbon steel. As in the case of the CSNF waste package, the carbon steel in the codisposal waste packages is calculated to drive the pH down at early times. After the carbon steel has been depleted, the pH steadily increases as HLW glass tends to dominate the effluent chemistry with release of alkalinity-generating species.

Calculations of total system performance using this supplemental in-package chemistry range are compared with the results using the base-case model in Figure 3.2.7.1-1. Figure 3.2.7.1-1a

compares the mean annual dose curves calculated with the two models, and Figure 3.2.7.1-1b shows the range of the realizations calculated using the supplemental model. The specific implementation of the modified chemistry range is given in Appendix A.

The results show significant effects after about 40,000 years when the contributions from neptunium-237 and other actinides begin to dominate the estimate of mean annual dose (see Section 3.1.1). The change in chemistry does not have a significant effect on the waste form degradation rate that controls the concentrations of technetium-99 or iodine-129, radionuclides that dominate the annual dose estimate in the first 40,000 years (see Section 3.1.1). The modified water chemistry, however, affects the solubility limits of neptunium, plutonium, and other actinides; and therefore, it affects the annual dose from the associated isotopes with concentrations that are determined by these solubility limits.

The effects of the supplemental in-package chemistry model depends on the time of waste package breaching, the rate of exposure of the waste form, and the flow of water through the waste package. Consequently, the effects in a model where these factors are different from those in the base-case model could be different than shown in Figure 3.2.7.1-1.

3.2.7.2 CSNF Cladding Degradation

The model for CSNF cladding degradation is described in the TSPA-SR (CRWMS M&O 2000 [DIRS 153246], Section 3.5.4). This model accounts for a number of factors. It considers the fraction of cladding that is perforated at the time of emplacement of the CSNF into the repository (e.g., during reactor operations and storage before emplacement). The model considers creep rupture of the cladding in the repository (e.g., due to creep and SCC under the high stresses at temperatures exceeding 300°C in the repository). The model includes a representation for localized corrosion of the cladding over time (e.g., pitting due to the presence of fluoride and chloride in water contacting the cladding). The model accounts for perforation of the cladding due to seismically induced vibratory ground motion. Finally, the model accounts for further degradation ("unzipping") of the cladding after perforation as exposed uranium oxide alters and swells.

Uncertainties in most of these factors are explicitly considered in the analyses using the TSPA-SR base-case model. In particular, probability distributions are used for the parameters describing the initial perforation of the cladding, creep and SCC in the potential repository, localized corrosion, and the cladding unzipping rate. The importance of this range of uncertainty has been examined in sensitivity analyses (CRWMS M&O 2000 [DIRS 153246], Section 5.3.4). Although, these uncertainties are among the most important contributors to overall uncertainty of the annual dose estimate, they only have a small impact on the estimate of mean annual dose: a factor of less than 10 in the first 100,000 years.

The supplemental TSPA analyses (BSC 2001 [DIRS 154657], Section 9.3.3) consider information regarding the range of uncertainties in models for cladding degradation processes in addition to that considered in the TSPA-SR (CRWMS M&O 2000 [DIRS 153246]). In particular, the probability distribution for creep and SCC during dry storage is modified to reflect a more realistic representation of creep failure. The result is a reduction in the estimate of early cladding failures: the mean fraction of early cladding failures is reduced from about 8 percent to

about 1 percent. The analyses (BSC 2001 [DIRS 154657], Section 9.3.3) also consider the probability distributions for localized corrosion and cladding unzipping. The ranges for these distributions are expanded to account for additional uncertainty considerations. The effect in this case is greater variance in the distribution of cladding failures. The analyses also consider perforations due to static loading by fallen rock. These considerations lead to increased degradation of the cladding after sufficient degradation of the waste package and drip shield occurs to permit the rocks to rest directly on the waste form.

The effects of the additional cladding degradation uncertainty on the annual dose estimate are shown in Figure 3.2.7.2-1. The conceptual model for the cladding degradation is summarized in SSPA Volume 1 (BSC 2001 [DIRS 154657], Section 9.4), and the implementation for these analyses is described in Appendix A. The small reduction in the mean annual dose in the period (Figure 3.2.7.2-1) arises largely from the reduction in early cladding failure. The other changes to the cladding degradation model do not result in significant changes to the estimate of mean annual dose in the first 100,000 years.

3.2.7.3 In-Package Radionuclide Solubility Limits

The model for dissolved radionuclide concentration limits is described in the TSPA-SR (CRWMS M&O 2000 [DIRS 153246], Section 3.5.5). These solubility limits are calculated from the in-package chemistry, specification of the phases that control the solubility of the elements under consideration, and the thermodynamic parameters that govern the stability of the aqueous species and elemental phases. Uncertainty taken into account in the estimate of the in-package chemistry is considered in developing the values for the solubility limits. For americium, neptunium, and uranium, the uncertainty in the chemistry is explicitly taken into account. For the others, bounding values are used for the in-package chemistry parameters. In addition, sensitivity to the selection of controlling phases is considered for neptunium and thorium.

The importance of the range of uncertainty explicitly accounted for in the solubility limits is examined in TSPA-SR base-case sensitivity analyses (CRWMS M&O 2000 [DIRS 153246], Section 5.3.4). The increased range of uncertainty has a modest effect on the estimate of long-term annual dose, which primarily is due to effects on the source terms for neptunium and thorium.

Supplemental analyses reported in SSPA Volume 1 (BSC 2001 [DIRS 154657], Section 9.3.2) consider a wider range for the uncertainty in the effect of the controlling phases for plutonium, neptunium, thorium, and technetium. The effects of the extended range of uncertainty in these concentration limits, along with the effects on in-package chemistry (e.g., pH), are shown in Figure 3.2.7.3-1. Figure 3.2.7.3-1a compares the mean annual dose taking these effects into account with the results using the base-case model. Figure 3.2.7.3-1b shows the contributions of the various radionuclides to the total mean annual dose estimate when these effects are taken into account. The implementation of the changes in the base-case model to account for these effects is summarized in Appendix A.

The results (Figure 3.2.7.3-1) show significant changes after the waste packages are breached. As indicated previously (see Section 3.1.1), neptunium-237 dominates the annual dose estimate

in the nominal scenario; therefore, changes to the solubility limit of this radionuclide have a large effect on the estimate of total mean annual dose. The estimates of mean annual dose for other radionuclides also are reduced by the changes in solubility limits. In particular, the mean annual dose from the plutonium isotopes is reduced by about a factor of three. The overall effect of these changes is to reduce the estimate of mean annual dose by a factor of more than five.

3.2.7.4 In-Package Colloid-Associated Radionuclide Concentrations

The model for colloid-associated radionuclide concentrations is described the TSPA-SR (CRWMS M&O 2000 [DIRS 153246], Section 3.5.6). The model considers three types of concentrations associated with colloids that form during degradation of HLW glass or corrosion of iron components of the waste package, or that occur naturally in UZ groundwater. The model accounts for uncertainty associated with each of these concentrations and with the characteristics for reversible and irreversible attachment of radionuclides to the colloids. The colloid-associated concentrations are not important in determining the annual dose in the base-case analyses. Sensitivity studies were not conducted to examine the importance of these concentrations over the range of quantified uncertainty.

The supplemental TSPA analyses (BSC 2001 [DIRS 154657], Section 9.3.4) extend the range of uncertainties in these concentrations and examined sensitivity over this range. First, the analyses consider the range of concentration of colloids formed during corrosion of iron components. The range used in the TSPA-SR used data for a site with groundwater adjacent to an iron-rich stock (CRWMS M&O 2000 [DIRS 153246], Section 3.5.6.1). This range is consistent with concentrations of other inorganic colloids at that and other sites. To account for uncertainties, the range for the iron-product colloid concentration extends this measured range upward by a factor of four (for conservatism), and extends below it based upon reasonable assumptions. The supplemental TSPA analyses (BSC 2001 [DIRS 154657]) considered the same data and concluded that, although the range used for the TSPA-SR base-case model was reasonable, the probability distribution should emphasize the measured concentrations.

Second, the analyses in SSPA Volume 1 (BSC 2001 [DIRS 154657], Section 9.3.4) consider the effect of ionic strength on the colloid concentrations. The base-case analyses consider this effect only to a limited extent. As a result, the range for the colloid concentrations in the SSPA Volume 1 analyses (BSC 2001 [DIRS 154657]) is wider than that in the TSPA-SR base-case model. In addition, the concentrations for low ionic strength and high ionic strength waters are different.

Finally, the analyses in SSPA Volume 1 (BSC 2001 [DIRS 154657], Section 9.3.4) consider the effect of the presence of iron oxide and iron hydroxide corrosion products in the water on the sorption characteristics of colloidally transported radionuclides. These analyses also consider the measurements of actinide sorption and conclude that the range of sorption should be extended in the lower direction as well. Accordingly, a wider range is proposed for the sorption coefficients.

The effect of using the colloid concentration and sorption model, considered in SSPA Volume 1 (BSC 2001 [DIRS 154657]), is shown in Figure 3.2.7.4-1, and the specific implementation for the analyses is described in Appendix A. Figure 3.2.7.4-1a compares the mean annual dose curves for the base case and the new colloid models, and Figure 3.2.7.4-1b shows the range of

the results for the new colloid model. There is little difference between the mean annual doses calculated using these models. In part, the small difference reflects the fact that the mean annual dose is dominated by dissolved radionuclides. However, even the comparison of the results for the colloids alone would show little change in the mean annual dose because the mean values of the probability distribution in the two models are virtually the same.

3.2.8 Analyses of Radionuclide Transport in the EBS

The TSPA-SR base-case model for radionuclide transport in the EBS is described in the TSPA-SR (CRWMS M&O 2000 [DIRS 153246], Section 3.6.1.2). This model accounts for transport of dissolved and colloid-associated radionuclides and considers advective and diffusive transport of these radionuclides in the waste package and drift invert. Supplemental analyses of radionuclide transport in the EBS are described in SSPA Volume 1 (BSC 2001 [DIRS 154657], Section 10.3). These analyses include the treatment of diffusion and sorption in the EBS.

The TSPA-SR base-case model does not account for diffusive transport processes within the waste package. A model for diffusive transport on thin films on the surface of in-package components is considered in SSPA Volume 1 (BSC 2001 [DIRS 154657], Section 10.3.1). Results implementing this effect are shown in Figure 3.2.8-1. The model is defined in SSPA Volume 1 (BSC 2001 [DIRS 154657], Section 10.4), and the implementation for this analysis is described in Appendix A. There is little difference between the dose calculated using the base-case model and the model including in-package diffusive transport in the EBS.

One possible reason for the small difference in these two estimates is the diffusion coefficient used for transport within the waste package. The diffusion coefficient used in the analysis is conservative and sensitivity analyses generally show this conservatism to be important. For example, sensitivity analyses (CRWMS M&O 2000 [DIRS 153246], Section 5.3.5) for the diffusion coefficient of the drift invert show that diffusion plays a key role in the EBS transport even after the drip shield and waste package have breached. This conclusion is sensitive to the diffusion properties assumed for the EBS. The TSPA-SR base-case model uses a conservative representation for the invert diffusivity, and these sensitivity analyses indicate a diffusive transport component that exceeds the advective transport in the early times and is comparable to it in the long term. Analyses using a more realistic diffusivity have a lower diffusive component. As in the analysis of the invert diffusion properties, a conservatively high diffusion coefficient results in limited diffusion resistance to radionuclide transport.

The second consideration is the effect of sorption on radionuclide transport in the EBS, in particular, the effect of iron corrosion products on reversible and irreversible sorption in the invert. The TSPA-SR base-case model assumes no sorption of dissolved species within the EBS. However, SSPA Volume 1 (BSC 2001 [DIRS 154657], Section 10.3.4) considers the conservative nature of this assumption and develops a model for the sorption of radionuclides in the EBS. This model includes sorption partition coefficients (K_ds) for corrosion products and other materials within the waste package and drift invert and fractions of radionuclides irreversibly sorbed onto these materials. Results using these K_ds are shown in Figure 3.2.8-2. The models are defined in SSPA Volume 1 (BSC 2001 [DIRS 154657], Section 10.4), and the implementation for this analysis is described in Appendix A.

The reduction in mean annual dose from the TSPA-SR base case derives from two principal effects. The first is the reduction in concentrations in the liquid phase due to the partitioning of the concentrations between the liquid phase and the solid phases not considered in the TSPA-SR base-case model, the result of which reduces the source term of many of the contributing radionuclides. The second is the effect of sorption on the diffusive transport, which effectively reduces the diffusion coefficient and increases the diffusion resistance of in-package transport. These two effects combine to decrease the source term and the resulting mean annual dose estimate.

3.2.9 Evaluation of Unsaturated Zone Transport

UZ transport refers to the movement of radionuclides from the potential repository, through the UZ, and to the water table. Water flow in the UZ is discussed in Section 3.2.1. Further movement of the radionuclides below the water table in the SZ is discussed in Section 3.2.10. UZ transport is the first natural barrier to radionuclides that escape from the potential repository. UZ transport acts as a barrier by delaying radionuclide movement. If the transport time is large compared to the half-life of a radionuclide, then the UZ can have a large effect on decreasing the dose from that radionuclide at the biosphere. The UZ-transport component of the TSPA is summarized in the TSPA-SR (CRWMS M&O 2000 [DIRS 153246], Section 3.7).

In Section 3.2.9.1, the UZ-transport results for TSPA-SR (CRWMS M&O 2000 [DIRS 153246], Section 3.7) are summarized. In Section 3.2.9.2, results of recent work on the effect of the drift shadow zone are presented. As shown in Table 1.3-1, additional analyses related to UZ transport are discussed in SSPA Volume 1 (BSC 2001 [DIRS 154657], Section 11), but the drift-shadow-zone analysis (BSC 2001 [DIRS 154657], Section 11.3.1) is the only one that was included in TSPA simulations. The other UZ-transport analyses provide useful information about UZ transport and its uncertainties, but they do not present new abstractions for use in TSPA simulations (BSC 2001 [DIRS 154657], Sections 11.3.2.6, 11.3.3.6, 11.3.4.7, and 11.3.5.5).

3.2.9.1 Review of Previous Results

Within a TSPA simulation, UZ flow is modeled as a sequence of steady states. (UZ flow is discussed in Section 3.2.1.) The transport calculation itself is fully transient, with radionuclides moving downward from the potential repository as they are released. In the TSPA-SR base-case model, each realization uses a set of flow fields representing a sequence of three climate states: present-day, monsoon, and glacial-transition climates (see Section 3.2.1). For each climate state, there are three infiltration cases: low, medium, and high. In the TSPA model, the water table is higher in wetter future climates (CRWMS M&O 2000 [DIRS 153246], Section 3.2.3.1). When the present-day climate changes to a monsoon climate at 600 years in the future in the TSPA-SR base case (CRWMS M&O 2000 [DIRS 153246], Section 3.2.1.4) and the water table rises, any radionuclides in the interval below the new water table are immediately sent to the SZ for transport to potential receptors (CRWMS M&O 2000 [DIRS 153246], Section 3.7.2).

A dual-continuum conceptual model is used for transport, with fractures and rock matrix represented as two interacting continua. Radionuclides from the EBS are released into the fracture continuum of the UZ transport model (CRWMS M&O 2000 [DIRS 153246], Section 3.7.2); therefore, radionuclide transport through the UZ initially is through fractures in

the model. This choice of transport mechanism is conservative in that transport through fractures is generally much faster than transport through the matrix (CRWMS M&O 2000 [DIRS 153246], Section 3.7.1.1). Perturbation of flow caused by the presence of the drifts (i.e., the diversion of flow around the drift openings) is conservatively neglected in the TSPA-SR base-case model (CRWMS M&O 2000 [DIRS 153246], Section 3.7.2), but it is discussed below in Section 3.2.9.2.

Breakthrough curves for UZ transport (CRWMS M&O 2000 [DIRS 153246], Figures 3.7-9 and 3.7-10) show that the transport-time distribution is bimodal, with some of the particles arriving at the water table relatively quickly and the rest spread out over time. The proportion of particles in each mode depends on several factors, including the climate, the infiltration rate, and radionuclide transport properties such as sorption coefficients and parameters related to colloidal transport. The early part of the breakthrough curves represents particles that travel very quickly in fractures from the potential repository to the water table (CRWMS M&O 2000 [DIRS 153246], Figures 3.7-9 and 3.7-10). The late part of the breakthrough curves represents particles that spend at least part of their time transporting through the matrix. For a nonsorbing species such as technetium-99, the initial breakthrough at the water table occurs in the model in a few years or less after release from the potential repository. The figures also indicate that the 50-percent breakthrough for a nonsorbing species is typically between a few hundred years and a few thousand years, but a small fraction of the transport times are over a million years (CRWMS M&O 2000 [DIRS 153246], Figures 3.7-9 and 3.7-10). Transport times for sorbing species, such as neptunium-237, can be much longer than for nonsorbing species, as shown in the figures.

Irreversible colloids have the fastest transport in the base-case UZ transport model, with 50 percent of plutonium irreversible colloids reaching the water table in about 500 years for present-day climate (CRWMS M&O 2000 [DIRS 153246], Figure 3.7-12). In comparison, the reversible colloids have the slowest transport in the model, taking about 300,000 years to reach a 50-percent breakthrough for plutonium reversible colloids even though the wetter glacial-transition climate is in effect for most of that period; only 70 percent of the plutonium reversible colloids reach the water table within 1 million years (CRWMS M&O 2000 [DIRS 153246], Section 3.7.4).

3.2.9.2 Effects of the Drift Shadow Zone

In the TSPA-SR base-case model, radionuclide releases from the EBS are released into the fracture continuum of the UZ transport model (CRWMS M&O 2000 [DIRS 153246], Section 3.7.2). This choice is conservative in that fracture transport is faster than matrix transport. Some of the radionuclides may transfer from fractures to matrix during their transport through the UZ, which can increase their transport time significantly (see Section 3.2.9.1). The region directly beneath an emplacement drift is expected to be drier than ambient conditions for the host formation at this depth because of the diversion of water around the drift opening due to the drift capillary-barrier effect (BSC 2001 [DIRS 154657], Section 11.3.1). The drift capillary-barrier effect is important to seepage, which is discussed in Section 3.2.2 and in BSC 2001 [DIRS 154657], Section 4. Such perturbations of flow caused by the presence of the drifts are neglected in the UZ-transport component of the TSPA model. Neglecting the flux

"shadow" below the drift is conservative because the drier conditions at the interface between the EBS and the UZ would increase transport times if included.

As an initial estimate of the effect of the presence of the drift on UZ transport, a sensitivity analysis was performed in which advective releases from the potential repository were released into the fracture continuum of the UZ transport model, as in the TSPA-SR base case, but diffusive releases were released into the matrix continuum of the model rather than into fractures (BSC 2001 [DIRS 154657], Section 11.3.1.6.1). The rationale for placement of diffusing radionuclides into the matrix rather than the fractures is that the area for diffusion at the drift boundary is roughly proportional to the water content, and the matrix water content is approximately 1,000 times greater than the fracture water content (BSC 2001 [DIRS 154657], Section 11.3.1.6). This approximation for including the drift shadow may be somewhat conservative because the ambient fracture and matrix flow fields are used for transport (i.e., the reduction in flow below the drifts is not taken into account). In contrast, another aspect of the method related to the implementation of matrix diffusion (radionuclides that have entered the matrix are not allowed to diffuse to the fractures) may be nonconservative (BSC 2001 [DIRS 154657], Section 11.3.1.6.1).

This sensitivity analysis still uses the TSPA-SR base-case assumption of a zero-concentration boundary condition at the drift wall for calculating diffusive releases from the EBS (CRWMS M&O 2000 [DIRS 153246], Section 3.6.2.2). This assumption is conservative because it maximizes the concentration gradient that drives the diffusive releases. A potentially less-conservative method of determining the concentration boundary condition was discussed in SSPA Volume 1 (BSC 2001 [DIRS 154657], Section 11.3.1.6.2). That method was not included in this analysis; if it is implemented in the future, it would likely result in an additional reduction in the diffusive component of engineered-barrier-system releases.

The results of this sensitivity analysis are shown in a comparison of the mean annual dose for this case with that of the TSPA-SR base case (Figure 3.2.9-1). The results show a delay of approximately 10,000 years in the mean annual dose for the drift-shadow case as compared to the TSPA-SR base case. The effect is as large as it is because a large portion of the radionuclide releases are diffusive, especially for technetium-99 (CRWMS M&O 2000 [DIRS 153246], Figure 4.1-13), and because transport through the matrix is slower than transport through the fractures.

3.2.10 Analyses of SZ Flow and Transport

The major purpose of the flow-and-transport component of the TSPA for the SZ is to evaluate the migration of radionuclides from their introduction at the water table below the potential repository to the release point to the biosphere. Radionuclides can move through the SZ either as solute (i.e., in the dissolved state) or associated with colloids (i.e., particles small enough to remain suspended indefinitely in water) (CRWMS M&O 2000 [DIRS 153246], Section 3.8.2). The input to the SZ flow-and-transport calculations is the spatial and temporal distribution of mass flux of radionuclides from the UZ (CRWMS M&O 2000 [DIRS 153246], Section 3.7). The SZ outputs a mass flux of radionuclides to the biosphere (CRWMS M&O 2000 [DIRS 153246], Section 3.9), where the concentration of radionuclides in the groundwater is calculated by dispersing this mass flux of radionuclides in the water used by a hypothetical

farming community. Radionuclide concentrations in the water-usage volume are used to calculate the potential radiation dose rates incurred by potential receptors.

In this section, a brief overview of TSPA-SR (CRWMS M&O 2000 [DIRS 153246]) results related to the SZ, referred to as the TSPA-SR base case, is followed by a discussion of five new analyses. The first new analysis (see Section 3.2.10.2.1) concerns several changes made to define more precisely the uncertainty in the SZ flow and transport model, as part of the examination of the unquantified uncertainty inherent in the model. The remaining analyses are sensitivity studies that examine specific parameter values. The second and third new analyses are concerned with the question of how the results of TSPA-SR change if there was no matrix diffusion in the volcanic rocks in the SZ (see Section 3.2.10.2.2) and how the results would change if there was more matrix diffusion than currently accounted for in TSPA-SR (see Section 3.2.10.2.3). The fourth analysis (see Section 3.2.10.2.4) examines how the TSPA-SR results change if the flow paths in the SZ missed the alluvial uncertainty zone in the southern half of the model domain. The fifth analysis (see Section 3.2.10.2.5) estimates how the results change if greater uncertainty were included in the parameters for the two models describing colloid-facilitated transport. Finally, the updated SZ flow and transport model for use in the supplemental TSPA model is described (see Section 3.2.10.2.6).

3.2.10.1 Review of TSPA-SR Results

The TSPA-SR uses two models of SZ flow and transport: a three-dimensional process-level model that calculates, in detail, the transport of individual radionuclides that are tracked in the TSPA analyses (CRWMS M&O 2000 [DIRS 153246], Section 3.5.1) (this model is also called the site-scale SZ flow and transport model), and a one-dimensional flow-tube model that is used to calculate the transport of daughter radionuclides (radionuclides that form by the decay of other radionuclides). Results from these models that are directly related to the performance of a potential repository at Yucca Mountain involve the transport time from the vicinity of Yucca Mountain to the interface of the geosphere and biosphere, located 20 km (12.4 miles) away. Dilution, another important effect of the SZ, is handled by the manner described in the guidance related to the proposed regulation (10 CFR 63, p. 8646 (64 FR 8640 [DIRS 101680])), and is not discussed in this report. Transport time through the SZ for dissolved, nonsorbing, nonreactive radionuclides can be short, less than 100 years; however, the median transport time for the present-day climate is about 600 years (CRWMS M&O 2000 [DIRS 153246], Section 3.8.2.6). In the volcanic rocks, these short transport times are mainly caused by fast transport through widely spaced flowing intervals, with limited interactions with water in the matrix. In the alluvium, the short transport times are mainly caused by the lack of sorption to retard the migration. Transport time for dissolved, sorbing radionuclides such as neptunium-237 is typically longer, on the order of thousands to tens-of-thousands of years (BSC 2001 [DIRS 154657], Figure 12.5.2-3). Radionuclides such as plutonium-239, with transport associated with colloids, also show similarly long or longer transport times. However, approximately 20 percent of all realizations have transport times of less than 1,000 years for irreversible colloids (DTN: SN0004T0501600.004 [DIRS 149288]). This wide range in radionuclide transport times is principally due to the uncertainty in SZ parameters that are used to estimate groundwater velocity, matrix diffusion, sorption, and colloid properties. A comparison of a degraded SZ (i.e., SZ model parameters chosen to reduce radionuclide transport time through the SZ) with an enhanced SZ (i.e., SZ model parameters chosen to

increase radionuclide transport time through the SZ) shows that the uncertainty in the SZ translates into an uncertainty in the calculated annual dose of approximately a factor of 10 to a factor of 100 in the 100,000 years following repository closure (CRWMS M&O 2000 [DIRS 153246], Figure 5.3-13).

3.2.10.2 New Results

3.2.10.2.1 Unquantified Uncertainties in the SZ

The SZ flow-and-transport model (CRWMS M&O 2000 [DIRS 139440]) was evaluated with respect to unquantified uncertainty to determine the parts of the model to change to provide a better representation of the SZ. Several changes to the parameters in the SZ model were made as a part of this effort, and the most important changes for SZ transport calculations are briefly described here. A detailed discussion of the changes made to the SZ modeling is presented in SSPA Volume 1 (BSC 2001 [DIRS 154657], Section 12.5.1 and Table 12.5.1-1).

For the evaluation of unquantified uncertainty in the SZ, the bulk density of the alluvium, a factor in determining the amount of sorption that a radionuclide undergoes, was changed from a constant to an uncertain variable and represented by a probability distribution. The sorption coefficients in the alluvium for technetium and iodine were set to 0; they were previously represented with uncertainty distributions with low values. The sorption-coefficient distribution for neptunium in the alluvium was assigned lower values (mean value of about 14 ml/g for the unquantified uncertainty evaluation versus about 18 ml/g for TSPA-SR); the sorption-coefficient distribution of uranium in the alluvium was set equal to that of neptunium, and the two distributions were correlated in the alluvium. The diffusion coefficient for radionuclides was changed from a log-uniform distribution to a log-triangular distribution with the same range, but with a mode of 3.2×10^{-11} m^2/s. The amount of uncertainty in the SZ groundwater flux was reduced. For TSPA-SR (CRWMS M&O 2000 [DIRS 153246], Table 3.8-2), the three SZ fluxes that were considered (high, medium, and low) each differed by a factor of 10; 6 m/year, 0.6 m/year, and 0.06 m/year, respectively, in the vicinity of the repository. For the evaluation of unquantified uncertainty, the high, medium, and low fluxes differed by a factor of 3 (1.8 m/year, 0.6 m/year, and 0.2 m/year, respectively).

The impact of the changes made to the SZ flow and transport model by the evaluation of unquantified uncertainty is shown in Figures 3.2.10-1a and 3.2.10-1b. Figure 3.2.10-1a shows the mean annual dose for the TSPA-SR base case (CRWMS M&O 2000 [DIRS 153246]) compared with the mean annual dose calculated using the unquantified uncertainty SZ model. Figure 3.2.10-1b shows the results for the multiple realizations of the unquantified uncertainty SZ model. Figure 3.2.10-1a shows that there is virtually no difference between the mean annual doses calculated using the TSPA-SR SZ model results and the unquantified uncertainties SZ model results. The changes made with respect to unquantified uncertainty offset one another from a total-system perspective. The increase in bulk density increased retardation in some radionuclides, but this was partially offset by the setting of the sorption coefficient to 0 for technetium-99 and iodine-129. Reducing the range in the flux distribution reduced the mean flux, but not the median. The mean annual doses primarily are controlled by factors external to the SZ (e.g., waste-package corrosion). The changes made for the unquantified uncertainty SZ model are insignificant (less than a few percent difference in annual dose) to the total repository

system performance. This uncertainty evaluation provides confidence that the SZ modeling used in TSPA-SR is a relatively robust description of uncertainty in the SZ system, and that the uncertainty included in the modeling was adequate for the TSPA-SR nominal case.

3.2.10.2.2 No Matrix Diffusion in the SZ

The SZ flow and transport model used in TSPA-SR is a dual-porosity model; the volcanic units are modeled as fractured continua and matrix continua. The advective movement of radionuclides is restricted to the fractures. The matrix can act as a temporary storage volume and delay the transport of radionuclides. The two continua interact by diffusion. To negate matrix diffusion in this sensitivity study, the diffusion coefficient was reduced by 10 orders of magnitude. A more detailed discussion of the changes made to the SZ modeling is contained in SSPA Volume 1 (BSC 2001 [DIRS 154657], Section 12.5.2.1).

Figure 3.2.10-2a shows the mean annual dose calculated in TSPA-SR base case (CRWMS M&O 2000 [DIRS 153246], Figure 4.1-5) compared with the mean annual dose calculated without the effects of matrix diffusion in the SZ. Figure 3.2.10-2b shows the results of the multiple realizations of the TSPA for the SZ transport model without matrix diffusion. The differences between the models with and without matrix diffusion are not discernable by visual inspection of the plots. The most likely reason for this situation is that approximately half of the TSPA-SR realizations have little or no matrix diffusion because of a low diffusion coefficient, large flowing-interval spacing, or a high groundwater flux. The mean annual dose in TSPA-SR is influenced primarily by the realizations that produce the high annual dose values, particularly for neptunium-237, and many of high-dose realizations include a SZ representation that has little or no matrix diffusion. Thus, reducing matrix diffusion in the half of the realizations that have matrix diffusion does little to increase the mean annual dose. It should also be remembered that the mean annual dose in TSPA-SR is controlled by factors external to the SZ for most of the first 100,000 years after repository closure.

3.2.10.2.3 Increased Matrix Diffusion in the SZ

This sensitivity study is intended to address the effect of using a conceptual model for greater matrix diffusion similar to that proposed by the Electrical Power Research Institute (EPRI 2000 [DIRS 154149], Section 7.2.3). To create an enhanced-matrix-diffusion model, the flowing-interval spacing in the site-scale SZ flow and transport model was reduced; in particular the mean of the distribution was reduced by a factor of 100. A more detailed discussion of the changes made to the SZ modeling is presented in SSPA Volume 1 (BSC 2001 [DIRS 154657], Section 12.5.2.2).

Figure 3.2.10-3a shows the mean annual dose calculated in the TSPA-SR base case compared with the mean annual dose calculated with enhanced matrix diffusion in the SZ transport model, as described in SSPA Volume 1 (BSC 2001 [DIRS 154657], Section 12.5.2.2). Figure 3.2.10-3b shows the results of the multiple realizations of the TSPA for the SZ transport model with enhanced matrix diffusion. As shown in Figure 3.2.10-3a, the differences in expected annual dose between the model with matrix diffusion and the model with enhanced matrix diffusion are generally less than 20 percent, and the simulated doses are somewhat lower for the model with enhanced matrix diffusion, as expected. Approximately half of the TSPA-SR realizations have

little or no matrix diffusion because of a low diffusion coefficient or a high groundwater flux. Reducing the flowing-interval spacing does not address these other factors. The mean annual dose in TSPA-SR (CRWMS M&O 2000 [DIRS 153246], Figure 4.1-5) is primarily influenced by the realizations that produce the high annual dose values, particularly for neptunium-237. The sorption coefficient for neptunium-237 in the volcanic matrix averages 0.5 ml/g (CRWMS M&O 2000 [DIRS 153246], Table 3.8-3). Thus, even if neptunium-237 diffuses into the matrix, there is little retardation because of the relatively low sorption coefficient for this radionuclide. The combination of high groundwater fluxes, low diffusion coefficient, and a low neptunium-237 sorption coefficient tends mostly to override the effect of a reduced flowing-interval spacing, at least for the calculation of the mean annual dose. This sensitivity study is an example how a change in a subcomponent model can have impact in that subcomponent model, but not a large impact on the total system. Also, the TSPA-SR shows that the mean annual dose is controlled by factors external to the SZ for most of the first 100,000 years after repository closure.

3.2.10.2.4 Minimum Flow-Path Length in the Alluvium

The alluvial-uncertainty zone is a region in the site-scale SZ model that encompasses the area where flow paths from the potential repository might enter alluvial deposits in southern Jackass Flats (CRWMS M&O 2000 [DIRS 147972], Section 6.2). The alluvial-uncertainty zone is approximately 5 km wide by 8 km long in the north-south direction. For this sensitivity study, the length of the alluvial-uncertainty zone was set to zero in the SZ model (BSC 2001 [DIRS 154657], Section 12.5.2.3), but there still was approximately 1 km of flow path length in alluvium prior to reaching the 20-km boundary in the model. This sensitivity study is meant to address the impact of the alluvium on the results of the total-system model. In particular, it is of interest to know the impact of virtually no alluvium in the SZ flow path on the TSPA-SR results. The length of the SZ flow path in the alluvium is potentially important to performance of the potential repository because of the generally slower transport of radionuclides in this unit relative to the volcanic units. A more detailed discussion of the changes to the alluvial-uncertainty zone made to the SZ modeling is presented in SSPA Volume 1 (BSC 2001 [DIRS 154657], Section 12.5.2.3).

Figure 3.2.10-4a shows the mean annual dose calculated for the TSPA-SR base case compared with the mean annual dose calculated with minimal alluvium in the groundwater transport path. The figure shows only a slight difference (generally less than 10 percent difference) in results, with the minimal-alluvium case showing slightly higher simulated dose, as expected. Figure 3.2.10-4b shows the results of the multiple realizations of the TSPA for the SZ transport model with minimal alluvium. As the mean annual dose is dependent to a large extent on neptunium-237 in TSPA-SR, and neptunium-237 transport is thought to be significantly retarded in the alluvium (CRWMS M&O 2000 [DIRS 153246], Table 3.8-3), this result is at first perplexing. However, the median transport time of neptunium-237 through the SZ (based on the median of the distribution of the 100 SZ breakthrough curves used in the supplemental TSPA model) is approximately 20,000 years for the present climate, based on the site-scale SZ model (BSC 2001 [DIRS 154657], Figure 12.5.2-3). For future climates, the model calculates a median transport time of approximately 5,000 years for neptunium-237 in the medium-specific-discharge case. In addition, for the high-specific-discharge case, the groundwater flux is a factor of ten higher, reducing the median transport time for neptunium-237 to approximately 500 years for

these cases that correspond to many of the higher-dose realizations in the TSPA analyses. In the figure, 500 years would separate the two annual-dose curves only slightly at times greater than 50,000 years, when simulated dose is dominated by neptunium-237. The results of the sensitivity analysis examining the minimum flow path length in the alluvium are approximately consistent with the expected behavior of the system, when the impacts of glacial climatic conditions and higher specific discharge are considered. Note that other factors external to the SZ model control the mean annual dose before 100,000 years, and therefore the median transport-time comparison cannot be used to explain all the factors that go into a calculation of the mean annual dose (e.g., other realizations might become more important in the calculation of the mean because of the absence of the alluvial-uncertainty zone).

3.2.10.2.5 Increased Uncertainty in the Colloid-Facilitated Transport Models

For the TSPA-SR (CRWMS M&O 2000 [DIRS 153246], Section 3.5.6), the colloid concentrations for radionuclides that irreversibly sorbed to colloids (irreversible colloids) and radionuclides that reversibly sorbed to colloids (reversible colloids) were calculated from functions of ionic strength that included no uncertainty. The sensitivity study defined here is for the colloid-facilitated transport (BSC 2001 [DIRS 154657], Sections 9.3.4 and 10.3.5). This model includes probability distributions for colloid concentrations (whereas colloid concentration was a deterministic parameter in the TSPA-SR) and an expanded probability distribution for the sorption coefficient for radionuclides onto colloids. Some conservatisms were left in the model, however, as described below.

For irreversible colloids (which only apply to the DOE HLW glass), the mass flux of plutonium and americium radionuclides associated with these colloids is introduced to the SZ at the interface of the UZ and SZ, and their transport is tracked for 20 km to the biosphere. In the volcanic units, these colloids are restricted to the fractures where they undergo transport and retardation as in TSPA-SR. In the alluvium, a new distribution of the retardation factor for radionuclides irreversibly sorbed onto colloids is used in this sensitivity study (BSC 2001 [DIRS 154657], Section 12.3.2.4.5). This uncertainty distribution is for lower values of the retardation factor (more conservative with regard to repository performance) compared to the retardation distribution used in TSPA-SR (BSC 2001 [DIRS 154657], Figure 12.3.2.4.4).

For reversible colloids (which primarily come from spent nuclear fuel), the mass flux of radionuclides associated with these colloids is also tracked from the interface of the UZ and SZ for 20 km to the biosphere. In a sensitivity study (BSC 2001 [DIRS 154657], Sections 9.3.4 and 10.3.5), the irreversible colloids also serve as reversible colloids in the HLW glass; any radionuclide that can sorb to colloids is allowed to sorb to the irreversible colloids. The reversible-colloid model is also called the K_c model, because the K_c parameter is the name of the partitioning coefficient between aqueous and colloidal radionuclides. The K_c parameter is the product of the colloid concentration and the radionuclide sorption coefficient onto a colloid (CRWMS M&O 2000 [DIRS 153246], Section 3.8.2.1.2). The sorption coefficient for americium is used for all radionuclides subject to reversible colloid-facilitated transport. Using the sorption coefficient for americium is done for simplicity and because americium has the largest sorption coefficient. Using this sorption coefficient would tend to maximize mobility of all the radionuclides associated with colloids, and thus be conservative. Similarly, only one generic colloid type is used in the sensitivity study. This colloid type has the properties of a

waste-form colloid with the greatest affinity for sorption of radionuclides and is thus conservative from the perspective of repository performance.

One final adjustment is made to the reversible-colloid model in the SZ. For TSPA-SR (CRWMS M&O 2000 [DIRS 153246], Section 3.8.2), protactinium was included in the strongly sorbing category of radionuclides. This inclusion required setting the sorption coefficient for the strongly sorbing group to a distribution with a conservative lower bound (a uniform distribution between 0 ml/g and 100 ml/g, the distribution for protactinium in vitric tuff). For this sensitivity study, protactinium was moved to the moderately strongly sorbing category of radionuclides, as befits its moderately sorbing character. The uncertainty distribution for the sorption coefficient of moderately strongly sorbing radionuclides was kept as a uniform distribution between 0 ml/g and 50 ml/g. This move allows the strongly sorbing category to have a distribution of sorption coefficient with higher values. The sorption-coefficient distribution for this category is now the K_d for plutonium on devitrified tuff, which has a strong central tendency of 50 ml/g (CRWMS M&O 2001 [DIRS 154024], Table 2b).

The results of the colloid sensitivity study for the SZ are presented in Figures 3.2.10-5 and 3.2.10-6. The simulated dose for changes only in the SZ flow-and-transport model are shown in Figures 3.2.10-5a and 3.2.10-5b. Doses for changes in all relevant components of the TSPA model (with regard to colloid-facilitated transport) are shown in Figures 3.2.10-6a and 3.2.10-6b. There is virtually no difference discernable by visual inspection in the mean annual dose using the representation of colloid-facilitated transport with increased uncertainty compared with the base-case colloid model used in TSPA-SR. The two radionuclides that comprise greater than approximately 70 percent of the annual dose in TSPA-SR (CRWMS M&O 2000 [DIRS 153246], Figure 4.1-5) are technetium-99 at earlier times and neptunium-237 at later times. Both of these radionuclides are transported as solute and thus are unaffected by the new colloid model. Also, in the new colloid model the means of the distributions (for colloid concentrations, sorption coefficients for radionuclides onto colloids, and sorption coefficients for radionuclides onto the rock matrix and alluvium) are similar to values used in TSPA-SR, and thus the mean behavior is not expected to be significantly different.

3.2.10.2.6 Updated Saturated Zone Flow and Transport Model for Supplemental TSPA Model Analyses

The SZ flow and transport modeling was modified to include new information for incorporation into the supplemental TSPA model analyses (see Section 4). These modifications were based on insights from the uncertainty analyses and to include new information developed since completion of TSPA-SR.

The updated SZ flow and transport model was changed to incorporate two new sources of information relevant to radionuclide transport. The model was updated to provide a more realistic representation of the bulk density of the alluvium (BSC 2001 [DIRS 154657], Section 12.3.2.4.4). Borehole gravimeter data are used to develop an uncertainty distribution for this parameter that has a higher mean value than the fixed value used in TSPA-SR (CRWMS M&O 2000 [DIRS 153246]) and other documents (CRWMS M&O 2000 [DIRS 147972], Section 6.9; BSC 2001 [DIRS 154657], Section 12.3.2.4.4). Continuing data collection from batch and column sorption experiments for iodine-129 and technetium-99 with alluvium samples

indicates that the sorption coefficients for these radionuclides are zero under oxidizing conditions (BSC 2001 [DIRS 154657], Section 12.3.2.2). Consequently, the sorption coefficients for iodine-129 and technetium-99 are a constant value of zero in the updated SZ flow and transport modeling, in contrast to the uncertainty distributions with small mean values used in TSPA-SR.

Simulated mean annual doses for the TSPA-SR base-case model (CRWMS M&O 2000 [DIRS 143665]) are compared to the results of the same TSPA model using the updated SZ flow and transport model in Figure 3.2.10-7. These results indicate that the changes to the updated SZ flow and transport model have little overall impact on the simulated mean annual dose in the TSPA analyses. The influences of higher values of bulk density in the alluvium and lower sorption coefficients for iodine-129 and technetium-99 on the simulated annual dose tend to counteract one another. In addition, the mean annual dose is influenced by a few of the highest-dose realizations at any particular time in a TSPA simulation. If these highest-dose realizations are the ones in which the importance of the retardation of key radionuclides is diminished (e.g., by low sorption coefficients or short path length in the alluvium), then the impact of the updated values of alluvial bulk density on the mean annual dose would be minimal.

3.2.11 Analyses of the Biosphere

The biosphere is that part of the crust, waters, and atmosphere of the earth that support life. The biosphere includes all living organisms in the soil, surface water, and the air. As opposed to this understanding of the biosphere as a global feature, the Yucca Mountain reference biosphere is limited in spatial extent, that at a minimum should include all biosphere-related features, events and processes applicable to the Yucca Mountain region. Living organisms (including humans) residing in the biosphere could be affected by radionuclide release from a potential repository at Yucca Mountain only if these contaminants reach the biosphere. The biosphere component of TSPA-SR is designed to support predictions of dose from radiation exposure to a person living in the general vicinity of the potential repository if there is release of radioactive material after closure of the potential repository.

The biosphere component includes the characteristics of the human receptor and the reference biosphere. The human receptor and the reference biosphere are consistent with the proposed NRC rule (10 CFR 63.115 (64 FR 8640 [DIRS 101680])). The preamble to the proposed regulation permits dilution to be calculated for the radionuclides transported in groundwater by mixing them in the annual water usage of a hypothetical farming community (10 CFR 63, p. 8646 (64 FR 8640 [DIRS 101680])). Radionuclides build up in soils because of continuing periods of irrigation with contaminated water, and this process is considered in the analyses. Estimates of soil and radionuclide removal by erosion, leaching, crop removal, and radioactive decay are incorporated into the biosphere modeling. The biosphere is the last component in the chain of TSPA-SR modeling subsystem components. In the TSPA-SR modeling there are two means by which radionuclides could be introduced into the biosphere. One is for the groundwater irrigation scenario (nominal scenario), in which the biosphere is coupled to the SZ flow-and-transport model; the other is for the disruptive scenario in which the biosphere is coupled to the model for the dispersal of contaminated volcanic ash resulting from the volcanic-eruption scenario (see Section 3.3.1).

Biosphere modeling provides an estimate of the dose incurred by the defined receptor if a unit of activity concentration of a radionuclide in groundwater reaches the geosphere-biosphere boundary or the unit of activity concentration is deposited on the soil surface. These estimates, BDCFs, are expressed in a probability distribution to reflect parametric uncertainty. In the TSPA-SR model, when a concentration of a radionuclide in groundwater has been calculated (within the computer program a mass flux is calculated and converted to a concentration at the downstream end of the SZ model), the BDCF sampled from the distribution is used as a multiplier to convert the radionuclide concentration into annual dose. For the direct releases by volcanic eruption, the annual dose is calculated by multiplying the volcanic eruption BDCF by the radionuclide mass loading in the ash layer per unit area.

3.2.11.1 Review of TSPA-SR Results

The primary result of the biosphere modeling for TSPA-SR is the construction of BDCF distributions for radionuclides of interest, for the groundwater-release exposure scenario (for use in the nominal scenario, human-intrusion case, and igneous-intrusion groundwater transport) and the volcanic-eruption exposure scenario (see Section 3.3.1). The BDCF distributions tended to have lower mean values for the radionuclides that are fission products than those that are actinides (CRWMS M&O 2000 [DIRS 153246], Table 3.9-2). For example, the geometric mean for carbon-14 is 0.5536×10^{-3} mrem/year per pCi/L with a geometric standard deviation of 1.5177; the geometric mean for neptunium-237 is 6.738 mrem/year per pCi/L, with a geometric standard deviation of 1.163. Soil buildup is not an important consideration for most radionuclides; the largest soil-buildup factor is 2.85 for thorium-229 (CRWMS M&O 2000 [DIRS 153246], Table 3.9-2). Additional analyses in the TSPA-SR (CRWMS M&O 2000 [DIRS 153246], Section 3.9.2.5) include sensitivity studies to determine the most important parameters in the model that contribute the most to the variance in the BDCF distributions (i.e., the parameters that cause the most spread in the BDCF uncertainty distributions), and a pathway analysis to identify which exposure pathways are the most important contributors to the BDCFs. For most radionuclides, the majority of the dose could be attributed to two pathways in the groundwater-release scenario: drinking water and the consumption of leafy vegetables (CRWMS M&O 2000 [DIRS 153246], Section 3.9.2.5). The parameters that contributed most to uncertainty in the BDCFs include: the crop interception fraction (the fraction of contamination in rainfall, irrigation water, or aerosols that adheres to plant surfaces) and the soil-plant-transfer scale factor (a factor representing uncertainty in the amount of radionuclides taken up by plants) (CRWMS M&O 2000 [DIRS 153246], Section 3.9.2.5).

Biosphere modeling of volcanic eruption BDCF distributions for TSPA-SR (CRWMS M&O 2000 [DIRS 153246], Section 3.10.3.4) includes the same major pathways as those considered for the groundwater release BDCF. In these analyses, it is assumed that only ash particles smaller than 10 microns are available for inhalation into the lungs (CRWMS M&O 2000 [DIRS 153246], Section 3.10.3.4) and that the uncertainty distribution in this air-mass load ranges from 30 to 1000 micrograms/m^3. The total suspended-particle concentration in the air, including particles larger than 10 microns, is about three times larger than the air-mass load of particles smaller than 10 microns (CRWMS M&O 2000 [DIRS 153246], Section 3.10.3.4).

3.2.11.2 New Results

Since the biosphere modeling for TSPA-SR, much of the supporting documentation for the biosphere has been revised, including updates of some parameter values. A more detailed discussion of the changes made to the biosphere modeling is contained in SSPA Volume 1 (BSC 2001 [DIRS 154657], Section 13.4). These new data were used to generate revised uncertainty distributions of BDCFs. The new parameter values are applicable to the two exposure scenarios evaluated. These two cases are the nominal scenario, in which radionuclides are introduced to the biosphere by groundwater, and the volcanic-eruption scenario, in which radionuclides are also introduced to the biosphere by volcanic ash. The most significant changes include:

- Parameters defining employment and recreational behavior (duration of inhalation and external exposure times) were revised (both exposure scenarios) (BSC 2001 [DIRS 154657], Section 13.2.1.4)

- Particulate concentrations in the air were changed (from PM_{10}, particles with mean diameter of less than 10 microns) to be based on measurement of total suspended particles at Yucca Mountain and PM_{10} measurements from arid farming communities in the southwestern United States and the Yucca Mountain area (groundwater release exposure scenario) (BSC 2001 [DIRS 154657], Section 13.2.1.4)

- The distribution of particulate concentrations in air for the volcanic scenario was revised to be based on measurement from Mount St. Helens and Cerro Negro (volcanic-eruption exposure scenario) (BSC 2001 [DIRS 154657], Section 13.2.1.4)

- A new set of particle-resuspension factors was developed for use after a volcanic event (volcanic eruption exposure scenario) (BSC 2001 [DIRS 154657], Section 13.2.1.6)

- The consumption rates of locally grown food for the critical group were represented by distributions (both exposure scenarios) (BSC 2001 [DIRS 154657], Section 13.3.1)

- The parameters associated with the ingestion pathway for the current climate were modified and new values were developed for the cooler and wetter climate (glacial transition) (both exposure scenarios) (BSC 2001 [DIRS 154657], Section 13.2.1.5).

3.2.11.2.1 Nominal Scenario

Several factors influencing the uncertainty in BDCFs for the groundwater-release scenario are reevaluated for incorporation into TSPA-SR analyses (BSC 2001 [DIRS 154657], Section 13.2.2). For the nominal scenario, the most significant contributing pathway to exposure is ingestion (CRWMS M&O 2001 [DIRS 152539], Section 6.7). The changes made to the updated input data had little impact on this pathway. Thus, there was only a small net effect on the mean value of the BDCFs. Comparing the mean values of BDCFs used in the TSPA-SR (given in CRWMS M&O 2000 [DIRS 144055], Table 3) with the new data in CRWMS M&O 2001 [DIRS 153207], Table 3 gives the magnitude of the change in BDCFs. TSPA-SR identified the radionuclides contributing most to annual dose as technetium-99, iodine-129,

neptunium-237, and plutonium-239 (CRWMS M&O 2000 [DIRS 153246], Figure 4.1-6). As an indication of the relative differences for technetium-99, iodine-129, and neptunium-237, the new mean values of the BDCFs are no more than 20 percent lower that those used in TSPA-SR. For plutonium-239, the change in the mean value of the BDCF is less than 20 percent.

The relatively small effect of these changes to the biosphere model on the expected annual dose for the nominal scenario is reflected in the TSPA results shown in Figure 3.2.11-1a. The mean annual dose using the new uncertainty distributions for the BDCFs (BSC 2001 [DIRS 154657], Section 13.4.) is compared to the results calculated in the TSPA-SR (CRWMS M&O 2000 [DIRS 153246], Figure 4.1-5) base case in this figure. The mean annual dose is slightly lower for the new nominal-scenario BDCFs for all times shown in the plot. The differences between the previously calculated annual dose (TSPA-SR base-case results) and the new results of less than 10 percent in simulated annual dose for most times do not constitute a large change.

3.2.11.2.2 Volcanic Eruption Scenario

Reevaluation of factors influencing the BDCFs for the volcanic eruption scenario (BSC 2001 [DIRS 154657], Section 13.4.3), resulted in updated TSPA input for the uncertainty distributions of BDCFs that is potentially significant to simulated doses. For the direct releases by volcanic eruption, inhalation is the dominant pathway when integrated over time. The particulate concentration in air was increased by a factor of 2.5 (BSC 2001 [DIRS 154657], Section 13.3.6), resulting in an increase in BDCFs that propagated through to the new predicted dose. Whereas BDCFs were developed for three phases during and following the volcanic eruption (eruption, transition, and steady-state), the BDCF distributions for the transition phase (BSC 2001 [DIRS 154657], Section 13.4.3) are used in the TSPA calculations. The BDCFs that are applicable for the eruption phase were not used in TSPA analyses because of the short duration of the eruptive phase. The transition phase BDCFs are conservative relative to the BDCFs for the steady-state phase following eruption because the volcanic ash is more available for resuspension in air during the transition phase. The case with the highest values for BDCFs (i.e., the 1-cm thick ash layer with annual average airborne particulate concentration) is used for the new volcanic eruption BDCFs.

The results of the TSPA model using the new volcanic eruption BDCFs are shown in Figure 3.2.11-2. The mean annual dose using the new uncertainty distributions for the volcanic eruption BDCFs is compared to the results calculated in TSPA-SR in this figure. These results indicate that, at all times, the expected mean annual dose is approximately 2.5 times greater for the new volcanic BDCFs relative to the previous TSPA-SR igneous model. This represents a significant increase in the mean dose rate relative to previous results and is primarily due to the increase in the respirable fraction of particulate concentration in air within the model (BSC 2001 [DIRS 154657], Section 13.3.6.2). However, the higher expected annual dose from direct exposure to contaminated volcanic ash using the new volcanic eruption BDCFs is still lower than the expected annual dose from the igneous groundwater pathway at later times (compare to the TSPA-SR (CRWMS M&O 2000 [DIRS 153246], Figure 4.2-1)).

3.3 EVALUATION OF DISRUPTIVE EVENTS

In this section, analyses conducted to examine the sensitivity of performance to new information related to disruptive events developed since the TSPA-SR (CRWMS M&O 2000 [DIRS 153246]) are described. Two potentially disruptive events are addressed: volcanism (i.e., igneous activity; see Section 3.3.1) and seismic events (see Section 3.3.2). Igneous activity is treated as a separate scenario from nominal performance, and models and input parameters that are specific to the scenario are used. Seismic activity is treated as an aspect of nominal performance, in the sense that some level of seismic activity is certain to occur, with uncertain magnitude and frequency during the postclosure performance period.

For igneous and seismic activity, results in this section are compared to results of the TSPA-SR base case (CRWMS M&O 2000 [DIRS 153246]). Sensitivity analyses are conducted as one-off analyses, only changing the model or parameters of interest. All other models and parameters are identical to those used in the TSPA-SR.

3.3.1 Igneous Disruption

The purpose of igneous activity disruptive-events modeling within the TSPA analysis is to evaluate the effect of the interaction of an unexpected igneous event with the potential repository. Conceptual models for eruptive and intrusive igneous disruptions are documented in the *Igneous Consequence Modeling for the TSPA-SR* report (CRWMS M&O 2000 [DIRS 151560]).

The eruptive (or direct) release scenario considers an igneous dike rising through the crust of the earth to the land surface and intersecting one or more drifts in the potential repository. One or more eruptive conduits form somewhere along the dike and feed a volcano. Waste packages in the path of the conduit are damaged to the extent that they provide no further protection for the waste, and waste particles become entrained in the eruptive material. Damage to packages outside the immediate path of the conduit is addressed in the intrusive release analysis and is not included in the eruption. The contaminated volcanic ash is erupted through the surface and transported downwind toward the receptor. The ash settles out of the plume, resulting in an ash layer on the land surface. The volcanic eruption and subsequent transport of radioactive material in the ash plume are modeled within the TSPA-SR using ASHPLUME V1.4LV-dll. For all analyses conducted for the SSPA, wind direction is assumed to be fixed in the direction of the receptor (south) at all times. This assumption was used in the TSPA-SR (CRWMS M&O 2000 [DIRS 153246], Section 3.10.4) to provide a reasonably conservative approach to compensate for uncertainty regarding possible surface redistribution of contaminated ash following an eruption. The receptor receives a radiation dose from various pathways associated with the contaminated ash. A set of BDCFs, specifically calculated for the eruptive release scenario using the GENII-S V1.4.8.5 computer program, is used to calculate annual doses that are then weighted by event probability.

The intrusive (or indirect) groundwater release scenario describes the effects of an igneous dike that intersects a section of the potential repository without necessarily developing a volcanic eruption at the surface. Like the waste packages directly in the path of the eruptive conduit, packages near the point of intersection are assumed to be damaged to the extent that they provide

no further protection for the waste. Unlike the waste in the path of a conduit, which potentially is entrained in an eruption, waste in packages near an intrusion is not entrained in an eruption, but is fully exposed to groundwater. Other waste packages in the intruded drift are assumed to be partially damaged, but they still provide some protection for the waste. Radionuclide releases from waste packages damaged by the intrusion then are available for transport in groundwater to the receptor. The igneous intrusion groundwater transport model consists of a set of model assumptions and input parameters characterizing damage to the drip shield, waste package, and cladding that are used to modify the source term to the flow and transport models developed for the nominal case. Groundwater transport away from the damaged packages is calculated using the nominal-scenario models, and annual doses from contaminated groundwater are determined using nominal BDCFs (CRWMS M&O 2000 [DIRS 153246], Section 3.9.2.5).

3.3.1.1 Review of TSPA-SR Results

Figure 3.3.1-1 shows the results of the TSPA-SR (CRWMS M&O 2000 [DIRS 153246], Section 4.2.2) calculations in terms of a range of probability-weighted annual dose histories representing possible doses to an exposed individual following disruption of the potential repository by igneous activity. The figure shows results from 500 of 5,000 realizations of sampled values for uncertain input parameters in the model. In addition, the mean, median, and 95^{th} and 5^{th} percentile results for probability-weighted annual dose are also shown. The 5^{th} percentile probability-weighted doses do not occur until close to the end of the 50,000-year simulation. Simulations of igneous disruption were limited to 50,000 years in the TSPA-SR for computational efficiency (CRWMS M&O 2000 ([DIRS 153246], Section 4.2).

For approximately the first 2,000 years, the annual dose history is a smooth curve (Figure 3.3.1-1). During this time, the annual dose is dominated by the effects of a volcanic eruption. The probability-weighted mean annual dose during this period reaches a peak of approximately 0.004 mrem/yr at about 300 years after closure of the potential repository, and then it decreases due to radioactive decay of the relatively shorter-lived radionuclides that contribute to annual doses from the ashfall exposure pathway. From approximately 2,000 years after closure onward, the mean igneous annual dose is dominated by groundwater releases from waste packages damaged by igneous intrusion. The relatively irregular shape of the curve after approximately 2000 years is partially a result of the complex groundwater transport processes, and partially reflects the combination of intrusive events that occur at random times, rather than the prescribed intervals used for the eruptive simulations. The first appearance of groundwater doses in the mean curve at approximately 2,000 years reflects retardation during transport, rather than the absence of intrusions at earlier times (CRWMS M&O 2000 [DIRS 153246] Section 4.2.2).

The combined probability-weighted mean annual dose calculated in the TSPA-SR (CRWMS M&O 2000 [DIRS 153246], Section 4.2) for eruptive and intrusive igneous releases reaches an initial peak during the first 10,000 years of approximately 0.08 mrem/yr at 10,000 years (Figure 3.3.1-1). At later times, the calculated mean igneous annual dose rate increases slowly to approximately 0.2 mrem/yr at the end of the 50,000-year period. This late-time igneous peak mean annual dose is dominated entirely by the groundwater releases following igneous intrusion (CRWMS M&O 2000 [DIRS 153246], Section 4.2.2).

An uncertainty importance analysis was carried out for the TSPA-SR results (CRWMS M&O 2000 [DIRS 153246], Section 5.1) using various statistical methods to identify the most important contributors to the spread in the overall model results and to identify contributors to the extreme, or outlier, outcomes in the model results. The analysis showed that the most important parameters affecting the spread in model results (Figure 3.3.1-1) are annual frequency of igneous intrusion and wind speed

3.3.1.2 Supplemental Results

3.3.1.2.1 Igneous Event Wind-Speed Sensitivity

As described in SSPA Volume 1 (BSC 2001 [DIRS 154657], Section 14.3.3.5), wind speed data collected from the Desert Rock Airstrip (approximately 40 km southeast of Yucca Mountain) between 1978 and 1995 (NOAA n.d. [DIRS 154435]) provide an alternative to the wind speed data used in the TSPA-SR (CRWMS M&O 2000 [DIRS 153246], Section 3.10.2.2.3). The CDF for the new data is given in SSPA Volume 1 (BSC 2001 [DIRS 154657], Table 14.3.3.5-1). Because the new data include winds from a higher elevation than those used to develop the TSPA-SR inputs, speeds are somewhat higher. The median value of the new data set is approximately 1,000 cm/s, compared to the median value of approximately 650 cm/s from the data used in the TSPA-SR. The maximum value of 5,683 cm/s is approximately 2.4 times faster than the highest value used in the TSPA-SR. Because the higher altitudes included in the Desert Rock Airstrip data are consistent with the upper range of column heights proposed to be possible for eruptions at Yucca Mountain (e.g., see column heights proposed in NRC 2000 [DIRS 149372], Section 4.3.2.3.1), these data are used in the supplemental TSPA analyses reported in Section 4.

Figure 3.3.1.2-1a shows mean probability-weighted annual doses for the eruptive case only, comparing results from TSPA-SR with the mean of a set of 300 realizations that are identical in all regards to the TSPA-SR case except that the alternative distribution for wind speed has been used. Using the Desert Rock Airstrip data as described in SSPA Volume 1 (BSC 2001 [DIRS 154657], Section 14.3.3.5) increases the probability-weighted annual doses by a factor of approximately 2 from TSPA-SR. Figure 3.3.1.2-1b shows the set of realizations calculated with the Desert Rock wind speed data, with the 95^{th} and 50^{th} (median) curves shown with the mean. Note that the 5^{th} percentile curve plots below the lowest value shown on the y-axis.

3.3.1.2.2 Igneous Event Waste-Particle-Size Sensitivity

As described in SSPA Volume 1 (BSC 2001 [DIRS 154657], Section 14.3.3.4), supplementary analyses performed since the TSPA-SR (CRWMS M&O 2000 [DIRS 153246]) have defined a set of alternative waste particle size distributions to be examined in sensitivity analyses. Specifically, the log-triangular distribution for waste particle diameter that is used in ASHPLUME V1.4LV-dll has been modified to consider cases in which the maximum and minimum values are increased and decreased by a factor of 2, and the modal value is increased and decreased by a factor of 10. These alternative distributions were chosen to allow testing the sensitivity of performance to the form of the distribution within a range of reasonable maximum and minimum values.

Figure 3.3.1.2-2 shows probability-weighted mean annual doses from the eruptive case only, calculated for the seven waste-particle size distributions in SSPA Volume 1 (BSC 2001 [DIRS 154657], Table 14.3.3.4-1) and the TSPA-SR base-case distribution (CRWMS M&O 2000 [DIRS 153246], Section 3.10.2.2.2). All other input parameters in each case are identical to those used in TSPA-SR (CRWMS M&O 2000 [DIRS 153246], Sections 3.10.2 through 3.10.4). Calculated annual doses only vary by a factor of approximately 1.3 or less, and performance is relatively insensitive to uncertainty in waste particle diameter within the range considered in these analyses. Consistent with this observation, the distribution used in the supplemental TSPA analyses (see Section 4) is unchanged from that used in the TSPA-SR (CRWMS M&O 2000 [DIRS 153246], Section 3.10.2.2.2).

3.3.1.2.3 Igneous Event Zone 1 and Zone 2 Sensitivity

As described in SSPA Volume 1 (BSC 2001 [DIRS 154657], Section 14.3.3.3), additional analyses have been conducted to examine the relative contributions to the annual dose due to groundwater transport following igneous intrusion from damage to Zone 1 and Zone 2. As defined in the TSPA-SR (CRWMS M&O 2000 [DIRS 153246], Sections 3.10.2.3 and 5.2.9.7) and summarized in SSPA Volume 1, Zone 1 includes waste packages that are close to the intrusive dike or directly in its path. Zone 2 includes the remainder of the waste packages in the drifts that are intersected by the dike. Damage in Zone 1 is anticipated to be extensive, and packages, drip shields, and cladding are conservatively assumed to be sufficiently damaged that they provide no further protection for the waste. Damage in Zone 2 is less extensive and is characterized by removal of drip shields, failure of cladding, and failure of welds on the package lids.

Figure 3.3.1.2-3a shows probability-weighted mean annual doses for the igneous intrusion groundwater release pathway only, comparing doses due to releases from Zone 1 and Zone 2 together with the releases from Zone 1 and Zone 2 calculated separately. Figures 3.3.1.2-3b and 3.3.1.2-3c show the set of realizations calculated for Zones 1 and 2 separately, with the 95^{th} and 50^{th} (median) curves shown with the mean. Note that the 5^{th} percentile curve plots below the lowest value shown on the y-axis. All model inputs are the same as those used in TSPA-SR (CRWMS M&O 2000 [DIRS 153246], Sections 3.10.2.2 through 3.10.2.4). The total probability-weighted annual dose from this pathway is dominated almost entirely by the Zone 1 releases, with the annual doses from Zone 2 being almost a factor of 10 lower.

Analyses conducted since completion of the TSPA-SR resulted in revisions of the CDFs characterizing the number of packages damaged in Zone 1 and Zone 2. Specifically, the TSPA-SR used input from the original *Igneous Consequences Modeling for the TSPA-SR* AMR (CRWMS M&O 2000 [DIRS 139563]) that addressed the igneous consequences modeling for the Enhanced Design Alternative-II repository design (CRWMS M&O 2000 [DIRS 107292]). This AMR was subsequently updated (CRWMS M&O 2000 [DIRS 151560]) to address the site recommendation subsurface layout for the 70,000 metric tons of heavy metal repository design ([DIRS 146021]) and to include changes in the output from the calculation *Number of Waste Packages Hit by Igneous Intrusion* (CRWMS M&O 2000 [DIRS 153097]). Summary measures for distributions used in the TSPA-SR and the revised distributions reported in of the igneous consequences modeling AMR are presented in Table 3.3.1.2-1. Complete distributions can be found in the *Igneous Consequence Modeling for the TSPA-SR* AMR (CRWMS

M&O [DIRS 151560], Attachment 1) and DTN: SN0006T0502900.002 [DIRS 150856]. Because the revised distributions allow sampling of the extreme upper end of the possible distributions, these distributions are used in the supplementary TSPA analyses (see Section 4.3). The upper bound for the revised Zone 1 distribution is nearly eight times greater than the upper bound in TSPA-SR, and the upper bound for Zone 2 now includes all packages in the potential repository.

Figure 3.3.1.2-4a shows a comparison of the 20,000-year probability-weighted mean annual doses calculated for Zone 1 for the TSPA-SR distribution and for the revised distribution. All other models and input parameters used in these cases are the same as those used in the TSPA-SR (CRWMS M&O 2000 [DIRS 153246], Sections 3.10.2.2 through 3.10.2.4). The revised distribution results in an increase in the calculated annual dose at all times, with a maximum change of a factor of approximately 2. Figure 3.3.1.2-4b shows the set of realizations calculated for Zone 1 with the revised distribution, with the 95^{th} and 50^{th} (median) curves shown with the mean. Note that the 5^{th} percentile curve plots below the lowest value shown on the y-axis. Figures 3.3.1.2-5a and 3.3.1.2-5b (the same comparison for Zone 2) show little or no change in the mean annual dose from Zone 2.

3.3.1.2.4 Conditional Igneous Events

All dose histories for the igneous disruption scenario in the TSPA-SR (CRWMS M&O 2000 [DIRS 153246], Sections 4.2 and 5.2.9) were displayed as probability-weighted annual doses resulting from events occurring at uncertain times throughout the period of simulation. As described in the TSPA-SR (CRWMS M&O 2000 [DIRS 153246], Section 4.2), this approach to calculating and displaying the probability-weighted annual doses is consistent with the approach specified by the NRC (NRC 2000 [DIRS 149372]) and is required for determination of the overall expected annual dose. However, displays of the probability-weighted annual dose do not allow direct interpretation of the conditional annual dose, which is the annual dose an individual would receive if a volcanic event occurred at a specified time. For conditional analyses, the probability of the event is set equal to an unrealistic value of 1 (i.e., the calculation is conditional on the occurrence of the event), and the time of the event must be specified. Conditional results do not provide a meaningful estimate of the overall risk associated with igneous activity at Yucca Mountain, but they provide insights into the magnitude of possible consequences for specific sets of assumptions. The following sections describe conditional annual dose calculations for the eruptive and intrusive pathways. Annual doses are calculated using the same models and parameter values used in TSPA-SR (CRWMS M&O 2000 [DIRS 153246]), with event probabilities fixed at 1. For the eruptive pathway, the event probability (the probability that an intrusive dike will intersect the potential repository) and the vent probability (the probability that the intrusion will result in an eruptive vent through the potential repository) are set at 1, and the event times are fixed at 100, 500, 1,000, and 5,000 years. For the intrusive pathway, the event times are the same as those sampled in TSPA-SR (CRWMS M&O 2000 [DIRS 153246], Appendix G, simulation SR00_005im4). Although results are displayed in terms of annual dose, they are not suitable for comparison with the expected annual dose standard in proposed 10 CFR 63.113b (64 FR 8640 [DIRS 101680]), which requires all doses to be weighted by their annual probability.

Conditional Eruptive Annual Dose Histories–Three hundred realizations of eruptive annual doses were calculated assuming that an eruption intersects the potential repository 100 years after closure (Figure 3.3.1.2.4-1). The distribution in annual doses in the first year is due entirely to uncertainty in the sampled values for input parameters in ASHPLUME V1.4LV-dll and BDCFs. The rapid decline in annual dose in subsequent years is due primarily to soil removal and, to a lesser extent, to radioactive decay. Variability in the rate at which annual dose decreases is caused by uncertainty in the soil removal rate. A discussion of ASHPLUME inputs, eruptive BDCFs, and soil removal is presented in the TSPA-SR (CRWMS M&O 2000 [DIRS 153246], Sections 3.10.2 through 3.10.4).

Conditional mean annual dose histories were calculated for eruptive events at 100, 500, 1,000, and 5,000 years (Figure 3.3.1.2.4-2). The mean annual dose history for an event at 100 years is repeated from Figure 3.3.1.2.4-1, and the mean annual dose histories for events at later times are each derived from 300 realizations analogous to those shown for the 100-year event (Figure 3.3.1.2.4-1). The similarity of the curves is consistent with the use of the same sampling of input parameters, and the differences in the initial annual dose at different times is due entirely to radioactive decay. The conditional mean dose in the first year for an eruptive event at 100 years is approximately 13 rems/year (1.3×10^4 mrem/year). The first-year conditional dose decreases to approximately one half this level by 500 years after closure, and is approximately 10 percent of this value after 5,000 years.

The conditional eruptive annual doses described here (Figure 3.3.1.2.4-2) do not include any dose that might be incurred by direct inhalation of the ash cloud during the eruptive event. As discussed in the TSPA-SR (CRWMS M&O 2000 [DIRS 153246], Section 5.2.9.9), conditional inhalation doses to people who do not evacuate during the eruptive event are estimated to be 3.7 rem/day for an event conservatively assumed to happen in the first year after closure of the potential repository. For a median-value eruptive event duration of 8.2 days, this could result in an additional non-evacuation conditional dose of 30.3 rem during the first year, and smaller values during subsequent years. As explained in the TSPA-SR (CRWMS M&O 2000 [DIRS 153246], Section 5.2.9.9), the non-evacuation dose is an insignificant contributor to the total probability-weighted annual dose because of the low annual probability of eruption, and therefore it is not included in the TSPA calculations of expected annual dose.

Figure 3.3.1.2.4-3 shows the same four annual dose histories as those shown in Figure 3.3.1.2.4-2, with the addition of a conditional mean annual dose history calculated for an eruption occurring at 100 years and with the soil removal rate set to zero. This additional case was calculated to provide graphical confirmation of the relative roles of soil removal and radioactive decay, and it is not intended to represent a realistic estimate of annual doses following a conditional eruption. Soil removal due to agricultural processes is included as part of the set of realistic and reasonable models used in the TSPA-SR and the SSPA. This final calculation confirms that the decrease in annual dose in the years following an eruption primarily is due to soil removal. The gradual decrease in annual dose after year 100 in this calculation is due entirely to radioactive decay, and the curve therefore intersects the first-year annual doses calculated for events at later times.

Conditional Igneous Intrusion Dose Histories–Calculation and display of the conditional doses resulting from groundwater transport following igneous intrusion is simpler than that for the eruptive releases because of the approach taken in TSPA-SR (CRWMS M&O 2000 [DIRS 153246], Section 4.2.1.2) to incorporate event probability by sampling on the time of the event. Figure 3.3.1.2.4-4 shows 500 out of the 5,000 realizations of 50,000-year igneous intrusion annual dose histories calculated for TSPA-SR (CRWMS M&O 2000 [DIRS 153246], Section 4.2). Results shown on Figure 3.3.1.2.4-4 are identical to those in Figure 3.3.1-1, except that the eruptive releases have been removed. Groundwater releases for each realization are shown weighted by the probability of the intrusive event occurring. In Figure 3.3.1.2.4-5, the same set of realizations are shown without probability-weighting. Peak mean annual dose from the igneous intrusion pathway increases from approximately 0.1 mrem/year in the probability-weighted case to approximately 500 mrem/year, consistent with the overall mean probability of an intrusive igneous event during the 50,000-year simulation of 8×10^{-4}.

Comparison of Eruptive and Intrusive Conditional Annual Doses–Peak conditional annual doses associated with volcanic eruption are significantly higher than those associated with igneous intrusion (compare Figures 3.3.1.2.4-1 and 3.3.1.2.4-5). This is a reversal of the relative importance of the two pathways in the probability-weighted igneous annual dose results (Figure 3.3.1-1). This change in importance is due to the probability weighting and the duration of the time following the volcanic event during which annual doses are high. Eruptive annual doses decrease quickly following the event. Thus, for a person to receive a relatively high eruptive annual dose, the event would have to occur during their lifetime or during the first several hundred years before their birth. For the groundwater pathway, annual doses may remain relatively unchanged for thousands of years following the event, and a person therefore could receive an annual dose from events occurring during a relatively long period of time. Probability-weighting therefore has the effect of emphasizing the more likely groundwater doses from a prior intrusive event, while de-emphasizing the eruptive doses that require the less likely occurrence of an eruption in a short time interval.

3.3.1.2.5 A Bounding Estimate of the Consequences of Surficial Redistribution of Volcanic Ash

The approach taken in the TSPA-SR (CRWMS M&O 2000 [DIRS 153246], Sections 3.10.2 through 3.10.4) and the SSPA does not explicitly include the effects of possible surface redistribution of contaminated ash following deposition. Specifically, aeolian and fluvial processes may result in transport of sediment from other regions within the area of the ashfall to the location of the receptor. Instead of explicitly including these processes, TSPA-SR analyses used a conservative approach (CRWMS M&O 2000 [DIRS 153246], Section 3.10.4) in which the wind direction was fixed toward the receptor for all eruptive events, overestimating the amount of ash initially deposited at the location receptor. Furthermore, the transition-phase BDCFs used for calculating eruptive annual dose at all times following ash deposition used high air-mass loading values applicable for fresh, unconsolidated ash, rather than the more appropriate long-term BDCFs calculated for stabilized soils. This overestimate of long-term air-mass loading, combined with the assumption for the purposes of calculating the inhalation dose that all radionuclides were concentrated in the upper 1 cm of the ash layer regardless of its thickness, formed the basis of the assertion in TSPA-SR that the overall treatment is conservative with respect to ash redistribution processes (CRWMS M&O 2000 [DIRS 153246], Section 3.10.4).

The conditional eruptive annual dose analyses conducted for the SSPA and described previously in this section provide useful insights into an upper bound on the possible consequences of ash redistribution following an eruption. Specifically, the no-soil removal case (Figure 3.3.1.2.4-3) provides an upper bound on conditional annual doses that might result if surficial redistribution processes cause deposition of contaminated sediment at the location of the receptor, as long as concentrations of radionuclides in the redeposited sediments are equal to or less than concentrations in the initial ash layer. This conclusion applies to redeposition by aeolian and fluvial processes, and it is not affected if the rate of redeposition at the location of the receptor exceeds the rate of soil removal by agricultural processes. Even if the layer of contaminated sediment grew in thickness through time, doses still would be derived from the upper 15 cm of the contaminated layer. The thin-layer transition-phase BDCFs used in this calculation result in greater annual doses than would be derived from layers of contaminated ash 15 cm or greater in thickness, because all radionuclides in the thin layer are assumed to be concentrated in the upper 1 cm where they are available for resuspension and inhalation (CRWMS M&O 2000 [DIRS 153246], Sections 5.2.9.10 and 3.10.3.3). Thus, regardless of the rate of redeposition of contaminated ash at the location of the receptor, the eruptive-pathway conditional annual dose calculated using the TSPA-SR model and parameters (CRWMS M&O 2000 [DIRS 153246], Sections 3.10.2 through 3.10.4) will not exceed the annual doses for the no-soil removal case (Figure 3.3.1.2.4-3) as long as surficial processes do not concentrate radionuclides within the sediment to levels above those calculated for the initial ashfall.

3.3.2 Seismic Activity Analyses

No new analyses of seismic events were conducted in SSPA Volume 1 (BSC 2001 [DIRS 154657]). Consequently, supplemental analyses of direct, disruptive effects of seismic events on the estimate of mean annual dose are not provided here. However, potential effects of seismic activity can be inferred from supplemental TSPA analyses regarding drift degradation, rock fall, and damage to CSNF cladding (which may be exacerbated by seismic activity).

Drift degradation and rock fall are considered in SSPA Volume 1 (BSC 2001 [DIRS 154657], Section 6.3.4), and effects of the additional considerations on the estimate of annual dose are discussed in this volume (see Section 3.2.4.1). These analyses do not indicate any significant effect on drip shield or waste package performance.

The effect of vibratory ground motion on CSNF cladding is considered in SSPA Volume 1 (BSC 2001 [DIRS 154657], Section 9.3.3), which notes that the TSPA-SR base-case model addresses this effect in terms of a discrete event in which cladding is damaged due to seismic activity. The frequency assumed for this event in the base-case model is 1.1×10^{-6} per year. Such a seismic event would occur randomly and is sampled in the TSPA-SR base-case analysis. When the vibratory ground motion event occurs, all CSNF cladding in the potential repository is assumed to fail by perforation, and further cladding degradation (i.e., unzipping) is calculated according to the cladding degradation model. Analyses in the TSPA-SR (CRWMS M&O 2000 [DIRS 153246], Section 3.3.1) indicate no effect on the estimate of mean annual dose as long as waste packages remain unbreached, and only minor effects at later times.

These effects are examined further in SSPA Volume 1 (BSC 2001 [DIRS 154657], Section 9.3.3), which considers a broad range of events and accounts for additional uncertainty in the magnitude of damage during the vibratory ground motion event. The SSPA Volume 1 analyses (BSC 2001 [DIRS 154657]) consider the probability distribution shown in Table 3.3.2-1. The results using this distribution are compared with the TSPA-SR base-case results in Figure 3.3.2.1-1. The differences between these estimates of mean annual dose are small and the uncertainty and extended range for the probability distribution for damage due to seismic activity have a negligible effect on the estimate of mean annual dose.

INTENTIONALLY LEFT BLANK

Table 3.3.1.2-1. Summary Information for Revised Distributions for the Number of Packages Damaged by Volcanic Activity

Source Document	Cumulative Distribution Function	
	Zone 1	Zone 1 + 2 Combined
TSPA-SR (CRWMS M&O 2000 [DIRS 153246], Section 3.10.2.3). See also DTN: SN0006T0502900.002 [DIRS 150856] for full distribution.	Range: 105 to 227 Median = 192	Range: 0 to 11,180 Median = 1,720
Igneous Consequences Modeling for the TSPA-SR (CRWMS M&O 2000 [DIRS 151560], Attachment 1).	Range: 98 to 1,785 Median = 197	Range: 0 to 11,184 Median = 1,838

NOTE: Full distributions, rather than the range and median values, are used in the TSPA calculations.

Table 3.3.2-1. Complementary Cumulative Distribution Function for Frequency of Seismic Cladding Failure for Supplemental Analyses

Complementary Cumulative Distribution Function	Frequency (/year)
1.00	4.90 E-06
0.95	4.90 E-06
0.85	1.10 E-06
0.50	6.40 E-08
0.15	6.20 E-10
0.05	2.70 E-12
0.00	2.70 E-12

Source: BSC 2001 [DIRS 154657], Table 9-8.

INTENTIONALLY LEFT BLANK

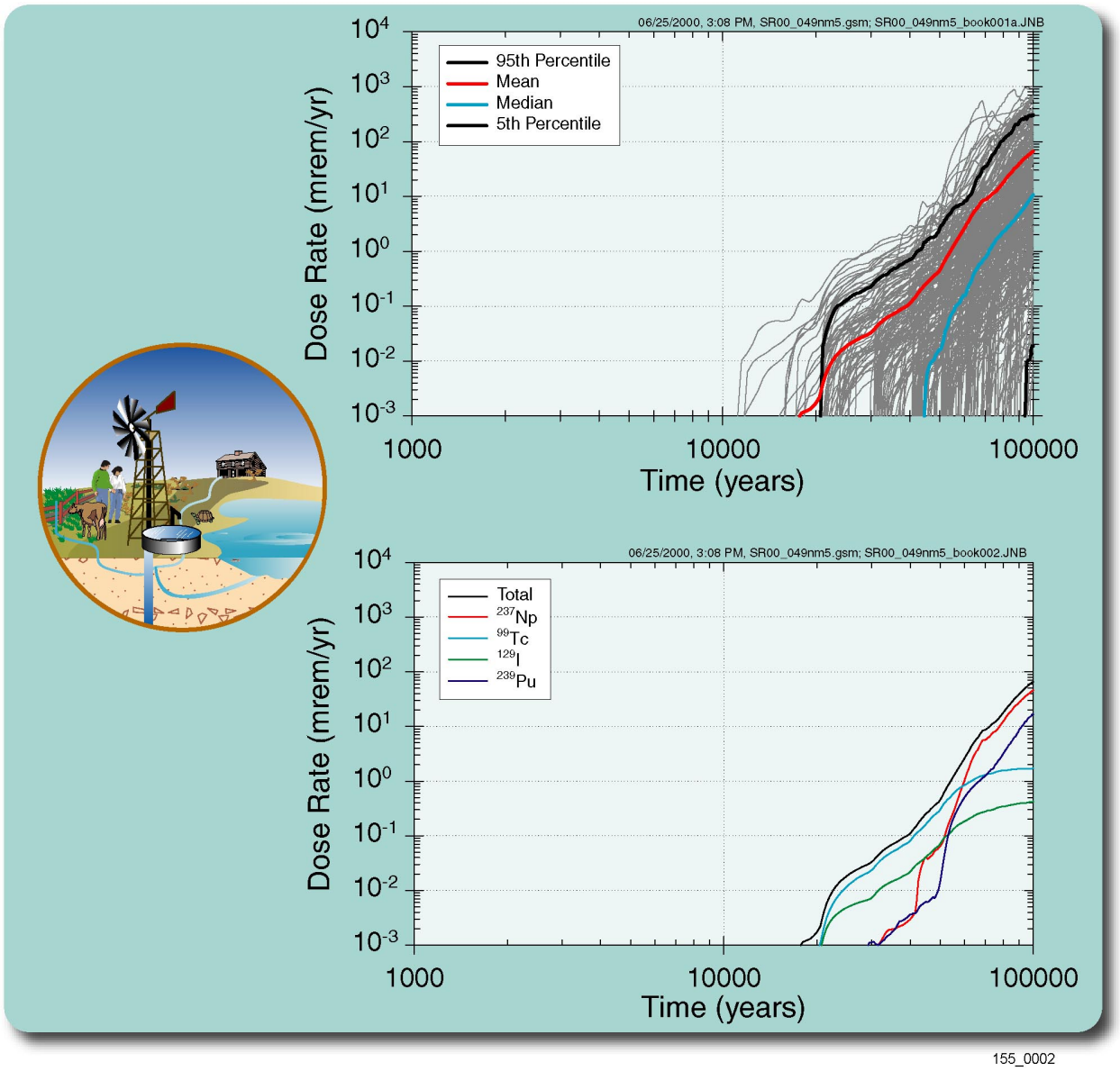

155_0002

Source: CRWMS M&O 2000 [DIRS 153246], Figure 4.1-5.

NOTE: Nominal scenario data from TSPA-SR. ^{237}Np = neptunium-237, ^{99}Tc = technetium-99, ^{129}I = iodine-129, ^{239}Pu = plutonium-239.

Figure 3.1.1-1. Simulated Annual Dose Histories for the TSPA-SR Nominal Scenario

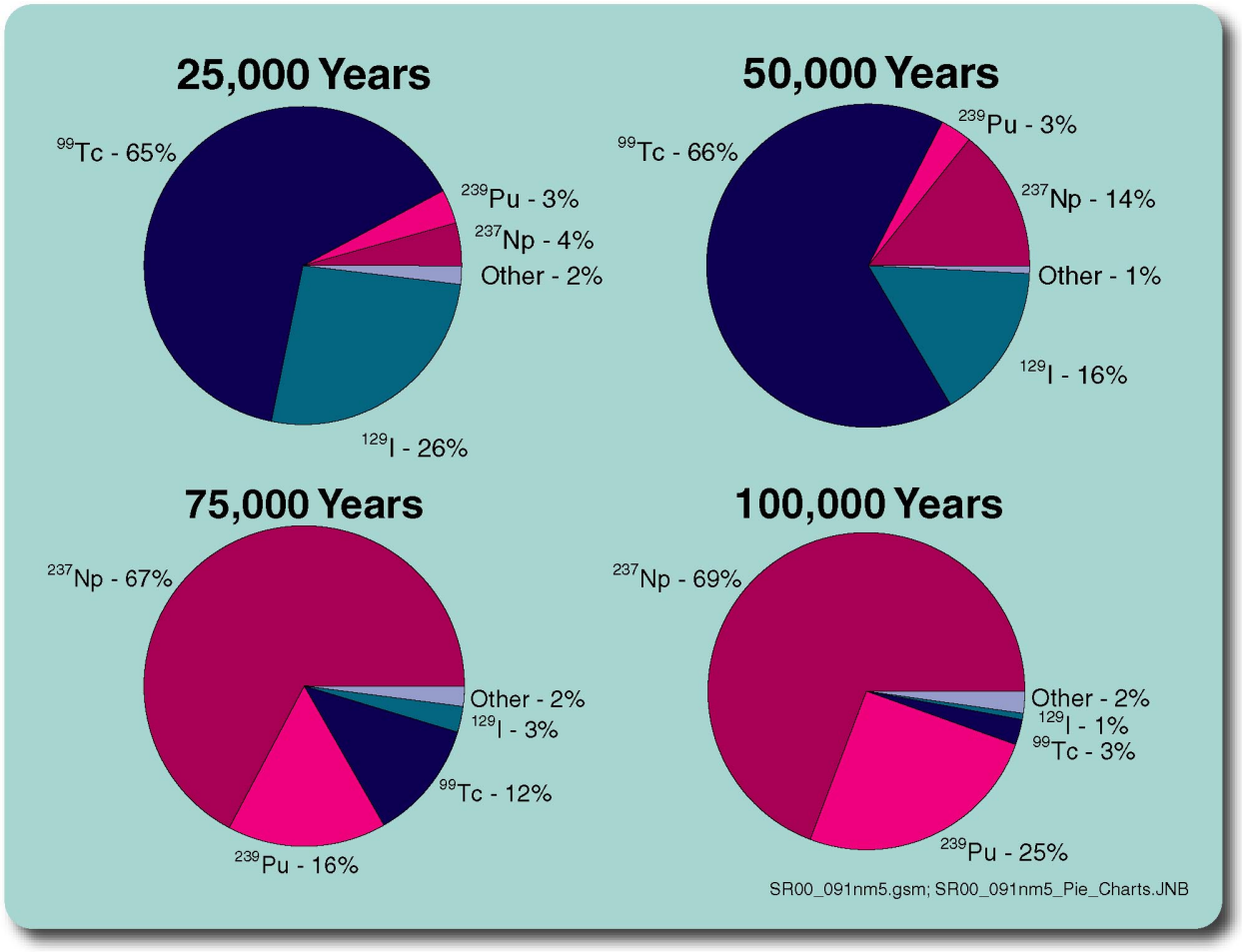

155_0003

155_0003

Source: CRWMS M&O 2000 [DIRS 153246], Figure 4.1-6.

NOTE: ^{237}Np = neptunium-237, ^{99}Tc = technetium-99, ^{129}I = iodine-129, ^{239}Pu = plutonium-239.

Figure 3.1.1-2. Contribution of Radionuclides to the TSPA-SR Mean Annual Dose at Four Times

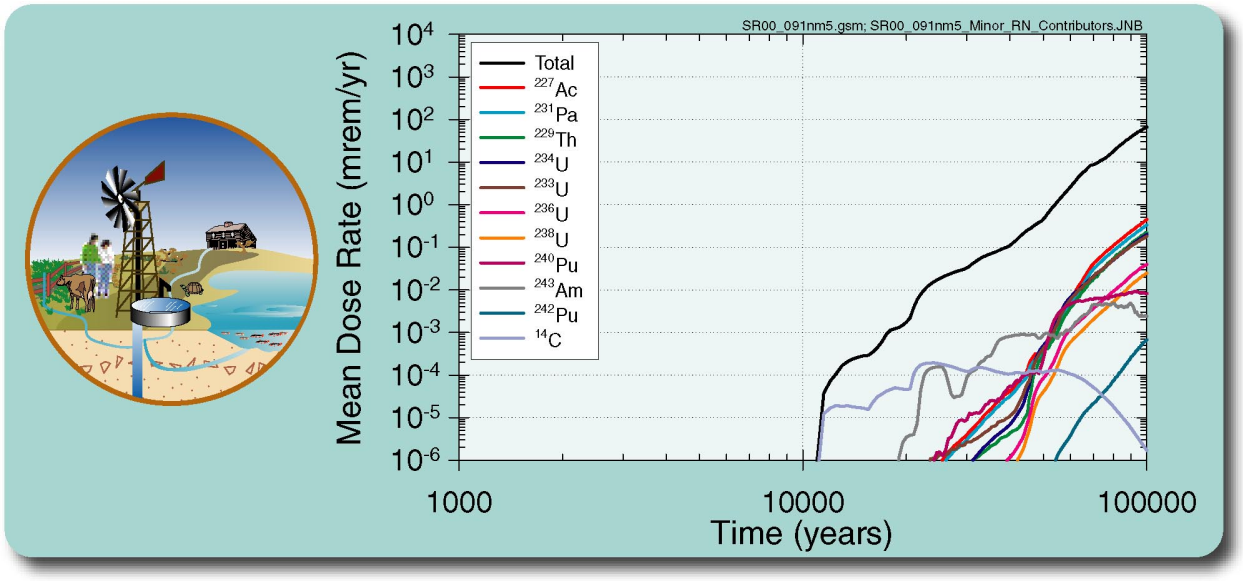

155_0004

Source: CRWMS M&O 2000 [DIRS 153246], Figure 4.1-7.

NOTE: Ac = actinium; Am = americium; C = carbon; Pa = protactinium; Pu = plutonium; Th = thorium; U = uranium.

Figure 3.1.1-3. Mean Annual Dose Histories for the TSPA-SR Less-Important Radionuclides

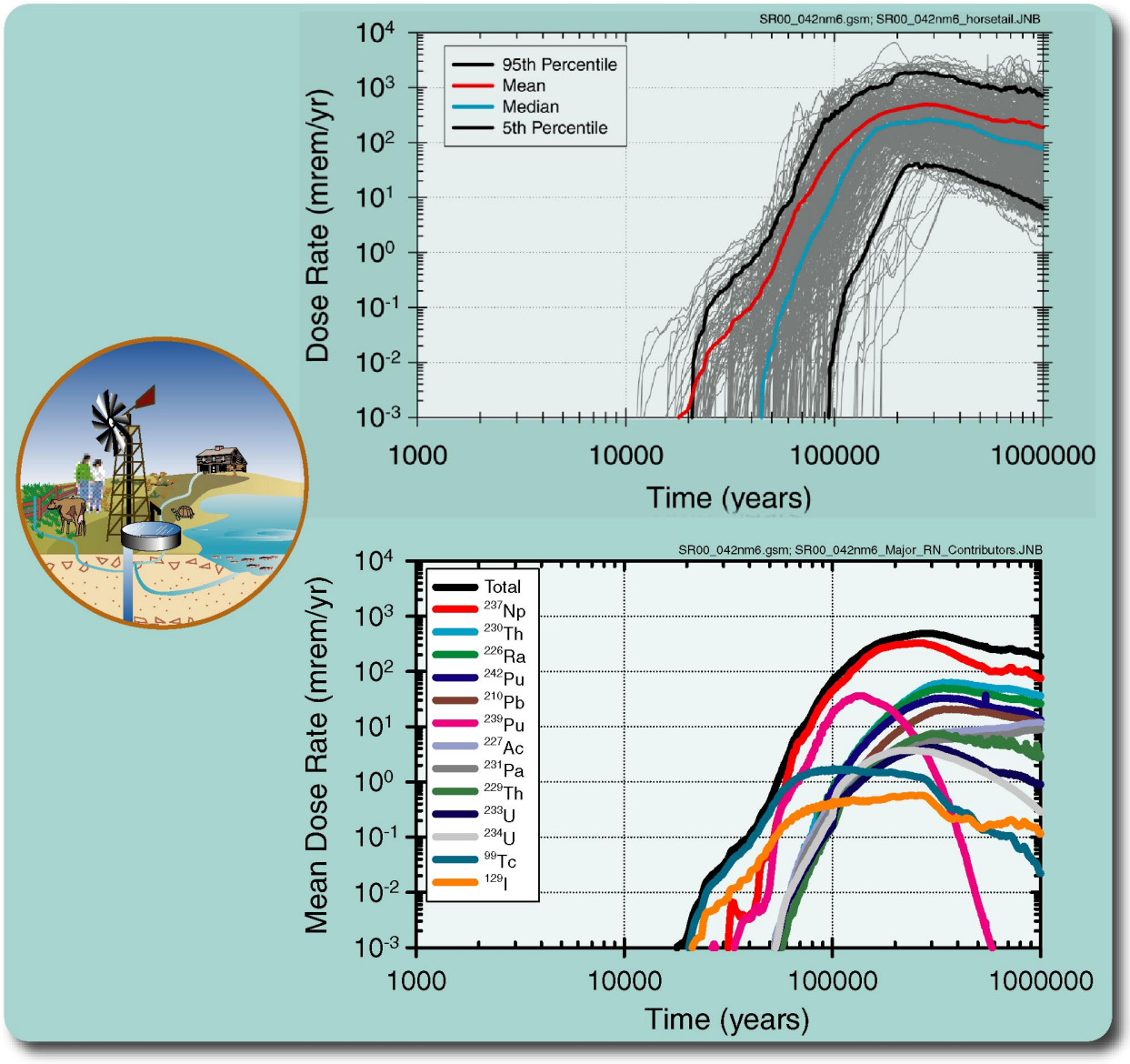

155_0005.ai

Source: CRWMS M&O 2000 [DIRS 153246], Figure 4.1-19a.

NOTE: Ac = actinium; Np = neptunium; Pa = protactinium; Pb = lead; Pu = plutonium; Ra = radium; Tc = technetium; Th = thorium; U = uranium; I = iodine.

Figure 3.1.2-1. Simulated Annual Dose Histories for the Nominal Scenario over 1,000,000 Years using the TSPA-SR Base-Case Models

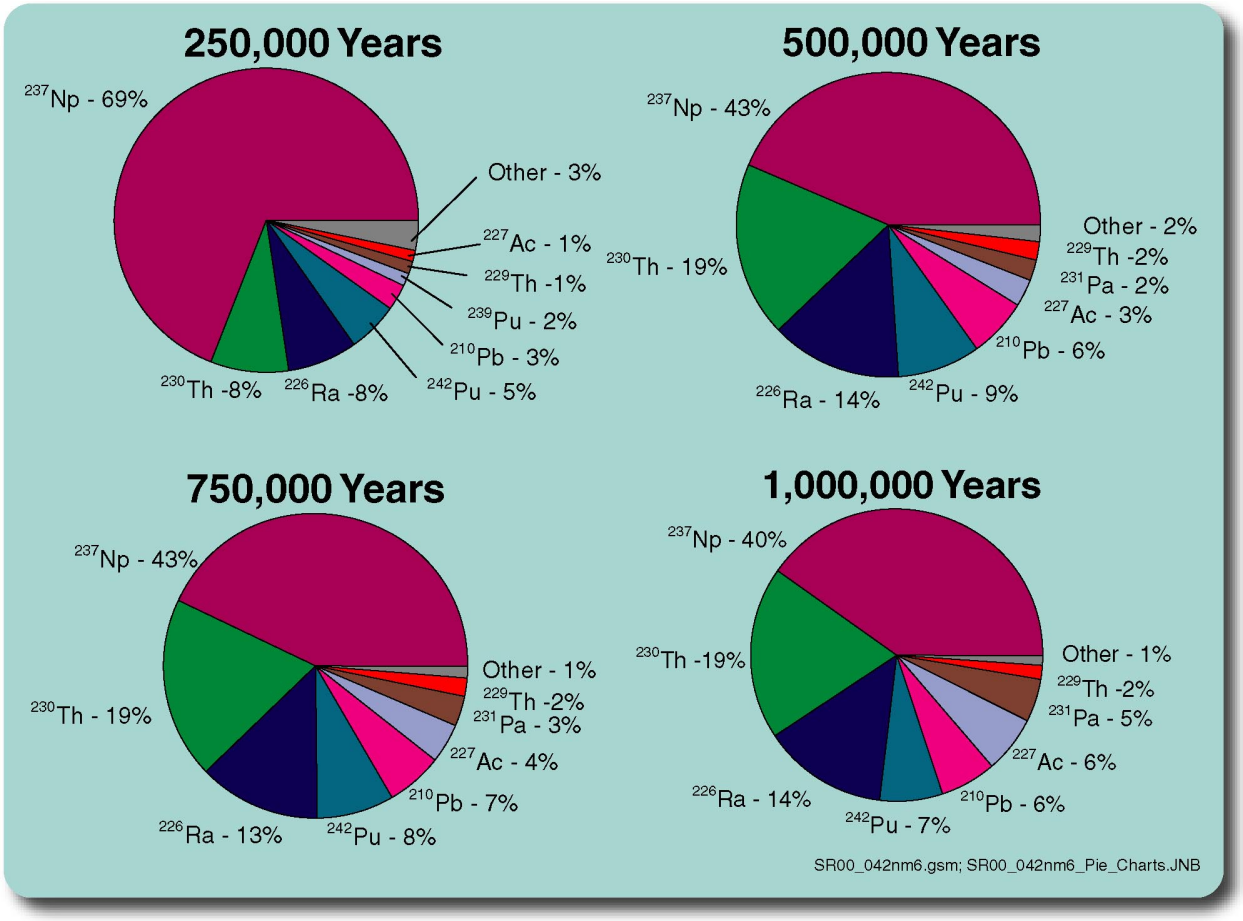

155_0006.ai

Source: CRWMS M&O 2000 [DIRS 153246], Figure 4.1-19b.

NOTE: Ac = actinium; Np = neptunium; Pa = protactinium; Pb = lead; Pu = plutonium; Ra = radium; Th = thorium.

Figure 3.1.2-2. Key Radionuclides Affecting Mean Annual Dose for the Nominal Scenario over 1,000,000 Years Using the TSPA-SR Base-Case Models

(a)

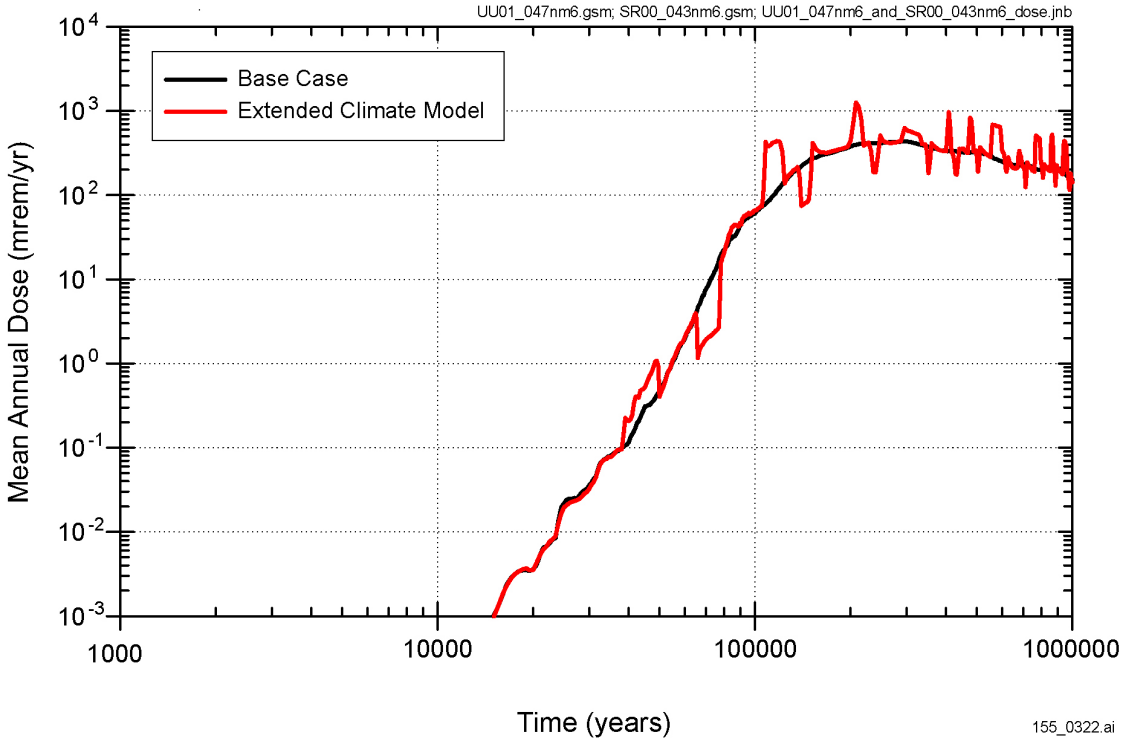

(b)

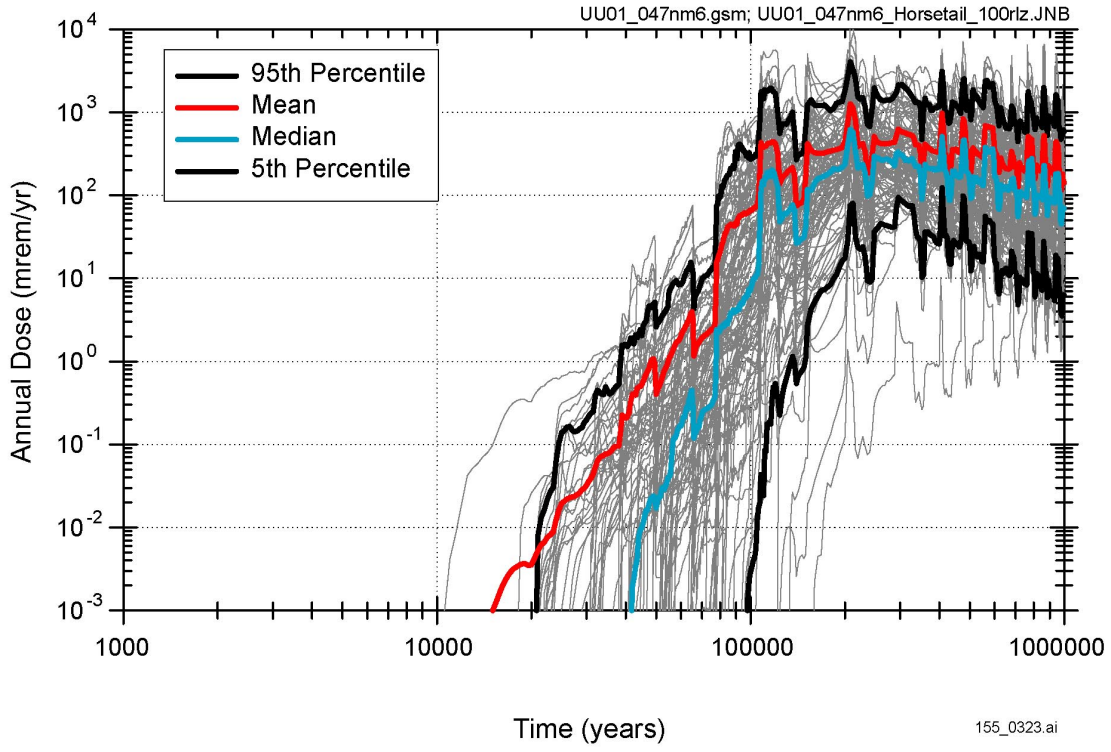

155_0322.ai / 155_0323.ai

NOTE: (a) Comparison of two cases. (b) All realizations and statistics for the extended climate model.

Figure 3.2.1-1. Annual Dose Histories for the Extended Climate Model and the Base Case

(a)

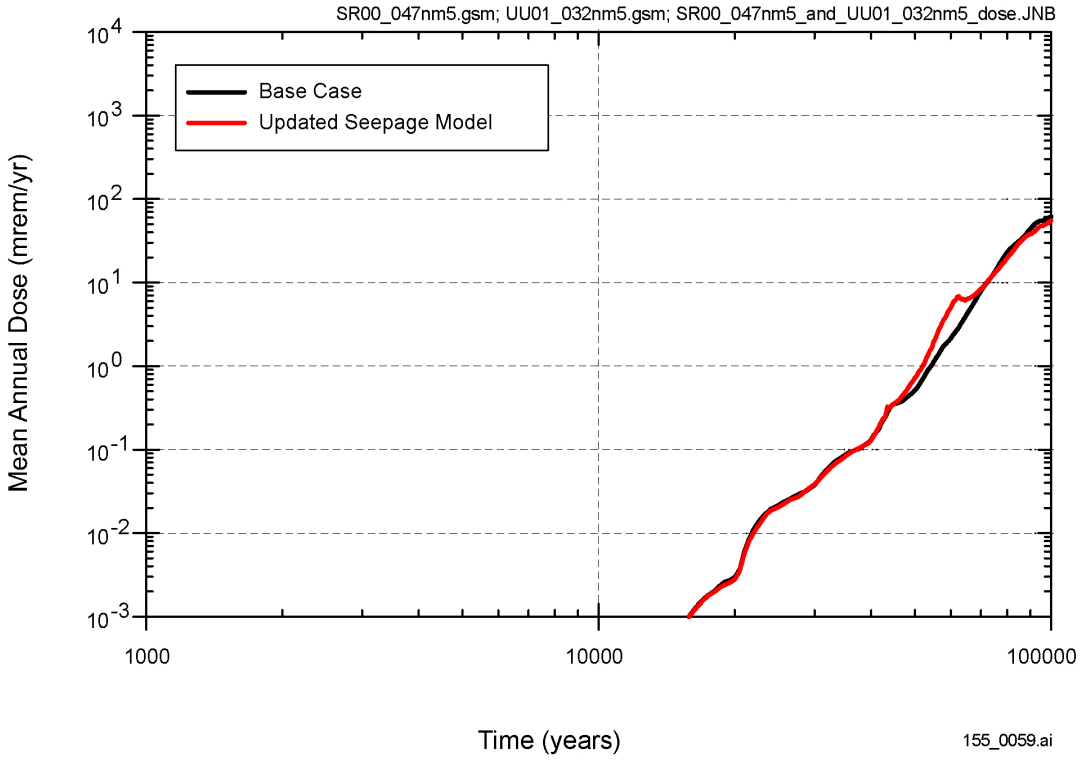

(b)

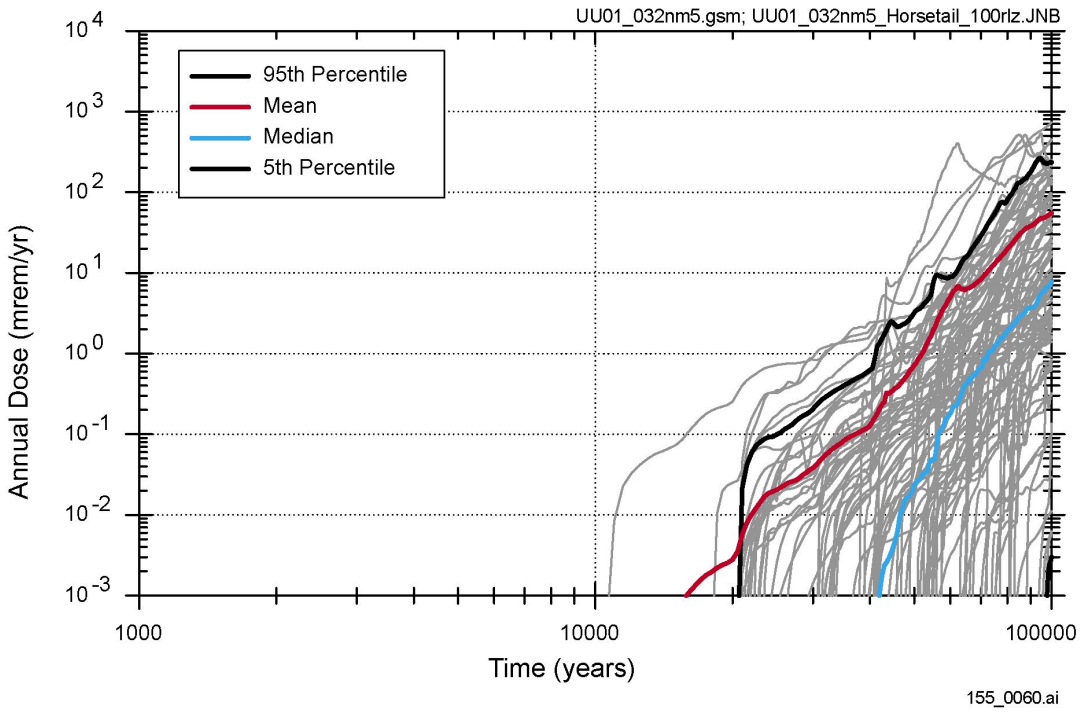

155_0059.ai / 155_0060.ai

NOTE: (a) Comparison of two cases. (b) All realizations and statistics for the updated seepage model.

Figure 3.2.2-1. Annual Dose Histories for the Updated Seepage Model and Base Case

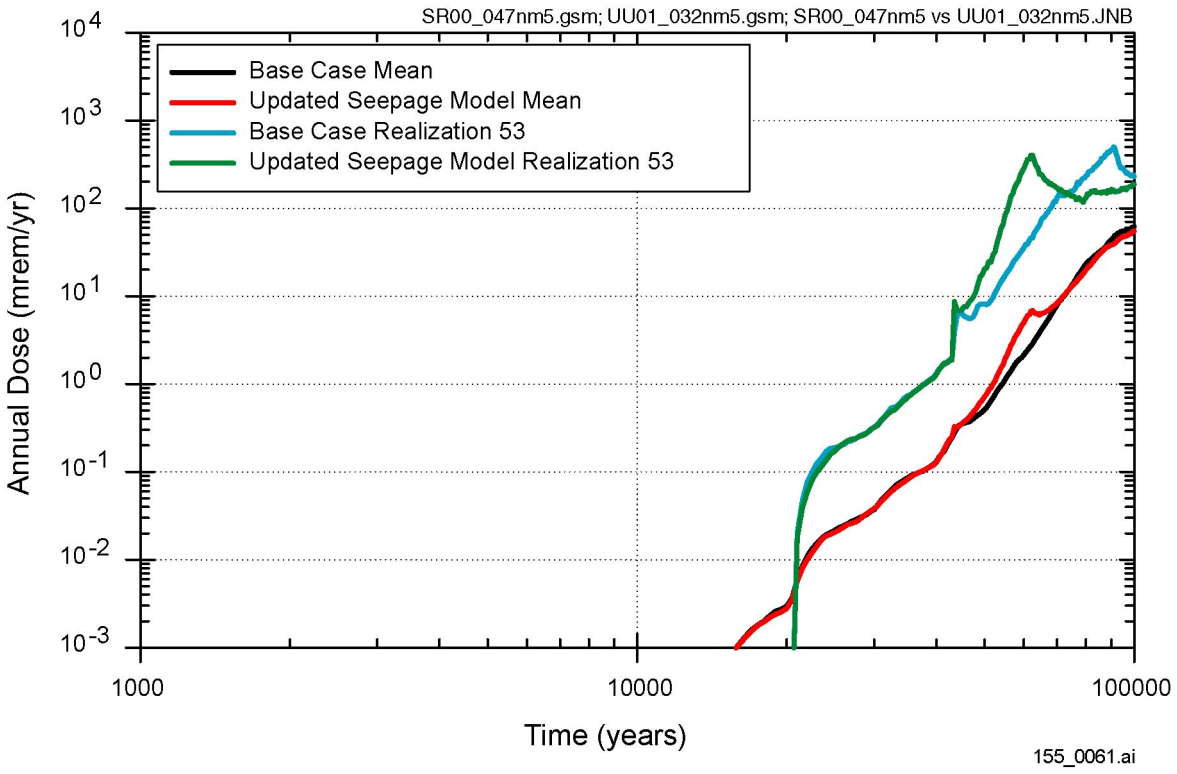

155_0061.ai

Figure 3.2.2-2. Realization 53 for the Updated Seepage Model and the Base Case

(a)

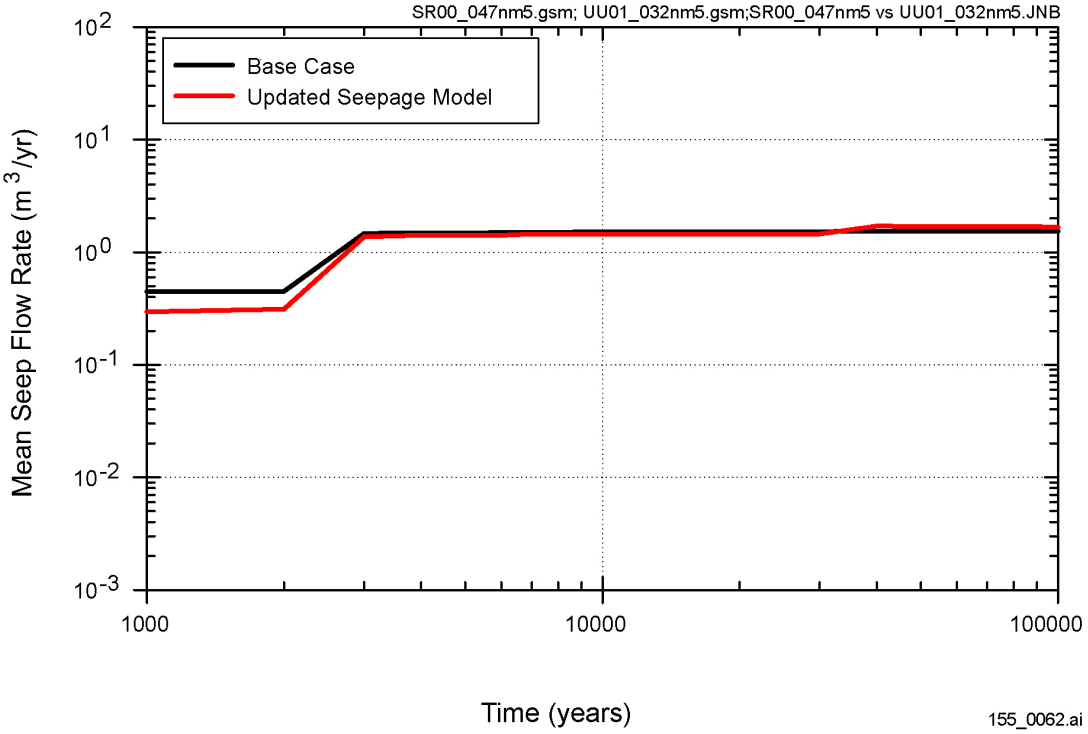

(b)

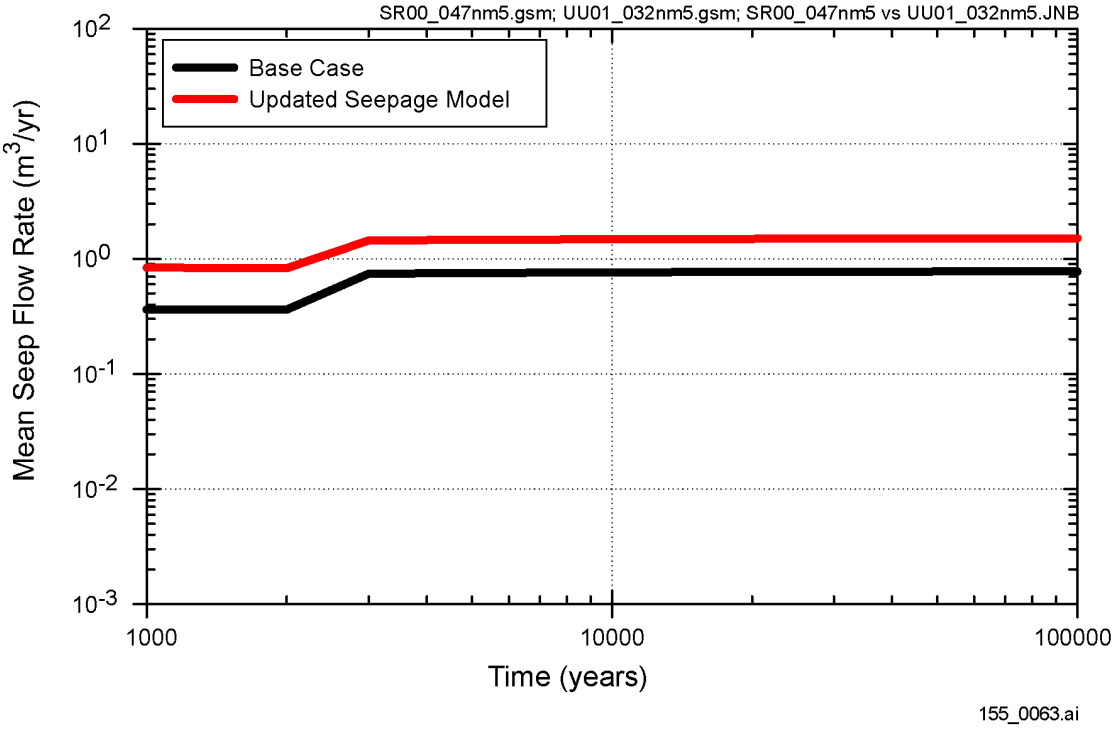

155_0062.ai / 155_0063.ai

NOTE: CSNF, 20 to 60 mm/yr infiltration. (a) Seepage some of the time. (b) Seepage all of the time.

Figure 3.2.2-3. Comparison of Seepage for the Updated Seepage and Base Case

(a)

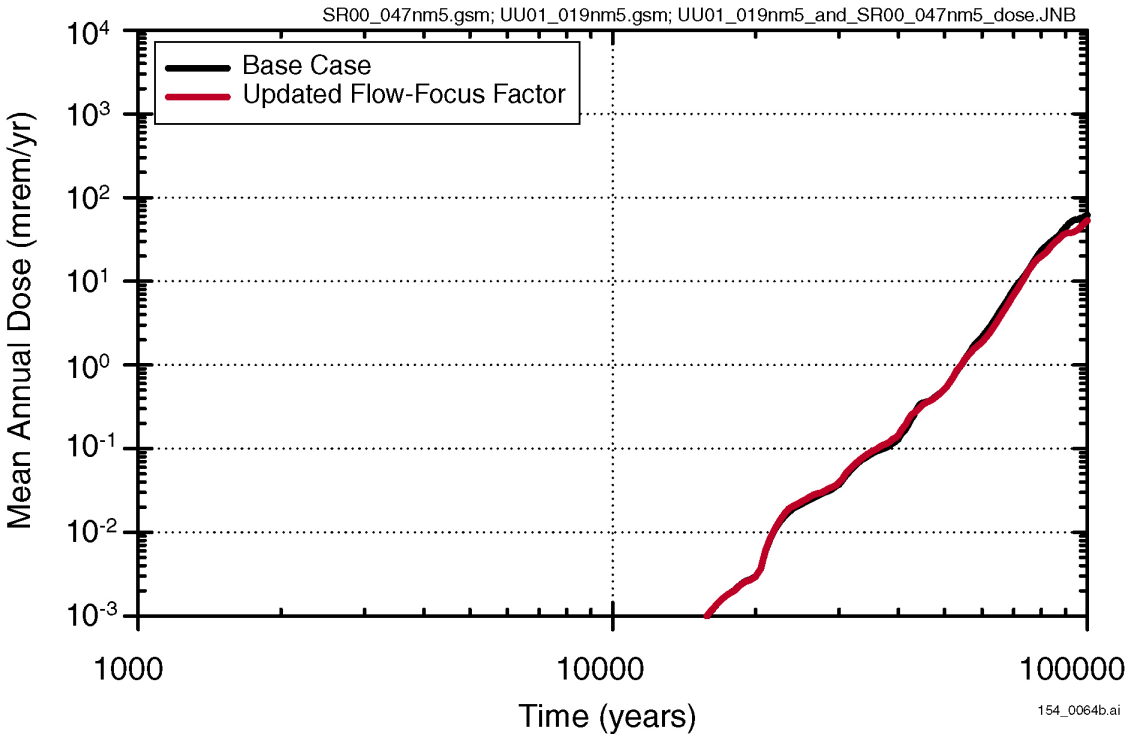

(b)

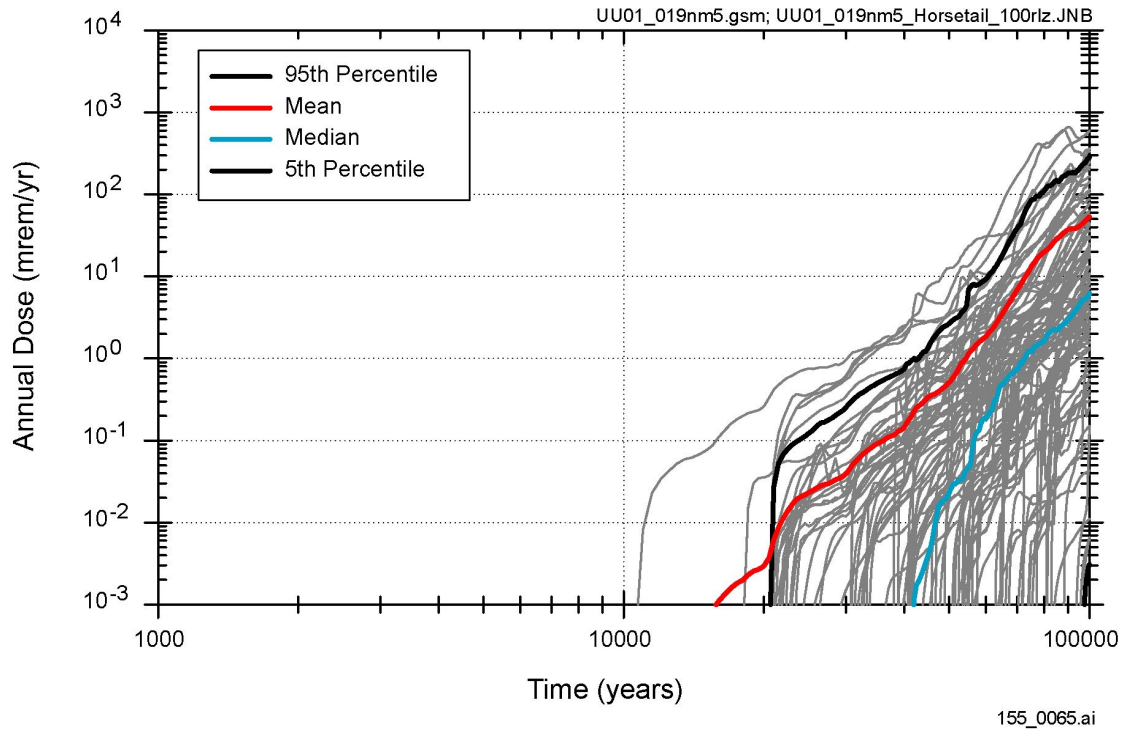

155_0064b.ai / 155_0065.ai

NOTE: (a) Comparison of two cases. (b) All realizations and statistics for the updated flow-focusing case.

Figure 3.2.2-4. Annual Dose Histories for the Updated Flow-Focusing and Base Cases

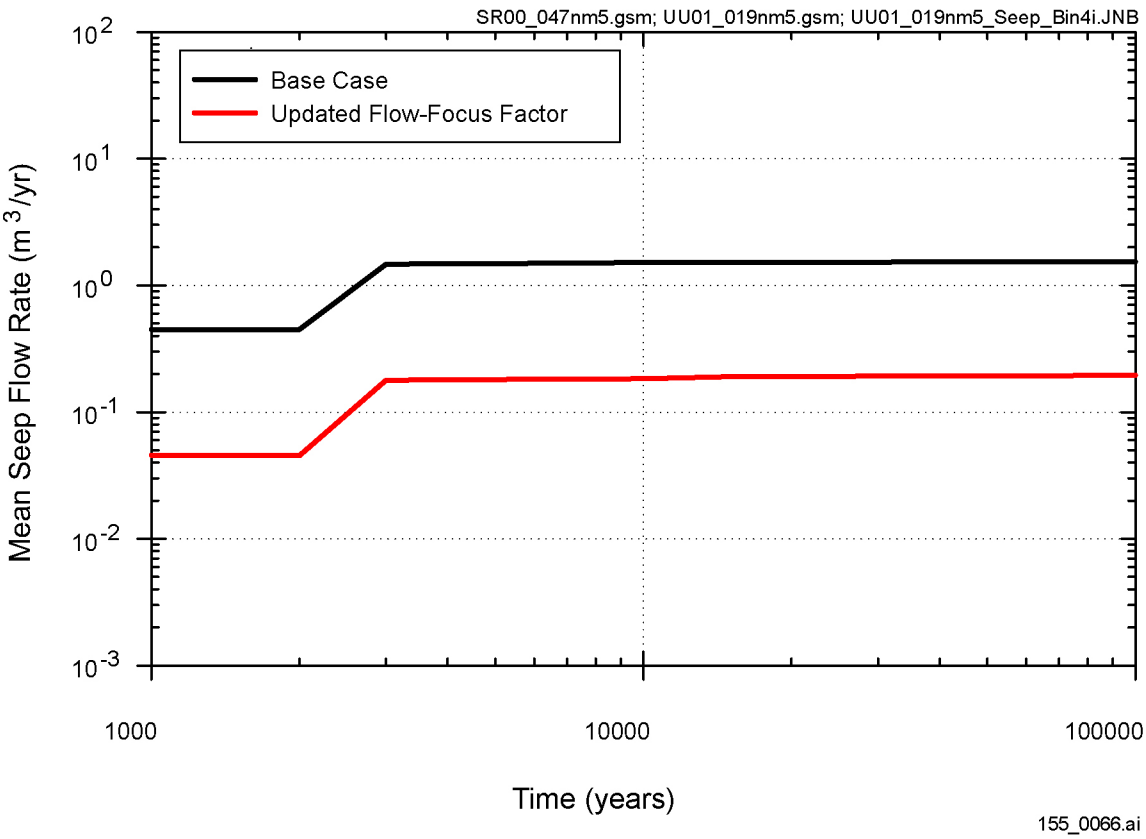

155_0066.ai

NOTE: CSNF, 20 to 60 mm/yr. Seepage some of the time.

Figure 3.2.2-5. Comparison of Seepage for the Updated Flow-Focusing and Base Cases

(a)

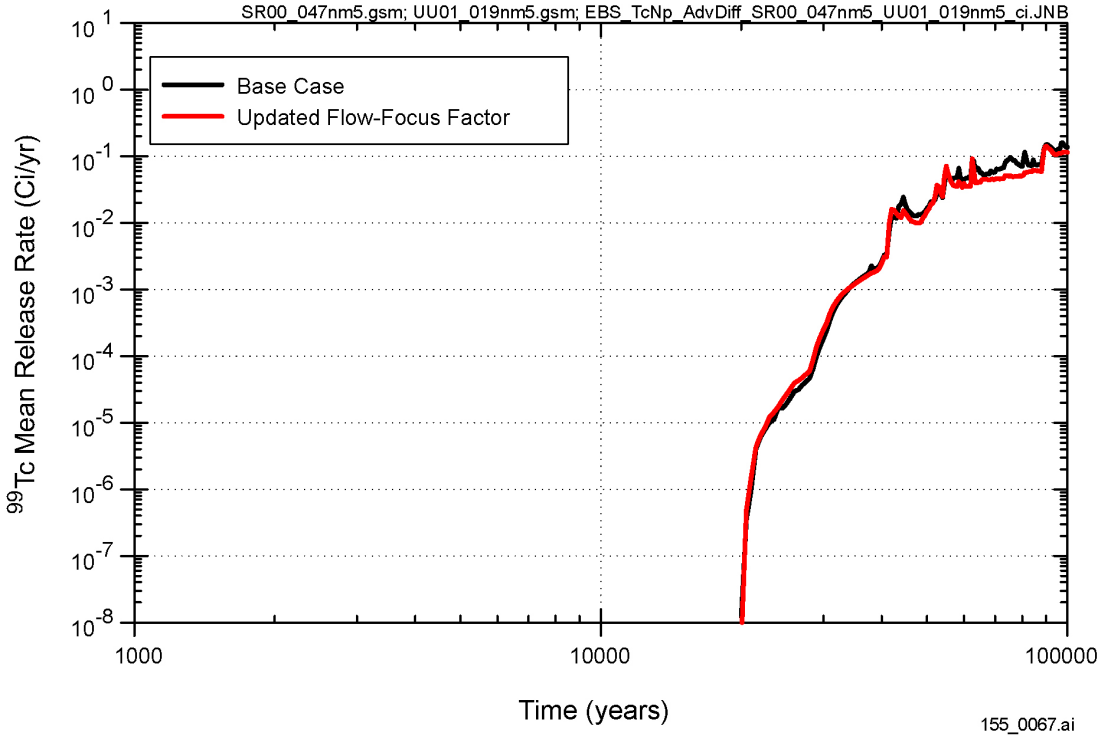

(b)

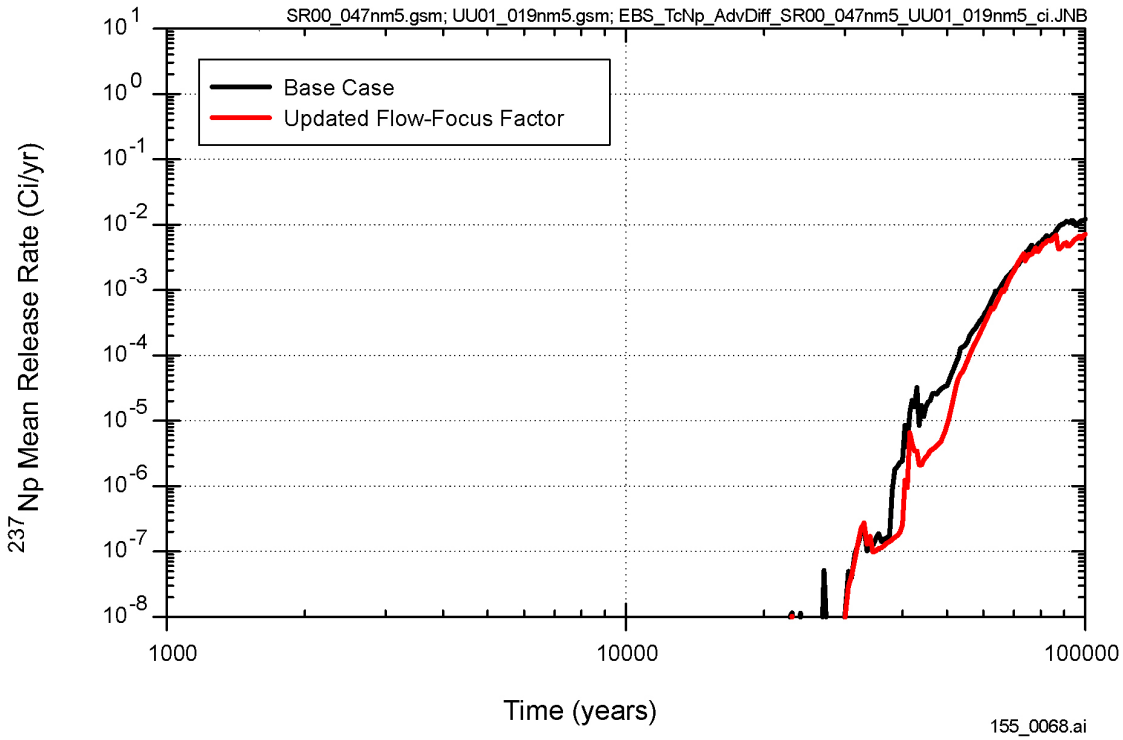

155_0067.ai / 155_0068.ai

NOTE: Release rates for CSNF. (a) Technetium (^{99}Tc). (b) Neptunium (^{237}Np).

Figure 3.2.2-6. Comparison of Advective Releases from the Engineered Barrier System for the Updated Flow-Focusing and Base Cases

(a)

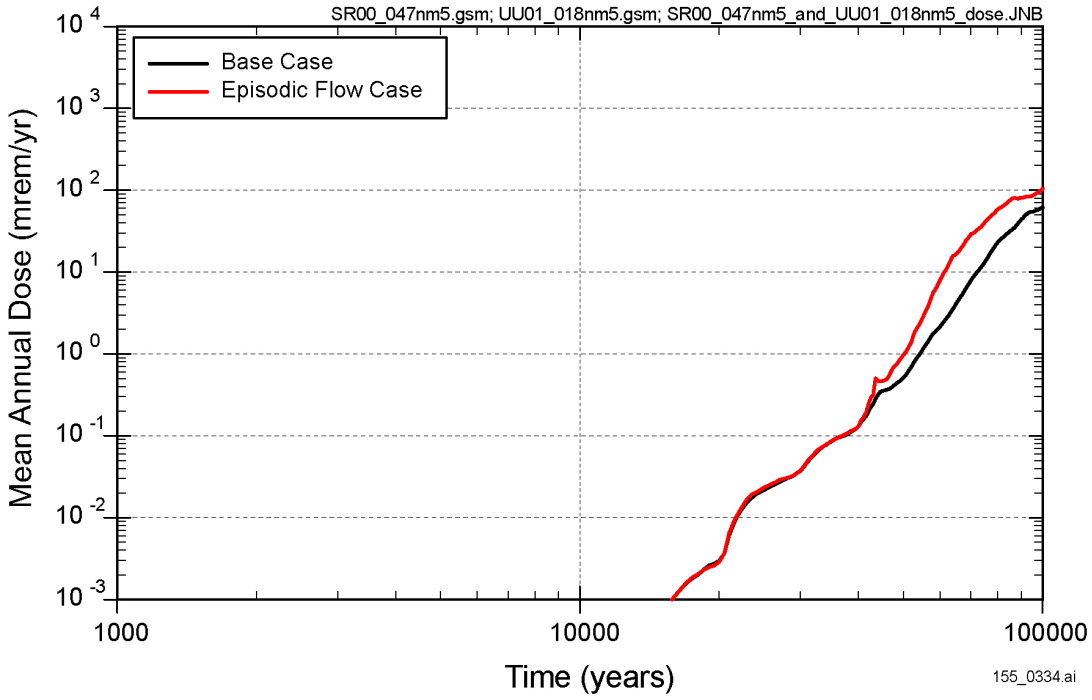

(b)

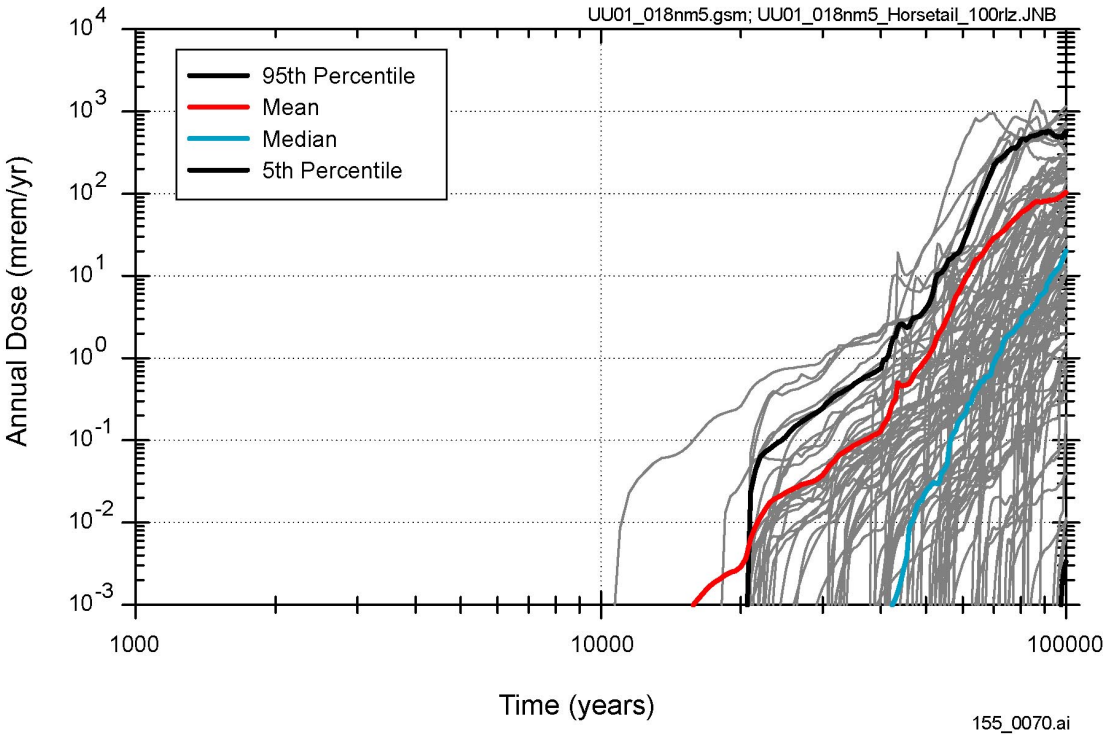

155_0334.ai/155_0070.ai

NOTE: (a) Comparison of two cases. (b) All realizations and statistics for the episodic-flow case.

Figure 3.2.2-7. Annual Dose Histories for the Episodic-Flow and Base Cases

(a)

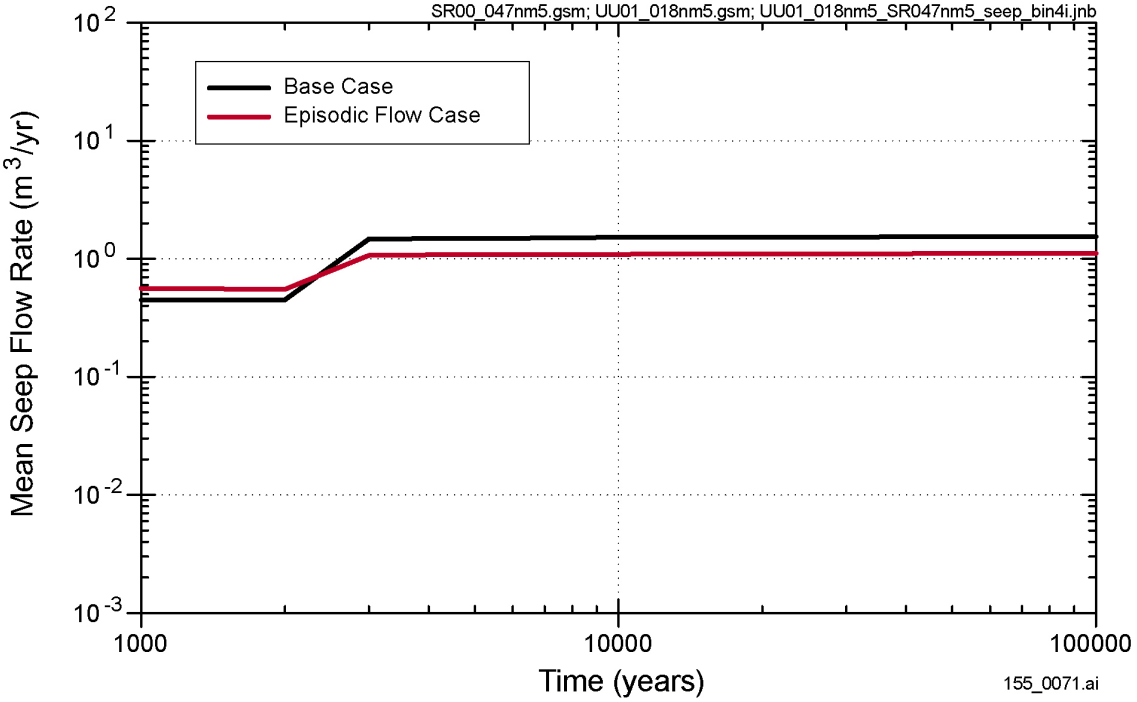

(b)

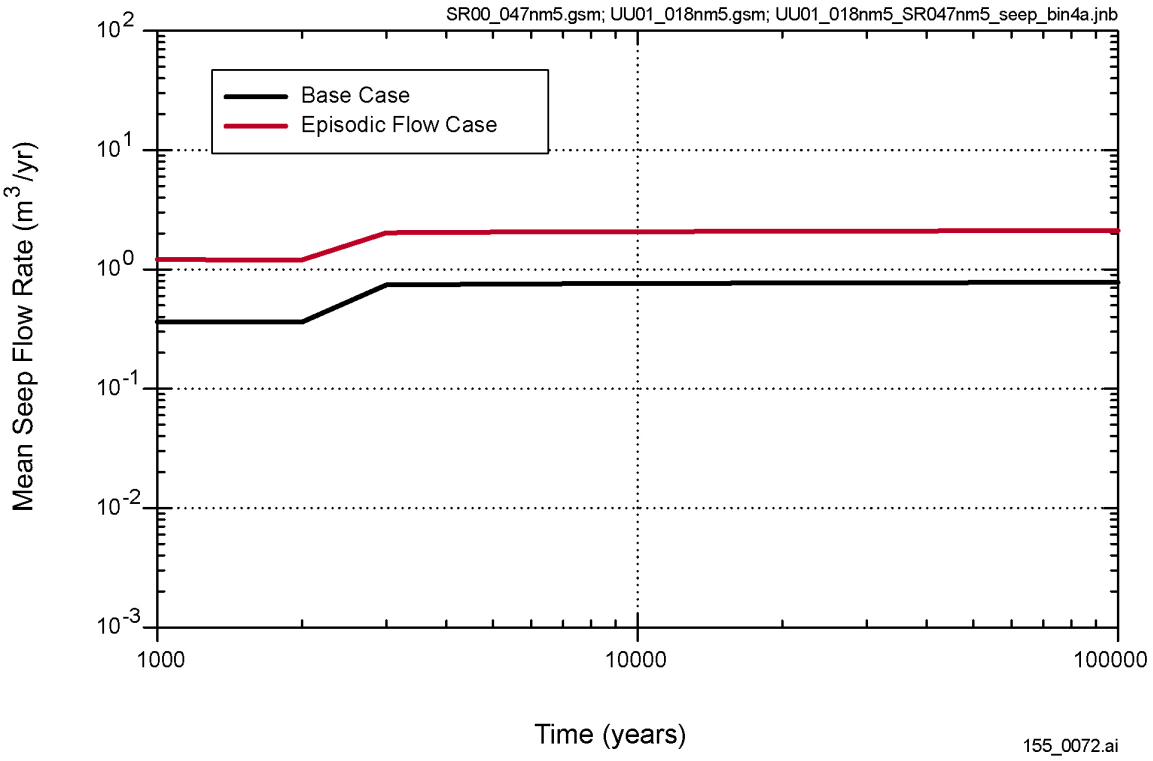

155_0071.ai / 155_0072.ai

NOTE: CSNF, 20 to 60 mm/yr infiltration. (a) Seepage some of the time. (b) Seepage all of the time.

Figure 3.2.2-8. Comparison of Seepage for the Episodic-Flow and Base Cases

(a)

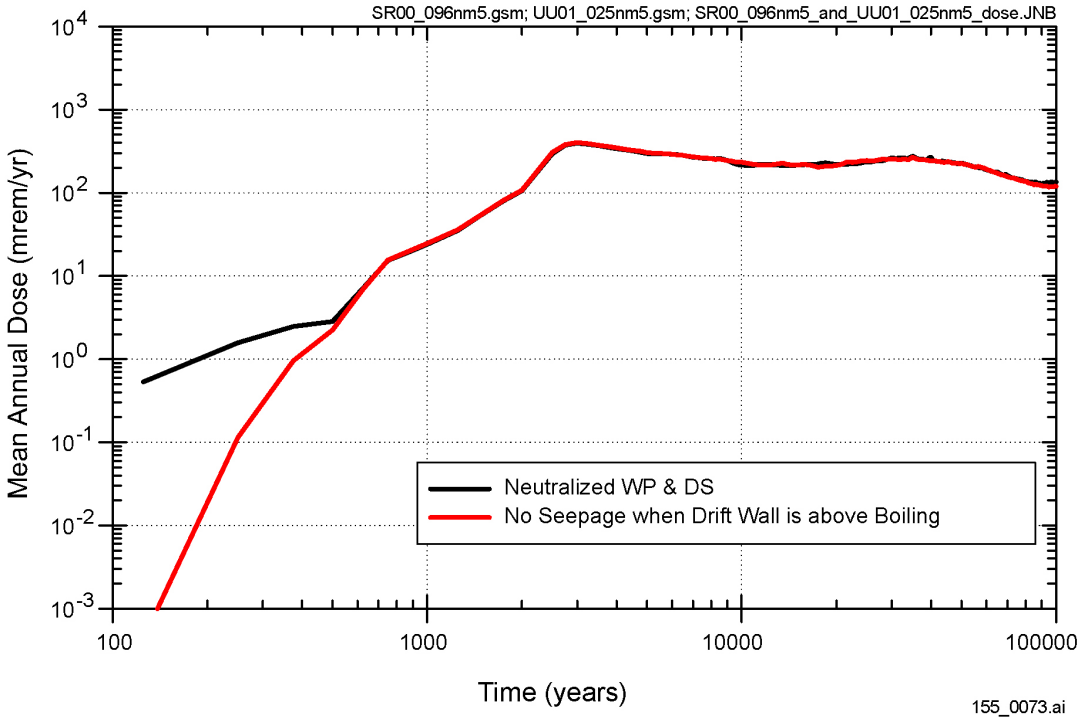

(b)

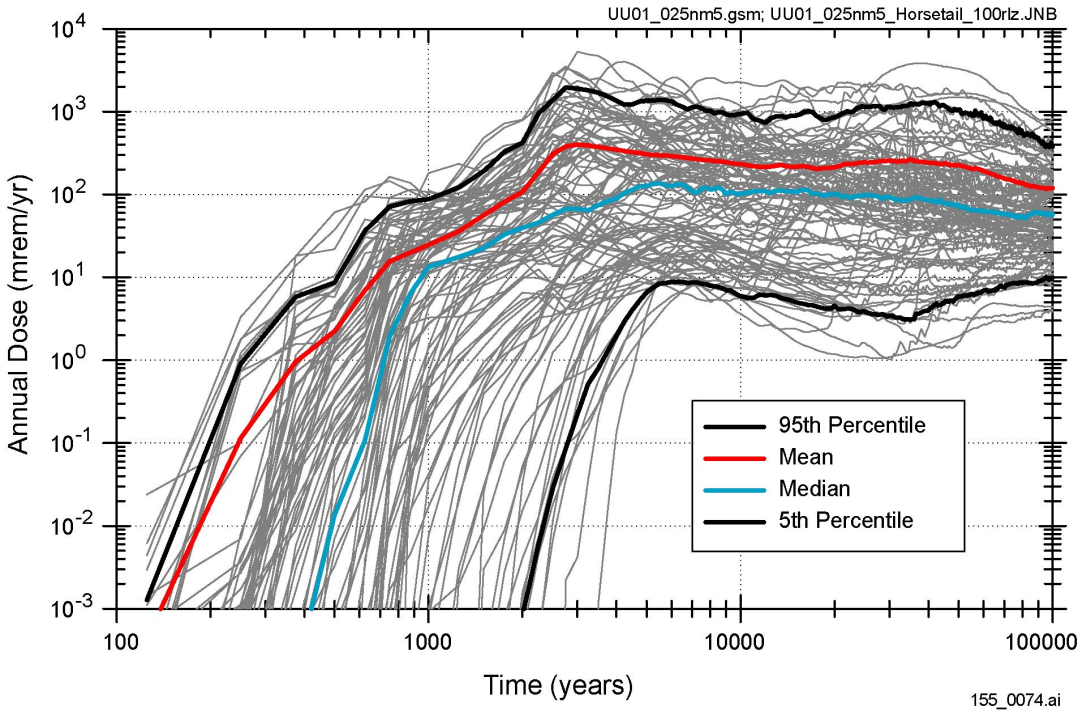

155_0073.ai / 155_0074.ai

NOTE: (a) Comparison of two cases. (b) All realizations and statistics for the case with no seepage during the boiling period. WP = waste package. DS = drip shield.

Figure 3.2.2-9. Annual Dose Histories with and without Seepage during the Boiling Period for the Case with Neutralized Waste Packages and Drip Shields

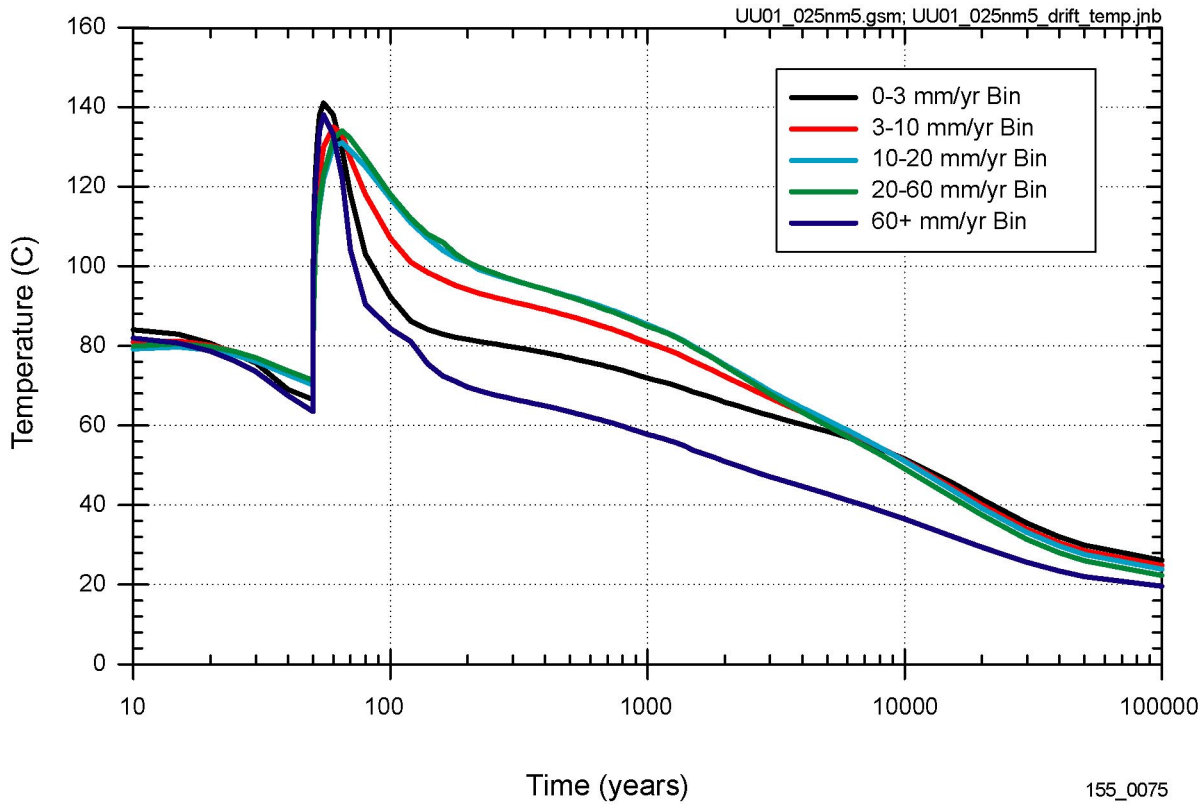

155_0075

NOTE: Curves apply to base case and sensitivity cases.

Figure 3.2.2-10. Bin-Averaged Drift-Wall Temperature for Commercial Spent Nuclear Fuel in the Medium-Infiltration Case

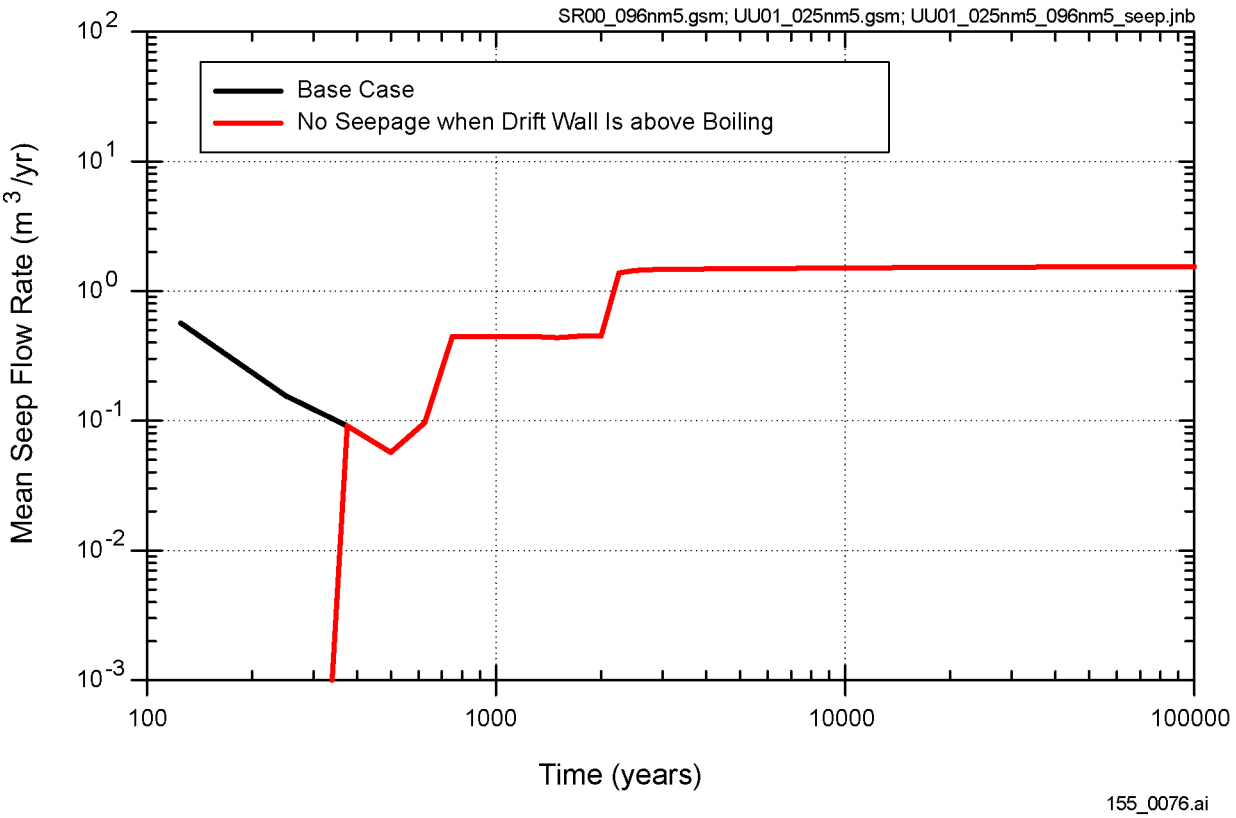

155_0076.ai

NOTE: CSNF, 20 to 60 mm/yr infiltration. Seepage some of the time.

Figure 3.2.2-11. Comparison of Seepage Models (TSPA-SR Base-Case and Alternate Seepage Models) for the Case with Neutralized Waste Packages and Drip Shields

(a)

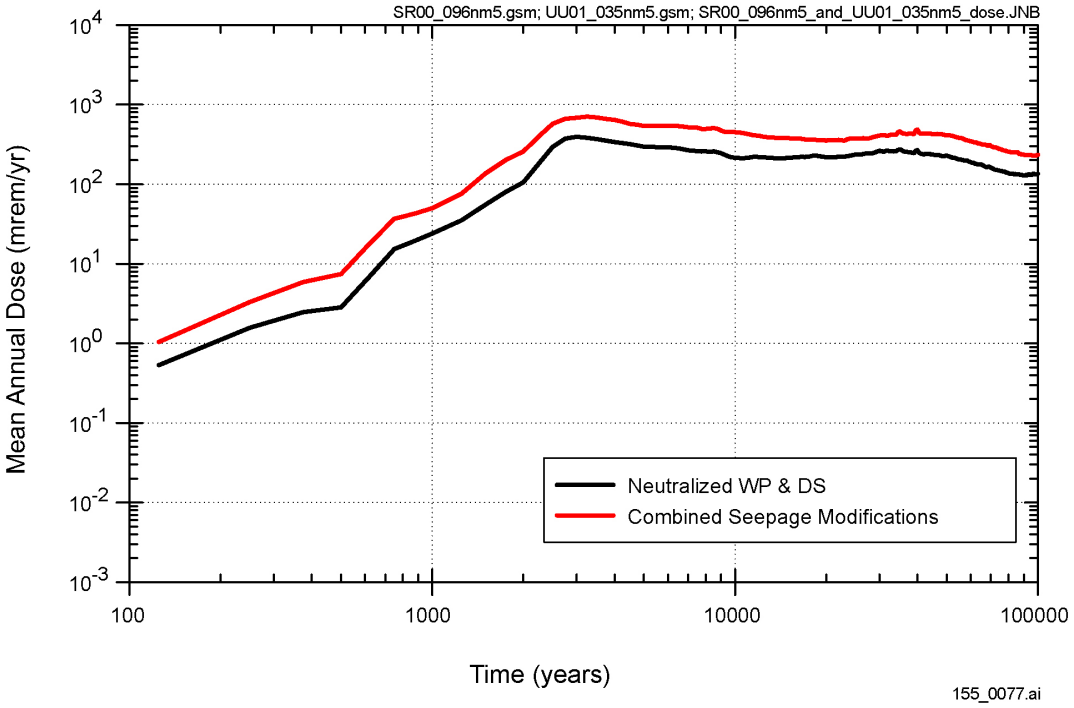

(b)

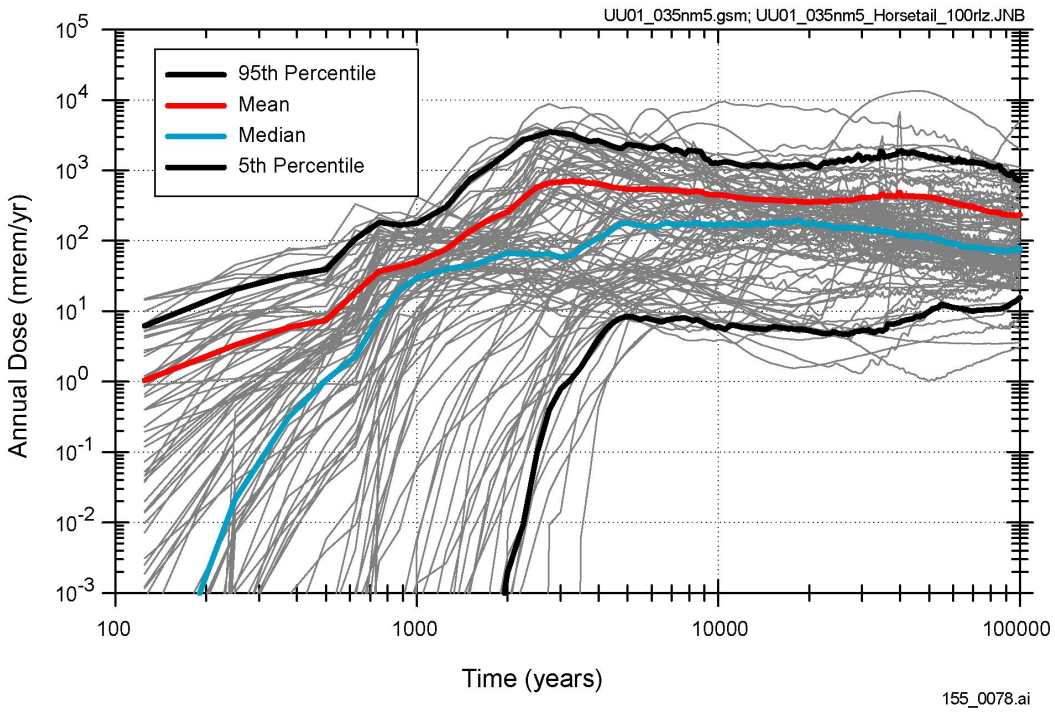

155_0077.ai / 155_0078.ai

NOTE: (a) Comparison of two cases. (b) All realizations and statistics for the case with combined seepage modifications. WP = waste package. DS = drip shield.

Figure 3.2.2-12. Annual Dose Histories with the Combined Seepage Modifications and the Base-Case Seepage Model for the Case with Neutralized Waste Packages and Drip Shields

(a)

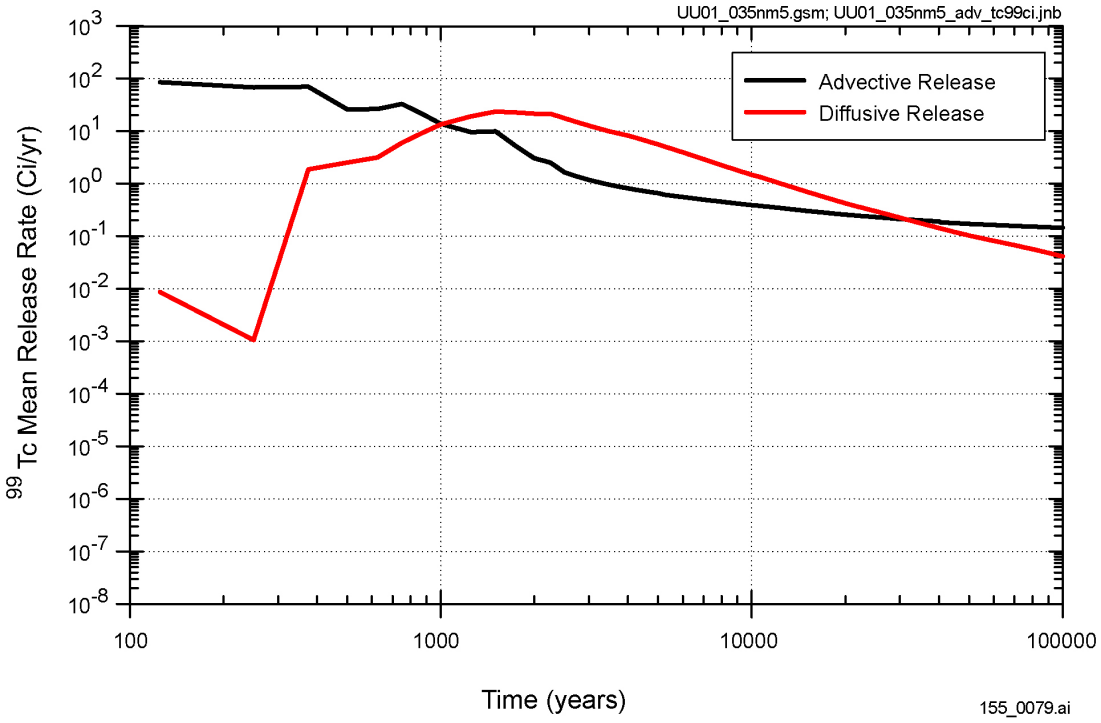

(b)

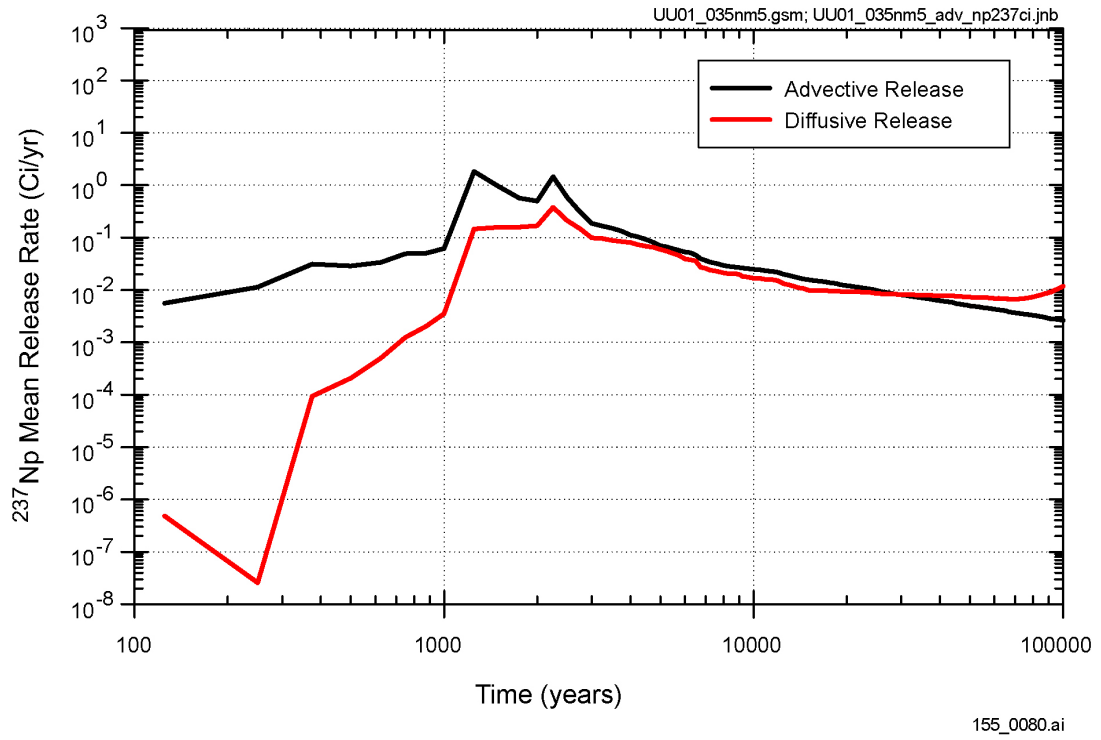

155_0079.ai / 155_0080.ai

NOTE: Release rates for CSNF. (a) Technetium (^{99}Tc). (b) Neptunium (^{237}Np).

Figure 3.2.2-13. Advective and Diffusive Releases from the Engineered Barrier System with the Combined Seepage Modifications

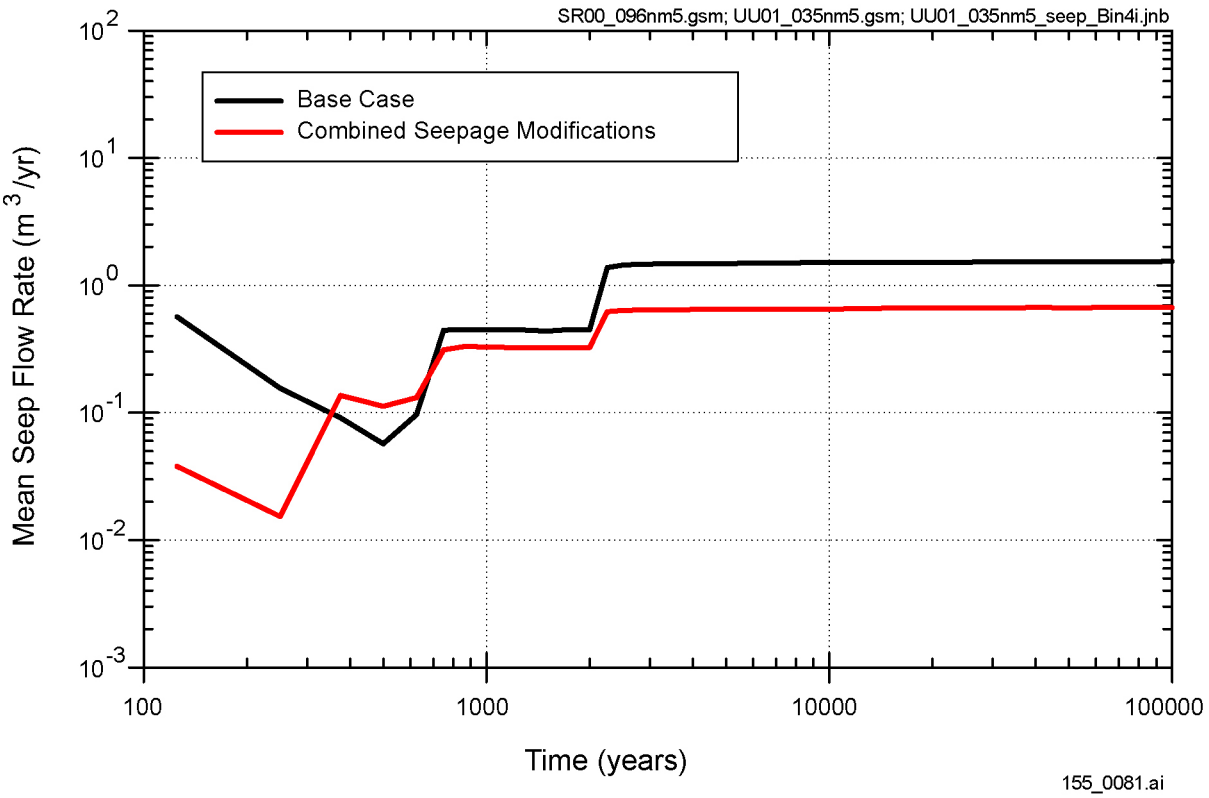

155_0081.ai

NOTE: CSNF, 20 to 60 mm/yr infiltration. Seepage some of the time.

Figure 3.2.2-14. Comparison of Seepage with the Combined Seepage Modifications and the Base-Case Seepage Model

(a)

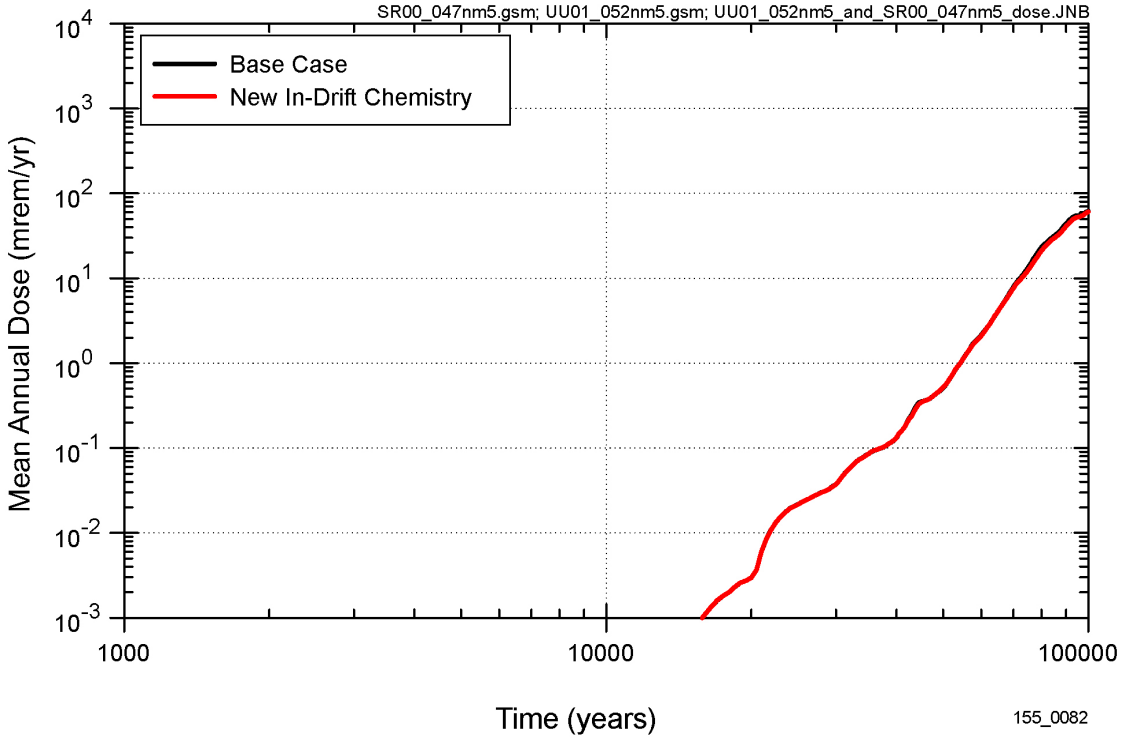

(b)

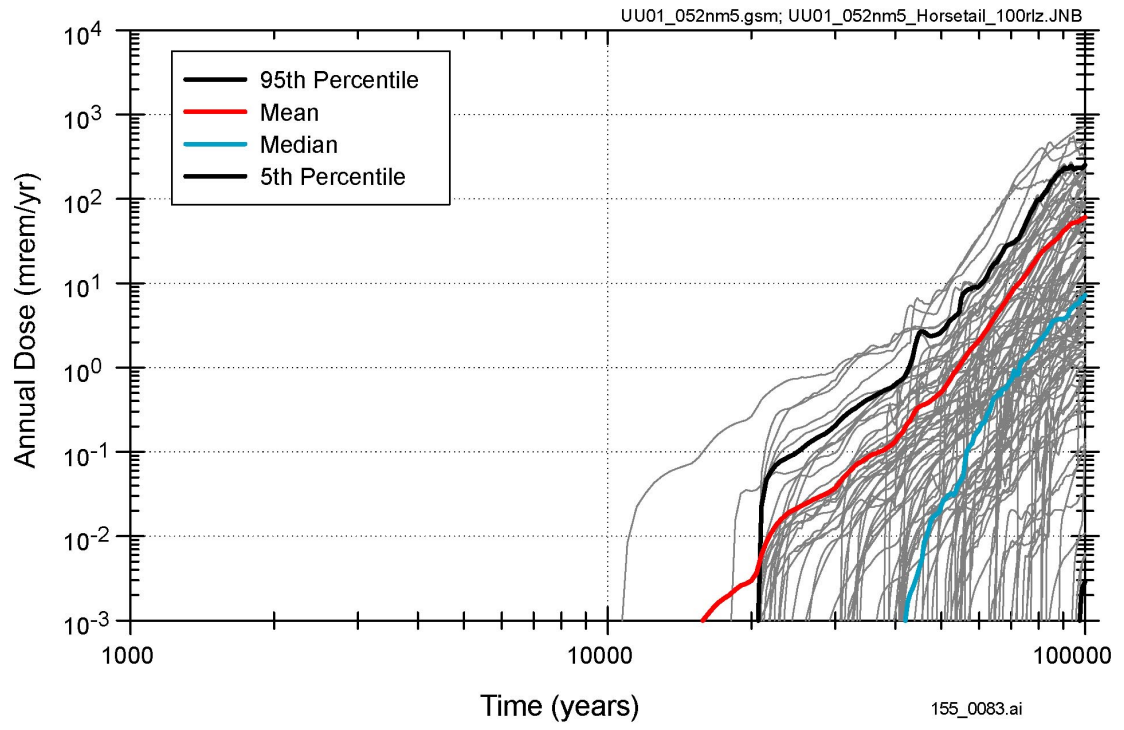

155_0082 / 155_0083.ai

NOTE: (a) Comparison of one-off sensitivity analysis with the mean annual dose calculated with the TSPA-SR base-case model. (b) Range of the results for all realizations for the one-off sensitivity analysis.

Figure 3.2.4-1. Sensitivity of Annual Dose to Uncertainty in In-Drift Chemistry

(a)

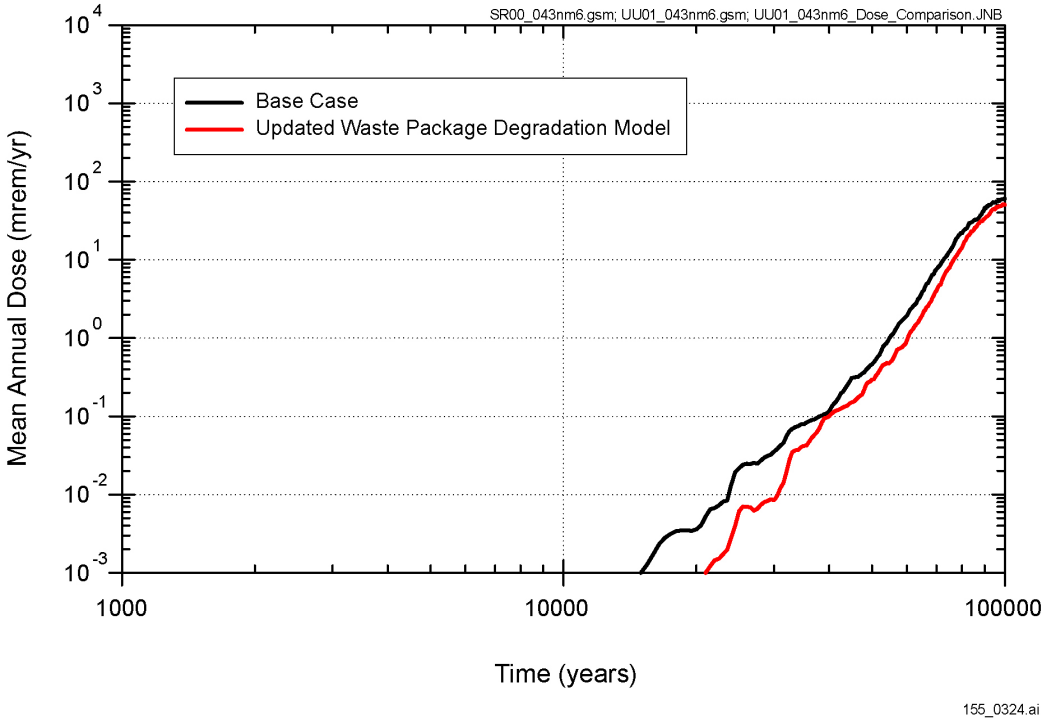

(b)

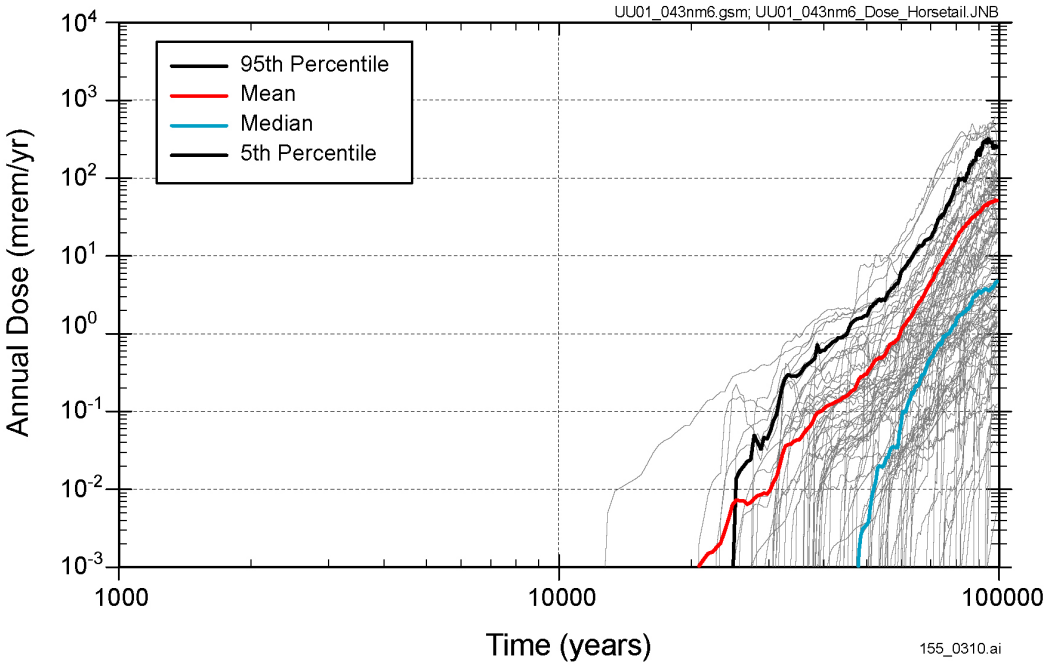

155_0324.ai / 155_0310.ai

NOTE: (a) Comparison of results with the updated waste-package degradation model with the mean annual dose calculated with the TSPA-SR base-case model. (b) Range of the results for all realizations for the analysis with the updated waste package degradation model.

Figure 3.2.5-1. Effect of Updates in the Waste Package Degradation Model on the Estimate of Annual Dose

(a)

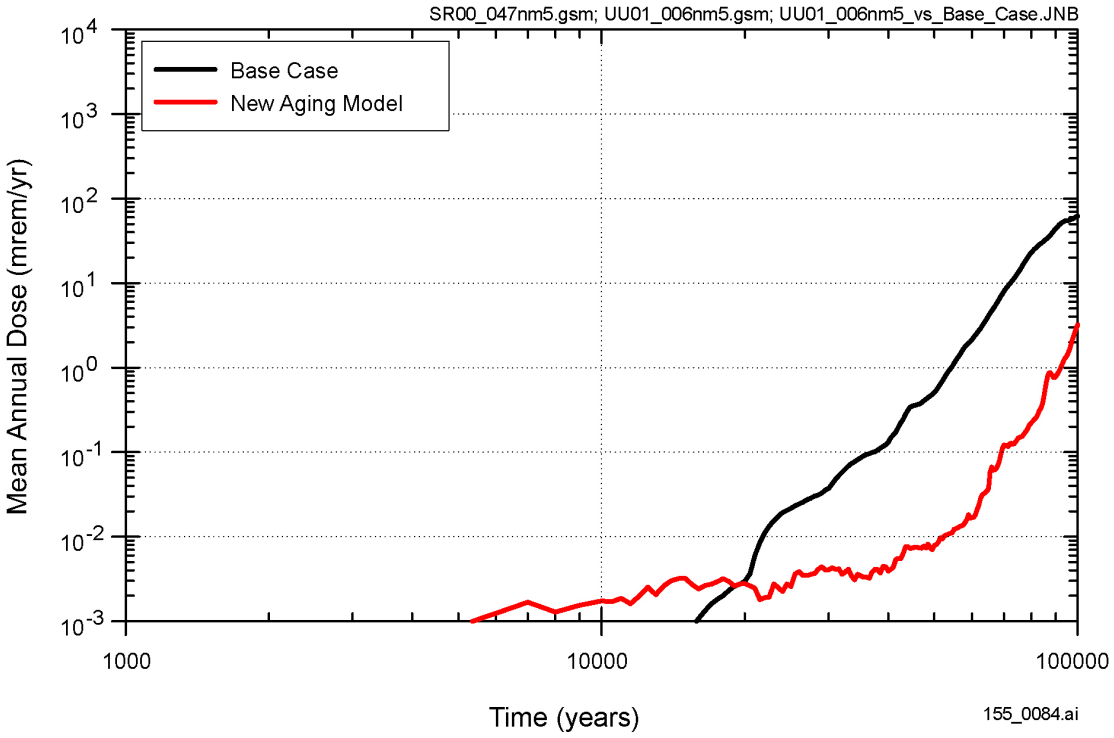

(b)

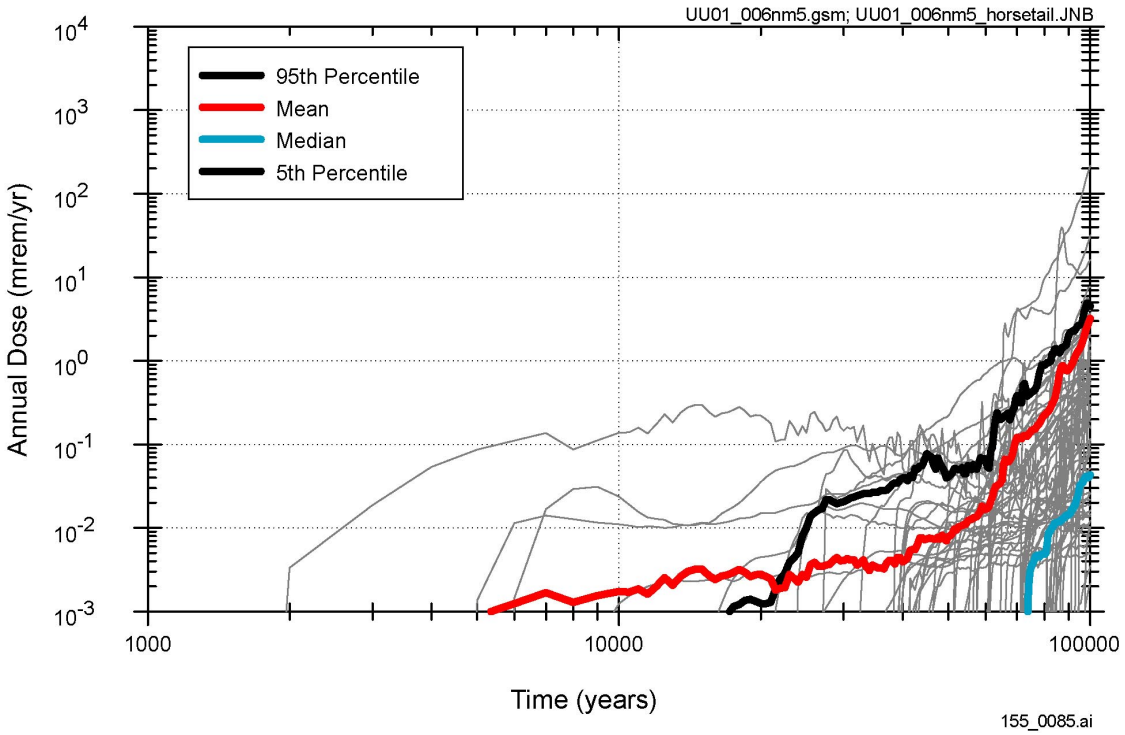

155_0084.ai / 155_0085.ai

NOTE: (a) Comparison of one-off sensitivity analysis with the mean annual dose calculated with the TSPA-SR base-case model. (b) Range of the results for all realizations for the one-off sensitivity analysis.

Figure 3.2.5.1-1. Sensitivity of Annual Dose to the Model for Aging of Alloy 22

(a)

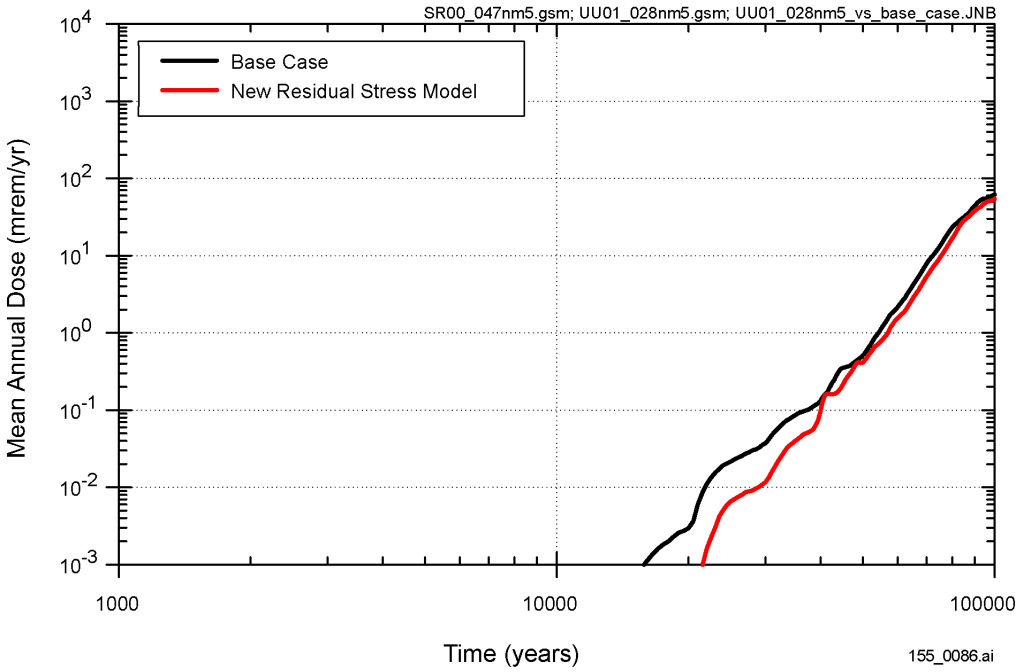

(b)

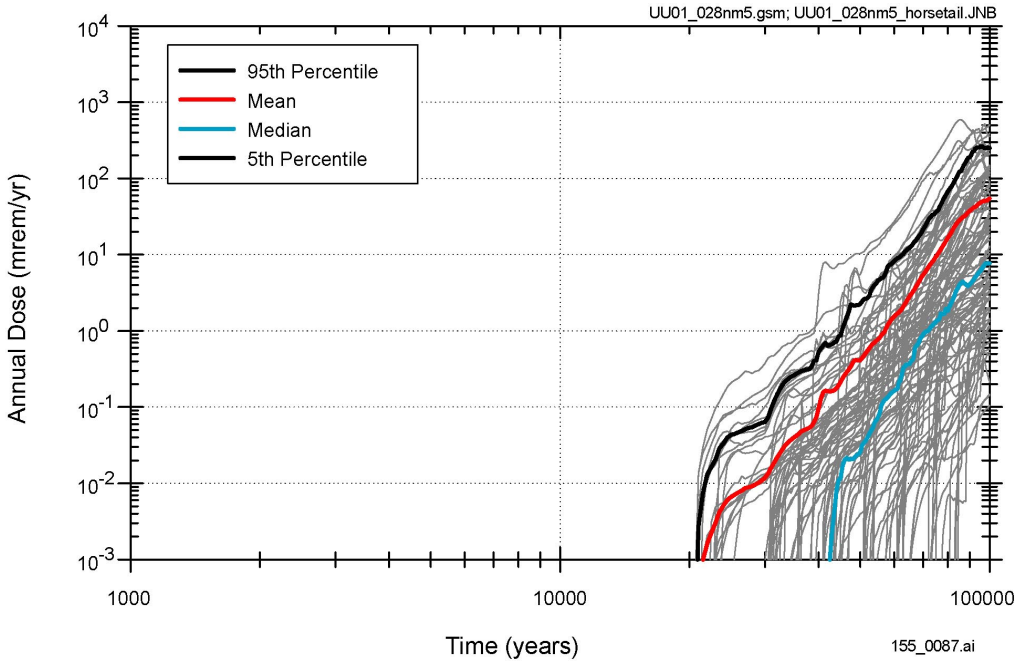

155_0086.ai / 155_0087.ai

NOTE: (a) Comparison of one-off sensitivity analysis with the mean annual dose calculated with the TSPA-SR base-case model. (b) Range of the results for all realizations for the one-off sensitivity analysis.

Figure 3.2.5.2-1. Sensitivity of Annual Dose to Additional Uncertainties Associated with Residual Stress Profile and Effect on Alloy 22 Stress Corrosion Cracking

(a)

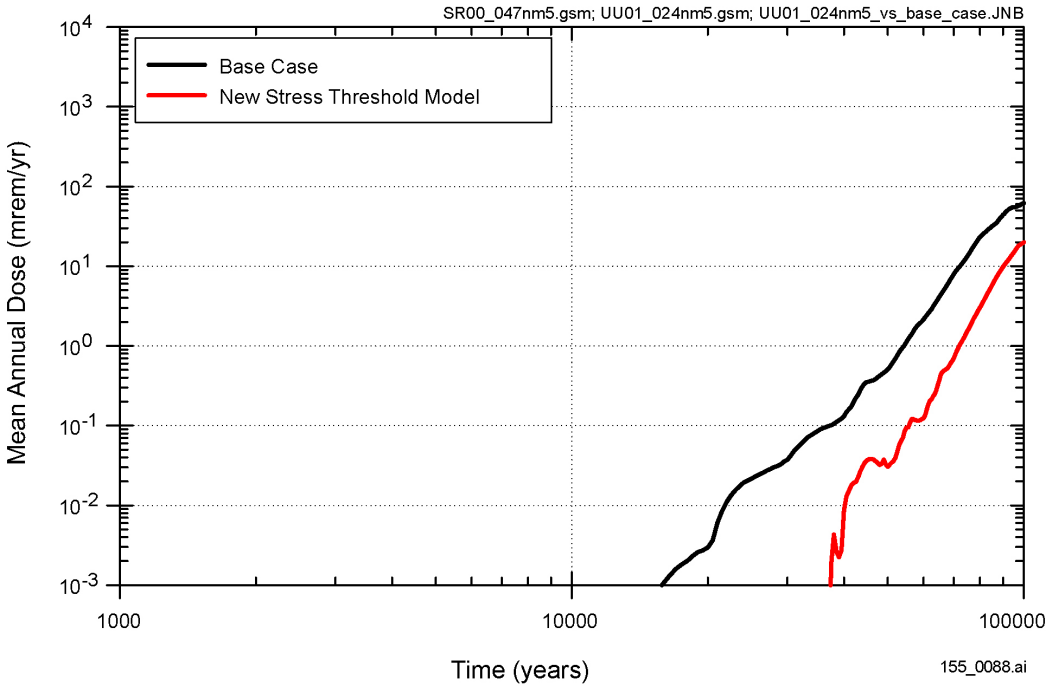

(b)

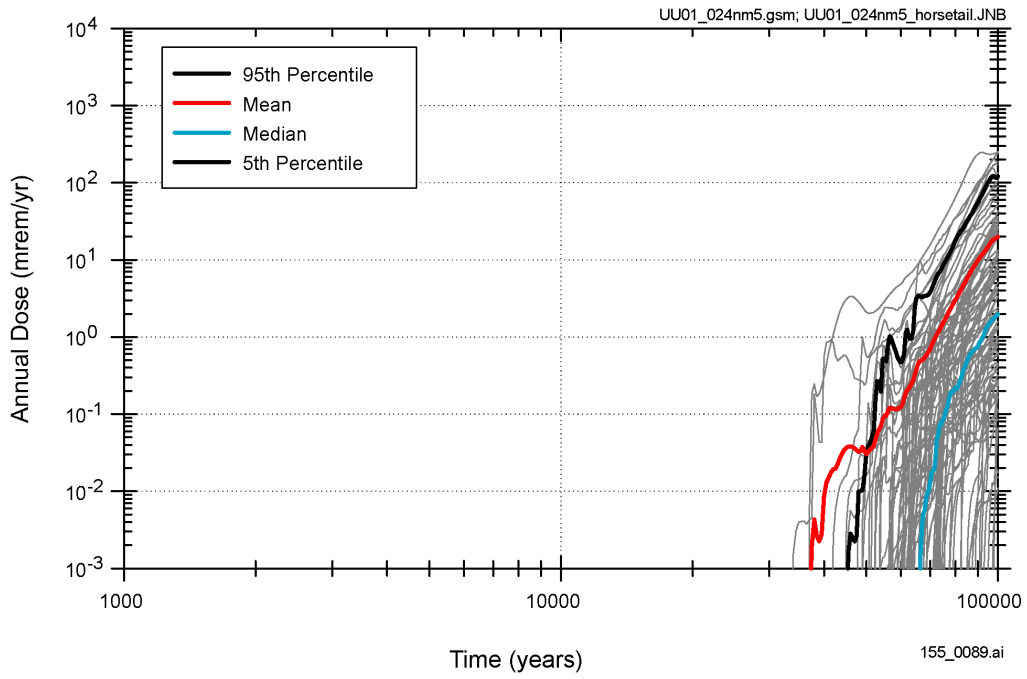

155_0088.ai / 155_0089.ai

NOTE: (a) Comparison of one-off sensitivity analysis with the mean annual dose calculated with the TSPA-SR base-case model. (b) Range of the results for all realizations for the one-off sensitivity analysis.

Figure 3.2.5.2-2. Sensitivity of Annual Dose to Additional Uncertainties Associated with Stress Initiation and Effect on Alloy 22 Stress Corrosion Cracking

(a)

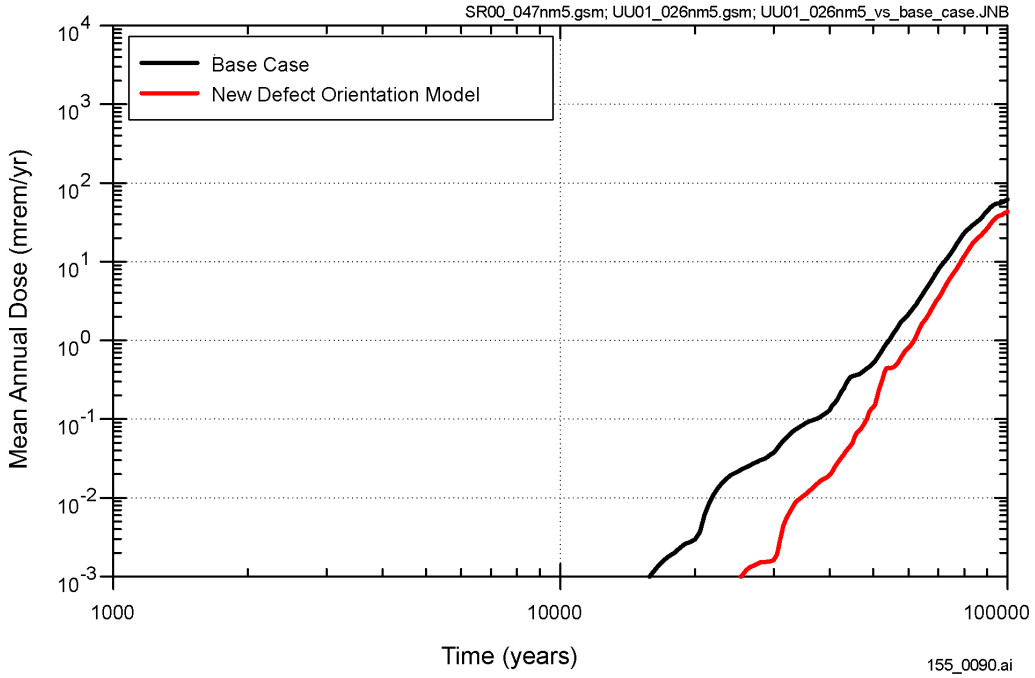

(b)

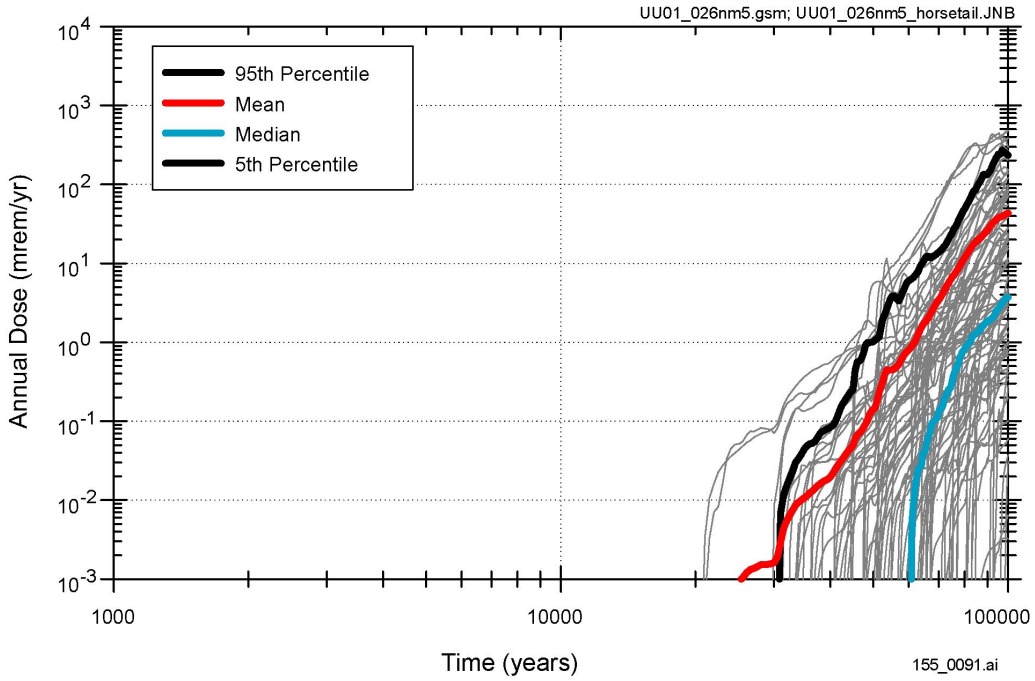

155_0090.ai / 155_0091.ai

NOTE: (a) Comparison of one-off sensitivity analysis with the mean annual dose calculated with the TSPA-SR base-case model. (b) Range of the results for all realizations for the one-off sensitivity analysis.

Figure 3.2.5.2-3. Sensitivity of Annual Dose to Additional Uncertainties Associated with Defect Orientation and Effect on Alloy 22 Stress Corrosion Cracking

(a)

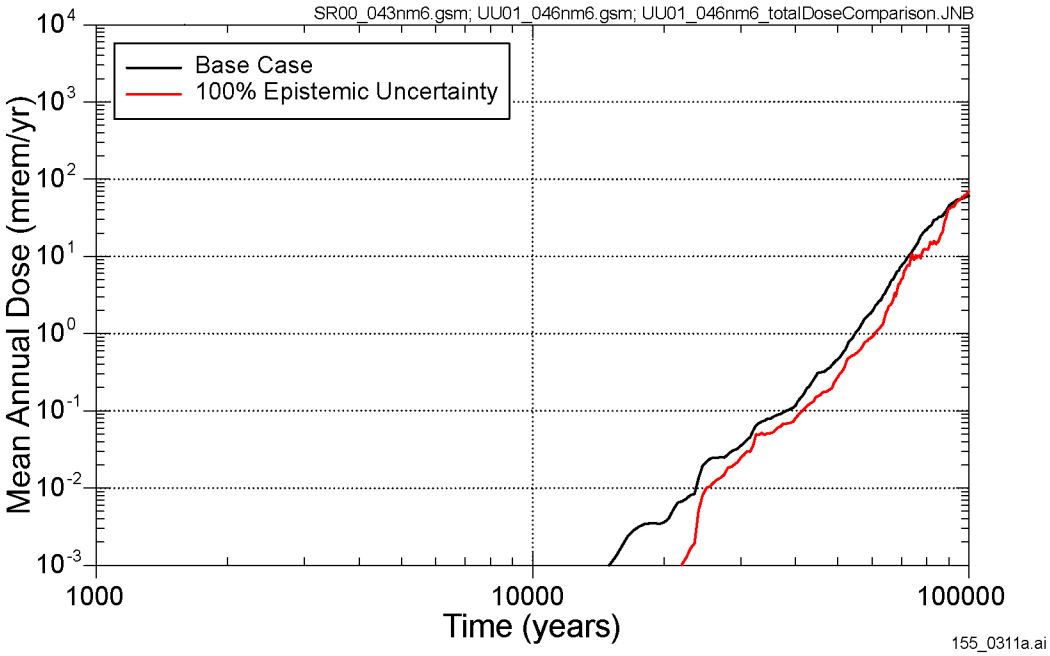

(b)

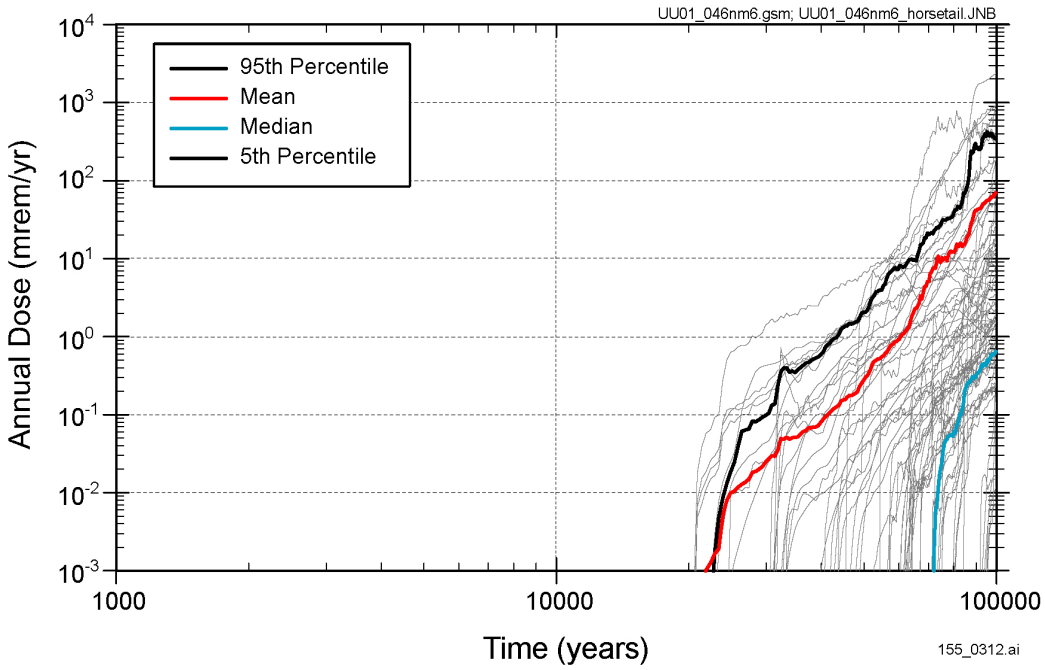

155_0311a.ai / 155_0312.ai

NOTE: (a) Comparison of one-off sensitivity analysis with the mean annual dose calculated with the TSPA-SR base-case model. (b) Range of the results for all realizations for the one-off sensitivity analysis.

Figure 3.2.5.3-1. Sensitivity of Annual Dose to Partitioning of Uncertainty in General Corrosion

(a)

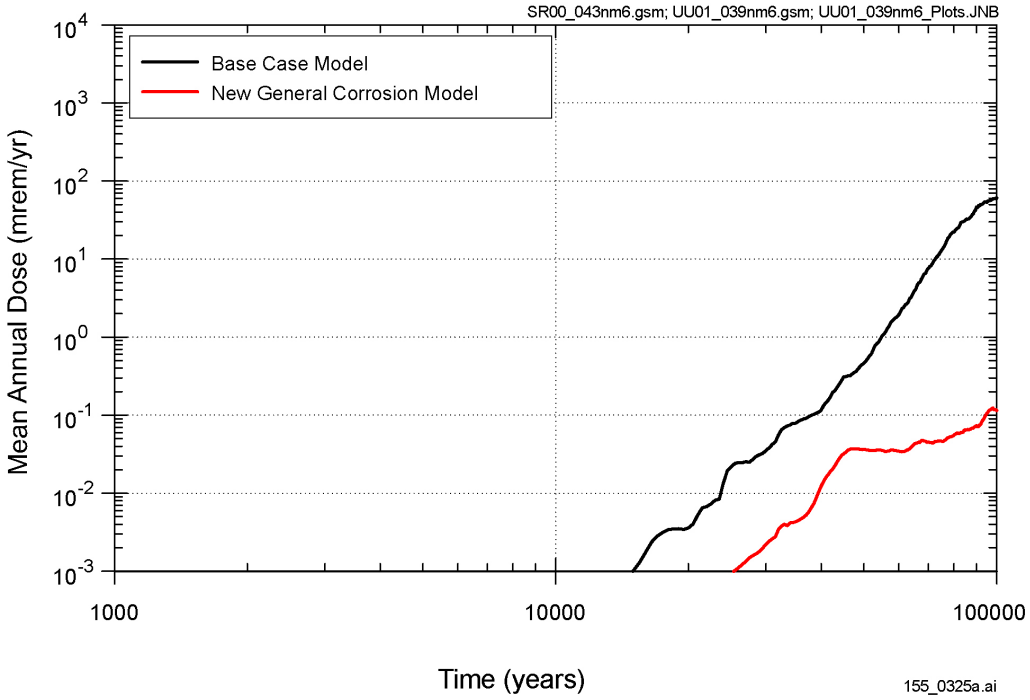

(b)

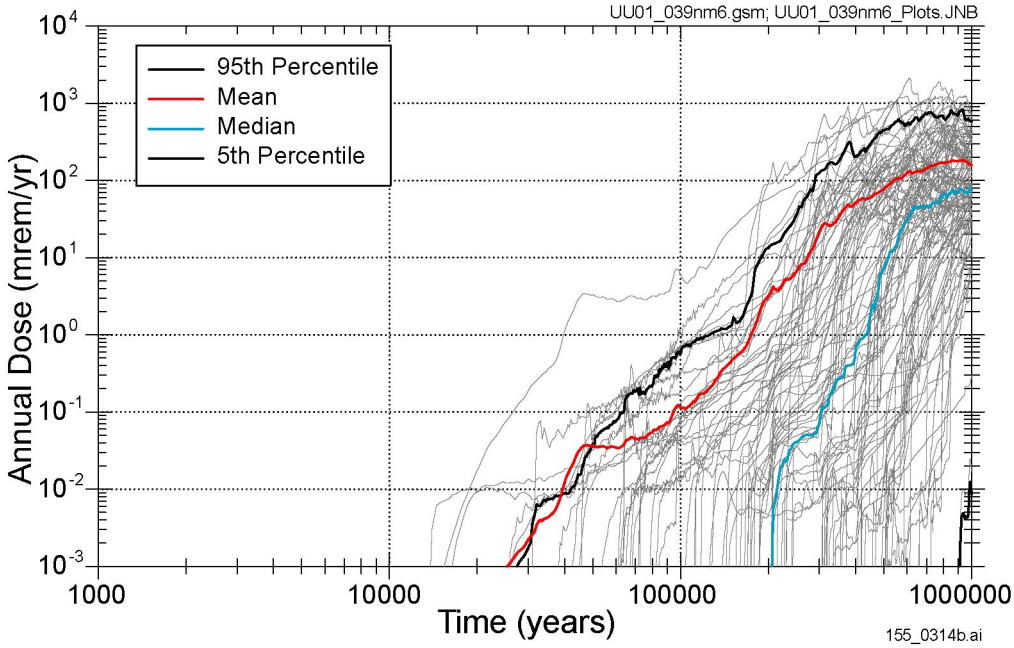

155_0325a.ai / 155_0314b.ai

NOTE: (a) Comparison of one-off sensitivity analysis with the mean annual dose calculated with the TSPA-SR base-case model. (b) Range of the results for all realizations for the one-off sensitivity analysis.

Figure 3.2.5.3-2. Sensitivity of Annual Dose to Treatment of Temperature Dependence of Alloy 22 General Corrosion

(a)

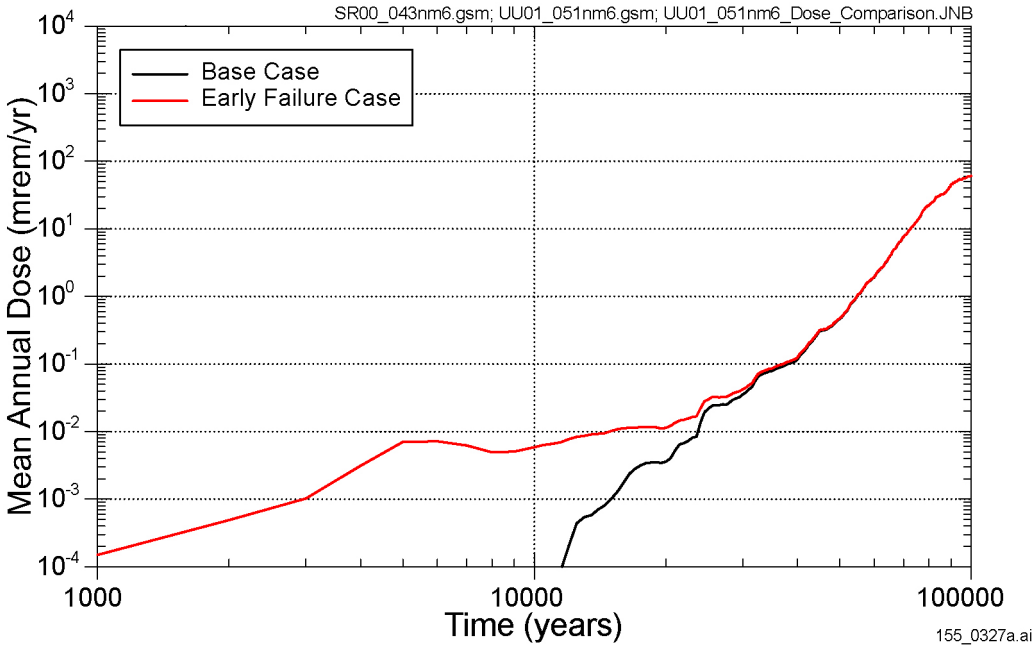

(b)

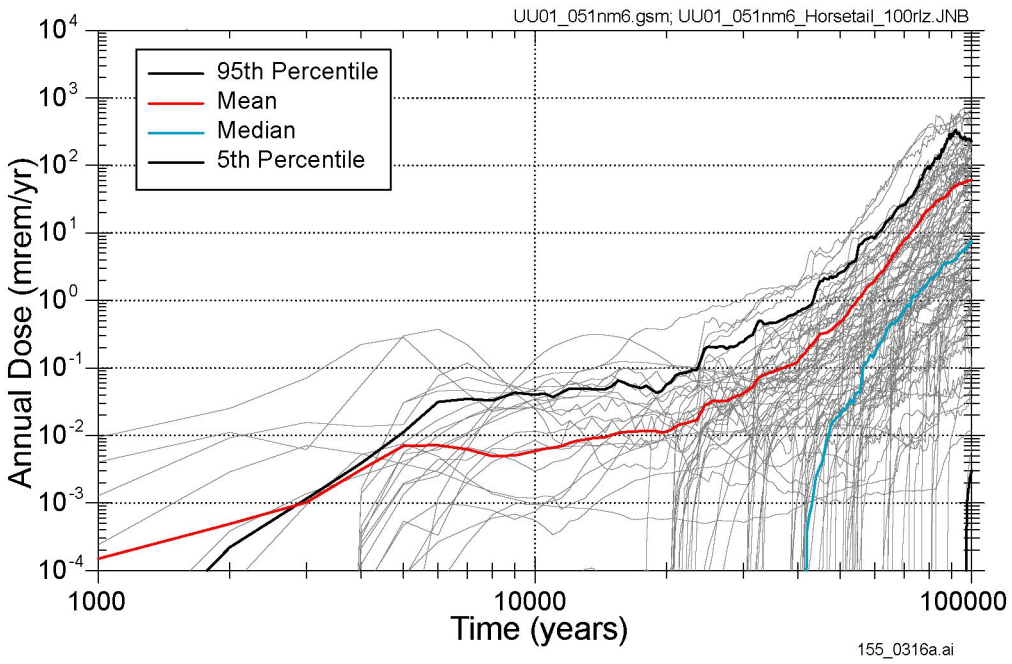

155_0327a.ai / 155_0316a.ai

NOTE: (a) Comparison of one-off sensitivity analysis with the mean annual dose calculated with the TSPA-SR base-case model. (b) Range of the results for all realizations for the one-off sensitivity analysis.

Figure 3.2.5.4-1. Sensitivity of Annual Dose to Additional Uncertainties Associated with Early Waste Package Failure Due to Improper Heat Treatment

(a)

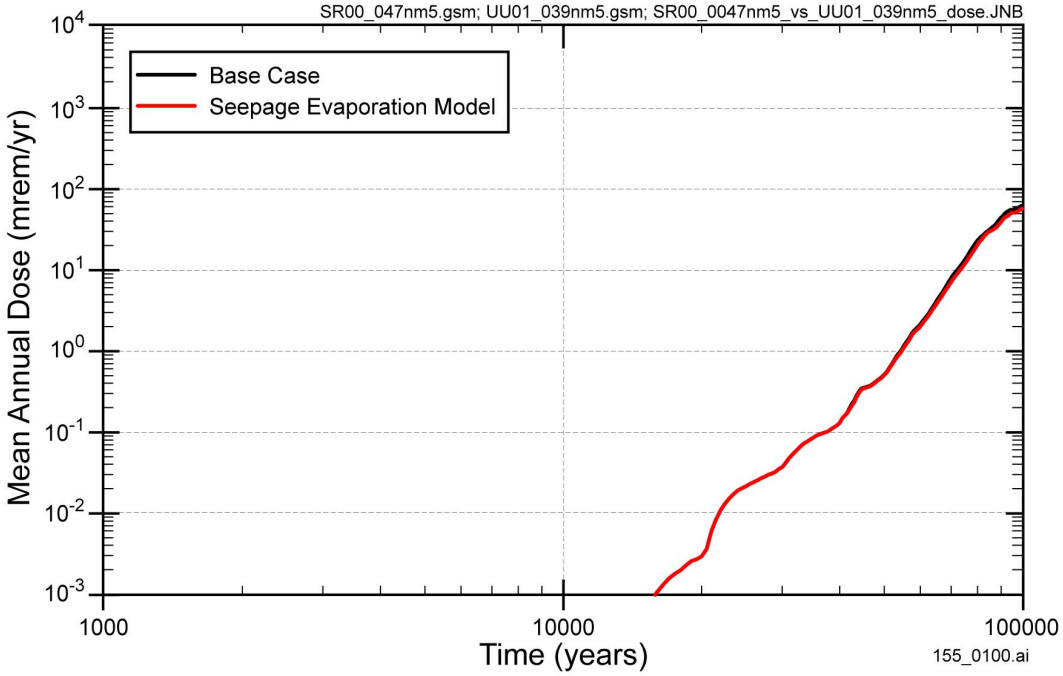

(b)

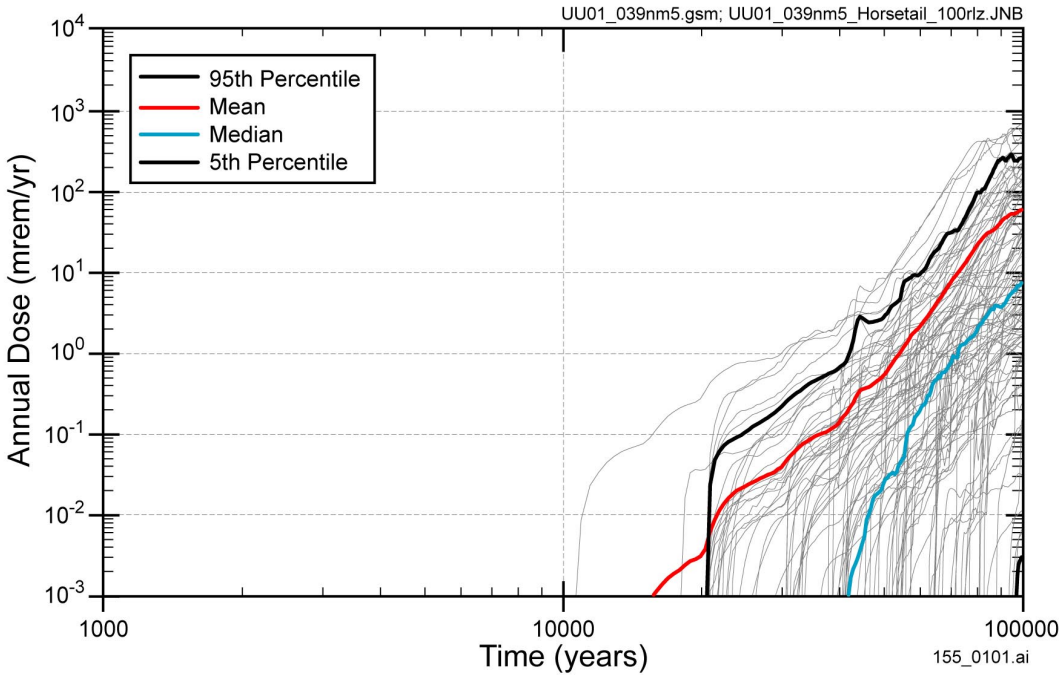

155_0100.ai / 155_0101.ai

NOTE: (a) Comparison of one-off sensitivity analysis with the mean annual dose calculated with the TSPA-SR base-case model. (b) Range of the results for all realizations for the one-off sensitivity analysis.

Figure 3.2.6.1-1. Sensitivity of Annual Dose to Uncertainties Associated with Evaporation of Seepage in the Engineered Barrier System

(a)

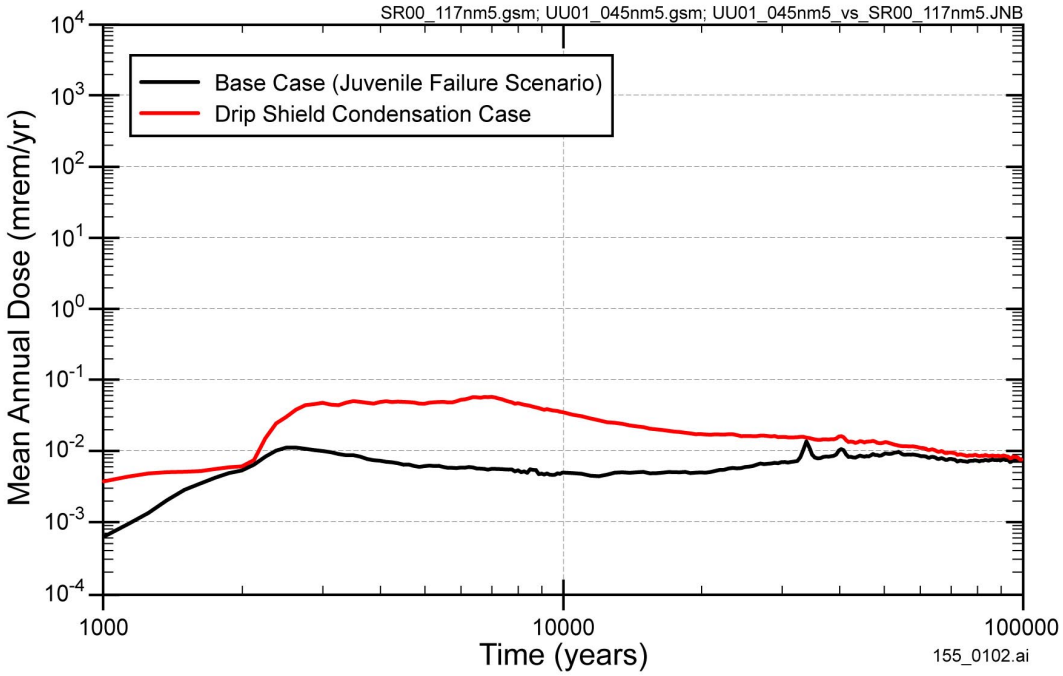

(b)

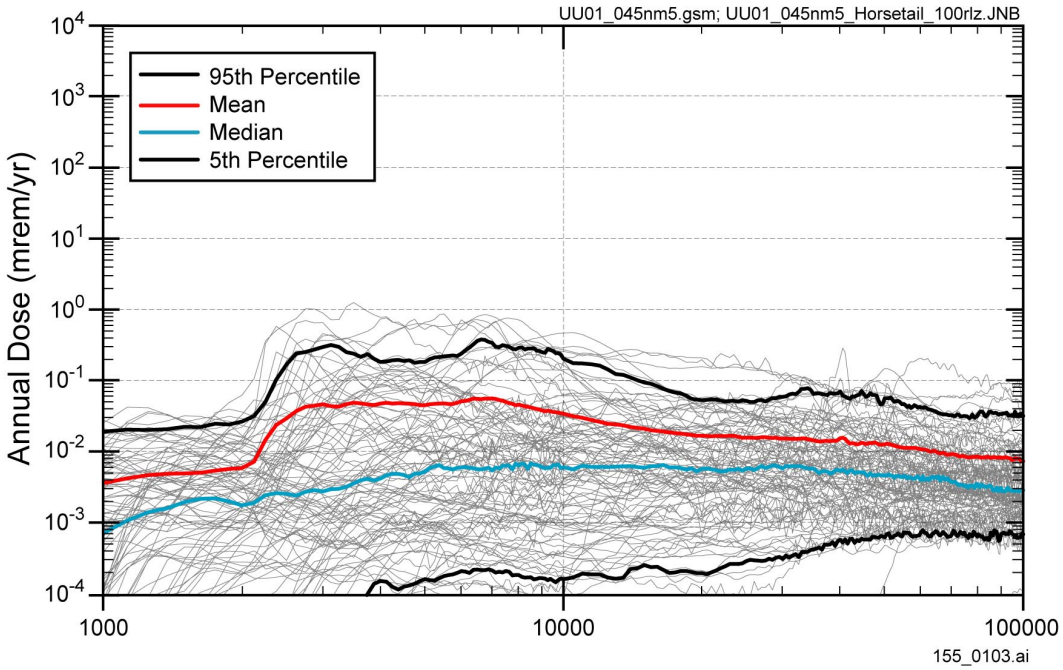

155_0102.ai / 155_0103.ai

NOTE: (a) Comparison of one-off sensitivity analysis with the mean annual dose calculated with the TSPA-SR base-case model. (b) Range of the results for all realizations for the one-off sensitivity analysis.

Figure 3.2.6.2-1. Sensitivity of Annual Dose to Uncertainties Associated with Condensation on the Under-Side of the Drip Shield

(a)

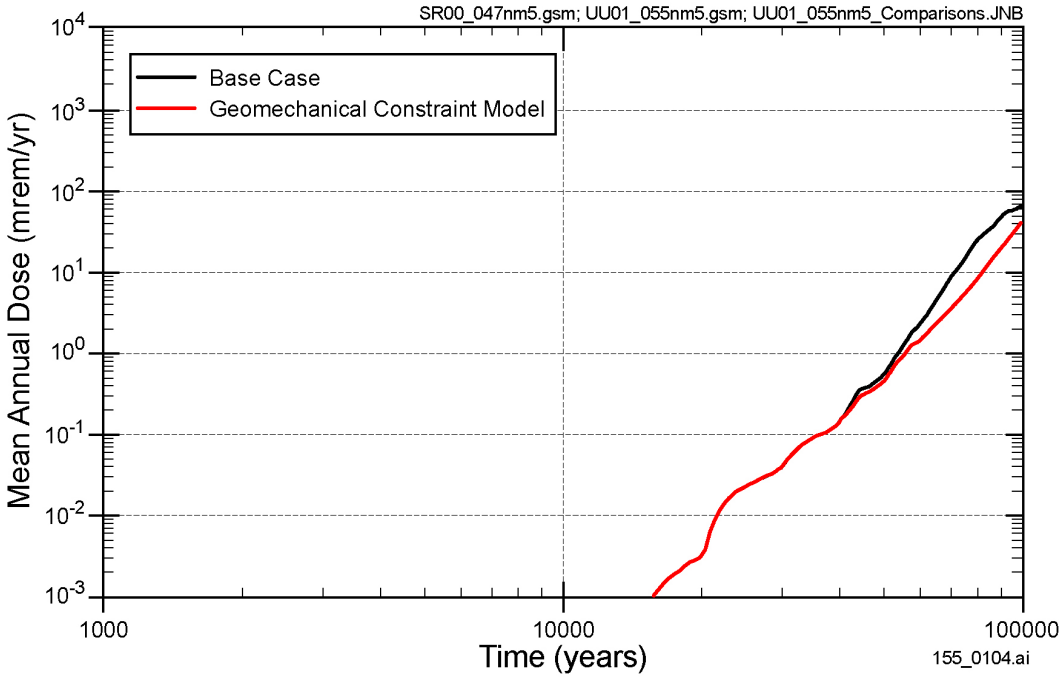

(b)

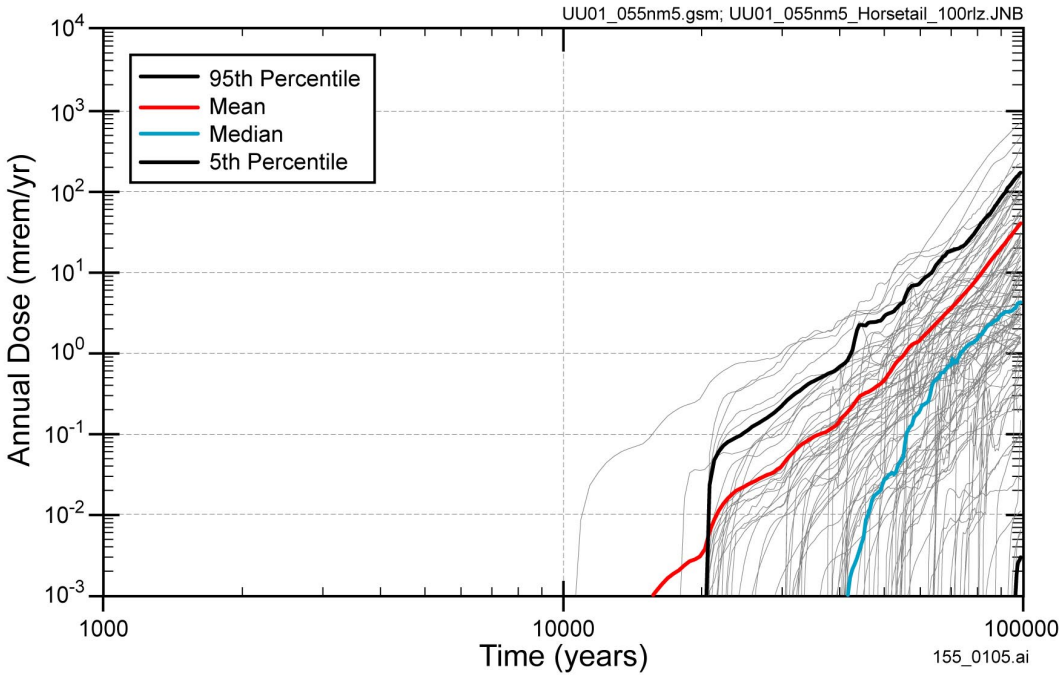

155_0104.ai / 155_0105.ai

NOTE: (a) Comparison of one-off sensitivity analysis with the mean annual dose calculated with the TSPA-SR base-case model. (b) Range of the results for all realizations for the one-off sensitivity analysis.

Figure 3.2.6.3-1. Sensitivity of Annual Dose to Geometry of Breaches in the Drip Shield and Waste Package

(a)

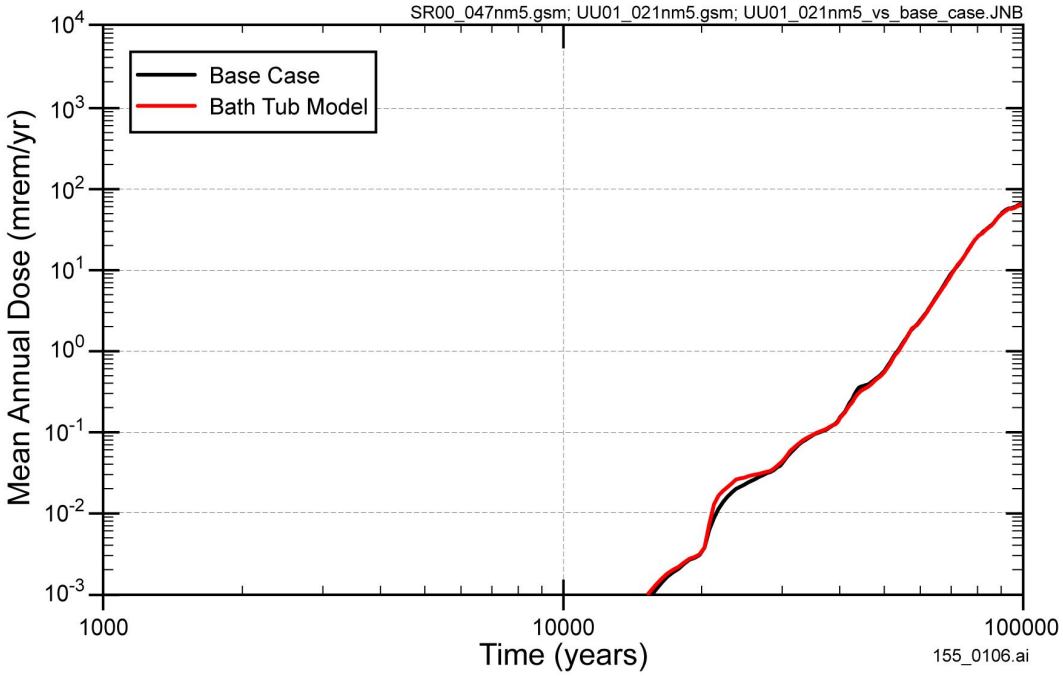

(b)

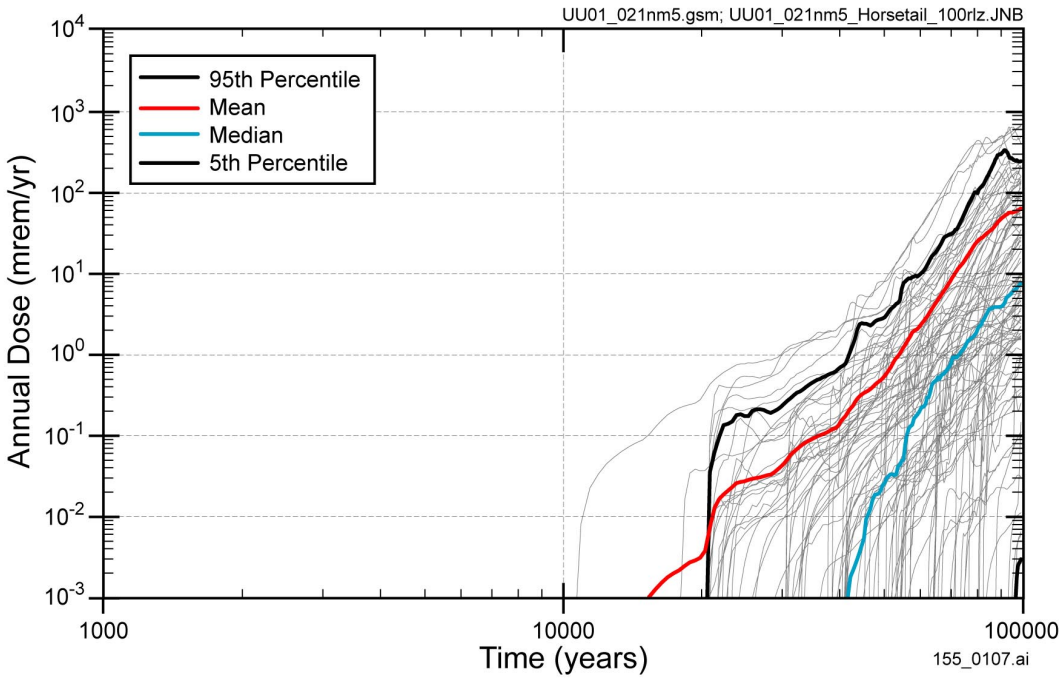

155_0106.ai / 155_0107.ai

NOTE: (a) Comparison of one-off sensitivity analysis with the mean annual dose calculated with the TSPA-SR base-case model. (b) Range of the results for all realizations for the one-off sensitivity analysis.

Figure 3.2.6.4-1. Sensitivity of Annual Dose to Timing of Breaches in Bottom and Top of Waste Package (Bathtub Effect)

(a)

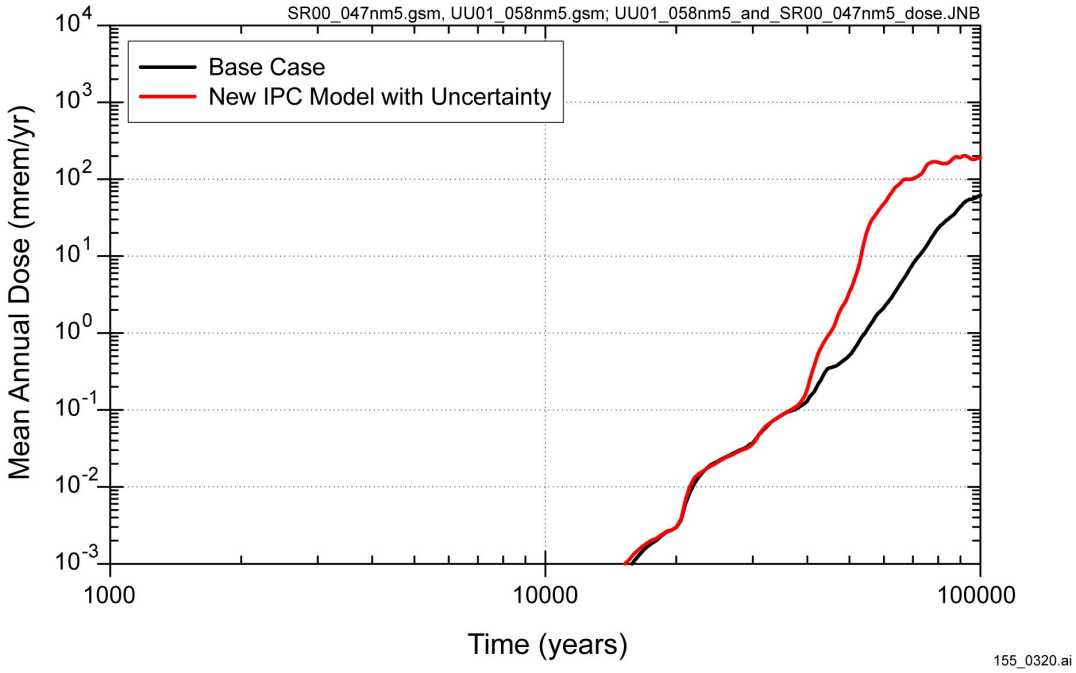

(b)

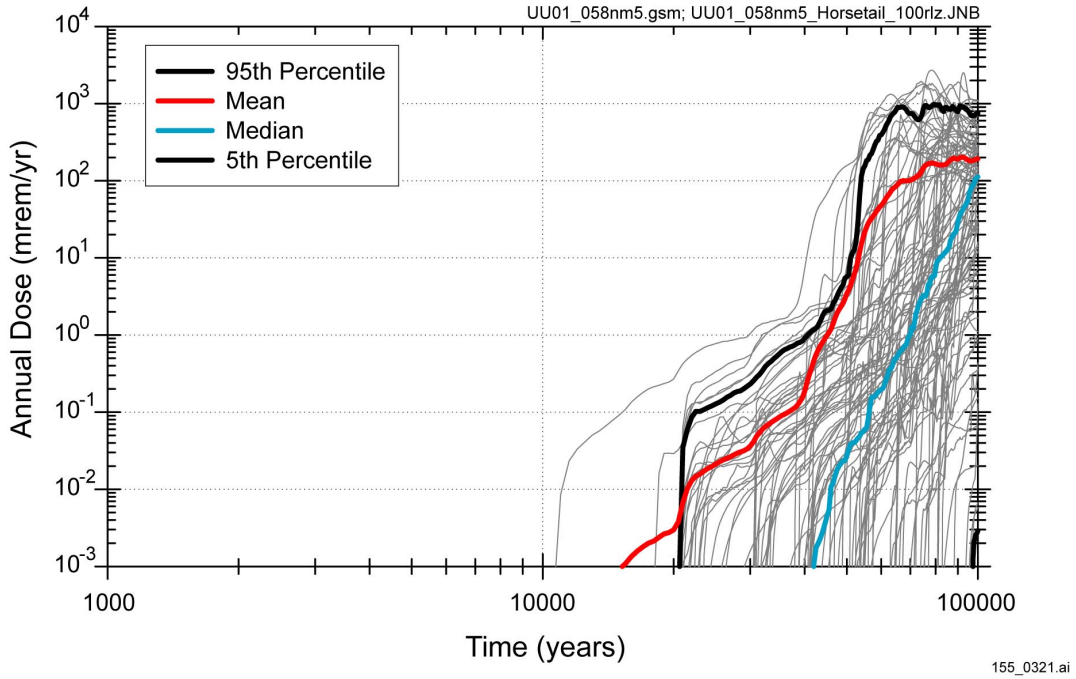

155_0320.ai / 155_0321.ai

NOTE: (a) Comparison of one-off sensitivity analysis with the mean annual dose calculated with the TSPA-SR base-case model. (b) Range of the results for all realizations for the one-off sensitivity analysis. IPC = in-package chemistry.

Figure 3.2.7.1-1. Supplemental Analyses of Effect of In-Package Chemistry Radionuclide Solubility Limits

(a)

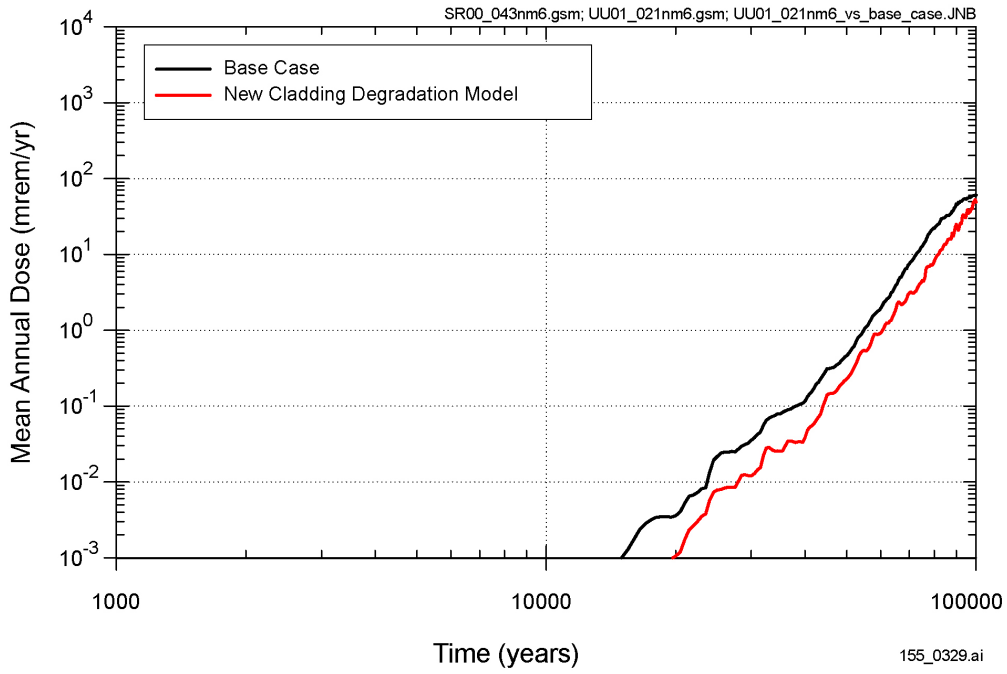

(b)

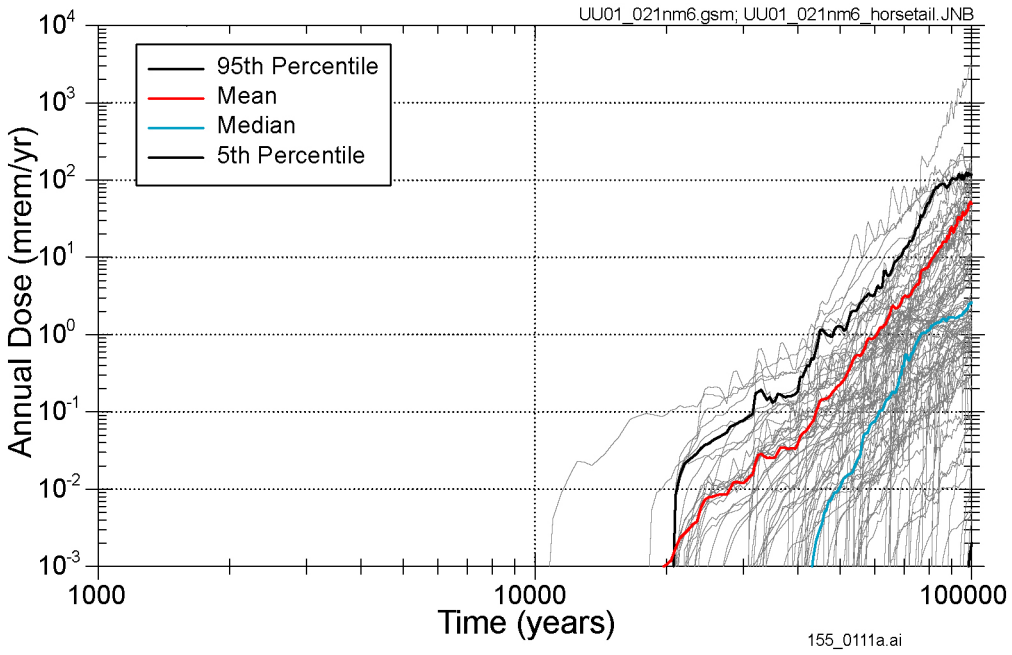

155_0329.ai / 155_0111a.ai

NOTE: (a) Comparison of one-off sensitivity analysis results with the mean annual dose calculated with the TSPA-SR base-case model. (b) Range of the results for all realizations for the one-off sensitivity analysis.

Figure 3.2.7.2-1. Supplemental Analyses of Commercial Spent Nuclear Fuel Cladding Degradation

(a)

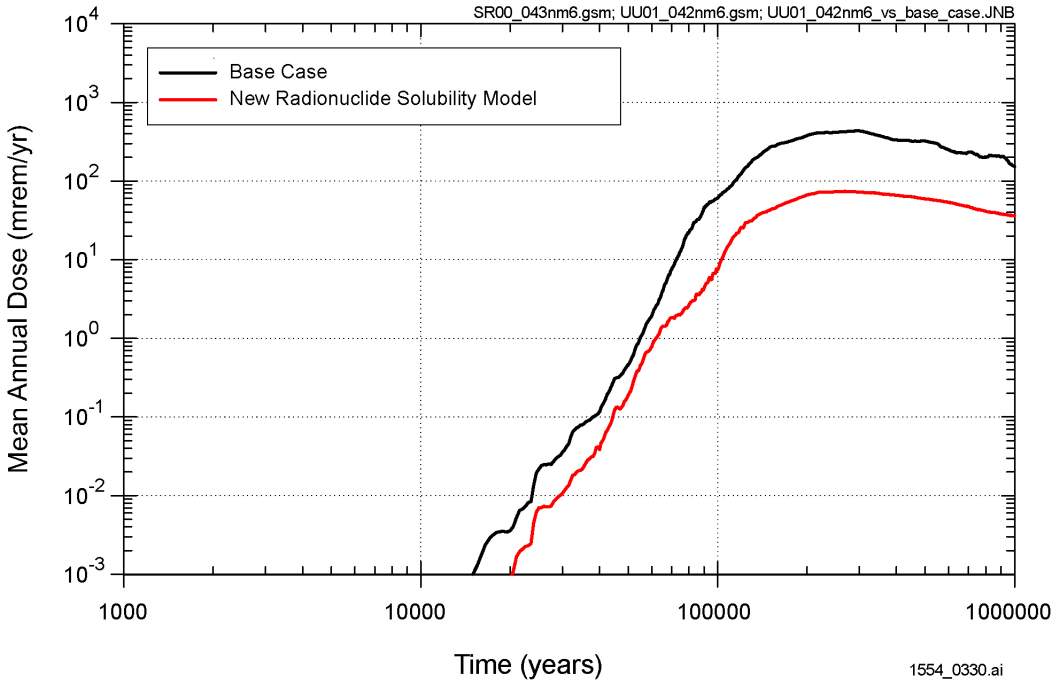

(b)

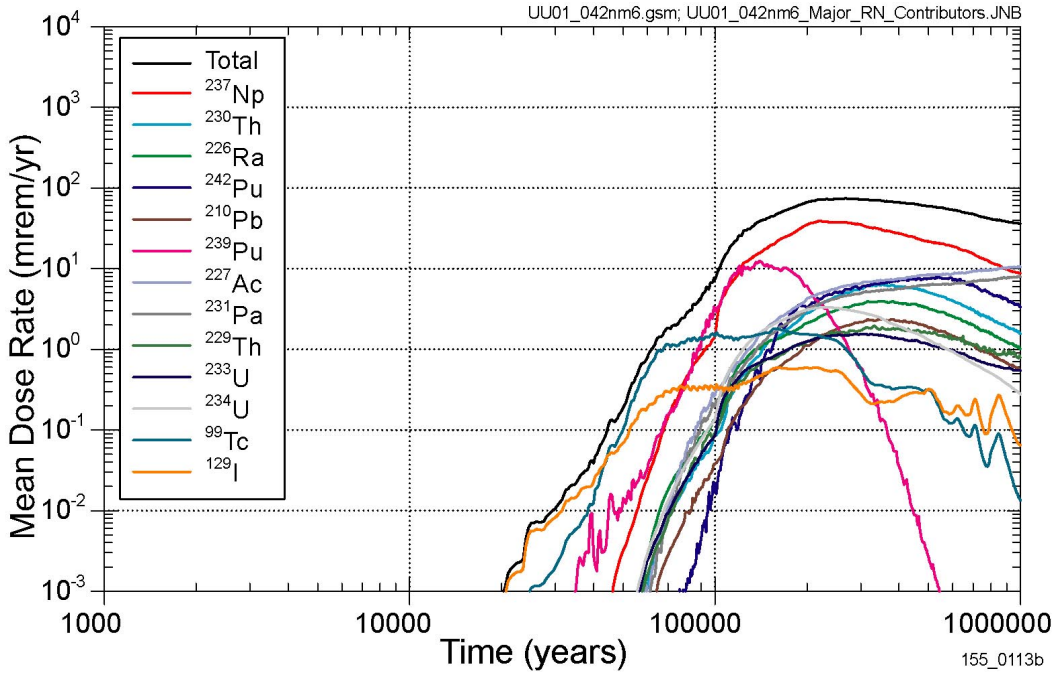

1554_0330.ai / 155_0113b

NOTE: (a) Comparison of mean annual dose estimates including (new model) and excluding (TSPA-SR base-case model) the effects of radionuclide solubility. (b) Contribution of individual radionuclides to the mean annual dose taking radionuclide solubility effects into account.

Figure 3.2.7.3-1. Supplemental Analyses of the Effect of Radionuclide Solubility Limits

(a)

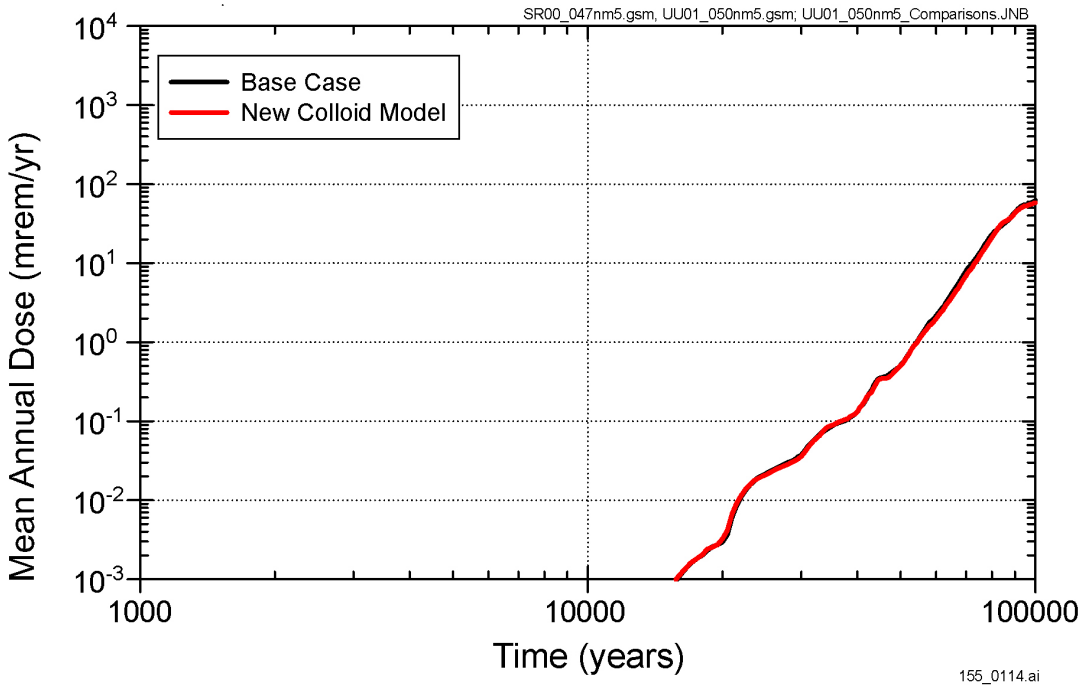

(b)

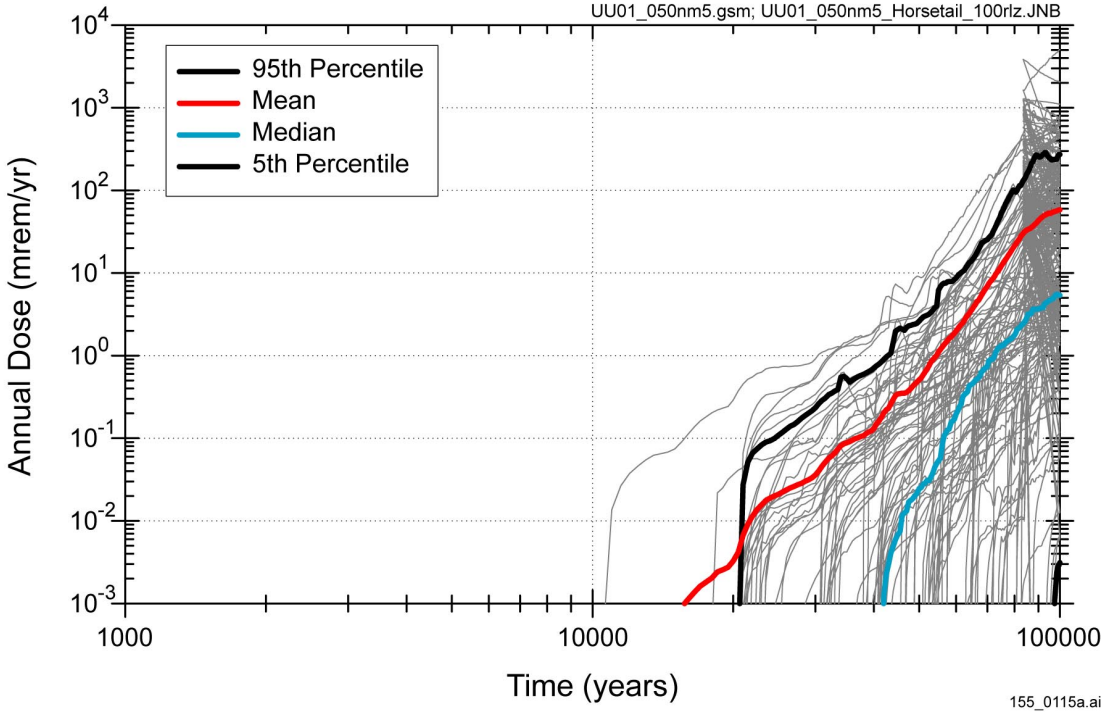

155_0114.ai / 155_0115a.ai

NOTE: (a) Comparison of one-off sensitivity analysis with the mean annual dose calculated with the TSPA-SR base-case model. (b) Range of the results for all realizations for the one-off sensitivity analysis.

Figure 3.2.7.4-1. Supplemental Analyses of the Effect of Colloid-Associated Radionuclide Concentrations

(a)

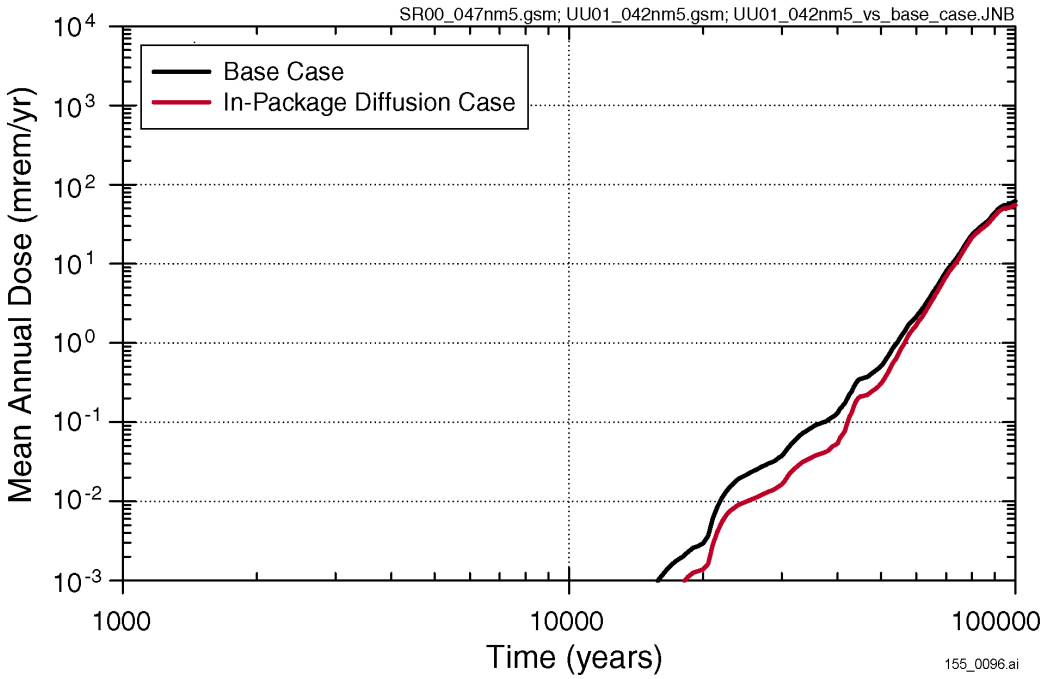

(b)

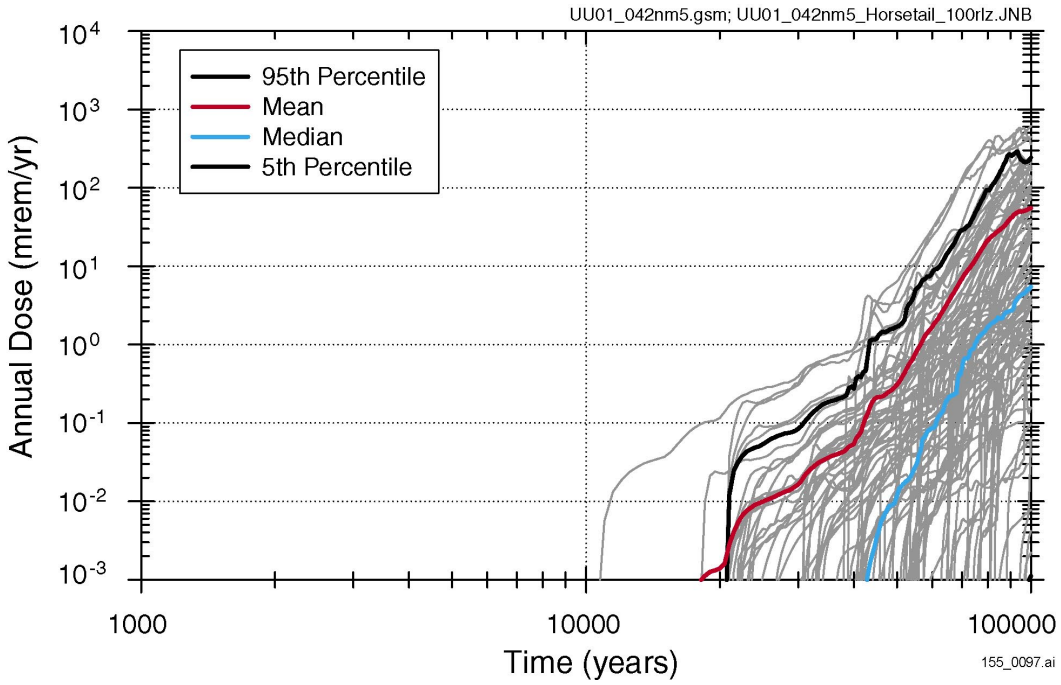

155_0096.ai / 155_0097.ai

NOTE: (a) Comparison of one-off sensitivity analysis with the mean annual dose calculated with the TSPA-SR base-case model. (b) Range of the results for all realizations for the one-off sensitivity analysis.

Figure 3.2.8-1. Sensitivity of Annual Dose to In-Package Diffusion

(a)

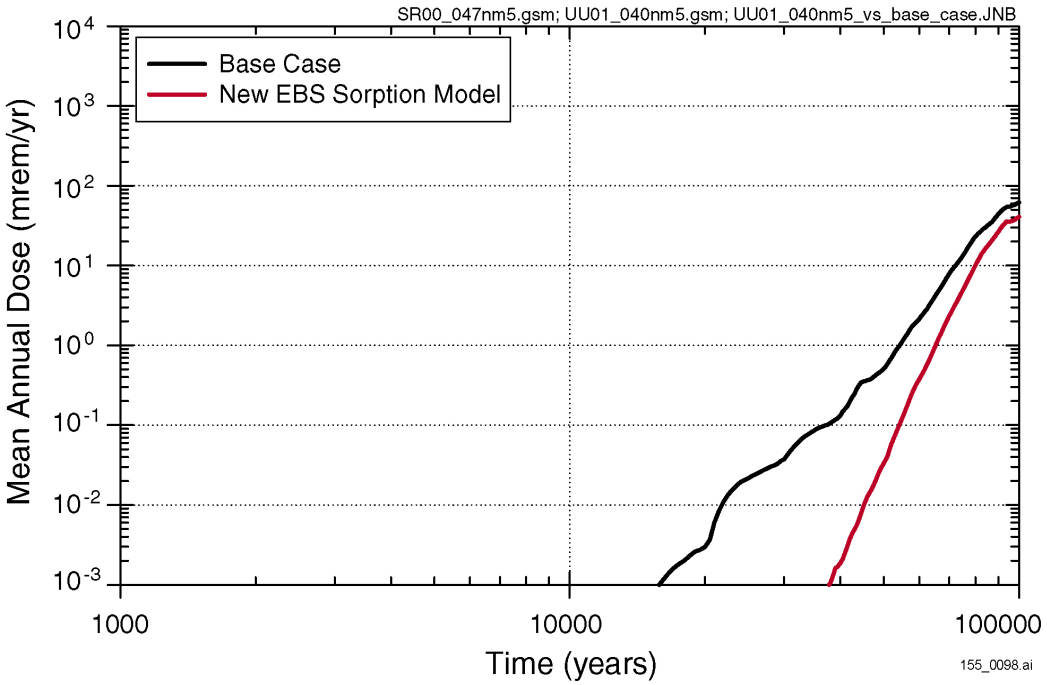

(b)

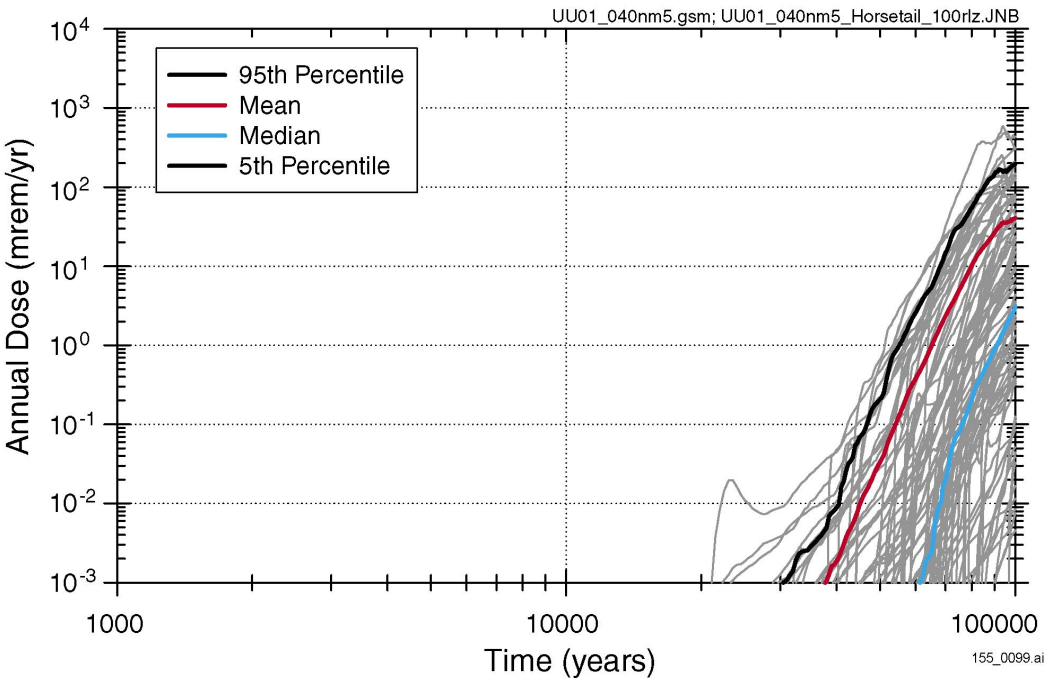

155_0098.ai / 155_0099.ai

NOTE: (a) Comparison of one-off sensitivity analysis with the mean annual dose calculated with the TSPA-SR base-case model. (b) Range of the results for all realizations for the one-off sensitivity analysis.

Figure 3.2.8-2. Sensitivity of Annual Dose to Radionuclide Sorption in the Engineered Barrier System

(a)

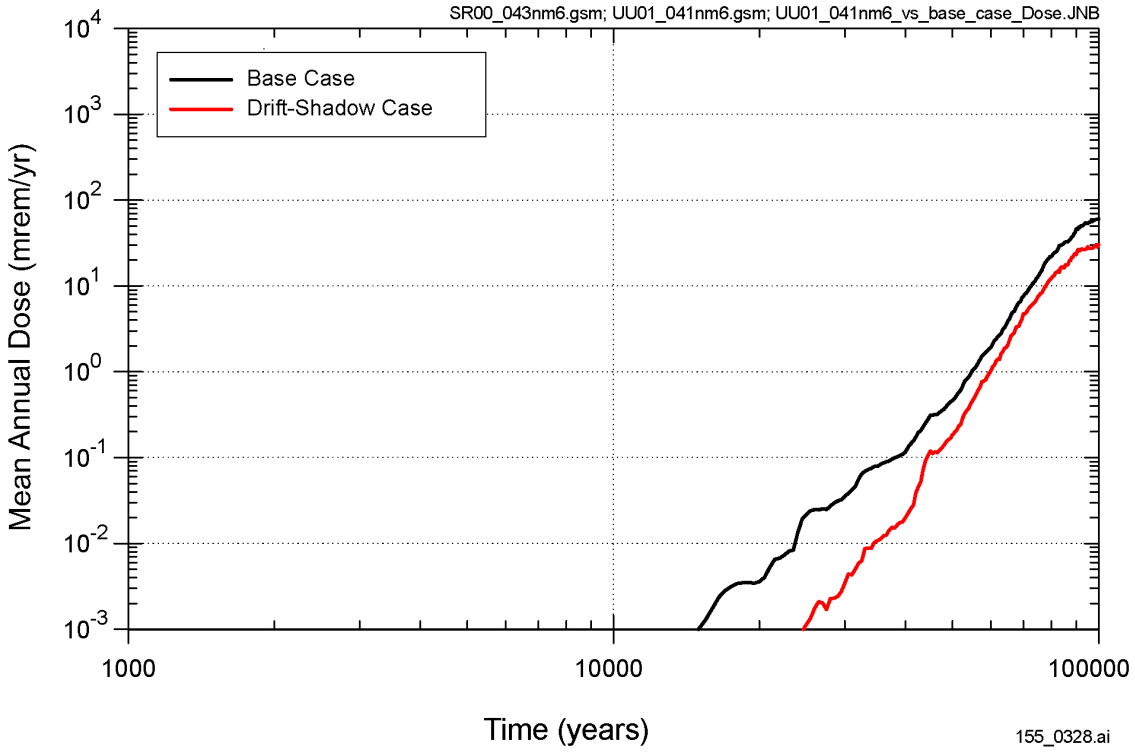

(b)

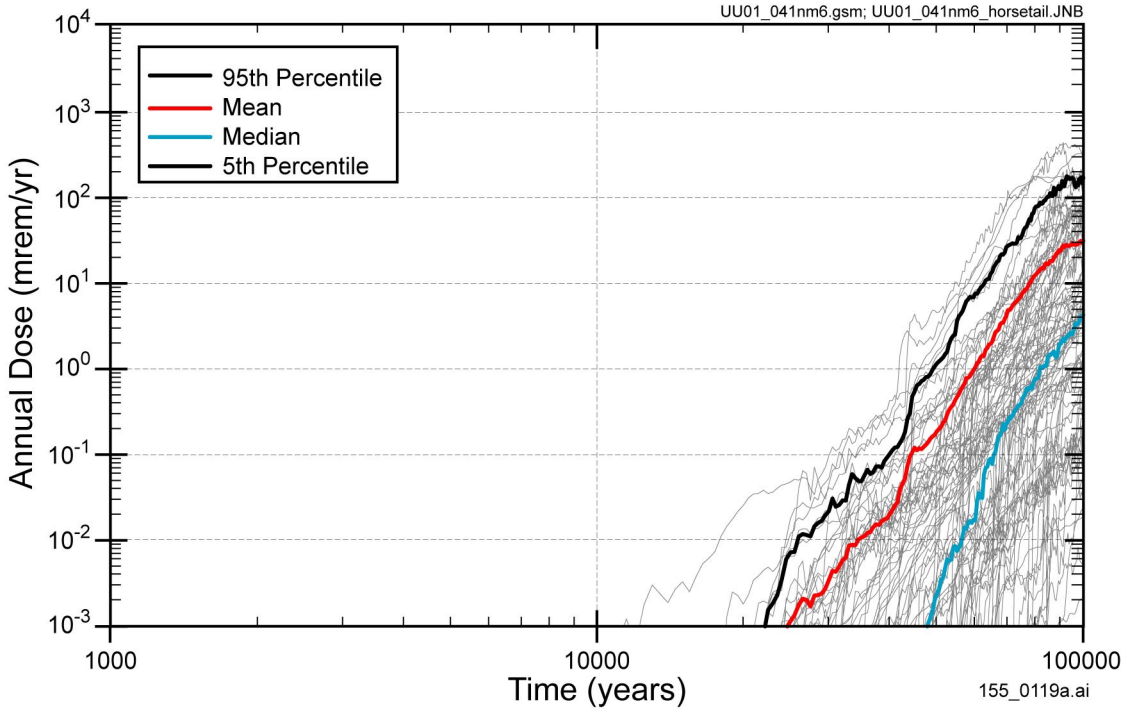

155_0328.ai / 155_0119a.ai

NOTE: (a) Comparison of two cases. (b) All realizations and statistics for the drift-shadow case. Fifth percentile curve does not appear because it is below the lower limit of the plot.

Figure 3.2.9-1. Annual Dose Histories for the Drift-Shadow and Base Cases

(a)

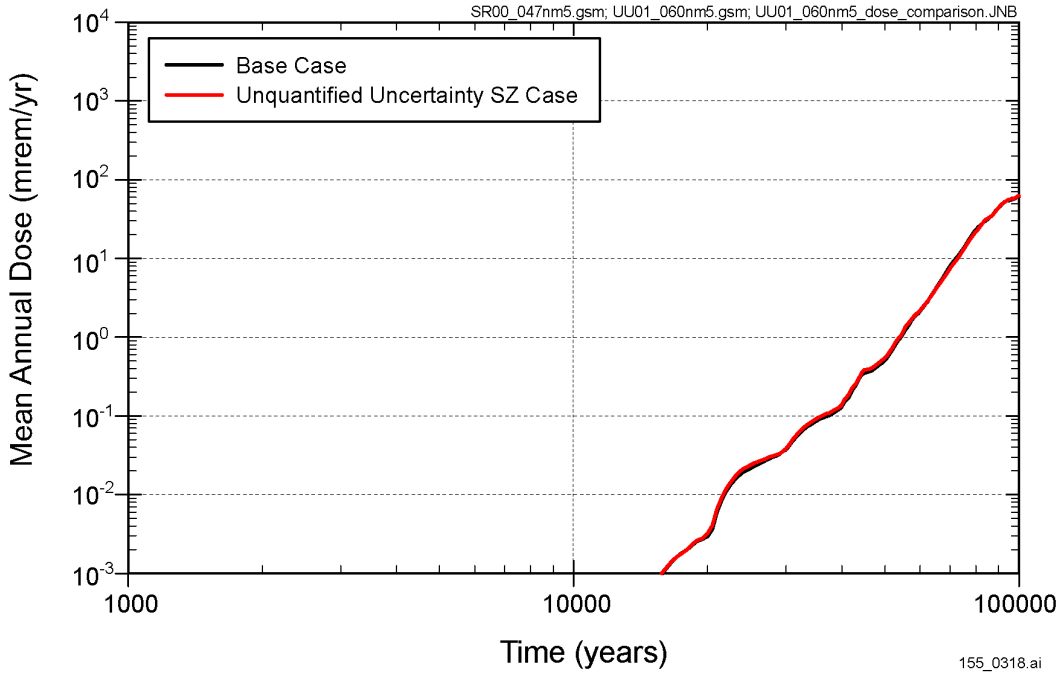

(b)

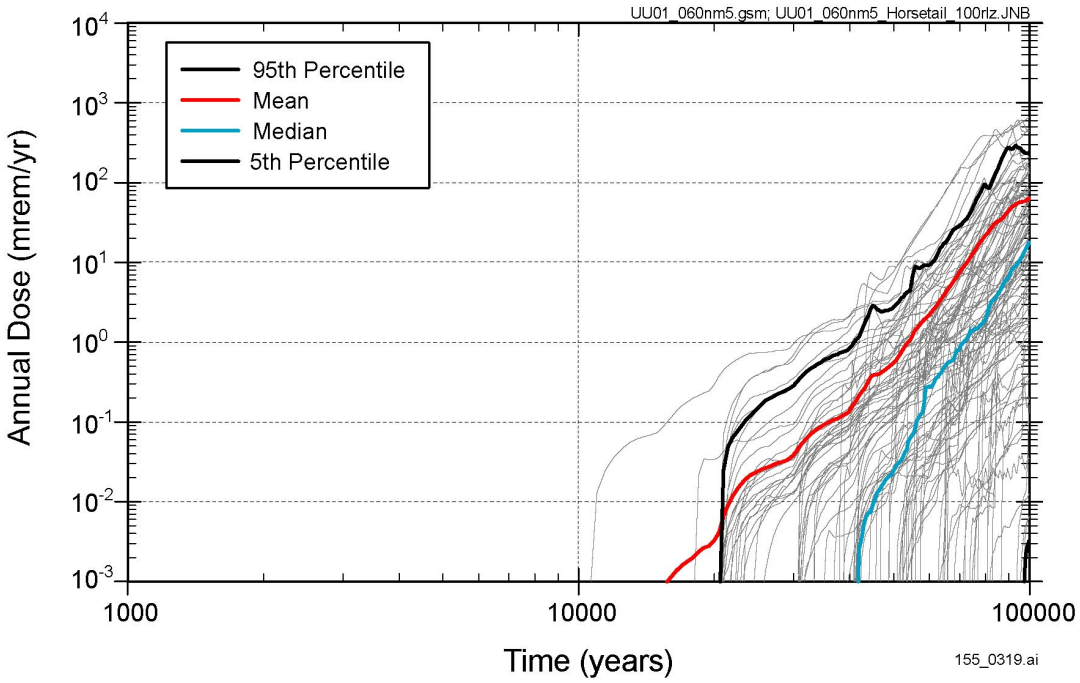

155_0318.ai/155_0319.ai

Source: Base case model from TSPA-SR (CRWMS M&O 2000 [DIRS 153246]).

NOTE: (a) Mean annual dose for the TSPA-SR base-case and for the unquantified uncertainties case for SZ flow and transport. (b) Simulated annual dose for the unquantified uncertainties case for SZ flow and transport.

Figure 3.2.10-1. Simulated Total System Performance Assessment Dose Rates for the Base Case and the Unquantified Uncertainties Case for Saturated Zone Flow and Transport

(a)

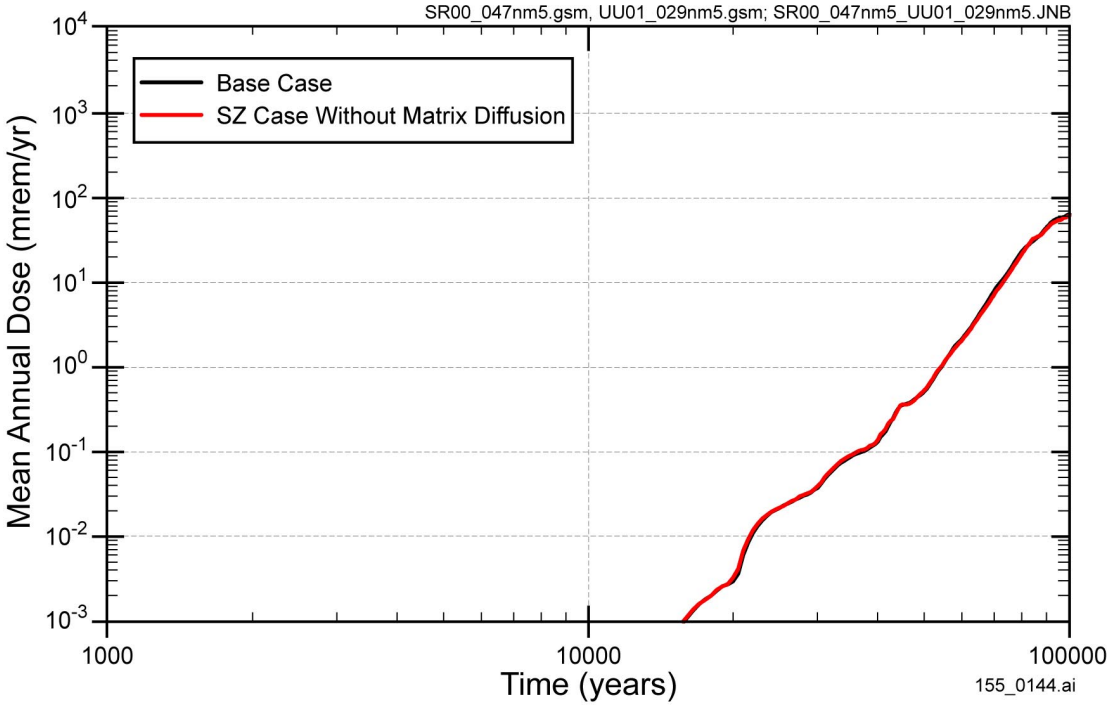

(b)

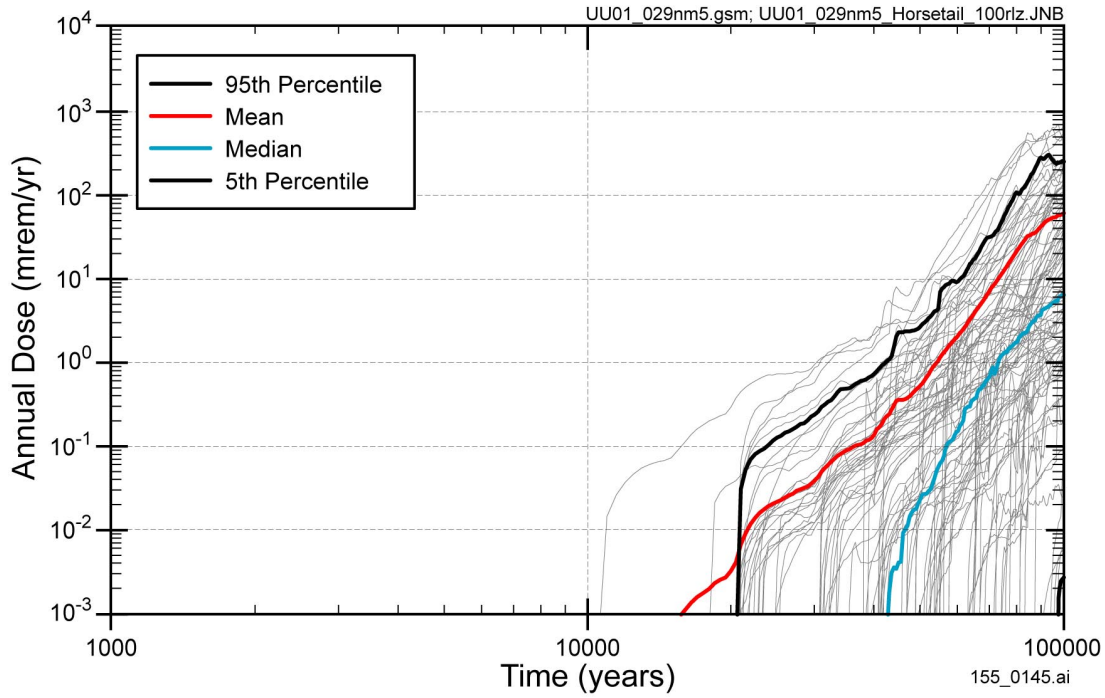

155_0144.ai / 155_0145.ai

Source: Base case model from TSPA-SR (CRWMS M&O 2000 [DIRS 153246]).

NOTE: (a) Mean annual dose for the TSPA-SR base-case and for the no matrix diffusion case for SZ flow and transport. (b) Simulated annual dose for no matrix diffusion.

Figure 3.2.10-2. Simulated Total System Performance Assessment Dose Rates for the Base Case and the No Matrix-Diffusion Case for Saturated Zone Flow and Transport

(a)

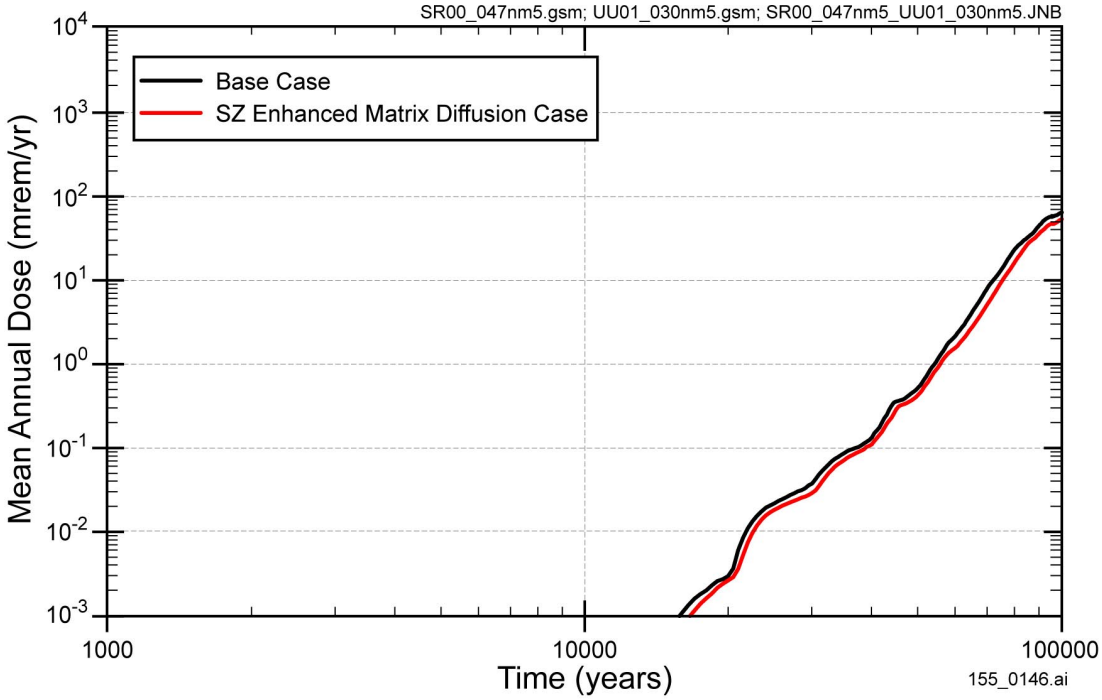

(b)

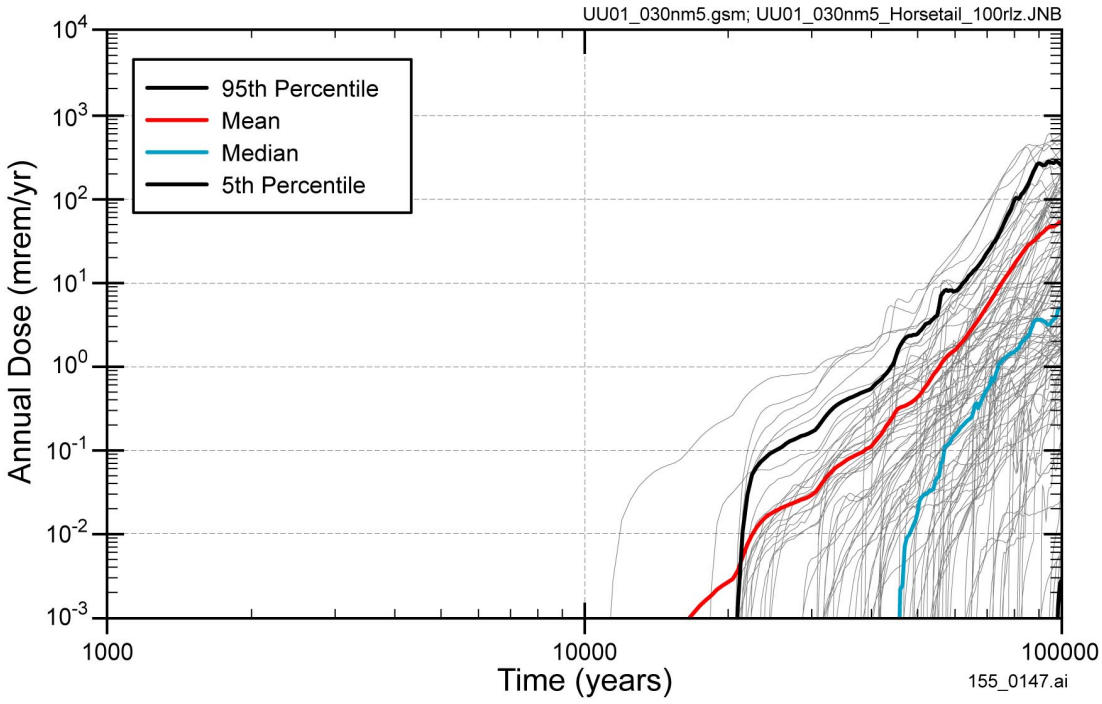

155_0146.ai / 155_0147.ai

Source: TSPA-SR (CRWMS M&O 2000 [DIRS 153246]).

NOTE: (a) Mean annual dose for the TSPA-SR base-case and for the enhanced matrix diffusion case for SZ flow and transport. (b) Simulated annual dose for the enhanced matrix diffusion case for SZ flow and transport.

Figure 3.2.10-3. Simulated Total System Performance Assessment Dose Rates for the Base Case and the Enhanced Matrix-Diffusion Case for Saturated Zone Flow and Transport

(a)

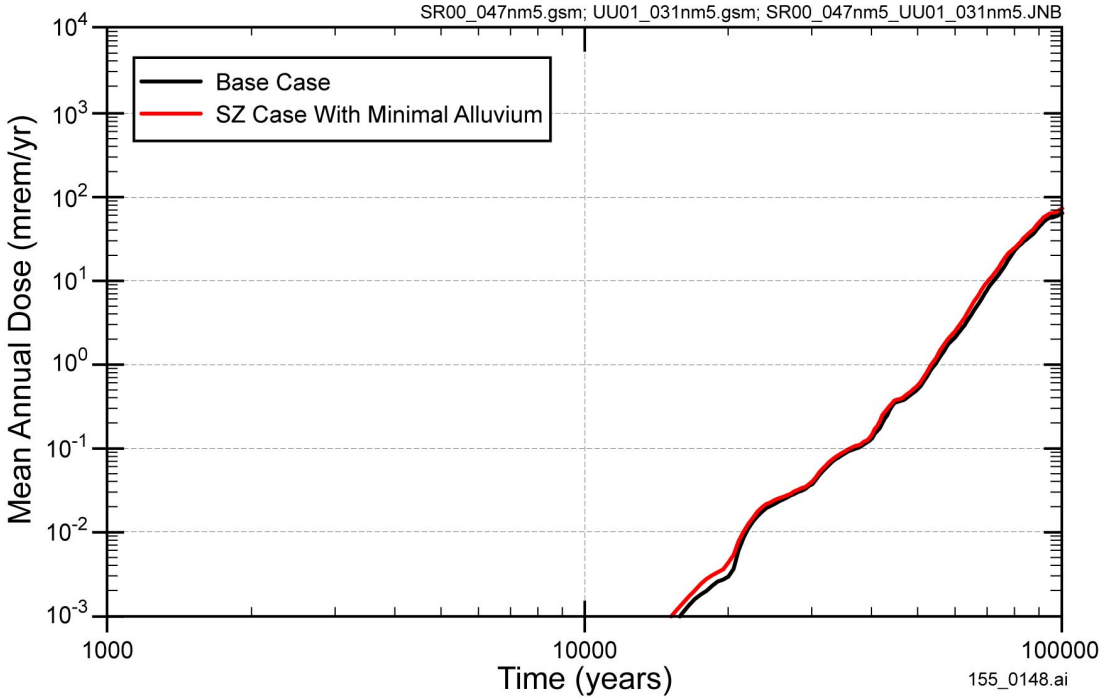

(b)

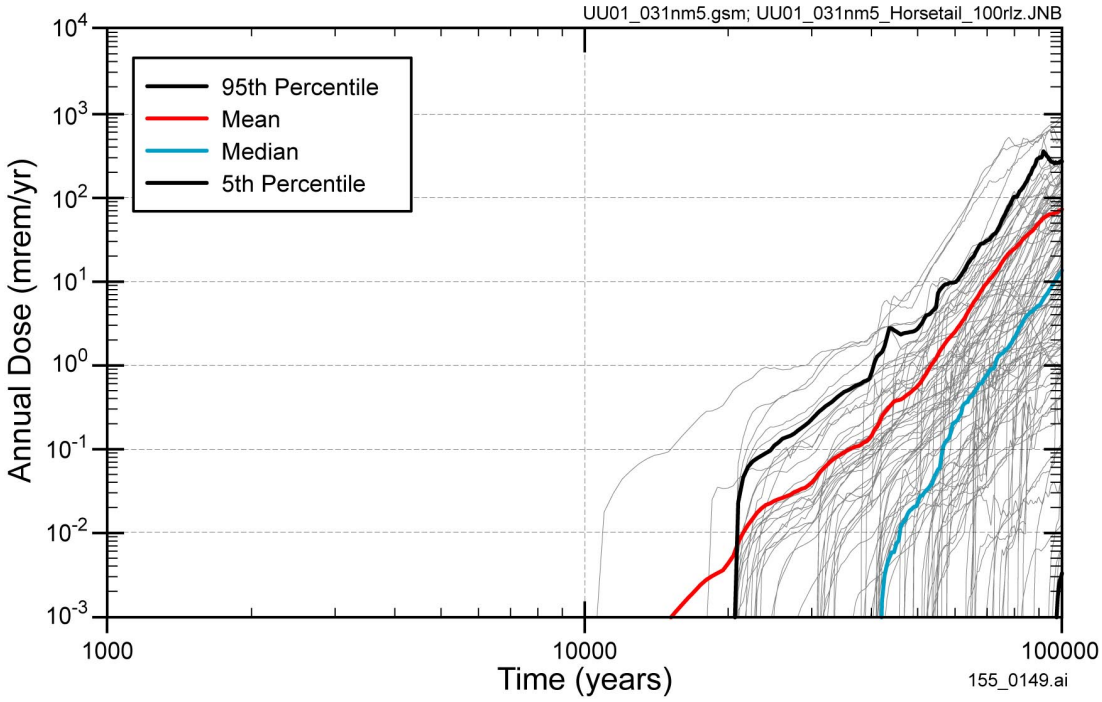

155_0148.ai / 155_0149.ai

Source: TSPA-SR (CRWMS M&O 2000 [DIRS 153246]).

NOTE: (a) Mean annual dose for the TSPA-SR base-case and for the minimum alluvium case for SZ flow and transport. (b) Simulated annual dose for the minimum alluvium case for SZ flow and transport.

Figure 3.2.10-4. Simulated Total System Performance Assessment Dose Rates for the Base Case and the Minimum-Alluvium Case for Saturated Zone Flow and Transport

(a)

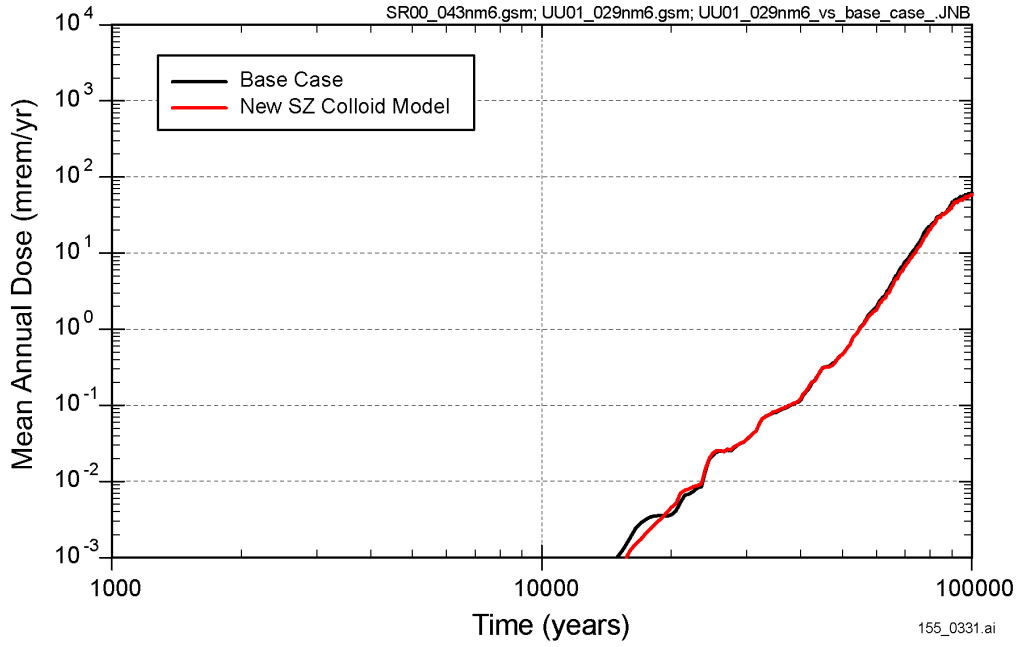

(b)

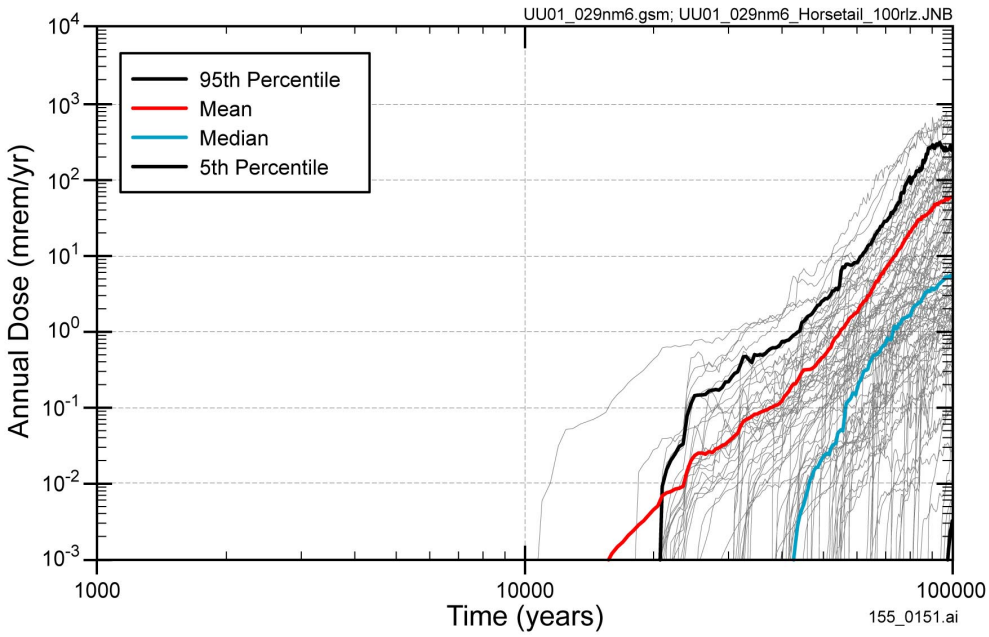

155_0331.ai / 155_0151.ai

Source: TSPA-SR (CRWMS M&O 2000 [DIRS 153246]).

NOTE: (a) Mean annual dose for the TSPA-SR base-case and for the increased uncertainty in colloid-facilitated-transport case for SZ flow and transport (only changes in the SZ transport model). (b) Simulated annual dose for the increased uncertainty in colloid-facilitated-transport case for SZ flow and transport (only changes in the SZ transport model).

Figure 3.2.10-5. Simulated Total System Performance Assessment Dose Rates for the Base Case and the Increased Uncertainty in Colloid-Facilitated-Transport Case for Saturated Zone Flow and Transport

(a)

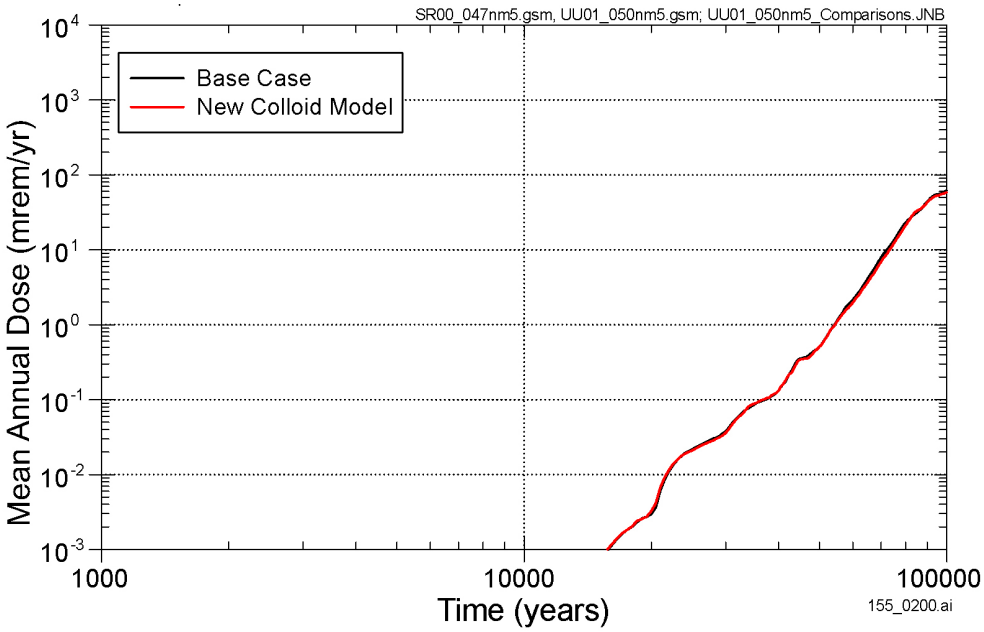

(b)

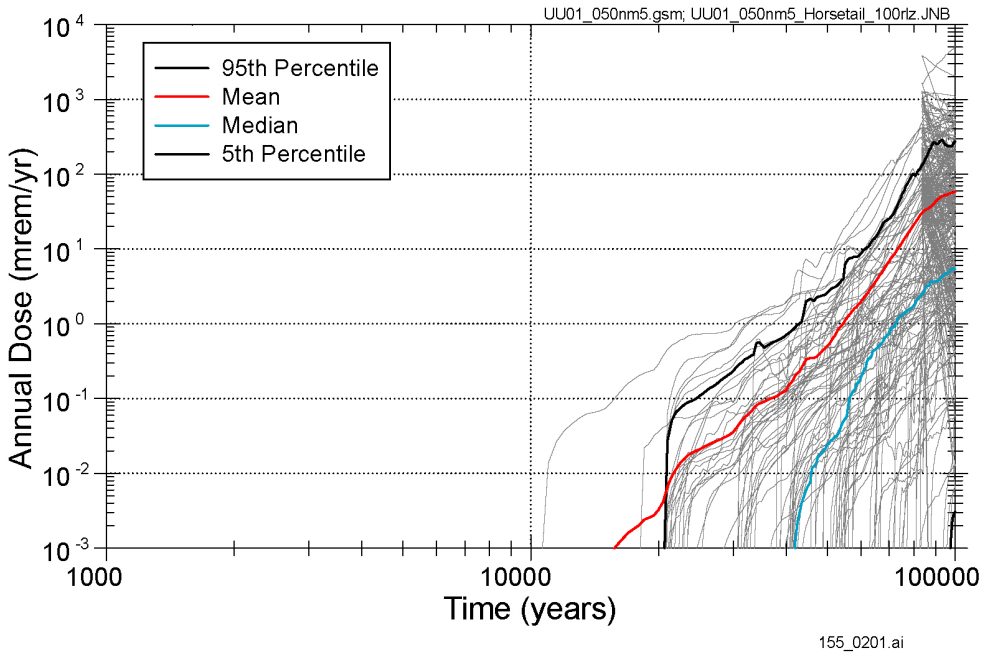

155_0200.ai / 155_0201.ai

Source: TSPA-SR (CRWMS M&O 2000 [DIRS 153246]).

NOTE: (a) Mean annual dose for the TSPA-SR base-case and for the increased uncertainty in colloid-facilitated-transport case for SZ flow and transport (changes in the EBS, UZ, and SZ transport model). (b) Simulated annual dose for the increased uncertainty in colloid-facilitated-transport case for SZ flow and transport (changes in the EBS, UZ, and SZ transport model).

Figure 3.2.10-6. Simulated Total System Performance Assessment Dose Rates for the Base Case and the Increased Uncertainty in Colloid-Facilitated-Transport Case for Saturated Zone Flow and Transport

(a)

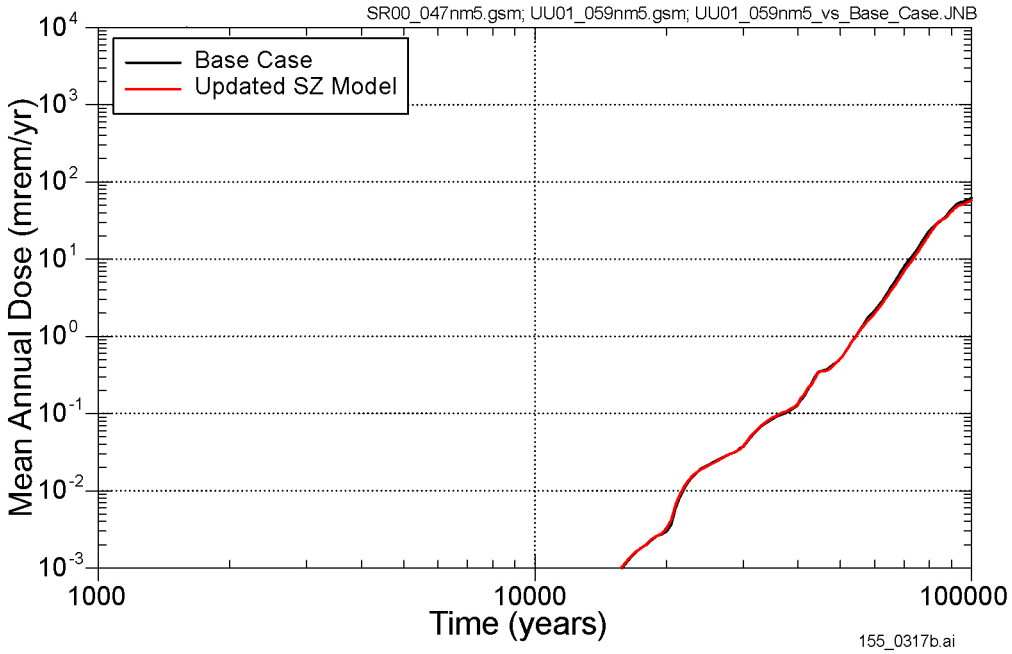

(b)

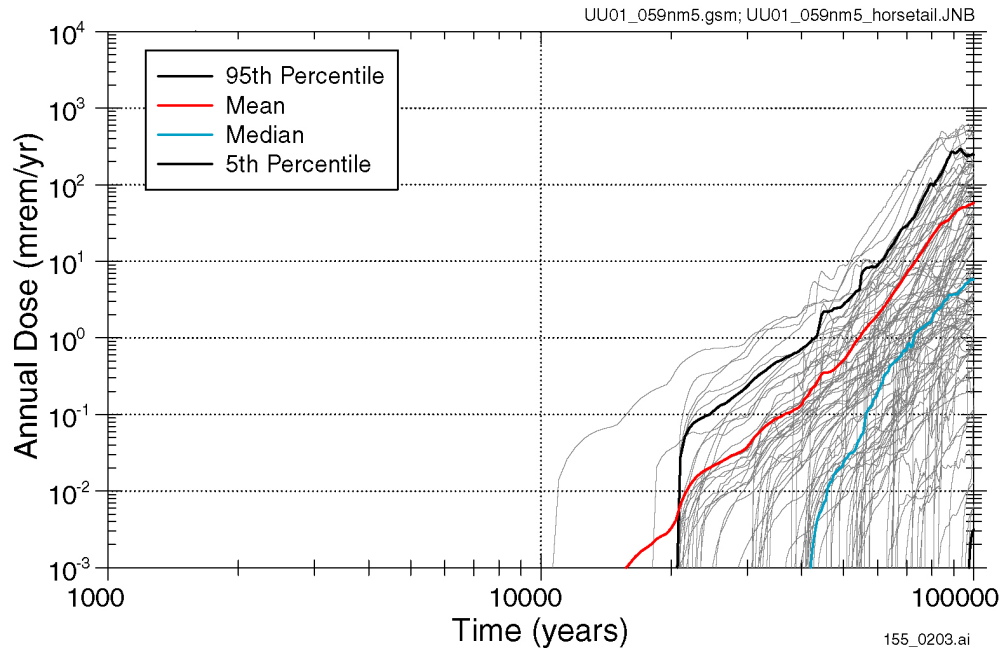

155_0317b.ai / 155_0203.ai

NOTE: (a) Mean annual dose for the TSPA-SR base-case and for the updated SZ flow and transport model for the supplemental TSPA analyses. (b) Simulated annual dose for the updated SZ flow and transport model for the supplemental TSPA analyses.

Figure 3.2.10-7. Simulated Total System Performance Assessment Dose Rates for the Base Case and the Simulated Annual Dose for Saturated Zone

(a)

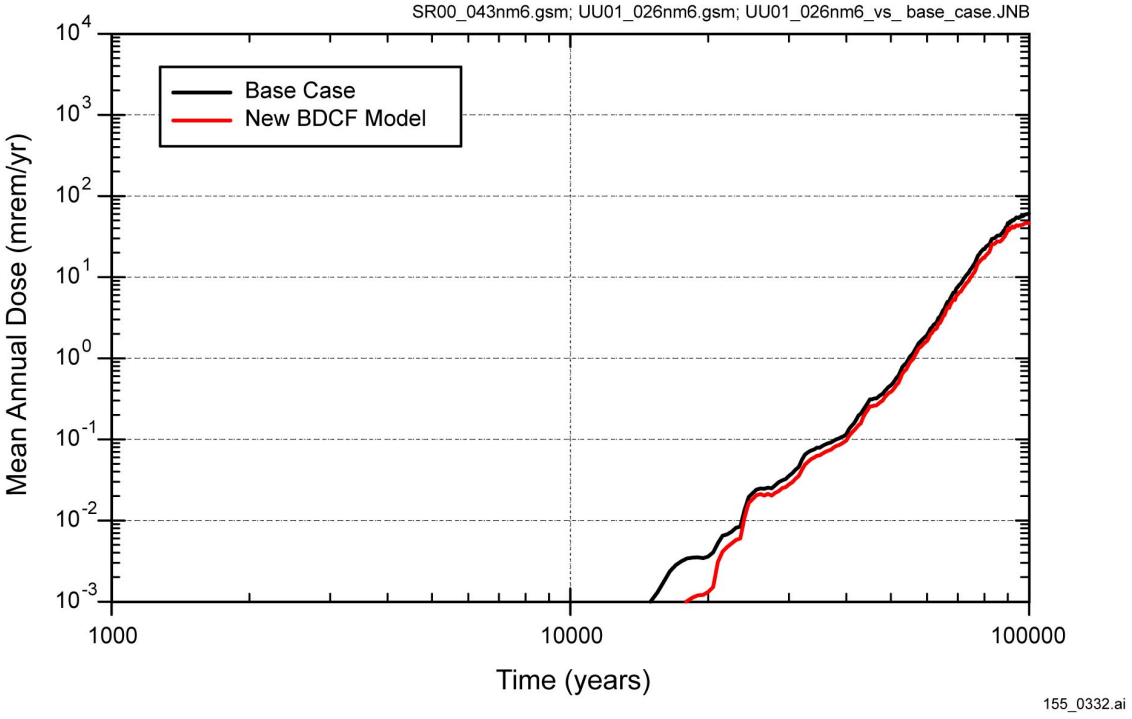

(b)

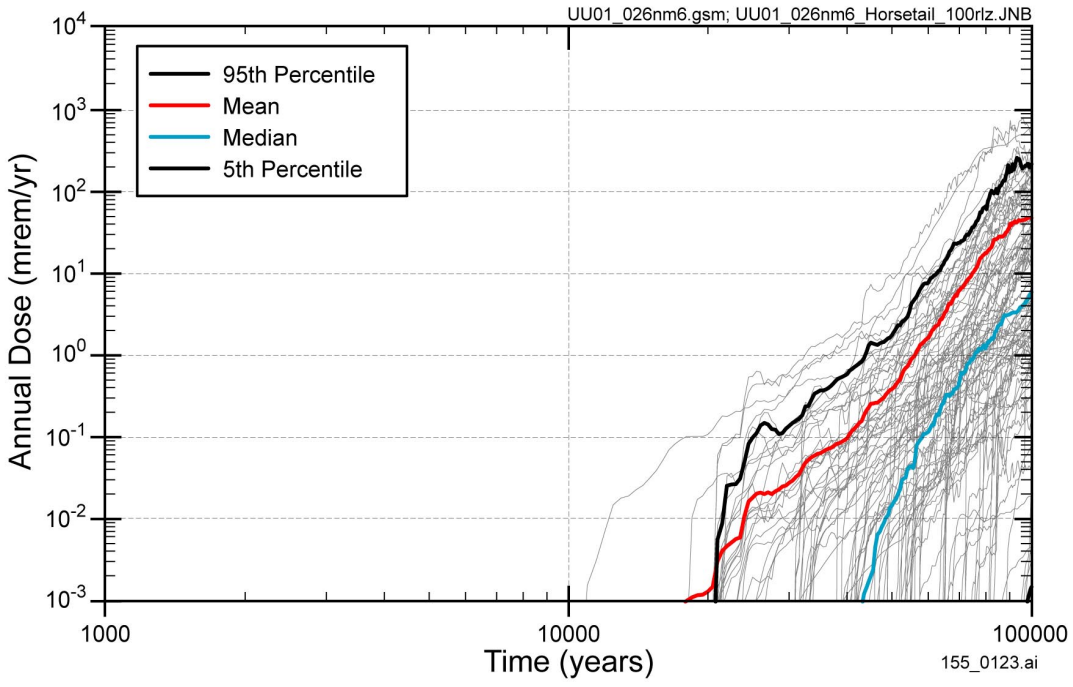

155_0332.ai / 155_0123.ai

Source: TSPA-SR (CRWMS M&O 2000 [DIRS 153246]).

NOTE: (a) Mean annual dose for the TSPA-SR base-case and for the new nominal case BDCFs. (b) Simulated annual dose for the new nominal case BDCFs.

Figure 3.2.11-1. Simulated Dose Rates for the Base Case and New Nominal Case Biosphere Dose Conversion Factors

(a)

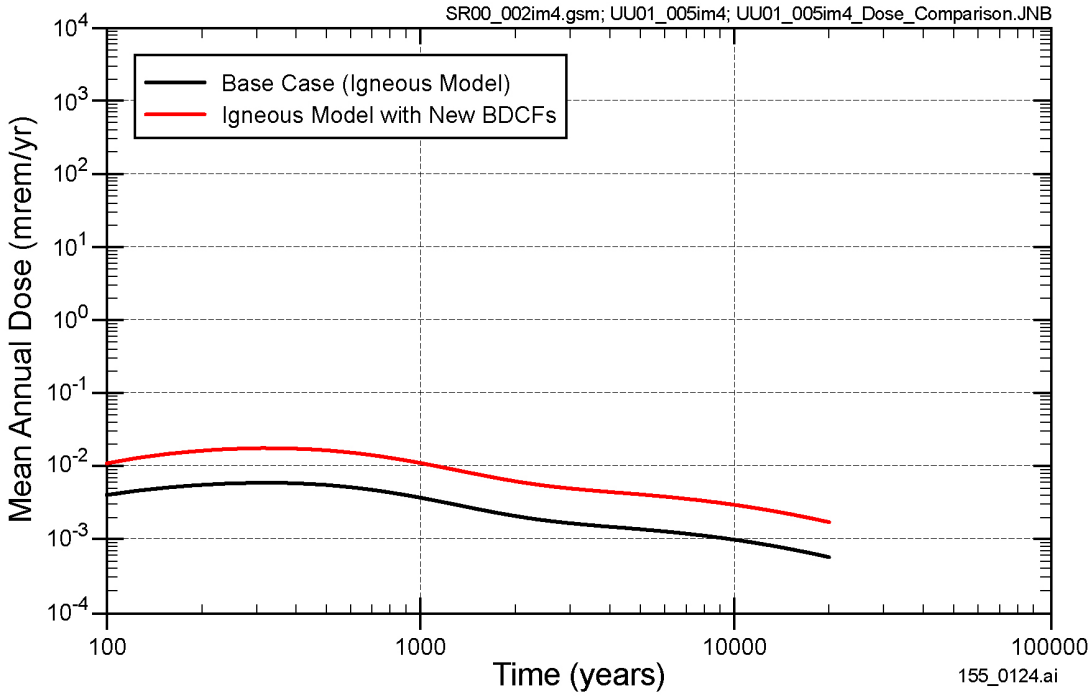

(b)

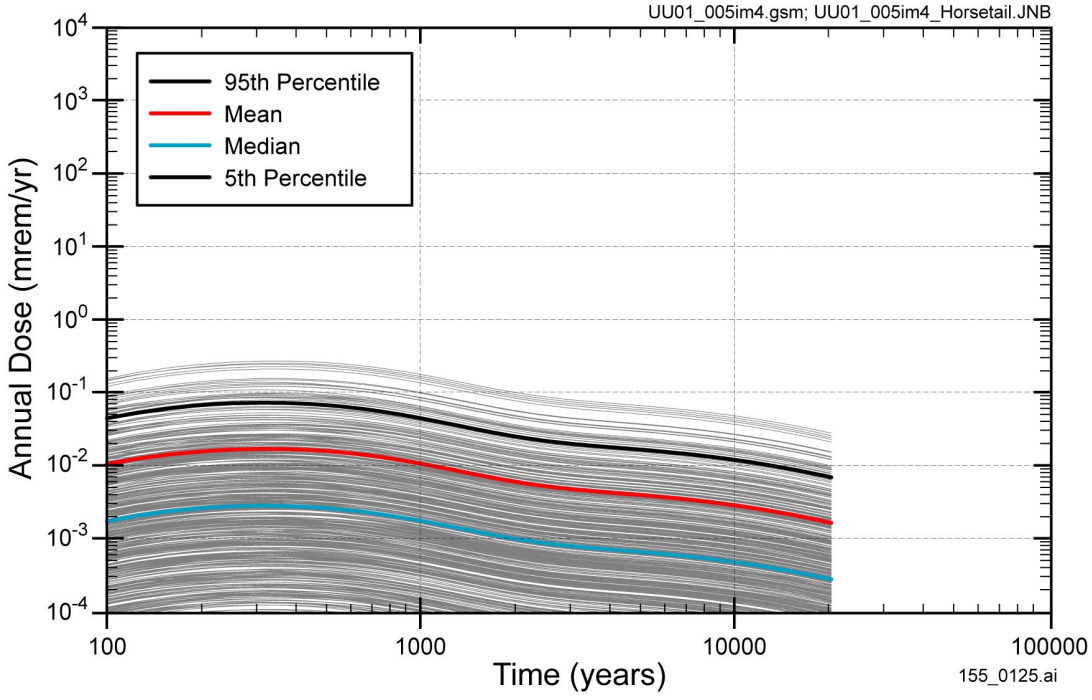

155_0124.ai / 155_0125.ai

Source: TSPA-SR (CRWMS M&O 2000 [DIRS 153246]).

NOTE: (a) Mean annual dose for the volcanic-eruption scenario from the TSPA-SR base-case and for the new volcanic-eruption case BDCFs. (b) Simulated annual dose for the new volcanic-eruption case BDCFs.

Figure 3.2.11-2. Simulated Dose Rates for the Base Case and the New Volcanic Eruption Case Biosphere Dose Conversion Factors

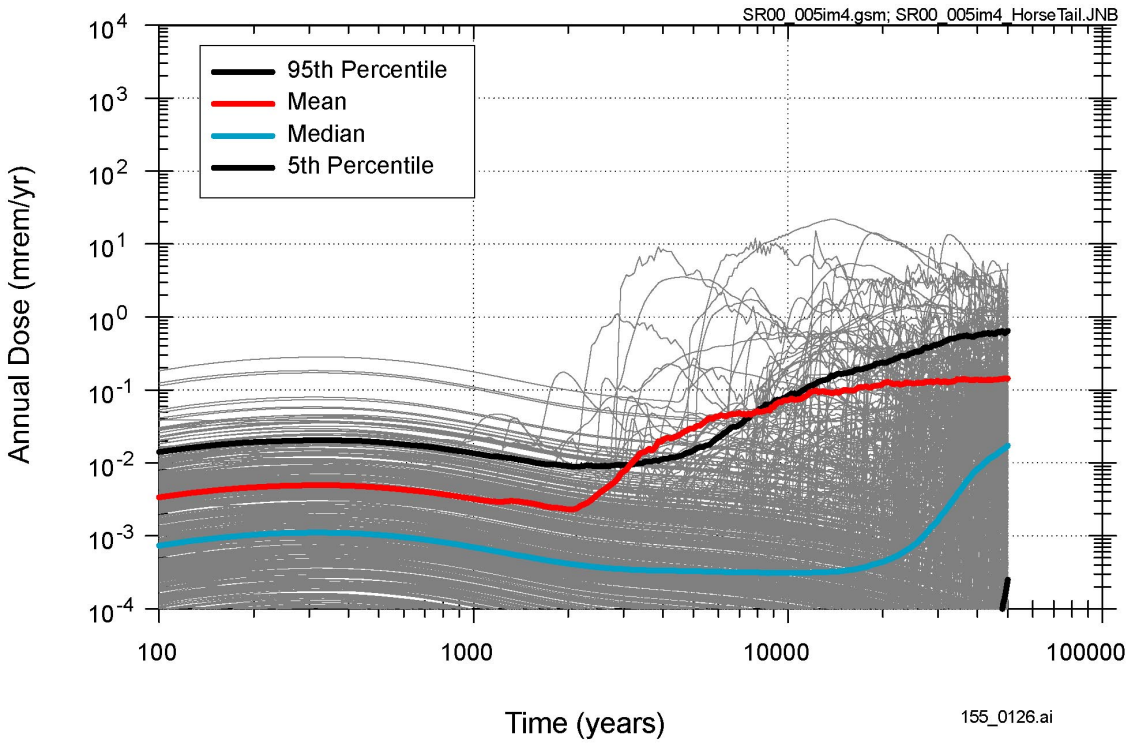

155_0126.ai

Source: TSPA-SR (CRWMS M&O 2000 [DIRS 153246], Figure 4.2-1).

NOTE: The 5th percentile curve does not occur until close to the end of the 50,000-year simulation.

Figure 3.3.1-1. Total Probability-Weighted Annual Dose Rate from Igneous Disruption

(a)

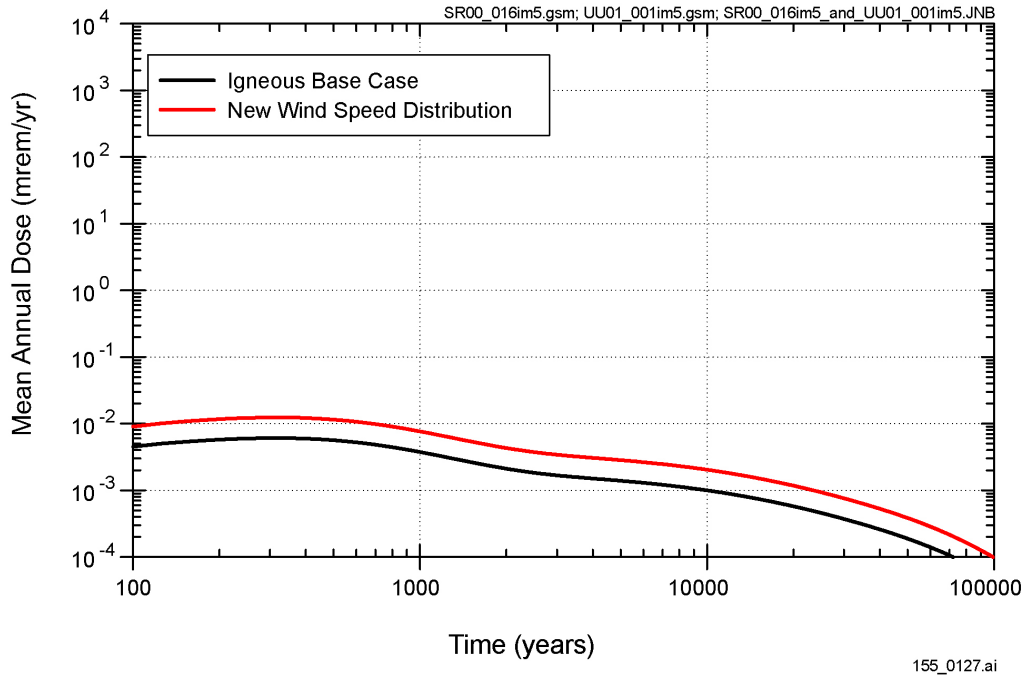

(b)

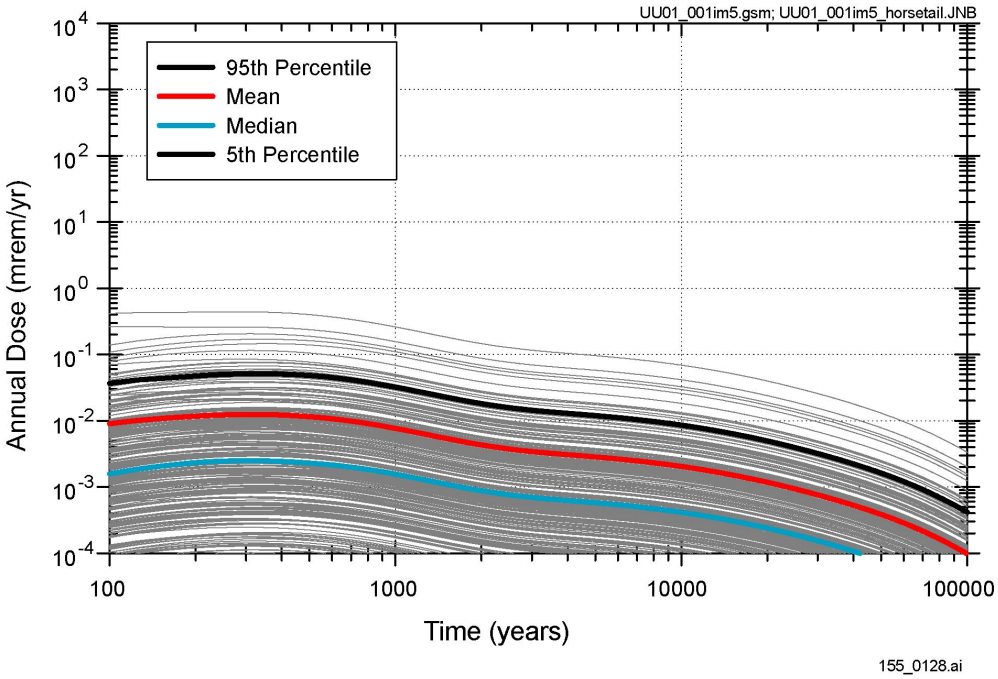

155_0127.ai / 155_0128.ai

Source: TSPA-SR (CRWMS M&O 2000 [DIRS 153246], Section 3.10.2.2 through 3.10.2.4).

NOTE: All models and input parameters, except the alternative wind speed data, are identical to those used in the TSPA-SR. In (b), the 5th percentile curve plots below the lowest value shown on the y-axis.

Figure 3.3.1.2-1. Sensitivity of Probability-Weighted Mean Annual Dose from Volcanic Eruption to the Use of an Alternative Set of Wind Speed Data

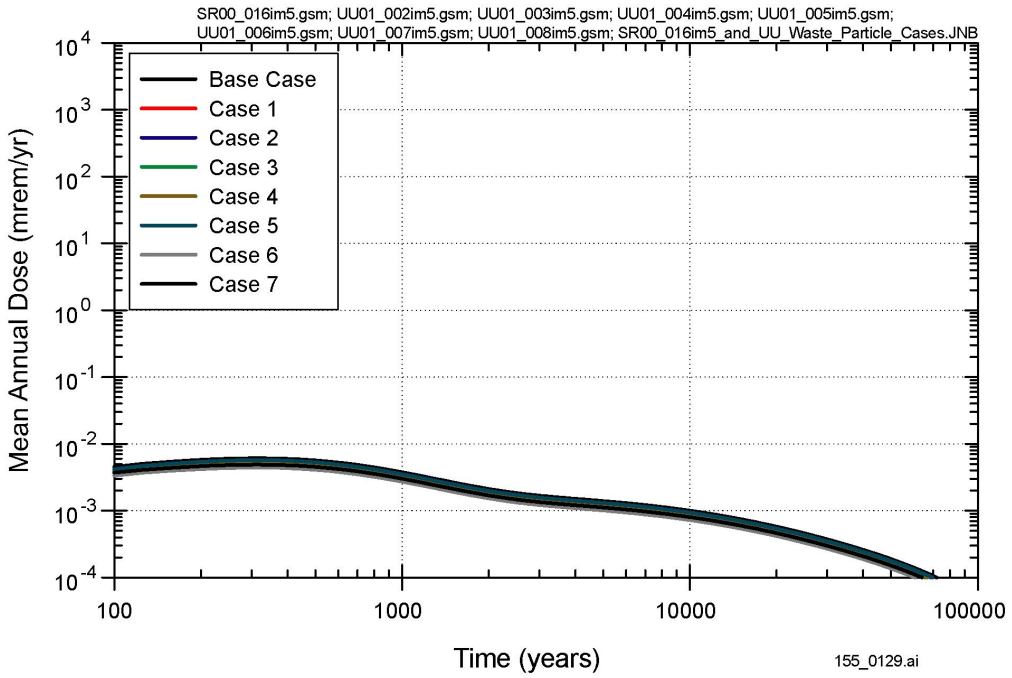

155_0129.ai

Source: TSPA-SR (CRWMS M&O 2000 [DIRS 153246], Sections 3.10.2.2 through 3.10.2.4).

NOTE: All models and input parameters, except the alternative waste particle diameter distributions, are identical to those used in the TSPA-SR.

Figure 3.3.1.2-2. Sensitivity of Probability-Weighted Mean Annual Dose from Volcanic Eruption to Waste Particle Diameter

(a)

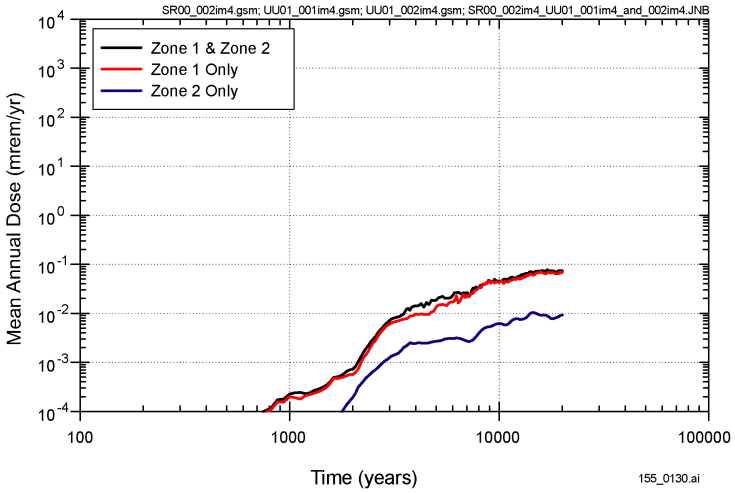

(b)

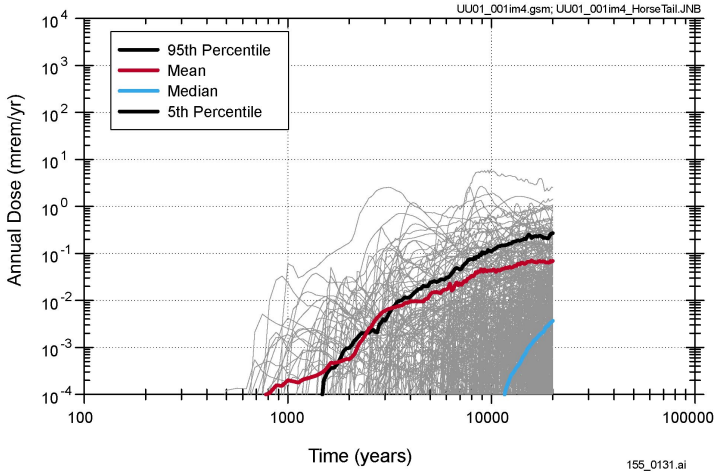

(c)

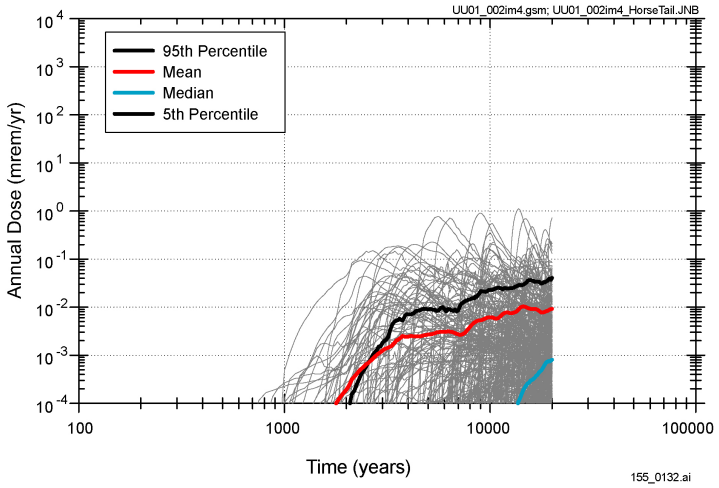

155_0130.ai / 155_0131.ai / 155_0132.ai

Source: TSPA-SR (CRWMS M&O 2000 [DIRS 153246], Sections 3.10.2.2 through 3.10.2.4).

NOTE: All models and input parameters are identical to those used in TSPA-SR. In (b) Zone 1 and (c) Zone 2, the 5th percentile curve plots below the lowest value shown on the y-axis.

Figure 3.3.1.2-3. Relative Contributions of Releases from Zones 1 and 2 to Probability-Weighted Mean Annual Dose from Igneous Intrusion

(a)

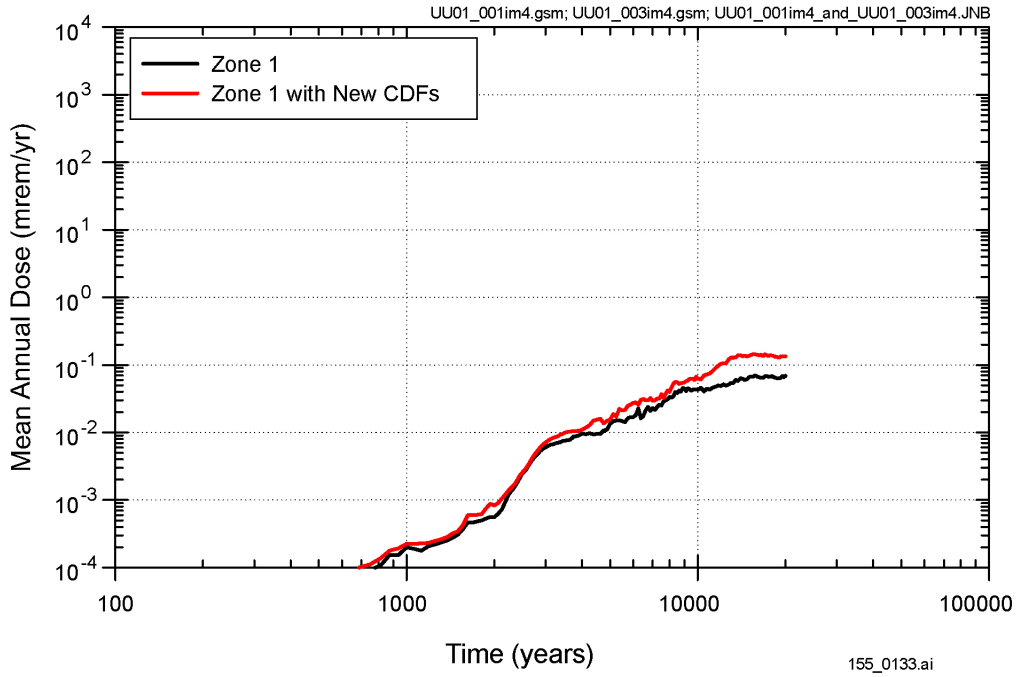

(b)

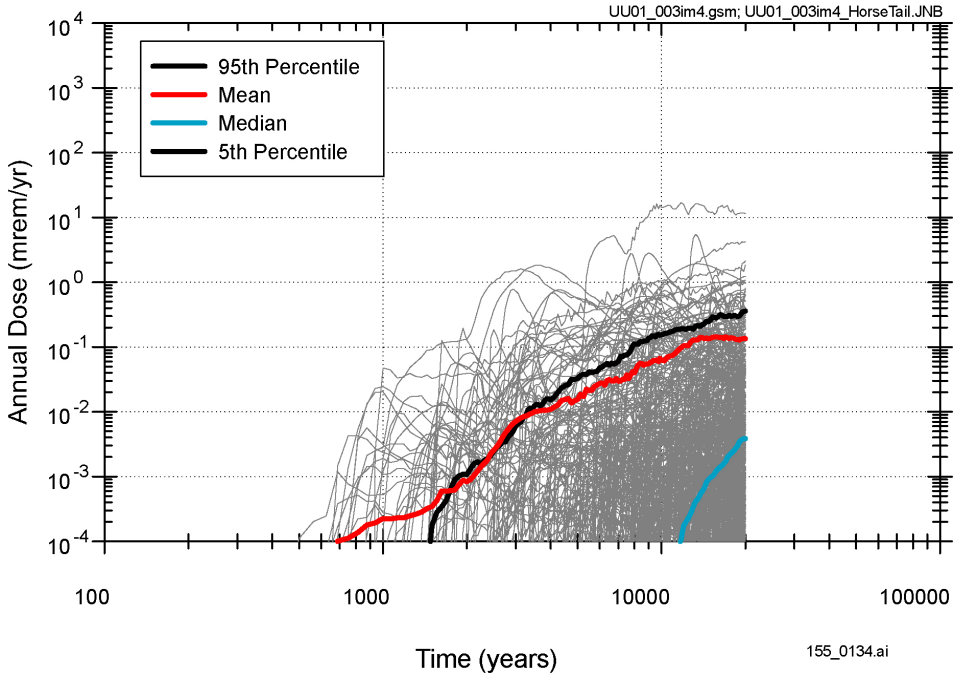

155_0133.ai / 155_0134.ai

Source: TSPA-SR (CRWMS M&O 2000 [DIRS 153246], Sections 3.10.2.2 through 3.10.2.4).

NOTE: All other models and input parameters are identical to those used in the TSPA-SR. In (b), the 5th percentile curve plots below the lowest value shown on the y-axis.

Figure 3.3.1.2-4. Comparison of Probability-Weighted Mean Annual Doses from Igneous Intrusion, Zone 1 Releases Only, Calculated using the TSPA-SR and Revised Distributions for the Number of Packages Damaged in Zone 1

(a)

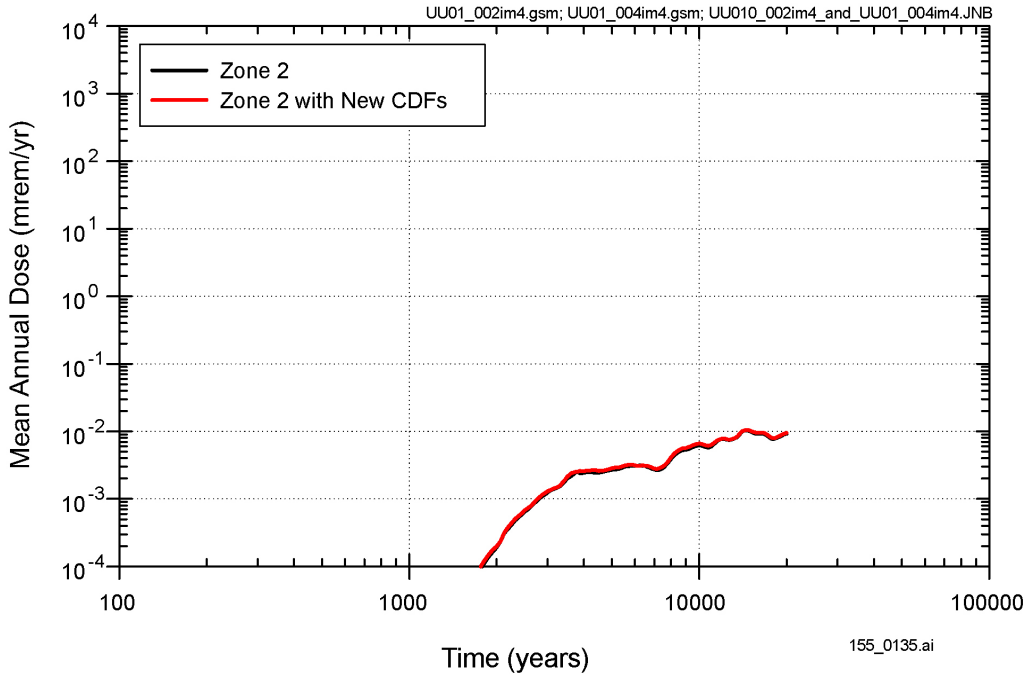

(b)

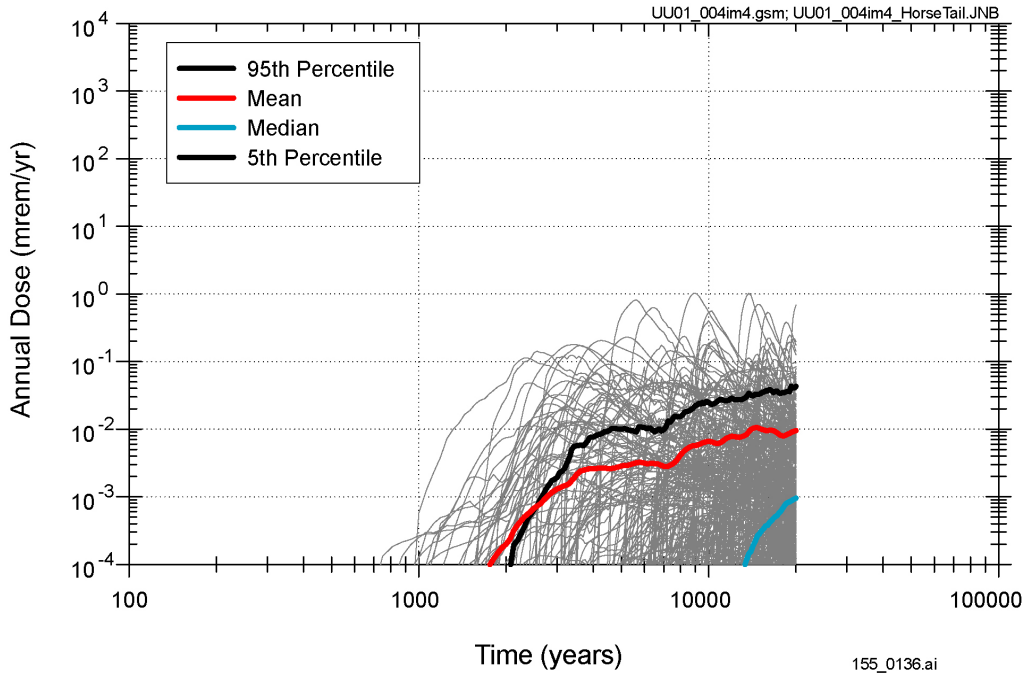

155_0135.ai / 155_0136.ai

Source: TSPA-SR (CRWMS M&O 2000 [DIRS 153246], Sections 3.10.2.2 through 3.10.2.4).

NOTE: All other models and input parameters are identical to those used in TSPA-SR. In (b), the 5th percentile curve plots below the lowest value shown on the y-axis.

Figure 3.3.1.2-5. Comparison of Probability-Weighted Mean Annual Doses from Igneous Intrusion, Zone 2 Releases Only, Calculated Using the TSPA-SR and Revised Distributions for the Number of Packages Damaged in Zone 2

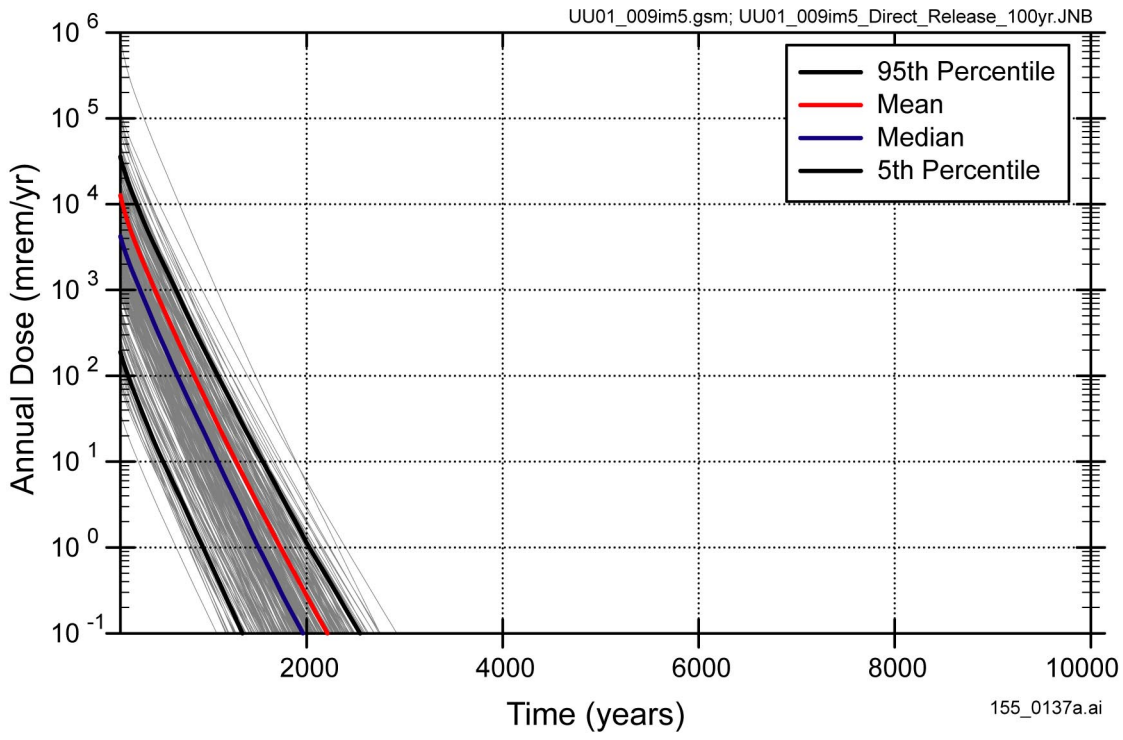

155_0137a.ai

Source: TSPA-SR (CRWMS M&O 2000 [DIRS 153246], Sections 3.10.2 through 3.10.4).

NOTE: Conditional annual doses due to a volcanic eruption 100 years after closure of the potential repository. Annual doses calculated using the TSPA-SR models and parameters, with the probability of an eruptive event at the repository set to 1. Because annual doses are not shown weighted by the probability of the occurrence of the eruptive event, they are not suitable for comparison to proposed regulatory standards.

Figure 3.3.1.2.4-1. Non-Probability Weighted Mean Annual Dose Due to Volcanic Eruption

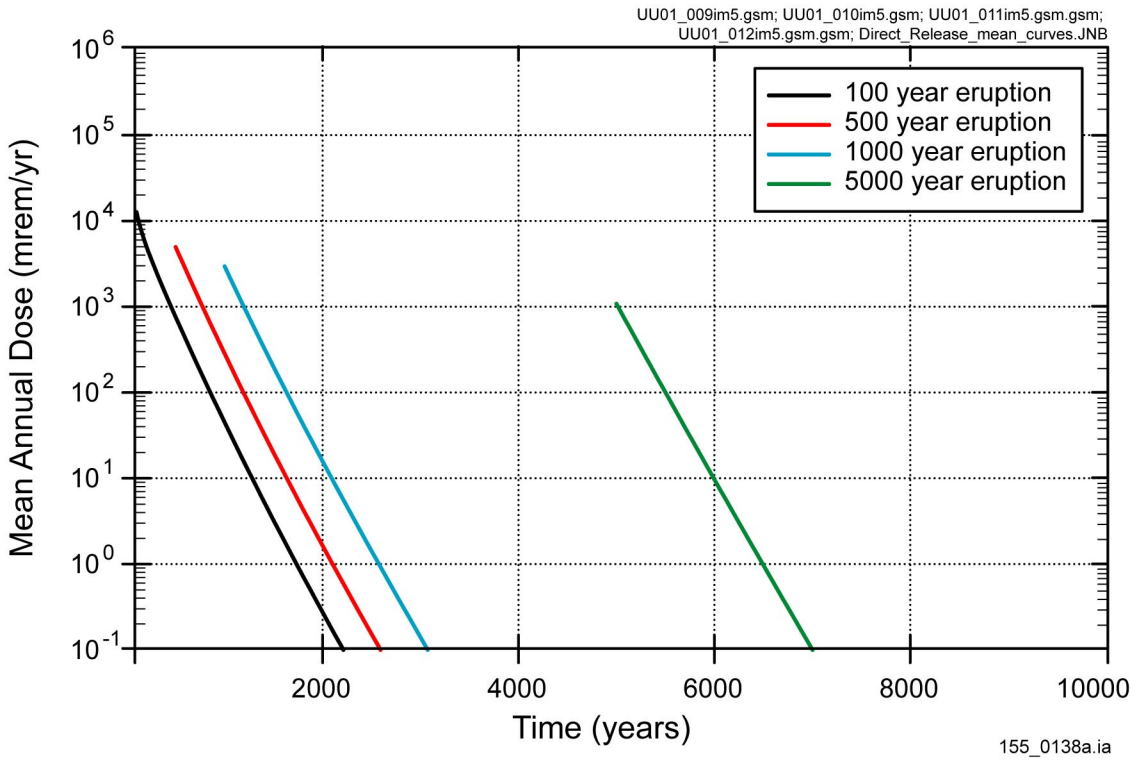

155_0138a.ai

Source: TSPA-SR (CRWMS M&O 2000 [DIRS 153246], Sections 3.10.2 through 3.10.4).

NOTE: Mean conditional annual doses due to a volcanic eruption 100, 500, 1000, and 5000 years after closure of the repository. Mean annual doses are calculated using the TSPA-SR base-case models and parameters, with the probability of an eruptive event at the repository set to 1. Because annual doses are not shown weighted by the probability of the occurrence of the eruptive event, they are not suitable for comparison to proposed regulatory standards.

Figure 3.3.1.2.4-2. Non-Probability Weighted Mean Annual Dose Due to Volcanic Eruption

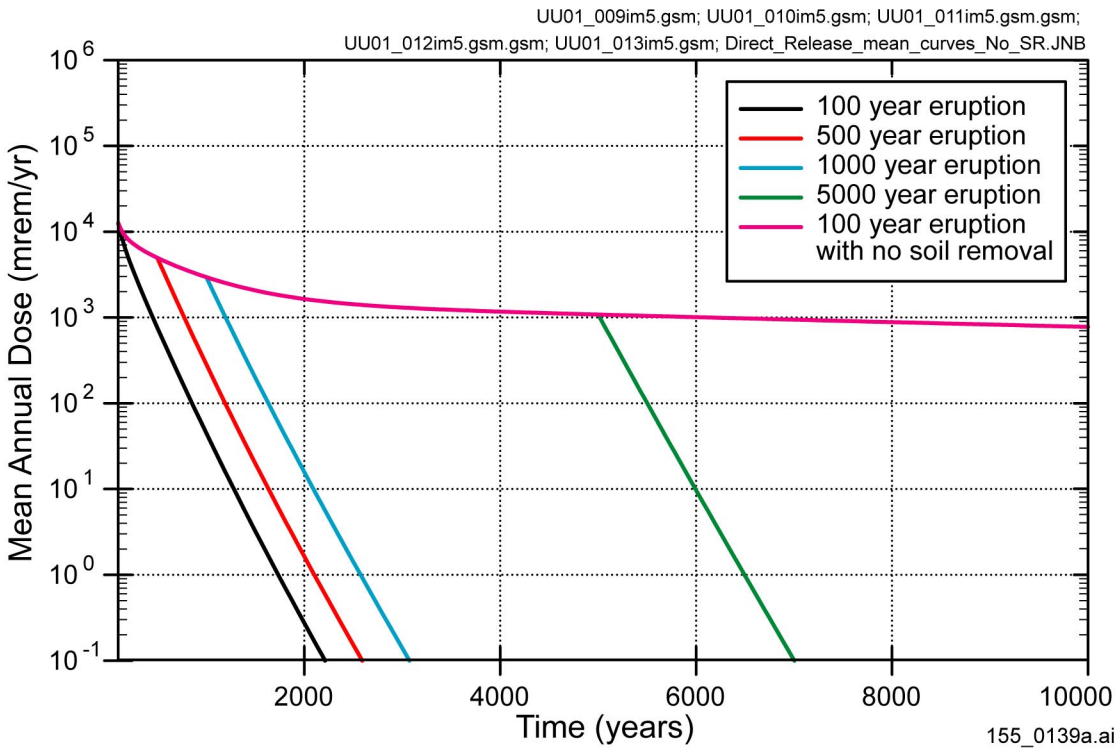

155_0139a.ai

Source: TSPA-SR (CRWMS M&O 2000 [DIRS 153246], Sections 3.10.2 through 3.10.4).

NOTE: Mean conditional annual doses due to a volcanic eruption 100, 500, 1000, and 5000 years after closure of the potential repository, with an additional case showing the mean annual dose from an eruptive event 100 years after closure with the soil removal rate set to zero. Mean annual doses are calculated using the TSPA-SR base-case models and parameters, except for the no-soil-removal case, with the probability of an eruptive event at the repository set to 1. Because annual doses are not weighted by the probability of the occurrence of the eruptive event, they are not suitable for comparison to proposed regulatory standards.

Figure 3.3.1.2.4-3. Non-Probability Weighted Mean Annual Dose Due to Volcanic Eruption with the No-Soil-Removal Case

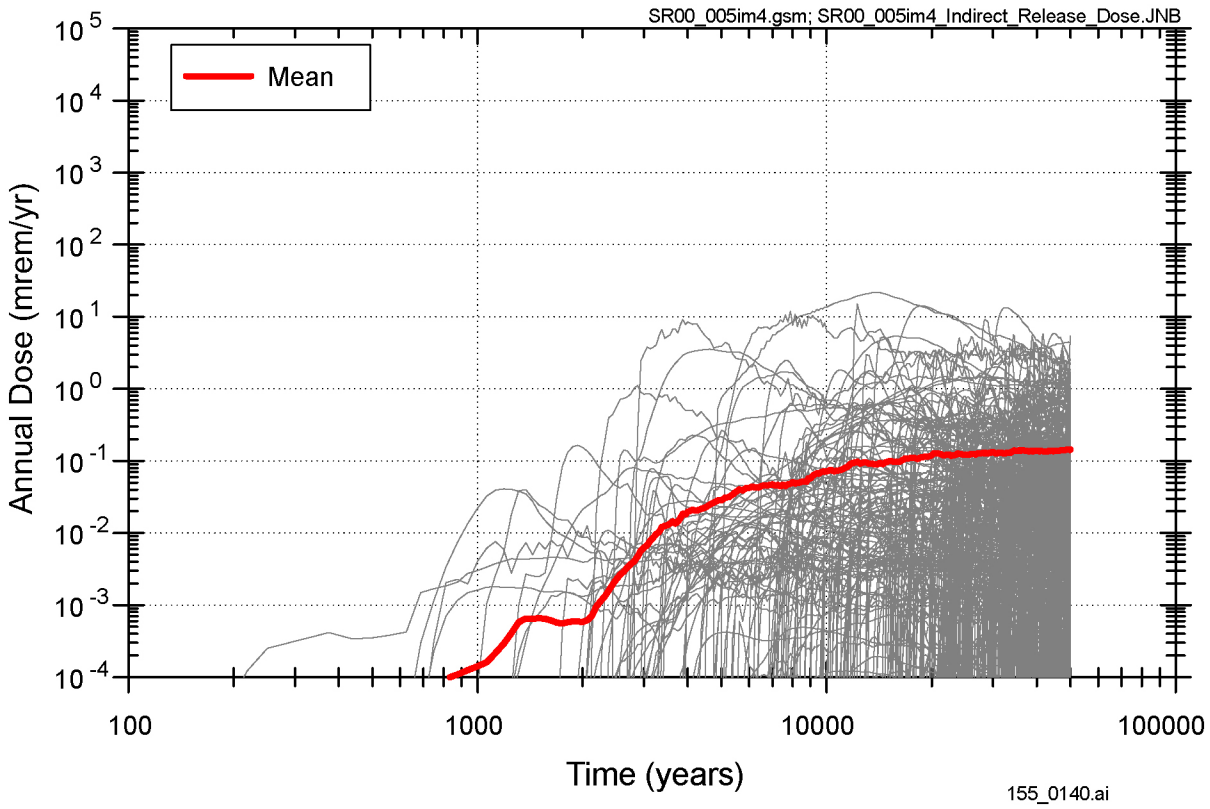

155_0140.ai

NOTE: Probability-weighted annual dose histories due to groundwater transport following an igneous intrusion. This figure displays the same results as in Figure 3.3.1-1, except without the addition of doses due to the eruptive pathway.

Figure 3.3.1.2.4-4. Probability-Weighted Dose for Igneous Groundwater Release Scenario

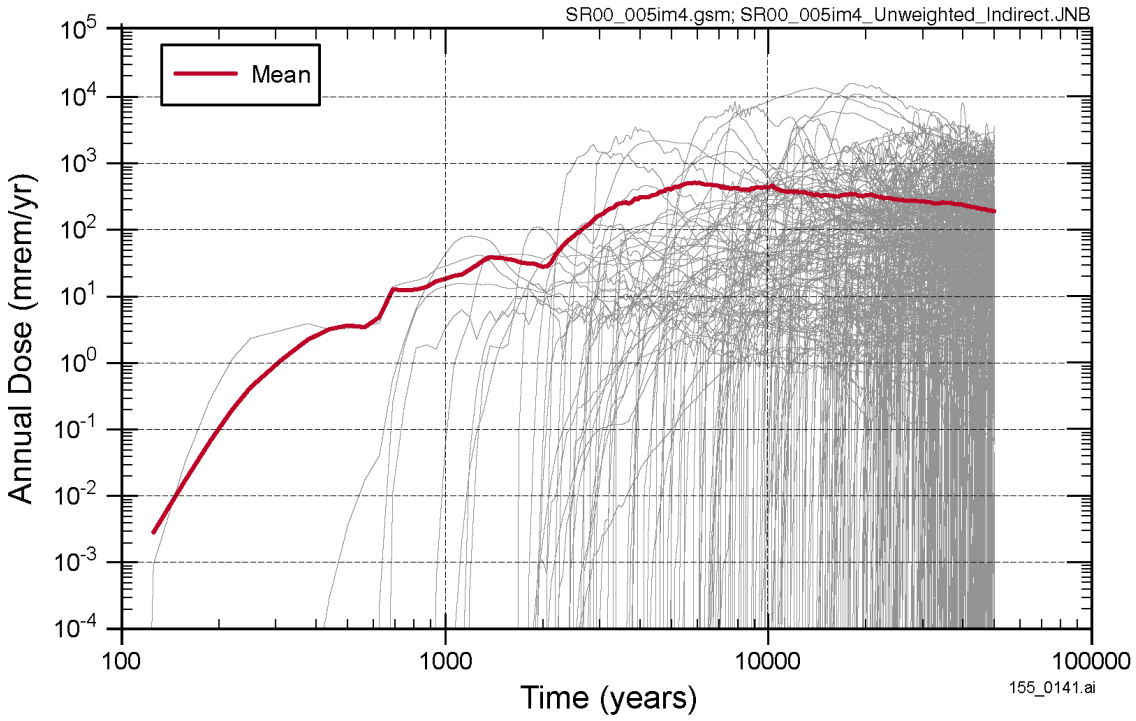

155_0141.ai

NOTE: Conditional annual dose histories due to groundwater transport following an igneous intrusion. This figure displays the same results as in Figure 3.3.1.2.4-4, except that the probability of the occurrence of an igneous intrusion during the simulation is set to 1.

Figure 3.3.1.2.4-5. Unweighted Dose for Igneous Groundwater Release Scenario

(a)

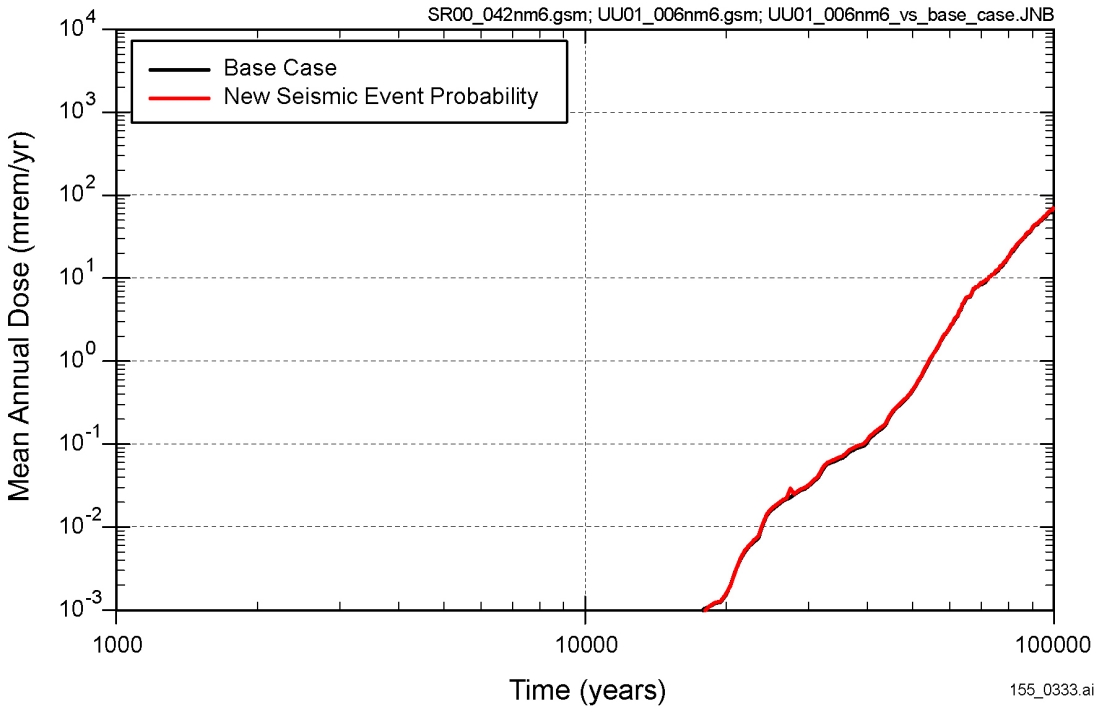

(b)

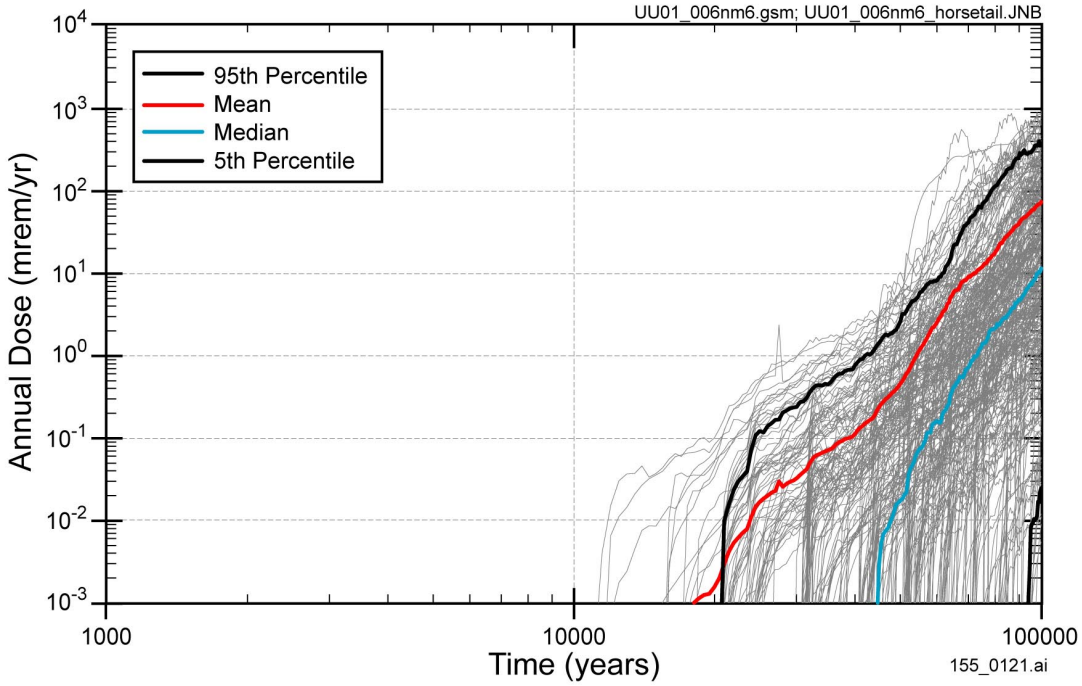

155_0333.ai / 155_0121.ai

NOTE: (a) Comparison of one-off sensitivity analysis with the mean annual dose calculated with the TSPA-SR base-case model. (b) Range of the results for all realizations for the one-off sensitivity analysis.

Figure 3.3.2.1-1. Supplemental Analyses of Sensitivity of Annual Dose Estimate to Uncertainty in Seismic Event Frequency

INTENTIONALLY LEFT BLANK

4. SUPPLEMENTAL TSPA MODEL

This section documents results of supplemental TSPA analyses conducted using a modification of the TSPA-SR model that incorporates new models and input parameter values for some components. These modifications have been made based on insights from uncertainty analyses (see Section 3) and on new information developed since completion of the TSPA-SR (CRWMS M&O 2000 [DIRS 153246]), as described in SSPA Volume 1 (BSC 2001 [DIRS 154657], Sections 3-14) and summarized in Table 1.3-1.

Unlike the one-off analyses (see Section 3), these supplemental TSPA model analyses represent a complete resampling of all input parameters for the TSPA-SR. Therefore, results include a full representation of uncertainty associated with all model components and display the overall impact on performance of the newly quantified uncertainties and other new information developed since TSPA-SR.

Results are discussed for system-level nominal performance (Section 4.1), subsystem nominal performance (Section 4.2), and the igneous disruption scenario (Section 4.3). Results are shown for HTOM and LTOM cases (BSC 2001 [DIRS 154657], Section 2.3.4). Analyses of nominal performance are based on 300 realizations of the supplemental TSPA model. Analyses of igneous disruption are based on 5000 realizations of the supplemental TSPA model. Where appropriate, supplemental TSPA model results are shown in comparison with results from the TSPA-SR.

Appendix A specifies the simulation runs corresponding to the figures in this section. GoldSim calculations have been archived in the Record Information System and are listed in Appendix A with their respective reference identification for accessibility. The electronic media tapes referenced in Appendix A, which can be retrieved using the references documented, identify the source file information used to produce the figures. Appendix A also provides a brief discussion of the process necessary to run the GoldSim simulations. Calculations conducted as part of TSPA-SR are archived in the Technical Data Management System and are listed with their Data Tracking Numbers in the TSPA-SR (CRWMS M&O (2000 [DIRS 153246], Appendix G).

4.1 SYSTEM-LEVEL ANALYSES OF NOMINAL PERFORMANCE

Model and parameter changes for the supplemental TSPA model are described in detail in SSPA Volume 1 (BSC 2001 [DIRS 154657], Sections 3 through 14) and summarized here. For the model and parameter changes that have been examined with one-off sensitivity analyses, references are provided to the relevant portions of Section 3 of this volume.

Supplemental Climate Model–The supplemental TSPA model is updated to include climate changes after 10,000 years in the future (BSC 2001 [DIRS 154657], Section 3.3.1 and Table 3.3.1-3). The updated climate model continues the current climate model until 38,000 years, when a full glacial period begins. The next full glacial period begins at 106,000 years in the updated model. Full glacial periods are anticipated to last 8,000 to 40,000 years in duration, and recur approximately every 90,000 years on average. The repository-average net infiltration for the full glacial states ranges from 17 mm/yr to 110 mm/yr. Interglacial climates represent present-day conditions. Intermediate climates are also represented

in the model and are equivalent to the glacial-transition climate of the TSPA-SR model. The impacts of this updated model on the TSPA-SR results are discussed in Section 3.2.1.2 of this volume.

Supplemental Seepage Model–The seepage model is changed to reflect new seepage data for the Topopah Spring lower lithophysal unit, in which most of the potential repository would be located (BSC 2001 [DIRS 154657], Section 4.3.1). Previously, seepage data were only available for the Topopah Spring middle nonlithophysal unit. These new data indicate that the seepage threshold (the percolation flux above which seepage occurs) is higher in the lower lithophysal unit than in the middle nonlithophysal unit. The revised seepage abstraction takes into account differences between the units by developing distributions of uncertainty and spatial variability separately for the lithophysal and nonlithophysal units. To do so, the two sets of results are combined and weighted by the fraction of the repository in each rock type: approximately 80 percent in the lithophysal unit and 20 percent in the nonlithophysal unit (see Section 3.2.2.2). Inclusion of results for the lower lithophysal unit, with its higher seepage threshold, results in lower estimates of the seepage fraction (the fraction of waste-package locations with seepage) in the revised seepage abstraction. The impact of this update on the TSPA-SR results is discussed in Section 3.2.2.2 of this volume.

Supplemental Seepage Flow Focusing Model–The updated distribution of the flow-focusing factor for seepage is based on simulations of unsaturated-zone flow that were performed using heterogeneous permeability fields (BSC 2001 [DIRS 154657], Section 4.3.2). The resulting flow enhancements are not as large as in the original model, usually less than a factor of 3 and always less than a factor of about 6. The flow-focusing factor is exponentially distributed, with a minimum focusing factor of 1 and a mean focusing factor of 2. Because of the lower degree of flow focusing, the average seepage rate in the regions that have seepage is lower than in the original model by nearly a factor of 10. At the same time, approximately 50 percent more waste packages are exposed to seepage. The impacts of the updated model on the TSPA-SR results are discussed in Section 3.2.2.3 of this volume.

Supplemental Model for Episodic Seepage–Episodicity in seepage induced by accumulation and subsequent release of water at fracture asperities is accounted for by an episodicity factor, which is the fraction of time that flow occurs (BSC 2001 [DIRS 154657], Section 4.3.5.6.2). The distribution of episodicity factors used for this sensitivity analysis is a log-uniform distribution between 10^{-4} and 10^{0}. This factor increases the mean seepage rate during the time seepage occurs. The impact of this factor on the TSPA-SR results is discussed in Section 3.2.2.4 of this volume.

Supplemental Model for Thermal Properties–The model for thermal properties of the host rock has been updated to integrate new information obtained for the Topopah Spring lower lithophysal unit (BSC 2001 [DIRS 154657], Section 4.3.5.6). In addition, thermal properties of the drift invert are updated to take into account the effects of carbon steel in the invert (BSC 2001 [DIRS 154657], Section 5.3.1). These changes result in small changes to the temperature in the host rock and in the emplacement drifts and in the RH in the emplacement drifts. Because changes in thermal properties may affect multiple components of the modeling system, these changes were not examined through one-off sensitivity analyses in Section 3 of

this volume, and their impact on performance is shown through examination of the system and subsystem-level results (see Section 4.1 and 4.2).

Supplemental Model for Thermal Hydrologic Effects on Seepage–The model is modified to take into account the changes in the thermal properties discussed above (BSC 2001 [DIRS 154657], Section 4.3.5.6.1). In addition, the model is modified to incorporate direct effects of higher temperatures on seepage into the emplacement drifts. This model is slightly different from the model considered in the sensitivity analyses (see Section 3.2.2.6). In that case, seepage is reduced to zero when the drift wall is above boiling. The model used in this case is less extreme. In this case, when the temperature at the drift wall exceeds 96ºC, the seepage is multiplied by a reduction factor between 0 and 0.2. The factor is distributed uniformly between these two values. The impact of these changes on performance is shown through examination of the system and subsystem-level results (see Sections 4.1 and 4.2).

Supplemental Model for In-Drift Chemistry–The supplemental TSPA model utilizes better-constrained thermodynamic and kinetic data to improve the representation of the ambient water chemistry and the temperature dependence of that chemistry (BSC 2001 [DIRS 154657], Section 6.3.3). The model also takes into account new information from the Topopah Spring lower lithophysal unit to provide a more representative host rock mineralogy; in particular, it includes contributions from fluorides not considered previously. The supplemental TSPA model also improves the representation of evolution of solids and water during the thermal period due to evaporation of water occurring in the emplacement drifts. In the low humidity range, bounding simplifications are used to overcome limitations in the model formerly used to make the estimates. Impacts of the new model on the TSPA-SR results are discussed in Section 3.2.4.2 of this volume.

Supplemental Model for Stress Corrosion Cracking of Alloy 22–The modified SCC model takes into account four changes (BSC 2001 [DIRS 154657], Section 7.3.3). The first is a changed representation for the fraction of the weld flaws that can propagate. The supplemental TSPA model provides an updated estimate of this fraction. The second change addresses repassivation at the crack tip. The new model is based on new information for Alloy 22. The third change is in the representation of uncertainty in the residual stress profile for the closure welds region of the outer waste package barriers. The representation makes use of updated values for the upper bounds of the uncertainty distributions. The fourth change is an updated distribution of the threshold stress for crack initiation. The new representation provides an updated probability distribution. The impacts of these changes on the TSPA-SR results are discussed in Section 3.2.5.2 of this volume.

Supplemental General Corrosion Model–The supplemental TSPA model takes into account temperature dependence of the general corrosion rate of the Alloy 22 outer waste package barrier (BSC 2001 [DIRS 154657], Section 7.3.5). This temperature dependence is developed from potentiostatic polarization tests. In addition, the uncertainty in the degradation due to general corrosion is assumed to be due entirely to uncertainty in the corrosion process itself and not to variability in conditions or structure. The impact of these modifications on the TSPA-SR results is discussed in Section 3.2.5.3 of this volume.

Supplemental Model for Early Failure of the Waste Package–The supplemental TSPA model includes an increased probability for early waste package failure due to improper heat treatment (BSC 2001 [DIRS 154657], Section 7.3.6). The impacts of this model on the TSPA-SR results are discussed in Section 3.2.5.4 of this volume.

Supplemental Model for Evaporative Reduction of Seepage–A model for evaporative reduction of seepage through the EBS is included in the supplemental TSPA model (BSC 2001 [DIRS 154657], Section 8.3.1). The impacts of this model on the TSPA-SR results are discussed in Section 3.2.6.1 of this volume.

Supplemental Model for Geometrical Constraints on Flow through the Waste Package–The supplemental TSPA model takes into account the fact that breaches in the drip shield may not occur directly over breaches in the waste package and that flow through the drip shield may not all enter the waste package (BSC 2001 [DIRS 154657], Section 8.3.3). The impacts of the geometrical constraints on flow through the waste package on TSPA-SR results are discussed in Section 3.2.6.3 of this volume.

Supplemental Model for In-Package Chemistry–The supplemental TSPA model has been modified to take into account the effect of waste form and iron degradation products on the in-package chemistry (BSC 2001 [DIRS 154657], Section 9.3.1). The impacts of the model on the TSPA-SR results are discussed in Section 3.2.7.1 of this volume.

Supplemental CSNF Cladding Degradation Model–The supplemental TSPA model incorporates new probability distributions for creep and SCC parameters, for localized corrosion, and for cladding unzipping (BSC 2001 [DIRS 154657], Section 9.3.3). In addition, ranges for failures due to rockfall and for the frequency of seismic events are taken into account. The impacts of the modified model on the TSPA-SR results are discussed in Section 3.2.7.2 of this volume.

Supplemental Model for In-Package Radionuclide Solubility Limits–The supplemental TSPA model is modified to increase the range for the uncertainty in the effect of the controlling phases for plutonium, neptunium, and thorium (BSC 2001 [DIRS 154657], Section 9.3.2). The impacts of this increased range on the TSPA-SR results are discussed in Section 3.2.7.3 of this volume.

Supplemental Model for Diffusive Transport within the Engineered Barrier System–The supplemental TSPA model is modified to include a component for diffusive transport on thin films on the surface of in-package components (BSC 2001 [DIRS 154657], Section 10.1 through 10.3). The model for the diffusivity of the drift invert is also updated. Impacts of these changes on the TSPA-SR results are discussed in Section 3.2.8 of this volume.

Supplemental Model for Radionuclide Sorption within the Engineered Barrier System–The supplemental TSPA model includes the effect of sorption within the waste package and in the drift invert (BSC 2001 [DIRS 154657], Section 10.3.4). The model explicitly represents sorption partition coefficients (K_ds) for corrosion products and other materials within the waste package and drift invert and fractions of radionuclides irreversibly sorbed onto these materials. Impacts of the model changes on the TSPA-SR results are discussed in Section 3.2.8 of this volume.

Supplemental Model for Radionuclide Transport in the Unsaturated Drift Shadow Zone-The transfer of radionuclides from the EBS to the UZ uses a modified representation of diffusive and advective flux (BSC 2001 [DIRS 154657], Section 11.3.1.6). Diffusive EBS releases are transferred to UZ matrix transport rather than to fracture transport. The impact of this model on the TSPA-SR results is discussed in Section 3.2.9 of this volume.

Supplemental Model for Radionuclide Transport in the Saturated Zone–The supplemental TSPA model uses a modified representation of the bulk density of the alluvium (BSC 2001 [DIRS 154657], Section 12.3.2.4). This factor helps determine the amount of retardation that a radionuclide undergoes during transport through the alluvium. In addition, the sorption coefficients for iodine and technetium have been changed to zero in the alluvium to reflect new experimental data, as described in SSPA Volume 1 (BSC 2001 [DIRS 154657], Section 12.3.2.2.2). The impacts of these updates on the TSPA-SR results are discussed in Section 3.2.10.2 of this volume.

Supplemental Biosphere Dose Conversion Factors–The supplemental TSPA model includes modified information regarding the biosphere dose conversion factors for key radionuclides (BSC 2001 [DIRS 154657], Section 13.4). Impacts of this change on the TSPA-SR results are discussed in Section 3.2.11 of this volume.

4.1.1 Million-Year Dose Histories for Nominal Performance

Figure 4.1-1 shows the million-year mean annual dose for nominal performance for the supplemental TSPA model for the HTOM and LTOM cases. The mean annual dose histories are compared to the mean annual dose for nominal performance from TSPA-SR. Figures 4.1-2, 4.1-3, and 4.1-4 show the full display of 300 realizations contributing to each mean.

The highest mean annual dose during the period between 10,000 and 100,000 years is substantially lower for the supplemental TSPA model HTOM and LTOM cases than for the TSPA-SR base case, dropping from about 70 mrem/yr to about 0.0001 mrem/yr. The largest contributions to this decrease in peak come from the updated treatment of waste package degradation used in the supplemental TSPA model that takes into account temperature-dependent corrosion rates (see Section 3.2.5). Peak mean doses during the entire 1-million-year period of simulation are also lower for the supplemental TSPA model, reaching a peak of about 35 mrem/yr, as opposed to about 490 mrem/yr in the TSPA-SR base case. Time of peak mean dose shifts from about 270,000 years to about 1 million years, with doses still trending slightly upward at the end of the simulation. As discussed in Sections 3.2.5 and 3.2.7, the decrease in peak mean dose and shift toward later times is due in large part to the updated treatments of waste package degradation (BSC 2001 [DIRS 154657], Section 7.4) and radionuclide solubility limits, in particular neptunium, plutonium, and thorium (BSC 2001 [DIRS 154657], Section 9.3.2). The increase in temporal variability (i.e., the spikiness of the curve) in the supplemental TSPA model results is due primarily to the additional resolution provided by the updated climate model.

Unlike the TSPA-SR base case, the supplemental TSPA model shows nonzero annual doses from nominal performance during the first 10,000 years. These doses result from early failures of a small number of waste packages (see Section 3.2.5), consistent with model changes that expand

the uncertainty associated with the effects of possible improper heat treatment of lid welds. Peak mean annual doses from these early waste package failures are small, reaching a maximum of about 0.0002 mrem/yr for the HTOM case and 0.00006 mrem/yr for the LTOM case. These small doses from early failures are the only significant contributors to the nominal mean annual dose until about 80,000 years, when waste package degradation processes begin to cause additional failures (see Section 3.2.5).

The mean annual dose for the supplemental TSPA model LTOM case is generally slightly less than the mean annual dose for the supplemental TSPA model HTOM case throughout the simulation (Figure 4.1-1). Differences are greatest in the first 20,000 years and again after 100,000 years, but the effect is small at most times. Only between 1,000 and 2,000 years after closure and again at nearly 120,000 years are LTOM annual doses as much as a factor of 10 less than those from the HTOM case.

4.1.2 Individual Radionuclides Contributing to Total Dose, Nominal Performance

Figures 4.1-5, 4.1-6, and 4.1-7 reproduce the total mean annual dose histories for the three cases shown in Figure 4.1-1 together with mean annual dose histories for individual radionuclides that contribute to those total mean annual doses. Results are similar for the supplemental TSPA model HTOM and LTOM cases. Annual doses during the first 10,000 years are dominated by groundwater transport of carbon-14 and technetium-99 from waste packages that have undergone early failure. For the purposes of this analysis, carbon-14 is assumed to be transported in groundwater without chemical reactions or isotopic exchange with water or rock. This assumption provides an unrealistically conservative bound on the possible transport of carbon-14 in groundwater, and the carbon-14 doses should be interpreted accordingly. Total doses from early waste package failures are greatly overestimated during the first approximately 2,000 years, when carbon-14 is the only contributor. Radioactive decay causes the carbon-14 contribution to decline after 10,000 years, and supplemental model doses between 10,000 and 100,000 years are dominated by technetium-99, with lesser contributions from neptunium-237 and iodine-129. After 100,000 years, annual doses calculated from the supplemental model are dominated by the long-lived radionuclide neptunium-237. Figure 4.1-8 shows the same information displayed in pie charts showing contributions to annual dose for the supplemental TSPA model HTOM and LTOM, and for the TSPA-SR base case at selected time during the simulation.

In general, results from the supplemental TSPA model are consistent with those from the TSPA-SR base case. The most noticeable change is the appearance of carbon-14 in the supplemental TSPA model during the first 10,000 years. However, the groundwater transport model for carbon-14 is based on bounding assumptions, and the use of a more realistic treatment of reactive transport would have shown lower doses in the supplemental TSPA model. Carbon-14 is not a contributor in the TSPA-SR base-case results due to its relatively short half-life, 5,730 years (CRWMS M&O 2000 [DIRS 151947], Table 5-4), and the waste package performance model that prevents releases during the first 10,000 years.

4.1.3 Significance of Unquantified Uncertainties and Updated Models, Nominal Performance

One of the goals of the SSPA is to provide insights into the significance of the unquantified uncertainties and the impact of updated scientific results and models (see Section 1). Section 3 documents results of one-off sensitivity analyses conducted using modifications of the TSPA-SR model that incorporate newly quantified uncertainties, new models, or new input parameter values for some components. This section further evaluates the system-level results to provide additional insight into the significance of the previously-unquantified uncertainties and updated scientific information, as well as the degree of conservatism in the overall assessment of the performance of the potential repository.

4.1.3.1 Annual Dose at Particular Times

In the nominal case, the range of uncertainties incorporated into the TSPA is captured by the range of 300 realizations of sampled models and parameters. Further, the mean, median, 5^{th}, and 95^{th} percentiles of the annual dose probability distribution provide information regarding the expected dose rate at a given time and the time to attain a given annual dose. Uncertainties in those mean estimates, represented by the percentiles, can provide insight on the differences between the TSPA-SR and the supplemental TSPA models.

An important consideration in the interpretation of the annual dose probability distribution is the sensitivity of the mean estimate to the number of realizations having zero or nonzero annual doses. This is illustrated by the dose rate histories showing the mean annual dose and individual realizations (Figures 4.1-2 through 4.1-4). At earlier times, most of the 300 realizations provide estimates of zero dose, while a relatively small number of realizations provide estimates of nonzero doses. Because the mean estimate is an average of all realizations at any given point in time, if any realizations have a nonzero dose, the mean estimate will likewise be nonzero. Further, if only a few realizations have annual doses that are significantly higher than the remaining realizations, the mean will likely be closer in value to the few higher values. This effect is seen in the annual dose histories. At early times when relatively few realizations have a finite dose rate, the mean lies close in value to the upper percentiles of the distribution. At later times, the number of realizations having finite dose rates increases and the mean moves closer to the central part of the distribution (that is, toward the median estimates). However, in the case of the supplemental TSPA model (Figures 4.1-2 and 4.1-3), even at times as late as several hundred thousand years there are still many realizations leading to zero dose and, as a result, the difference between the mean and median estimates is notable. In the subsequent discussion, it is important to keep in mind these characteristics of the mean estimates.

Examining the annual dose histories from the standpoint of the probability distribution of realizations can provide insights into the aggregate or system-level significance of the uncertainties in the inputs. Consider first the distribution of dose rates at particular times, which is the same as taking "vertical slices" through the annual dose history plots (Figures 4.1-2, 4.1-3, and 4.1-4). Figures 4.1-9 through 4.1-11 are plots showing the distribution of realizations at three particular points in time: 10,000 years, 30,000 years, and the time of the peak in the mean dose (approximately 1,000,000 years). These plots are constructed by looking at the distribution of realizations at a given time and progressively summing the number of realizations at particular

dose rates to form a cumulative distribution function or summing the number of realizations within various dose-rate increments to form histograms.

The nominal performance annual dose at 10,000 years is zero for all (100 percent) realizations in TSPA-SR, and for about 77 percent of the realizations for the supplemental TSPA model (Figure 4.1-9). The supplemental TSPA model includes a consideration of the uncertainty associated with possible improper heat treatment of the lid welds, and this leads to waste package failures prior to 10,000 years. The wider range of quantified uncertainty in the supplemental TSPA model, in this case, leads to a broader range of outcomes, expressed by the range of realizations.

By 30,000 years (Figure 4.1-10), waste package failures begin to occur according to the TSPA-SR model. A comparable percentage of realizations show failure (about 20 percent), but the annual doses for the TSPA-SR model are significantly higher. This is primarily because the TSPA-SR model shows failures occurring in tens to hundreds of packages by 30,000 years (CRWMS M&O 2000 [DIRS 153246], Figure 4.1-9), while the early failures in the supplemental TSPA model due to improper heat treatment of welds are limited to one or two packages.

The distribution of annual doses at the time of the peak of the mean annual dose is shown in Figure 4.1-11. The peak of the mean dose rate during the period of simulation occurs at about 276,000 years for the TSPA-SR model, and it is close to 1,000,000 years for the supplemental TSPA model, with doses still climbing slightly (Figure 4.1-1). All of the realizations in the TSPA-SR model show a nonzero dose, as do about 90 percent of the realizations for the supplemental TSPA model. The median (50^{th} percentile) dose rate for the supplemental TSPA model is about 10 mrem/yr, and it is about 200 mrem/yr for the TSPA-SR model. As can be seen in the plots, the additional quantified uncertainties and updated models in the supplemental TSPA model lead not only to a reduction in the peak dose at this time, but also a broader spread in the range of annual doses.

4.1.3.2 Time to Particular Annual Doses

Another way to compare the results of the TSPA-SR model and the supplemental TSPA model for nominal performance is to examine the distribution of realizations for the time to reach particular annual doses. This is comparable to taking a series of "horizontal slices" through the dose history plots (Figures 4.1-2 through 4.1-4) at given dose rates. Shown in Figures 4.1-12 through 4.1-15 are cumulative distribution functions and histograms that were constructed in the same way as discussed in Section 4.1.3.1 using the distribution of 300 realizations for each case. Shown are the times at which each realization first reaches a particular annual dose for dose rates of 0.00001, 0.001, 0.1, and 10 mrem/yr. These values are chosen to provide insight into trends, and do not carry specific programmatic or regulatory connotations. The cumulative distribution function is first shown, followed by histograms out to 1,000,000 years and out to 100,000 years.

Beginning with the time to reach 0.00001 mrem/yr (Figure 4.1-12), in general, the time for most of the realizations to reach this annual dose in the TSPA-SR model is considerably shorter than for the supplemental TSPA model. For example, the median or 50 percent of the realizations reach this dose rate by about 50,000 years for the TSPA-SR model, and it is about 400,000 years for the supplemental TSPA model. Similarly, over 90 percent of the TSPA-SR realizations reach

0.00001 mrem/yr in the first 100,000 years, whereas only approximately 20 percent of the realizations in the supplemental TSPA model reach this value in the first 100,000 years (Figure 4.1-12b). Most of realizations in the supplemental TSPA model that reach 0.00001 mrem/yr during the first 100,000 years, do so during the first 50,000 years, with the largest number occurring in the first 10,000 years (Figure 4.1-12c). These early releases are due to improper heat treatment of the waste package lid welds (Section 3.2.5.4). The earliest annual doses of 0.00001 mrem/yr are generally from the unrealistically rapid transport of carbon-14, and if results were adjusted to show only the early doses due to technetium-99, there would be fewer realizations reaching this level in the first 10,000 years. In contrast, the TSPA-SR model has no releases in the first 10,000 years. The net effect of the additional quantified uncertainties and updated models in the supplemental TSPA model is to broaden the range of times at which this dose is reached, relative to the TSPA-SR model.

The same conclusion holds true at the other annual doses (Figures 4.1-13 through 4.1-15). As the dose rate of interest increases from 0.001 to 10 mrem/yr, the difference between the two models in the time to reach that dose level remains about one order of magnitude at the 50^{th} percentile level. At the relatively lower doses of 0.00001 and 0.001 mrem/yr, the supplemental TSPA model has early realizations that reach these levels; at relatively higher doses of 0.1 and 10 mrem/yr, only the TSPA-SR model has early realizations that reach these levels. The first realizations of the supplemental TSPA models do not reach these levels until 200,000 years or later.

4.1.3.3 Conclusions Regarding Uncertainties and Conservatism in Simulations of Nominal Performance

Comparisons at the system (Section 4.1) and subsystem levels (Section 4.2) between the TSPA-SR process models and the supplemental TSPA models and unquantified uncertainties developed for this SSPA provide insight into the ways that uncertainties have been addressed and quantified. Likewise, the one-off sensitivity analyses (see Section 3) provide information regarding the potential effects of the uncertainties and supplemental TSPA models on performance at an individual process model level. In this section, the aggregate effect of all quantified uncertainties and updated scientific information on system performance are presented and compared to the TSPA-SR model. Further, the effects of thermal operating mode on the supplemental TSPA model results are compared.

Comparison of dose histories over 1,000,000 years for the TSPA-SR base case and the supplemental TSPA model shows the following two characteristics. First, the supplemental TSPA model shows significantly wider ranges of doses at a given time, and of times to reach given doses. Second, except at early times, the magnitude of the dose rate is less for the supplemental TSPA model and it occurs later in time.

The first observation is best illustrated by the comparisons in Figures 4.1-9 through 4.1-15. In every case, the supplemental TSPA model produces a broader range of annual doses or times to specific annual dose values than does the TSPA-SR model. This is represented quantitatively by the distribution of realizations at particular dose rates and particular times. The broader range is a result of the additional uncertainties and updated models that have been incorporated into the supplemental TSPA model. In many cases, simplified or bounding models have been replaced

with more physically representative models that include quantified uncertainties in their parameters. For example, a bounding solubility model for neptunium in TSPA-SR (CRWMS M&O 2000 [DIRS 153246], Section 3.5.5) has been replaced with a more complex model that accounts for the solubility of secondary phases that control the solubility (BSC 2001 [DIRS 154657]), Section 9.3.4). The updated solubility model is believed to be more realistic, but the uncertainties in the model lead to a broader range of neptunium concentrations than the previous model. Propagation of these uncertainties, as well as those of all of the other updated process models, results in the broad ranges that are seen in results of the supplemental TSPA model.

The second observation is based on a comparison of the estimates of mean performance (dose rate and time to dose) for the TSPA-SR case and the supplemental TSPA cases (Figure 4.1-1), which shows that, after approximately 10,000 years, the mean annual dose for the supplemental TSPA model is always less than the mean for the TSPA-SR model. The difference between the mean estimates is one measure of the magnitude of the conservatism in the TSPA-SR model. For example, at 30,000 years, the difference between the mean estimates of dose rate is about three orders of magnitude (Figure 4.1-10a), and at time of peak mean dose the difference is about one order of magnitude (Figure 4.1-11a). The magnitude of conservatism can also be estimated by the difference in the mean time to reach particular dose levels. For example, the delay in reaching a mean annual dose of 0.1 mrem/yr in the supplemental TSPA model is about 200,000 years, and the delay in reaching 10 mrem/yr is over 400,000 years (Figures 4.1-1, 4.1-14a and 4.1-15a).

During the period prior to 10,000 years, the small annual doses (less than about 0.0002 mrem/yr) indicated by the supplemental TSPA nominal model clearly exceed the zero annual doses calculated in TSPA-SR, and the supplemental TSPA model could be interpreted as being nonconservative with respect to the TSPA-SR model during this time. However, these small doses, resulting from the revised treatment of uncertainty regarding the potential for improper heat treatment of lid welds on waste packages, are more than a factor of one thousand below applicable regulatory limits. Differences between the supplemental TSPA model and TSPA-SR have essentially no impact on conclusions that might be drawn with respect to comparisons with quantitative regulatory limits.

From the standpoint of uncertainties at the total system level, the supplemental TSPA model HTOM and LTOM cases show essentially comparable nominal performance, and both are significantly different from the TSPA-SR model. One potentially significant difference between the two operating modes is seen in the plots of the time for individual realizations to reach 0.1 and 10 mrem/yr (Figures 4.1-14a and 4.1-15a). supplemental TSPA model LTOM realizations reach those levels several tens of thousands of years later than HTOM realizations. This is due to the temperature dependency of the general corrosion rate for the waste package, resulting in lower corrosion rates for the LTOM.

4.1.4 One-Million-Year Nominal Performance Results: Groundwater Concentrations and Critical Organ Doses from Beta and Photon Emitters

Figure 4.1-16 shows the mean combined radium-226 and radium-228 concentrations and the mean gross alpha-activity concentration (including radium-226, but excluding radon and

uranium) calculated for nominal performance. Figure 4.1-17 shows the mean critical organ dose associated with beta and photon emitting radionuclides (iodine-129, technetium-99, and carbon-14), calculated for nominal performance. The critical organs for these three radionuclides are the thyroid (iodine-129), the gastrointestinal tract (technetium-99), and fat (carbon-14). As described in following paragraphs, each figure contains three separate plots: one each for the TSPA-SR results (CRWMS M&O 2000 [DIRS 153246], Section 4.1.5); the supplemental TSPA model HTOM; and the supplemental TSPA model LTOM. Carbon-14 doses should be interpreted as a conservative upper bound, consistent with the unrealistic simplifying assumption in the TSPA-SR and supplemental TSPA models that carbon-14 is transported as a nonreactive species. All results are calculated for a location 20 km south of the potential repository, and all results are based on a representative volume of groundwater of 1,285 acre-ft/yr, consistent with the requirements of proposed 40 CFR 197.36 (64 FR 46976 [DIRS 105065]). As discussed in SSPA Volume 1 (BSC 2001 [DIRS 154657], Section 12.5.3) and summarized in Section 5.4, implementation of the final EPA requirement of 18 km (40 CFR 197.31, 66 FR 32074 [DIRS 155216]) will shift the peak mean concentrations and mean doses to somewhat earlier times, but will not affect the magnitude of the peaks. Implementation of the final EPA requirement of 3,000 acre-ft/yr (40 CFR 197.31, 66 FR 32074 [DIRS 155216]) will cause a reduction in concentrations and critical organ doses equal to a 2.3 dilution factor introduced by the increase in the size of the representative volume.

The overall peak mean concentrations during the period of simulation are delayed and reduced in the supplemental TSPA model for total radium activity and gross alpha activity, relative to the TSPA-SR results (Figure 4.1-16). Changes in mean radionuclide concentrations between the TSPA-SR results and the supplemental TSPA model are consistent with the changes observed in the mean annual dose described in Section 4.1. Small concentrations occur at relatively early times in the supplemental TSPA model, consistent with early waste package failures resulting from the expanded range of uncertainty associated with heat treatment of lid welds. The delay of peak concentrations in the supplemental TSPA model is consistent with the modified treatment of waste package corrosion. Peak mean concentrations of gross-alpha activity are reduced (from about 14 pCi/L in the TSPA-SR, to about 7 pCi/L in the supplemental TSPA model HTOM case, and to 5 pCi/L in the supplemental TSPA model LTOM case), consistent with reductions in the mean solubility of neptunium and plutonium. Peak mean concentrations of total radium activity are similar in the supplemental TSPA model (about 0.09 pCi/L for HTOM and 0.07 pCi/L for LTOM) to the values from TSPA-SR (about 0.06 pCi/L). During the time period of regulatory concern (10,000 years), when the only releases come from the low-probability early waste package failures, concentrations are extremely small but higher than the zero values in TSPA-SR. The highest mean concentrations of gross-alpha activity during the first 10,000 years are approximately 7×10^{-8} pCi/L for the supplemental TSPA model, occurring in the HTOM case. The highest mean concentrations of total radium activity during the first 10,000 years are approximately 7×10^{-11} pCi/yr, also occurring in the supplemental TSPA model HTOM case.

Natural background concentrations of radionuclides are not included in the results shown in Figure 4.1-16. As discussed in the TSPA-SR (CRWMS M&O 2000 [DIRS 153246], Section 4.1.5), available data indicate that gross alpha background concentrations at the point of compliance are 0.4 ± 0.7 pCi/L, and that total radium background concentrations are no greater than 1.04 pCi/L. For comparison to the EPA limits of 15 pCi/L for gross alpha concentration and 5 pCi/L for total radium during the first 10,000 years of performance (40 CFR 197.30,

66 FR 32074 [DIRS 155216]), the TSPA-SR and supplemental TSPA model results should be adjusted to include naturally occurring background concentrations.

Peak mean critical organ doses from iodine-129 and technetium-99 are delayed in the supplemental TSPA model relative to the TSPA-SR model (Figure 4.1-17). Consistent with the changes observed in the mean annual dose (see Section 4.1), small doses occur at relatively early times in the supplemental TSPA model due to early waste package failures resulting from the expanded range of uncertainty associated with heat treatment of lid welds. The delay in peak doses is consistent with the more realistic treatment of waste package corrosion. Peak mean doses from iodine-129 are similar (about 7 mrem/yr in the supplemental TSPA model for the HTOM and LTOM cases, versus about 9 mrem/yr in TSPA-SR), and peak mean technetium-99 doses are lower (about 0.3 mrem/yr in the supplemental TSPA model for the HTOM and LTOM cases, versus about 3 mrem/yr in TSPA-SR). Small carbon-14 doses occur earlier in the supplemental TSPA model, consistent with the small number of early waste package failures in the model. Peak mean carbon-14 doses are smaller (about 0.0002 mrem/yr in TSPA-SR to about 0.000005 mrem/yr for the supplemental TSPA model) due to the longer lifetime of most waste packages that allows for the decay of most carbon-14 before it is released. During the time period of regulatory concern (10,000 years) when the only releases come from the low-probability early waste package failures, calculated critical organ doses from carbon-14 reach a maximum of about 0.00005 mrem/yr for the HTOM case and 0.00002 for the LTOM case.

4.2 SUBSYSTEM-LEVEL ANALYSES OF NOMINAL PERFORMANCE

This section documents subsystem-level analyses of the supplemental TSPA model for nominal performance. Sections are organized by individual model components, paralleling the organization of Section 3.2. However, the results in these sections are not the result of one-off sensitivity studies as in the case of Section 3.2. The analyses in this case are intermediate outputs of the system-level analysis of nominal performance discussed in Section 4.1. Results are expressed in terms of subsystem intermediate performance measures (e.g., seepage flux, temperature, RH, drip shield, and waste package failure) calculated using the supplemental TSPA model for the HTOM and LTOM cases. As appropriate, intermediate performance measures are compared to the analogous results from the TSPA-SR base-case model.

4.2.1 Evaluation of Unsaturated Zone Flow

In Section 4.1, the supplemental TSPA model is described, and results for two thermal operating modes are presented. In this section, information is presented about UZ flow in the supplemental TSPA model. The only change from the TSPA-SR base case to the supplemental TSPA model related to UZ flow is the use of the extended climate model (CRWMS M&O 2000 [DIRS 153246], Section 3.2.5; see also Section 3.2.1.2), rather than the TSPA-SR base-case climate model (CRWMS M&O 2000 [DIRS 153246], Section 3.2.1; see also Section 3.2.1.1). The climate in the supplemental TSPA model is the same as that in the TSPA-SR base-case climate model until 38,000 years, when the first glacial period is estimated to begin. After 38,000 years, the supplemental TSPA model includes alternating intermediate, glacial, and interglacial climates to 1,000,000 years in the future (BSC 2001 [DIRS 154657], Table 3.3.1-3), whereas the TSPA-SR base-case model retains an intermediate climate for this duration.

Climate, infiltration, and UZ flow are independent of potential repository thermal operating mode, so they are the same for both modeled thermal operating modes. In principle, UZ flow is affected by heat from the potential repository, and therefore is affected by the thermal operating mode, but thermal effects on mountain-scale flow are neglected in the TSPA-SR models (CRWMS M&O 2000 [DIRS 153246], Section 3.2.3.1.)

Climate change affects modeled net infiltration (Figure 4.2.1-1), as illustrated with curves showing average net infiltration averaged over the potential repository area and over the three infiltration cases (low, medium, and high). For example, the curve for the supplemental TSPA model is the weighted average of the three curves in CRWMS M&O (2000 [DIRS 153246], Figure 3.2-16), weighted by the probabilities in the TSPA-SR (CRWMS M&O 2000 [DIRS 153246], Table 3.2-2). The TSPA-SR base case has no climate changes after 2,000 years. The increases in net infiltration after that time in the supplemental TSPA model occur during glacial climate periods, and the decreases occur during interglacial periods.

4.2.2 Evaluation of Seepage

In this Section, information is presented about seepage in the supplemental TSPA model. For seepage, the supplemental TSPA model includes several changes from the TSPA-SR base case (BSC 2001 [DIRS 154657], Section 4.3.1.3; CRWMS M&O 2000 [DIRS 153246], Section 3.2.4; see also Section 3.2.2.1). The changes are discussed in Section 3.2.2.7. In summary, the changes are:

- The updated seepage abstraction (updated distributions for seepage fraction and the mean and standard deviation of seep flow rate) (BSC 2001 [DIRS 154657], Section 4.3.1.6; see also Section 3.2.2.2)

- The updated distribution for the flow-focusing factor (BSC 2001 [DIRS 154657], Section 4.3.2.6; see also Section 3.2.2.3)

- The distribution of the episodicity factor (BSC 2001 [DIRS 154657], Section 4.3.5.6.2; see also Section 3.2.2.4)

- The modified model for TH effects on seepage (reduction in seepage by a sampled factor between 0 and 0.2 when the drift wall is above boiling) (BSC 2001 [DIRS 154657], Section 4.3.5.6.1; see also Section 3.2.2.6).

In addition, a change was made in the way the environmental groups of waste packages are defined (see Section 3.2.2.1). The distinction between seepage some of the time and seepage all of the time was eliminated because no significant differences in their behavior have been found (CRWMS M&O 2000 [DIRS 153246], Section 4.1.2). Thus, there are 20 environmental groups in the supplemental TSPA model instead of 30. These groups are based on five infiltration bins, times two waste packages, times two seepage states (see Section 3.2.2.1).

The average number of waste packages in each environmental group is given in Table 4.2.2-1 for the HTOM case and in Table 4.2.2-2 for the LTOM case. The numbers in the tables represent averages over all 300 TSPA realizations. The differences between the operating modes are

caused by differences in the potential repository area and differences in the percolation flux above the drifts during the thermal period.

For reasons discussed in Section 3.2.2.7 (primarily, the reduction in the flow-focusing factor and the inclusion of episodic flow), the number of waste packages in locations with seepage is significantly higher in the supplemental TSPA model as compared to the TSPA-SR base case (CRWMS M&O 2000 [DIRS 153246], Table 4.1-1). The overall average fraction of waste packages in locations with seepage is 48 percent for the HTOM case (Table 4.2.2-1) and 45 percent for the LTOM case (Table 4.2.2-2). The corresponding average fraction for the TSPA-SR base case (CRWMS M&O 2000 [DIRS 153246], Section 4.1.2) is 13 percent.

Figures 4.2.2-1 through 4.2.2-4 show the mean seep flow rate for the 10 environmental groups with seepage, averaged over the 300 TSPA realizations. The plots show that, after the thermal period, the mean seep flow rate is higher for the higher infiltration bins, and the mean seep flow rate is highest during the glacial climates and lowest during the interglacial climates. Seep flow rates, in Figures 4.2.2-1 through 4.2.2-4, have been reduced to account for evaporation in the drift (part of the water-diversion performance of the EBS discussed in BSC 2001 [DIRS 154657], Section 8.3.1; see also Section 3.2.6.1), in addition to being reduced to account for evaporation of water when there is a vaporization zone around the drift (BSC 2001 [DIRS 154657], Section 4.3.5.6.1; see also Section 3.2.2.6).

A direct comparison between the two operating modes and the TSPA-SR base case for one of the environments (CSNF locations with seepage in the 20 to 60 mm/yr infiltration bin) is presented in Figure 4.2.2-5. This environment is presented because it has the greatest number of waste packages of all groups with seepage (Tables 4.2.2-1 and 4.2.2-2). For this environment, seep flow is suppressed during the first few hundred years in the HTOM case because a boiling zone develops around the drifts (Figures 4.2.2-6 and 4.2.2-8). No boiling zone develops in the LTOM case (Figures 4.2.2-7 and 4.2.2-9). In Figure 4.2.2-5, the mean seep flow rate is essentially the same in both operating modes after about 1,000 years. The mean seep flow rate is lower than the TSPA-SR base case except during the glacial climates.

4.2.3 Analyses of In-Drift Thermal-Hydrologic Conditions

Calculated temperature and RH in the emplacement drifts are shown in Figures 4.2.3-1 and 4.2.3-2). The analyses that have produced these results and source file information traceable to particular simulation runs are discussed in Section 4.

Waste package temperatures are shown in Figure 4.2.3-1. This analysis compares average waste package temperatures calculated for the TSPA-SR base-case HTOM case (CRWMS M&O 2000 [DIRS 153246], Section 3.3.3) with those calculated using the supplemental TSPA model for the HTOM and the LTOM cases. Figure 4.2.3-1a shows the results for the codisposal waste packages, and Figure 4.2.3-1b shows the results for CSNF packages.

For each type of waste, comparison of the temperature histories (Figure 4.2.3-1) shows small differences between the results for the two models for the HTOM case. The peak waste package and invert temperatures for the supplemental TSPA model are somewhat higher than the peak temperatures calculated with the TSPA-SR base-case model, reflecting the changes in the

thermal and TH models. Temperatures for the LTOM case are substantially lower than those for the HTOM cases during the thermal period (the first several thousand years after closure of the potential repository). The peak waste package temperature is reduced from about 160ºC to less than 85ºC.

Figure 4.2.3-2 shows the analogous comparison for RH calculated next to the waste package. Figure 4.2.3-2a compares the average RH for codisposal waste packages, and Figure 4.2.3-2b compares the average RH for CSNF waste packages. In these analyses, the estimate of RH accounts for temperature changes with time, but it does not account for the removal of moisture by ventilation air in the period before permanent closure. In general, the comparison shows differences between the RH calculated with the TSPA-SR (CRWMS M&O 2000 [DIRS 153246]) base-case model and with the supplemental TSPA model for the HTOM design that reflect the difference in waste package temperatures calculated with these two models. The RH is inversely proportional to the saturated vapor pressure, and this quantity increases with temperature. This dependence on the temperatures shown in Figure 4.2.3-1 is reflected in the relative humidities shown in Figure 4.2.3-2.

Up to the time of permanent closure (50 years for the HTOM; 300 years for the LTOM), the RH comparison for the HTOM and LTOM designs also reflects the difference between the waste package temperatures. After this time, however, the RH for the LTOM is calculated to be lower than that for the HTOM, in spite of the fact that the waste package temperature is lower for the LTOM. The reason for this inversion is that, in addition to the higher saturated vapor pressure due to higher temperature, the HTOM reflects a higher vapor pressure than the LTOM. The vapor pressure is sufficiently high that the RH, which is the ratio of the vapor pressure to the saturated vapor pressure, is higher for the HTOM than for the LTOM.

The calculated temperature and RH are included in the evaluation of total system performance, and the difference between the results for the different models is taken into account in the estimates of annual dose for the system as a whole. The comparison among these estimates is discussed in Section 4.1.

4.2.4 Analyses of In-Drift Physical and Chemical Environments

Calculated pH in the emplacement drift is shown in Figure 4.2.4-1. The analyses that produced these results are described in Section 4.1. The model analyses and source file information traceable to the particular simulation runs used to produce these results are discussed in Section 4.

Figure 4.2.4-1 shows the pH for the drift invert calculated using the TSPA-SR base-case and supplemental TSPA models. Figure 4.2.4-1a compares the mean drift invert pH calculated using the TSPA-SR base-case model for the HTOM case (CRWMS M&O 2000 [DIRS 153246], Section 3.3.4) with those calculated with the supplemental TSPA model for the HTOM and the LTOM cases. To provide perspective, Figure 4.2.4-1b shows the range of invert pH calculated for the HTOM using the TSPA-SR base-case model.

As explained in Volume 1, the pH in the LTOM model falls to around 5 or slightly lower as evaporation produces ionic strengths above 1 molal (DIRS 154657, Section 6.3.3.6.1). These

lower pH predictions are caused by the differences in the abstracted seepage and gas compositions used as input and varying (high or low) pCO2 starting values (DIRS 154657, Section 6.3.1).

The comparison of the temperature histories (Figure 4.2.4-1a) shows that the changes in the TSPA-SR base-case model lead to large changes in the pH in the first several thousand years when temperatures are elevated. The main effect of the invert pH is to modify the transport characteristics of radionuclides released from breached waste packages; however this change appears to have no effect on total overall performance. Consequently, this large difference would not have a large impact for those waste packages that do not fail during this early period. The invert pH calculated in the supplemental TSPA model also differs somewhat from the base-case model results at later times; however the difference in this case is on the order of the range of uncertainty in the pH (e.g., in the range shown in Figure 4.2.4-1b). Accordingly, although the models and operating modes differ, the impact on the estimate of system performance of the in-drift chemistry may not be important.

4.2.5 Analyses of Waste Package and Drip Shield Degradation

Calculated drip shield and waste package degradation rates are shown in Figures 4.2.5-1 through 4.2.5-3. The analyses that produced these results are described in Section 4.1. The model analyses and source file information traceable to the particular simulation runs used to produce these results are discussed in Section 4.

Figure 4.2.5-1 shows the fraction of drip shields calculated to have failed using the TSPA-SR base-case model and the supplemental TSPA model. The mean fraction of failed drip shields for the HTOM calculated using the TSPA-SR base-case model (CRWMS M&O 2000 [DIRS 153246], Section 3.4.2) is compared with the fractions calculated using the supplemental TSPA model for the HTOM and the LTOM cases in Figure 4.2.5-1a. To provide perspective, Figures 4.2.5-1b, 4.2.5-1c, and 4.2.5-1d show the range of realizations for the estimate of the fraction of drip shield failures calculated for each of these three calculations. The ranges do not differ widely among the three cases.

There is no apparent difference between the results for the LTOM and the HTOM cases calculated with the supplemental TSPA model, indicating that the drip shield corrosion model is not sensitive to temperature or other environmental parameters. In contrast, there is a large difference between the results of the TSPA-SR base-case and supplemental TSPA models. This difference is due entirely to the different approach to the treatment of uncertainty in the two models. The probability distribution for the drip shield corrosion rate in the supplemental TSPA model does not include any uncertainty due to variability in environmental conditions or microstructure across the drip shield. The uncertainty in the degradation rate, therefore, only reflects the uncertainty in the corrosion rate. The TSPA-SR base-case model, however, does account for the additional uncertainty due to variability across the drip shield. Therefore, the TSPA-SR base-case probability distribution for the drip shield degradation has a broader range than that in the supplemental TSPA model. The way in which this modification affects the time of occurrence of initial breaching of the drip shield is described in Section 3.2.5.3. Accordingly, the drip shield failure fraction is shifted out to later times in the supplemental TSPA model analyses.

Figure 4.2.5-2 shows the fraction of waste packages calculated to have failed using the TSPA-SR base-case and supplemental TSPA models. The mean fraction of failed waste packages for the TSPA-SR base case (CRWMS M&O 2000 [DIRS 153246], Section 3.4.2) is compared with those calculated with the supplemental TSPA model for the HTOM and the LTOM in Figure 4.2.5-2a. To provide perspective, Figures 4.2.5-2b, 4.2.5-2c, and 4.2.5-2d show the range of the estimate of the fraction of failed waste packages calculated in each of these models.

Figure 4.2.5-3 shows the estimates of the fraction of patch failures on those waste packages that failed using the TSPA-SR base-case and supplemental TSPA models. The mean fraction of failed patches on failed waste packages calculated with the TSPA-SR base-case model (CRWMS M&O 2000 [DIRS 153246], Section 3.4.2) is compared with those calculated with the supplemental TSPA model for the HTOM and the LTOM in Figure 4.2.5-3a. Figures 4.2.5-3b, 4.2.5-3c, and 4.2.5-3d show the range of this estimate for the three cases. In Figures 4.2.5-2 and 4.2.5-3, the difference between the results using the TSPA-SR base-case model and the supplemental TSPA model is significant. Aside from the small fraction of potential early failures in the supplemental TSPA model, the waste package failures generally occur later in this model than in the TSPA-SR base-case model. At the same time, the differences between the HTOM and LTOM results using the supplemental TSPA model are smaller than the differences between the results for the TSPA-SR base-case and supplemental TSPA models, suggesting the main source of difference between these results is the change in the corrosion model and not the difference in the environments on the waste package. The updates to the SCC model and the temperature dependence of the general corrosion model increase the time to first failure and breaching after initial failure. The temperature dependence of the Alloy 22 general corrosion model explains the difference between the results for the HTOM and LTOM in the supplemental TSPA model. Finally, the supplemental TSPA model includes the model for early failure due to improper heat treatment that is not included in the TSPA-SR base-case model. This combination of effects results in the changes in failure characteristics relative to the TSPA-SR base-case model.

Sensitivities to individual changes in the model are illustrated in Figures 4.2.5-4 and 4.2.5-5. Figure 4.2.5-4a shows the mean fraction of waste packages calculated to have failed using the TSPA-SR base-case model along with several sensitivity studies. The sensitivity studies are conducted for the LTOM. These sensitivity studies are designed to show the effect of individual changes incorporated into the supplemental TSPA model on the waste package failure. The corresponding mean annual dose histories are shown in Figure 4.2.5-4b. To provide additional insight, the ranges for the realizations calculated for the LTOM sensitivity analyses are shown in Figure 4.2.5-5.

The first LTOM sensitivity analysis is for a model incorporating all the components of the supplemental TSPA model except the waste package degradation model. The waste package degradation model in this case corresponds to that of the TSPA-SR base-case model. As shown in Figure 4.2.5-4a, the waste package degradation profile for this case differs little from that obtained using the entire TSPA-SR base-case model. Figure 4.2.5-4b shows the mean annual dose history for this model. The curve shows a small annual dose at earlier times than did the TSPA-SR base-case model because of the incorporation of early waste package failures. However, the onset of increased annual dose is delayed by about 20,000 years from the result for

the TSPA-SR base-case model. This delay is due to differences between the TSPA-SR base-case and supplemental TSPA models other than the waste package degradation model.

The second LTOM sensitivity analysis considers the same situation except that the waste package degradation model is modified to include the supplemental model for weld flaw orientation (see Section 3.2.5.2). That is, all components of the supplemental TSPA model are invoked except that the waste package degradation model corresponds to the TSPA-SR base-case model with the supplemental weld flaw model incorporated. The results in Figure 4.2.5-4a show a delay in the onset of waste package degradation to 30,000 years. The corresponding mean annual dose curve in Figure 4.2.5-4b shows the delay in the onset of increased annual dose of about 50,000 years relative to the result from the TSPA-SR base-case model.

The third LTOM sensitivity analysis considers additional effects in the waste package degradation model. In this case, all components of the supplemental TSPA model are incorporated except that the waste package degradation model corresponds to the TSPA-SR base-case model with the supplemental SCC model incorporated. This model includes all of the SCC effects discussed in Section 3.2.5.2 (including the supplemental weld flaw model). The results in Figure 4.2.5-4 show the waste package failure profile and mean annual dose history obtained using this particular model. The effects accounted for in this analysis delay the onset of waste package degradation 40,000 years relative to the TSPA-SR base-case model. The time at which the mean annual dose deviates from the early failure-only mean annual dose is about 60,000 years later than that calculated with the TSPA-SR base-case model.

The remaining analysis in this comparison examines the full supplemental TSPA model. In particular, this analysis includes the effect of temperature dependence of the general corrosion model (see Section 3.2.5.3), as well as the effects accounted for in the other curves in this figure. The curve in Figure 4.2.5-4a is the same as that shown in Figure 4.2.5-2a, and the curve in Figure 4.2.5-4b is the same as that shown in Figure 4.1-1. It is clear from this figure that the temperature-dependence of the general corrosion rate plays a major role in determining the onset of increased mean annual dose in this analysis.

These figures suggest that the mean annual dose is closely related to waste package failure. The general features of the profiles in Figure 4.2.5-4 suggest a correlation between the mean annual dose and the mean waste package failure rate. For example, the early ledge in both curves shows the correlation between early waste package failure due to the improper heat treatment and the early release of radionuclides in this analysis. Then, the increase in waste package failures due to general and other corrosion mechanisms is correlated with an associated increase in the annual dose rate. Other factors play a role (for example, processes affecting delay in the transport of radionuclides from the repository to the accessible environment); however, the correlation between the mean failure rate and the mean annual dose profiles is clearly apparent.

Evaluation of the magnitude of the mean annual dose provides additional evidence for this correlation because this magnitude generally scales with the total number of waste package patch breaches. For example, the mean number of patch breaches associated with the early waste package failures is approximately 8 (see Section 3.2.5.4). Figure 4.2.5-4b indicates the magnitude of the mean annual dose associated with these early waste package failures is on the order of 10^{-4} mrem/year. The mean annual dose per breach failure in this case is therefore on the

order of 10^{-5} mrem/year. At 1,000,000 years, Figure 4.2.5-3 indicates that the mean number of patch failures on those packages that have failed is estimated in the full supplemental TSPA-SR model for the LTOM to be about 15 percent of the 1,000 patches per waste package, or about 150 patch breaches per failed waste package. Figure 4.2.5-4a indicates that approximately 60 percent of the 11,000 waste packages, or about 6,600 waste packages, are failed by this time in this same model. These quantities support a total mean annual dose of about 10 mrem/year for the entire repository ($6{,}600 \times 150 \times 10^{-5}$) if the mean annual dose scales with number of patch breaches. This value is consistent with the supplemental TSPA-SR model estimate of the mean annual dose at 1,000,000 years in Figure 4.2.5-4b for the LTOM. In general, the magnitude of the mean annual dose correlates well with the rate and degree of waste package failure.

4.2.6 Analyses of Water Diversion Performance of the Engineered Barrier System

Calculated flow through the EBS is shown in Figures 4.2.6-1 and 4.2.6-2. The analyses that produced these results are described in Section 4.1. The model analyses and source file information traceable to the particular simulation runs used to produce these results are discussed in Section 4.

Figure 4.2.6-1 shows the average seepage through a drip shield calculated using the three models (i.e., the TSPA-SR base-case model (CRWMS M&O 2000 [DIRS 153246]), the supplemental TSPA model for the HTOM case, and the supplemental TSPA model for the LTOM case). The supplemental TSPA model generally predicts a lower flux than does the conservative estimate in the TSPA-SR base-case model. Increases in net infiltration during times of higher precipitation, taken into account in the supplemental climate model, result in higher fluxes during those times; however, the average is lower. There is virtually no difference between results of the higher-temperature and lower-temperature cases using the supplemental TSPA model. This suggests that evaporation of the flux and other temperature-dependent effects, taken into account in the model, have little influence on the results.

Figure 4.2.6-2 shows fluid flux through a single waste package calculated using the TSPA-SR base-case model (CRWMS M&O 2000 [DIRS 153246], Section 3.6.3.1) and the supplemental TSPA model for the HTOM and the LTOM cases. These results indicate a substantial delay before water flows into and through the waste package in the supplemental TSPA model relative to the fraction calculated for the TSPA-SR base-case model. As in the case of fluid flux through the drip shield, the largest effect is due to the difference in the estimate of seepage into the emplacement drift. However, there is an additional reduction in the in-package flux due to the geometrical constraint provided by the difference between waste package breaches and drip shield breaches (see Section 3.2.6.3).

4.2.7 Analyses of Waste Form Degradation and Radionuclide Release

Calculated waste form release rates for the codisposal waste are shown in Figure 4.2.7-1. The analyses that produced these results are described in Section 4.1. The model analyses and source file information traceable to the particular simulation runs used to produce these results are discussed in Section 4.

Performance of the system is indicated in this section in terms of estimates of the rate of radionuclide release of technetium-99 and neptunium-237 from the waste form. Although other radionuclides contribute to the overall performance of the system (see Figures 4.1-5 through 4.1-7), only these key contributors are shown because they represent two important categories of radionuclides that reveal the characteristics of the waste form release rate. Technetium-99 indicates the performance of the waste form for radionuclides where release is limited by the waste form degradation rate (e.g., carbon-14 and iodine-129). Neptunium-237 indicates the performance of the waste form for radionuclides whose release is limited by the radionuclide solubility (e.g., plutonium-239 and thorium-230).

Figure 4.2.7-1 compares selected codisposal waste-form release curves calculated using the TSPA-SR base-case (CRWMS M&O 2000 [DIRS 153246]) and supplemental TSPA models. Figure 4.2.7-1a shows the results for technetium-99 and Figure 4.2.7-1b shows the results for neptunium-237. For both radionuclides, the figures shows the mean codisposal waste form radionuclide release history calculated for the HTOM using the TSPA-SR base-case model (CRWMS M&O 2000 [DIRS 153246], Section 4.1.2) and the waste form release histories calculated for the HTOM and the LTOM with the supplemental TSPA model. The waste form release history calculated with the supplemental TSPA model differs from the results using the TSPA-SR base-case model in each case. However, comparison of the curves in Figure 4.2.7-1a and 4.2.7-1b shows that the curves for the two radionuclides, each with different waste form release characteristics, are similar for each model calculation. This similarity suggests the nature of the differences among the models does not depend strongly on the particular characteristics of the radionuclides. In fact, the shape of the waste form release curve depends almost entirely on the waste package failure rate. Detailed comparison of the waste package failure curves (Figure 4.2.5-2) shows that the climb of the waste form release curve tracks the climb in the rate of waste package failure, consistent with the conclusions of the previous section. Therefore, the differences in the results reflect differences among the waste package failure rates for these cases. In particular, the waste form release curves reflect the influence of the small fraction of potential early waste package failures that is modeled and the delay to failure of the majority of the waste package due to the relatively slow general corrosion rate in the supplemental model.

Figure 4.2.7-2 provides similar waste form release histories for the CSNF waste form. As in the case of the codisposal waste form, the shape of the CSNF waste form release curves does not depend upon individual radionuclide properties. The radionuclide release curves depend on the waste package failure rate; however, they also depend upon the amount of waste exposed to water as a result of the CSNF cladding breaches. As indicated in the TSPA-SR base-case model (CRWMS M&O 2000 [DIRS 153246], Section 3.2.7.2), slightly more than eight percent of the CSNF cladding fails early, while in the supplemental TSPA model, the early cladding failure fraction is about one percent. The sharp spikes in the supplemental TSPA model results reflect cladding failure due to seismic events (which occur more frequently in that model than in the TSPA-SR base-case model). Aside from this difference, differences among the curves in Figure 4.2.7-2 largely reflect the differences among the waste package failure rates and the difference between the representations of early cladding failure.

4.2.8 Analyses of Radionuclide Transport in the Engineered Barrier System

Calculated rates of release from the waste package are shown in Figures 4.2.8-1 through 4.2.8-4. The analyses that produced these results are described in Section 4.1. The model analyses and source file information traceable to the particular simulation runs used to produce these results are discussed in Section 4.

Figures 4.2.8-1 through 4.2.8-4 compare results of analyses using the TSPA-SR base-case (CRWMS M&O 2000 [DIRS 153246]) and supplemental TSPA models. Figures 4.2.8-1 and 4.2.8-2 show the mean waste package release rates for codisposal waste and CSNF, respectively. The figures show the results for technetium-99 and neptunium-237, the two radionuclides considered in Section 4.2.7. These results reflect the relative concentrations of these radionuclides in the waste packages and the emplacement drifts. Fluctuations in the waste package release rate result from build up of concentrations in the emplacement drift as radionuclides are transported away from the waste package, and changes in the concentrations as the chemistry changes in the waste package. A particular example is shown in Figure 4.2.8-1b, where the supplemental TSPA model HTOM waste package release rate becomes negative (and thus cannot be shown on the logarithmic scale) when the concentration of neptunium-237 in the emplacement drift exceeds that in the waste package, and the radionuclide diffuses back into the waste package in the calculation model.

In each case, the results using the TSPA-SR base-case model differ significantly from those using the supplemental TSPA model. The results from the TSPA-SR base-case model generally show releases beginning at about 10,000 years (when the waste packages begin to fail in that model). The release rate peaks at about 100,000 years when most of the waste packages have breached, and then diminishes as the radionuclide inventory is removed from these waste packages. The results from the supplemental TSPA model generally show two distinct release events. The first is a low level of release from the small number of waste packages (fewer than an average of 0.25 waste packages) that fail early in this model. Then, a second release becomes apparent, beginning at about 100,000 years, when the waste packages and drip shields show significant failure in this model. This second release peaks after about 500,000 years in this model. The peak release rate is lower in the TSPA-SR base-case model than in the supplemental TSPA model, the difference depending upon the radionuclide.

In Section 4.2.7, the waste form release curves in each model are similar for different radionuclides (Figures 4.2.7-1 and 4.2.7-2). However, the two models give radionuclide-dependent shapes for the waste package release rates. This effect is consistent with the conclusions in the TSPA-SR (CRWMS M&O 2000 [DIRS 153246], Section 4.1.2), which indicates that, unlike the waste-form release rates, the waste package and EBS release rates depend on the radionuclide characteristics, in particular the solubility of the radionuclides within the waste package and in the drift invert. This effect is also seen in the supplemental TSPA model. In general, differences between the waste package release curves reflect more than the waste package degradation rates (that determine the waste form release rates).

Comparing results for the supplemental TSPA model HTOM and LTOM cases shows smaller differences than those between the results for the two models (TSPA-SR base-case and supplemental TSPA models) for the same HTOM case. There are differences due to different

waste package lifetimes in the two cases that change the time of the peak release rate, but they do not have a substantial effect on the peak release rate. The waste package lifetime reflects differences between corrosion rates in the early thermal period for the HTOM and LTOM, but the release rate itself occurs well after the thermal period and thus does not reflect differences in the two cases.

Figures 4.2.8-3 and 4.2.8-4 show comparisons for the mean EBS release rates. Differences between Figures 4.2.8-1 through 4.2.8-4 indicate the effects due to transport through the drift invert. The calculated EBS release rates generally follow the waste package release rates. The exception to this general statement is the neptunium-237 release rate that is calculated with the supplemental TSPA model for the period before significant waste package degradation (i.e., in the period when the only radionuclide release in this model is from the small number of waste packages assumed to fail early). In particular, the EBS release rates are lower than the waste package release rates in the period between approximately 10,000 years and 100,000 years.

The reason for this difference is that the supplemental TSPA model predicts a higher neptunium-237 concentration in the hot waste package than the solubility limit in the drift invert. Consequently, the neptunium-237 concentration in the water moving from the waste package to the drift invert is reduced, resulting in the lower rate of release from the invert than from the waste package. This effect is not seen for technetium-99 because the solubility limit for this radionuclide in the drift invert is higher and is not constraining. Other than this, processes in the drift invert play little role in the EBS release rate in the TSPA-SR base-case or supplemental TSPA models.

Additional insight into the rate of release from the EBS is shown in Figures 4.2.8-5 through 4.2.8-7. Figure 4.2.8-5 shows the total EBS release rate (i.e., for codisposal and CSNF waste) for technetium-99 and neptunium-237. Figure 4.2.8-6 shows the decomposition of the total technetium-99 EBS release rate into advective and diffusive release rates. Comparison of these two components with the total technetium-99 release rate in Figure 4.2.8-5a shows that EBS release in the first 80,000 to 100,000 years results from the small number of waste packages that fail early in this model. The release in this case generally is diffusive because the drip shields remain intact for most of this period and limit advective flow through the EBS. After this time, the drip shields begin to fail and additional waste packages fail. Consequently, advective and diffusive transport increases.

The advective component of the EBS release rate calculated in the supplemental TSPA model, although delayed substantially relative to that calculated in the TSPA-SR base-case model (due to the longer waste package lifetime), has approximately the same peak value as in the TSPA-SR base-case model. Consequently, the addition of sorption to the supplemental TSPA model does not have a significant affect on the advective EBS release rate of technetium-99. The peak diffusive release rate, in contrast, shows a reduction by a factor of approximately ten. This reduction is due to the reduced diffusivity of the drift invert in the supplemental TSPA model. This reduction is modest compared to that evaluated in the TSPA-SR (CRWMS M&O 2000 [DIRS 153246], Section 5.2.5.1), nevertheless, even the small change incorporated into the supplemental TSPA model appears to have an impact.

Figure 4.2.8-7 shows the decomposition of the neptunium-237 EBS release rate into advective and diffusive release rates. In this case, the peak values calculated for the advective and diffusive components are reduced in the supplemental TSPA model: the peak advective EBS release rate is reduced by approximately one order of magnitude, and the peak diffusive EBS release rate is reduced by approximately two orders of magnitude. The additional change, relative to that for the technetium-99 comparison, is due to the reduction in the neptunium solubility limit in the supplemental TSPA model. This solubility limit affects the diffusive and advective components.

The EBS release rate provides the source term for calculating radionuclide transport through the UZ and the SZ, and the release to the accessible environment. Comparing the two models indicates the following characteristics:

TSPA-SR base-case model

- EBS releases from early waste package failures are negligible.
- EBS releases begin at about 10,000 years when waste packages begin to fail.
- EBS releases are diffusive until the drip shields begin to fail.
- Peak EBS release rate occurs at about 100,000 years, and the diffusive EBS release rate is comparable to, or larger than, the advective EBS release rate.

Supplemental TSPA Model

- The only EBS release in the first 80,000 to 100,000 years (before the drip shields begin to fail) is diffusive release from the small number of packages that fail early in this model.
- Advective and diffusive EBS releases increase substantially at about 100,000 years after the waste packages and drip shield begin to fail.
- The peak EBS release rate occurs after about 500,000 years, and the peak release rate is reduced one or two orders of magnitude below that computed with the TSPA-SR base-case model.
- The release rate is somewhat different for the HTOM and LTOM cases, largely due to differences in the waste package corrosion rate during the early thermal period and resulting differences in waste package failure characteristics.

These summaries for the two models are compatible. For both models, the timing of the EBS release rate in each model reflects the rate of drip shield and waste package failure. The increase in magnitude of the EBS release rate is determined largely by the waste package failure characteristics, the waste package and drift invert water chemistry (in particular the pH of the water), and the diffusivity model for diffusive releases. While details are different in the two models, these tendencies described here are preserved. Further, the mean EBS release rate estimated in the supplemental TSPA model lies within the range of uncertainty estimated for the

TSPA-SR base-case model. Consequently, these results suggest that the estimates using the TSPA-SR base-case model are reasonable.

4.2.9 Evaluation of Unsaturated Zone Transport

In Section 4.1, the supplemental TSPA model is described, and results for two thermal operating modes are presented. In this section, additional information is presented about UZ transport in the supplemental TSPA model. For UZ transport, the only change from the TSPA-SR base-case (CRWMS M&O 2000 [DIRS 153246], Section 3.2.7) to the supplemental TSPA model is the inclusion of the drift-shadow modification (BSC 2001 [DIRS 154657], Section 11.3.1.6.1; see also Section 3.2.9.2). To address the drift-shadow effect, advective releases from the potential repository are released into the fracture continuum of the UZ transport model, but diffusive releases are released into the matrix continuum of the model.

The role of UZ transport in the TSPA results can be illustrated by plots comparing average radionuclide release rates from the EBS and the UZ. For the TSPA-SR base case, this comparison can be seen in the TSPA-SR (CRWMS M&O 2000 [DIRS 153246], Figure 4.1-11). That figure includes four plots, for technetium-99, neptunium-237, plutonium-239 transporting as solute with reversible attachment to colloids, and plutonium-239 transporting irreversibly attached to colloids. These radionuclides are among the most important to calculated mean annual dose (Section 4.1.2) and cover a range of transport behaviors. The analogous plots for the supplemental TSPA model are shown in Figures 4.2.9-1 through 4.2.9-4 for the HTOM case and in Figures 4.2.9-5 through 4.2.9-8 for the LTOM case.

At early times, the UZ releases of technetium-99 are lower than the EBS releases because of delay in the UZ (Figures 4.2.9-1 and 4.2.9-5). After about 20,000 years, there is no longer a visible delay and the release rate from the UZ is nearly the same as that from the EBS. Some effects of the climate changes are visible in the plots for technetium-99. For example, the UZ release rate increases from a little before 40,000 years to about 50,000 years (during the first glacial climate) and the UZ release rate decreases starting between 60,000 and 70,000 years and extending to about 80,000 years (this is an interglacial climate).

The UZ releases of neptunium-237 have a visible lag compared to the EBS releases for 100,000 years or more, indicating a greater UZ transport time for neptunium than for technetium (Figures 4.2.9-2 and 4.2.9-6). In comparison, the effect of UZ transport is even greater for reversible plutonium-239, for which the UZ and EBS release rates remain different for several hundred thousand years (Figures 4.2.9-3 and 4.2.9-7). In contrast to reversible plutonium, the UZ and EBS release rates for irreversible plutonium-239 are similar (Figures 4.2.9-4 and 4.2.9-8), indicating that transport by irreversible colloids is faster than transport by reversible colloids in the supplemental TSPA model.

The same conclusions were reached for the TSPA-SR base case: irreversible colloids were found to have the fastest transport, followed by technetium and neptunium, with reversible colloids having the slowest transport (CRWMS M&O 2000 [DIRS 153246], Sections 3.7.4 and 4.1.2; see also Section 3.2.9.1).

4.2.10 Analyses of Saturated Zone Flow and Transport

The SZ flow and transport modeling for the supplemental TSPA model is changed relative to the base case to incorporate bulk density in the alluvium as an uncertain parameter and to set the sorption coefficients for technetium-99 and iodine-129 in the alluvium to zero. These changes to the SZ transport modeling are the result of additional information available from borehole data in the alluvium and continuing laboratory sorption experiments on alluvium samples (BSC 2001 [DIRS 154657], Sections 12.3.2.2 and 12.3.2.4; see also Section 3.2.10.2). Saturated-zone flow and radionuclide transport are similar for the HTOM and LTOM cases (BSC 2001 [DIRS 154657], Section 12.3.2.3.1).

The impact of SZ flow and transport on the TSPA results is shown by comparing the radionuclide mass-release rates from the UZ to the release rates from the SZ for the supplemental TSPA model. The release-rate curves for technetium-99 from the UZ and the SZ are shown for the HTOM and LTOM in Figures 4.2.10-1a and 4.2.10-1b, respectively. The separation between the mean release curves in Figure 4.2.10-1 indicates a delay of several hundred years in the SZ during the influence of monsoonal climatic conditions that are predicted from 600 to 2,000 years in the future (as indicated by the first "step" in the infiltration model shown in Figure 4.2.1-1). In addition, the release-rate curve from the SZ shows some dampening of the peaks in the UZ release-rate curve that are discernible at times of less than 10,000 years due to dispersion during transport in the SZ. Release rates from the SZ may exceed the release rate from the UZ at a particular time due to the delay in transport through the SZ. Similarly, Figures 4.2.10-2a and 4.2.10-2b show the release rate curves for neptunium-237 from the UZ and the SZ for the HTOM and LTOM, respectively. The breakthrough of neptunium-237 from the UZ occurs later than the breakthrough of technetium-99. As an example of the delay in the SZ, the separation between the mean release-rate curves (Figure 4.2.10-2; at 90,000 to 100,000 years) indicates a delay in release of about 8,000 years due to sorption of neptunium-237 in the SZ. The delay between the UZ and SZ release curves for technetium-99 and neptunium-237 is generally not discernable in Figures 4.2.10-1 and 4.2.10-2 on the log-time scale at times of greater than 100,000 years. The delays in radionuclide release, particularly for wetter climatic conditions in which transport occurs more rapidly in the SZ, are not large in relation to longer time scales.

4.2.11 Analyses of the Biosphere

The biosphere modeling for the supplemental TSPA model was changed relative to the base case for the groundwater pathway. Biosphere modeling now incorporates evaluation of parameter values related to several aspects of the biosphere system (BSC 2001 [DIRS 154657], Section 13.4.1; see also Section 3.2.11.2). The impact of these changes is relatively small for the groundwater pathway, as shown on Figure 3.2.11-1 by comparing the simulated mean annual dose for the base case calculated in TSPA-SR (using the TSPA-SR BDCFs) with the BDCFs used in the supplemental TSPA model. The supplemental TSPA model also includes changes to the biosphere model for the volcanic-eruption scenario (BSC 2001 [DIRS 154657], Section 13.4.3; see also Section 3.2.11.2). The impact of these changes for the volcanic-eruption scenario is an approximately one-half order of magnitude increase in the mean dose as shown on Figure 3.2.11-2 by comparing the simulated mean annual dose for the base case calculated in TSPA-SR (using the TSPA-SR BDCFs) and the BDCFs for the supplemental TSPA model.

4.3 SYSTEM-LEVEL ANALYSES OF IGNEOUS DISRUPTION PERFORMANCE

The model and parameter changes for the supplemental TSPA model for the igneous disruption scenario class are described in detail in SSPA Volume 1 (BSC 2001 [DIRS 154657], Sections 13 and 14) and are summarized here.

As described in SSPA Volume 1 (BSC 2001 [DIRS 154657], Section 13.4), the BDCFs for eruptive and groundwater pathways were modified to account for new information developed since completion of the TSPA-SR (CRWMS M&O 2000 [DIRS 153246]). Impacts of these changes on the nominal scenario class BDCFs used for the groundwater pathway are slight (see Section 3.2.11). Changes in the volcanic eruptive BDCFs, however, are more extensive and increase the probability-weighted annual dose by a factor of approximately 2.5 (Section 3.2.11).

Several input parameters to the TSPA models used to calculate consequences of igneous disruption were changed (BSC 2001 [DIRS 154657], Section 14.3.3.7). Consistent with new information regarding the probability of an eruption at the location of the potential repository given an igneous intrusive event, the conditional probability of an eruption at the potential repository was revised from 0.36 (CRWMS M&O 2000 [DIRS 153246], Table 3.10-4) to 0.77. Changes also were made in the probability distribution for an intrusive event, consistent with revisions in the potential repository footprint since inputs were compiled for TSPA-SR. New distributions were provided for the number of waste packages affected by eruptive and intrusive events, consistent with the new event probability information. Changes have been made in the input data used to determine the wind speed during an eruption (see Section 3.3.1.2.1). Additional changes in inputs to the TSPA-SR igneous consequence model are listed in SSPA Volume 1 (BSC 2001 [DIRS 154657], Section 14.3.3.7, Tables 14.3.3.7-1 and 14.3.3.7-2). Other model inputs and assumptions, including the assumption that wind direction is fixed toward the location of the receptor at all times, are the same as those used in the TSPA-SR (CRWMS M&O 2000 [DIRS 153246] Section 3.10).

4.3.1 One-Hundred-Thousand-Year Dose Histories for Igneous Disruption

The TSPA-SR model for igneous disruption calculates doses from eruptions that entrain waste in volcanic ash and from igneous intrusions that damage waste packages and allow releases of radionuclides into groundwater (see Section 3.3.1). Figure 4.3-1 shows the probability-weighted mean annual dose for igneous disruption for the supplemental TSPA model for the HTOM and the LTOM. The 100,000-year supplemental analyses use 5,000 realizations for each case, and are compared to the 5,000-realization, 50,000-year base case from the TSPA-SR (CRWMS M&O 2000 [DIRS 153246], Figure 4.2-1). Figures 4.3-2 through 4.3-4 show 500 of the 5,000 realizations (i.e., every tenth realization) for each case.

The probability-weighted annual dose for the igneous disruption scenario class is significantly different in the supplemental model as shown in Figure 4.3-1. Eruptive doses, which dominated in TSPA-SR for only approximately the first 2,000 years (see Section 3.3.1.1), are now the main contributor to annual dose for more than 10,000 years. Peak mean annual eruptive dose still occurs approximately 300 years after closure, but it is increased by a factor of approximately 25, to approximately 0.1 mrem/yr. Doses from groundwater transport following igneous intrusion are decreased (generally by a factor of 5 or more), and the peak mean intrusive dose (which

occurs in the LTOM case between 40,000 and 50,000 years) is approximately 0.05 mrem/yr, roughly one-quarter of the comparable peak mean dose in the TSPA-SR. The time of the peak mean annual igneous dose corresponds to the onset of the first full glacial climate at 38,000 years.

The largest single contributor to the 25-fold increase in the probability-weighted mean eruptive dose comes from changes in BDCFs (a factor of approximately 2.5; see Section 3.2.11). Other major factors are the change in wind speed (a factor of approximately 2; see Section 3.3.1.2.1), and the increase in the conditional probability of an eruption at the location of the potential repository (a factor of approximately 2, from 0.36 to 0.77). An increase in the total number of eruptive conduits possible within the potential repository (from 5 to 13) accounts for most of the remainder of the change (parameter values from CRWMS M&O 2000 [DIRS 153246], Table 3.10-4; BSC 2001 [DIRS 154657], Table 14.3.3.7-1).

Decreases in the probability-weighted annual dose due to igneous intrusion are due to changes in the nominal performance models for radionuclide mobilization and transport. The distributions used to characterize uncertainty in the number of waste packages affected by igneous intrusion were modified, resulting in a larger number of packages damaged for the supplemental analyses (BSC 2001 [DIRS 154657], Section 14.3.3.7 and Table 14.3.3.7-2). This increase, however, is more than offset by decreases in radionuclide mobilization and transport (see Section 3.2.7).

As modeled, thermal operating conditions have no effect on the eruptive doses, and the curves for the HTOM and LTOM cases overlie each other until groundwater pathway releases cause minor divergence beginning about 10,000 years. Differences between LTOM and HTOM performance in the igneous scenario class are negligible until after 20,000 years, when mean annual LTOM doses become up to a factor of 3 greater than HTOM doses (Figure 4.3-1). However, the probability of igneous disruption is assumed to be the same for the LTOM and HTOM cases in these analyses, and possible changes in drift and waste package spacing for alternative thermal designs are not evaluated. Increasing the area of the potential repository will proportionally increase the probability of igneous disruption, and changes in drift and package spacing could affect the number of packages damaged by igneous disruption. Analysis of a LTOM design that increases the length of the potential repository by 3,300 m shows a 70 percent increase in the probability of igneous intrusion and eruption at the potential repository (BSC 2001 [DIRS 154657] Section 14.3.3.2.2). Adjusting the probability of igneous disruption for the LTOM case would result in a corresponding increase of 70 percent in the probability-weighted annual dose. Increasing waste package spacing causes a proportional reduction in the number of packages damaged (BSC 2001 [DIRS 154657] Section 14.3.3.2.3). Neither correction has been made in any analyses reported in Section 4.3, and all LTOM and HTOM results shown here are calculated assuming the same potential repository footprint and emplacement geometry.

4.3.2 Individual Radionuclides Contributing to Total Probability-Weighted Dose, Igneous Disruption

Figures 4.3-5a through 4.3-5c show the major radionuclides contributing to the total probability-weighted mean annual dose for the HTOM and LTOM supplemental TSPA analyses and for the TSPA-SR base case (CRWMS M&O 2000 [DIRS 153246], Figure 4.2-1). Major

contributors for eruptive doses are similar for all three cases, and total doses are dominated by americium-241, plutonium-240, plutonium-239, and plutonium-238. At later times, intrusive doses are dominated by plutonium-239 in all three cases. Neptunium-237 is a less important contributor in the supplemental TSPA analyses, primarily due to a decrease in the mean solubility limit of this species in the nominal scenario class (see Section 3.2.7). Figures 4.3-6a through 4.3-6c display the same information in pie charts showing contributions to annual dose for the supplemental TSPA analyses HTOM, LTOM, and TSPA-SR base case at selected times during the simulation.

Table 4.2.2-1. Average Division of Waste Packages into Environmental Groups, HTOM

Waste Type	Seepage State	0–3 mm/yr	3–10 mm/yr	10–20 mm/yr	20–60 mm/yr	60+ mm/yr
CSNF	No Seepage	488	351	768	2,146	336
	Seepage	444	310	622	2,014	379
Co-Disposal Waste	No Seepage	243	174	381	1,073	168
	Seepage	219	156	308	998	191

Source: TSPA run SM01_029nm6; see Appendix A.

NOTE: Numbers add up to less than the actual number of waste packages in the model (11,770; CRWMS M&O 2000 [DIRS 153246], Section 3.5.1.1) because of rounding.

Table 4.2.2-2. Average Division of Waste Packages into Environmental Groups, LTOM

Waste Type	Seepage State	0–3 mm/yr	3–10 mm/yr	10–20 mm/yr	20–60 mm/yr	60+ mm/yr
CSNF	No Seepage	566	556	973	1,916	282
	Seepage	428	360	713	1,742	323
Co-Disposal Waste	No Seepage	281	275	487	955	141
	Seepage	214	179	353	866	158

Source: TSPA run SM01_030nm6; see Appendix A.

NOTE: Numbers add up to less than the actual number of waste packages in the model (11,770; CRWMS M&O 2000 [DIRS 153246], Section 3.5.1.1) because of rounding.

INTENTIONALLY LEFT BLANK

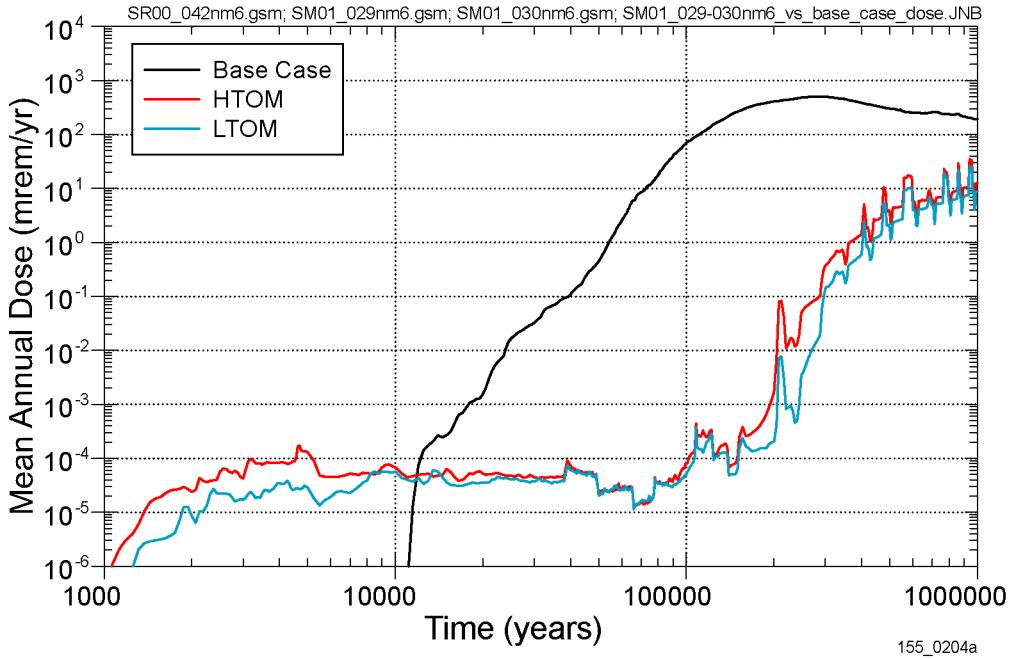

155_0204a

Source: TSPA-SR (CRWMS M&O 2000 [DIRS 153246]).

NOTE: Mean annual dose histories are shown for the supplemental TSPA model for HTOMs and LTOMs, and are compared to a base case showing the mean annual dose for nominal performance from the TSPA-SR.

Figure 4.1-1. Supplemental TSPA Model: Mean Million-Year Annual Dose Histories for Nominal Performance

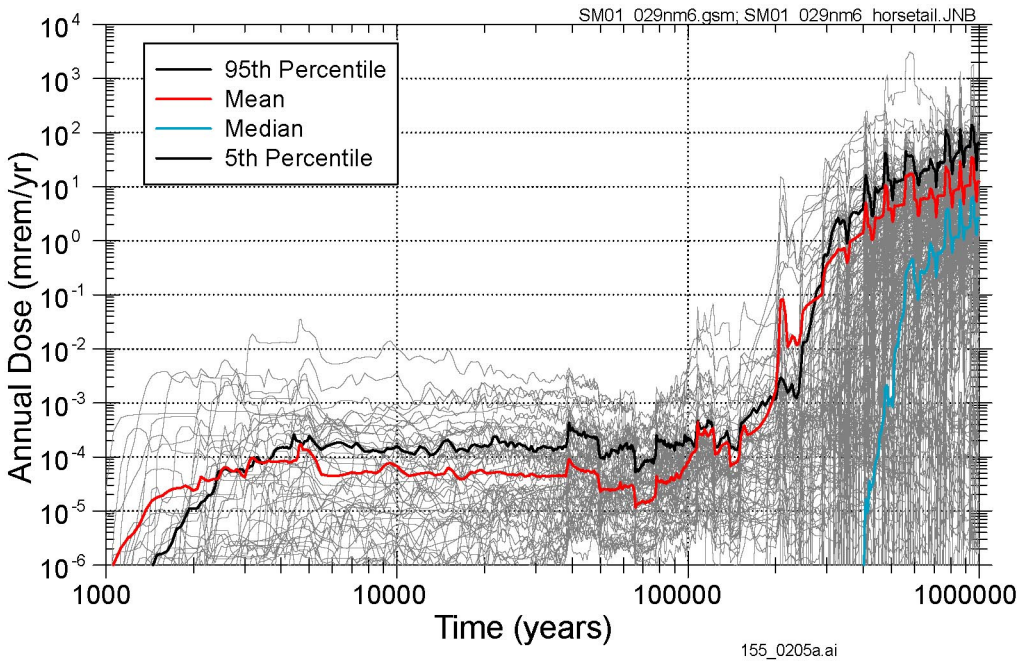

155_0205a.ai

NOTE: Summary curves show the 95th and 50th (median) percentiles, as well as the mean. The 5th percentile curve plots below the lowest values shown.

Figure 4.1-2. Supplemental TSPA Model: 300 Realizations of Million-Year Annual Dose Histories for Nominal Performance, Higher-Temperature Operating Mode

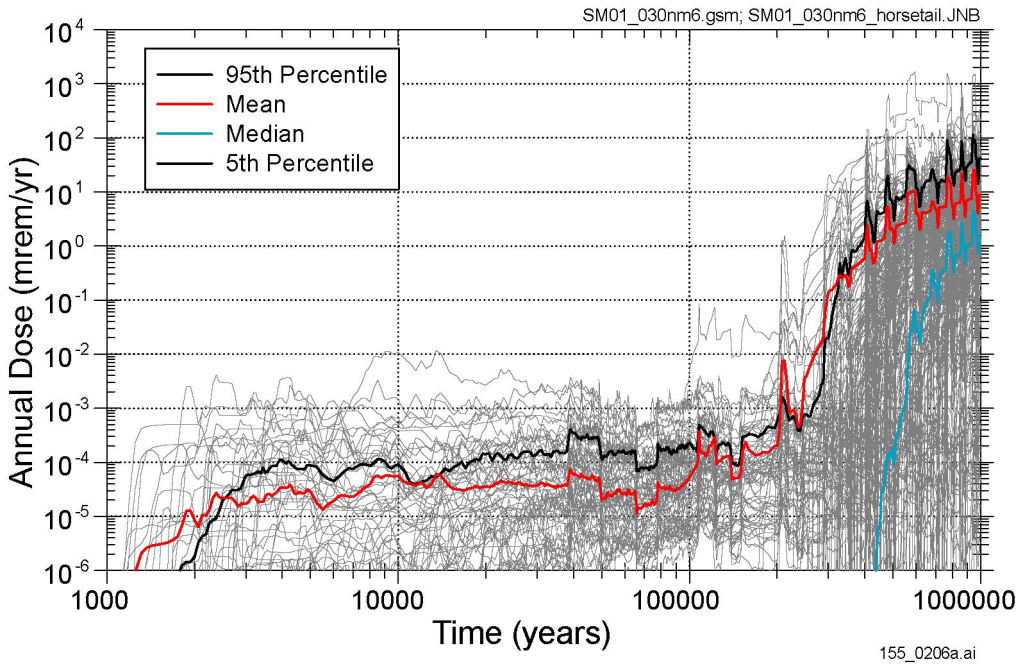

155_0206a.ai

NOTE: Summary curves show the 95th and 50th (median) percentiles, as well as the mean. The 5th percentile curve plots below the lowest values shown.

Figure 4.1-3. Supplemental TSPA Model: 300 Realizations of Million-Year Annual Dose Histories for Nominal Performance, Lower-Temperature Operating Mode

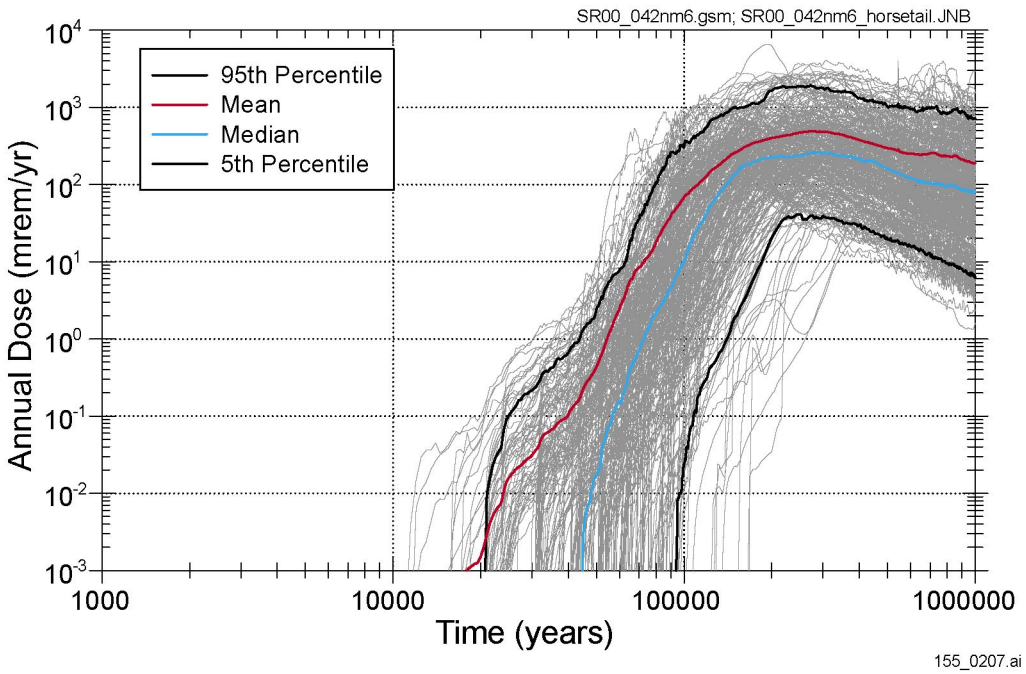

155_0207.ai

Source: TSPA-SR (CRWMS M&O 2000 [DIRS 153246], Figure 4.1-19a).

NOTE: Summary curves show the 95th, 50th (median), and 5th percentiles, as well as the mean. Results based on the TSPA-SR base-case model.

Figure 4.1-4. TSPA-SR Base-Case Model: 300 Realizations of Million-Year Annual Dose Histories for Nominal Performance

(a)

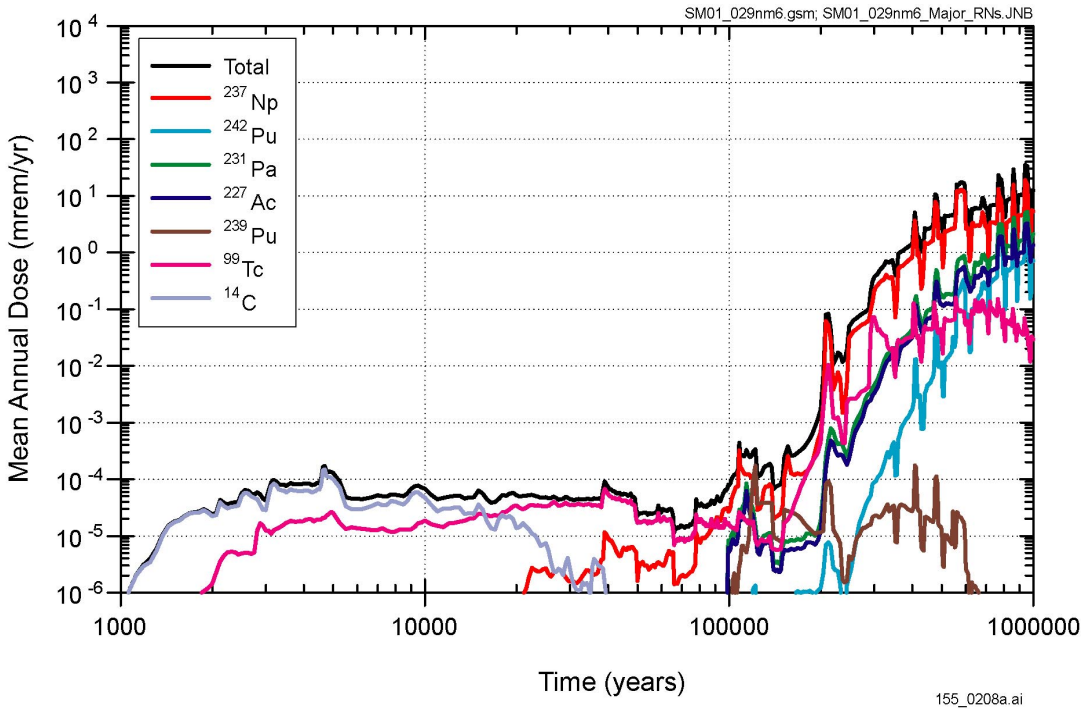

(b)

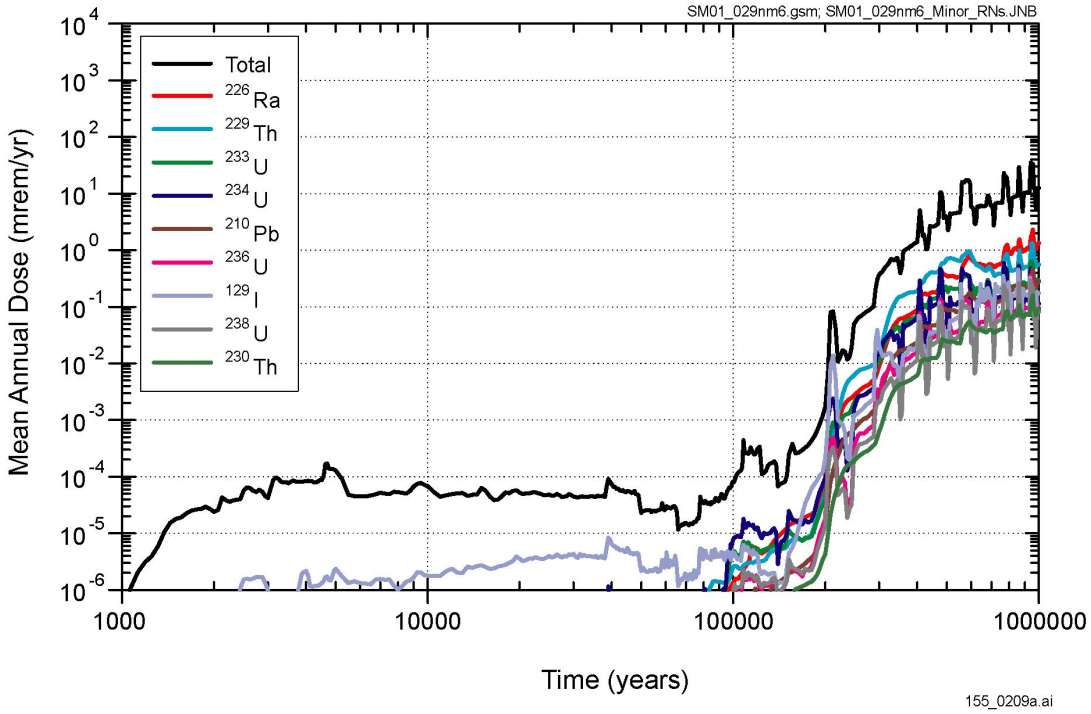

155_0208a.ai / 155_0209a.ai

NOTE: (a) Shows the major contributors. (b) Shows additional radionuclides of interest.

Figure 4.1-5. Supplemental TSPA Model: Mean Annual Dose Histories for Radionuclides Contributing to the Total Mean Annual Dose for 1 Million Years, Nominal Performance, Higher-Temperature Operating Mode

(a)

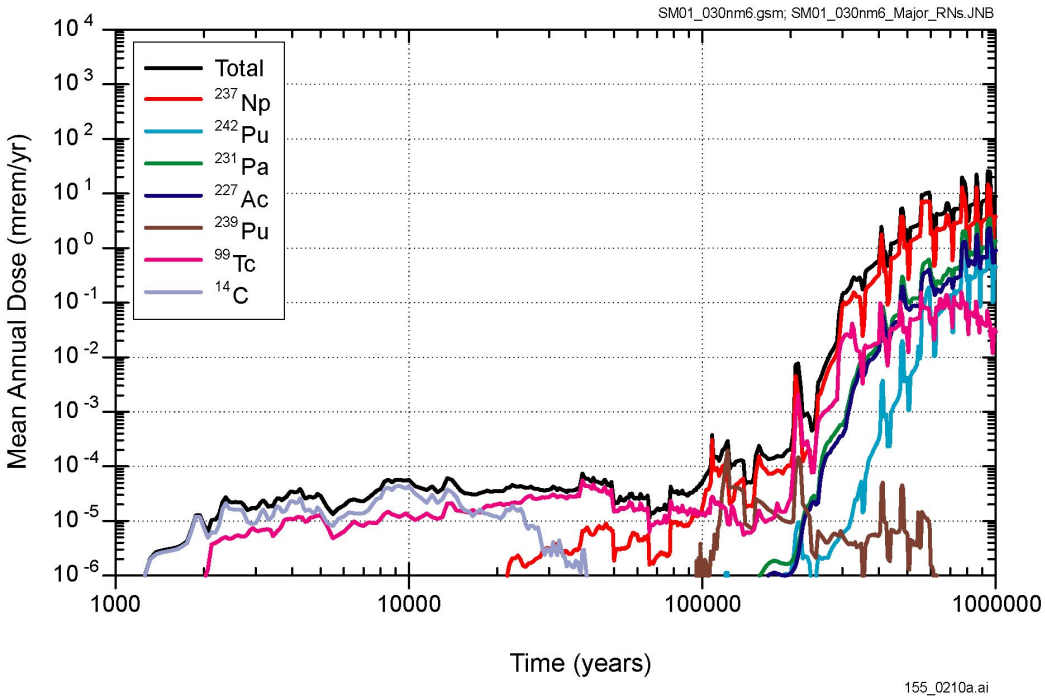

(b)

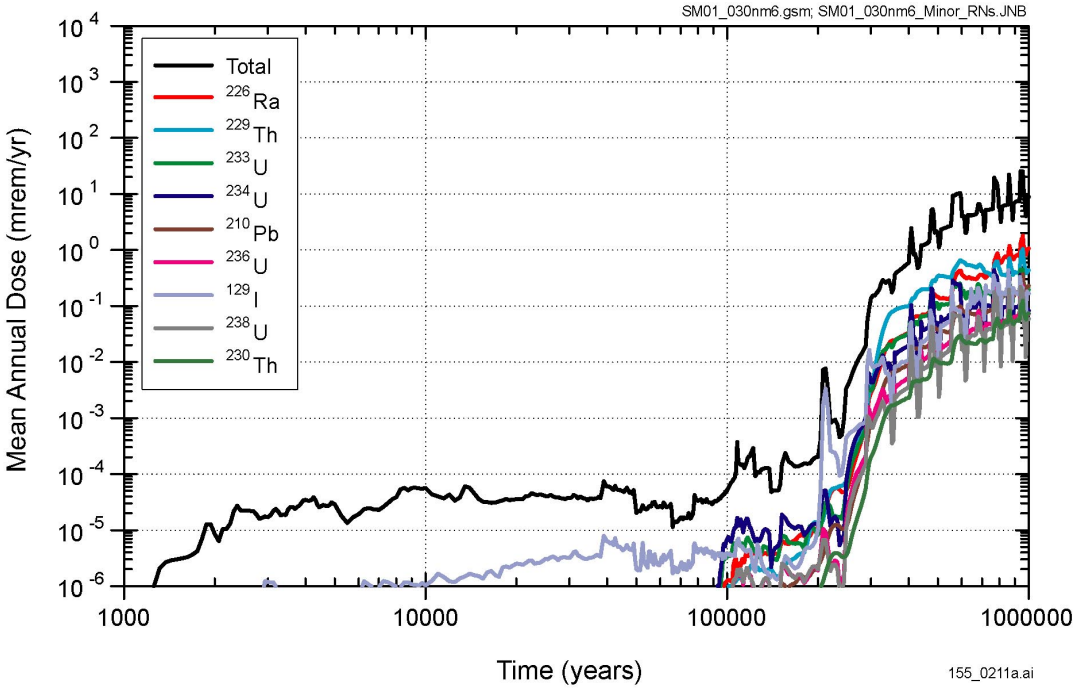

155_0210a.ai / 155_0211a.ai

NOTE: (a) Shows the major contributors. (b) Shows additional radionuclides of interest.

Figure 4.1-6. Supplemental TSPA Model: Mean Annual Dose Histories for Radionuclides Contributing to the Total Mean Annual Dose for 1 Million Years, Nominal Performance, Lower-Temperature Operating Mode

(a)

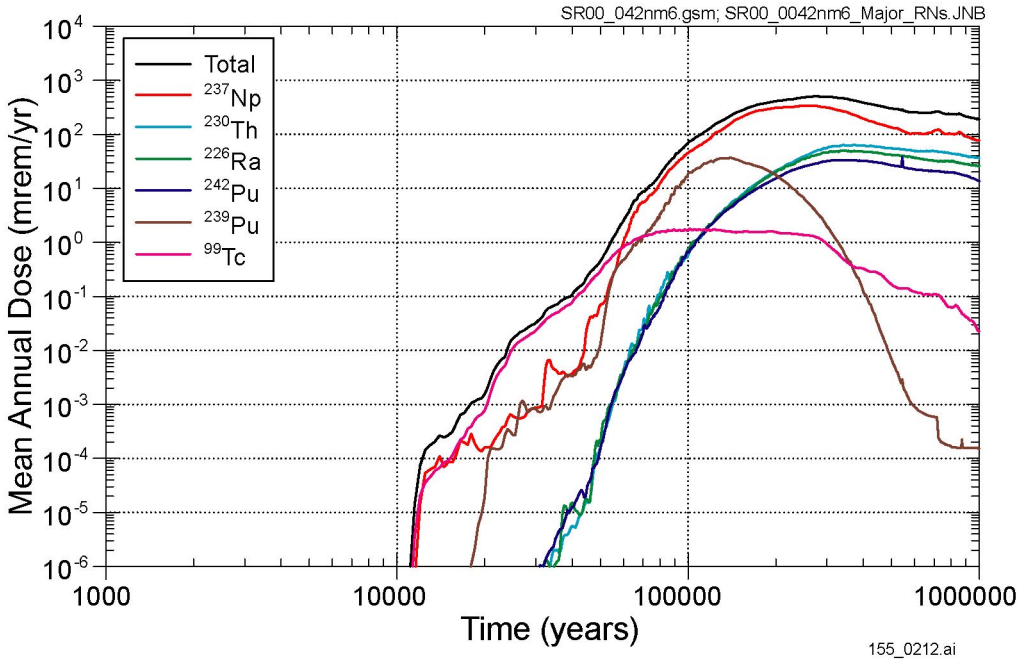

(b)

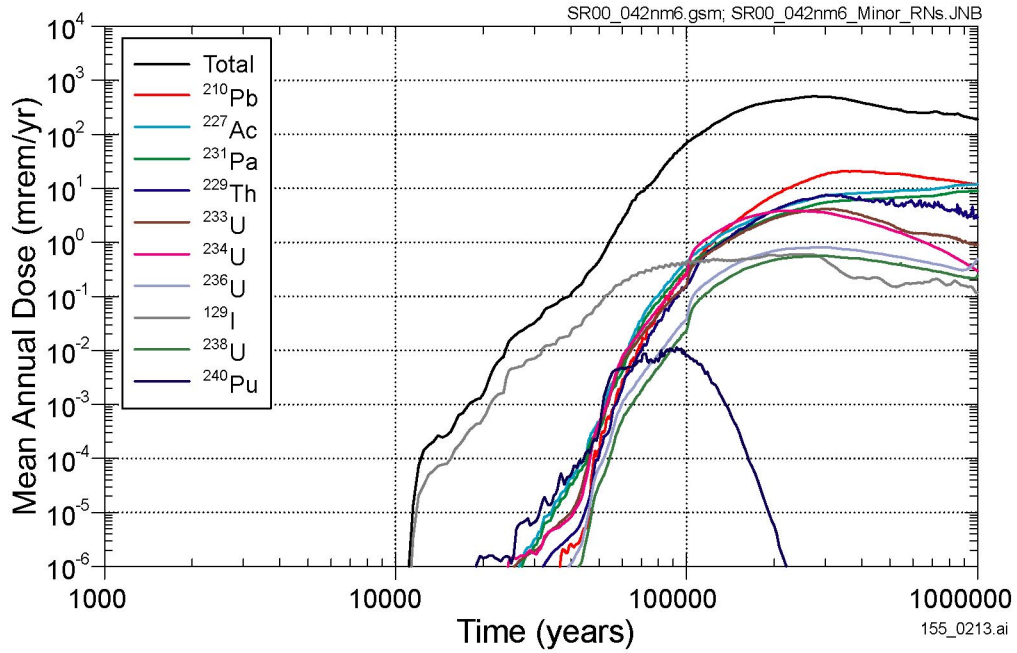

155_0212.ai / 155_0213.ai

Source: TSPA-SR (CRWMS M&O 2000 [DIRS 153246], Figure 4.1-19a).

NOTE: (a) Shows the major contributors. (b) Shows additional radionuclides of interest.

Figure 4.1-7. TSPA-SR Base-Case Model: Mean Annual Dose Histories for Radionuclides Contributing to the Total Mean Annual Dose for 1 Million Years, Nominal Performance

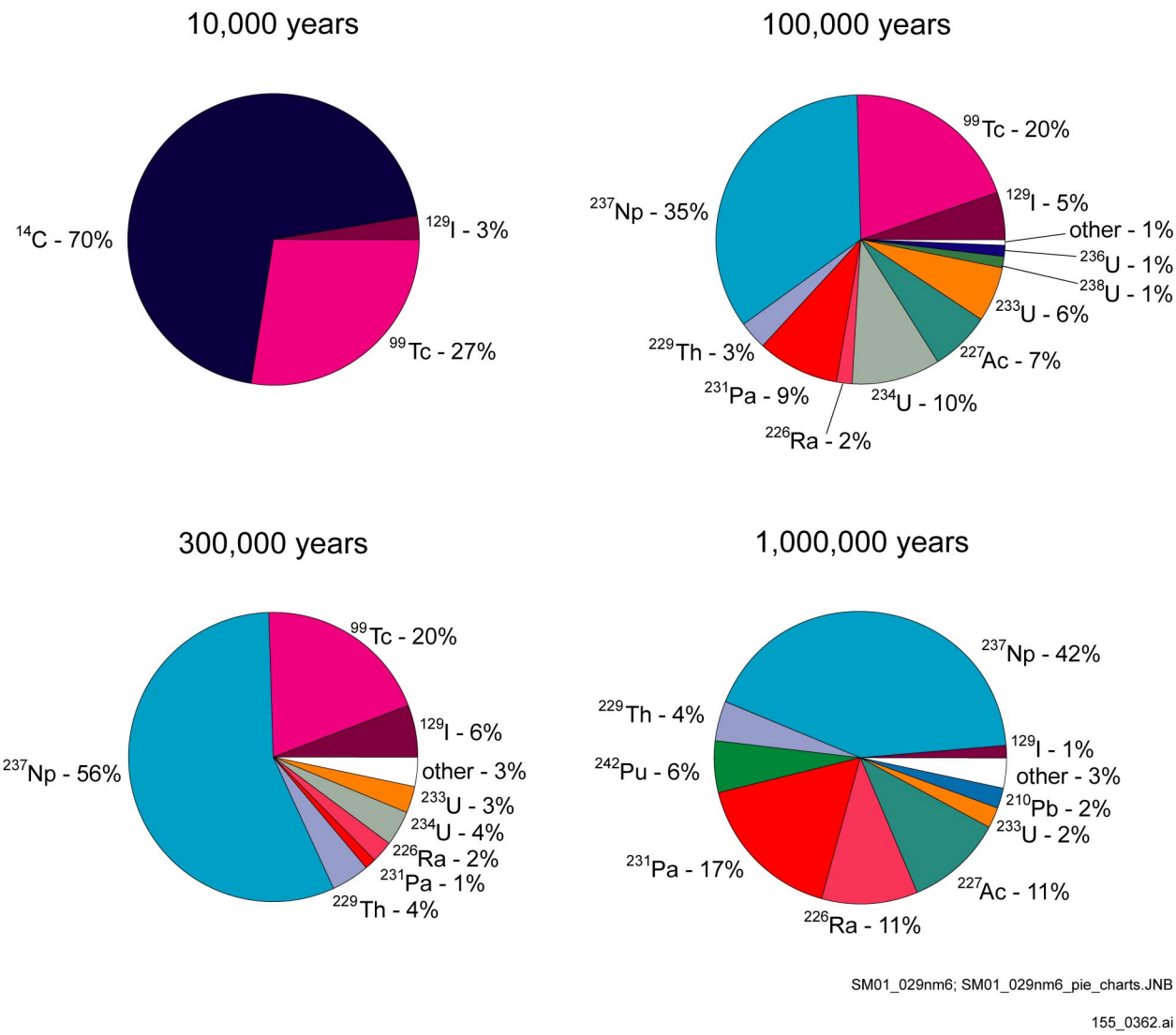

155_0362.ai

NOTE: Shows contributors to the HTOM mean annual dose.

Figure 4.1-8a. Radionuclides Contributing to Total Mean Annual Dose for Nominal Performance at Selected Times, Supplemental TSPA Model Higher-Temperature Operating Mode and Lower-Temperature Operating Mode and the TSPA-SR Base-Case Model

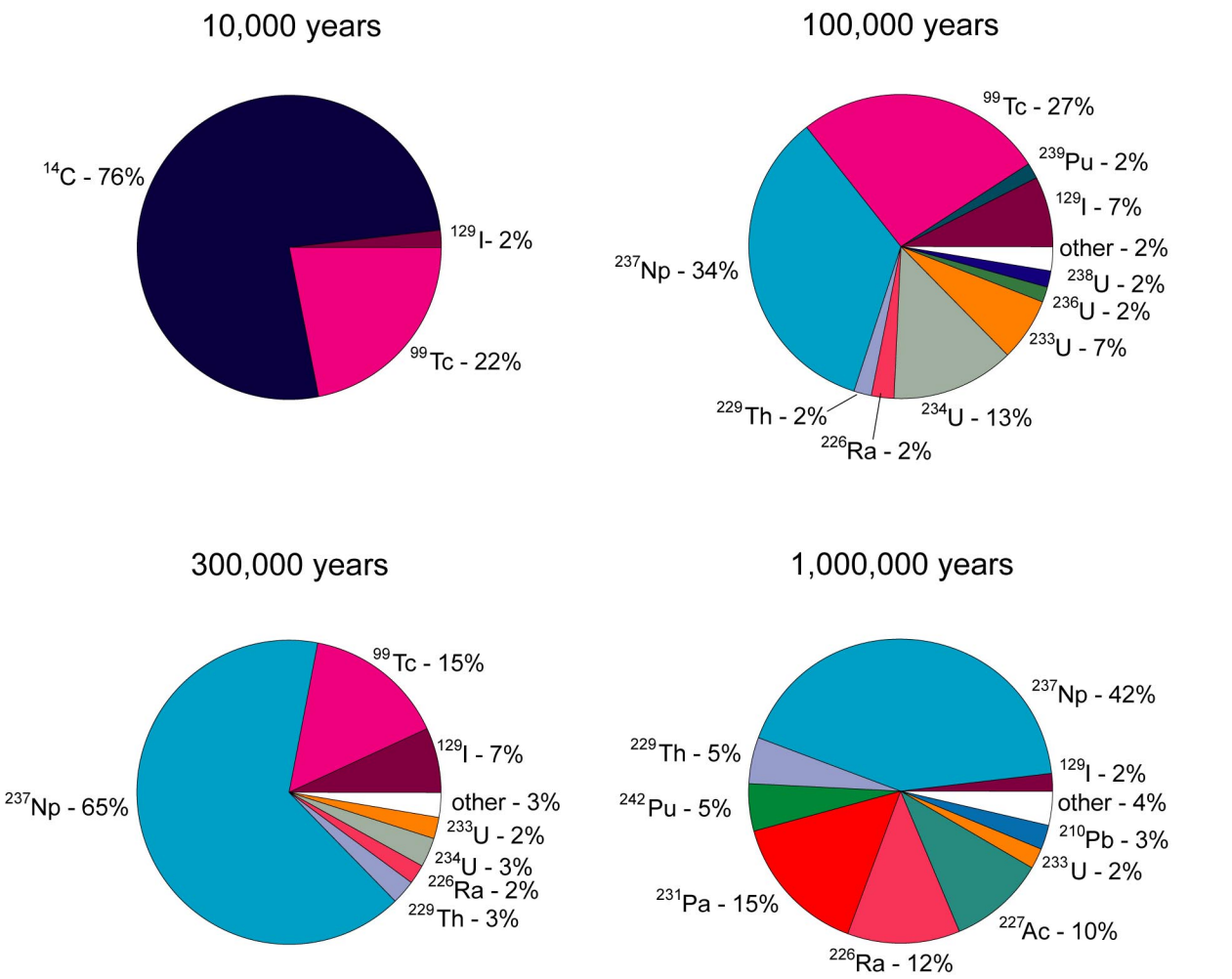

SM01_030nm6; SM01_030nm6_pie_charts.JNB

155_0363.ai

155_0363.ai

NOTE: Shows contributors to the LTOM mean annual dose.

Figure 4.1-8b. Radionuclides Contributing to Total Mean Annual Dose for Nominal Performance at Selected Times, Supplemental TSPA Model Higher-Temperature Operating Mode and Lower-Temperature Operating Mode, and the TSPA-SR Base-Case Model

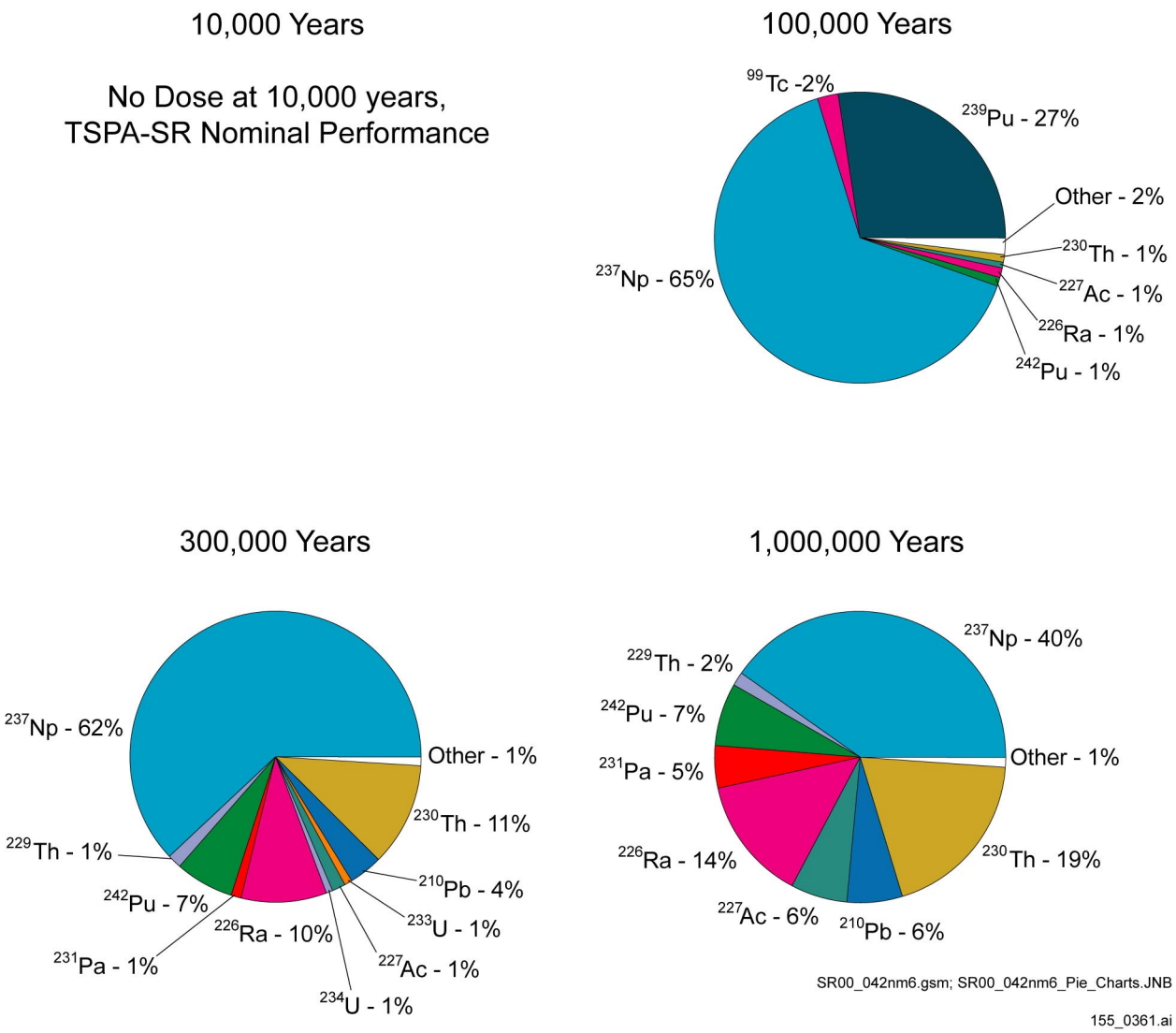

155_0361.ai

Source: TSPA-SR (CRWMS M&O 2000 [DIRS 153246]).

NOTE: Shows contributors to the TSPA-SR base-case model mean annual dose. Nominal performance for TSPA-SR had zero doses at 10,000 years.

Figure 4.1-8c. Radionuclides Contributing to Total Mean Annual Dose for Nominal Performance at Selected Times, Supplemental TSPA Model Higher-Temperature Operating Mode and Lower-Temperature Operating Mode, and the TSPA-SR Base-Case Model

(a)

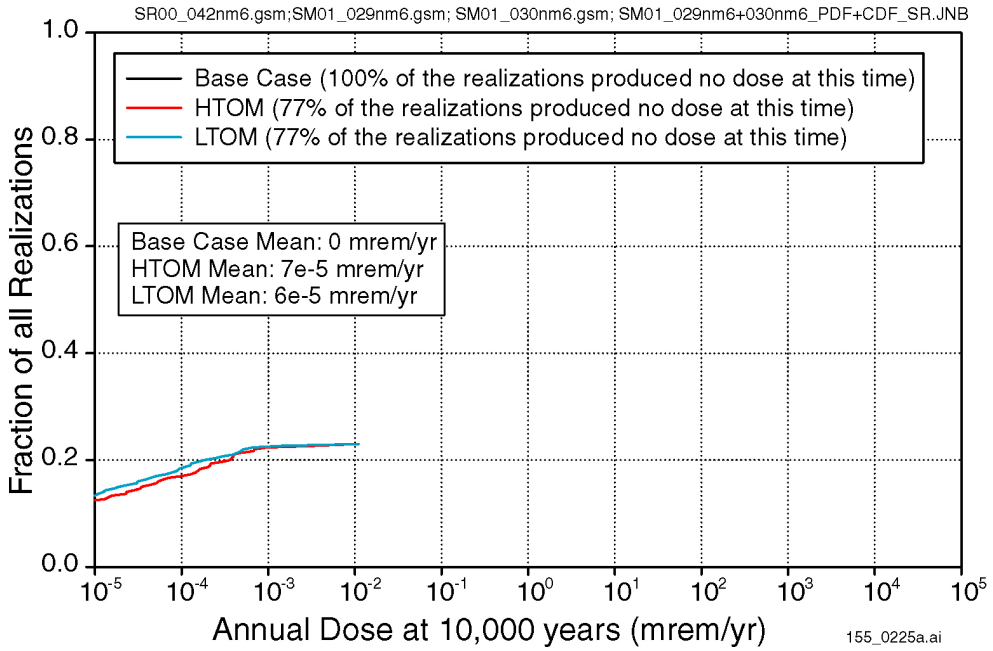

(b)

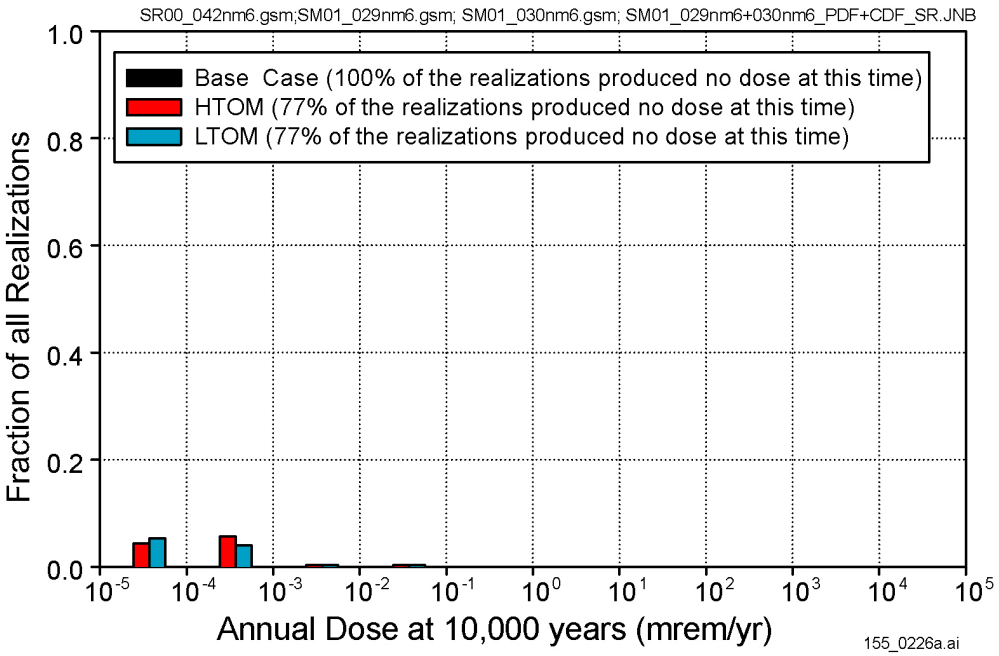

155_0225a.ai / 155_0226a.ai

NOTE: (a) Cumulative distribution function of fraction of realizations. (b) Histogram of fraction of realizations.

Figure 4.1-9. Fraction of Realizations Reaching Particular Annual Dose Rates at 10,000 Years

(a)

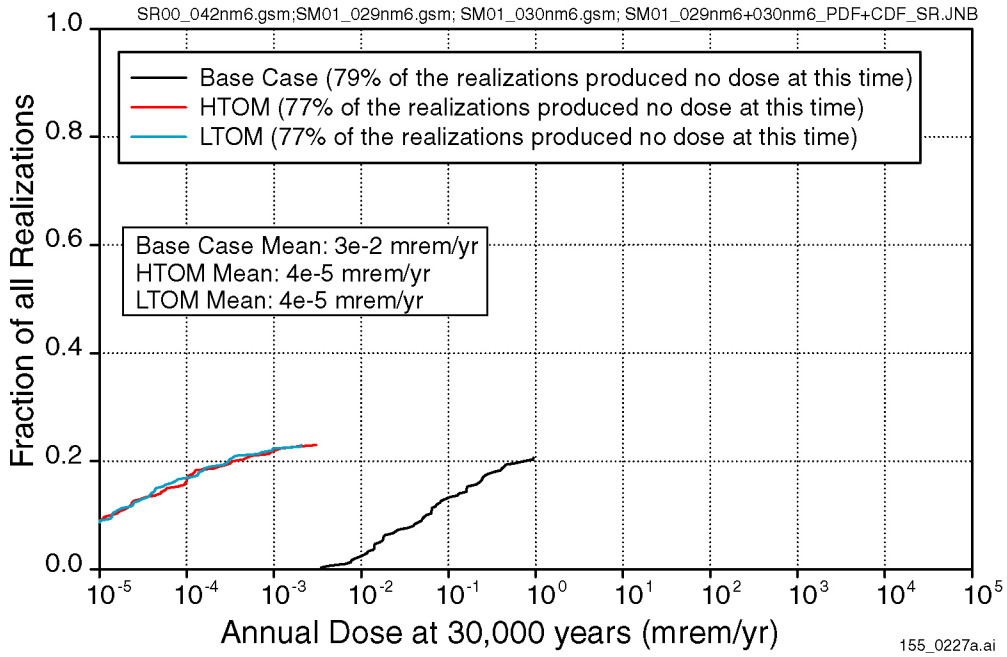

(b)

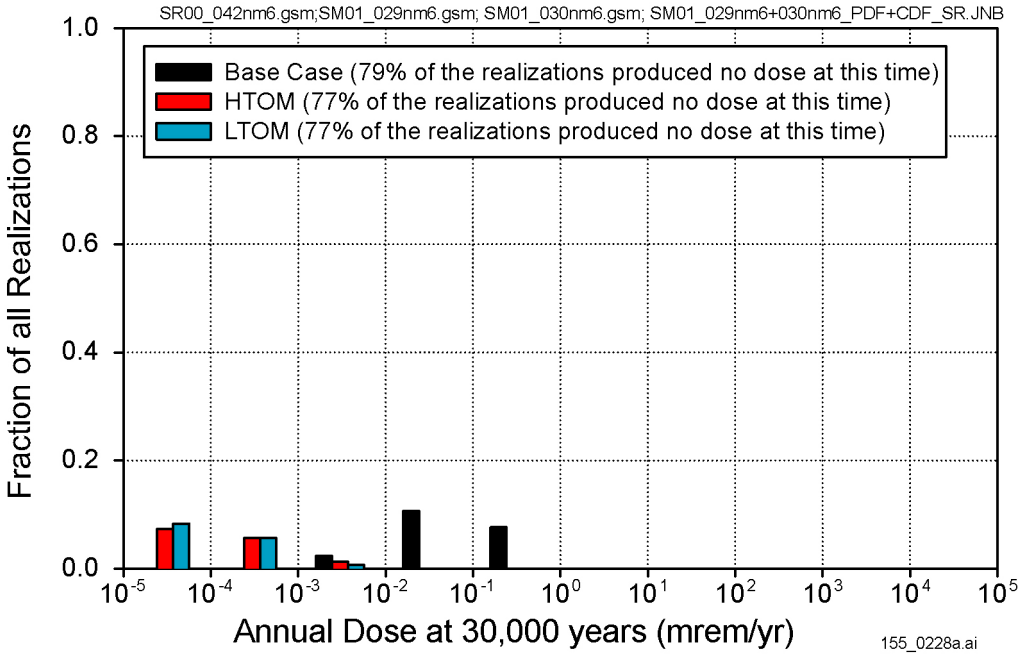

155_0227a.ai / 155_0228a.ai

NOTE: (a) Cumulative distribution function of fraction of realizations. (b) Histogram of fraction of realizations.

Figure 4.1-10. Fraction of Realizations Reaching Particular Annual Dose Rates at 30,000 Years

(a)

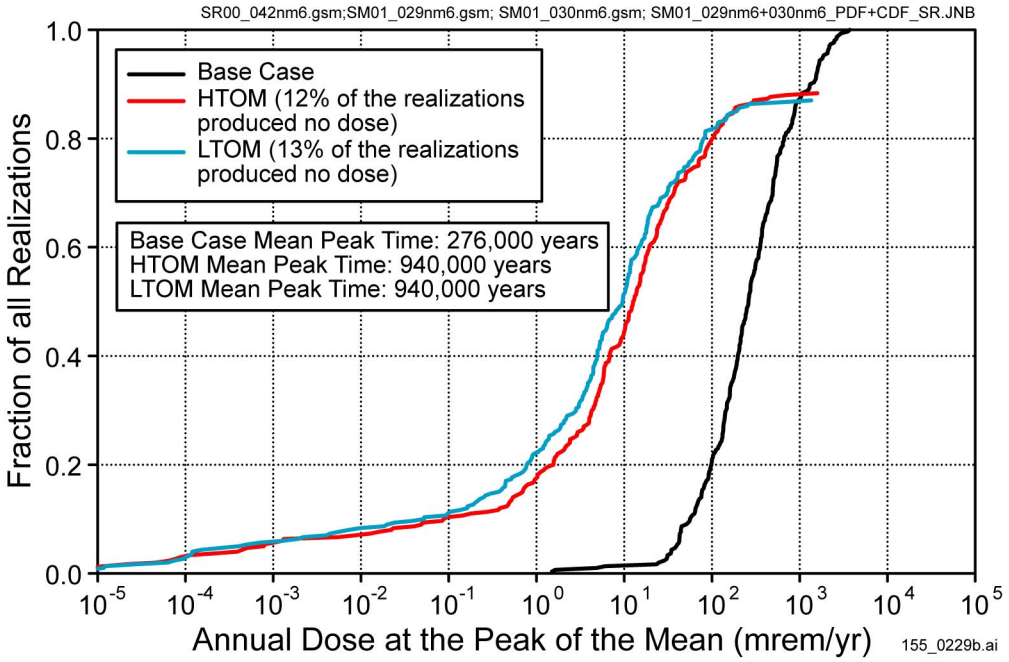

(b)

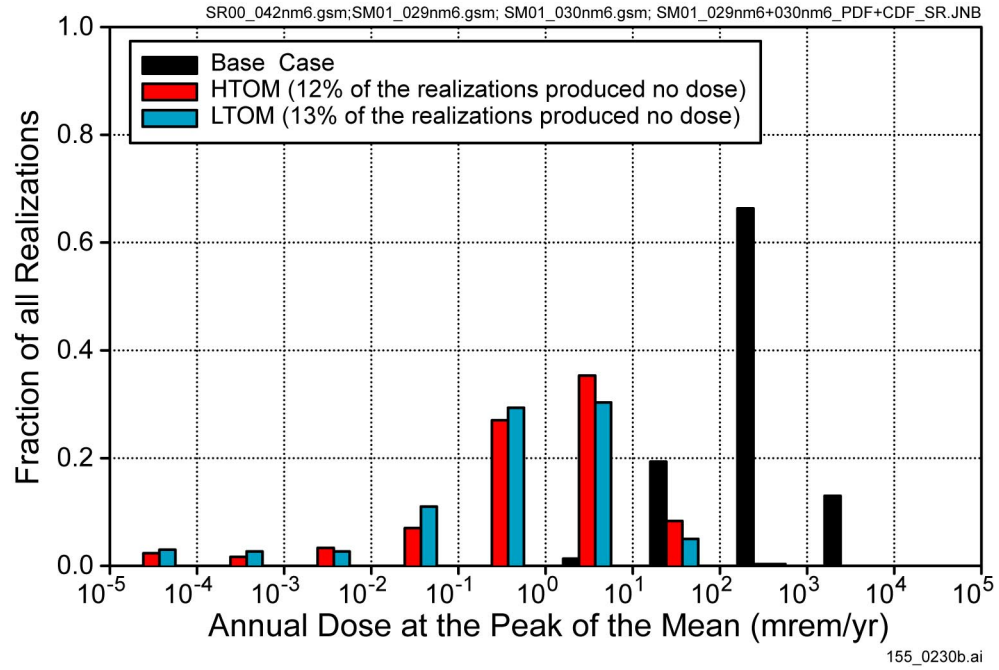

155_0229b.ai / 155_0230b.ai

NOTE: (a) Cumulative distribution function of fraction of realizations. (b) Histogram of fraction of realizations.

Figure 4.1-11. Fraction of Realizations Reaching Particular Annual Dose Rates at Time When Mean Dose Rate Peaks

(a)

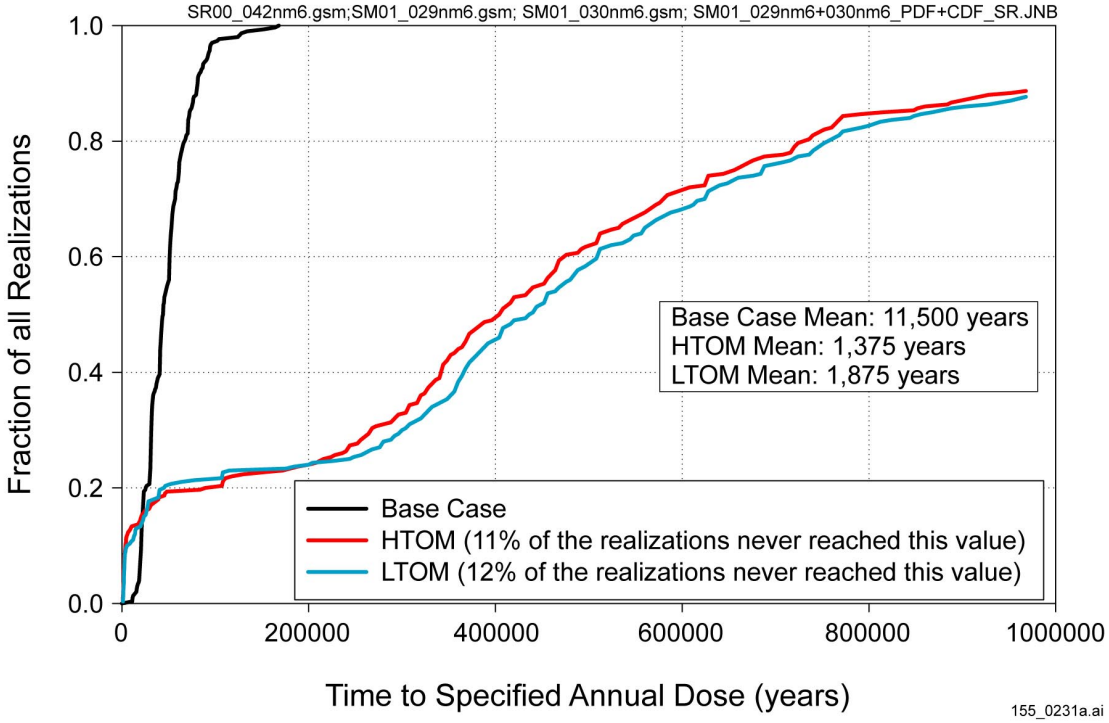

(b)

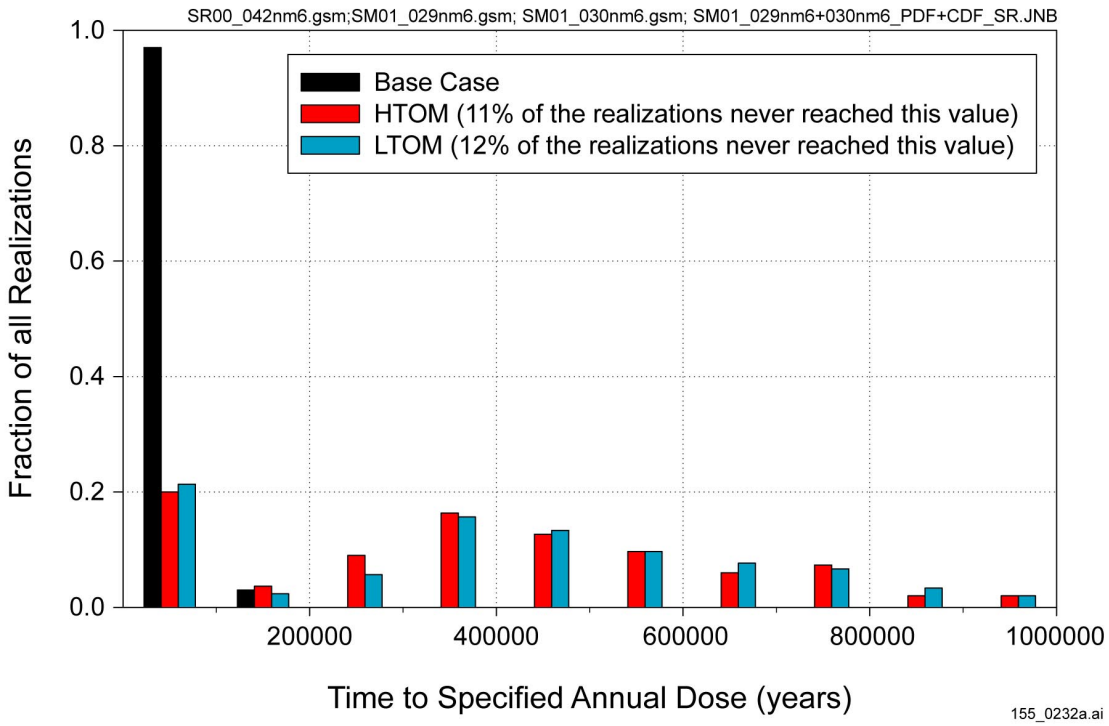

155_0231a.ai / 155_0232a.ai

NOTE: (a) Cumulative distribution function of time to dose rate of 10^{-5} mrem/yr. (b) Histogram of time to dose rate of 10^{-5} mrem/yr (to 1,000,000 years).

Figure 4.1-12a and b. Time that Fraction of Realizations Reaches Dose Rate of 10^{-5} mrem/yr

(c)

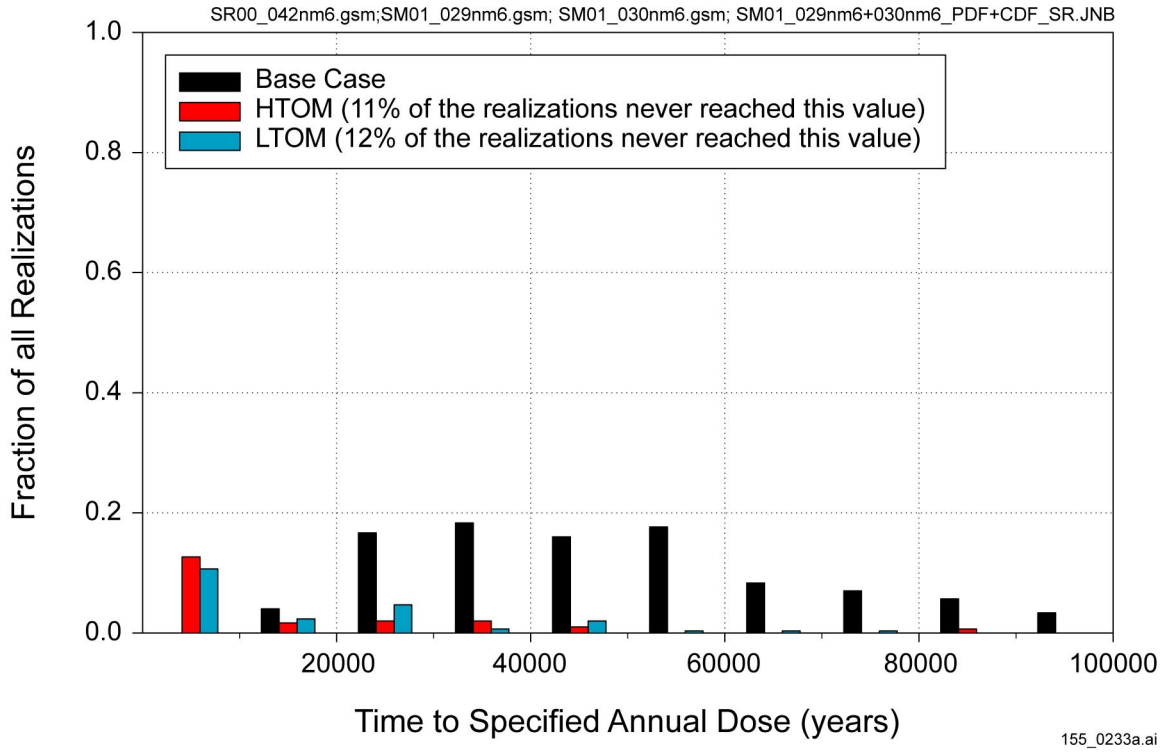

155_0233a.ai

NOTE: (c) Histogram of time to dose rate of 10^{-5} mrem/yr (to 100,000 years).

Figure 4.1-12c. Time that Fraction of Realizations Reaches Dose Rate of 10^{-5} mrem/yr

(a)

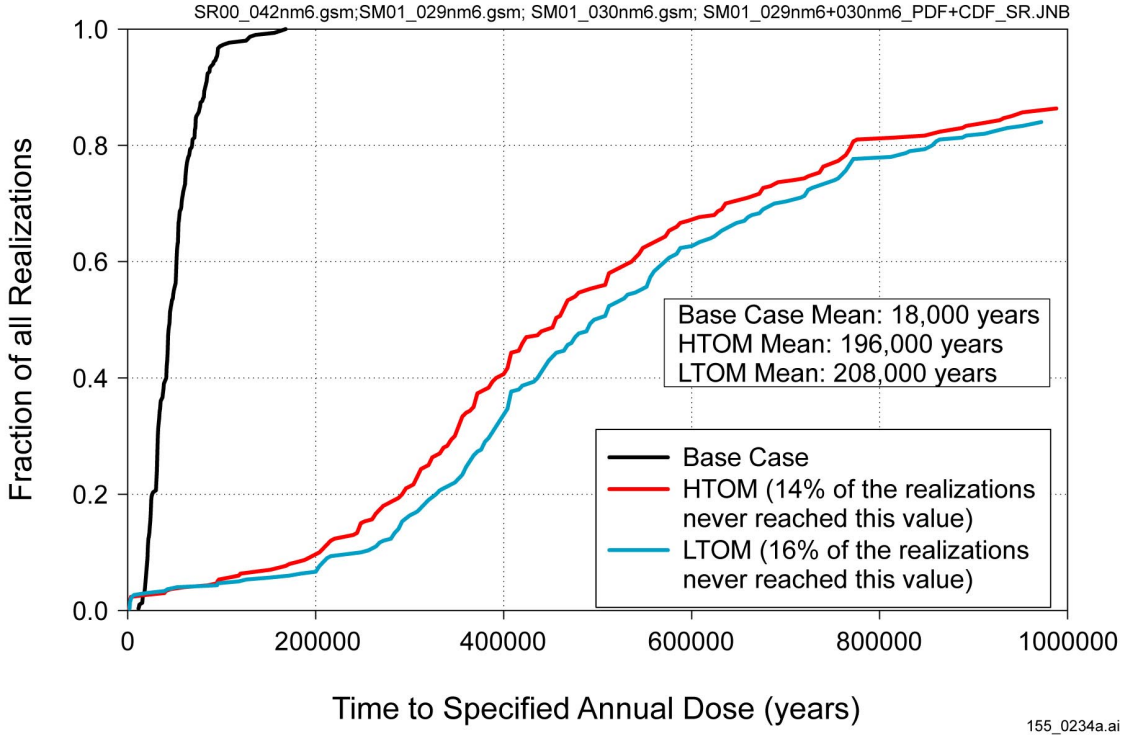

(b)

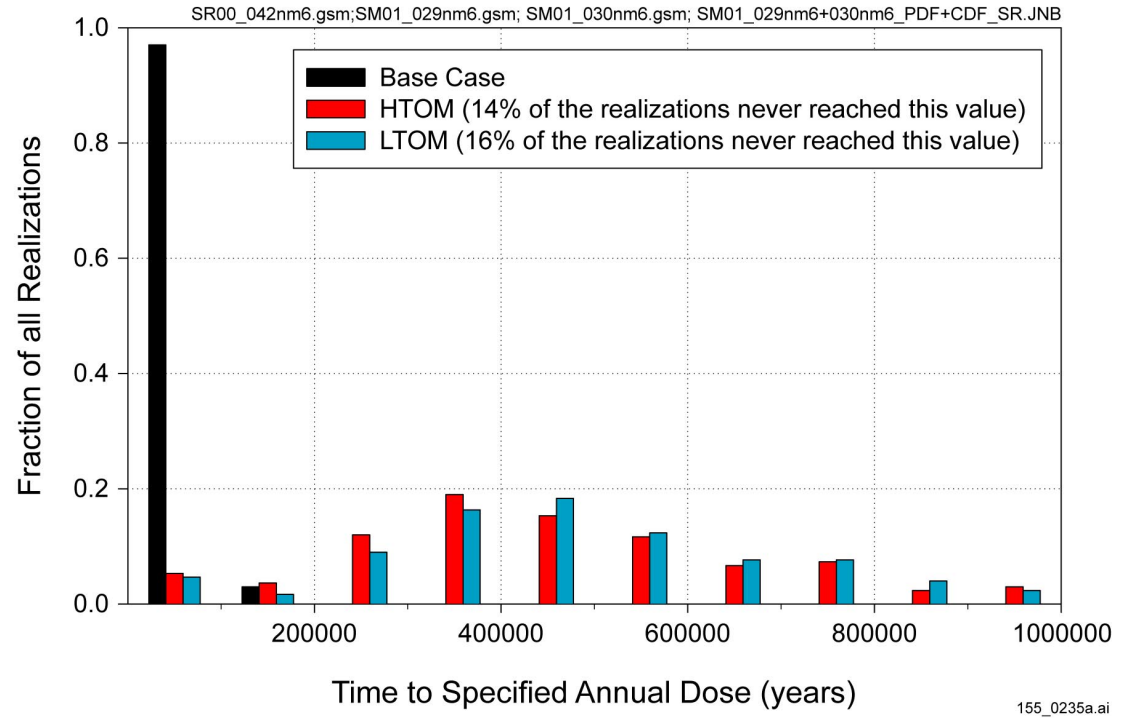

155_0234a.ai / 155_0235a.ai

NOTE: (a) Cumulative distribution function of time to dose rate of 10^{-3} mrem/yr. (b) Histogram of time to dose rate of 10^{-3} mrem/yr (to 1,000,000 years

Figure 4.1-13a and b. Time that Fraction of Realizations Reaches Dose Rate of 10^{-3} mrem/yr

(c)

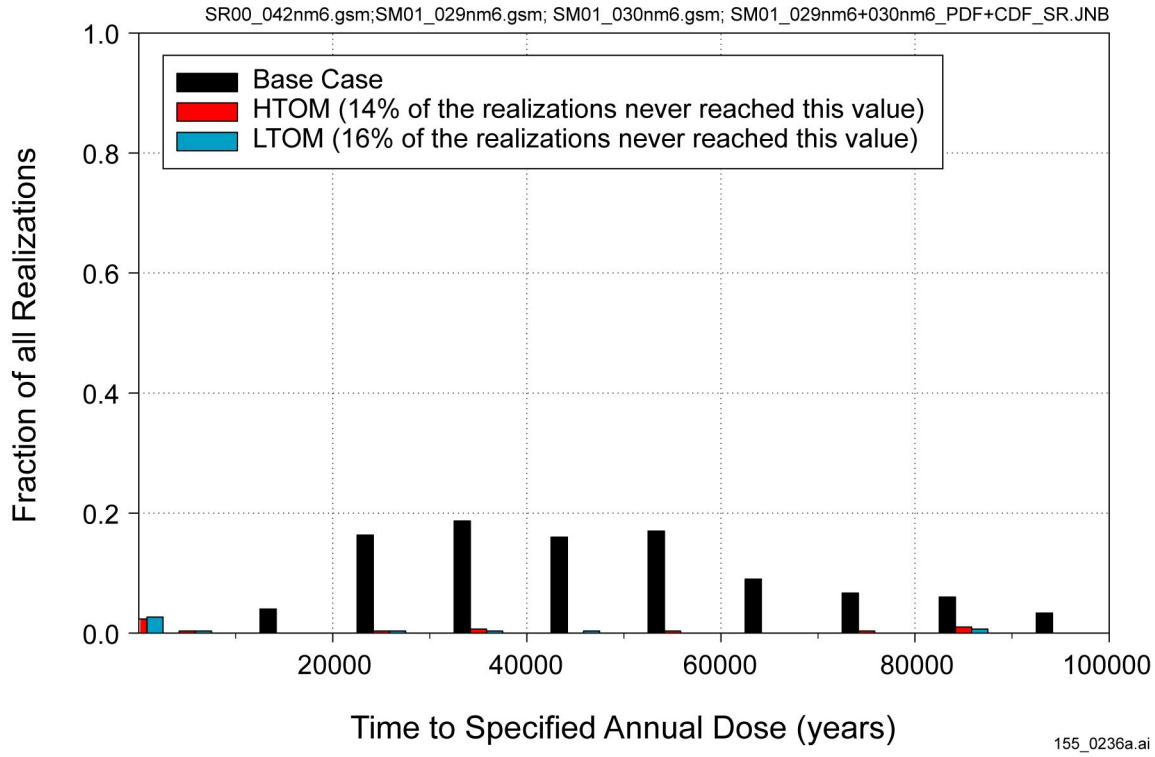

155_0236a.ai

NOTE: (c) Histogram of time to dose rate of 10^{-3} mrem/yr (to 100,000 years).

Figure 4.1-13c. Time that Fraction of Realizations Reaches Dose Rate of 10^{-3} mrem/yr

(a)

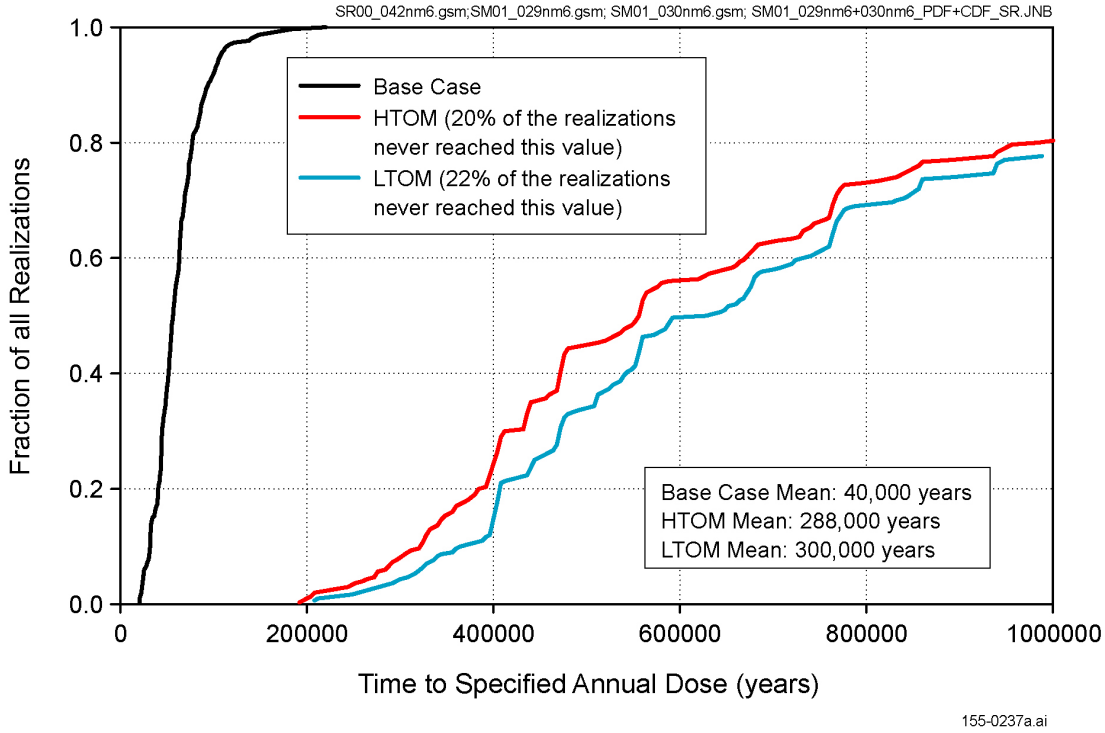

(b)

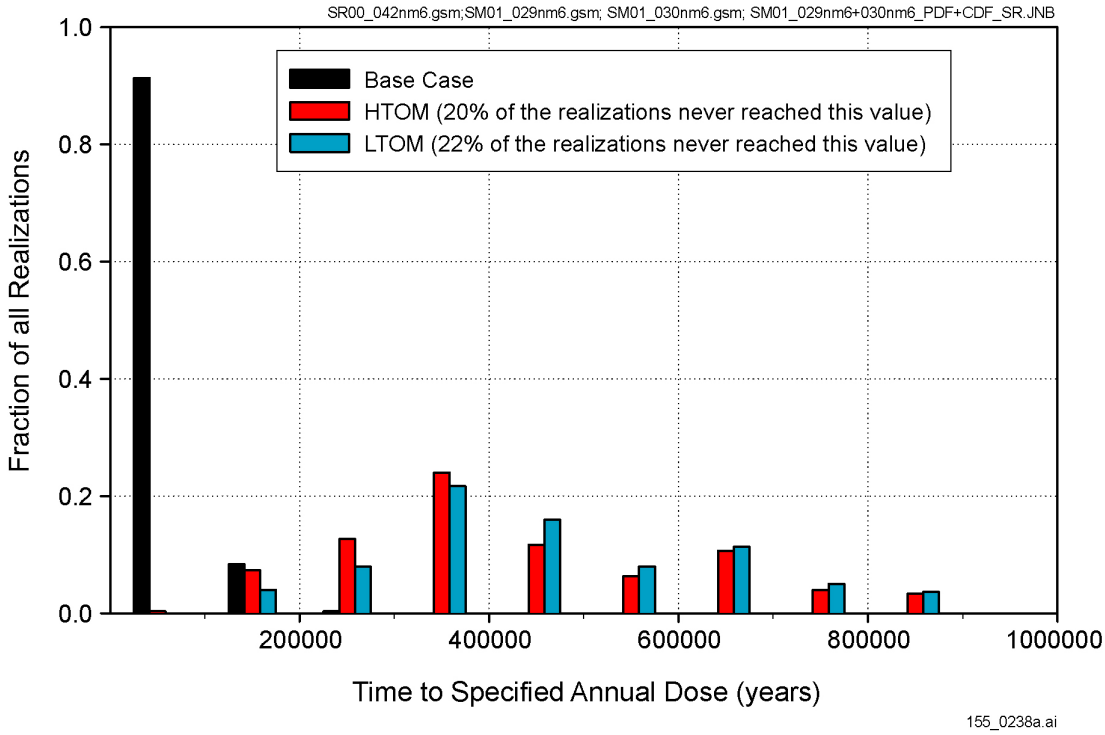

155_0237a.ai / 155_0238a.ai

NOTE: (a) Cumulative distribution function of time to dose rate of 10^{-1} mrem/yr. (b) Histogram of time to dose rate of 10^{-1} mrem/yr (to 1,000,000 years).

Figure 4.1-14a and b. Time that Fraction of Realizations Reaches Dose Rate of 10^{-1} mrem/yr

(c)

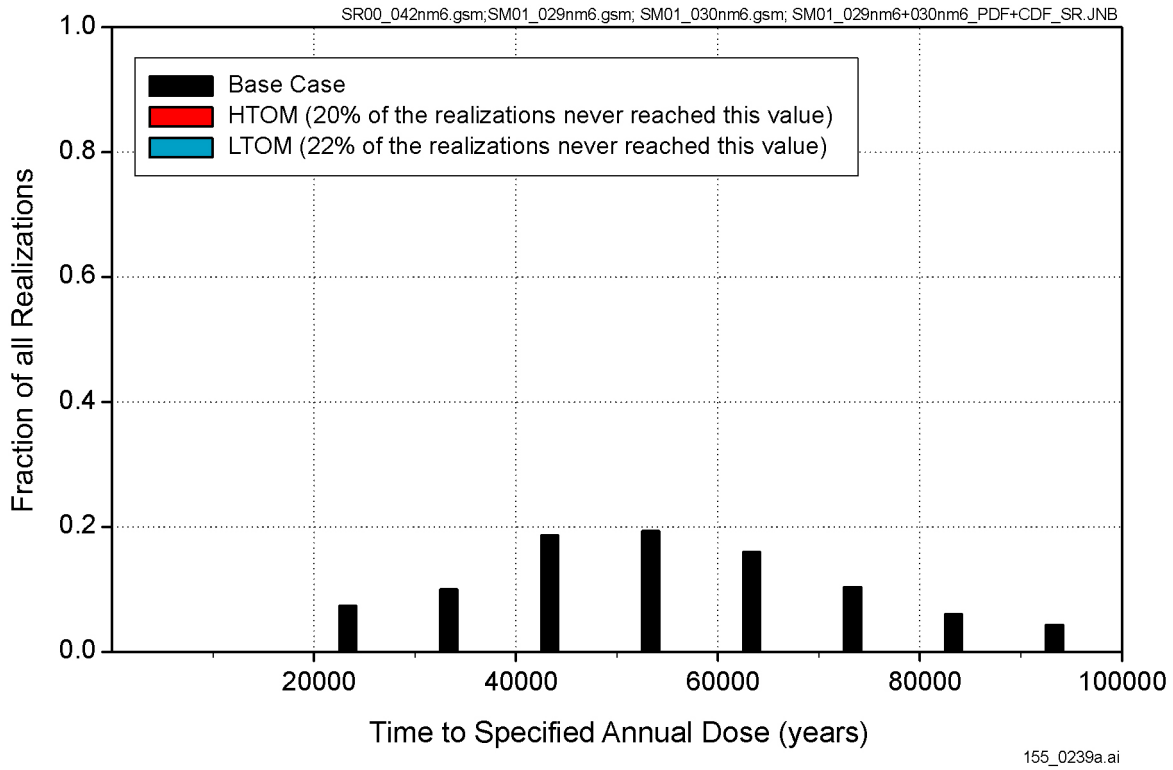

155_0239a.ai

NOTE: (c) Histogram of time to dose rate of 10^{-1} mrem/yr (to 100,000 years).

Figure 4.1-14c. Time that Fraction of Realizations Reaches Dose Rate of 10^{-1} mrem/yr

(a)

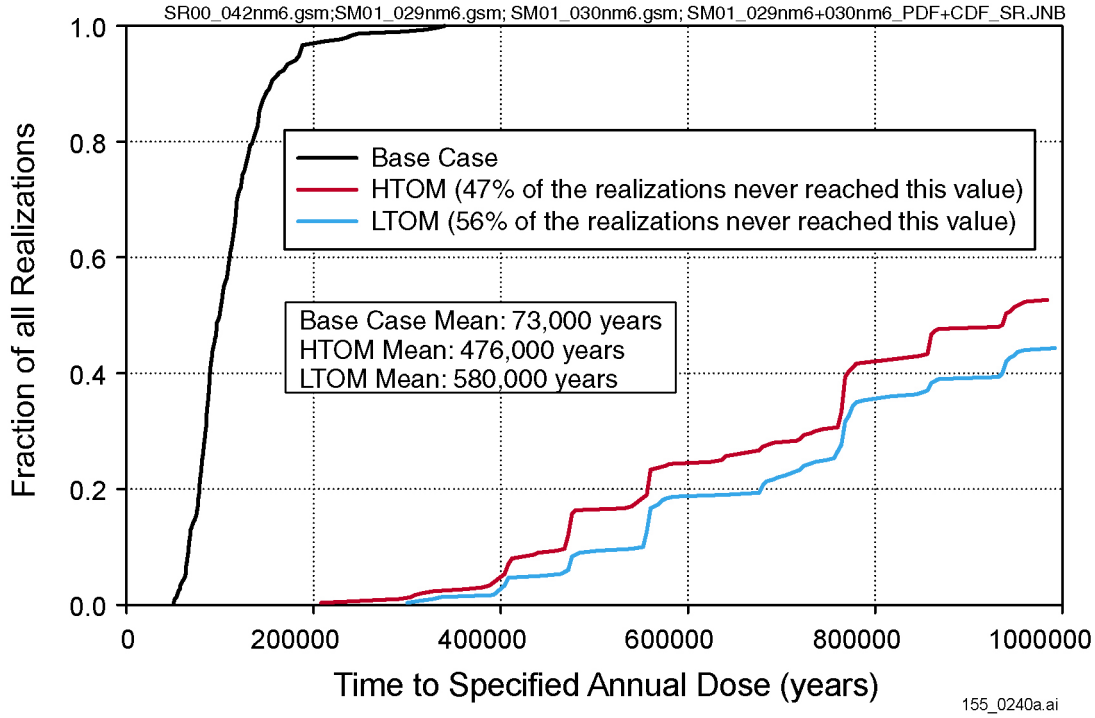

(b)

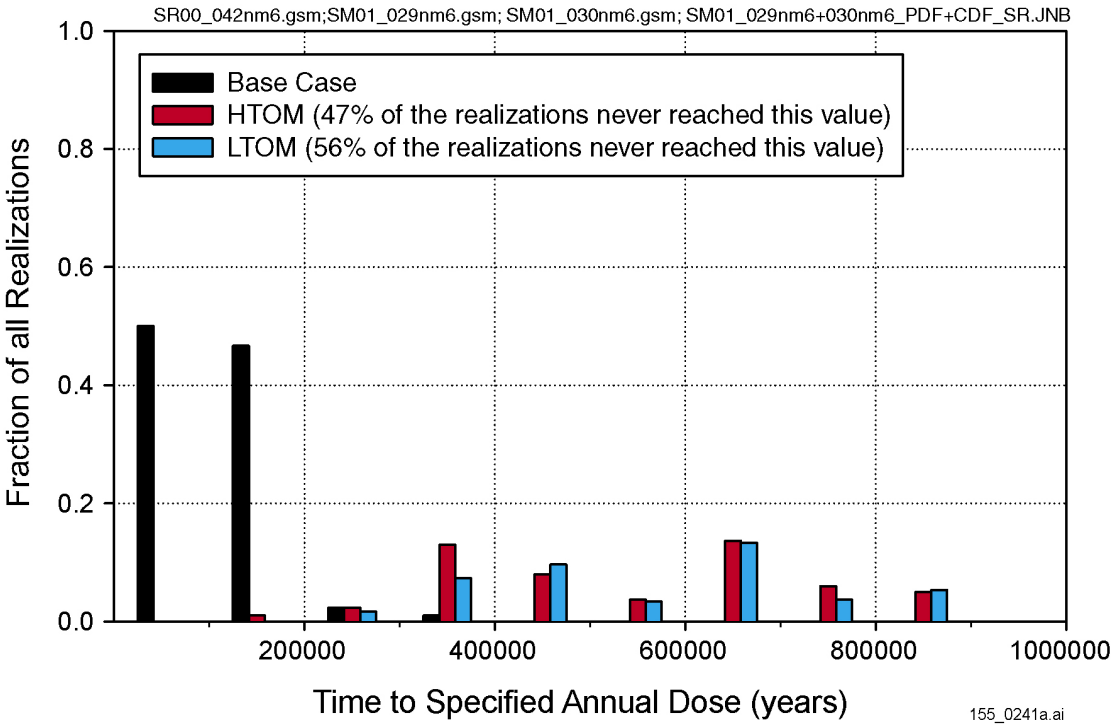

155_0240a.ai / 155_0241a.ai

NOTE: (a) Cumulative distribution function of time to dose rate of 10 mrem/y. (b) Histogram of time to dose rate of 10 mrem/yr (to 1,000,000 years).

Figure 4.1-15a and b. Time that Fraction of Realizations Reaches Dose Rate of 10 mrem/yr

(c)

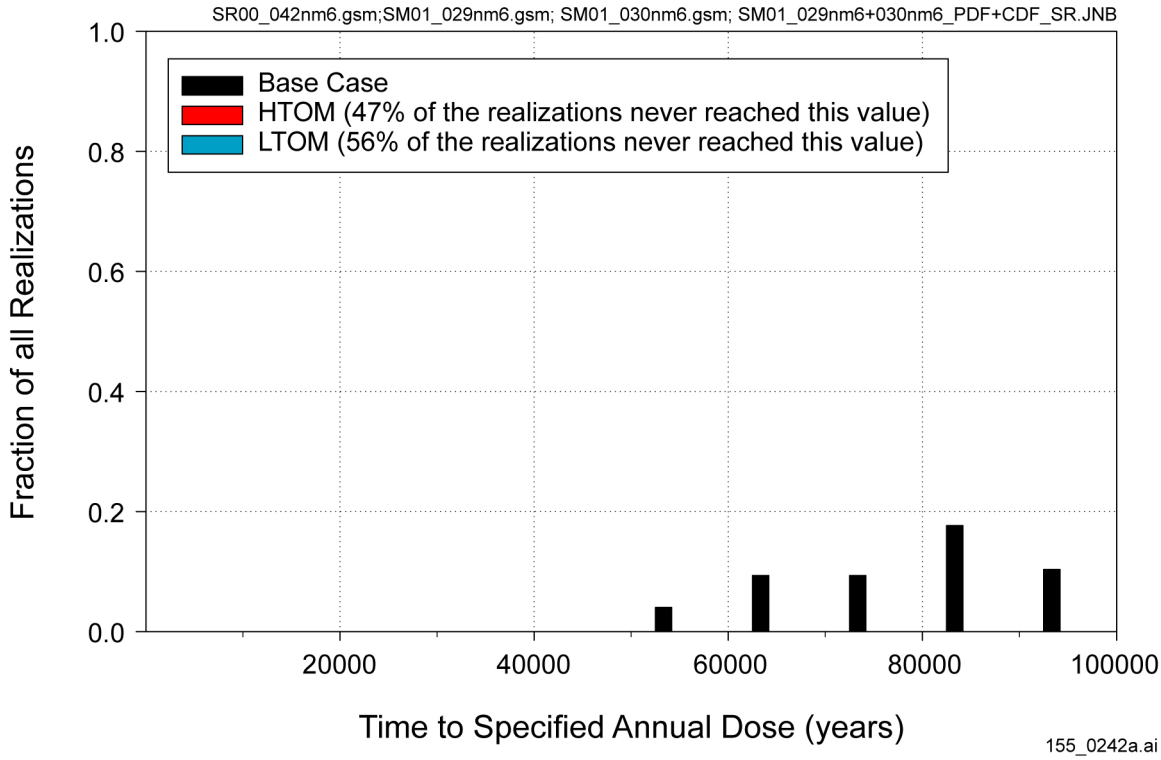

155_0242a.ai

NOTE: (c) Histogram of time to dose rate of 10 mrem/yr (to 100,000 years).

Figure 4.1-15c. Time that Fraction of Realizations Reaches Dose Rate of 10 mrem/yr

(a)

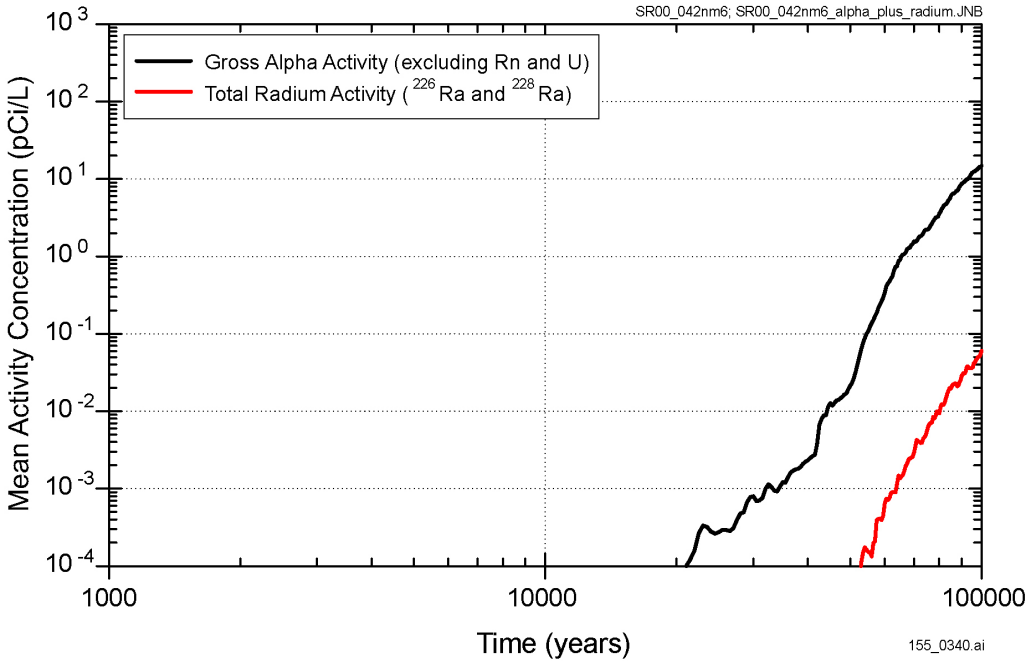

(b)

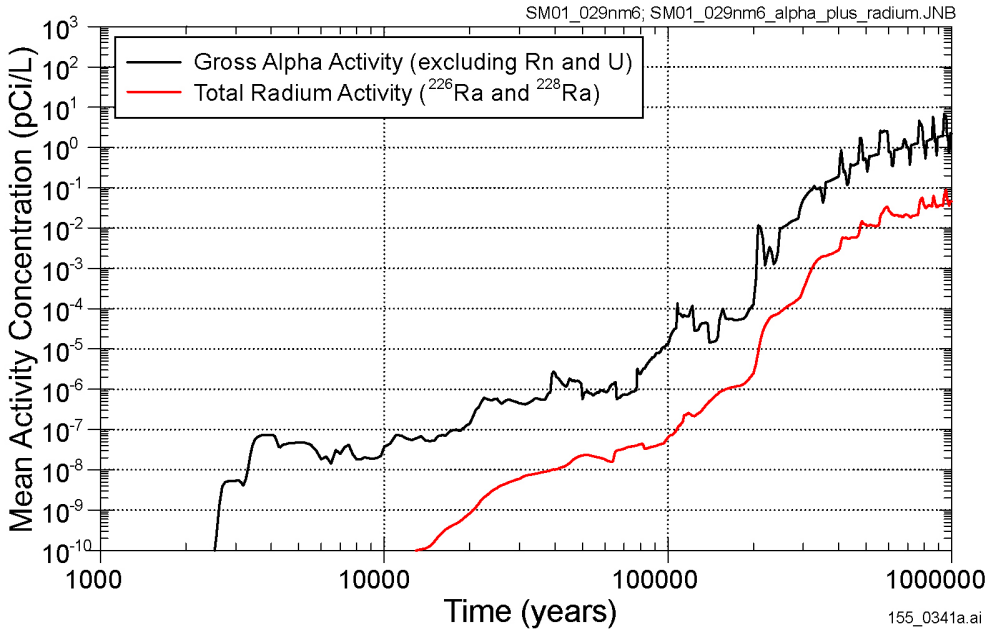

155_0340.ai / 155_0341a.ai

Source: CRWMS M&O 2000 [DIRS 153246].

NOTE: Concentrations calculated for a representative volume of water of 1,285 acre-ft/yr, 20 km from the potential repository. Naturally occurring background radionuclide concentrations are not included. (a) TSPA-SR results for 100,000 years of nominal performance. (b) Supplemental TSPA model results for 1,000,000 years of nominal performance, HTOM. Concentration axis expanded relative to Figure 4.1-16a to display low values.

Figure 4.1-16a and b. Mean Concentrations of Gross Alpha Activity and Total Radium in Groundwater

(c)

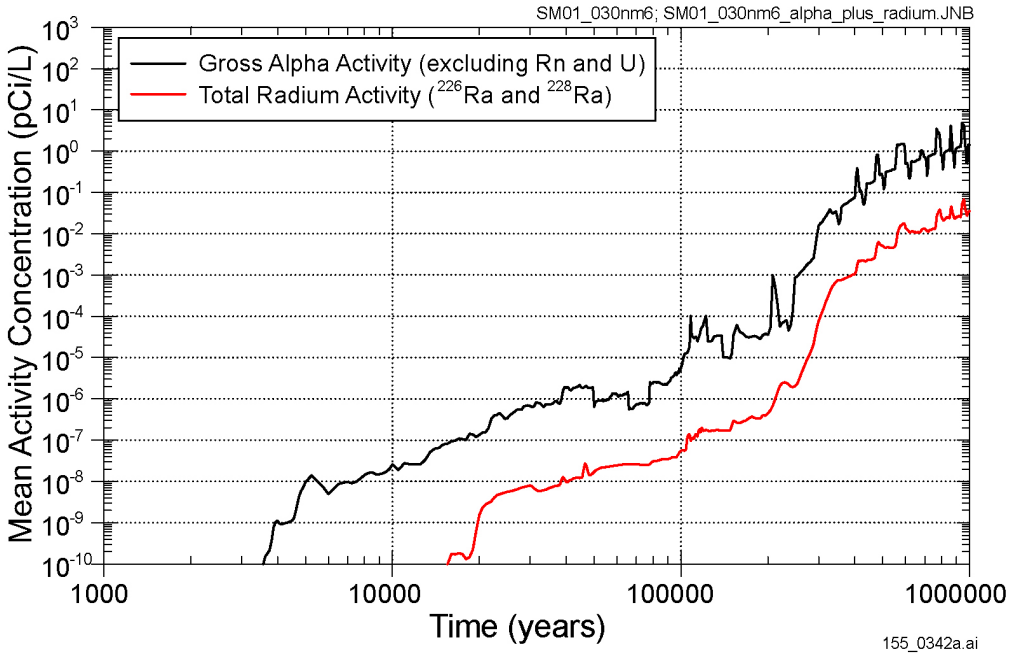

155_0342a.ai

Source: CRWMS M&O 2000 [DIRS 153246].

NOTE: Concentrations calculated for a representative volume of water of 1,285 acre-ft/yr, 20 km from the potential repository. Naturally occurring background radionuclide concentrations are not included. (c) Supplemental TSPA model results for 1,000,000 years of nominal performance, LTOM. Concentration axis expanded relative to Figure 4.1-16a to display low values.

Figure 4.1-16c. Mean Concentrations of Gross Alpha Activity and Total Radium in Groundwater

(a)

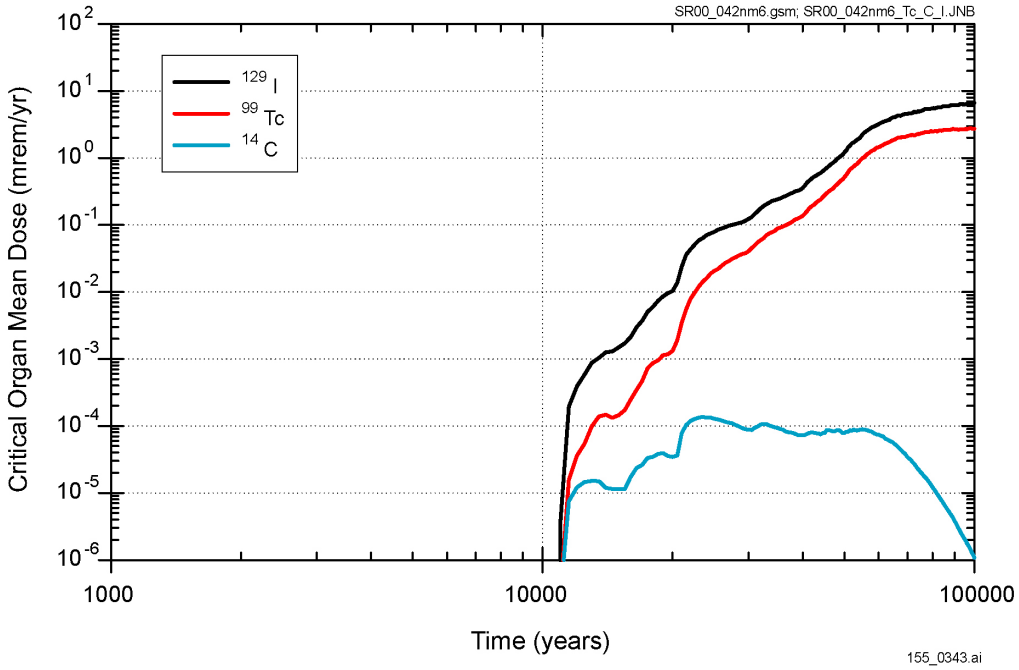

(b)

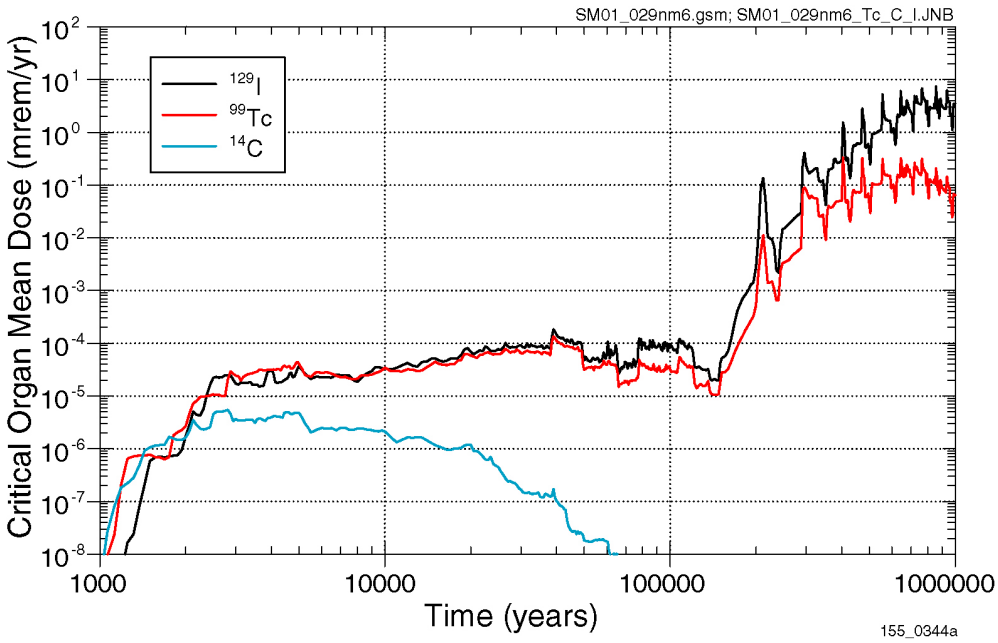

155_00343.ai / 155_0344.ai

NOTE: Concentrations calculated for a representative volume of water of 1,285 acre-ft/yr, 20 km from the potential repository. Naturally occurring background radionuclide concentrations are not included. (a) TSPA-SR results for 100,000 years of nominal performance. (b) Supplemental TSPA model results for 1,000,000 years of nominal performance, HTOM. Concentration axis expanded relative to Figure 4-17a to display low values.

Figure 4.1-17a and b. Mean Doses to Critical Organs Resulting from Beta and Photon Emitters in Groundwater

(c)

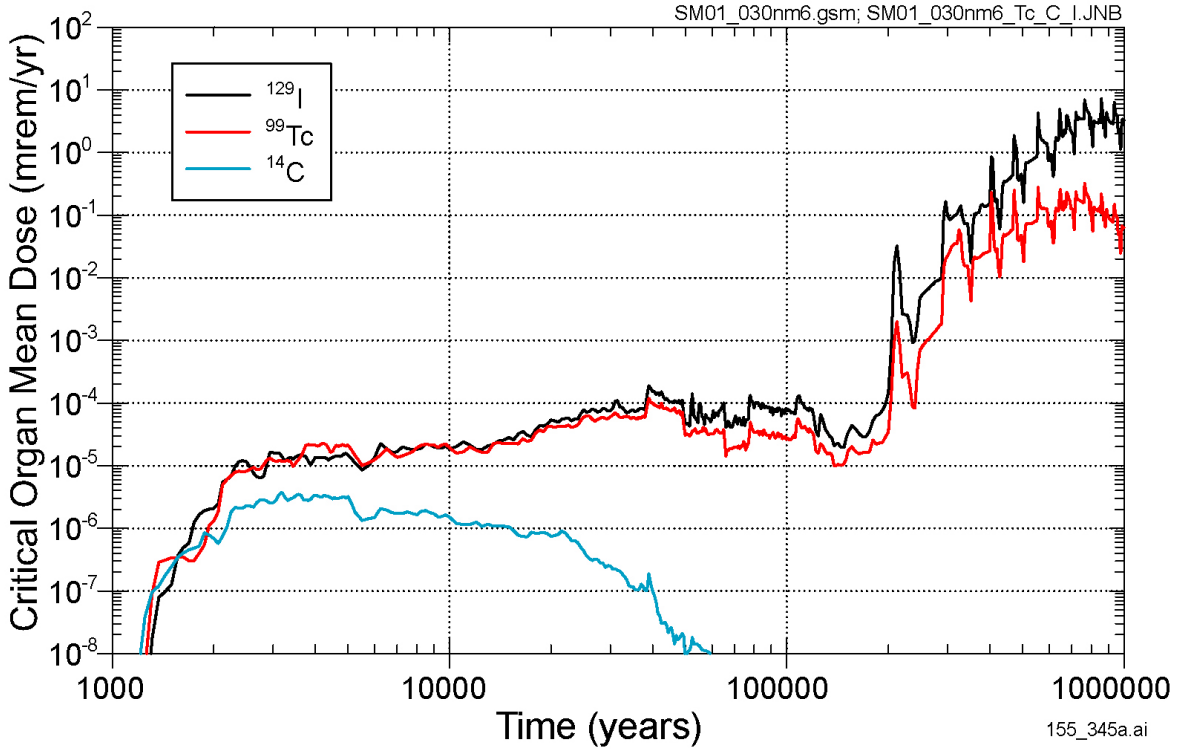

155_345a.ai

Source: CRWMS M&O 2000 [DIRS 153246].

NOTE: Concentrations calculated for a representative volume of water on 1,285 acre-ft/yr, 20 km from the potential repository. Naturally occurring background radionuclide concentrations are not included. (b) Supplemental TSPA model results for 1,000,000 years of nominal performance, LTOM. Concentration axis expanded relative to Figure 4-17a to display low values.

Figure 4.1-17c. Mean Doses to Critical Organs Resulting from Beta and Photon Emitters in Groundwater

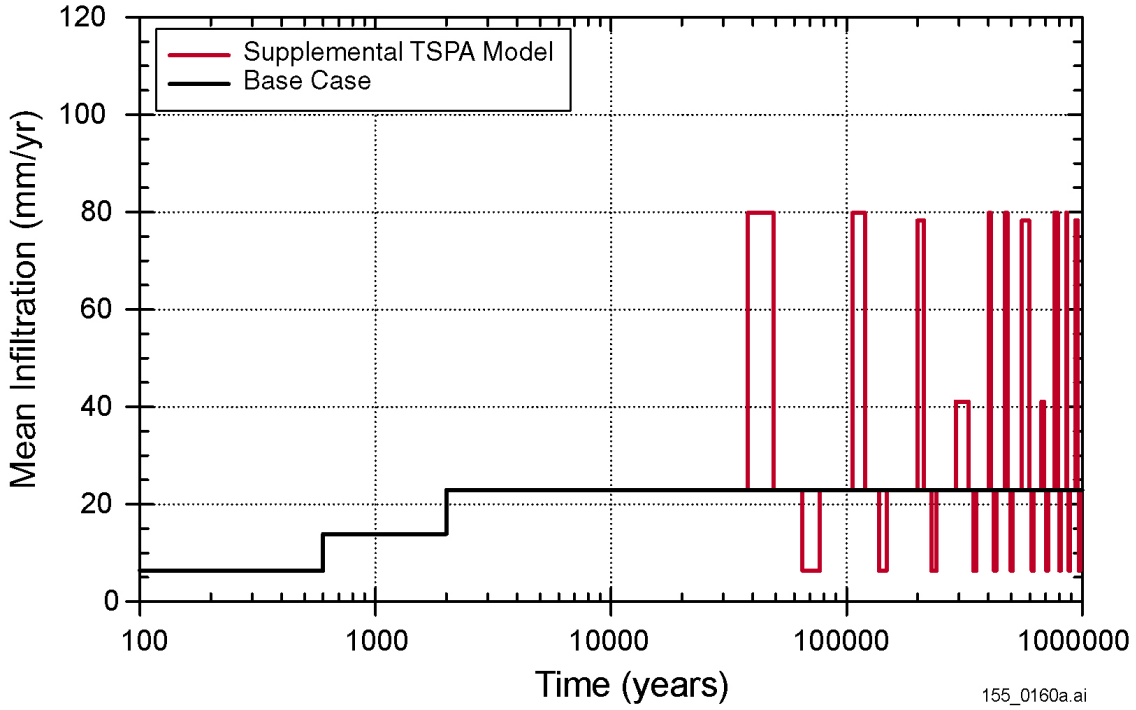

155_0160a.ai

Source: TSPA-SR (CRWMS M&O 2000 [DIRS 153246], Tables 3.2-1, 3.2-2, 3.2-4, and 3.2-6).

Figure 4.2.1-1. Net Infiltration, Averaged over the Repository Area and over the Three Infiltration Cases

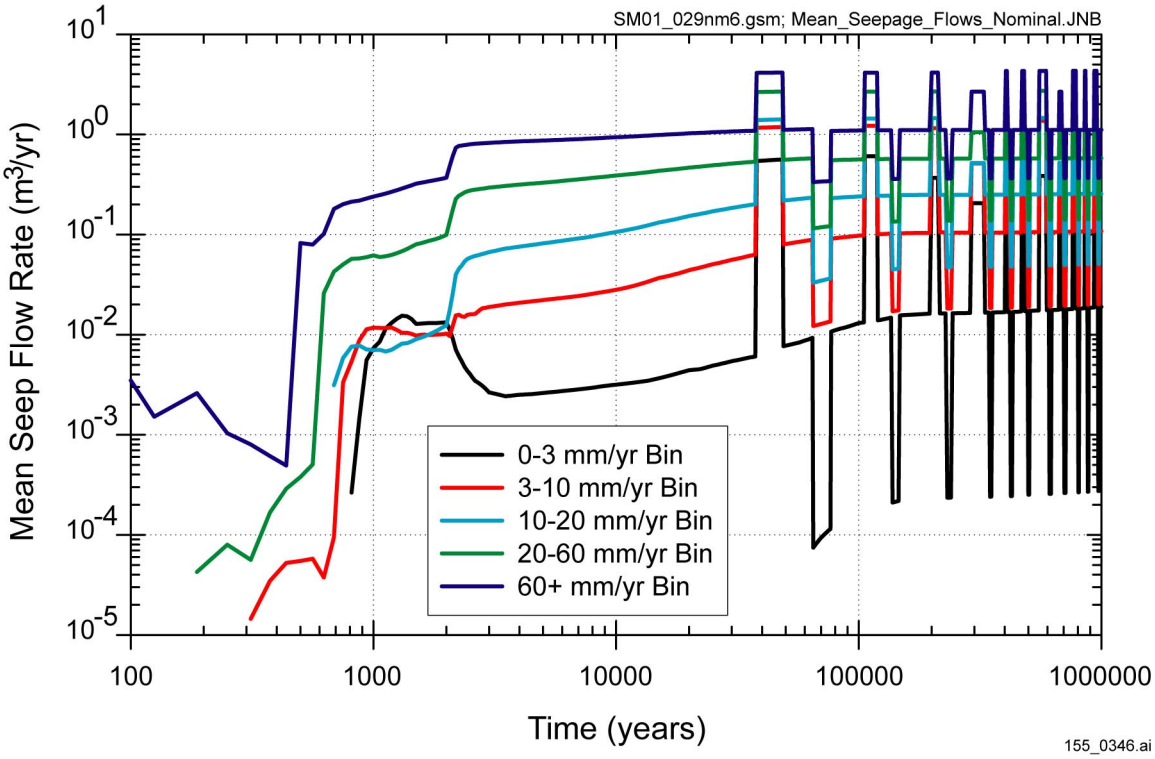

155_0346.ai

Figure 4.2.2-1. Mean Seep Flow Rate for Commercial Spent Nuclear Fuel, Higher-Temperature Operating Mode

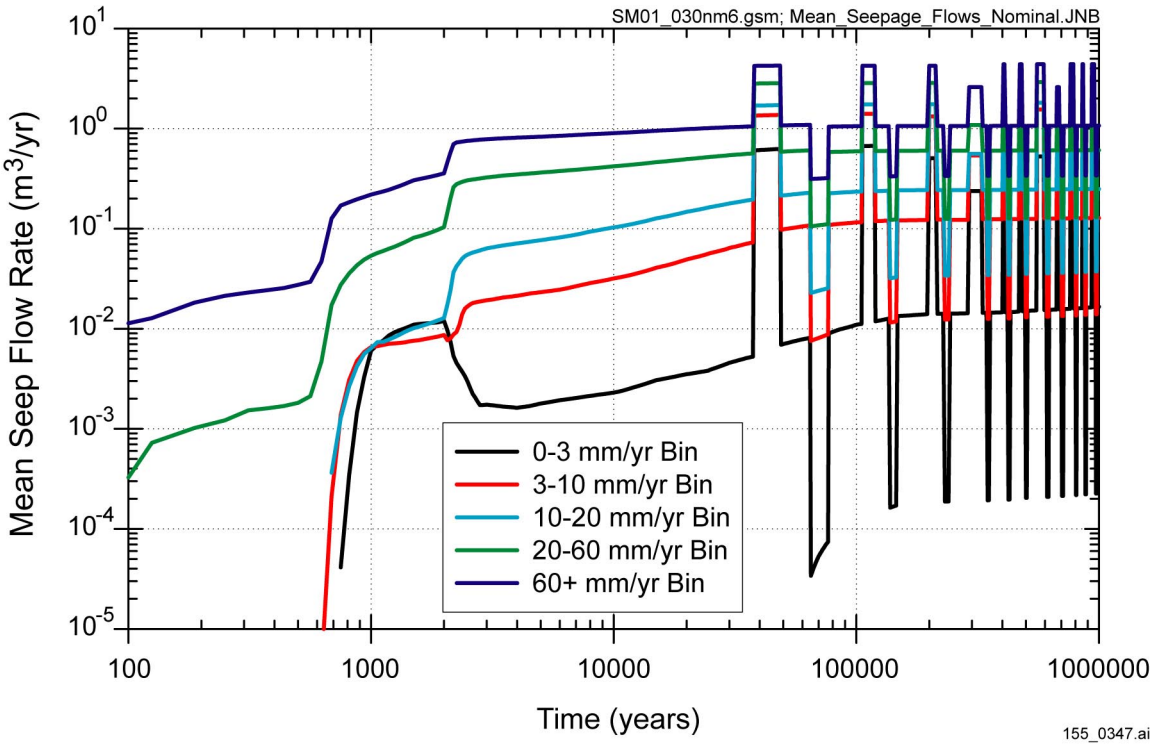

155_0347.ai

Figure 4.2.2-2. Mean Seep Flow Rate for Commercial Spent Nuclear Fuel, Lower-Temperature Operating Mode

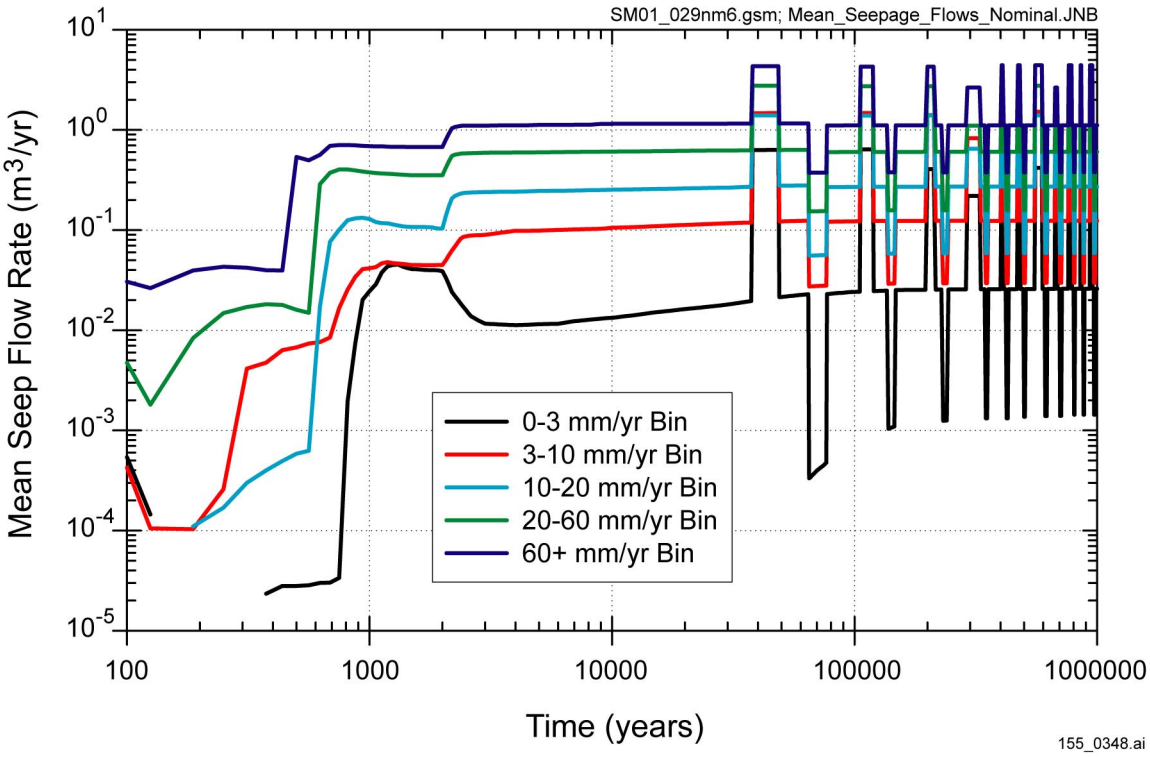

155_0348.ai

Figure 4.2.2-3. Mean Seep Flow Rate for Co-Disposal Waste, Higher-Temperature Operating Mode

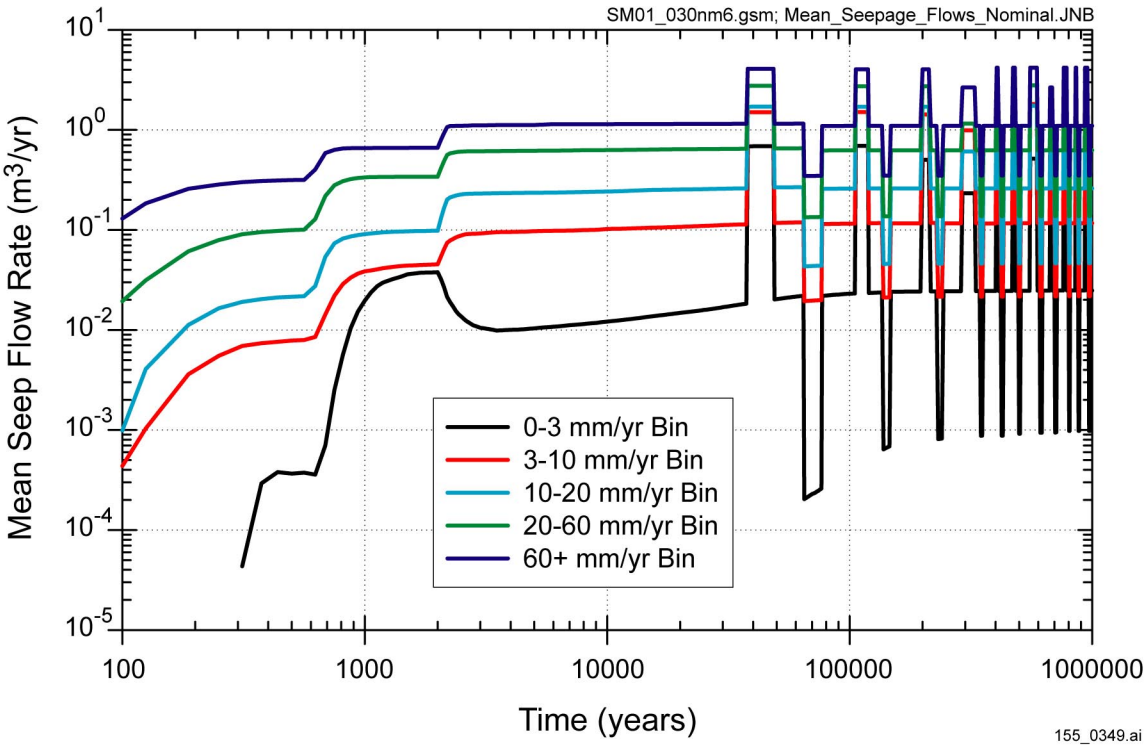

155_0349.ai

Figure 4.2.2-4. Mean Seep Flow Rate for Co-Disposal Waste, Lower-Temperature Operating Mode

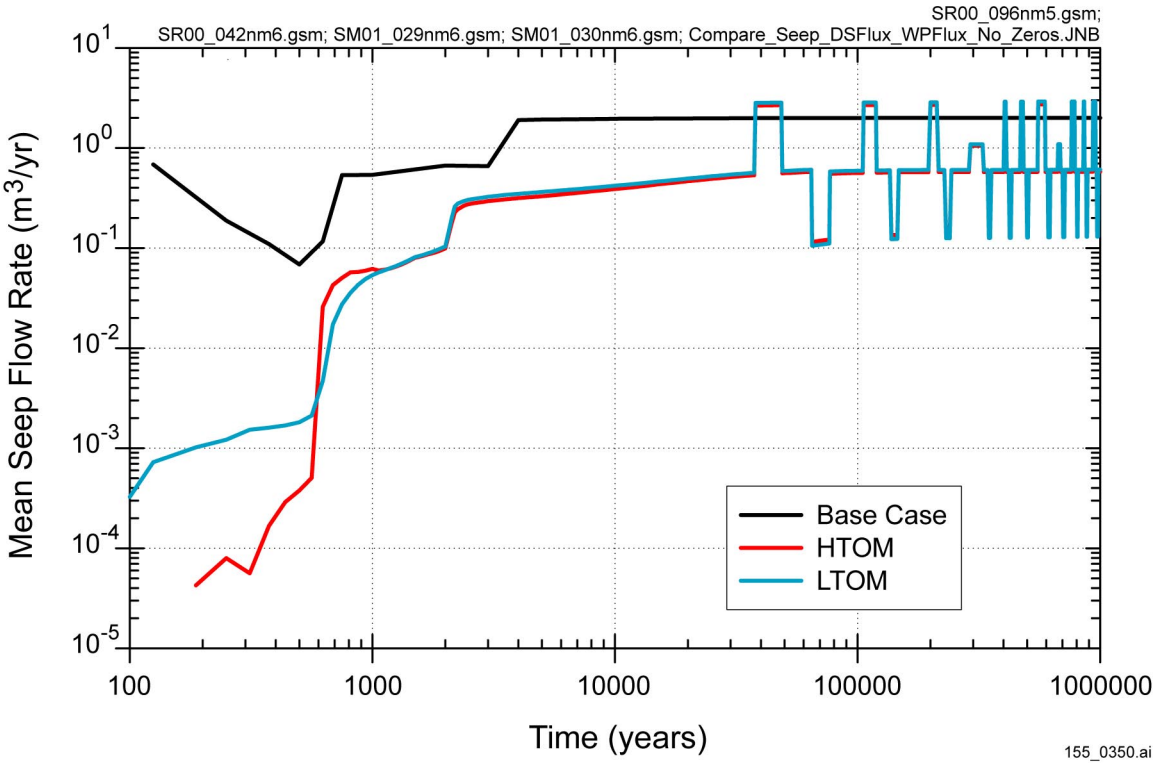

155_0350.ai

Figure 4.2.2-5. Comparison of Mean Seep Flow Rate in Three Cases for Commercial Spent Nuclear Fuel with 20 to 60 mm/yr Infiltration

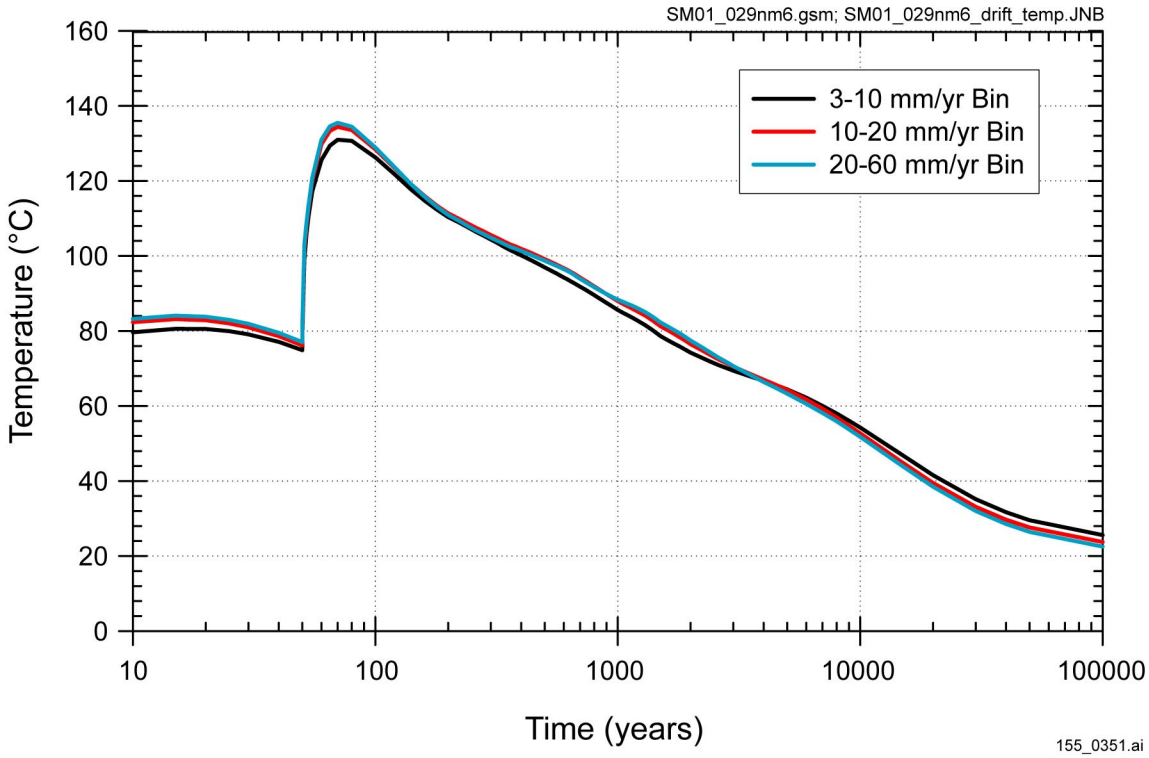

155_0351.ai

Figure 4.2.2-6. Bin-Averaged Drift-Wall Temperature for Commercial Spent Nuclear Fuel in the Medium-Infiltration Case, Higher-Temperature Operating Mode

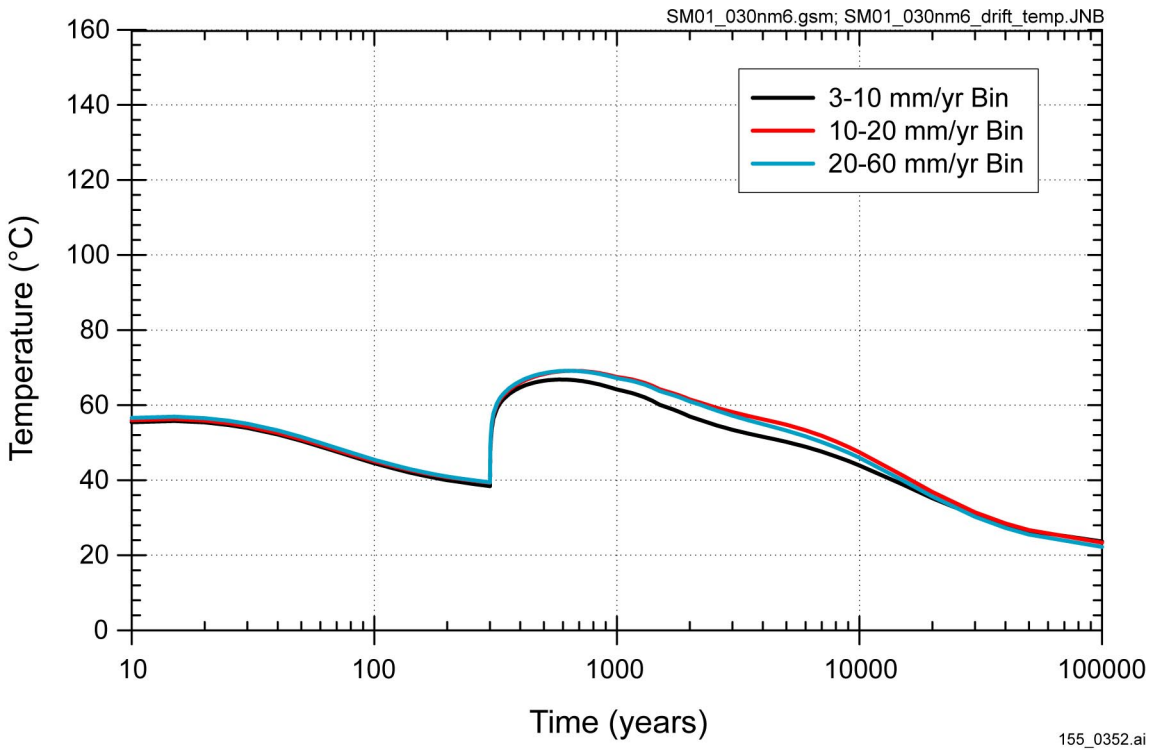

155_0352.ai

Figure 4.2.2-7. Bin-Averaged Drift-Wall Temperature for Commercial Spent Nuclear Fuel in the Medium-Infiltration Case, Lower-Temperature Operating Mode

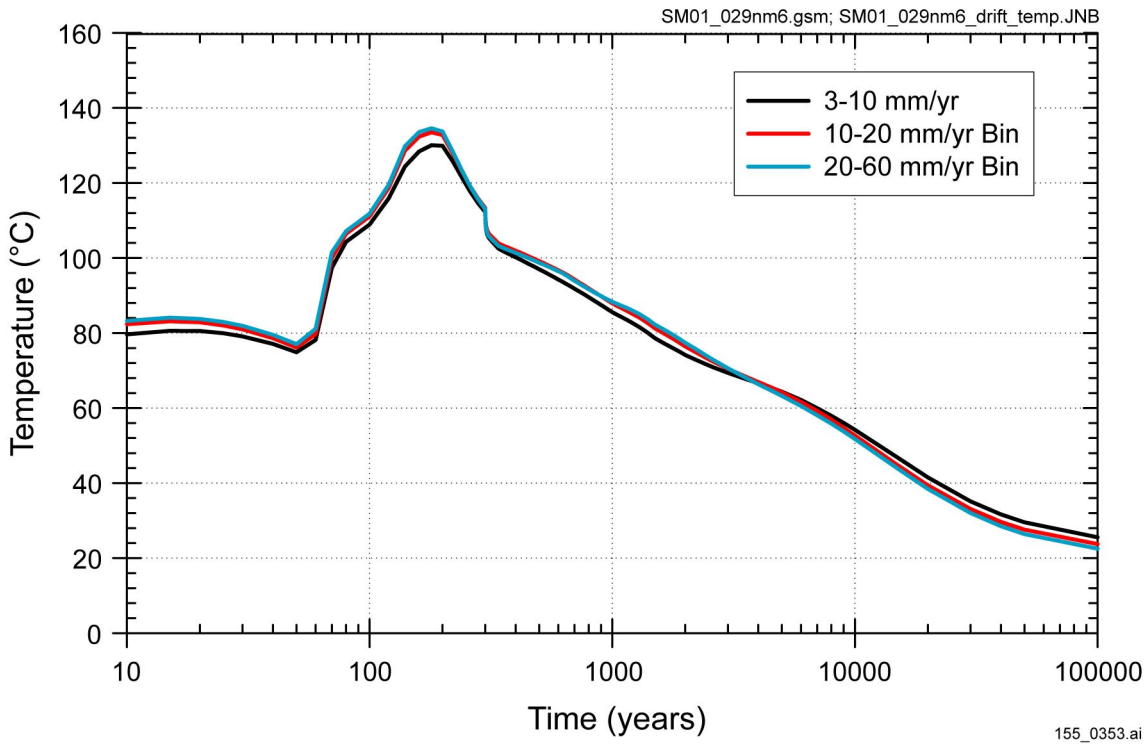

155_0353.ai

Figure 4.2.2-8. Bin-Averaged Drift-Wall Temperature for Co-Disposal Waste in the Medium-Infiltration Case, Higher-Temperature Operating Mode

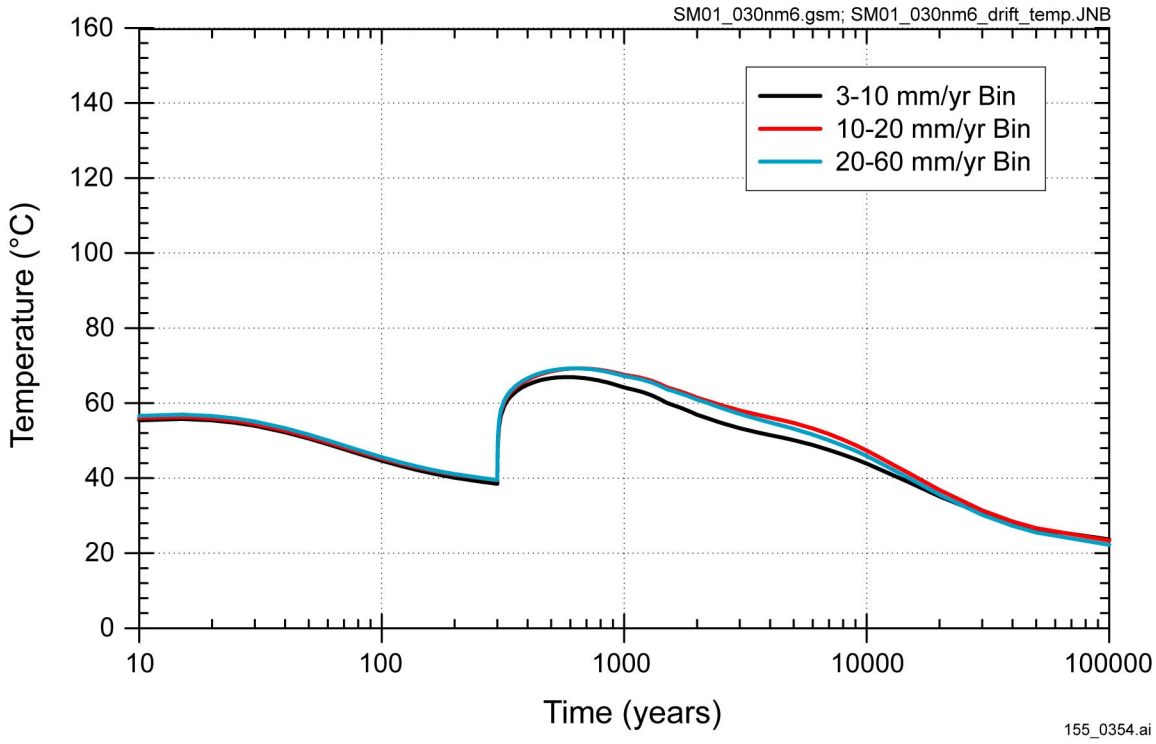

155_0354.ai

Figure 4.2.2-9. Bin-Averaged Drift-Wall Temperature for Co-Disposal Waste in the Medium-Infiltration Case, Lower-Temperature Operating Mode

(a)

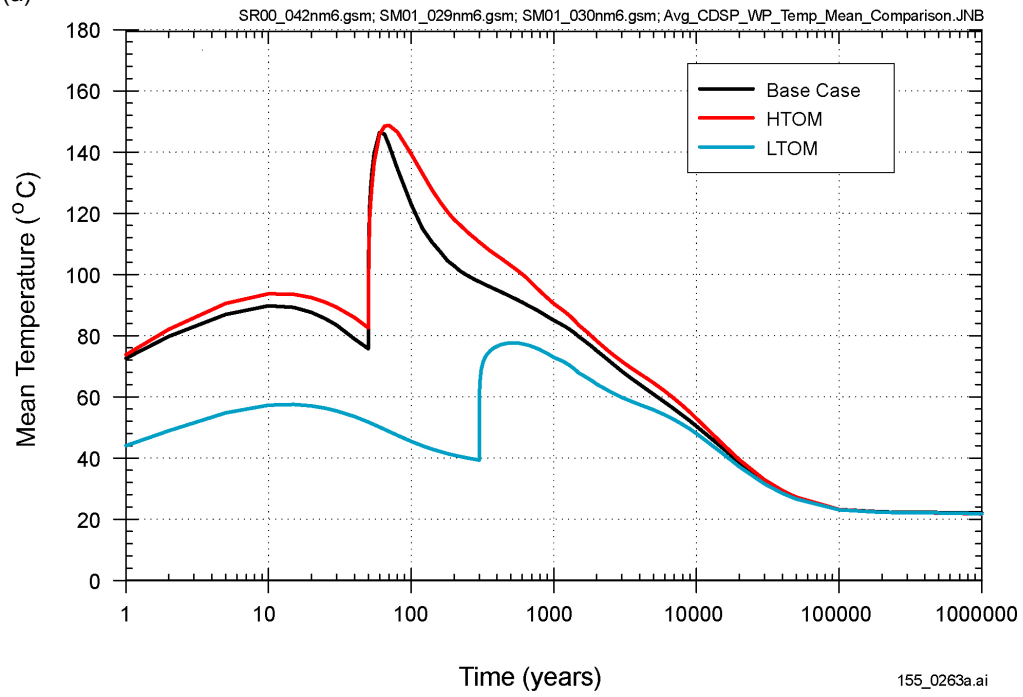

(b)

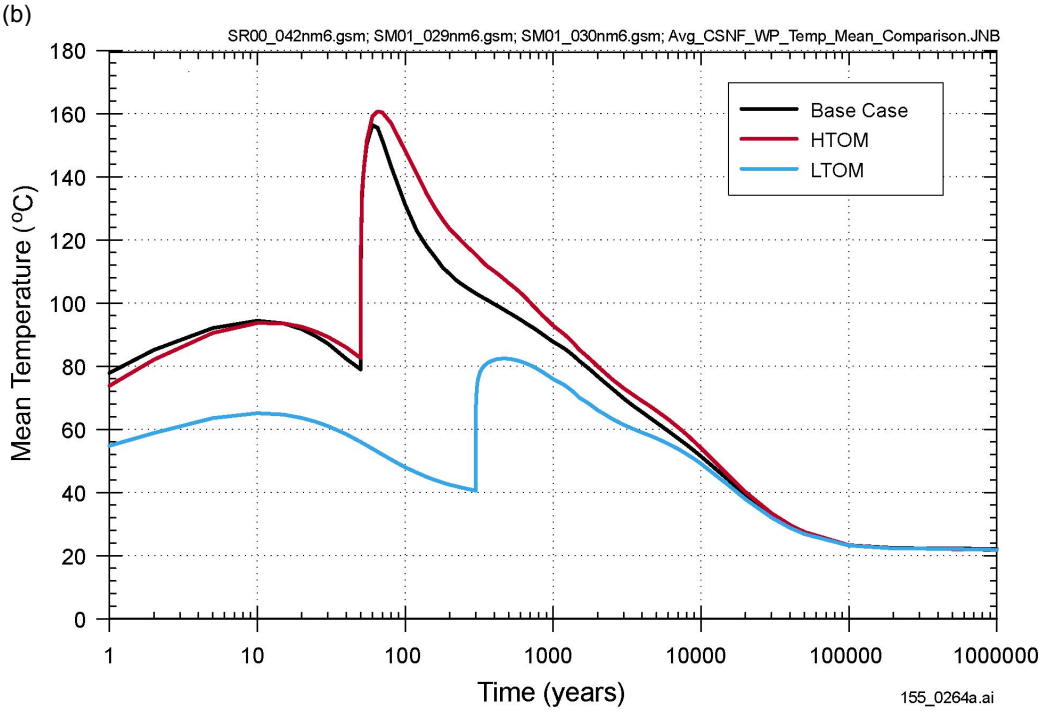

155_0263a.ai / 155_0264a.ai

NOTE: (a) Comparison of temperature histories for the average codisposal waste package in three cases: TSPA-SR base case model HTOM, supplemental TSPA model HTOM, and supplemental TSPA model LTOM. (b) Comparison of temperature histories for the average CSNF waste package in the same three cases.

Figure 4.2.3-1. Waste Package Temperature Calculated with the TSPA-SR Base-Case Model and the Supplemental TSPA Model

(a)

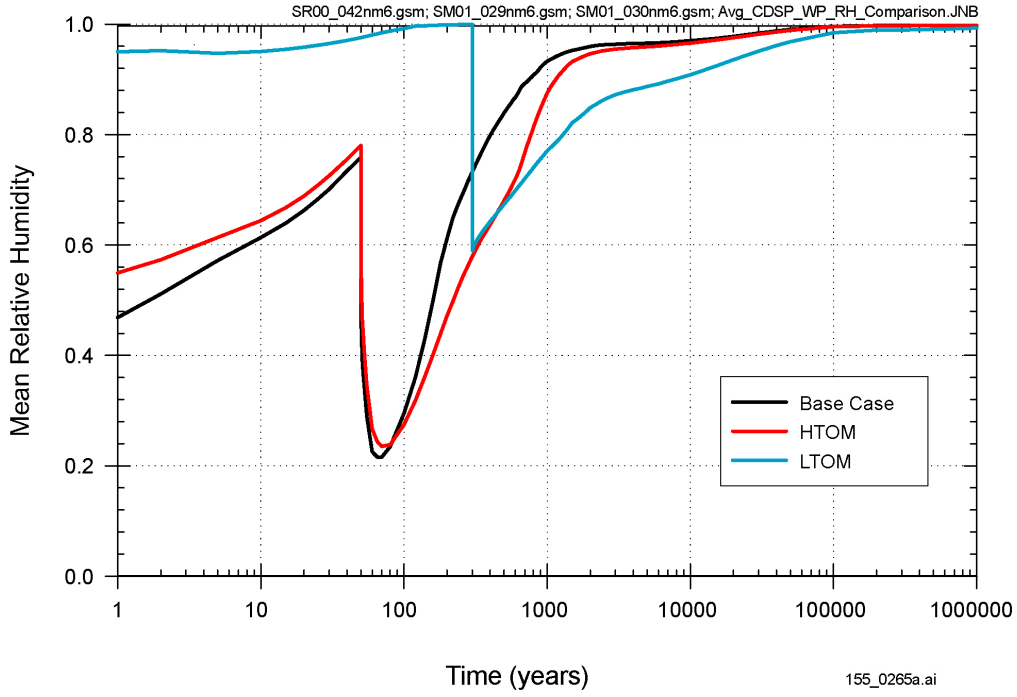

(b)

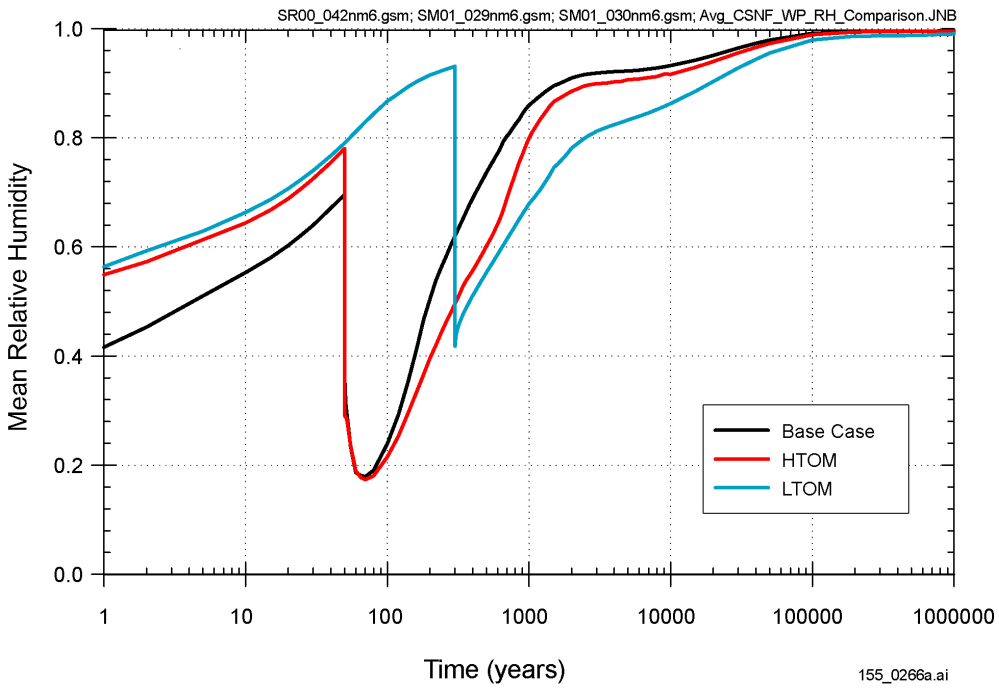

155_0265.ai / 155_0266a.ai

NOTE: (a) Comparison of the relative humidity histories for the average HLW waste package in three cases: TSPA-SR base-case model, supplemental TSPA model HTOM, and supplemental TSPA model LTOM. (b) Comparison of relative humidity histories for the average CSNF waste package for the same three cases.

Figure 4.2.3-2. Relative Humidity Near the Waste Package Calculated with the TSPA-SR Base-Case Model and the Supplemental TSPA Model

(a)

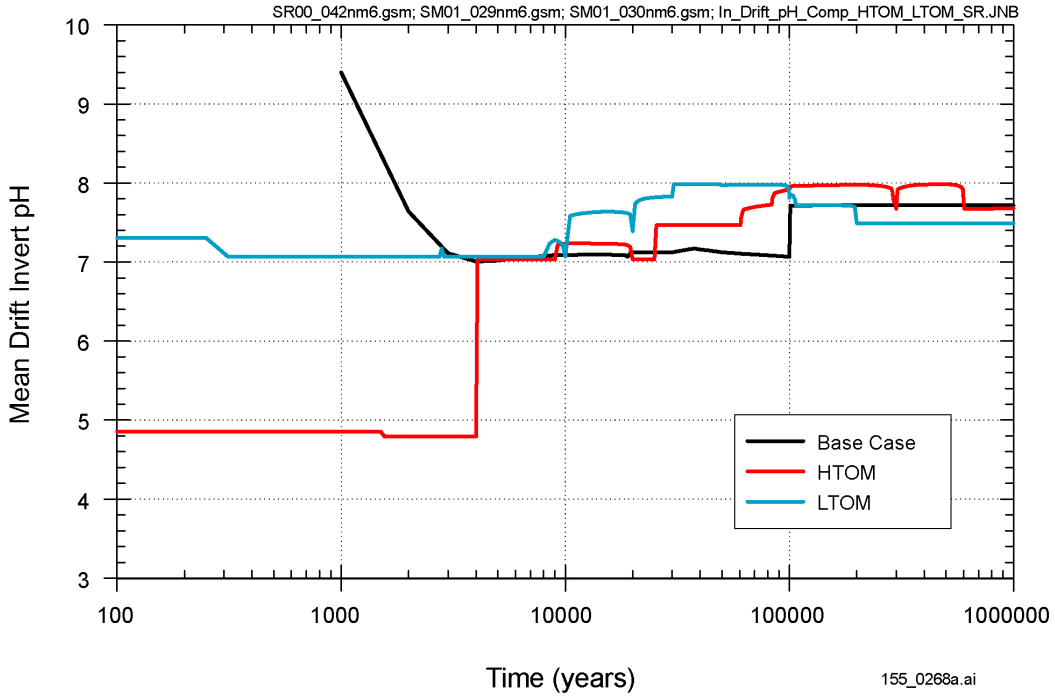

(b)

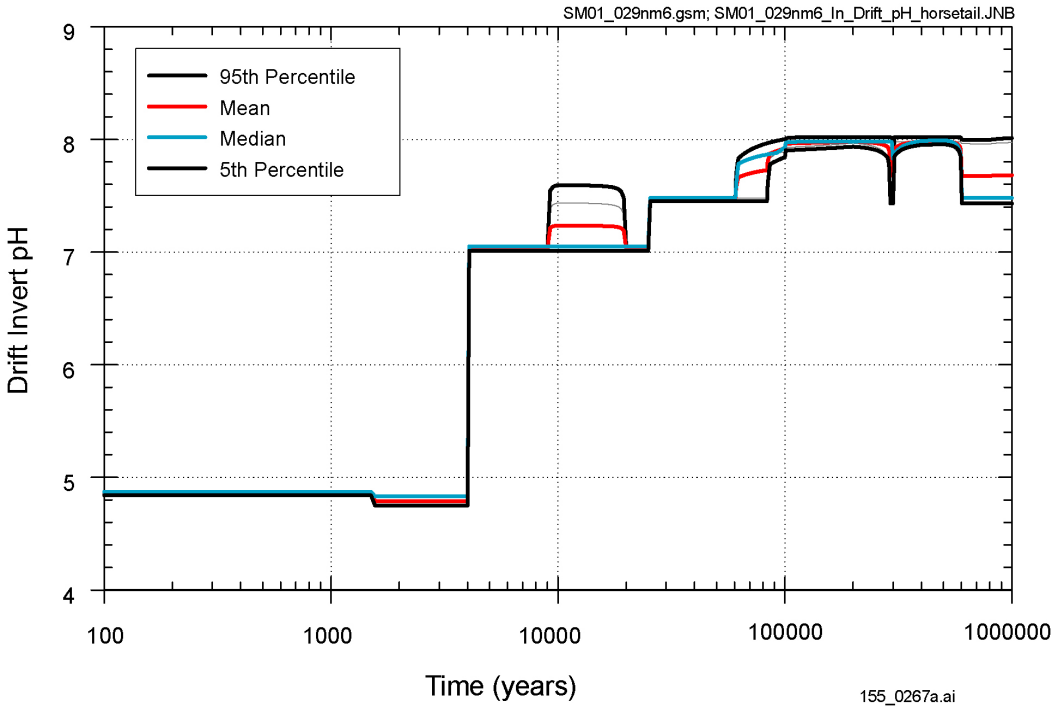

155_0268a.ai / 155_0267a.ai

NOTE: (a) Comparison of the mean drift invert pH for three cases: TSPA-SR base-case model HTOM, supplemental TSPA model HTOM, and supplemental TSPA model LTOM. (b) Range of the drift invert pH for the supplemental TSPA model HTOM.

Figure 4.2.4-1. Drift Invert pH Calculated with the TSPA-SR Base-Case Model and the Supplemental TSPA Model

(a)

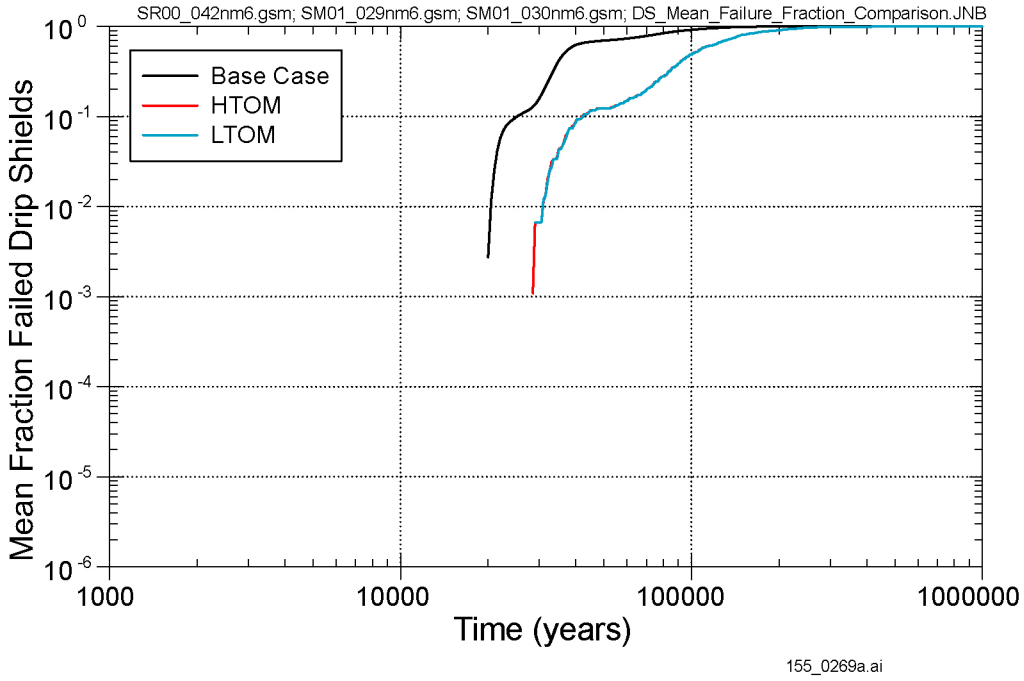

(b)

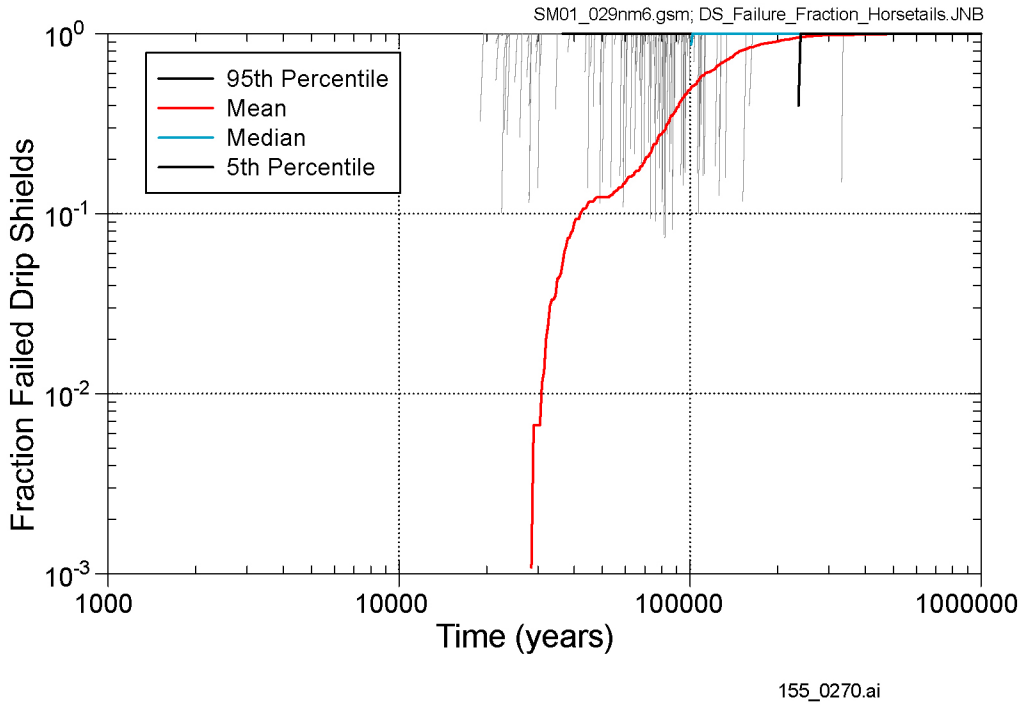

155_0269.ai / 155_0270.ai

NOTE: (a) Comparison of the mean fraction of failed drip shields for the three cases (TSPA-SR base-case model HTOM, supplemental TSPA model HTOM, and supplemental TSPA model LTOM). (b) Range of the fraction of failed drip shields for the supplemental TSPA model HTOM.

Figure 4.2.5-1. Fraction of Failed Drip Shields Using the TSPA-SR Base-Case and Supplemental TSPA Models

(c)

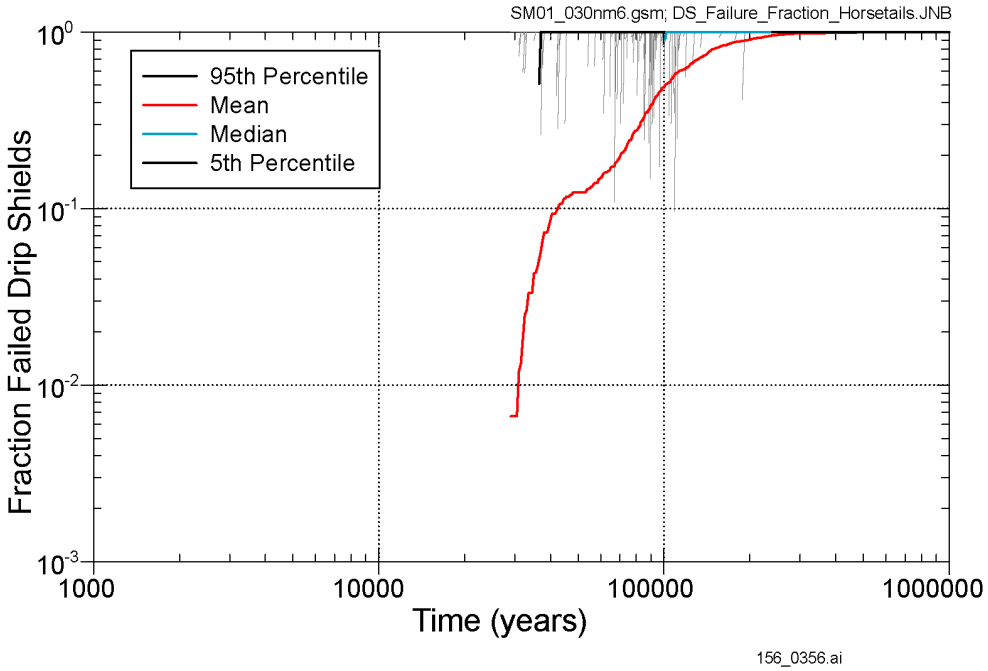

(d)

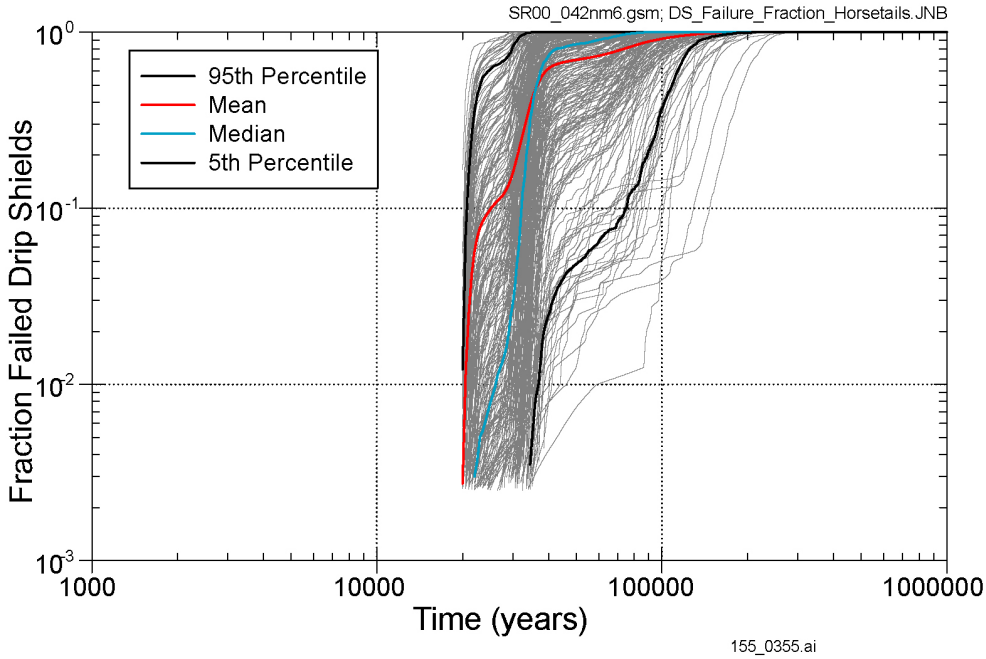

156_0356.ai / 155_0355.ai

NOTE: (c) Range of the fraction of failed drip shields for the supplemental TSPA model LTOM. (d) Range of the fraction of failed drip shields for the TSPA-SR base-case model.

Figure 4.2.5-1. Fraction of Failed Drip Shields Using the TSPA-SR Base-Case and Supplemental TSPA Models (Continued)

(a)

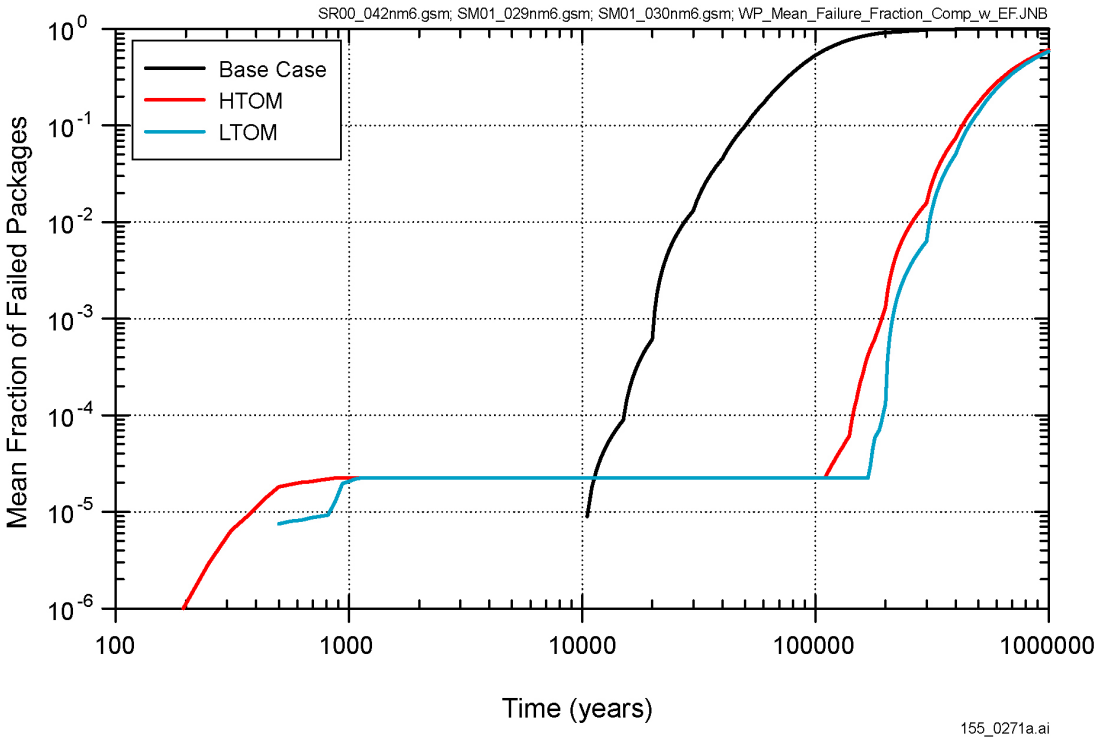

(b)

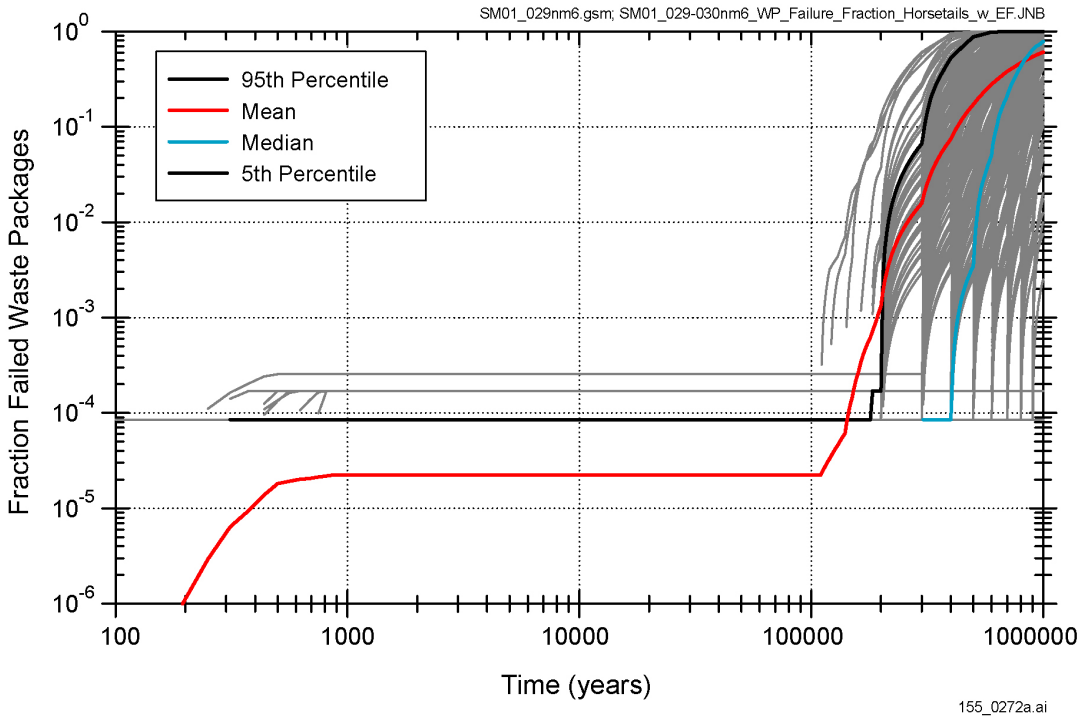

155_0271a.ai / 155_0272a.ai

NOTE: (a) Comparison of the mean fraction of failed waste packages for three cases: TSPA-SR Base-Case Model HTOM, supplemental TSPA model HTOM, and supplemental TSPA model LTOM. This comparison includes the effect of the potential early waste package failures. (b) Range of the failed waste packages for the supplemental TSPA model HTOM.

Figure 4.2.5-2. Fraction of Failed Waste Package Using the TSPA-SR Base-Case and Supplemental TSPA Models

(c)

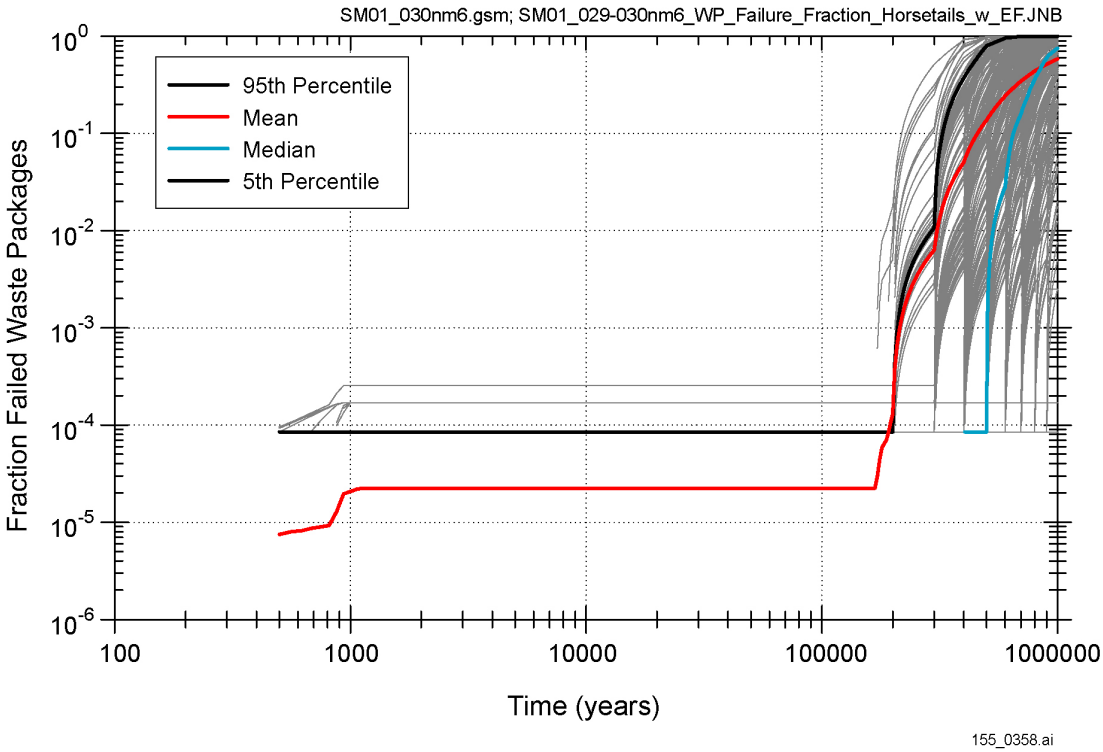

(d)

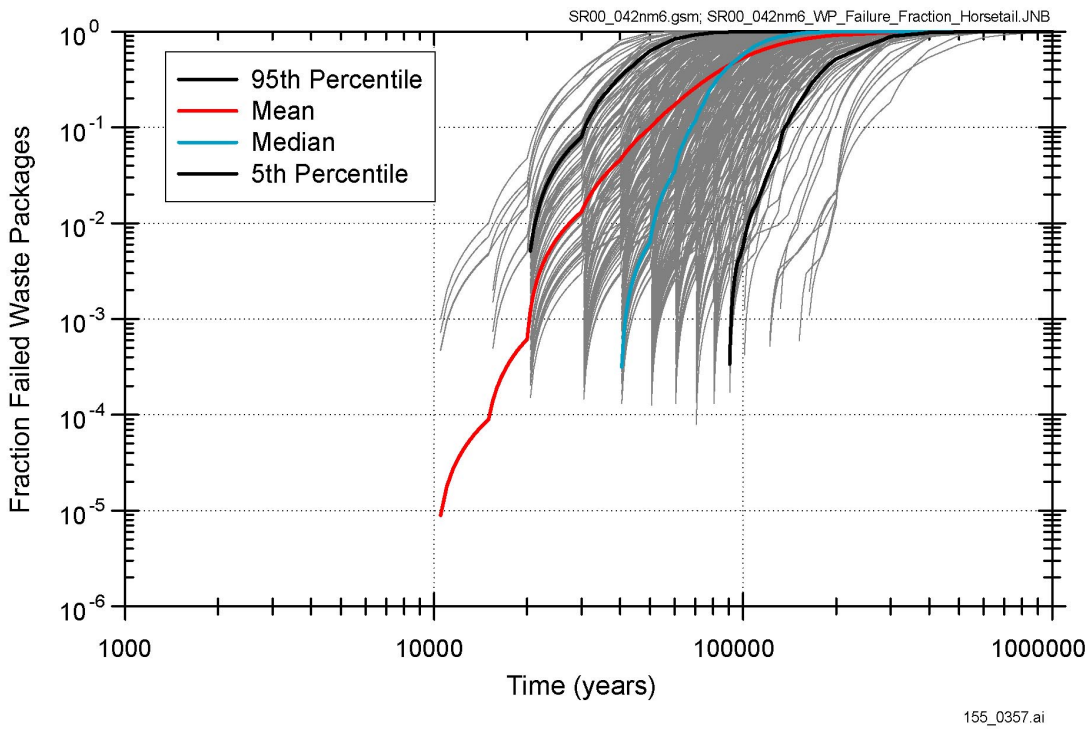

155_0358.ai / 155_0357.ai

NOTE: (c) Range of the failed waste packages for the supplemental TSPA model LTOM. (d) Range of the failed waste packages for the TSPA-SR base-case model.

Figure 4.2.5-2. Fraction of Failed Waste Package Using the TSPA-SR Base-Case and Supplemental TSPA Models (Continued)

(a)

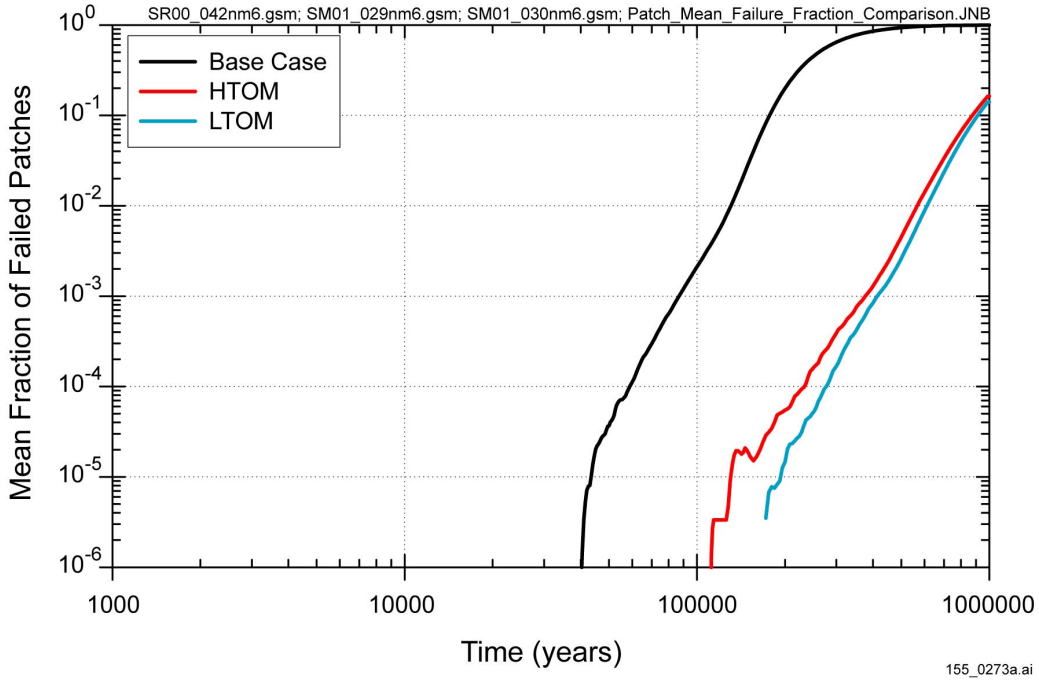

(b)

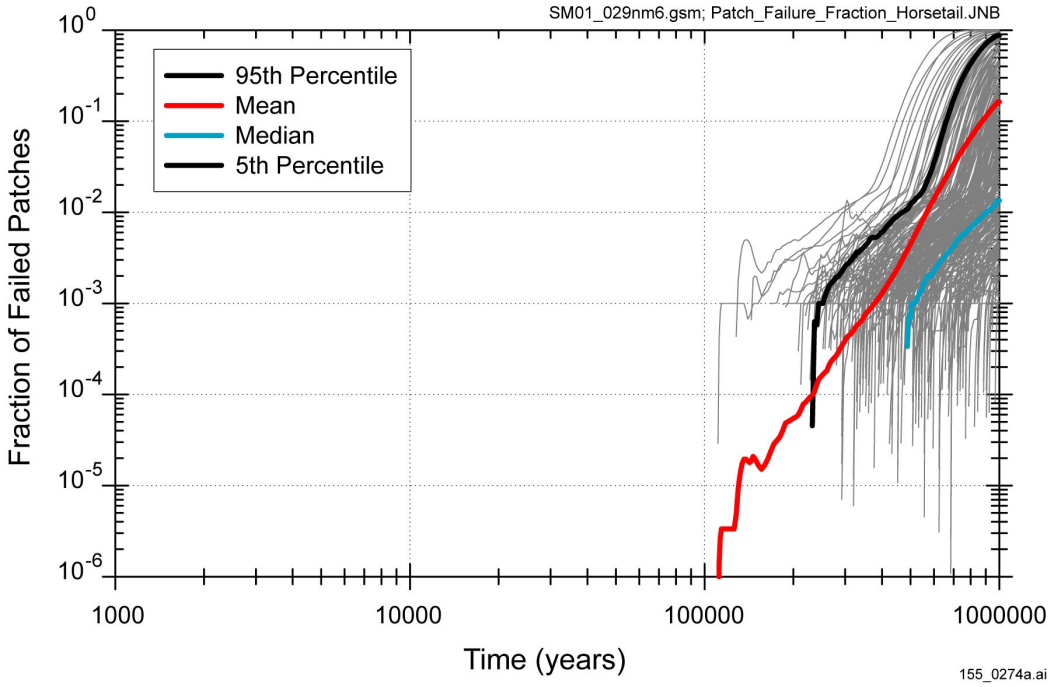

155_0273a.ai / 155_0274a.ai

NOTE: (a) Comparison of the mean fraction of patch failures on failed waste packages for three cases: TSPA-SR base-case model HTOM, supplemental TSPA model, and supplemental TSPA model LTOM. (b) Range of the patch failures on failed waste packages for the supplemental TSPA model HTOM.

Figure 4.2.5-3. Fraction of Patch Failures on Failed Waste Packages Using the TSPA-SR Base-Case and Supplemental TSPA Models

(c)

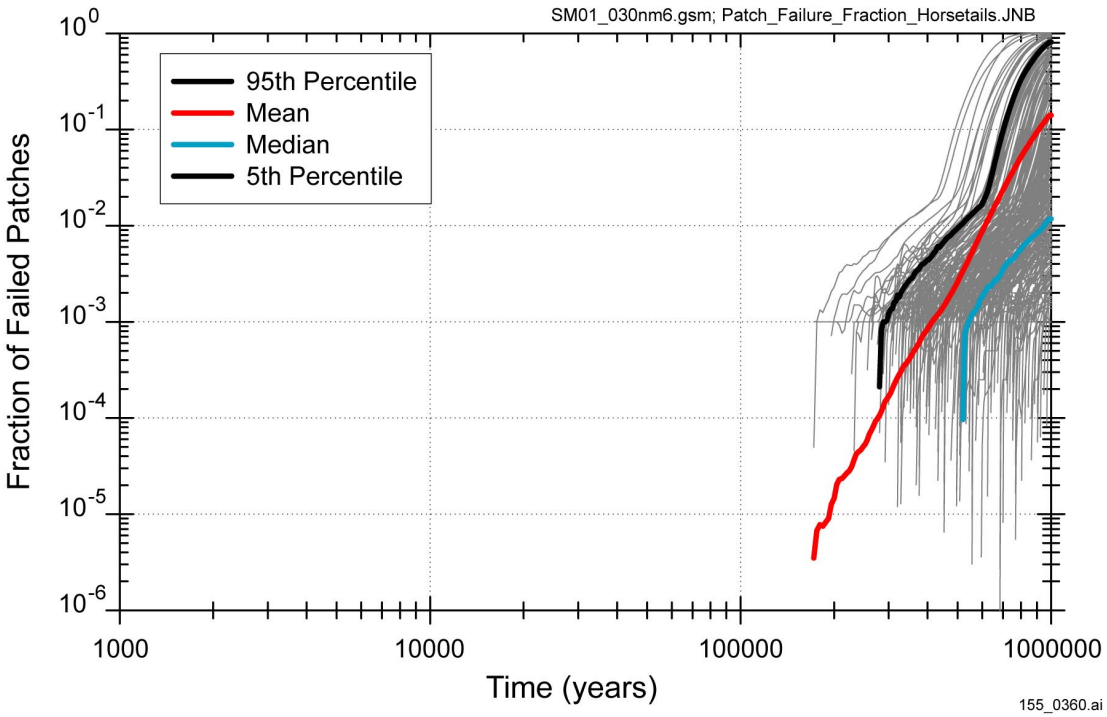

(d)

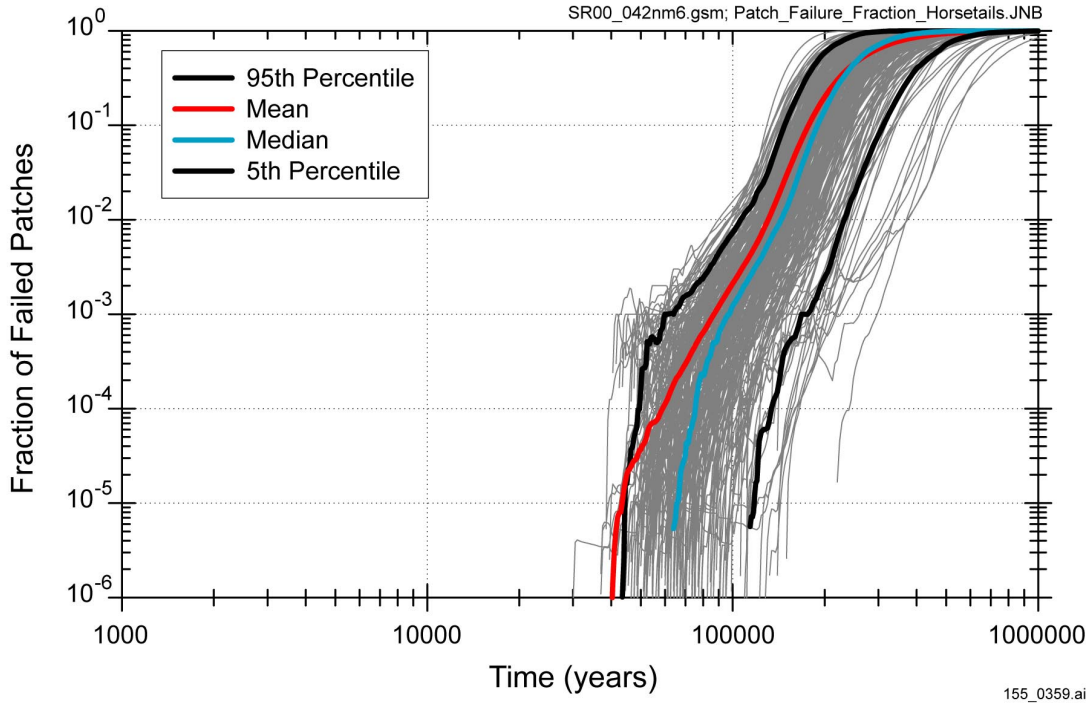

155_0360.ai / 155_0359.ai

NOTE: (c) Range of the patch failures on failed waste packages for the supplemental TSPA model LTOM. (d) Range of the patch failures on failed waste packages for the TSPA-SR base-case model. These results do not include the effect of early waste package failures due to improper heat treatment considered in the supplemental TSPA model.

Figure 4.2.5-3. Fraction of Patch Failures on Failed Waste Packages Using the TSPA-SR Base-Case and Supplemental TSPA Models (Continued)

(a)

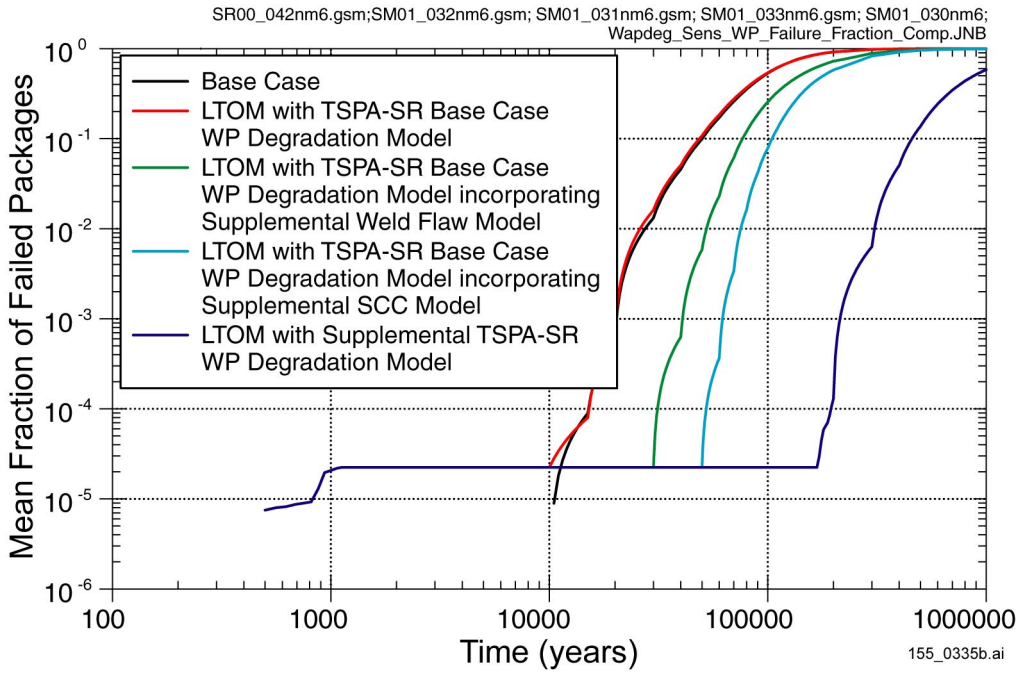

(b)

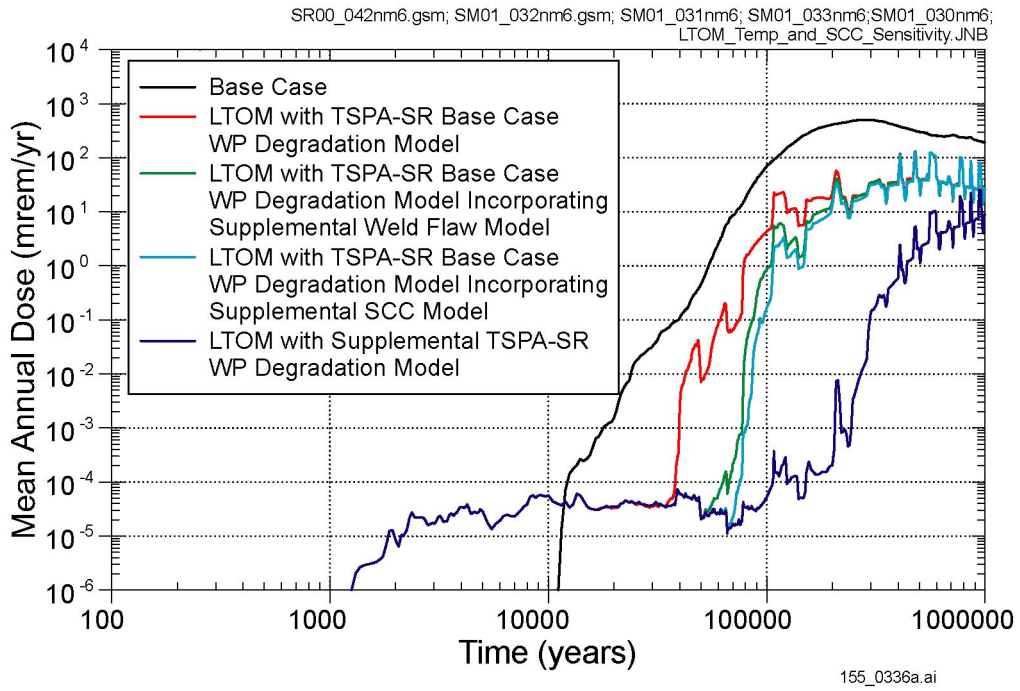

155_0335b.ai / 155_0336a.ai

NOTE: (a) Comparison of the mean fraction of failed waste packages for five cases: TSPA-SR base-case model, LTOM with TSPA-SR base-case waste package degradation model, LTOM with TSPA-SR base-case waste package degradation model incorporating supplemental weld flaw model, LTOM with TSPA-SR base-case waste package degradation model incorporating supplemental stress-corrosion cracking model, LTOM with supplemental waste package degradation model including temperature dependent general corrosion model. (b) Mean annual dose for the five cases considered.

Figure 4.2.5-4. Sensitivity to Waste Package Degradation Effects

(a)

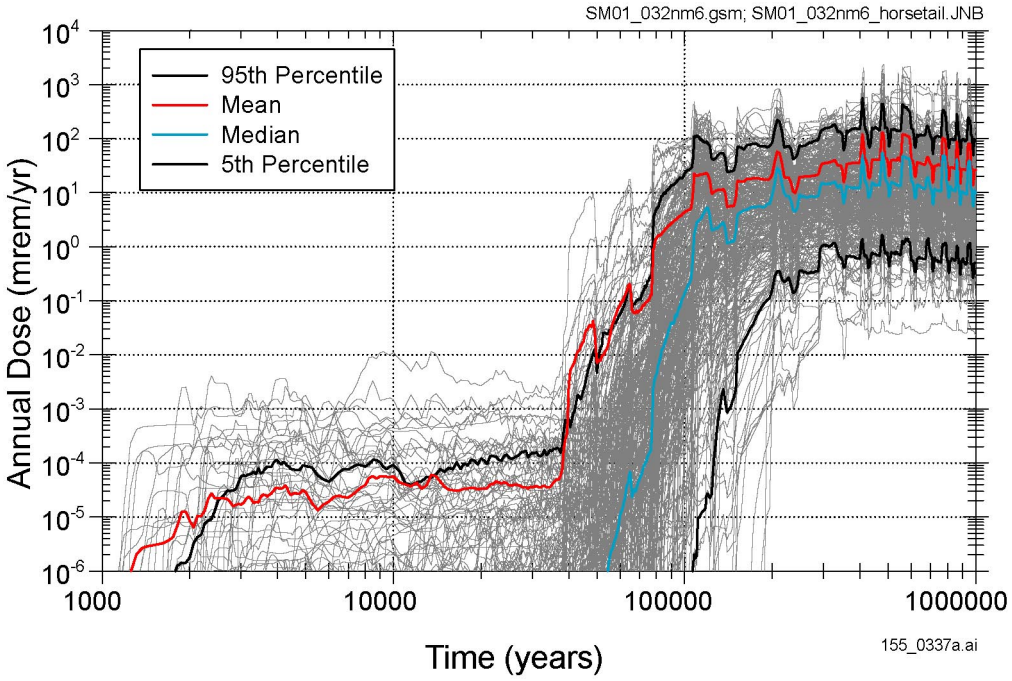

(b)

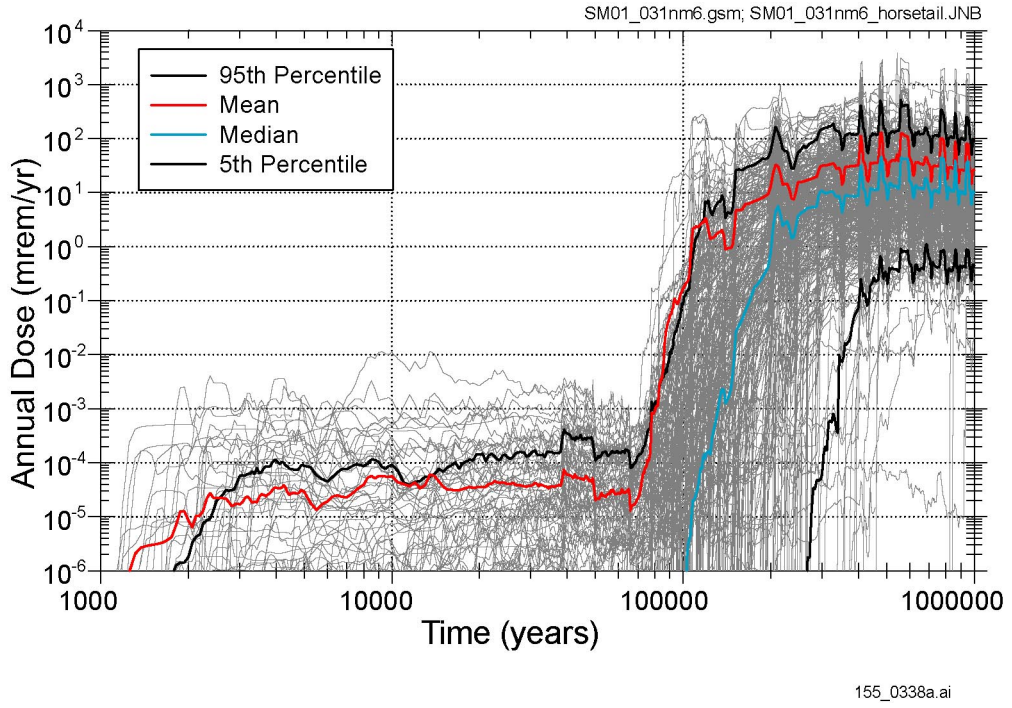

155_0337a.ai / 155_0338a.ai

NOTE: (a) LTOM with TSPA-SR base-case waste package degradation model incorporating supplemental weld flaw model. (b) LTOM with TSPA-SR base-case waste package degradation model.

Figure 4.2.5-5a and b. Range of Annual Dose Estimates for Three Models

(c)

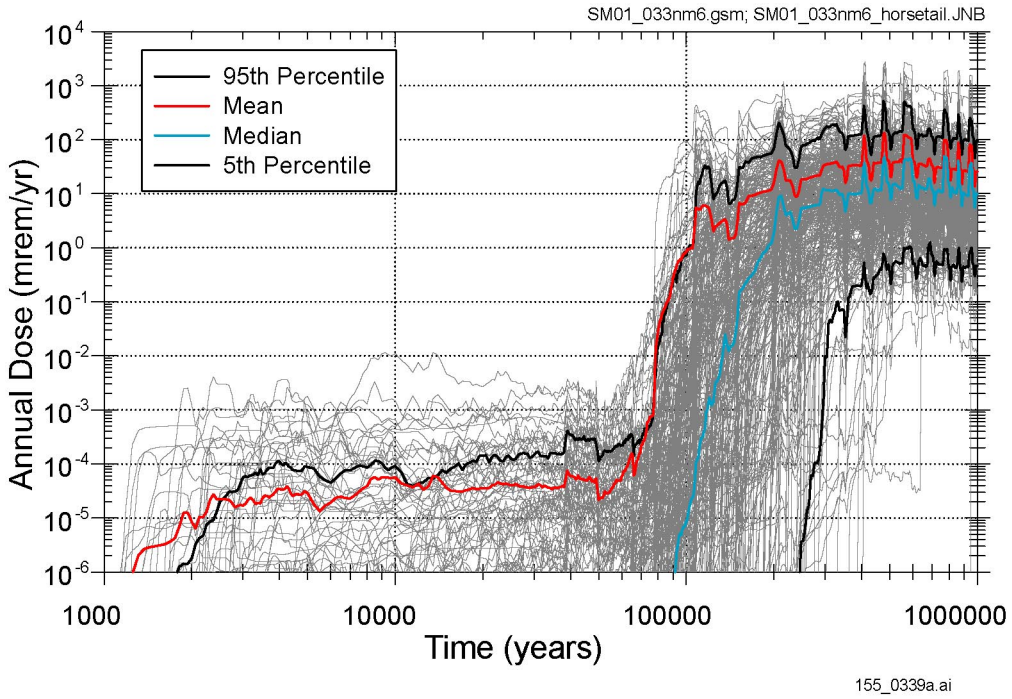

155_0339a.ai

NOTE: (c) LTOM with TSPA-SR base-case waste package degradation model incorporating supplemental stress-corrosion cracking model.

Figure 4.2.5-5c. Range of Annual Dose Estimates for Three Models

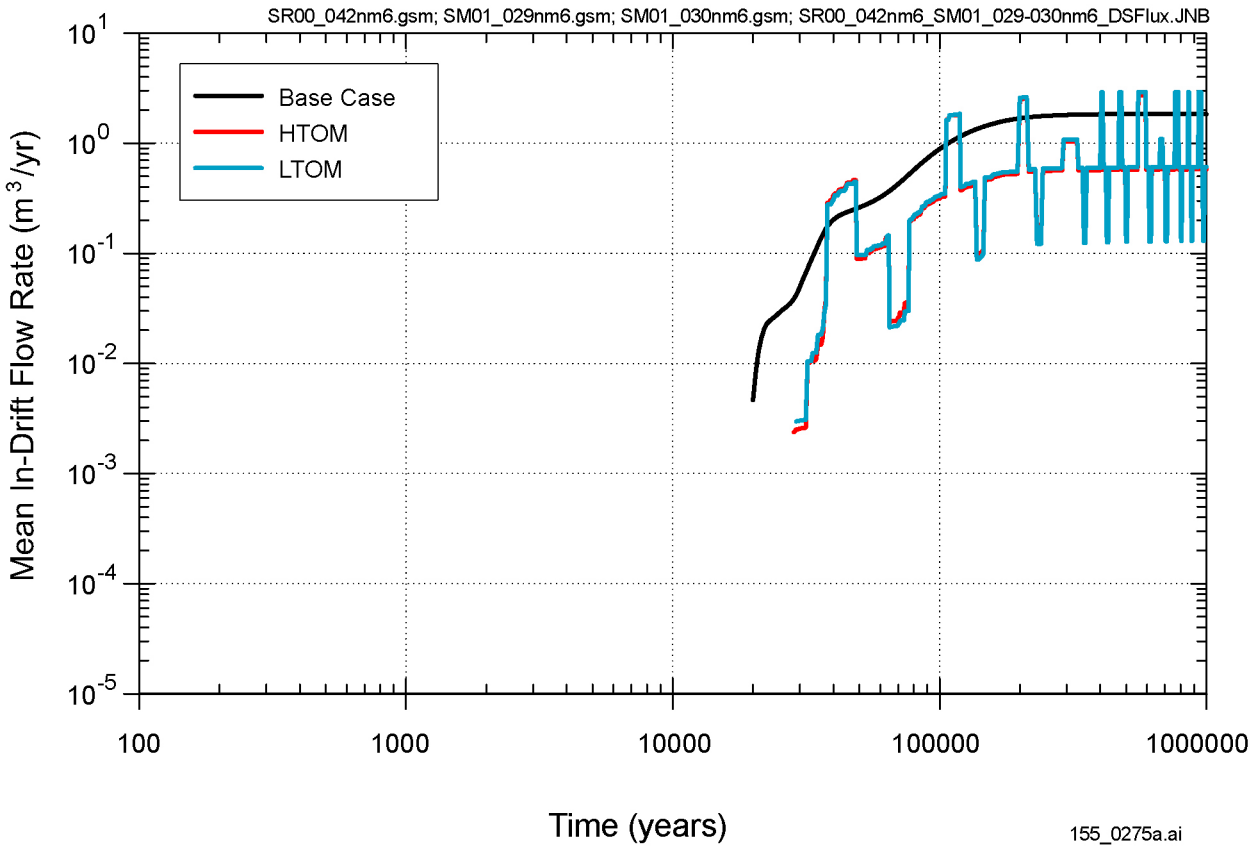

155_0275a.ai

NOTE: Comparison of the mean fluid flux per drip shield for three cases: TSPA-SR base-case model HTOM, supplemental TSPA model, and supplemental TSPA model LTOM.

Figure 4.2.6-1. Average Fluid Flux Through a Drip Shield Calculated with the TSPA-SR Base-Case and Supplemental TSPA Models

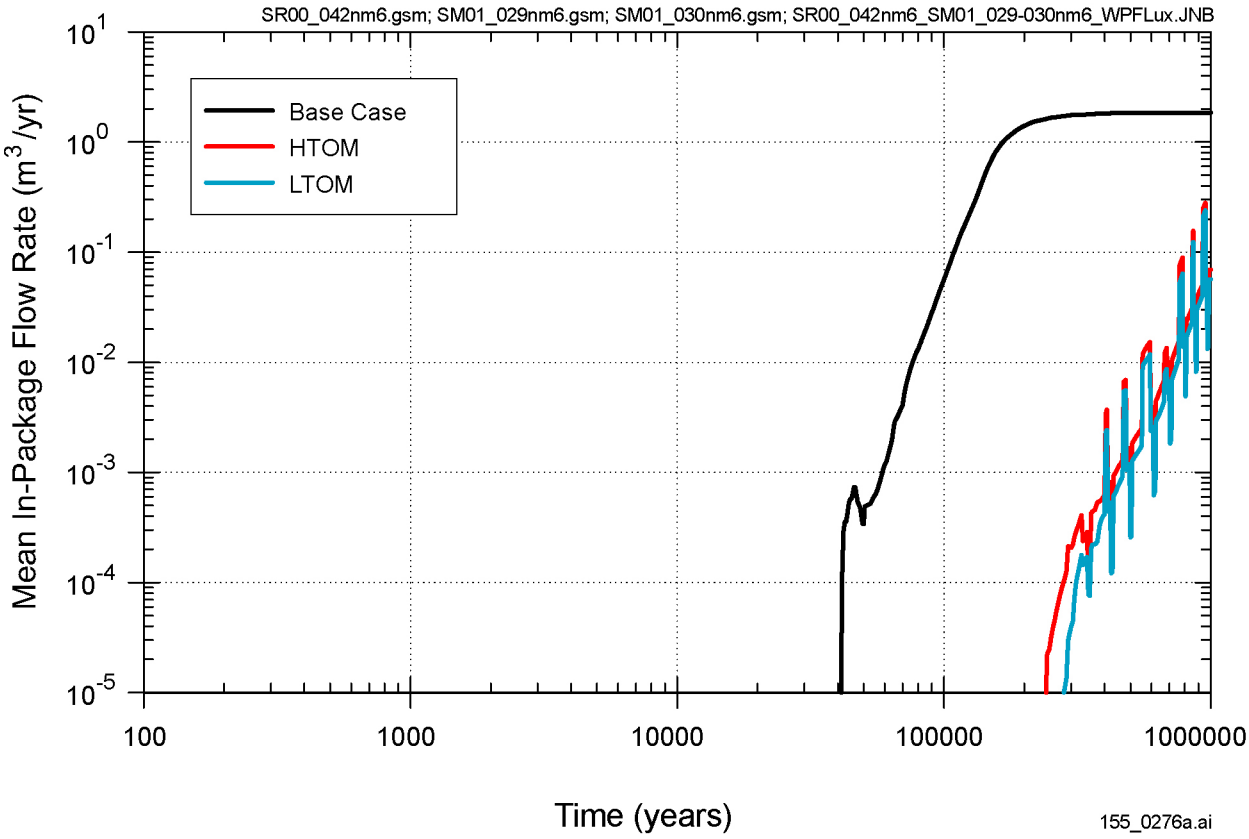

155_0276a.ai

NOTE: Comparison of the mean fluid flux per waste package for three cases: TSPA-SR base-case model HTOM, supplemental TSPA model HTOM, and supplemental TSPA model LTOM. The results for the supplemental TSPA model do not take into account the flux through the small fraction of packages that fail early in that model.

Figure 4.2.6-2. Fluid Flux Through a Single Waste Package Calculated with the TSPA-SR Base-Case and Supplemental TSPA Models

(a)

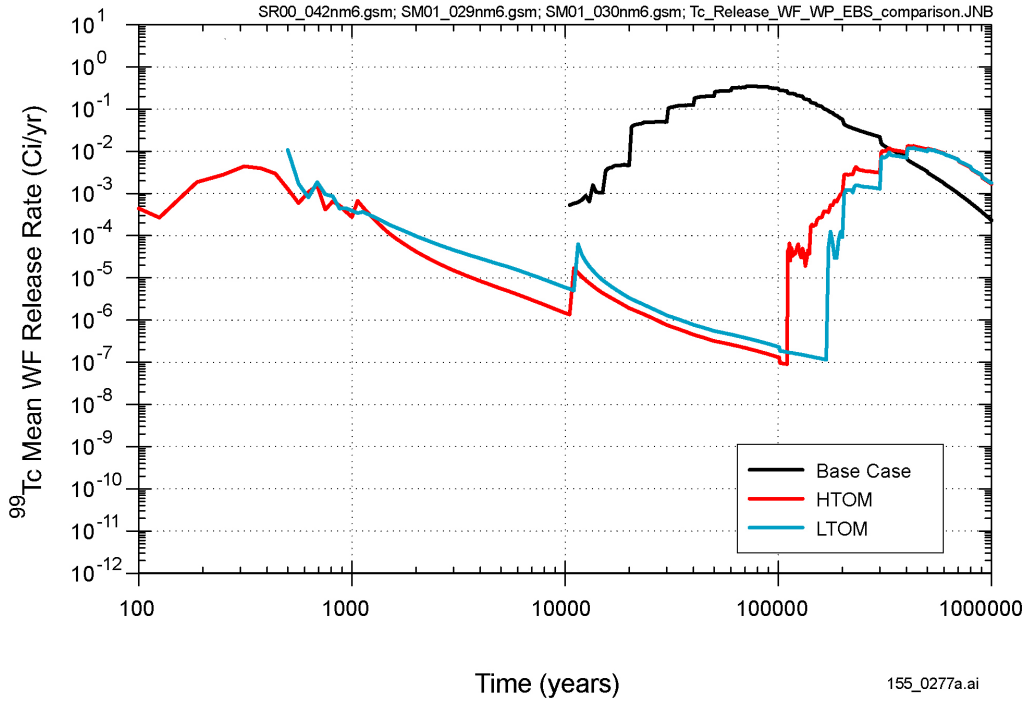

(b)

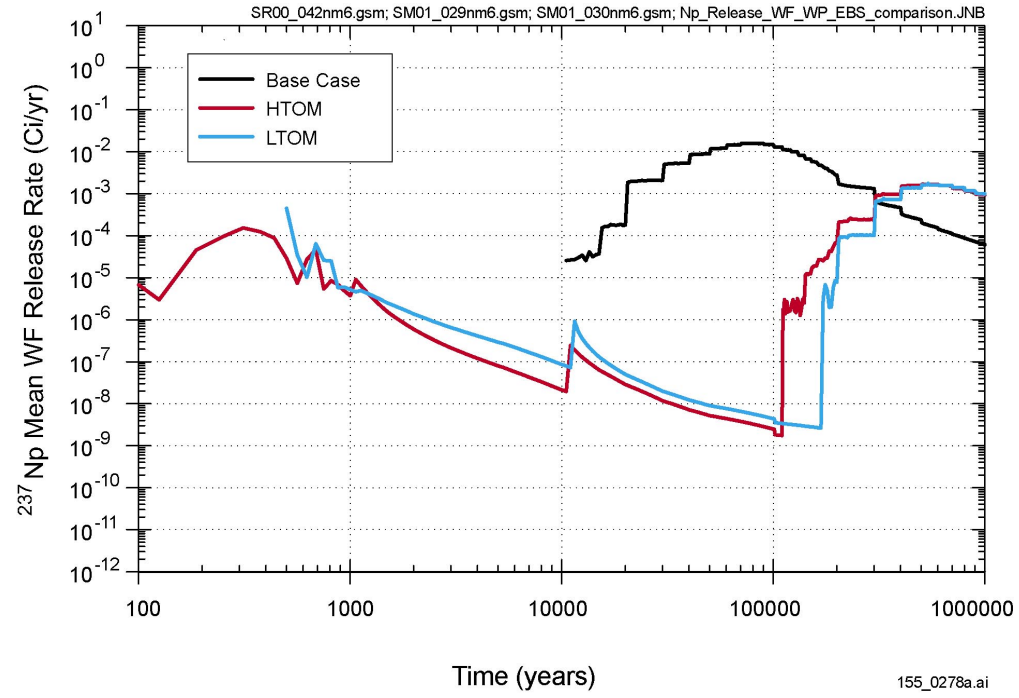

155_0277a.ai / 155_0278a.ai

NOTE: Comparison of the mean HLW form release of (a) technetium-99 and (b) neptunium-237 for the three cases: TSPA-SR base-case HTOM, supplemental TSPA model HTOM, and supplemental TSPA model LTOM.

Figure 4.2.7-1. High-Level Waste Form Release Rate Calculated with the TSPA-SR Base-Case Model and the Supplemental TSPA Model

(a)

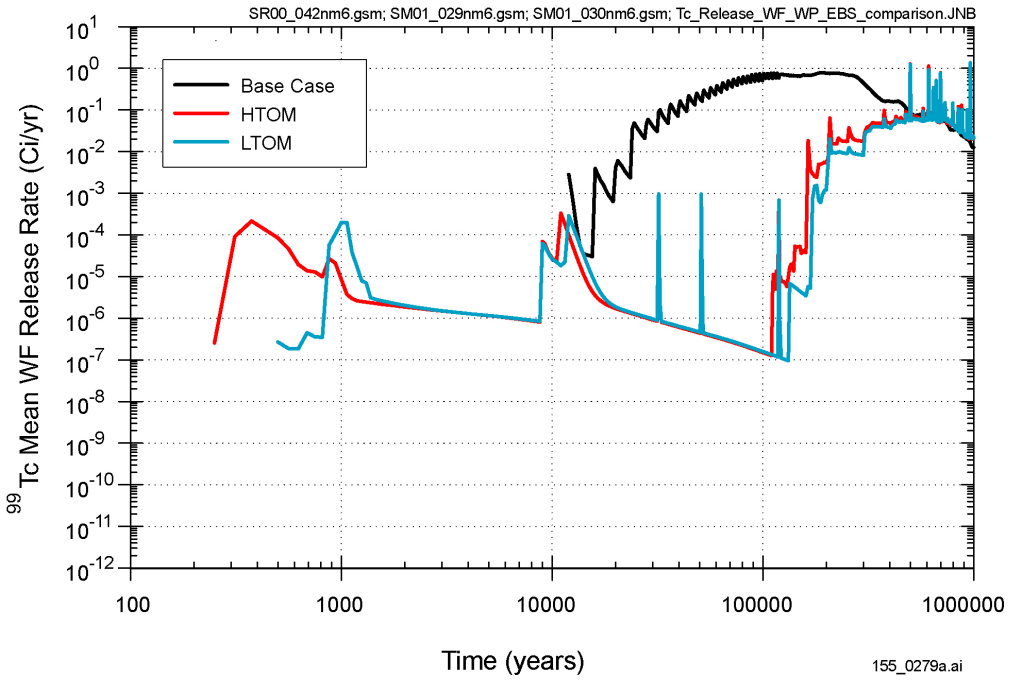

(b)

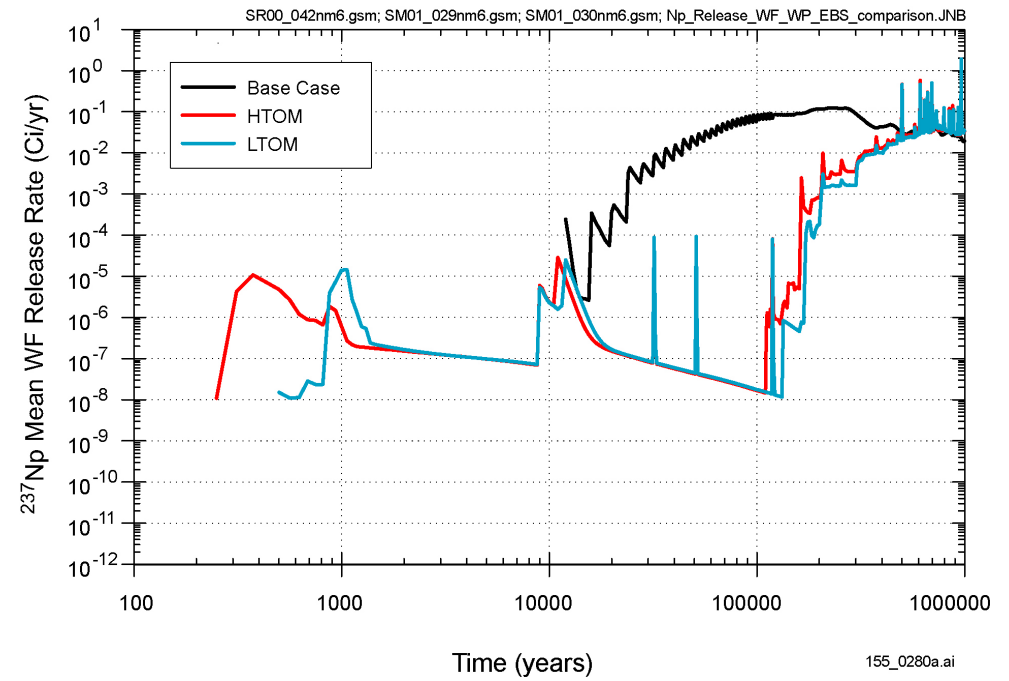

155_0279a.ai / 155_0280a.ai

NOTE: Comparison of the mean CSNF waste form release of (a) technetium-99 and (b) neptunium-237 for the three cases: TSPA-SR base-case HTOM, supplemental TSPA model HTOM, and supplemental TSPA model LTOM.

Figure 4.2.7-2. Commercial Spent Nuclear Fuel Waste Form Release Rate Calculated with the TSPA-SR Base-Case Model and the Supplemental TSPA Model

(a)

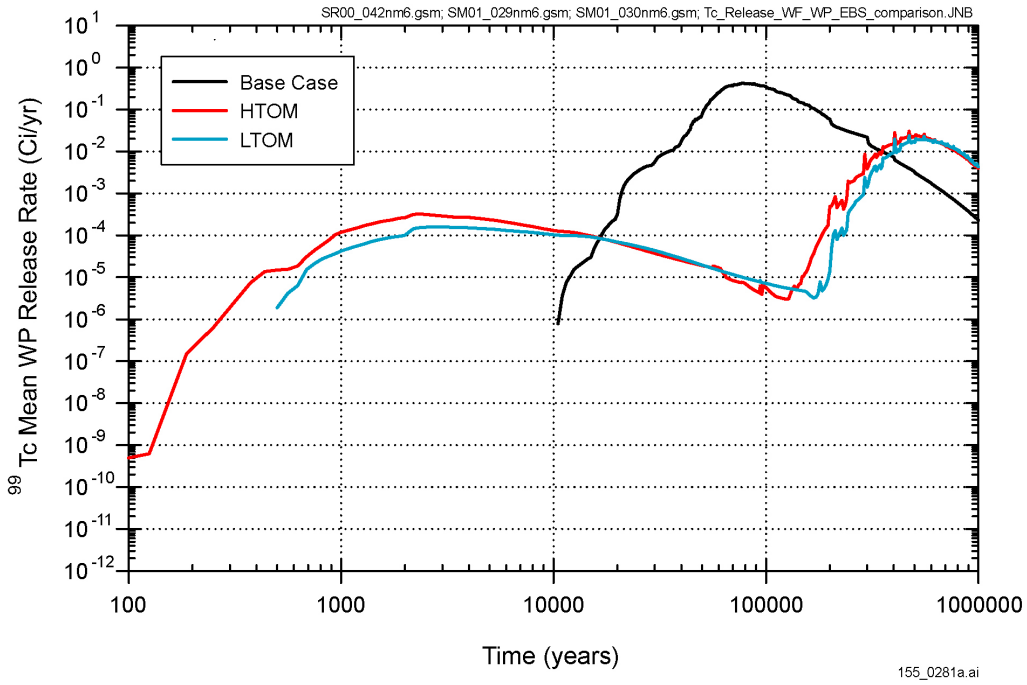

(b)

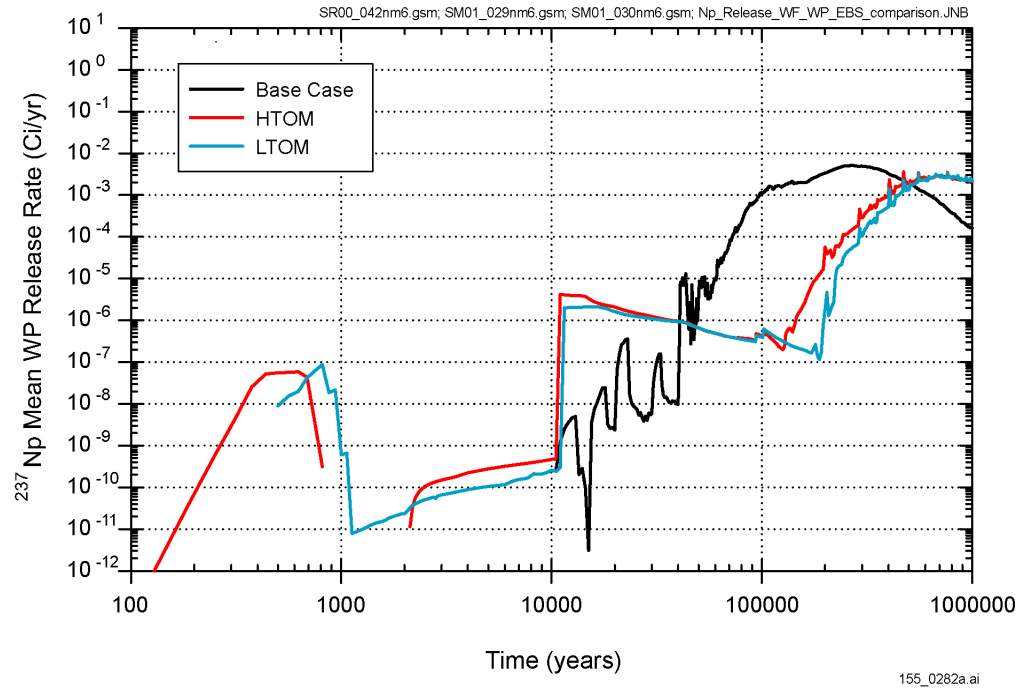

155_0281a.ai / 155_0282a.ai

NOTE: Comparison of the mean HLW package release of (a) technetium-99 and (b) neptunium-237 for the three cases: TSPA-SR base-case HTOM, supplemental TSPA model HTOM, and supplemental TSPA model LTOM.

Figure 4.2.8-1. High-Level Waste Package Release Rate Calculated with the TSPA-SR Base-Case Model and the Supplemental TSPA Model

(a)

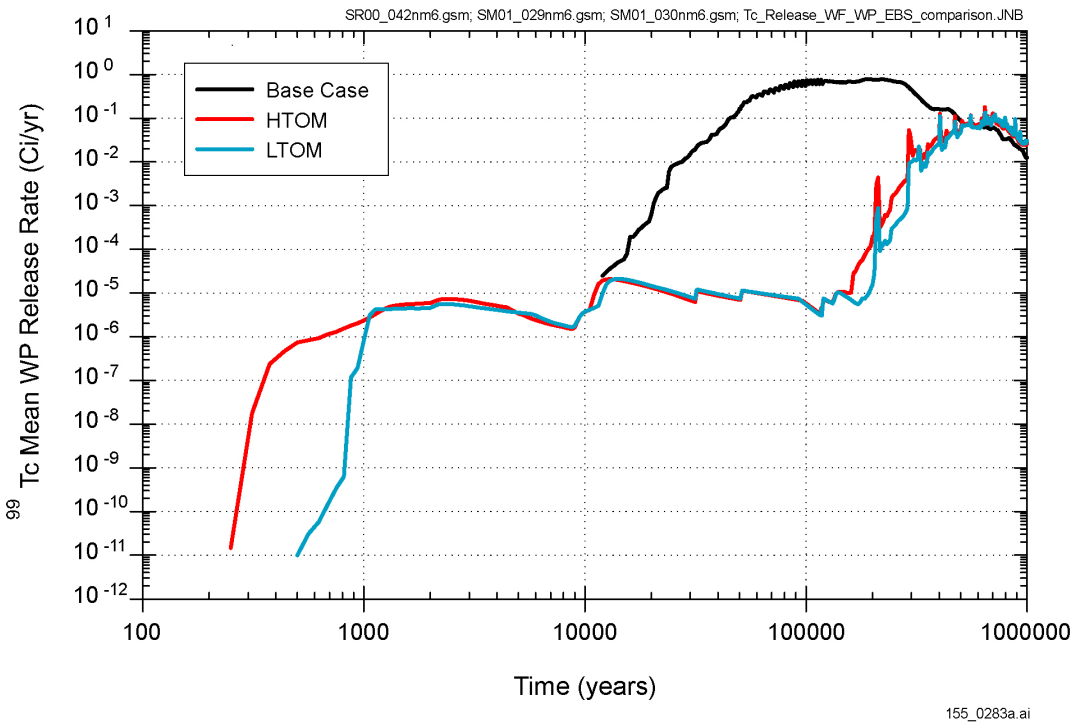

(b)

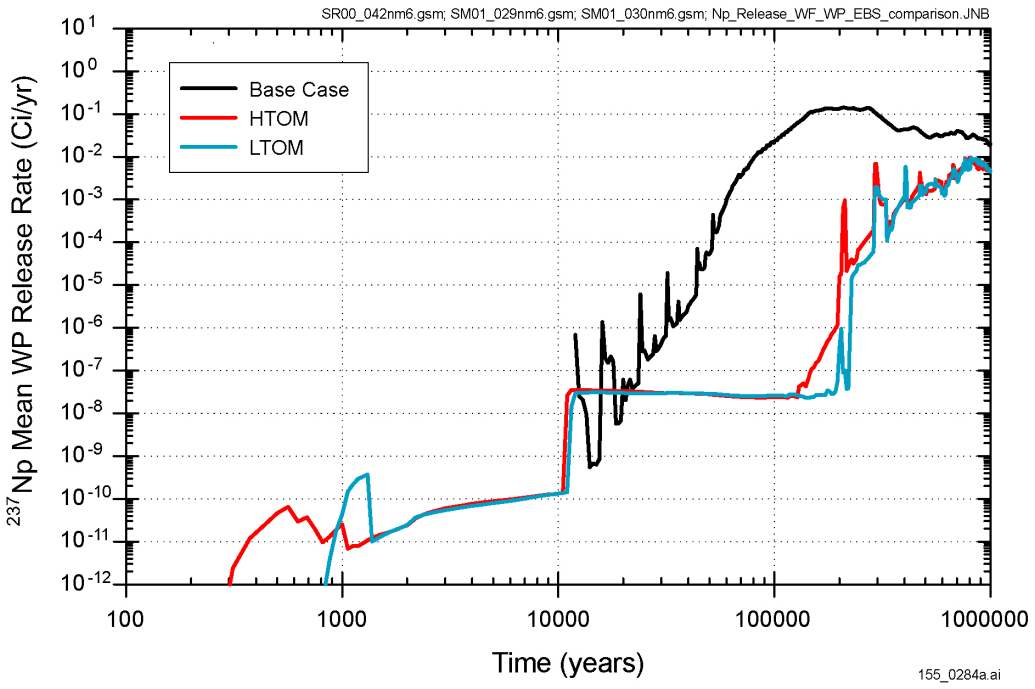

155_0283a.ai / 155_0284a.ai

NOTE: Comparison of the mean CSNF waste package release (a) technetium-99 and (b) neptunium-237 for the three cases: TSPA-SR base-case HTOM, supplemental TSPA model HTOM, and supplemental TSPA model LTOM.

Figure 4.2.8-2. Commercial Spent Nuclear Fuel Waste Package Release Rate Calculated with the TSPA-SR Base-Case Model and the Supplemental TSPA Model

(a)

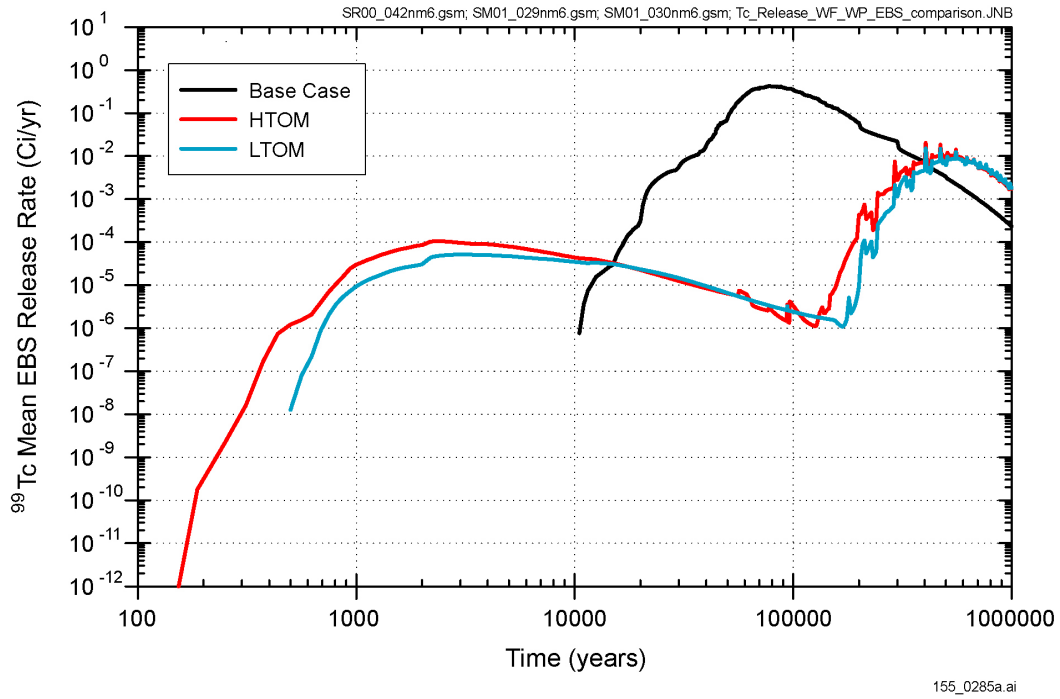

(b)

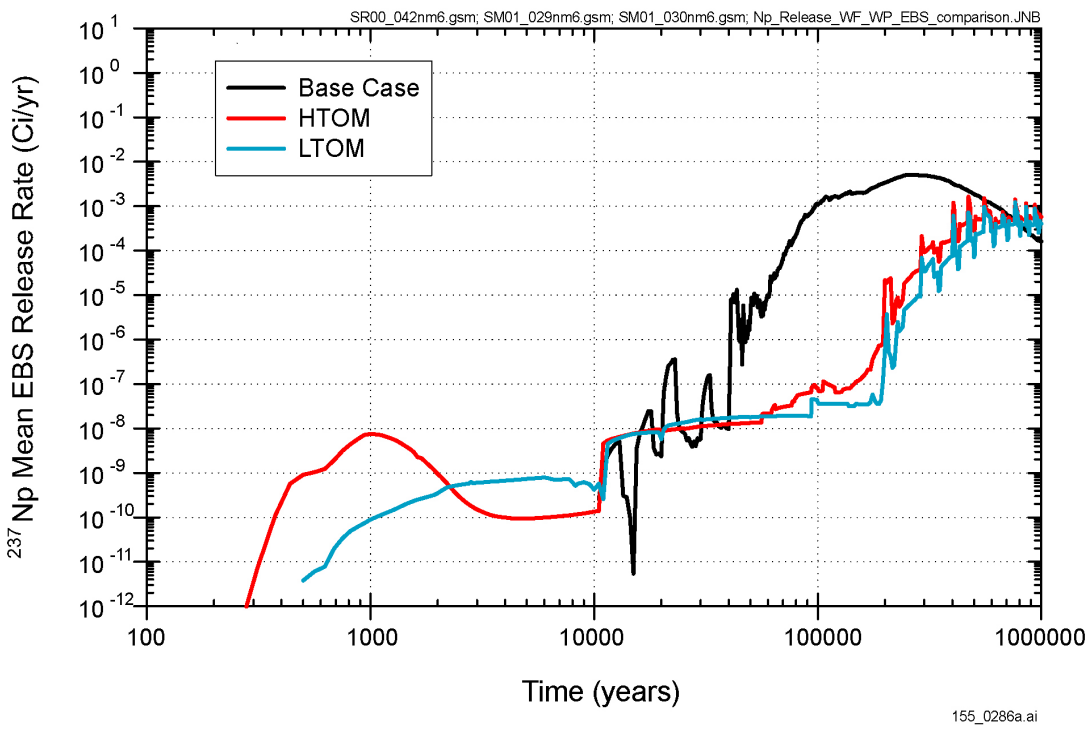

155_0285a.ai / 155_0286a.ai

NOTE: Comparison of the mean HLW EBS release of (a) technetium-99 and (b) neptunium-237 for the three cases: TSPA-SR base-case HTOM, supplemental TSPA model HTOM, and supplemental TSPA model LTOM.

Figure 4.2.8-3. High-Level Waste Engineered Barrier System Release Rate Calculated with the TSPA-SR Base-Case Model and the Supplemental TSPA Model

(a)

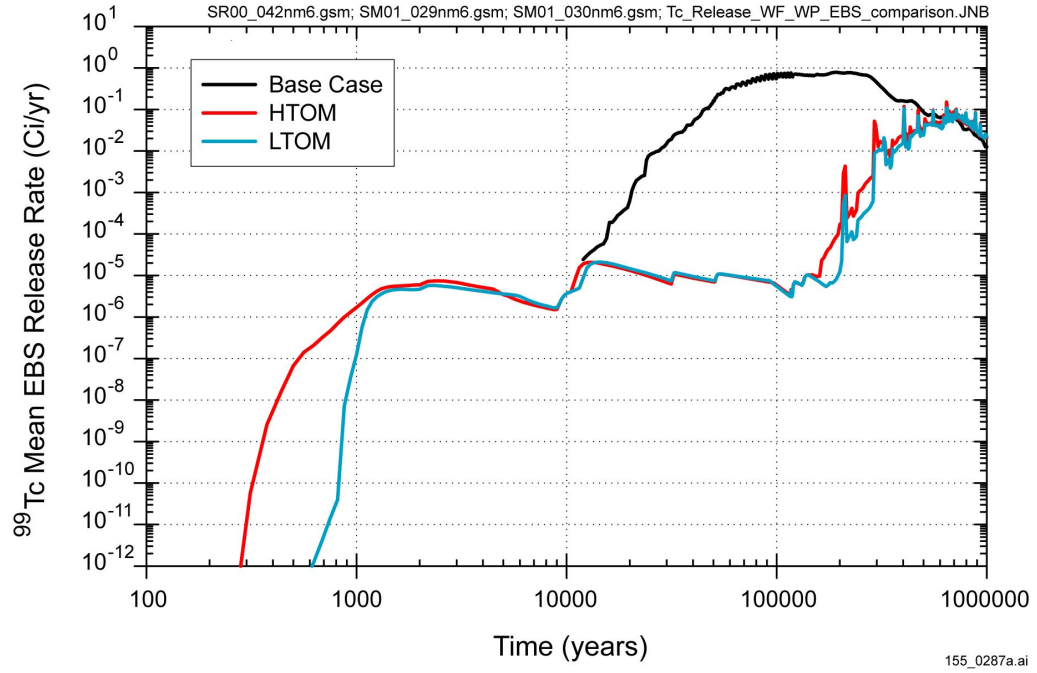

(b)

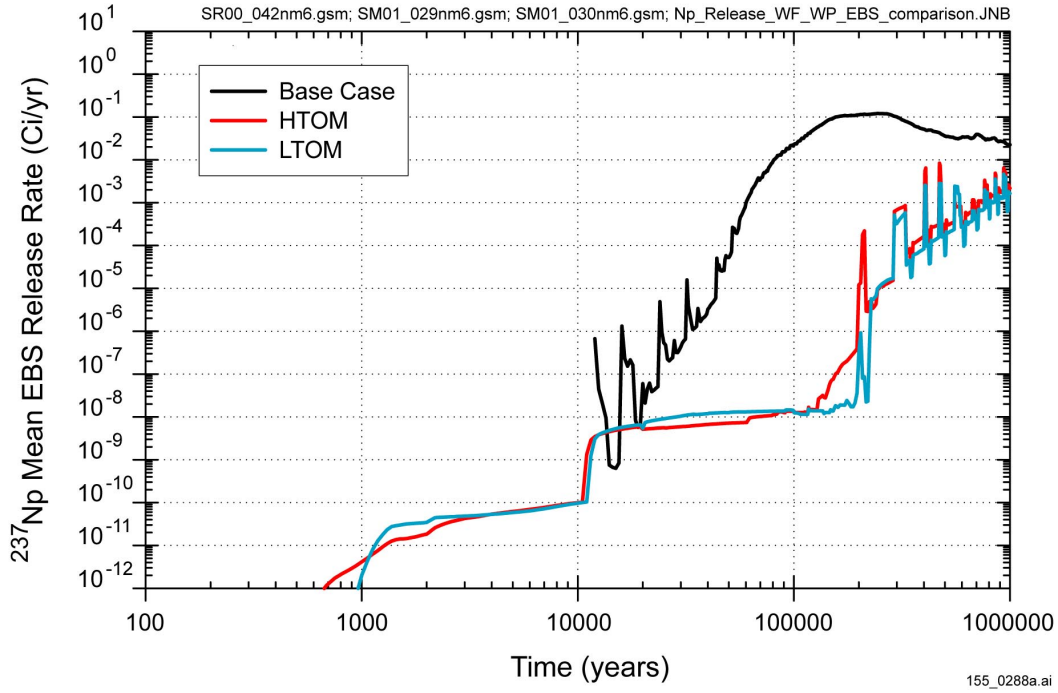

155_0287a.ai / 155_0288a.ai

NOTE: Comparison of the mean CSNF EBS release of (a) technetium-99 and (b) neptunium-237 for the three cases: TSPA-SR base-case HTOM, supplemental TSPA model HTOM, and supplemental TSPA model LTOM.

Figure 4.2.8-4. Commercial Spent Nuclear Fuel Engineered Barrier System Release Rate Calculated with the TSPA-SR Base-Case Model and the Supplemental TSPA Model

(a)

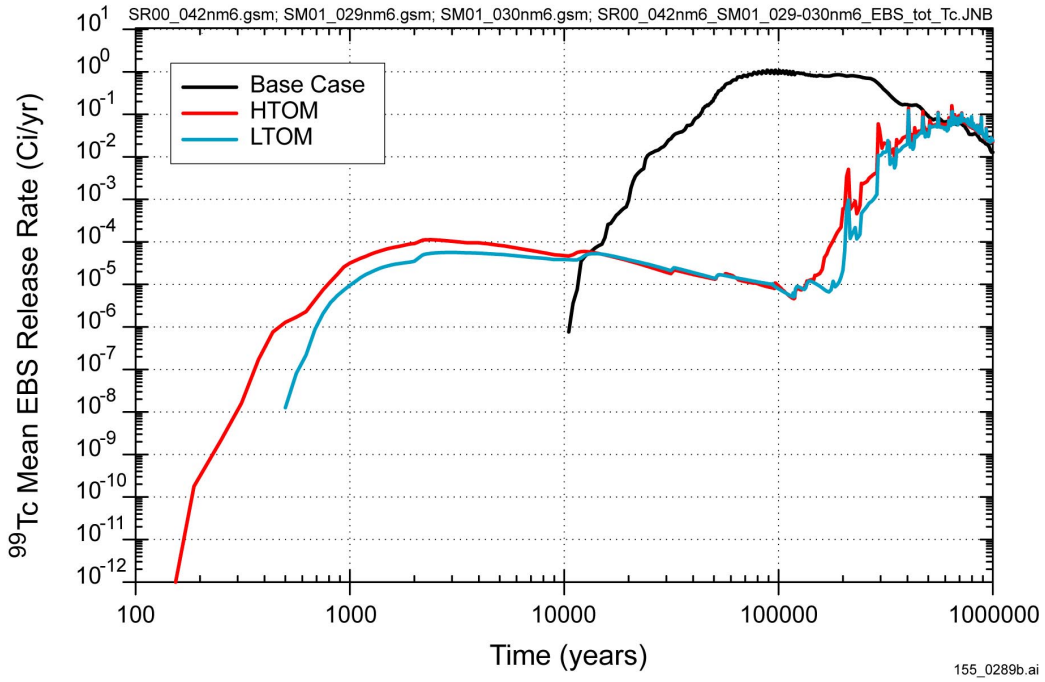

(b)

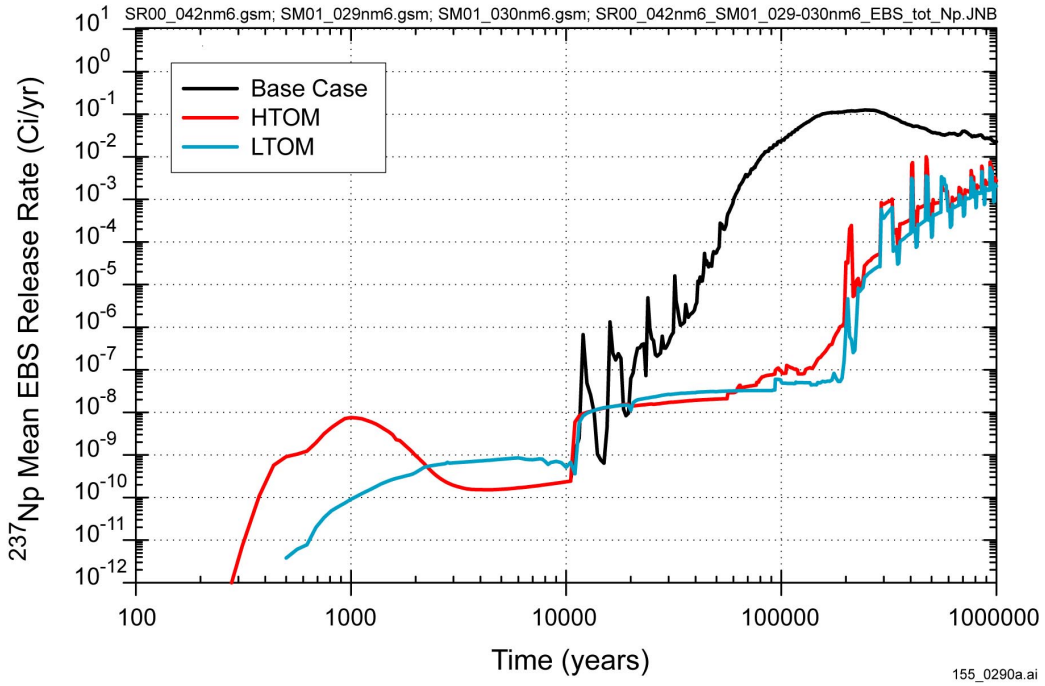

155_0289b.ai / 155_0290a.ai

NOTE: Comparison of the total (HLW + CSNF) mean EBS release of (a) technetium-99 and (b) neptunium-237 for the three cases: TSPA-SR base-case HTOM, supplemental TSPA model HTOM, and supplemental TSPA model LTOM.

Figure 4.2.8-5. Total Engineered Barrier System Release Rate Calculated with the TSPA-SR Base-Case Model and the Supplemental TSPA Model

(a)

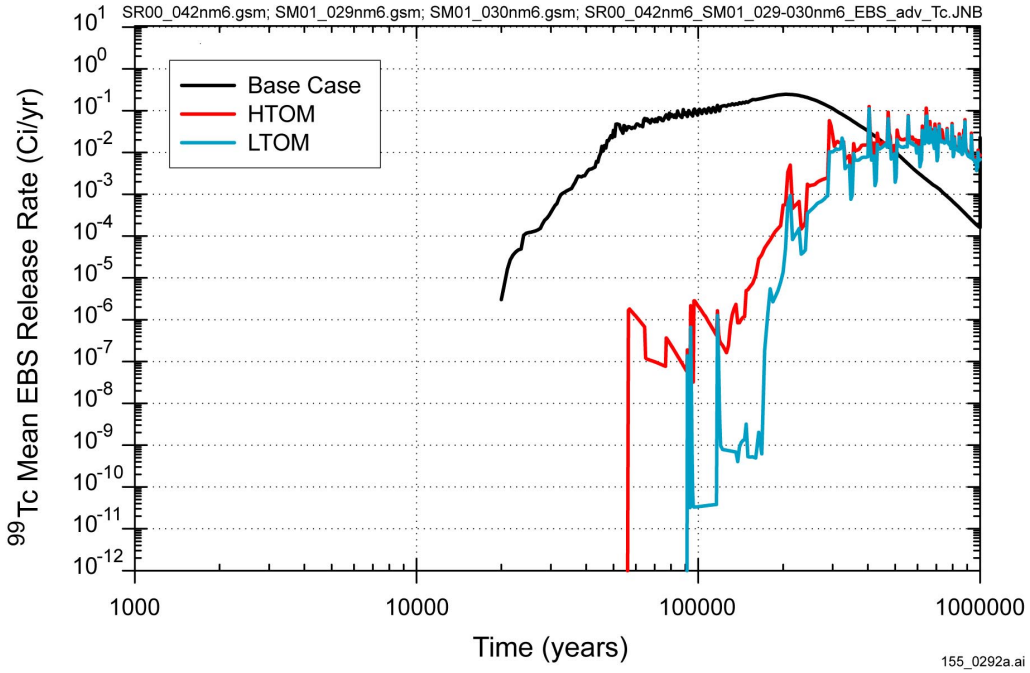

(b)

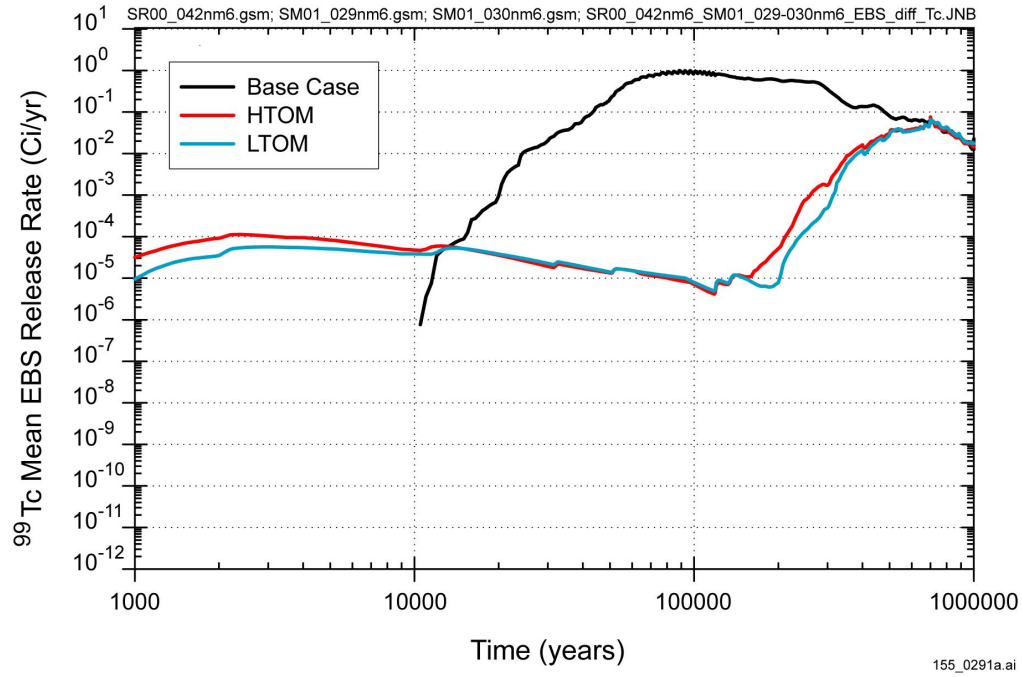

155_0292a.ai / 155_0291a.ai

NOTE: Comparison of the mean (a) advective and (b) diffusive EBS release of technetium-99 for the three cases: TSPA-SR base-case HTOM, supplemental TSPA model HTOM, and supplemental TSPA model LTOM.

Figure 4.2.8-6. Technetium-99 Advective and Diffusive Engineered Barrier System Release Rate Calculated with the TSPA-SR Base-Case Model and the Supplemental TSPA Model

(a)

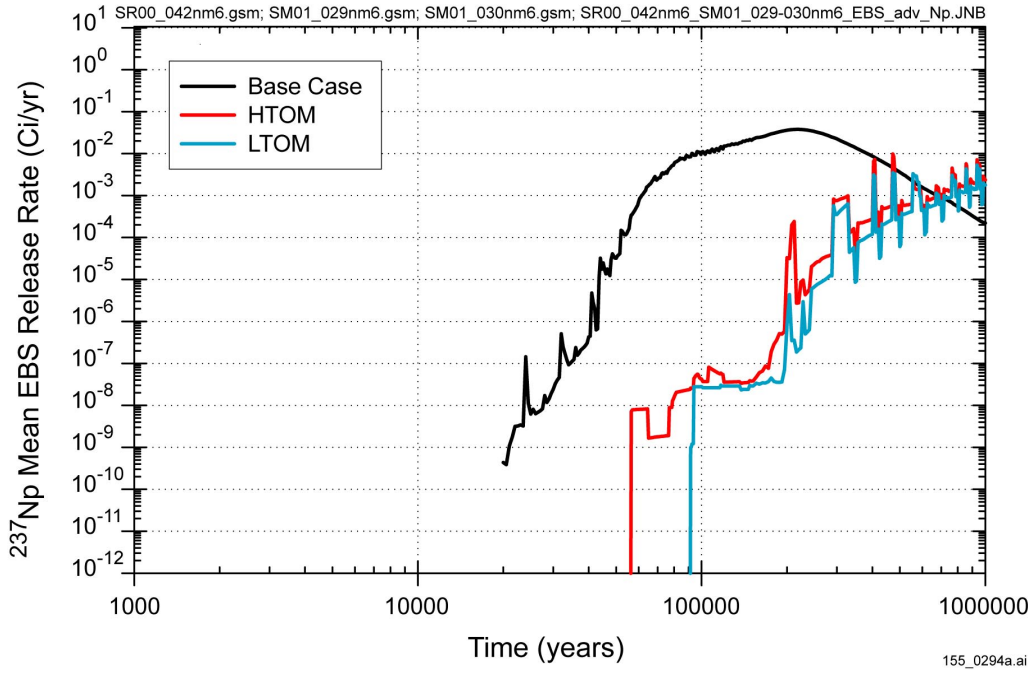

(b)

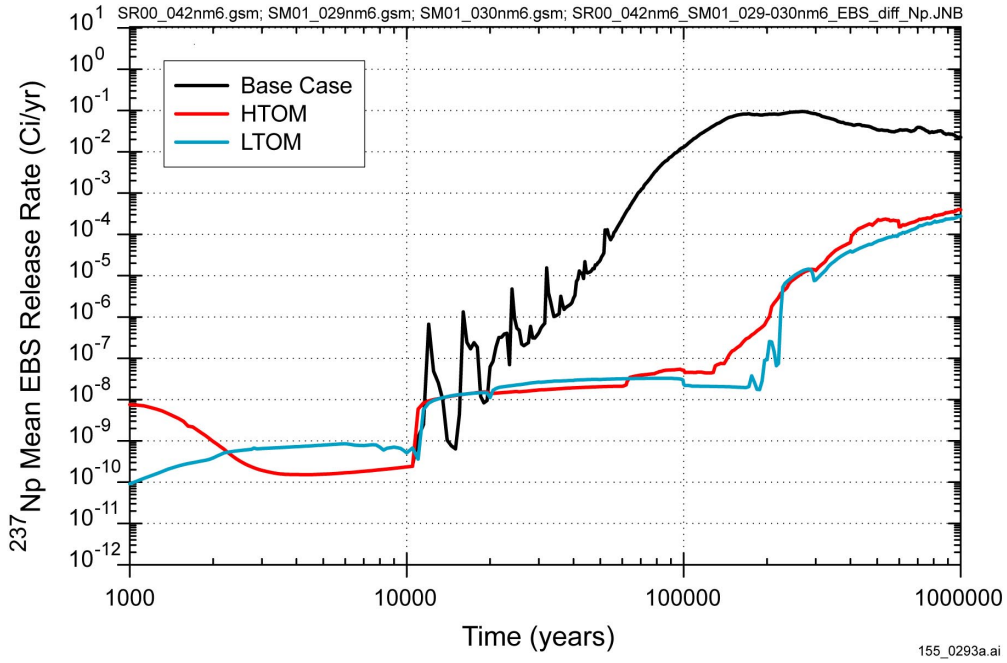

155_0294a.ai / 155_0293a.ai

NOTE: Comparison of the mean (a) advective and (b) diffusive EBS release of neptunium-237 for the three cases: TSPA-SR base-case HTOM, supplemental TSPA model HTOM, and supplemental TSPA model LTOM.

Figure 4.2.8-7. Neptunium-237 Advective and Diffusive Engineered Barrier System Release Rate Calculated with the TSPA-SR Base-Case and Supplemental TSPA Models

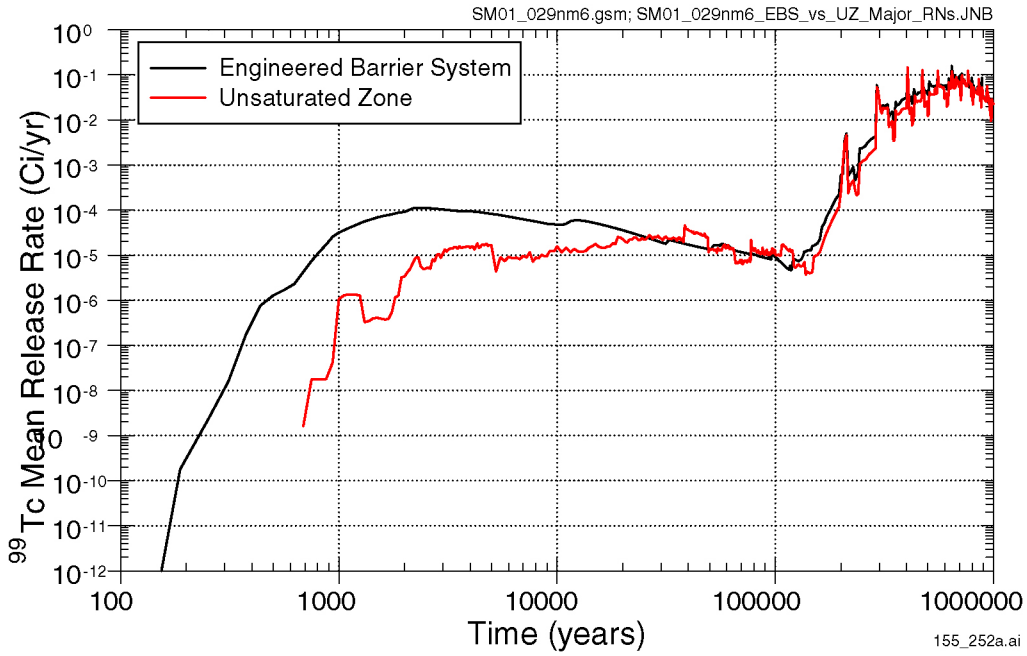

155_252a.ai

Figure 4.2.9-1. Mean Release Rate from the Engineered Barrier System and from the Unsaturated Zone for Technetium-99, Higher-Temperature Operating Mode

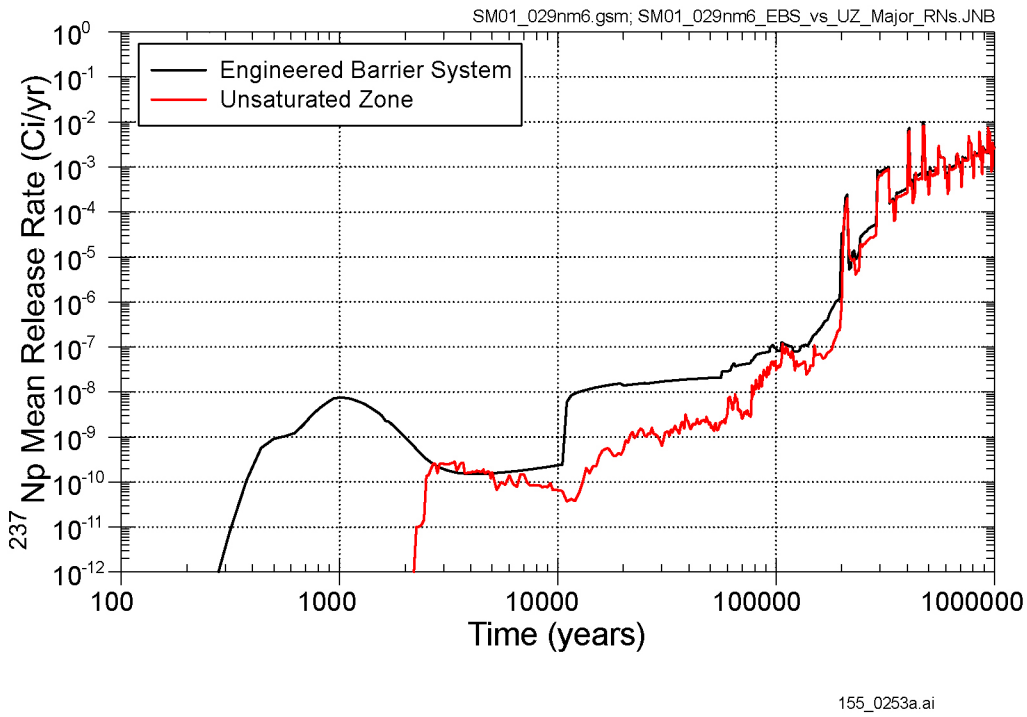

155_0253a.ai

Figure 4.2.9-2. Mean Release Rate from the Engineered Barrier System and from the Unsaturated Zone for Neptunium-237, Higher-Temperature Operating Mode

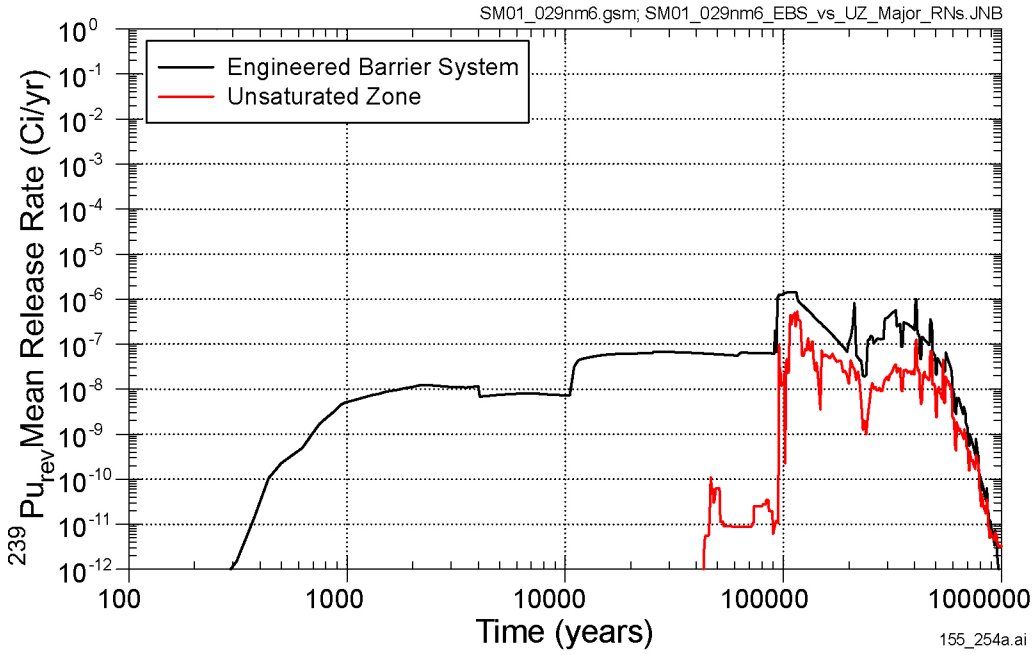

155_254a.ai

Figure 4.2.9-3. Mean Release Rate from the Engineered Barrier System and from the Unsaturated Zone for Reversible Plutonium-239, Higher-Temperature Operating Mode

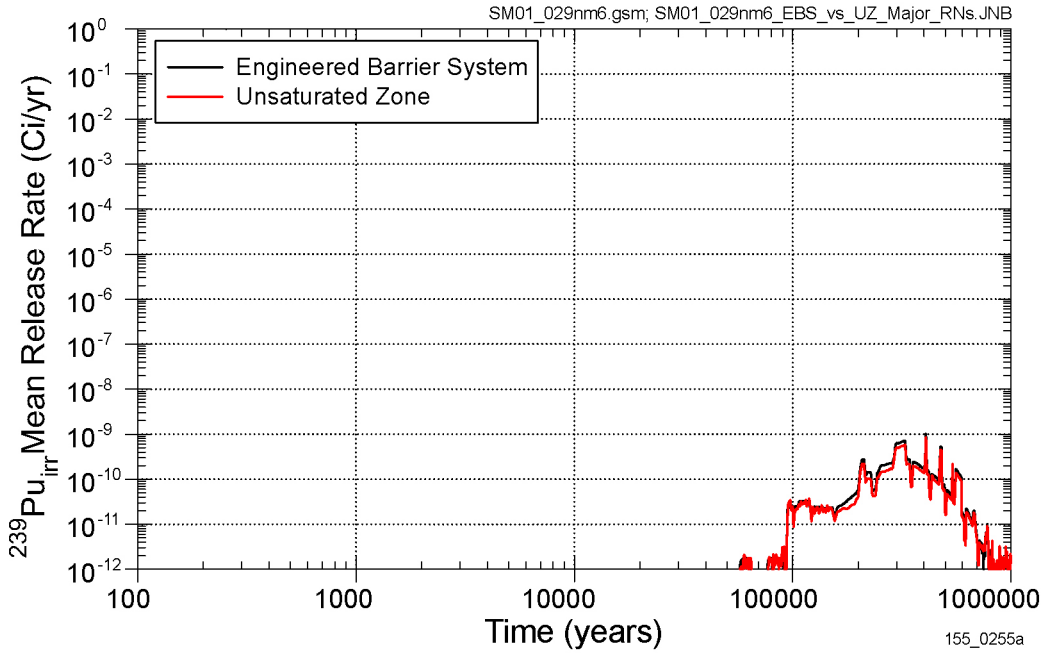

155_0255a

Figure 4.2.9-4. Mean Release Rate from the Engineered Barrier System and from the Unsaturated Zone for Irreversible Plutonium-239, Higher-Temperature Operating Mode

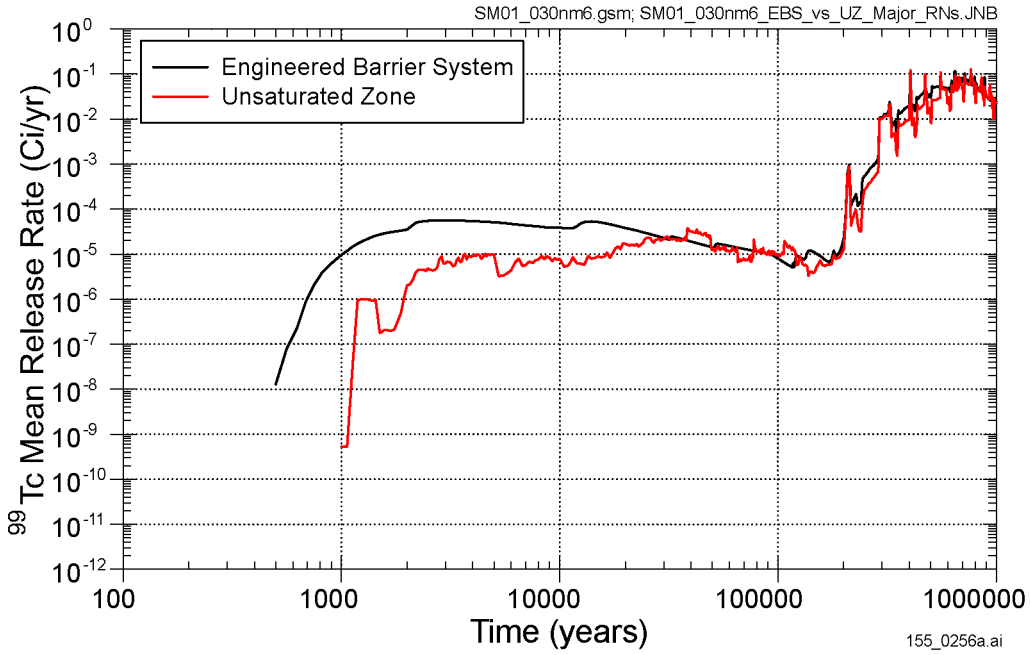

155_0256a.ai

Figure 4.2.9-5. Mean Release Rate from the Engineered Barrier System and from the Unsaturated Zone for Technetium-99, Lower-Temperature Operating Mode

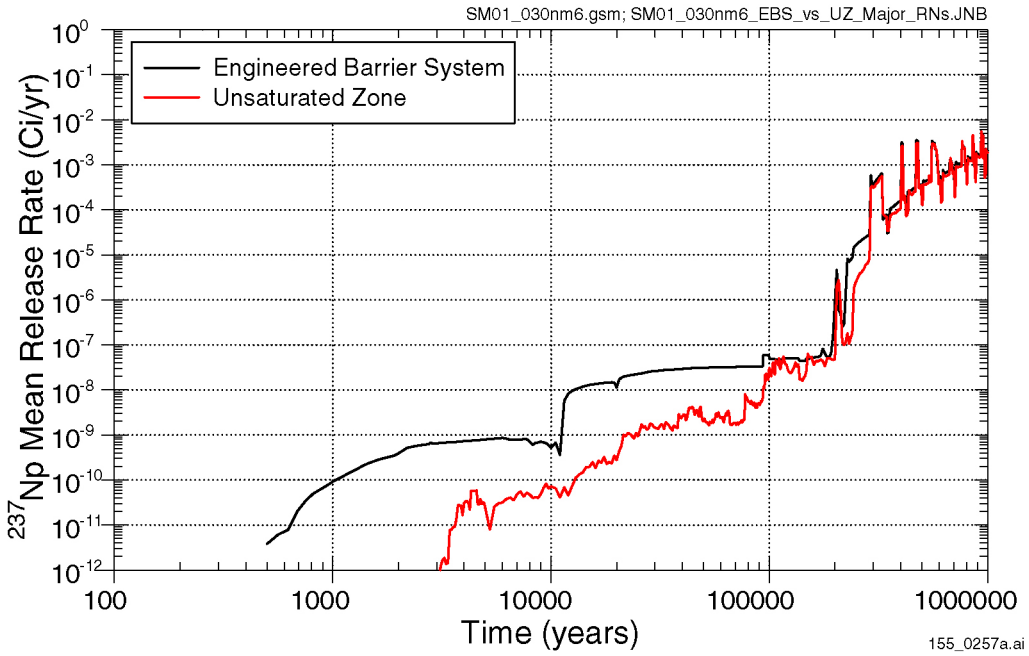

155_0257a.ai

Figure 4.2.9-6. Mean Release Rate from the Engineered Barrier System and from the Unsaturated Zone for Neptunium-237, Lower-Temperature Operating Mode

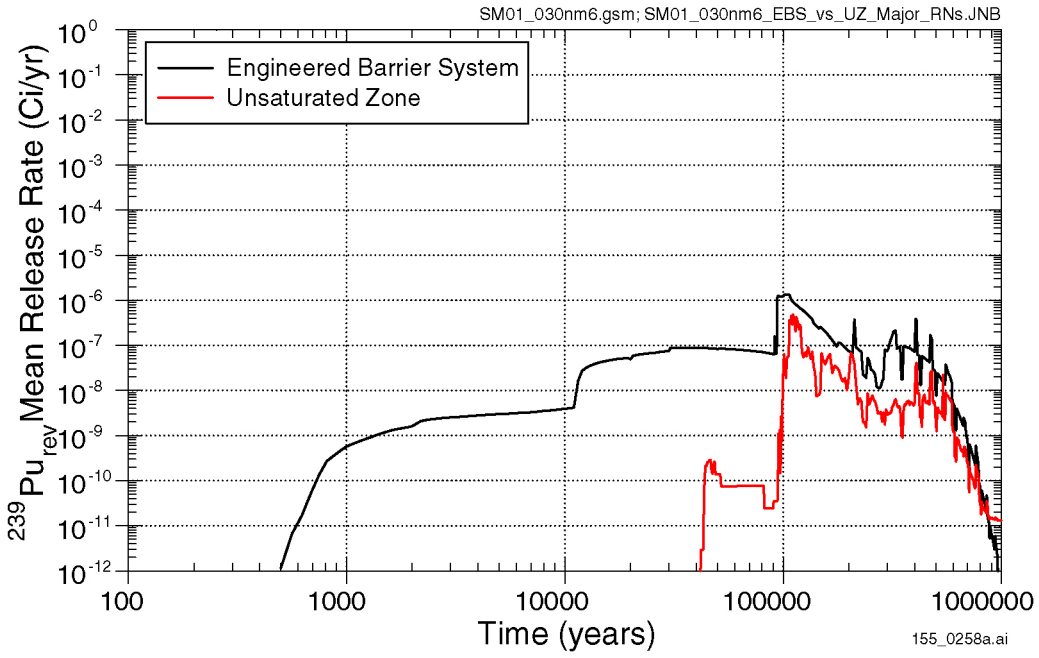

155_0258a.ai

Figure 4.2.9-7. Mean Release Rate from the Engineered Barrier System and from the Unsaturated Zone for Reversible Plutonium-239, Lower-Temperature Operating Mode

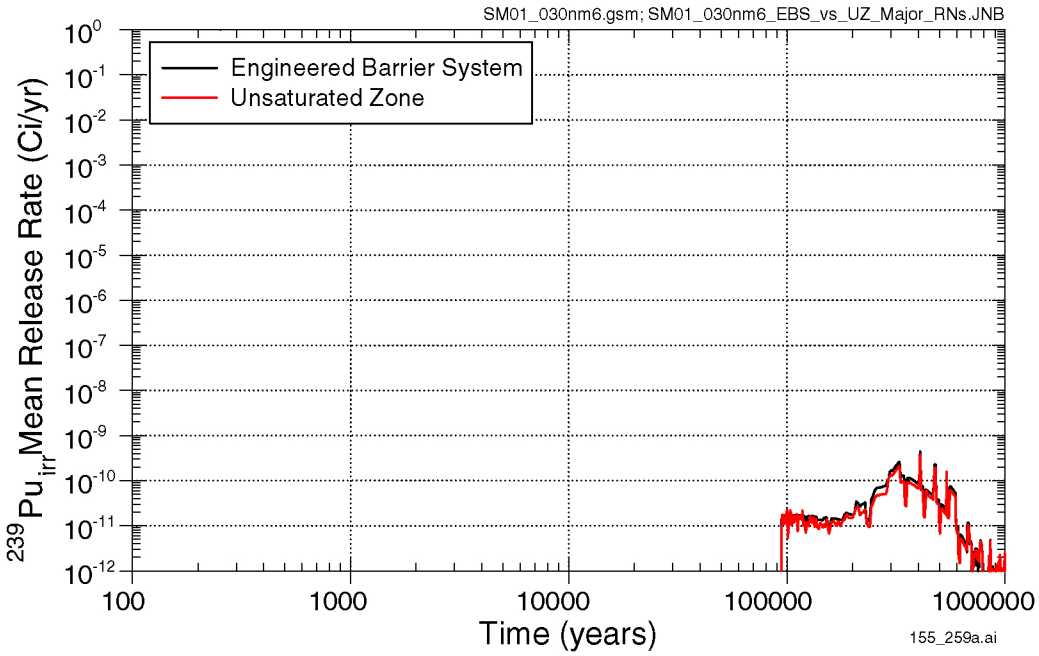

155_259a.ai

Figure 4.2.9-8. Mean Release Rate from the Engineered Barrier System and from the Unsaturated Zone for Irreversible Plutonium-239, Lower-Temperature Operating Mode

(a)

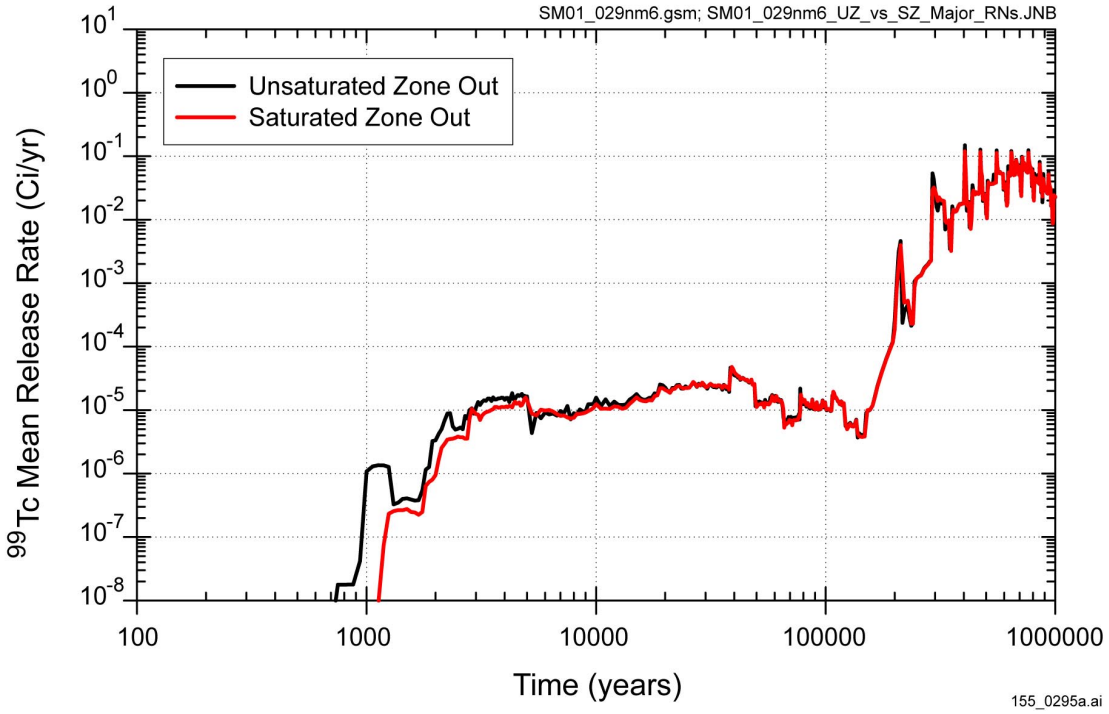

(b)

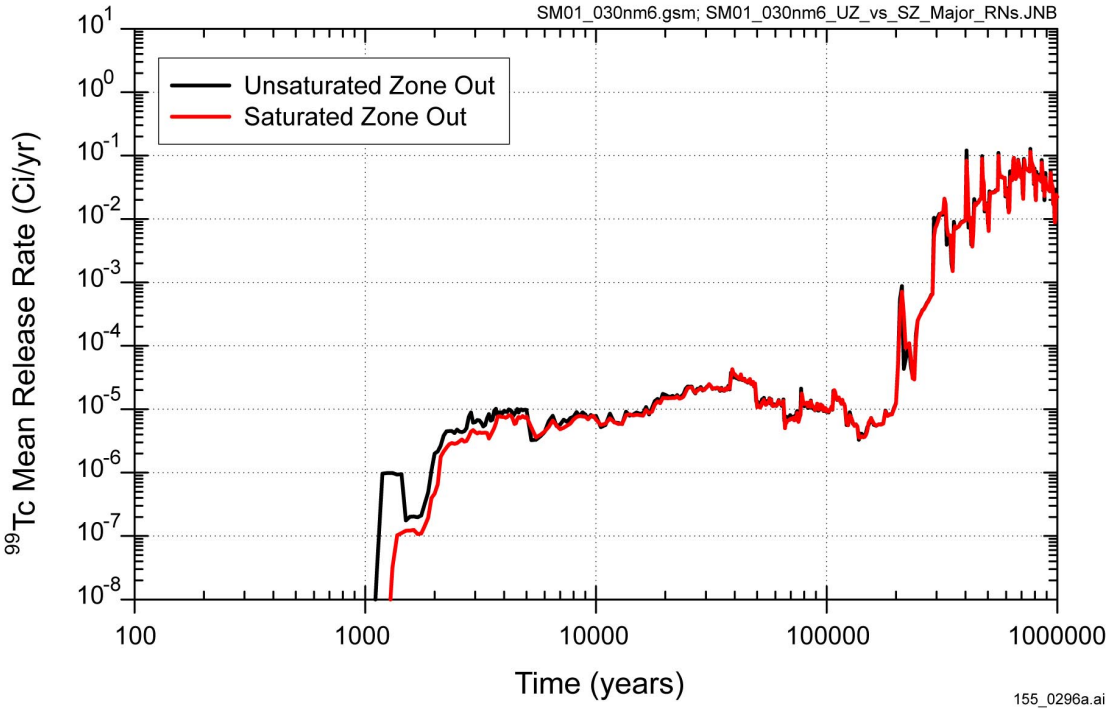

155_0295a.ai / 155_0296a.ai

NOTE: Mean annual release rate for technetium-99 from the UZ and the SZ with the supplemental TSPA model for (a) HTOM and (b) LTOM.

Figure 4.2.10-1. Release Rates for Technetium-99 from the Unsaturated Zone and Saturated Zone with the Supplemental TSPA Model for the Higher-Temperature Operating Mode and the Lower-Temperature Operating Mode

(a)

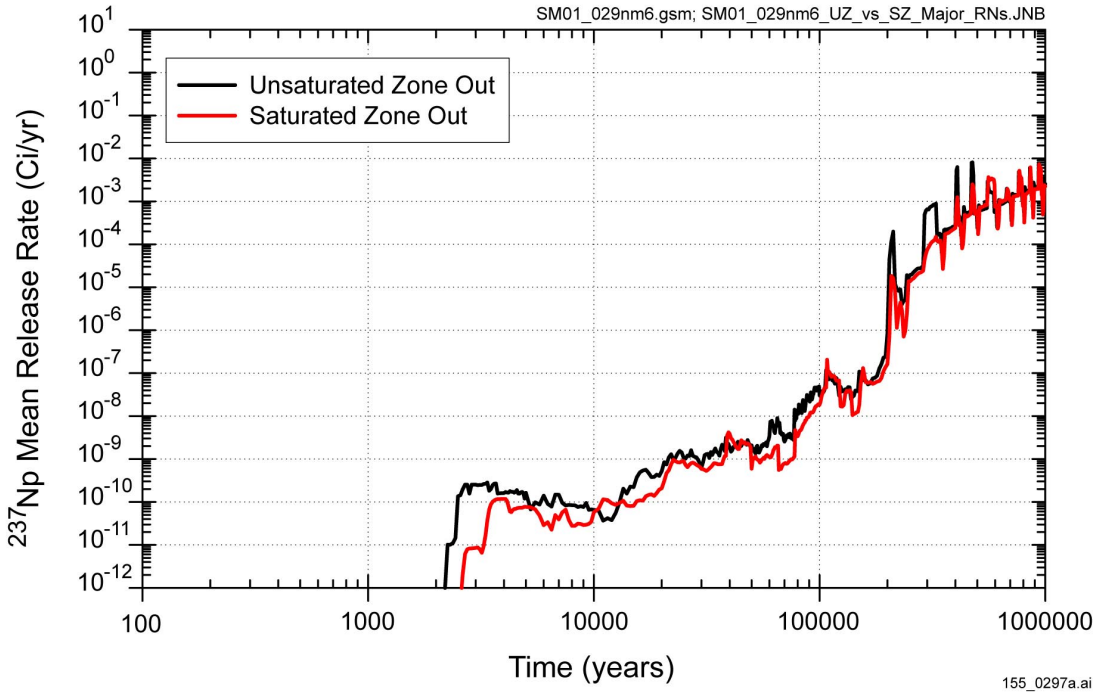

(b)

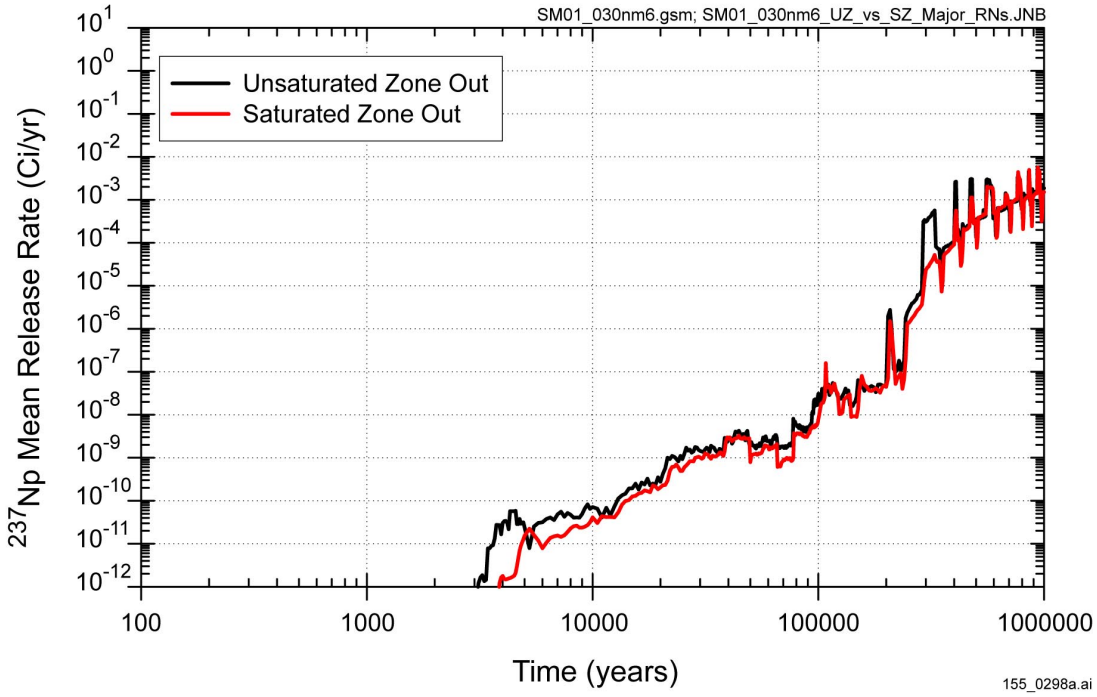

155_0297a.ai / 155_0298a.ai

NOTE: Mean annual release rate for neptunium-237 from the UZ and the SZ with the supplemental TSPA model (a) HTOM and (b) LTOM.

Figure 4.2.10-2. Release Rates for Neptunium 237 from the Unsaturated Zone and Saturated Zone with the Supplemental TSPA Model for the Higher-Temperature Operating Mode and the Lower-Temperature Operating Mode

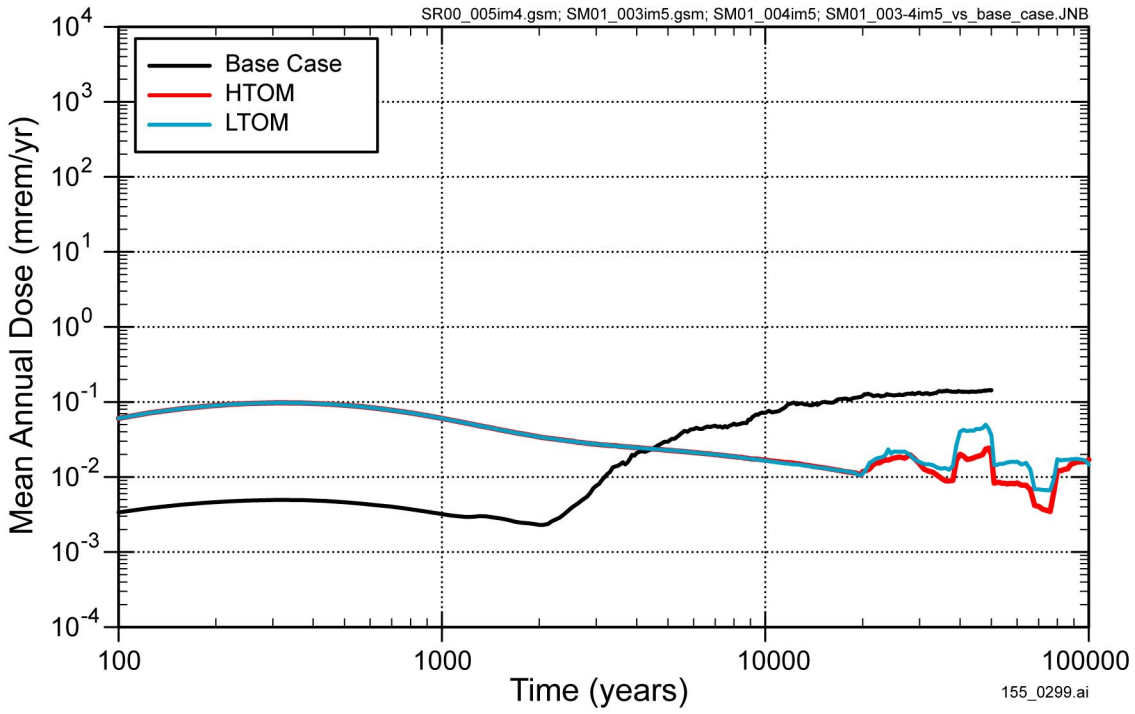

155_0299.ai

NOTE: Comparison of the mean annual does for three cases: TSPA-SR base-case HTOM, supplemental TSPA model HTOM, and supplemental TSPA model LTOM.

Figure 4.3-1. Probability-Weighted Mean Annual Dose for Igneous Disruption

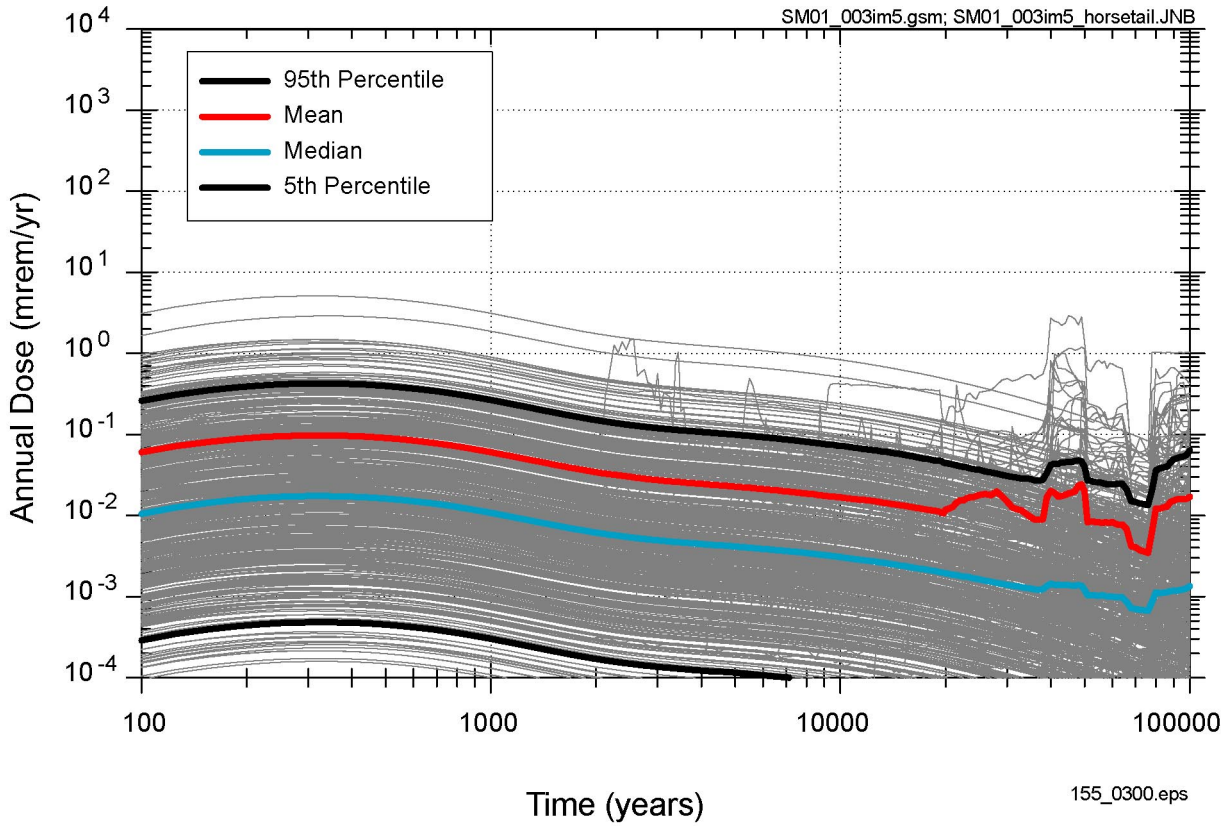

155_0300.eps

NOTE: Summary curves show the mean and the 95th, 50th (median), and 5th percentiles.

Figure 4.3-2. Supplemental TSPA Model: 500 (of 5,000) Realizations of Probability Weighted Annual Dose Histories for Igneous Disruption, Higher-Temperature Operating Mode

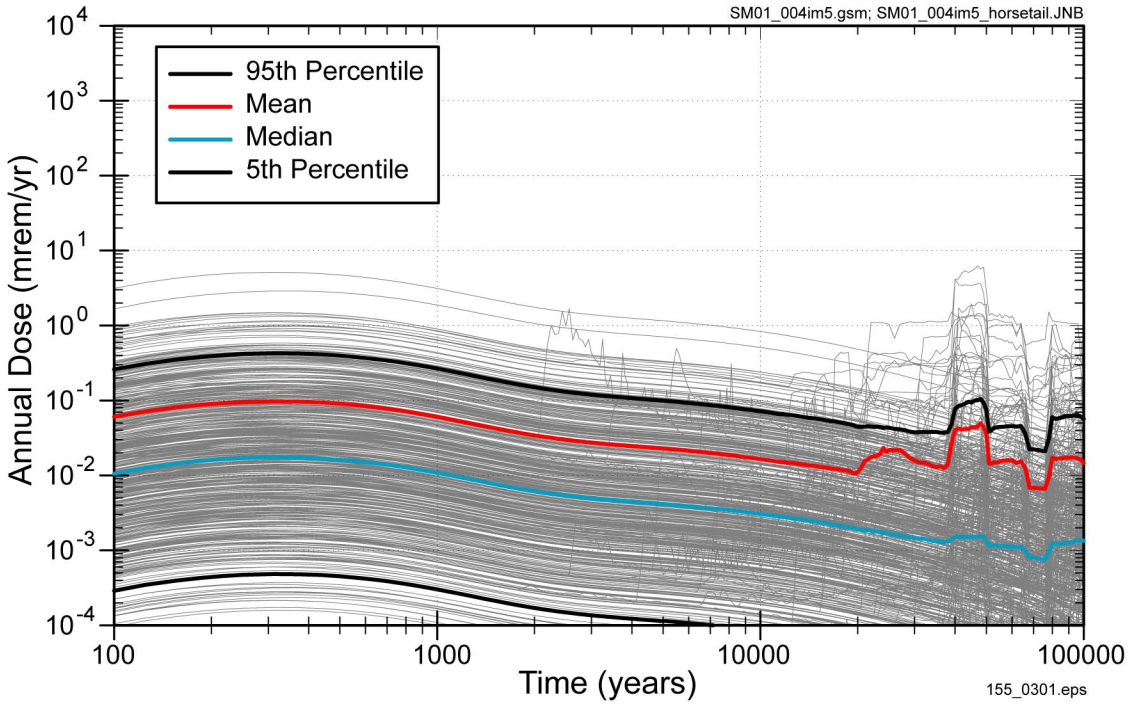

155_0301.eps

NOTE: Summary curves show the mean and the 95th, 50th (median), and 5th percentiles.

Figure 4.3-3. Supplemental TSPA Model: 500 (of 5,000) Realizations of Probability Weighted Annual Dose Histories for Igneous Disruption, Lower-Temperature Operating Mode

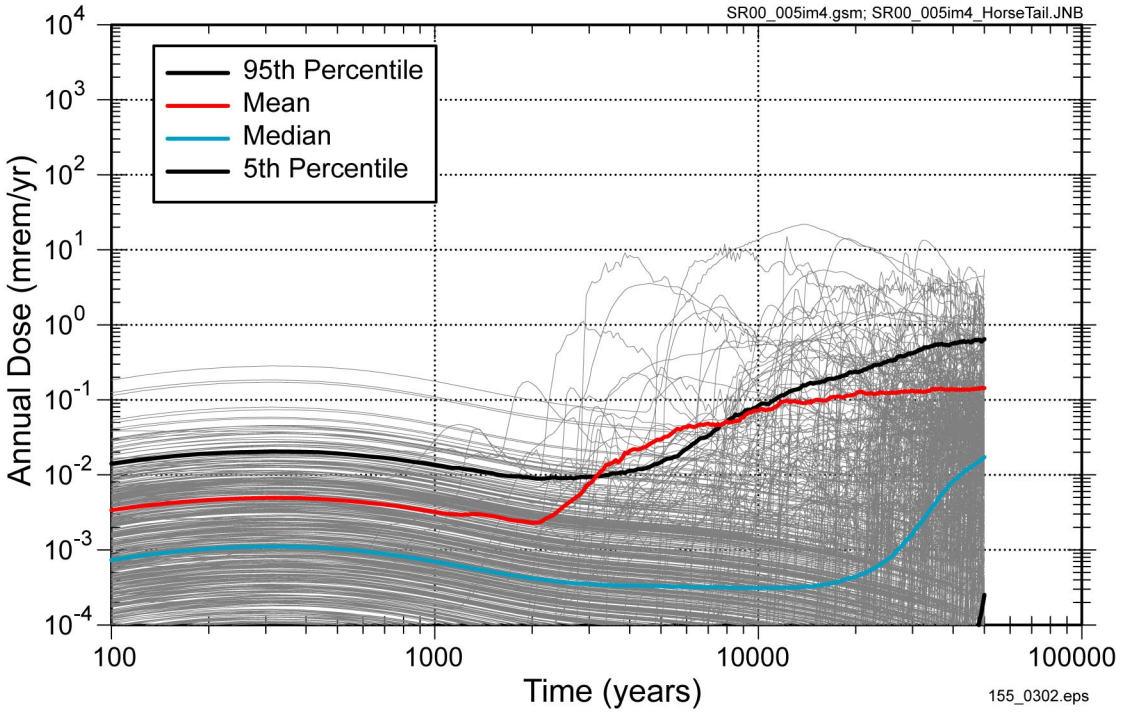

155_0302.eps

NOTE: Summary curves show the mean and the 95th, 50th (median), and 5th percentiles.

Figure 4.3-4. TSPA-SR: 500 (of 5,000) Realizations of Probability Weighted Annual Dose Histories for Igneous Disruption

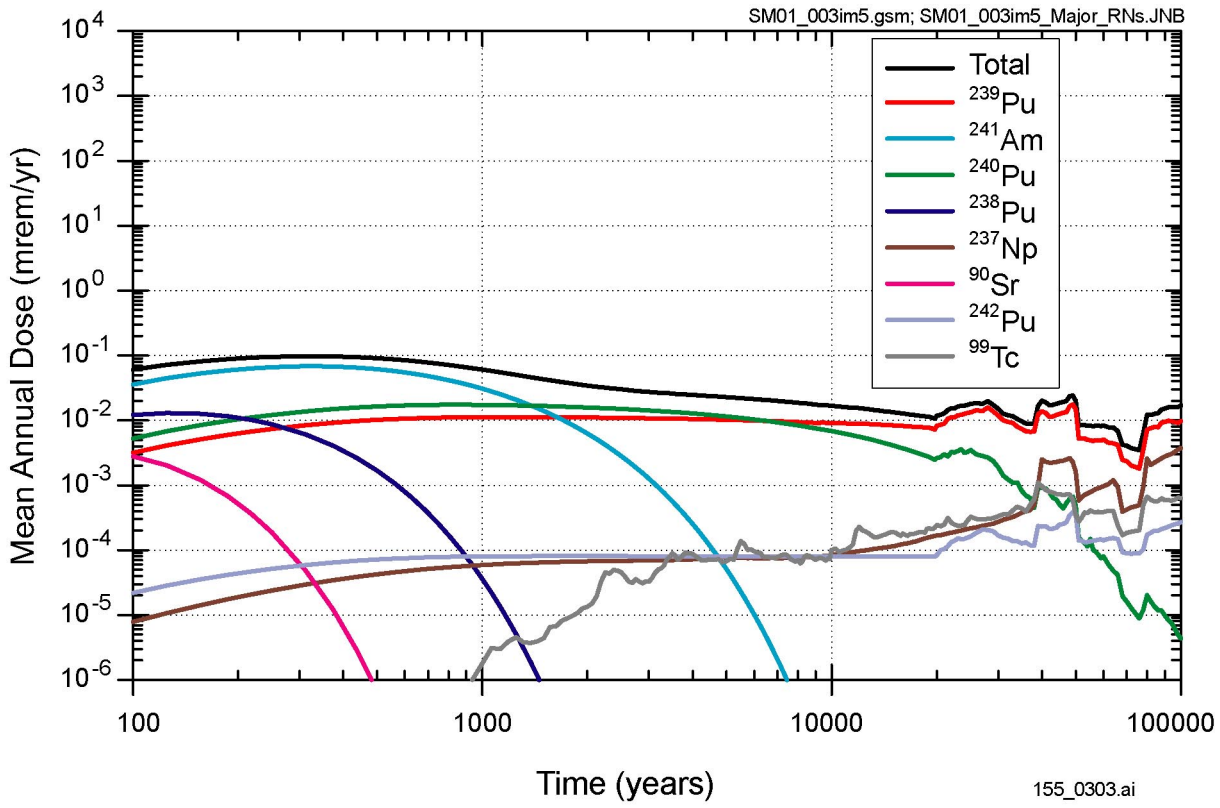

155_0303.ai

NOTE: Results for the supplemental TSPA analyses HTOM.

Figure 4.3-5a. Probability-Weighted Mean Annual Dose Histories for Radionuclides Contributing to the Total Probability-Weighted Igneous Disruption Mean Annual Dose

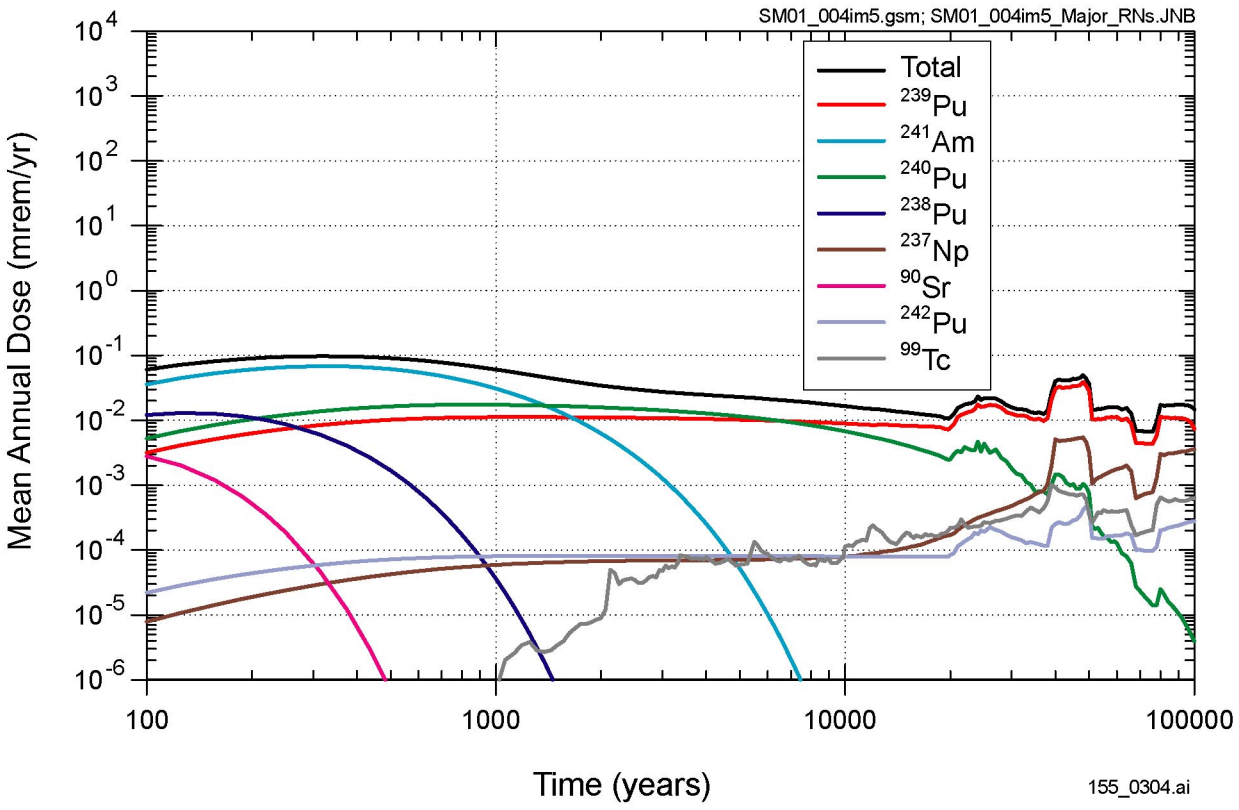

155_0304.ai

NOTE: Results for the supplemental TSPA analyses LTOM.

Figure 4.3-5b. Probability-Weighted Mean Annual Dose Histories for Radionuclides Contributing to the Total Probability-Weighted Igneous Disruption Mean Annual Dose

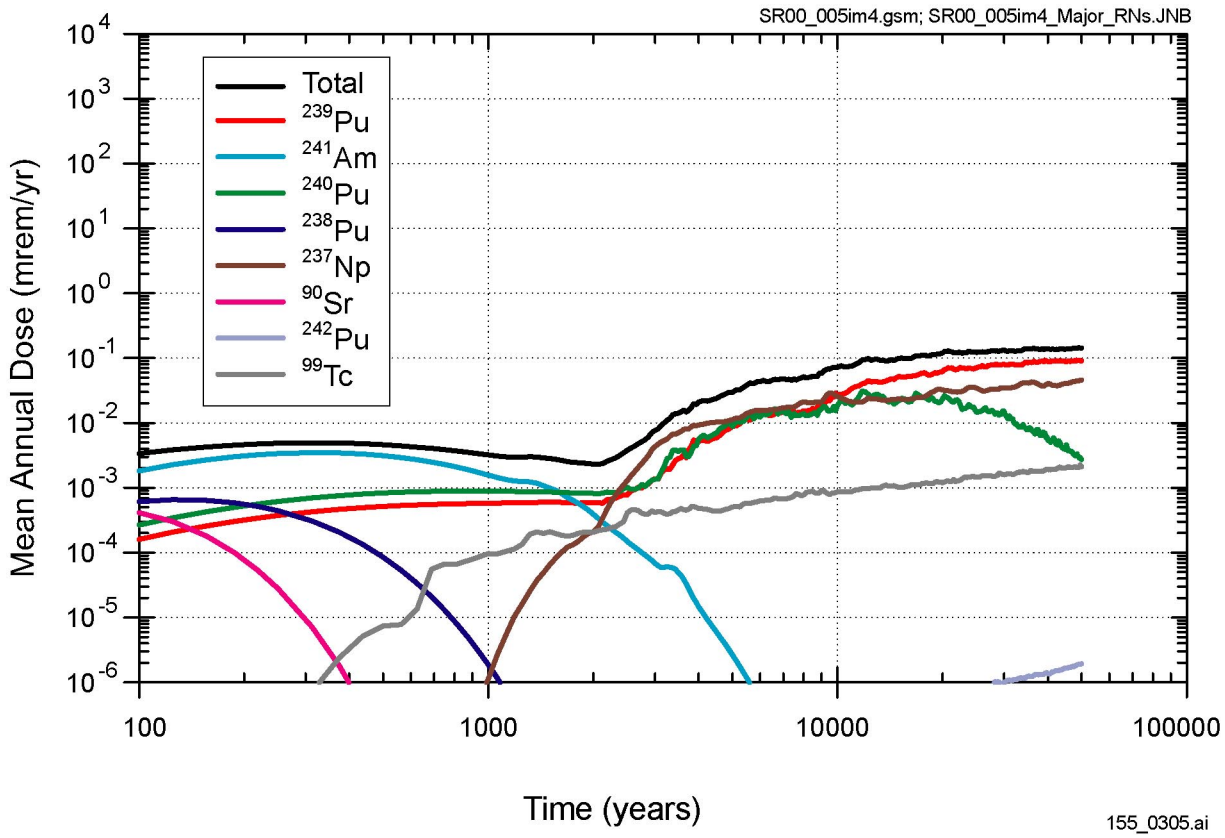

155_0305.ai

NOTE: Shows results from the TSPA-SR.

Figure 4.3-5c. Probability-Weighted Mean Annual Dose Histories for Radionuclides Contributing to the Total Probability-Weighted Igneous Disruption Mean Annual Dose

(a)

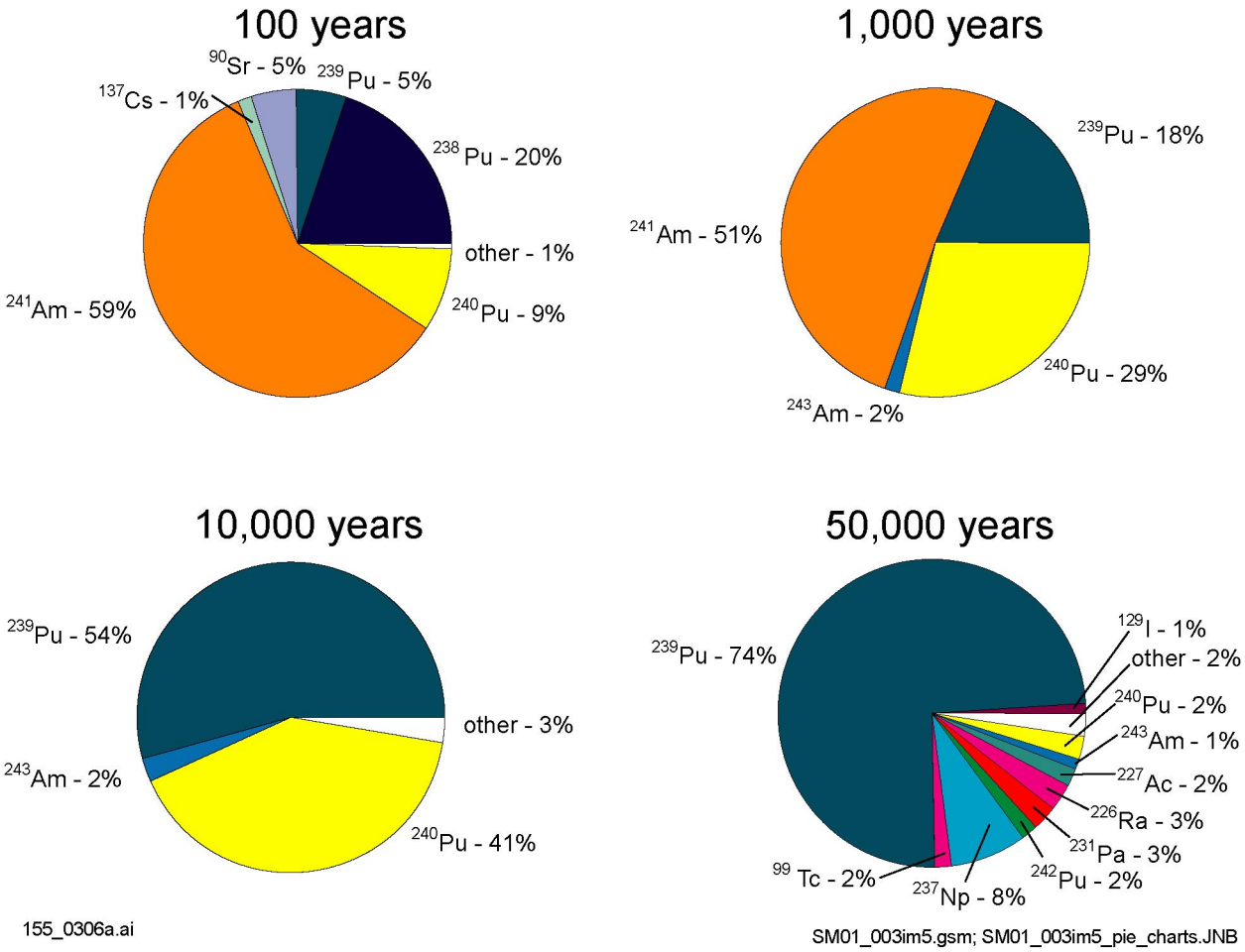

155_0306a.ai

Figure 4.3-6a. Radionuclides Contributing to Total Probability-Weighted Mean Annual Dose for the Igneous Disruption Scenario Class at Selected Times, Supplemental TSPA Model Higher-Temperature Operating Mode

(b)

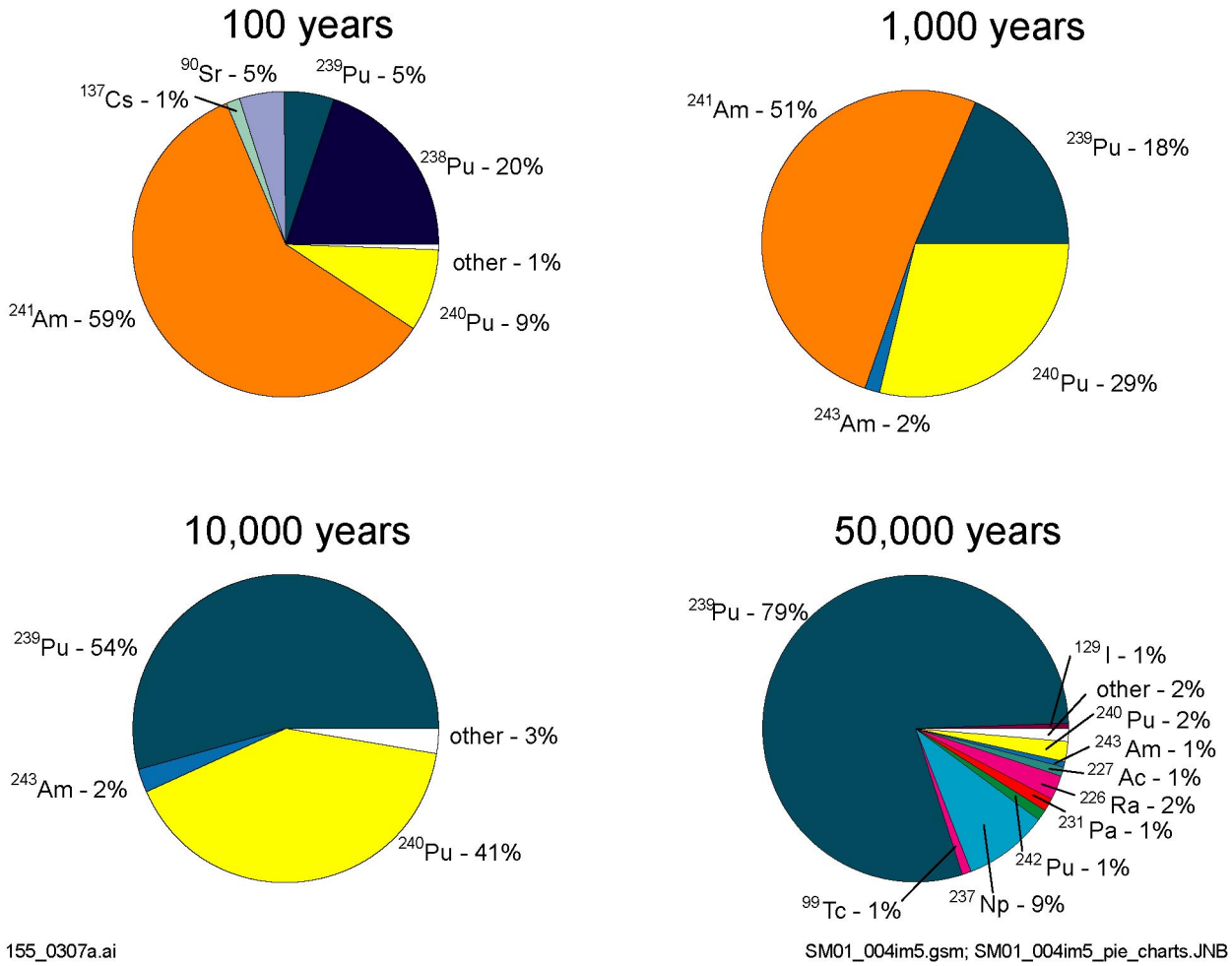

155_0307a.ai

Figure 4.3-6b. Radionuclides Contributing to Total Probability-Weighted Mean Annual Dose for the Igneous Disruption Scenario Class as Selected Times, Supplemental TSPA Model Lower-Temperature Operating Mode

(c)

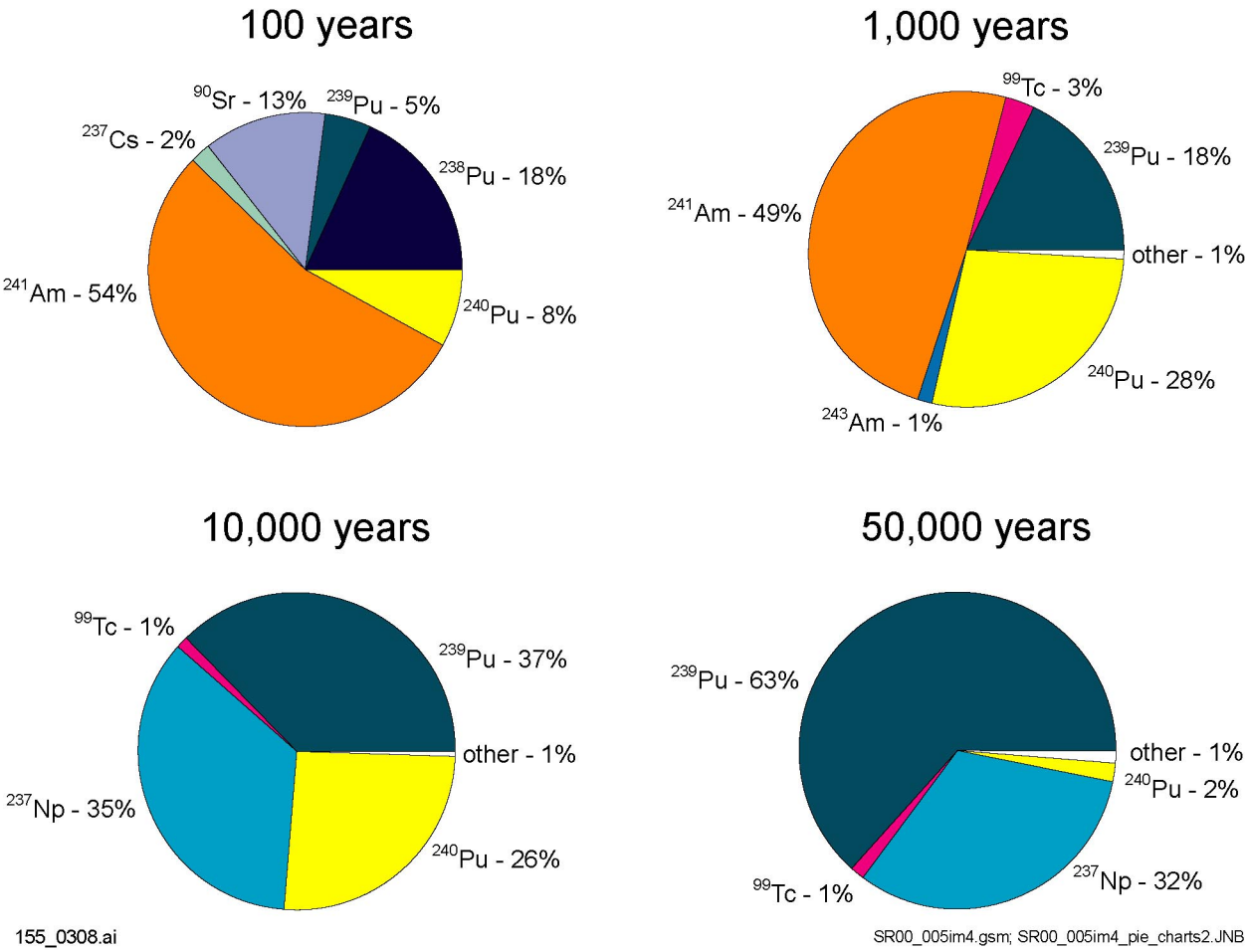

155_0308.ai

Figure 4.3-6c. Radionuclides Contributing to Total Probability-Weighted Mean Annual Dose for the Igneous Disruption Scenario Class at Selected Times, 100,000-Year TSPA-SR Base-Case Model

5. SUMMARY AND CONCLUSIONS

This volume of the *FY01 Supplementary Science and Performance Analyses* describes PA analyses conducted to examine the implications of information developed since completion of the S&ER (DOE 2001 [DIRS 153849]) and the TSPA-SR (CRWMS M&O 2000 [DIRS 153246]). As described in Section 1.1, the updated information has been grouped into three broad categories: consideration of uncertainties that were not fully quantified in TSPA-SR, consideration of new scientific information developed since completion of TSPA-SR, and evaluation of the performance of the disposal system for a range of thermal operating conditions. Table 1.3-1 provides a brief summary of the new information and how it has been carried forward into the performance assessment analyses and additional summaries are provided in Sections 3 and 4. Appendix A of this volume describes the supplemental TSPA model files and associated external files necessary to reproduce the documented results. The technical basis for the new information is provided in the SSPA Volume 1 (BSC 2001 [DIRS 154657], Sections 3 to 14).

Analyses described in this volume are of two types. Section 3 summarizes one-off analyses that compare the effects of individual model or parameter changes to the TSPA-SR (CRWMS M&O 2000 [DIRS 153246]) results. These analyses use models and input parameters that are identical to the models and parameters used in the TSPA-SR in all regards except for the specific model or parameters being varied. Results therefore allow direct interpretation of the effects of the specific change. Results of these one-off analyses do not allow interpretation of the possible coupled or aggregated effects of multiple changes in the modeling system. However, those insights are provided in Section 4, which summarizes the results of a set of analyses using the supplemental TSPA model that combines important new information for all model components into a single analysis. The results of performance analyses are provided in the SSPA to complement the TSPA-SR results by incorporating new information, further quantification of uncertainties, and by applying the supplemental TSPA model to the HTOM and LTOM cases.

5.1 NOMINAL PERFORMANCE

The supplemental TSPA model estimates of mean annual dose to a receptor are substantially lower for nominal performance than those reported in the TSPA-SR for most of the million-year period of simulation (Figure 4.1-1). During the first 10,000 years, results of the supplemental TSPA analyses are higher than those reported in the TSPA-SR, consistent with new information that expands the uncertainty associated with the effects of improper heat treatment of waste package lid welds. Consideration of this uncertainty leads to the failure of a small number of waste packages in 23 percent of the SSPA realizations, and releases from these early failures are the only contributor to nominal performance mean annual dose for approximately the first 80,000 years. Mean annual doses associated with these early failures are small, reaching a maximum during the first 10,000 years of approximately 0.0002 mrem/yr for the HTOM and 0.00006 mrem/yr for the LTOM. Peak mean annual doses between 10,000 and 100,000 years are substantially lower for the supplemental TSPA model than for the TSPA-SR, dropping from approximately 70 mrem/yr to approximately 0.0001 mrem/yr, primarily because of the modified treatment of waste package degradation in the supplemental TSPA model. Peak mean doses during the entire 1-million-year period of simulation also are lower for the supplemental TSPA model, reaching a peak of approximately 35 mrem/yr, as opposed to approximately 490 mrem/yr

in the TSPA-SR base case. Time of peak mean dose shifts from approximately 270,000 years to approximately 1-million years, with doses still trending slightly upward at the end of the simulation. The drop in peak annual dose is due largely to the modified treatment of radionuclide solubilities, particularly neptunium, thorium, and plutonium. Effects of other model changes, particularly the use of the supplemental TSPA model for long-term climate changes after 10,000 years, can be observed in the annual dose histories but do not have a major impact on the overall conclusions.

Evaluations of the HTOM and LTOM cases show thermal impacts on nominal performance at the subsystem level during the first thousand years (e.g., see Section 4.2.2 for a discussion of thermal effects on seepage). However, these subsystem effects have only a relatively minor impact on system level performance and expected annual dose (Figure 4.1-1; see also Section 4.1.3). For nominal performance, the LTOM yields mean annual dose estimates that are generally slightly less than those for the HTOM. The maximum differences in annual dose between the two operating modes are approximately a factor of 10, and the choice of thermal operating mode does not strongly influence overall conclusions from the supplemental analyses.

5.2 IGNEOUS DISRUPTION

Figure 4.3-1 compares the probability-weighted mean annual dose results for the supplemental TSPA analyses with those of the TSPA-SR. Overall, the peak igneous probability-weighted mean annual dose during the first 100,000 years is lower by a factor of approximately 2 for the supplemental TSPA analyses (approximately 0.1 mrem/yr) than for the TSPA-SR (approximately 0.2 mrem/yr). However, changes in several key input parameters have raised the annual dose during the first several thousand years by a factor of up to 25, and the peak mean annual dose of approximately 0.1 mrem/yr now occurs before 10,000 years (see Section 4.3). This increase is due to modifications in the input parameters for the volcanic eruption model, consistent with new scientific information developed since the completion of the TSPA-SR. Annual doses at later times are lower for the supplemental TSPA model, consistent with the modified treatment of radionuclide solubilities that result in lower doses from groundwater transport following igneous intrusion. These analyses do not include the effects of possible changes in the area of the potential repository or waste emplacement geometry associated with alternative thermal operating modes. Analysis of a representative lower-temperature design, one that increases the length of the potential repository by 3,300 m, shows a 70 percent increase in the probability of igneous disruption and would result in a corresponding increase of 70 percent in the probability-weighted annual dose from igneous disruption (BSC 2001 [DIRS 154657], Section 14.3.3.2.2).

5.3 IMPORTANCE OF NEW INFORMATION DEVELOPED SINCE THE TSPA-SR

The supplemental TSPA analyses using information developed since the TSPA-SR and the S&ER complement the postclosure performance results presented in those documents, and provide additional insights into the behavior of the disposal system. These analyses support the TSPA-SR conclusion that igneous disruption is the largest contributor to the overall expected annual dose during the first 10,000 years, and that releases from igneous disruption may come from eruptive and groundwater transport pathways. The analyses also support the TSPA-SR conclusions that the nominal performance is robust, and that waste package degradation is a key

process in determining the rate at which radionuclides are released from the disposal system and the time of the peak annual dose. As noted in the TSPA-SR, radionuclide solubilities have a major impact on the magnitude of the peak annual dose, with climate change also contributing. As described in SSPA Volume 1 (BSC 2001 [DIRS 154657], Sections 3 to 14), the supplemental TSPA analyses provide new insights regarding subsystem performance. At the system level, important observations are that overall performance remains robust even with early waste package failures associated with weld flaws, and that overall expected annual dose is not strongly sensitive to the choice of thermal operating conditions.

For the TSPA-SR and the supplemental TSPA model, probability-weighted mean annual doses from igneous disruption determine the magnitude of the overall mean annual dose from nominal and disruptive performance during the first 10,000 years. For the TSPA-SR, there are no nominal doses during the first 10,000 years, and the probability-weighted igneous mean annual dose and the total dose are the same. For the supplemental TSPA model, the nominal mean annual dose is hundreds to thousands of times smaller than the probability-weighted mean annual igneous dose throughout the first 10,000 years, and overall mean annual dose can be approximated as the probability-weighted mean annual dose during this period.

5.4 FINAL ENVIRONMENTAL PROTECTION AGENCY STANDARD 40 CFR PART 197

The models and analyses conducted to evaluate the TSPA used in the supplemental TSPA analyses were based on the requirements specified in the proposed EPA standard (40 CFR Part 197, 64 FR 46976 [DIRS 105065]) and the proposed NRC regulation (10 CFR Part 63, 64 FR 8640 [DIRS 101680]). Recently the EPA promulgated the final 40 CFR Part 197 (66 FR 32074 [DIRS 155216]). Key aspects of the final EPA standard were examined in SSPA Volume 1 (BSC 2001 [DIRS 154657], Section 13) and possible impacts on system performance are addressed qualitatively here.

The provisions of the final EPA standards that have been examined include the definition of the point of compliance, the definition of the food and water consumption habits of the reasonably maximally exposed individual, and the size of the representative volume used in the groundwater protection portion of the standard.

The point of compliance specified in the final standard is at the edge of the controlled area, which has a maximum southern extension to 36°40'13.6661" north latitude (40 CFR 197.12, 66 FR 32074 [DIRS 155216]). This is a distance of about 18 km from the potential repository (for the HTOM), and it is approximately 2 km north of the boundary used in the proposed EPA and NRC regulations. The effect of this shorter distance is to shorten the transport distance before radionuclides reach the potential receptor. The shorter distance implies shorter advective transport times for the dissolved radionuclides in the SZ.

To quantify the effect of these shorter transport times, two alternative analyses were conducted using the SZ flow and transport model. The results of these comparisons for a nonsorbing radionuclide and a sorbing radionuclide are illustrated in SSPA Volume 1 (BSC 2001 [DIRS 154657], Section 12.5.3). Carbon-14 is used in these calculations to represent possible behavior of nonsorbing species such as technetium-99 and iodine-129, although carbon-14 itself

is a reactive species, and is likely to be delayed during transport by chemical reactions with water and rock. For transport modeling, carbon-14 has been conservatively assumed to be nonsorbing. Neptunium-237 is used as a representative example of a sorbing species. These results indicate that the average median advective transport time (i.e., the time at which 50 percent of the contaminant has reached the location of the receptor) is reduced from the 20 km case by approximately 30 percent for nonsorbing species and less than 50 percent for neptunium-237. This reduction is more than would be anticipated for the case when the transport time is linear with transport distance because the last few kilometers of radionuclide transport are in the alluvium which has a higher porosity and therefore lower advective velocity (for sorbing and nonsorbing radionuclide species) than the corresponding fractured tuff rock units. Because the length of the transport path within the alluvium is determined primarily by the location of the boundary of the controlled area, rather than by the location of the southern edge of the potential repository, differences in transport time between the HTOM and LTOM cases are not likely to be strongly affected by the change in overall path length.

The effect of the reduced advective transport times (due to the shorter distance) used in the supplemental TSPA analyses compared to those used in the S&ER (DOE 2001 [DIRS 153849], Section 4.2.9.4) and the TSPA-SR (CRWMS M&O 2000 [DIRS 153246], Section 3.8.2]) is to shift the breakthrough curves to correspondingly earlier times. During the period of regulatory concern (10,000 years) when the only releases in the supplemental TSPA model for nominal performance come from the low-probability early waste package failures due to the possibility of improper heat treatment of the closure welds (see Section 3.2.5), annual doses are primarily due to nonsorbing radionuclides. Therefore, reducing the advective transport time by several hundred years would reduce the breakthrough of the radionuclides by this same amount of time. This reduction in the transport time would have no effect on the magnitude of the peak mean annual dose, as this is controlled by the temporally dispersed release from the EBS.

Similar conclusions can be drawn from the analysis of the doses at later times, when sorbing radionuclides such as neptunium-237 dominate. Advective transport times could be reduced by thousands to tens of thousands of years for the more sorbing species, again causing earlier breakthroughs. In both instances, the change in the transport distance of about 10 percent (from 20 to 18 km) effectively translates the plots along the time axis without significantly affecting the magnitude of the peak mean annual dose during the periods of interest.

The definition of the food and water consumption habits of a reasonably maximally exposed individual, as defined in the final EPA standard, are different from the values used in the analyses used to generate the BDCFs described in SSPA Volume 1 (BSC 2001 [DIRS 154657], Section 13.2). In particular, the promulgated standard specifies that the receptor consumes the mean amount of locally grown food (as determined from the survey of all individuals currently residing in the town of Amargosa Valley) and drinks two liters per day of groundwater pumped from the aquifer at the point of compliance (40 CFR 197.21, 66 FR 32074 [DIRS 155216]).

An analysis of the potential differences associated with the prescribed consumption of food and water compared to the consumption distributions used in the generation of the dose conversion factors is presented in SSPA Volume 1 (BSC 2001 [DIRS 154657], Section 13.3.1.3) for two time periods (25,000 and 100,000 years). These time periods correspond to times when the doses would be expected to be dominated by nonsorbing and sorbing radionuclides, respectively,

and therefore represent the sensitivity of the dose estimate to the food and water consumption assumptions. The analysis presented in SSPA Volume 1 (BSC 2000 [DIRS 154657], Tables 13.3-3 and 13.3-4, receptors 1 and 3) indicates that the difference in total annual dose between the two receptors is likely to be less than 30 percent, even though the difference in some foodstuff pathways is almost a factor of two. The difference is small compared to uncertainty from other sources in the TSPA modeling and would have little effect on the annual doses calculated in the supplemental TSPA analyses or the TSPA-SR (CRWMS M&O 2000 [DIRS 153246], Section 4.1).

The third aspect of the EPA final standard addressed here is the use of a representative volume of 3,000 acre-ft/yr (40 CFR 197.31(a)(3), 66 FR 32074 [DIRS 155216]), as opposed to the 1,285 acre-ft/yr specified in the proposed EPA standard (proposed 40 CFR 197.36(a)(3), 64 FR 46976 [DIRS 105065]). This difference effectively reduces the estimated radionuclide concentrations and critical organ doses used for comparison to the groundwater protection standard by a factor of 2.3, equal to the dilution factor introduced by the increase in the size of the representative volume of groundwater. Groundwater radionuclide concentrations and critical organ doses calculated for the SSPA are discussed in Section 4.1.4 and summarized in Section 5.5.

5.5 OTHER SYSTEM PERFORMANCE MEASURES

The supplemental TSPA analyses presented in this volume focus on evaluating the potential importance of unquantified uncertainties and on the performance-related effects of different thermal operating modes. Analyses included system calculations of the individual protection performance measure.

Potential effects of the supplemental science presented in SSPA Volume 1 (BSC 2001 [DIRS 154657]) on the performance projections for the stylized human intrusion scenario are expected to be negligible. The changes in the solubility limits would reduce the mean release rates for the lower solubility radionuclides, such as neptunium-237, thus lowering their annual doses during the compliance period. However, this effect would be offset to some extent by the reduced travel path length caused by the change in the location of the point of compliance. The net effect would not significantly affect the results of the stylized human intrusion scenario presented in the S&ER (DOE 2001 [DIRS 153849], Section 4.4.4).

Overall peak mean concentrations of total radium activity and gross alpha activity are delayed and reduced in the supplemental TSPA model, relative to the TSPA-SR results (Section 4.1.4). During the time of regulatory concern (10,000 years), when the only releases in nominal performance come from the low-probability early waste package failure, concentrations are small but higher than the zero values in the TSPA-SR. The highest mean concentrations of gross-alpha activity during the first 10,000 years are approximately 7×10^{-7} pCi/L for the supplemental TSPA model, and the highest mean concentrations of total radium activity during the first 10,000 years are approximately 7×10^{-11} pCi/L. Critical organ doses due to concentrations of beta and photon emitters in groundwater are also extremely small in the supplemental TSPA model, reaching a maximum of approximately 0.00005 mrem/yr during the first 10,000 years. As discussed in Section 4.1.4, these calculations do not include naturally-occurring background radiation, and groundwater concentration values should be adjusted accordingly for comparison

to the EPA limits of 15 pCi/L for gross alpha concentration and 5 pCi/L for total radium during the first 10,000 years of performance (40 CFR 197.30, 66 FR 32074 [DIRS 155216]). Available data indicate that gross alpha background concentrations at the point of compliance are 0.4 ± 0.7 pCi/L, and total radium background concentrations are no greater than 1.04 pCi/L (CRWMS M&O 2000 [DIRS 153246], Section 4.1.5).

6. REFERENCES

NOTE: The following references are sorted in numerical order using a unique Yucca Mountain Project identifier.

6.1 DOCUMENTS CITED

100550 DOE (U.S. Department of Energy) 1998. *Total System Performance Assessment.* Volume 3 of *Viability Assessment of a Repository at Yucca Mountain.* DOE/RW-0508. Washington, D.C.: U.S. Department of Energy, Office of Civilian Radioactive Waste Management. ACC: MOL.19981007.0030.

100987 Jarzemba, M.S.; LaPlante, P.A.; and Poor, K.J. 1997. *ASHPLUME Version 1.0—A Code for Contaminated Ash Dispersal and Deposition, Technical Description and User's Guide.* CNWRA 97-004, Rev. 1. San Antonio, Texas: Center for Nuclear Waste Regulatory Analyses. TIC: 239303.

101112 CRWMS M&O 1998. *Software Routine Report for SZ_CONVOLUTE V1.0.* CSCI: 30038 V1.0. DI: 30038-2999, Rev. 00. Las Vegas, Nevada: CRWMS M&O. ACC: MOL.19981103.0084.

107292 CRWMS M&O 1999. *License Application Design Selection Report.* B00000000-01717-4600-00123 REV 01 ICN 01. Las Vegas, Nevada: CRWMS M&O. ACC: MOL.19990908.0319.

117132 Sandia National Laboratories 2001. *Software Code: WTRISE V1.0.* V1.0. 10537-1.0-00. URN-0917

123650 USGS (U.S. Geological Survey) 2000. *Simulation of Net Infiltration for Modern and Potential Future Climates.* ANL-NBS-HS-000032 REV 00. Denver, Colorado: U.S. Geological Survey. ACC: MOL.20000801.0004.

132447 Los Alamos National Laboratory 2000. *Software Code: FEHM* . V2.10. SUN Ultra Sparc, PC. 10086-2.10-00.

139440 CRWMS M&O 2000. *Input and Results of the Base Case Saturated Zone Flow and Transport Model for TSPA.* ANL-NBS-HS-000030 REV 00. Las Vegas, Nevada: CRWMS M&O. ACC: MOL.20000526.0330.

139563 CRWMS M&O 2000. *Igneous Consequence Modeling for the TSPA-SR.* ANL-WIS-MD-000017 REV 00. Las Vegas, Nevada: CRWMS M&O. ACC: MOL.20000501.0225.

143244 CRWMS M&O 2000. *Analysis of Infiltration Uncertainty.* ANL-NBS-HS-000027 REV 00. Las Vegas, Nevada: CRWMS M&O. ACC: MOL.20000525.0377.

143665 CRWMS M&O 2000. *Total System Performance Assessment for the Site Recommendation.* TDR-WIS-PA-000001 REV 00. Las Vegas, Nevada: CRWMS M&O. ACC: MOL.20001005.0282.

144055 CRWMS M&O 2000. *Distribution Fitting to the Stochastic BDCF Data.* ANL-NBS-MD-000008 REV 00. Las Vegas, Nevada: CRWMS M&O. ACC: MOL.20000517.0258; MOL.20000601.0753.

146021 CRWMS M&O 2000. *Site Recommendation Subsurface Layout.* ANL-SFS-MG-000001 REV 00. Las Vegas, Nevada: CRWMS M&O. ACC: MOL.20000908.0276.

146973 Golder Associates 2000. *User's Guide, GoldSim, Graphical Simulation Environment.* Version 6.02. Manual Draft #4 (March 17, 2000). Redmond, Washington: Golder Associates. TIC: 247347.

147972 CRWMS M&O 2000. *Uncertainty Distribution for Stochastic Parameters.* ANL-NBS-MD-000011 REV 00. Las Vegas, Nevada: CRWMS M&O. ACC: MOL.20000526.0328.

148384 CRWMS M&O 2000. *Total System Performance Assessment (TSPA) Model for Site Recommendation.* MDL-WIS-PA-000002 REV 00. Las Vegas, Nevada: CRWMS M&O. ACC: MOL.20001226.0003.

148713 CRWMS M&O 2000. *Repository Safety Strategy: Plan to Prepare the Safety Case to Support Yucca Mountain Site Recommendation and Licensing Considerations.* TDR-WIS-RL-000001 REV 04. Three volumes. Las Vegas, Nevada: CRWMS M&O. ACC: MOL.20001003.0112.

149372 NRC (U.S. Nuclear Regulatory Commission) 2000. *Issue Resolution Status Report Key Technical Issue: Total System Performance Assessment and Integration.* Rev. 2. Washington, D.C.: U.S. Nuclear Regulatory Commission. TIC: 247614.

149540 DOE (U.S. Department of Energy) 2000. *Quality Assurance Requirements and Description.* DOE/RW-0333P, Rev. 10. Washington, D.C.: U.S. Department of Energy, Office of Civilian Radioactive Waste Management. ACC: MOL.20000427.0422.

151202 Golder Associates 2000. *Software Code: GoldSim.* 6.04.007. PC, Windows NT. 10344-6.04.007-00.

151395 Golder Associates 1999. *Software Code: RIP.* 5.19.01. 30055 V5.19.01.

151560 CRWMS M&O 2000. *Igneous Consequence Modeling for the TSPA-SR.* ANL-WIS-MD-000017 REV 00 ICN 01. Las Vegas, Nevada: CRWMS M&O. ACC: MOL.20001204.0022.

151940 CRWMS M&O 2000. *Unsaturated Zone Flow and Transport Model Process Model Report.* TDR-NBS-HS-000002 REV 00 ICN 02. Las Vegas, Nevada: CRWMS M&O. ACC: MOL.20000831.0280.

151947 CRWMS M&O 2000. *Source Terms for HLW Glass Canisters.* CAL-MGR-NU-000002 REV 01. Las Vegas, Nevada: CRWMS M&O. ACC: MOL.20000823.0004.

152539 CRWMS M&O 2001. *Nominal Performance Biosphere Dose Conversion Factor Analysis.* ANL-MGR-MD-000009 REV 01. Las Vegas, Nevada: CRWMS M&O. ACC: MOL.20010123.0123.

152624 CRWMS M&O 2000. *Software Routine: CWD* . V1.0. 10363-1.0-00.

153038 CRWMS M&O 2000. *Documentation of Million-Year TSPA.* Input Transmittal 00393.T. Las Vegas, Nevada: CRWMS M&O. ACC: MOL.20001110.0057; MOL.20001120.0173.

153045 CRWMS M&O 2001. *Seepage Calibration Model and Seepage Testing Data.* MDL-NBS-HS-000004 REV 01. Las Vegas, Nevada: CRWMS M&O. ACC: MOL.20010122.0093.

153097 CRWMS M&O 2000. *Number of Waste Packages Hit by Igneous Intrusion.* CAL-WIS-PA-000001 REV 01. Las Vegas, Nevada: CRWMS M&O. ACC: MOL.20001220.0041.

153207 CRWMS M&O 2001. *Distribution Fitting to the Stochastic BDCF Data.* ANL-NBS-MD-000008 REV 00 ICN 01. Las Vegas, Nevada: CRWMS M&O. ACC: MOL.20010221.0148.

153225 CRWMS M&O 2000. *Repository Safety Strategy: Plan to Prepare the Safety Case to Support Yucca Mountain Site Recommendation and Licensing Considerations.* TDR-WIS-RL-000001 REV 04 ICN 01. Two volumes. Las Vegas, Nevada: CRWMS M&O. ACC: MOL.20001122.0186.

153246 CRWMS M&O 2000. *Total System Performance Assessment for the Site Recommendation.* TDR-WIS-PA-000001 REV 00 ICN 01. Las Vegas, Nevada: CRWMS M&O. ACC: MOL.20001220.0045.

153314 CRWMS M&O 2000. *Seepage Model for PA Including Drift Collapse.* MDL-NBS-HS-000002 REV 01. Las Vegas, Nevada: CRWMS M&O. ACC: MOL.20010221.0147.

153849 DOE (U.S. Department of Energy) 2001. *Yucca Mountain Science and Engineering Report.* DOE/RW-0539. [Washington, D.C.]: U.S. Department of Energy, Office of Civilian Radioactive Waste Management. ACC: MOL.20010524.0272.

153940 CRWMS M&O 2000. *EBS Radionuclide Transport Abstraction.* ANL-WIS-PA-000001 REV 00 ICN 02. Las Vegas, Nevada: CRWMS M&O. ACC: MOL.20001204.0029.

154024 CRWMS M&O 2001. *Unsaturated Zone and Saturated Zone Transport Properties (U0100).* ANL-NBS-HS-000019 REV 00 ICN 1. Las Vegas, Nevada: CRWMS M&O. ACC: MOL.20010201.0026.

154149 EPRI (Electric Power Research Institute) 2000. *Evaluation of the Candidate High-Level Radioactive Waste Repository at Yucca Mountain Using Total System Performance Assessment, Phase 5.* 1000802. Palo Alto, California: Electric Power Research Institute. TIC: 249555.

154291 CRWMS M&O 2001. *Abstraction of Drift Seepage.* ANL-NBS-MD-000005 REV 01. Las Vegas, Nevada: CRWMS M&O. ACC: MOL.20010309.0019.

154435 NOAA (National Oceanic and Atmospheric Administration) n.d. *Upper Air Data: Desert Rock, Nevada, 1978-1995.* Reno, Nevada: National Oceanic and Atmospheric Administration, Western Regional Climate Center. TIC: 249335.

154594 CRWMS M&O 2001. *Abstraction of NFE Drift Thermodynamic Environment and Percolation Flux.* ANL-EBS-HS-000003 REV 00 ICN 02. Las Vegas, Nevada: CRWMS M&O. ACC: MOL.20010221.0160.

154657 BSC (Bechtel SAIC Company) 2001. *FY01 Supplemental Science and Performance Analyses, Volume 1: Scientific Bases and Analyses.* TDR-MGR-MD-000007 REV 00. Las Vegas, Nevada: Bechtel SAIC Company. Submit to RPC URN-0887

154748 CRWMS M&O 2000. *Software Code: ASHPLUME.* V1.4LV-dll. PC, Windows 95/NT. 10022-1.4LV-dll-00.

154921 BSC 2001. *Software Code: MkTable.* V1.00. PC, Windows NT. 10505-1.00-00.

155055 BSC (Bechtel SAIC Company) 2001. *Technical Work Plan for FY01 Supplemental Science and Performance Analyses: Volume 1 – Scientific Bases and Analyses, Volume 2 – Performance Analyses.* TWP-MGR-MD-000014 REV 01. Las Vegas, Nevada: Bechtel SAIC Company. ACC: MOL.20010601.0152.

155089 Golder Associates 2001. *Software Code: Goldsim.* V6.04.000. PC, Windows NT. 10310-6.04.000-00.

155163 Los Alamos National Laboratory 2001. *Software Code: WT_BINNING.* V1.0. PC, Windows NT. 10489-1.0-00.

155164 BSC (Bechtel SAIC Company) 2001. *Software Code: writefiles.* V1.0. 10527-1.0-00. URN-0888

155165 BSC (Bechtel SAIC Company) 2001. *Software Code: Bath_10.* V1.0. 10539-1.0-00. URN-0889

155166 CRWMS M&O 2000. *Software Code: WAPDEG.* V4.0. PC, Windows NT. 10000-4.0-00.

155168 BSC (Bechtel SAIC Company) 2001. *Software Code: Transform_Perc_files_into_Tables.* V1.0. 10530-1.0-00. URN-0891

155170 Los Alamos National Laboratory 2001. *Software Code: T2_BINNING.* V1.0. PC, Windows NT. 10490-1.0-00.

155171 BSC (Bechtel SAIC Company) 2001. *Software Code: SOILEXP.* V1.0. 10492-1.0-00. URN-0892

155172 BSC (Bechtel SAIC Company) 2001. *Software Code: Seepagedllv2.* V1.0. 10496-1.0-00. URN-0893

155174 BSC (Bechtel SAIC Company) 2001. *Software Code: Seepagedllv2uu.* V1.0. 10535-1.0-00. URN-0895

155175 Los Alamos National Laboratory 2001. *Software Code: MAKEPTRK.* V2.0. SUN, Solaris. 10491-2.0-00.

155176 BSC (Bechtel SAIC Company) 2001. *Software Code: Patch_Fail_Lag.* V1.0. 10532-1.0-00. URN-0896

155177 BSC (Bechtel SAIC Company) 2001. *Software Code: SeepagedllMk2_uu.* V1.0. 10534-1.0-00. URN-0897

155178 CRWMS M&O 2000. *Software Code: SCCD.* V2.0. PC, Windows NT. 10343-2.0-00.

155179 BSC (Bechtel SAIC Company) 2001. *Software Code: POST10K_BINS.* V1.0. 10538-1.0-00. URN-0898

155180 BSC (Bechtel SAIC Company) 2001. *Software Code: Rewrite_Perculation_Data.* V1.0. 10501-1.0-00. URN-0899

155181 BSC (Bechtel SAIC Company) 2001. *Software Code: PREWAP.* V1.0. 10533-1.0-00. URN-0900

155182 BSC (Bechtel SAIC Company) 2001. *Software Code: GoldSim.* V7.17.200. 10344-7.17.200-00. URN-0901

155316 BSC (Bechtel SAIC Company) 2001. *Software Code: WAPDEG.* V4.0. 10000-4.0-02. URN-0886

155412 LANL (Los Alamos National Laboratory) 2001. *Software Code: FEHM.* V2.12. 10086-2.12-00. URN-0909

155413 BSC (Bechtel SAIC Company) 2001. *Software Code: PDFCDF.* V1.0. 10558-1.0-00. URN-0907

155414 BSC (Bechtel SAIC Company) 2001. *Software Code: PROCESSBTC.* V1.0. 10556-1.0-00. URN-0908

155419 McNeish, J.A. 2001. "Delivery of Input and Output Files for the Supplemental TSPA Model." Memorandum from J.A. McNeish (BSC) to RPC, July 11, 2001, PROJ.07/01.021, with enclosures. Submit to RPC URN-0905

155420 McNeish, J.A. 2001. "Delivery of Input and Output Files for the Unquantified Uncertainty Sensitivity Analyses." Memorandum from J.A. McNeish (BSC) to RPC, July 11, 2001, PROJ.07/01.022, with enclosures. Submit to RPC URN-0904

155423 CRWMS M&O 2000. *Software Code: SZ_CONVOLUTE.* V2.0. PC, Windows NT. 10207-2.0-00.

155424 BSC 2001. *Software Code: SZ_CONVOLUTE.* V2.1. PC, Windows NT. 10207.2.1-00. URN-0906

155433 CRWMS M&O 2000. *Software Routine: GVP.* V1.02. PC, Windows NT. 10341-1.02-00.

155434 CRWMS M&O 2000. *Software Routine: MFD.* V1.01. PC, Windows NT. 10342-1.01-00.

155437 BSC 2001. *Software Code: WRITEFILES_NEW.* V1.0. PC, Windows NT. 10560-1.0-00. URN-0916.

6.2 CODES, STANDARDS, REGULATIONS, AND PROCEDURES

101680 64 FR 8640. Disposal of High-Level Radioactive Wastes in a Proposed Geologic Repository at Yucca Mountain, Nevada. Proposed rule 10 CFR Part 63. Readily available.

105065 64 FR 46976. Environmental Radiation Protection Standards for Yucca Mountain, Nevada. Proposed rule 40 CFR Part 197. Readily available.

146376 AP-SI.1Q, Rev. 2, ICN 4. *Software Management.* Washington, D.C.: U.S. Department of Energy, Office of Civilian Radioactive Waste Management. ACC: MOL.20000223.0508.

153202 AP-SV.1Q, Rev. 0, ICN 2. *Control of the Electronic Management of Information.* Washington, D.C.: U.S. Department of Energy, Office of Civilian Radioactive Waste Management. ACC: MOL.20000831.0065.

154517 AP-3.10Q, Rev. 2, ICN 4. *Analyses and Models.* Washington, D.C.: U.S. Department of Energy, Office of Civilian Radioactive Waste Management. ACC: MOL.20010405.0009.

154534 AP-2.21Q, Rev. 1, ICN 0, BSCN 001. *Quality Determinations and Planning for Scientific, Engineering, and Regulatory Compliance Activities.* Washington, D.C.: U.S. Department of Energy, Office of Civilian Radioactive Waste Management. ACC: MOL.20010212.0018.

154886 AP-SI.1Q, Rev. 3, ICN 1. *Software Management.* Washington, D.C.: U.S. Department of Energy, Office of Civilian Radioactive Waste Management. ACC: MOL.20010515.0126.

155216 66 FR 32074. 40 CFR Part 197, Public Health and Environmental Radiation Protection Standards for Yucca Mountain, NV; Final Rule. Readily available.

6.3 SOURCE DATA

149288 SN0004T0501600.004. Updated Results of the Base Case Saturated Zone (SZ) Flow and Transport Model. Submittal date: 04/10/2000.

150856 SN0006T0502900.002. Updated Igneous Consequence Data for Total System Performance Assessment-Site Recommendation (TSPA-SR). Submittal date: 06/15/2000.

154198 MO0012MWDNM601.033. Nominal 1,000,000-Year Base Case Contained in TDR-WIS-PA-000001 REV 00 ICN 01, Figure 4.1-19, Nominal Scenario, 1,000,000 Years, No Backfill. Constant Glacial Transition Climate After 2,000 Years. Submittal date: 12/12/2000. Submit to RPC URN-0830

154770 MO0012MWDNBC01.030. Nominal Base Cases Contained in TDR-WIS-PA-000001 REV 00 ICN 01, Nominal Scenario; 100,000 Years, No Backfill. Includes EBS-Only Simulation With All Chemistry Results Saved. Submittal date: 12/12/2000. Submit to RPC URN-0914

155415 MO0012MWDIM401.031. Igneous Scenario 5000-Realization Base Case Contained in TDR-WIS-PA-000001REV 00 ICN 01, Igneous Scenario; No Backfill; 5000 Realizations; 50,000 Years. Submittal date: 12/12/2000. Submit to RPC URN-0911

155416 MO0012MWDNEU01.025. Rss4 Neutralization Cases Contained in TDR-WIS-RL-000001 REV 04 ICN 01, Based On Nominal Scenario; No Backfill, 100,000 Years. Submittal date: 12/12/2000. Submit to RPC URN-0915

155417 MO0012MWDJUV01.026. Juvenile Failure Cases Contained in TDR-WIS-PA-000001 REV 00 ICN 01, Juvenile Failure Scenario; No Backfill, 100,000 Years. Submittal date: 12/12/2000. Submit to RPC URN-0913

155418 MO0012MWDIGN01.027. Igneous Sensitivity Cases Contained in TDR-WIS-PA-000001 REV 00 ICN 01, Igneous Scenario, Groundwater Release (Igneous Intrusion) Runs and Atmospheric Release (Volcanic Eruption) Runs. Submittal date: 12/12/2000. Submit to RPC URN-0910

155422 MO0012MWDIM501.029. Igneous Scenario 300-Realization Base Case Contained in TDR-WIS-PA-000001 REV 00 ICN 01, Igneous Scenario; No Backfill; 300 Realizations; 100,000 Years. Submittal date: 12/12/2000. Submit to RPC URN-0912

APPENDIX A

DATA TRACKING INFORMATION FOR SUPPLEMENTAL SCIENCE AND PERFORMANCE ANALYSES

APPENDIX A
DATA TRACKING INFORMATION FOR SUPPLEMENTAL SCIENCE AND PERFORMANCE ANALYSES

Listed in Table A-1 are the simulations conducted for SSPA Volume 2. These runs were performed using one of the GoldSim versions identified in Section 2.3 of this report along with associated dynamic link libraries, which model the potential Yucca Mountain repository. This table is designed to provide the information necessary to identify and compare results from the TSPA-SR (CRWMS M&O 2000 [DIRS 153246]) with results from the unquantified uncertainties analyses and the supplemental TSPA model.

All of the data for the uncertainties analyses (including SR00_043nm6) and supplemental TSPA model simulations (Table A-1) have been submitted on tape to the Records Information System under the references listed in Table A-1. The name of each simulation file is followed by a gsm extension identifying it as a GoldSim file. These gsm files contain all of the computer codes and associated input data used for the simulation. A Readme file is provided with each run explaining the particulars of the run, including run descriptions, run details, and GoldSim version used for each run. Instructions for operating and utilizing the GoldSim code are contained in the GoldSim Users Manual (Golder Associates 2000 [DIRS 146973]). Data from the GoldSim simulation file are exported to text files and then imported to SigmaPlot, which is used to plot the numerical data. The SigmaPlot files are denoted by a jnb extension. The upper-right corner of each figure in this report identifies the simulation number(s) (gsm extension) used to create the plot and the file name of the plot (jnb extension). In some cases a figure may contain data from more than one simulation. In these cases, the names of each simulation used are provided with the figure. SigmaPlot (jnb) files containing data used to create the horsetail plots are denoted with the word horsetail in the plot file name. Information on software (e.g., versions and references) is presented in Table 2.3-1.

The information in this table includes:

- Simulation number — This column contains the unique identifier assigned to each model run. The first two alpha characters (SR = TSPA-SR, UU = unquantified uncertainties, SM = supplemental TSPA model) denote the purpose of the run. In the data archived in the Records Information System, each simulation number is associated with a folder of the same number, which contains a gsm file that contains the results of the simulation.

- Scenario — This column identifies the basic scenario, nominal or igneous, on which the run was based. Base-case simulations refer to TSPA-SR scenarios.

- Description — This column contains a brief description of the runs, which are described in more detail in Sections 3 and 4 of this report. To review specifics of the modifications, retrieve the run records from the Records Information System under the reference identified.

- Figures — This column identifies the plots in this report incorporating data from this run.

- Reference — For the unquantified uncertainties and supplemental TSPA model runs, this column identifies the Records Information System references through which the model runs can be retrieved. For the TSPA-SR runs, this column identifies the reference (DTN) through which the model runs can be retrieved from the Technical Data Management System. These sources identify the model data and modified parameters associated with the model runs.

Table A-1. Listing of Simulations Conducted for Volume 2 of the SSPA

Simulation Number	Scenario	Description	Figures	Reference
SM01_003im5	Igneous	SSPA igneous-scenario base case for the HTOM (5000 realizations; 100,000 years)	Fig. 4.3-1 Fig. 4.3-2 Fig. 4.3-5a Fig. 4.3-6a	McNeish, J. 2001 [DIRS 155419]
SM01_004im5	Igneous	SSPA igneous-scenario base case for the LTOM (5000 realizations; 100,000 years)	Fig. 4.3-1 Fig. 4.3-3 Fig. 4.3-5b Fig. 4.3-6b	McNeish, J. 2001 [DIRS 155419]
SM01_029nm6	Nominal	SSPA nominal-scenario base case for the HTOM (300 realizations; 1,000,000 years)	Fig. 4.1-1 Fig. 4.1-2 Fig. 4.1-5a, b Fig. 4.1-8a Fig. 4.1-9a, b Fig. 4.1-10a, b Fig. 4.1-11a, b Fig. 4.1-12a, b, c Fig. 4.1-13a, b, c Fig. 4.1-14a, b, c Fig. 4.1-15a, b, c Fig. 4.1-16b Fig. 4.1-17b Fig. 4.2.2-1 Fig. 4.2.2-3 Fig. 4.2.2-5 Fig. 4.2.2-6 Fig. 4.2.2-8 Fig. 4.2.3-1a, b Fig. 4.2.3-2a, b Fig. 4.2.4-1a, b Fig. 4.2.5-1a, b Fig. 4.2.5-2a, b Fig. 4.2.5-3a, b Fig. 4.2.6-1 Fig. 4.2.6-2 Fig. 4.2.7-1a, b Fig. 4.2.7-2a, b Fig. 4.2.8-1a, b Fig. 4.2.8-2a, b Fig. 4.2.8-3a, b Fig. 4.2.8-4a, b Fig. 4.2.8-5a, b Fig. 4.2.8-6a, b Fig. 4.2.8-7a, b Fig. 4.2.9-1 Fig. 4.2.9-2 Fig. 4.2.9-3 Fig. 4.2.9-4 Fig. 4.2.10-1a Fig. 4.2.10-2a	McNeish, J. 2001 [DIRS 155419]

Table A-1. Listing of Simulations Conducted for Volume 2 of the SSPA (Continued)

Simulation Number	Scenario	Description	Figures	Reference
SM01_030nm6	Nominal	SSPA nominal-scenario base case for LTOM (300 realizations; 1,000,000 years)	Fig. 4.1-1 Fig. 4.1-3 Fig. 4.1-6a, b Fig. 4.1-8b Fig. 4.1-9a, b Fig. 4.1-10a, b Fig. 4.1-11a, b Fig. 4.1-12a, b, c Fig. 4.1-13a, b, c Fig. 4.1-14a, b, c Fig. 4.1-15a, b, c Fig. 4.1-16c Fig. 4.1-17c Fig. 4.2.2-2 Fig. 4.2.2-4 Fig. 4.2.2-5 Fig. 4.2.2-7 Fig. 4.2.2-9 Fig. 4.2.3-1a, b Fig. 4.2.3-2a, b Fig. 4.2.4-1a Fig. 4.2.5-1a, c Fig. 4.2.5-2a, c Fig. 4.2.5-3a, c Fig. 4.2.5-4a, b Fig. 4.2.6-1 Fig. 4.2.6-2 Fig. 4.2.7-1a, b Fig. 4.2.7-2a, b Fig. 4.2.8-1a, b Fig. 4.2.8-2a, b Fig. 4.2.8-3a, b Fig. 4.2.8-4a, b Fig. 4.2.8-5a, b Fig. 4.2.8-6a, b Fig. 4.2.8-7a, b Fig. 4.2.9-5 Fig. 4.2.9-6 Fig. 4.2.9-7 Fig. 4.2.9-8 Fig. 4.2.10-1b Fig. 4.2.10-2b	McNeish, J. 2001 (DIRS 155419]
SM01_031nm6	Nominal	Nominal LTOM with temperature-independent general corrosion	4.2.5-4a, b 4.2.5-5b	McNeish, J. 2001 [DIRS 155419]
SM01_032nm6	Nominal	Nominal LTOM with TSPA-SR base case waste package degradation model	4.2.5-4a, b 4.2.5-5a	McNeish, J. 2001 [DIRS 155419]
SM01_033nm6	Nominal	Nominal LTOM with temperature-independent general corrosion and TSPA-SR base case stress threshold and stress uncertainty	4.2.5-4a, b 4.2.5-5c	McNeish, J. 2001 [DIRS 155419]
SR00_002im4	Igneous	TSPA-SR igneous-scenario base case run (1000 realizations; 20,000 years)	Fig. 3.2.11-2a Fig. 3.3.1.2-3a	DTN MO0012MWDIGN01.027 [DIRS 155418]

Table A-1. Listing of Simulations Conducted for Volume 2 of the SSPA (Continued)

Simulation Number	Scenario	Description	Figures	Reference
SR00_005im4	Igneous	TSPA-SR igneous-scenario base case run (5000 realizations; 50,000 years)	Fig. 3.3.1-1 Fig. 3.3.1.2.4-4 Fig. 3.3.1.2.4-5 Fig. 4.3-1 Fig. 4.3-4 Fig. 4.3-5c Fig. 4.3-6c	DTN MO0012MWDIM401.031 [DIRS 155415]
SR00_016im5	Igneous	TSPA-SR igneous-scenario base case run (300 realizations; 100,000 years)	Fig. 3.3.1.2-1a Fig. 3.3.1.2-2	DTN MO0012MWDIM501.029 [DIRS 155422]
SR00_043nm6	Nominal	TSPA-SR nominal-scenario base case run (100 realizations; 1,000,000 years)	Fig. 3.2.1-1a Fig. 3.2.5-1a Fig. 3.2.5.3-1a Fig. 3.2.5.3-2a Fig. 3.2.5.4-1a Fig. 3.2.7.2-1a Fig. 3.2.7.3-1a Fig. 3.2.9-1a Fig. 3.2.10-5a Fig. 3.2.11-1a	McNeish, J. 2001 [DIRS 155420]
SR00_042nm6	Nominal	TSPA-SR nominal-scenario base case run (300 realizations; 1,000,000 years)	Fig. 3.3.2.1-1a Fig. 4.1-1 Fig. 4.1-4 Fig. 4.1-7a, b Fig. 4.1-8c Fig. 4.1-9a, b Fig. 4.1-10a, b Fig. 4.1-11a, b Fig. 4.1-12a, b, c Fig. 4.1-13a, b, c Fig. 4.1-14a, b, c Fig. 4.1-15a, b, c Fig. 4.1-16a Fig. 4.1-17a Fig. 4.2.2-5 Fig. 4.2.3-1a, b Fig. 4.2.3-2a, b Fig. 4.2.4-1a Fig. 4.2.5-1a, d Fig. 4.2.5-2a, d Fig. 4.2.5-3a, d Fig. 4.2.5-4a, b Fig. 4.2.6-1 Fig. 4.2.6-2 Fig. 4.2.7-1a, b Fig. 4.2.7-2a, b Fig. 4.2.8-1a, b Fig. 4.2.8-2a, b Fig. 4.2.8-3a, b Fig. 4.2.8-4a, b Fig. 4.2.8-5a, b Fig. 4.2.8-6a, b Fig. 4.2.8-7a, b	DTN MO0012MWDNM601.033 [DIRS 154198]

Table A-1. Listing of Simulations Conducted for Volume 2 of the SSPA (Continued)

Simulation Number	Scenario	Description	Figures	Reference
SR00_047nm5	Nominal	TSPA-SR nominal-scenario base case run (100 realizations; 100,000 years)	Fig. 3.2.2-1a Fig. 3.2.2-2 Fig. 3.2.2-3a, b Fig. 3.2.2-4a Fig. 3.2.2-5 Fig. 3.2.2-6a, b Fig. 3.2.2-7a Fig. 3.2.2-8a, b Fig. 3.2.4-1a Fig. 3.2.5.1-1a Fig. 3.2.5.2-1a Fig. 3.2.5.2-2a Fig. 3.2.5.2-3a Fig. 3.2.6.1-1a Fig. 3.2.6.3-1a Fig. 3.2.6.4-1a Fig. 3.2.7.1-1a Fig. 3.2.7.4-1a Fig. 3.2.8-1a Fig. 3.2.8-2a Fig. 3.2.10-1a Fig. 3.2.10-2a Fig. 3.2.10-3a Fig. 3.2.10-4a Fig. 3.2.10-6a Fig 3.2.10-7a	DTN MO0012MWDNBC01.030 [DIRS 154770]
SR00_096nm5	Nominal	Neutralized waste package and drip shield sensitivity (100 realizations; 100,000 years)	Fig. 3.2.2-9a Fig. 3.2.2-11 Fig. 3.2.2-12a Fig. 3.2.2-14	DTN MO0012MWDNEU01.025 [DIRS 155416]
SR00_117nm5	Nominal	Commercial spent nuclear fuel juvenile failure (100 realizations; 100,000 years)	Fig. 3.2.6.2-1a	DTN MO0012MWDJUV01.026 [DIRS 155417]
UU01_001im4	Igneous,	Indirect release, zone 1 only (1,000 realizations; 20,000 years)	Fig. 3.3.1.2-3a, b Fig. 3.3.1.2-4a	McNeish, J. 2001 [DIRS 155420]
UU01_001im5	Igneous	Direct release, wind speed sensitivity (300 realizations; 100,000 years)	Fig. 3.3.1.2-1a, b	McNeish, J. 2001 [DIRS 155420]
UU01_002im4	Igneous	Indirect release, zone 2 only (1000 realizations; 20,000 years)	Fig. 3.3.1.2-3a, c Fig. 3.3.1.2-5a	McNeish, J. 2001 [DIRS 155420]
UU01_002im5	Igneous	Direct release, waste particle size sensitivity case 1 (300 realizations; 100,000 years)	Fig. 3.3.1.2-2	McNeish, J. 2001 [DIRS 155420]
UU01_003im4	Igneous	Indirect release, zone 1 only, new cumulative distribution functions for the number of packages hit (1000 realizations; 20,000 years)	Fig. 3.3.1.2-4a, b	McNeish, J. 2001 [DIRS 155420]
UU01_003im5	Igneous	Direct release, waste particle size sensitivity case 2 (300 realizations; 100,000 years)	Fig. 3.3.1.2-2	McNeish, J. 2001 [DIRS 155420]
UU01_004im4	Igneous	Indirect release, zone 2 only, new cumulative distribution functions for number of packages hit (1,000 realizations; 20,000 years)	Fig. 3.3.1.2-5a, b	McNeish, J. 2001 [DIRS 155420]

Table A-1. Listing of Simulations Conducted for Volume 2 of the SSPA (Continued)

Simulation Number	Scenario	Description	Figures	Reference
UU01_004im5	Igneous	Direct release, waste particle size sensitivity case 3 (300 realizations; 100,000 years)	Fig. 3.3.1.2-2	McNeish, J. 2001 [DIRS 155420]
UU01_005im4	Igneous	Direct release, updated direct release biosphere dose conversion factors (1,000 realizations; 20,000 years)	Fig. 3.2.11-2a, b	McNeish, J. 2001 [DIRS 155420]
UU01_005im5	Igneous	Direct release, waste particle size sensitivity case 4 (300 realizations; 100,000 years)	Fig. 3.3.1.2-2	McNeish, J. 2001 [DIRS 155420]
UU01_006im5	Igneous	Direct release, waste particle size sensitivity case 5 (300 realizations; 100,000 years)	Fig. 3.3.1.2-2	McNeish, J. 2001 [DIRS 155420]
UU01_006nm5	Nominal	WAPDEG aging and phase stability sensitivity (100 realizations; 100,000 years)	Fig. 3.2.5.1-1a, b	McNeish, J. 2001 [DIRS 155420]
UU01_006nm6	Nominal	Seismic risk for cladding failure sensitivity (100 realizations; 1,000,000 years)	Fig. 3.3.2.1-1a, b	McNeish, J. 2001 [DIRS 155420]
UU01_007im5	Igneous	Direct release, waste particle size sensitivity case 6 (300 realizations; 100,000 years)	Fig. 3.3.1.2-2	McNeish, J. 2001 [DIRS 155420]
UU01_008im5	Igneous	Direct release, waste particle size sensitivity case 7 (300 realizations; 100,000 years)	Fig. 3.3.1.2-2	McNeish, J. 2001 [DIRS 155420]
UU01_009im5	Igneous	Direct release, single volcano occurs at 100 years, dose is not probability-weighted (300 realizations; 100,000 years)	Fig. 3.3.1.2.4-1 Fig. 3.3.1.2.4-2 Fig. 3.3.1.2.4-3	McNeish, J. 2001 [DIRS 155420]
UU01_010im5	Igneous	Direct release, single volcano occurs at 500 years, dose is not probability-weighted (300 realizations; 100,000 years)	Fig. 3.3.1.2.4-2 Fig. 3.3.1.2.4-3	McNeish, J. 2001 [DIRS 155420]
UU01_011im5	Igneous	Direct release, single volcano occurs at 1000 years, dose is not probability-weighted (300 realizations; 100,000 years)	Fig. 3.3.1.2.4-2 Fig. 3.3.1.2.4-3	McNeish, J. 2001 [DIRS 155420]
UU01_012im5	Igneous	Direct release, single volcano occurs at 5000 years, dose is not probability-weighted (300 realizations; 100,000 years)	Fig. 3.3.1.2.4-2 Fig. 3.3.1.2.4-3	McNeish, J. 2001 [DIRS 155420]
UU01_013im5	Igneous	Direct release, single volcano occurs at 100 years, no soil removal, dose is not probability-weighted (300 realizations; 100,000 years)	Fig. 3.3.1.2.4-3	McNeish, J. 2001 [DIRS 155420]
UU01_018nm5	Nominal	Episodic flow factor sensitivity (100 realizations; 100,000 years)	Fig. 3.2.2-7a, b Fig. 3.2.2-8a, b	McNeish, J. 2001 [DIRS 155420]
UU01_019nm5	Nominal	Flow focusing factor sensitivity (100 realizations; 100,000 years)	Fig. 3.2.2-4a, b Fig. 3.2.2-5 Fig. 3.2.2-6a, b	McNeish, J. 2001 [DIRS 155420]
UU01_021nm5	Nominal	Bathtub delay for advective release (100 realizations; 100,000 years)	Fig. 3.2.6.4-1a, b	McNeish, J. 2001 [DIRS 155420]

Table A-1. Listing of Simulations Conducted for Volume 2 of the SSPA (Continued)

Simulation Number	Scenario	Description	Figures	Reference
UU01_021nm6	Nominal	New cladding failure model (100 realizations; 1,000,000)	Fig. 3.2.7.2-1a, b	McNeish, J. 2001 [DIRS 155420]
UU01_024nm5	Nominal	WAPDEG stress corrosion cracking – stress threshold sensitivity (100 realizations; 100,000 years)	Fig. 3.2.5.2-2a, b	McNeish, J. 2001 [DIRS 155420]
UU01_025nm5	Nominal	No seepage when drift wall is above boiling (96ºC), plus waste package and drip shield neutralized (100 realizations; 100,000 years)	Fig. 3.2.2-9a, b Fig. 3.2.2-10 Fig. 3.2.2-11	McNeish, J. 2001 [DIRS 155420]
UU01_026nm5	Nominal	WAPDEG stress corrosion cracking – manufacturing defect sensitivity (100 realizations; 100,000 years)	Fig. 3.2.5.2-3a, b	McNeish, J. 2001 [DIRS 155420]
UU01_026nm6	Nominal	New groundwater biosphere dose conversion factors (100 realizations; 1,000,000 years)	Fig. 3.2.11-1a, b	McNeish, J. 2001 [DIRS 155420]
UU01_028nm5	Nominal	WAPDEG stress corrosion cracking – stress profiles sensitivity (100 realizations; 100,000 years)	Fig. 3.2.5.2-1a, b	McNeish, J. 2001 [DIRS 155420]
UU01_029nm5	Nominal	Saturated zone no matrix diffusion sensitivity (100 realizations; 100,000 years)	Fig. 3.2.10-2a, b	McNeish, J. 2001 [DIRS 155420]
UU01_029nm6	Nominal	Saturated zone colloids sensitivity (100 realizations; 1,000,000 years)	Fig. 3.2.10-5a, b	McNeish, J. 2001 [DIRS 155420]
UU01_030nm5	Nominal	Saturated zone enhanced matrix diffusion sensitivity (100 realizations; 100,000 years)	Fig. 3.2.10-3a, b	McNeish, J. 2001 [DIRS 155420]
UU01_031nm5	Nominal	Saturated zone no alluvium sensitivity (100 realizations; 100,000 years)	Fig. 3.2.10-4a, b	McNeish, J. 2001 [DIRS 155420]
UU01_032nm5	Nominal	Rev 01 seepage model sensitivity (100 realizations; 100,000 years)	Fig. 3.2.2-1a, b Fig. 3.2.2-2 Fig. 3.2.2-3a, b	McNeish, J. 2001 [DIRS 155420]
UU01_035nm5	Nominal	New seepage model for SSPA supplemental model (100 realizations; 100,000 years)	Fig. 3.2.2-12a, b Fig. 3.2.2-13a, b Fig. 3.2.2-14	McNeish, J. 2001 [DIRS 155420]
UU01_039nm5	Nominal	Seepage evaporation sensitivity (100 realizations; 100,000 years)	Fig. 3.2.6.1-1a, b	McNeish, J. 2001 [DIRS 155420]
UU01_039nm6	Nominal	New WAPDEG temperature-dependent general corrosion model (Case 13-23) with 36 kJ slope and MKTABLE.DLL, which samples temperature variability (100 realizations; 1,000,000 years)	Fig. 3.2.5.3-2a, b	McNeish, J. 2001 [DIRS 155420]
UU01_040nm5	Nominal	Sorption coefficients in waste package and Invert (americium, iodine, neptunium, plutonium, technetium, thorium, and uranium), with scaled volume of water for waste package and Invert (100 realizations; 100,000 years)	Fig. 3.2.8-2a, b	McNeish, J. 2001 [DIRS 155420]
UU01_041nm6.		Advection and diffusion unsaturated zone flux splitting (100 realizations; 100,000 years)	Fig. 3.2.9-1a, b	McNeish, J. 2001 [DIRS 155420]

Table A-1. Listing of Simulations Conducted for Volume 2 of the SSPA (Continued)

Simulation Number	Scenario	Description	Figures	Reference
UU01_042nm5	Nominal	In-package diffusion model for commercial spent nuclear fuel, no drip environments only (100 realizations; 100,000 years)	Fig. 3.2.8-1a, b	McNeish, J. 2001 [DIRS 155420]
UU01_042nm6	Nominal	New radionuclide solubilities for technetium, thorium, plutonium, uranium, and neptunium (100 realizations; 1,000,000 years)	Fig. 3.2.7.3-1a, b	McNeish, J. 2001 [DIRS 155420]
UU01_043nm6	Nominal	WAPDEG (Rev 01) Case 39-22 (100 realizations; 1,000,000 years)	Fig. 3.2.5-1a, b	McNeish, J. 2001 [DIRS 155420]
UU01_045nm5	Nominal	Dripshield condensation model (100 realizations; 100,000 years)	Fig. 3.2.6.2-1a, b	McNeish, J. 2001 [DIRS 155420]
UU01_046nm6	Nominal	100% uncertainty and WAPDEG (Rev 01) model, case 42-22 (100 realizations; 1,000,000 years)	Fig. 3.2.5.3-1a, b	McNeish, J. 2001 [DIRS 155420]
UU01_047nm6	Nominal	Long term climate with new saturated zone curves (6/18/01) and SZ convolute (SZ_Conv_6-6-01.dll) (100 realizations; 1,000,000 years)	Fig. 3.2.1-1a, b	McNeish, J. 2001 [DIRS 155420]
UU01_050nm5	Nominal	Glass waste form colloid (engineered barrier system, unsaturated zone, saturated zone) sensitivity (100 realizations; 100,000 years)	Fig. 3.2.7.4-1a, b Fig. 3.2.10-6a, b	McNeish, J. 2001 [DIRS 155420]
UU01_051nm6	Nominal	WAPDEG early failure (improper heat treatment of welds) model (100 realizations; 1,000,000 years)	Fig. 3.2.5.4-1a, b	McNeish, J. 2001 [DIRS 155420]
UU01_052nm5	Nominal	New in-drift chemistry and initial carbon dioxide values for HTOM (100 realizations; 100,000 years)	Fig. 3.2.4-1a, b	McNeish, J. 2001 [DIRS 155420]
UU01_055nm5	Nominal	New waste package/drip shield flux splitting (100 realizations; 100,000 years)	Fig. 3.2.6.3-1a, b	McNeish, J. 2001 [DIRS 155420]
UU01_058nm5	Nominal	New in-package chemistry model (100 realizations; 100,000 years)	Fig. 3.2.7.1-1a, b	McNeish, J. 2001 [DIRS 155420]
UU01_059nm5	Nominal	Saturated zone with 1/8/01 breakthrough curves (new distribution for bulk density of the alluvium and sorption coefficients for iodine and technetium set to zero in alluvium)	Fig. 3.2.10-7a, b	McNeish, J. 2001 [DIRS 155420]
UU01_060nm5	Nominal	Unquantified uncertainties saturated zone case. Replaced base case saturated zone curves with the unquantified uncertainties saturated zone curves (03-13-01).	Fig. 3.2.10-1a, b	McNeish, J. 2001 [DIRS 155420]

NOTE: HTOM = higher-temperature operating mode; LTOM = lower-temperature operating mode

INTENTIONALLY LEFT BLANK